Volume Editor H. Nagase

Chemistry of Opioids

Springer

299

Topics in Current Chemistry

Topics in Current Chemistry
Recently Published and Forthcoming Volumes

Chemistry of Opioids

Volume Editor: Hiroshi Nagase

With Contributions by

S.N. Calderon · N. Chida · H. Fujii · S. Hirono · S.M. Husbands ·
J.W. Lewis · K.M. Lovell · A. Lozama · H. Nagase ·
K.M. Prevatt-Smith · T.E. Prisinzano · H. Schmidhammer ·
M. Spetea · N. Yamaotsu

Springer

Editor
Prof. Dr. Hiroshi Nagase
Kitasato University
School of Pharmaceutical Sciences
Department of Medicinal Chemistry
Sirokane 5-9-1
108-8641 Tokyo
Minato-ku
Japan
nagaseh@pharm.kitasato-u.ac.jp

Cover design: WMXDesign GmbH, Heidelberg, Germany

Printed on acid-free paper

Springer is part of Springer Science+Business Media (www.springer.com)

Topics in Current Chemistry
Also Available Electronically

Topics in Current Chemistry is included in Springer's eBook package *Chemistry and Materials Science*. If a library does not opt for the whole package the book series may be bought on a subscription basis. Also, all back volumes are available electronically.

For all customers with a print standing order we offer free access to the electronic volumes of the series published in the current year.

If you do not have access, you can still view the table of contents of each volume and the abstract of each article by going to the SpringerLink homepage, clicking on "Chemistry and Materials Science," under Subject Collection, then "Book Series," under Content Type and finally by selecting *Topics in Current Chemistry*.

You will find information about the

– Editorial Board
– Aims and Scope
– Instructions for Authors
– Sample Contribution

at springer.com using the search function by typing in *Topics in Current Chemistry*.

Color figures are published in full color in the electronic version on SpringerLink.

Aims and Scope

The series *Topics in Current Chemistry* presents critical reviews of the present and future trends in modern chemical research. The scope includes all areas of chemical science, including the interfaces with related disciplines such as biology, medicine, and materials science.

The objective of each thematic volume is to give the non-specialist reader, whether at the university or in industry, a comprehensive overview of an area where new insights of interest to a larger scientific audience are emerging.

Thus each review within the volume critically surveys one aspect of that topic and places it within the context of the volume as a whole. The most significant developments of the last 5–10 years are presented, using selected examples to illustrate the principles discussed. A description of the laboratory procedures involved is often useful to the reader. The coverage is not exhaustive in data, but rather conceptual, concentrating on the methodological thinking that will allow the non-specialist reader to understand the information presented.

Discussion of possible future research directions in the area is welcome.

Review articles for the individual volumes are invited by the volume editors.

In references *Topics in Current Chemistry* is abbreviated *Top Curr Chem* and is cited as a journal.

Impact Factor 2009: 4.291; Section "Chemistry, Multidisciplinary": Rank 20 of 138

Preface

As part of the *Topics in Current Chemistry* series, this volume, entitled "Chemistry of Opioids," presents the progress made in opioid research over the past 5 years in the synthesis and pharmacology of opioids.

In 1803, morphine was first isolated by a German pharmacologist, Sertürner, and its structure was later determined. Since then, many research groups have tried to synthesize an ideal analgesic without addictive properties. In the course of those studies, a number of opioids were synthesized. Morphine has a unique 4,5-epoxymorphinan skeleton, which comprises five sequential asymmetric centers and a phenolic hydroxy group, a 4,5-epoxy ring, and a basic nitrogen. Due to this complex structure, early research groups could not synthesize morphine. Therefore, they tried to design drugs with simpler structures that could be manufactured as an industrial product. These trials produced many drugs, including pentazocine (benzomophan), butorphanol, levorphanol (morphinan), pethidine (phenylpiperidine), fentanyl (anilinopiperidine), etc. However, these compounds could not provide analgesics without addiction. In 1975, when endogenous opioids were isolated, many researchers expected to be able to produce a drug without addictive properties, and many peptide derivatives were synthesized. Unfortunately, these opioid peptide mimetics also had addictive properties, despite the fact that they were derived from endogenous substances.

Nevertheless, opioid researchers did not give up their dreams. The first clue was that there were three types of opioid receptors (μ, δ, κ). This explained the diverse pharmacological effects of the many synthetic drugs. Many of the syntheses and pharmacologies of drugs produced before the early 1980s have been described in detail in two excellent books published in 1986, entitled *Opioid Analgesics; Chemistry and Receptor* and *Opiates*. After that, research focused on the κ and δ opioid receptor types. In the 1990s, extensive research was conducted in multiple efforts to synthesize κ selective agonists. However, there is no current book regarding the progress in the whole opioid field of δ- and κ-type selective ligands. In particular, in the 1990s, a vast number of U-50,488H (discovered by Upjohn Company) derivatives were synthesized to produce a nonaddictive drug. Unfortunately, these derivatives showed aversive effects (psychotomimetics), and development was suspended in the early stages, both as an analgesic and as an antipruritic

drug. Consequently, there have been no reports on U-50,488H derivatives in the last 5 years.

This book describes the progress made in the opioid field over the last 5 years with a focus on the work of 14 representative researchers in the opioid field.

The first chapter, "Recent Advances in the Synthesis of Morphine and Related Alkaloids," by Noritaka Chida, presents the racemic synthesis of morphine and related alkaloids by four research groups, and the chiral synthesis of those alkaloids by four research groups. This work has greatly contributed to progress in Organic Chemistry and Medicinal Chemistry.

The second chapter, "Opioids in Preclinical and Clinical Trials," by Hiroshi Nagase and Hideaki Fujii, provides a short survey of opioid ligands in development. They also give a detailed history of the drugs, TRK-851(δ-antagonist) and TRK-820 (nalfurafine hydrochloride, κ-agonist), which were discovered by their team.

The third chapter, "Synthesis of 14-Alkoxymorphinan Derivatives and Their Pharmacological Actions," by Helmut Schmidhammer and Mariana Spetea, presents recent advances in the chemistry, ligand-based structure activity relationships, and pharmacology of 14-alkoxymorphinans.

The fourth chapter, "14-Amino-4,5-epoxymorphinan Derivatives and Their Pharmacological Actions," by John W. Lewis and Stephen M. Husbands, presents the recent extensive studies on the chemistry, structure–activity relationships, and pharmacology of 14-acylamino- and 14-alkylamino-derivatives.

The fifth chapter, "Nonpeptidic δ Opioid Agonists and Antagonists of the Diarylmethylpiperazine Class: What Have We Learned?" by Silvia N. Calderon, presents the major advances in the field of δ-opioid ligands and the extensive research performed to uncover the SAR of SNC-80 derivatives. Furthermore, synthetic methods are described for these compounds.

The sixth chapter, "Synthesis of Neoclerodane Diterpenes and Their Pharmacological Effects," by Kimberly M. Lovell, Katherine M. Prevatt-Smith, Anthony Lozama, and Thomas E. Prisinzano, describes the total synthesis of Salvinorin A and current research efforts focused on structure modifications of Salvinolin A derivatives.

The seventh chapter, "Synthesis of Novel Basic Skeletons Derived from Naltrexone," by Hiroshi Nagase and Hideaki Fujii, describes the many novel reactions that were discovered in the course of synthesizing naltrexone derivatives and the characteristics of those naltrexone derivatives. Some of the new reactions were expanded into general reactions.

The eighth chapter, "Twin and Triplet Drugs in Opioid Research," by Hideaki Fujii, presents opioid research that used dimer and trimer ligands as a tool for investigating opioid receptors. The dimer and trimer constructs were able to increase ligand activity and selectivity.

The ninth chapter, "3D-Pharmacophore Identification for κ-Opioid Agonists Using Ligand-Based Drug-Design Techniques," by Noriyuki Yamaotsu and Shuichi Hirono, presents a summary of previous efforts in identifying the pharmacophore in κ-opioid agonists and a proposal for a new model that encompasses the activities of all class κ-agonists.

I would like to thank all those who have contributed to making this volume a collection of expert articles. I hope that our readers find this volume a useful guide to the current progress in opioid research.

Tokyo, Summer 2010   Hiroshi Nagase

Contents

Recent Advances in the Synthesis of Morphine and Related Alkaloids

Noritaka Chida

Abstract Morphine, an alkaloid isolated from the opium poppy, has been widely used as an analgesic, and has been a fascinating synthetic target of organic chemists. After the first total synthesis reported in 1952, a number of synthetic studies toward morphine have been reported, and findings obtained in such studies have greatly contributed to the progress of synthetic organic chemistry as well as medicinal chemistry. This review provides an overview of recent studies toward the total synthesis of morphine and related alkaloids. Work reported in the literature since 2004 will be reviewed.

Keywords Chiral synthesis · Codeine · Morphine · Total synthesis

Contents

Abbreviations

aq   Aqueous
BHT   2,6-Di-*tert*-butyl4-methylphenol
Cy   Cyclohexyl

N. Chida (✉)
Department of Applied Chemistry, Keio University, 3-14-1 Hiyoshi, Kohoku-ku, Yokohama
223-8522, Japan
e-mail: chida@applc.keio.ac.jp

dba	Dibenzylideneacetone
DIAD	Diisopropyl azodicarboxylate
DMP	Dess–Martin periodinane
dppe	1,2-Bis(diphenylphosphino)ethane
dppf	1,1′-Bis(diphenylphosphino)ferrocene
dppp	1,3-Bis(diphenylphosphino)propane
MS3A	Molecular sieves 3A
o-tolyl	2-Methylphenyl
Troc	2,2,2-Trichloroethoxycarbonyl

1 Introductory Remarks

More than two hundred years have passed since the isolation of morphine (**1**) from the unripe seed pods of opium poppy, *Papaver somniferum* [1, 2]. A number of structurally related alkaloids, such as codeine (**2**), thebaine (**3**), and codeinone (**4**), have also been discovered in the same plant (Scheme 1) [3]. Due to its significant effectiveness as an analgesic and as an anesthetic, morphine has been used as an important medicine for a long time in spite of its serious addictive side effects. The structure of morphine, first proposed in 1925, is quite unique among alkaloids; it has a strained pentacyclic core (morphine skeleton) with five contiguous chiral centers including a benzylic quaternary carbon [4]. The significant biological activity as well as the highly challenging structure of morphine has naturally received considerable attention from synthetic chemists, and thus a huge number of synthetic
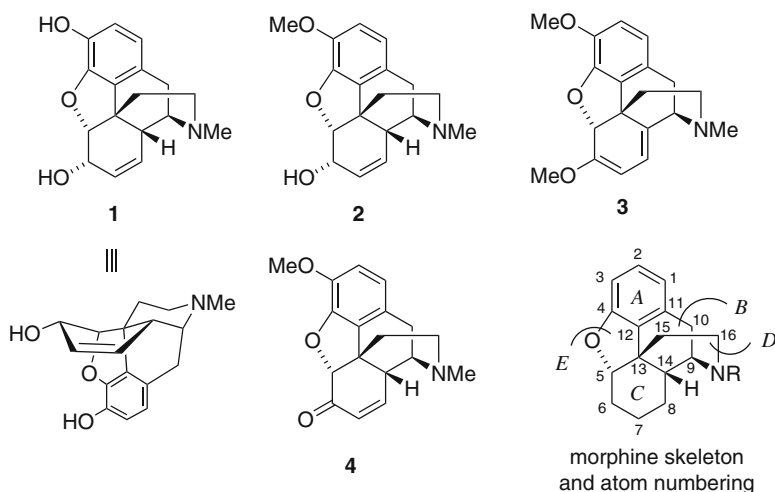
Scheme 1 Structures of morphine, codeine, thebaine, codeinone, and a morphine skeleton

studies and total syntheses have been reported after the first total synthesis by Gates and Tschudi in 1952 [5, 6]. During the extensive synthetic studies of morphine, many useful new reactions and innovative synthetic methodologies have been developed, bringing significant progress in the field of organic chemistry [7–9]. The developments of the novel and effective synthetic method of morphine and its related compounds are still an important task in modern synthetic organic chemistry. In this chapter we will deal with the recent synthetic studies of morphine and its related alkaloids in the literature since 2004, as the excellent and comprehensive reviews covering the literature prior to 2004 by Maier [7], Multzer [10], Blakemore and White [11], Hudlicky [12, 13], Taber [14], and Dalton [15] have been published.

2 Synthesis of Morphine and Related Alkaloids

Although a huge number of synthetic studies toward the total synthesis of morphine and related alkaloids have been reported to date, it is still important to establish the novel and efficient synthetic pathways to these alkaloids. In particular, developments of flexible synthetic methods, which can produce morphine analogs that are difficult to obtain by the chemical modification of natural alkaloids, are highly important for the generation of a novel morphine-type drug showing lower or no addictive effect. From the viewpoint of organic synthesis, the complex pentacyclic structure of morphine with multi stereogenic centers remains a challenging target. In this chapter, recent literature describing the total synthesis of morphine and related alkaloids reported from eight research groups during 2004–2009 will be reviewed. They are classified into two categories: racemic synthesis and chiral synthesis.

2.1 Racemic Synthesis

In this section, reports on the total synthesis of morphine-related compounds in racemic forms based on the novel and synthetically important methodologies disclosed by Fukuyama, Guillou, Stork, and Magnus will be discussed.

2.1.1 Fukuyama Group

In 2006 Fukuyama published a total synthesis of racemic morphine starting from isovanillin and a cyclohexene-epoxide [16, 17]. The key features in their synthesis are (1) a construction of the ether linkage between A and C rings by Tsuji-Trost coupling, (2) an intramolecular Heck reaction to construct A–C–E tricyclic system, and (3) an intramolecular Mannich-type reaction of a ketone with an aminal to provide the pentacyclic structure of morphine in a one-step reaction by double cyclization.
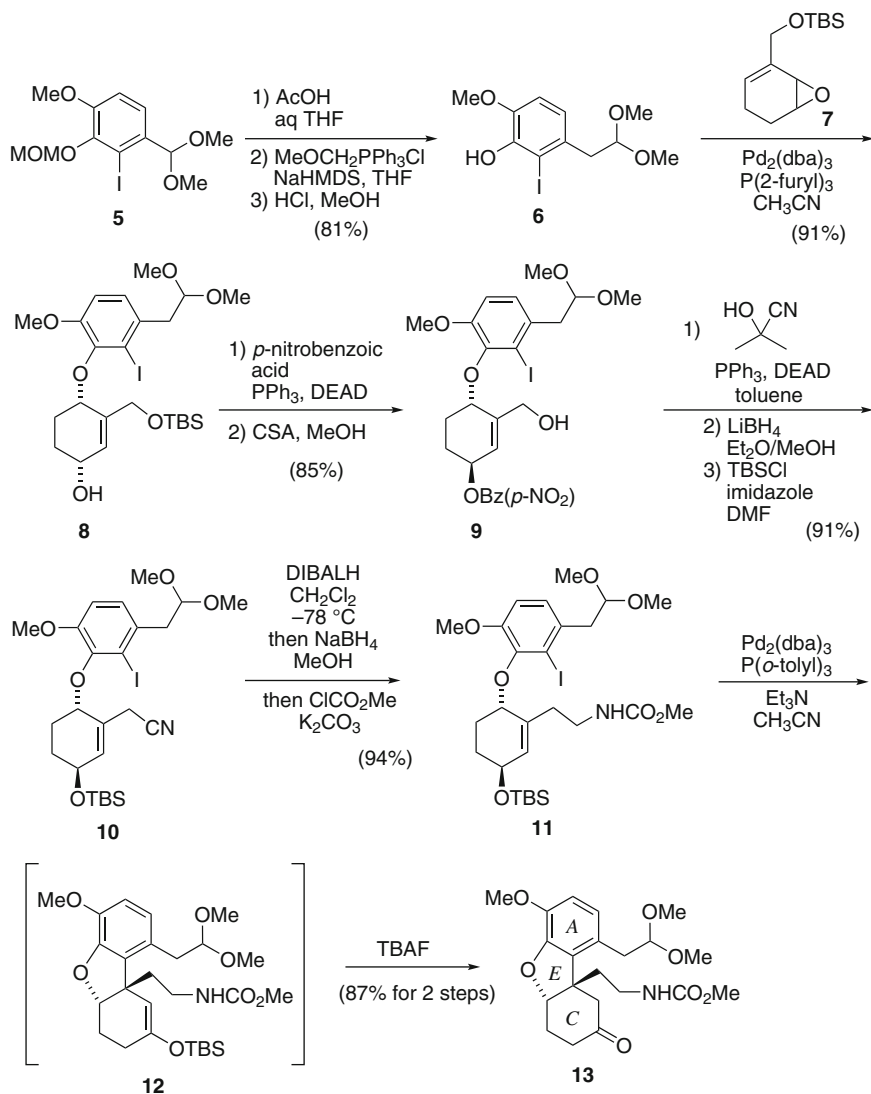
Scheme 2 Construction of the A–C–E ring of morphine by Fukuyama

Their synthesis begins with the known aryliodide **5** (Scheme 2). After one-carbon homologation of **5**, the resulting phenol **6** was treated under the Tsuji-Trost conditions [18] with cyclohexene-epoxide **7** to afford aryl ether **8** with complete regio- and stereoselectivity. After inversion of the stereochemistry of the secondary alcohol function in **8** by Mitsunobu reaction [19, 20] with *p*-nitrobenzoic acid, the primary hydroxy group in **9**, obtained by the deprotection of TBS group, was converted into a nitrile under the Mitsunobu conditions. Exchange of the protecting
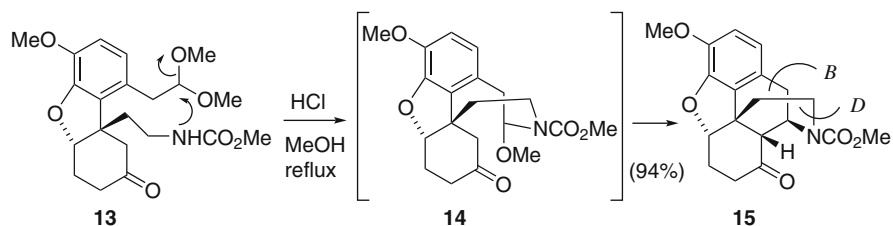
Scheme 3 Construction of D- and B-rings by way of the double cyclization via an intramolecular Mannich-type reaction

group of the hydroxy group afforded **10**. The nitrile function in **10** was reduced with DIBALH to give a crude imine, which was further reduced with NaBH$_4$ in methanol to give a primary amine. Protection of the amine as a methyl carbamate provided **11**.

The intramolecular Heck reaction to construct the polycyclic benzofuran skeleton in morphine was reported by Overman [21] in their synthesis of (+)- and (–)-dihydroisocodeine in 1993, and after that, the Heck cyclization has been extensively studied by Cheng [22], Hsin [23, 24], Hudlicky [25] (see Sect. 2.2.3), Trost (see Sect. 2.2.1), and Guillou (see Sect. 2.1.2). In Fukuyama's synthesis, the Heck reaction of **11** works well and successfully provided the A–C–E tricyclic ring system **13** in 87% yield after deprotection of the TBS group in the intermediary enol ether **12**.

When acetal **13** was treated with methanolic HCl at reflux temperature, double cyclization took place to give morphine skeleton **15** in 94% yield (Scheme 3). Since the formation of eight-membered aminal **14** was observed during the reaction, this intriguing cyclization is believed to proceed via an intramolecular Mannich-type reaction. It is important to note that the morphine skeleton was effectively constructed in high yield under simple reaction conditions.

For a conversion of **15** to morphine, compound **15** was first oxidized under Ito-Saegusa conditions [26] to give cyclohexenone derivative **16** (Scheme 4). After introduction of an epoxide ring, the ketone carbonyl in **17** was stereoselectively reduced to afford **18**. The rigid pentacyclic structure of a morphine skeleton allowed the approach of the reagent only from the less hindered *exo* (β-) face. The hydroxy group in **18** was converted into a thiocarbamate and tin-mediated radical conditions [27] induced the epoxide opening to provide allylic alcohol **19**. Oxidation of the alcohol function gave a cyclohexenone, which was treated with LiAlH$_4$. Under the reaction conditions, the ketone carbonyl was reduced stereoselectively and the methyl carbamate was also reduced to give codeine. Finally, by Rice's procedure [28], codeine was successfully converted into morphine.

2.1.2 Guillou Group

In 2008 the Guillou group disclosed the total synthesis of racemic codeine [29]. The key features in their synthesis are (1) a construction of the C-ring including a quaternary carbon by the intramolecular Heck reaction, (2) an oxy-Michael
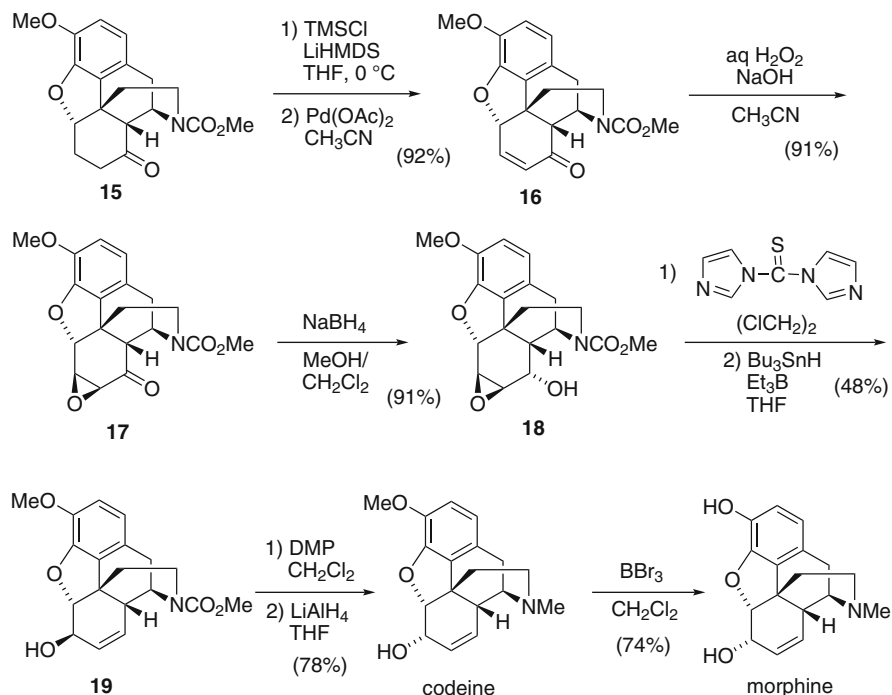
Scheme 4 Synthesis of morphine by Fukuyama

addition of phenol to cyclohexadienone to generate the A–C–E tricyclic system of morohine skeleton, (3) an Eschenmoser Claisen rearrangement for the stereoselective construction of a tertiary carbon at C-14, (4) a B-ring formation by intramolecular Friedel−Crafts-type cyclization/dehydration, and (5) a reductive hydroamination to make up the D-ring.

Condensation of carboxylic acid **20** with 2-iodo-6-methoxyphenol gave ester **21** (Scheme 5). When **21** was treated with Pd catalyst and Et$_3$N in DMF, the intramolecular Heck reaction successfully took place to provide spiro-compound **22**. It is interesting to note that, in this reaction, the absence of phosphine ligands is essential for the completion of the reaction in shorter reaction time. After hydrolysis of the dioxolane group, the resulting ketone was converted into dienone **23** by the oxidation with (PhSeO)$_2$O. Treatment of **23** with N-methylbenzylamine induced the lactone opening and the formation of an amide. Under the reaction conditions, an intramolecular oxy-Michael addition of the resulting phenol **24** to the dienone moiety occurred to afford the tricyclic benzofuran (A–C–E ring system) **25**.

Reaction of **25** with LiAlH$_4$ stereoselectively reduced the enone system in a 1,2-fashion as well as the amide carbonyl to give **26**. Eschenmoser Claisen rearrangement [30] of **26** afforded the desired rearranged product **27** in 49% yield. The major side product in the rearrangement was diene **28** (32%), and it was found that
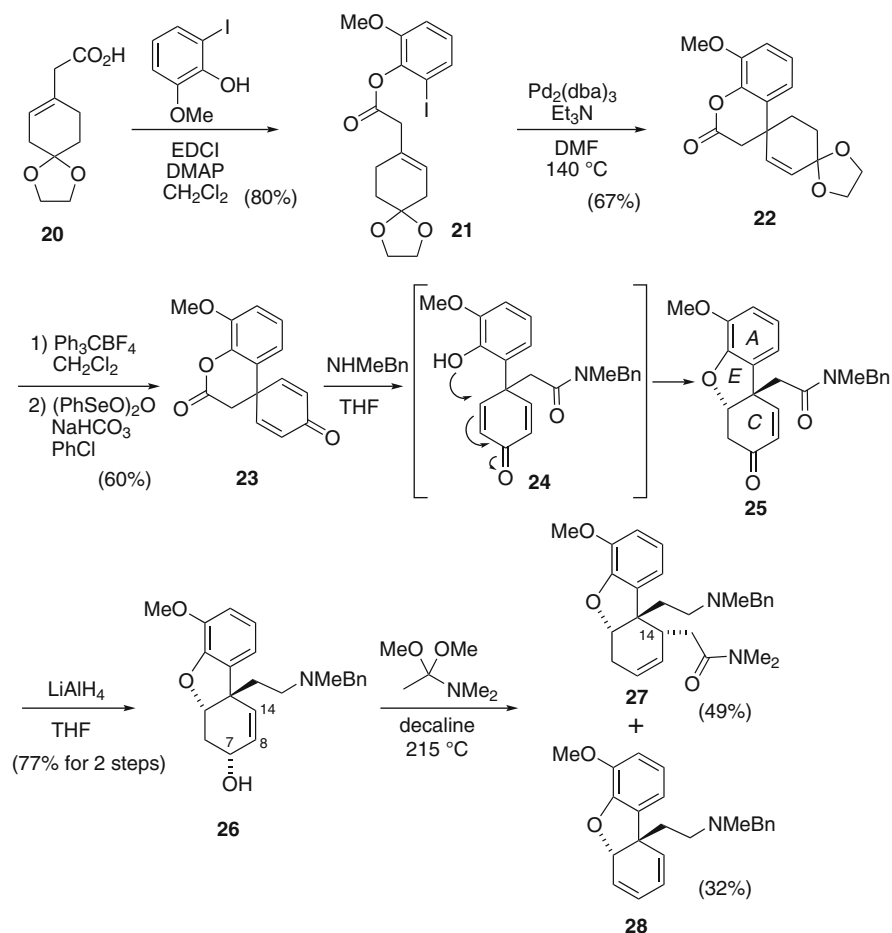
Scheme 5 Synthesis of A–C–E ring of codeine by Guillou

other variants of Claisen rearrangement [31] (Kazmaier [32], Ireland [33], and Johnson [34]) gave no rearranged product.

The dimethylamide function in **27** was reduced by the action of Ti(Oi-Pr)$_4$ and phenylsilane [35] to give aldehyde **29**, which was then treated with p-TsOH in toluene at room temperature (Scheme 6). Under these reaction conditions, the intramolecular Friedel−Crafts-type cyclization occurred, and the subsequent dehydration of a benzylic alcohol also took place to afford phenanthrofuran skeleton (A–B–C–E ring) **30**. The formation of the B-ring by way of intramolecular Friedel−Crafts acylation was first reported by Ginsburg in his synthesis of dihydrothebainone in 1954 [36]. This transformation was also employed by White in the synthesis of (+)-morphine [37], and by Multzer in the synthesis of dihydrocodeinone [38–40]. The Friedel−Crafts-type cyclization with an aldehyde function was used by Evans [41] in the formal synthesis of morphine and by Hudlicky in the
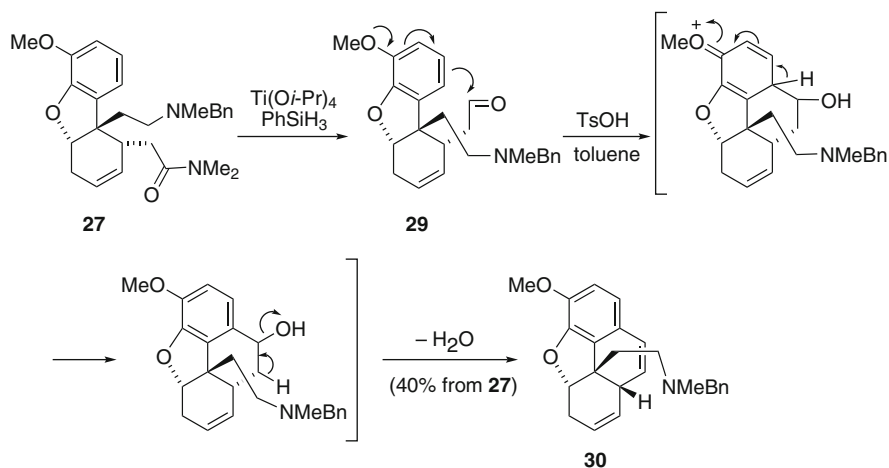
Scheme 6 Construction of the B-ring by the Friedel−Crafts-type cyclization

synthesis of 10-hydroxy-14-*epi*-dihydrocodeinone [25]. The Friedel−Crafts-type cyclization/dehydration with an aldehyde was reported by Ogasawara [42] in the synthesis of (–)-morphine, and later employed by Chida in the synthesis of (–)-dihydroisocodeine (see Sect. 2.2.4).

The *N*-benzyl group in **30** was removed by the action of 1-chloroethyl chloroformate [43], and the resulting secondary amine was protected as a sulfonamide to afford **31** (Scheme 7). Allylic oxidation of **31** with SeO$_2$ and *t*-BuOOH [44] gave allylic alcohol **32** in regio- and stereoselective manners. The similar allylic oxidation of phenanthrofuran compound has been reported by Trost (see Sect. 2.2.1). The stereochemistry of the allylic alcohol in **32** was inverted by oxidation−reduction procedure to give **33** in 28% yield from **31**. Final ring-closure of D-ring was carried out using the hydroamination of a nitrogen radical (or anion) with a styrene moiety, first reported by Parker in the synthesis of dihydroisocodeine (see Sect. 2.2.2). Thus, treatment of sulfonamide **32** with Li in liquid ammonia in the presence of *t*-BuOH removed the Ts group on the nitrogen and induced the D-ring cyclization to give racemic codeine in 51% yield. The similar cyclization reactions of the corresponding amine which also provided codeine by the action of LDA and visible light (Trost, see Sect. 2.2.1) and Hg(OAc)$_2$/LiAlH$_4$ (Hudlicky, see Sect. 2.2.3) have been reported.

2.1.3 Stork Group

The Stork group reported the synthesis of racemic codeine and thebaine utilizing the intramolecular Diels–Alder reaction as the key transformation in 2009 [45]. The key features of their synthesis are (1) a direct construction of a phenanthrofuran skeleton (A–B–C–E tetracyclic system) by the intramolecular Diels–Alder reaction of a diene tethered to the benzofuran ring and (2) a formation of the D-ring by the intramolecular S$_N$2 reaction of an amino-mesylate.
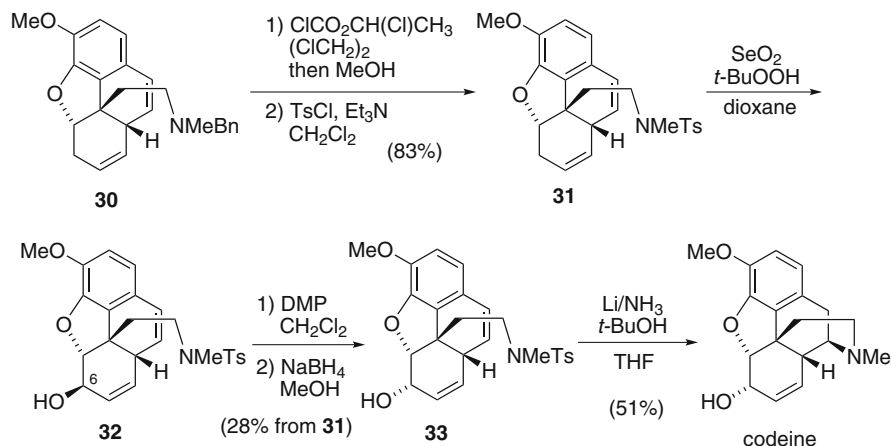
Scheme 7 Synthesis of racemic codeine by Guillou

Reaction of the known acetal **34** readily available from iodoisovanillin with methyl propiolate gave oxy-Michael product **35**, whose intramolecular Heck reaction cleanly provided benzofuran **36** (Scheme 8). One-carbon homologation of **36** gave **37**. Addition of an *E*-vinylzirconium species generated by hydrozirconation [46] of 3-buten-1-yne to aldehyde **37**, followed by *O*-silylation, afforded diene **38**. When a decaline solution of diene-benzofuran **38** was heated at 230°C in the presence of Et₃N in a sealed flask, the desired Diels–Alder reaction took place to afford phenanthrofuran **40** in 89% yield as an epimeric mixture at C-9. The cycloaddition reaction proceeded via the *endo*-benzofuran transition structure **39**, thus providing the adducts in a highly stereoselective manner. It is important to note that the intramolecular Diels–Alder reaction successfully constructed the highly functionalized phenanthrofuran (A–B–C–E ring of morphine), possessing the correct stereochemistry including the quaternary carbon, stereoselectively in a one-step reaction. The intramolecular Diels–Alder reaction of amidofurans tethered onto a benzofuran ring which delivered the simple model compound of an A–C–E ring in morphine skeleton was reported by Padwa [47]. The intermolecular version of Diels–Alder cycloaddition for the construction of A–B–C ring of morphine skeleton was employed by Gates [5, 6] and Tius [48] as the key reactions in their syntheses of morphine.

The ester group in **40** was converted into a vinyl ether to give **41**, the *O*-TES protecting group of which was removed and the resulting secondary alcohol was oxidized to afford ketone **42** (Scheme 9). As a tetracyclic structure of **42** allowed the approach of the reagent from the less hindered β-face, the reduction of the ketone carbonyl in **42** with structurally bulky L-selectride (lithium tri-*sec*-butylborohydride) gave the single α-alcohol, which was isolated as its *O*-methanesulfonate ester **43**. Hydrolysis of the vinyl ether function in **43**, followed by reductive amination with methylamine in the presence of NaBH₄, afforded ethanamine **44**.
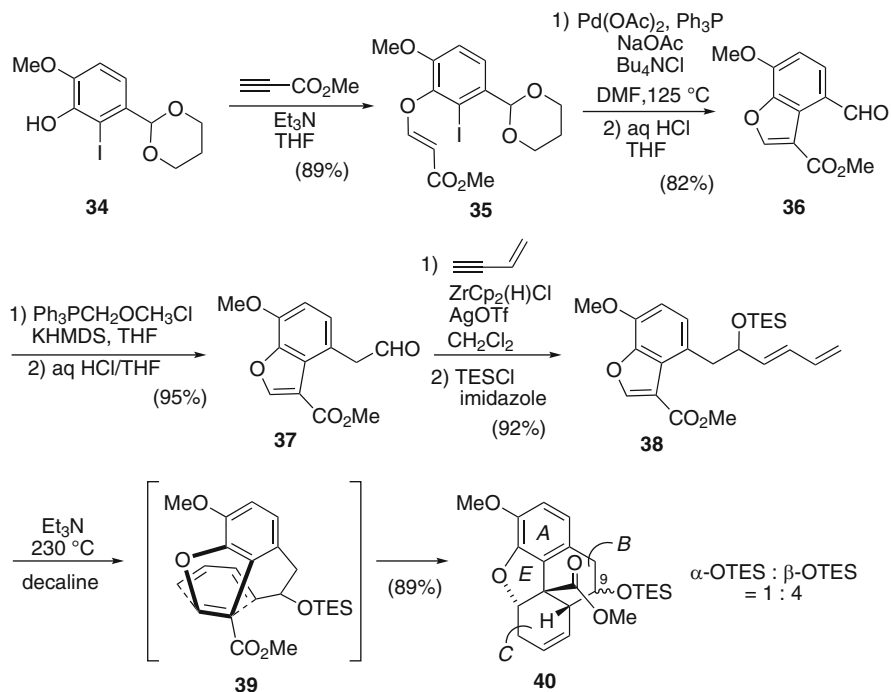
Scheme 8 Construction of a tetracycle of codeine by the intramolecular cycloaddition
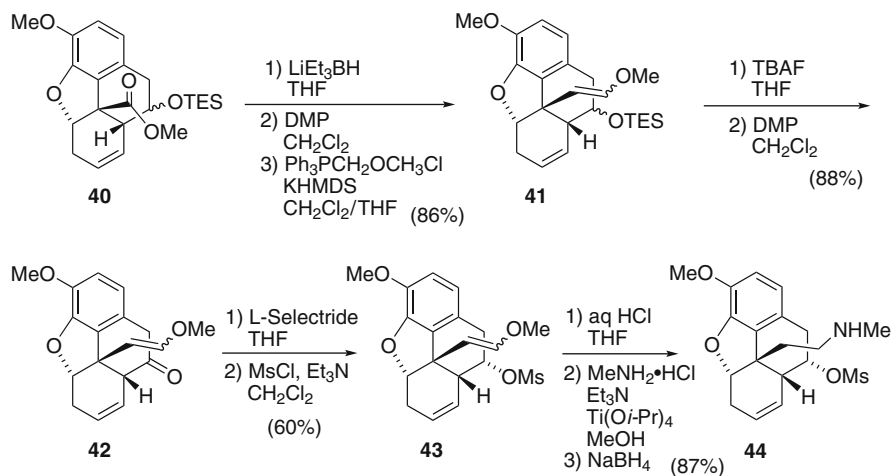
Scheme 9 Preparation of a tetracyclic amine
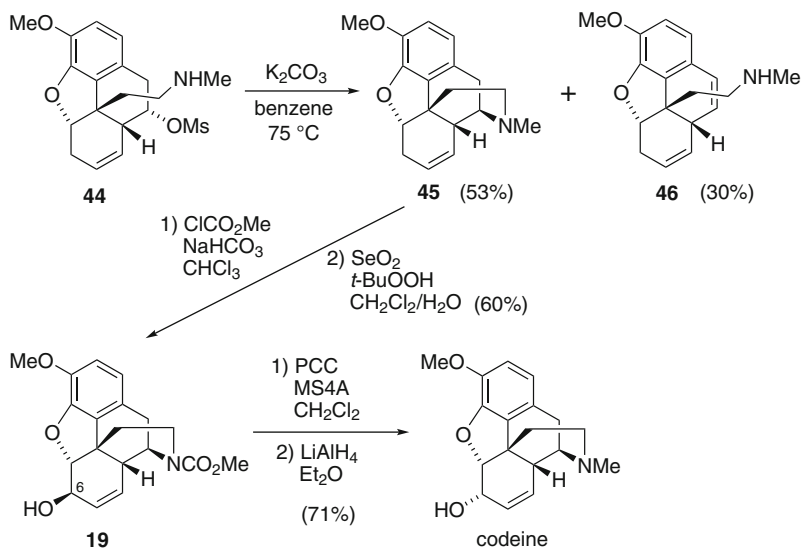
Scheme 10 Synthesis of codeine by Stork

Heating of the benzene solution of **44** and K_2CO_3 induced the intramolecular S_N2 reaction to afford 6-deoxycodeine **45** in 53% yield (Scheme 10). The major side product in this reaction was, as anticipated, diene **46** (30% yield), which was formed by elimination reaction. It was reported that the solvent effect is significant in the S_N2 reaction: when this reaction was carried out in acetonitrile, diene **46** was obtained as the major product. Treatment of **45** with methyl chloroformate provided a methyl carbamate, whose allylic oxidation with SeO_2 in the presence of *t*-BuOOH introduced the hydroxy group at C-6 to give **19**. PCC oxidation of **19**, followed by LiAlH$_4$ reduction, provided racemic codeine.

The more straightforward approach to codeine methyl ether (**52**) was also reported by the Stork group (Scheme 11). Hydrozirconation of 4-methoxy-3-butene-1-yne and in situ addition of the resulting organozirconate to aldehyde **37** afforded **47** after *O*-silylation. The intramolecular Diels–Alder reaction of **47** proceeded via the *endo*-benzofuran transition structure as observed in the reaction of **38**, to provide **48** in 69% yield as a mixture of epimeric alcohols at C-9. By this cycloaddition, the requisite four contiguous chiral centers including a quaternary carbon and an alcohol function at C-6 in codeine were successfully constructed stereoselectively. The same reaction sequence as employed for the conversion of **40** to **44** was applied to **48** to give amine **51** via **49** and **50**. Similar intramolecular S_N2 reaction of **51** as used for the ring closure of **44** afforded codeine methyl ether (**52**) in 73% yield. The presence of 6-*O*-methoxy group suppressed the undesired elimination reaction and gave the cyclized product **52** in good yield.

Codeine methyl ether (**52**) could be converted into thebaine by the known one-step procedure (MnO$_2$ oxidation) reported by Rapoport (Scheme 12) [49]. On the
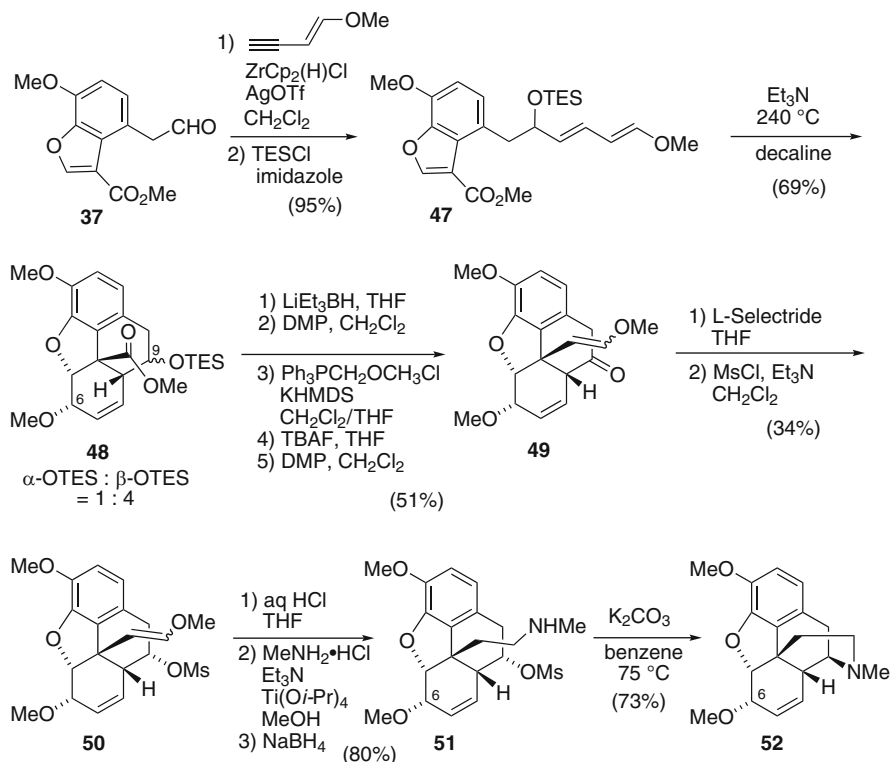
Scheme 11 Synthesis of codeine methyl ether by the Stork group
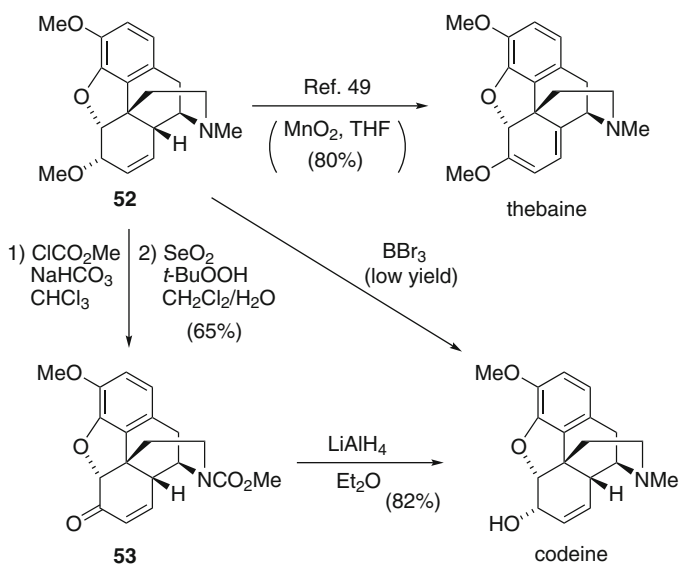
Scheme 12 Conversion of codeine methyl ether to thebaine and codeine

other hand, the attempted direct conversion of **52** into codeine by the cleavage of methyl ether with BBr$_3$ resulted in the low yield formation of codeine. To improve this transformation, compound **52** was first converted into methyl carbamate. Oxidation of the carbamate with SeO$_2$ and *t*-BuOOH provided ketone **53**. Finally, reduction of **53** with LiAlH$_4$ gave racemic codeine.

2.1.4 Magnus Group

In 2009, the Magnus group disclosed the synthesis of racemic codeine [50]. In their synthesis (1) an intramolecular phenol alkylation generating an A–C bicyclic ring system with a quaternary carbon, (2) a stereo-controlled, one-pot formation of a B-ring by way of the combination of Henry reaction and Michael addition of nitromethane with a cyclohexadienone-aldehyde, and (3) an introduction of the requisite functionalities in the C-ring by the epoxide-mediated selenylation followed by oxidation, were employed as the key transformations.

The Suzuki−Miyaura coupling of arylbromide **54** with the boronic acid tris anhydride **55** gave biphenyl **56**, which was then converted into bromo-acetal **57** (Scheme 13). Treatment of **57** with CsF in DMF at 130°C induced the intramolecular phenol alkylation to afford **58** in 96% yield. When cyclohexadienone-aldehyde **58** was reacted with nitromethane in acetic acid in the presence of NH$_4$OAc, the Henry reaction/dehydration [51] and the Michael addition of a carbanion of the nitromethane took place simultaneously to generate an A–B–C ring system of morphine **59** in 97% yield in a one-pot reaction. The 1,4-reduction of the nitroalkene moiety in **59** with NaCNBH$_3$ in acetic acid afforded **60** stereoselectively; the stereochemistry at C-9 was controlled by the axial protonation of the intermediary nitronate anion, giving the thermodynamically stable product. The intriguing approach using nitromethane as a one-carbon unit for the construction of B-ring and the masked amino functionality effectively generated the tricyclic system. Further reduction of **60** with LiAlH$_4$ provided amine-alcohol **61**. Treatment of **61** with NaCNBH$_3$ in acidic media caused the intramolecular reductive amination of an amine-aldehyde formed by the hydrolysis of an acetal group, as well as the formation of dihydrofuran ring presumably via an allylic cation intermediate generated by dehydration of an allylic alcohol moiety, to afford the pentacyclic morphine skeleton **62**. It is important to note that the pentacyclic core structure of morphine was stereoselectively constructed in relatively short reaction steps and with good overall yield (seven steps and 38% yield from **54**). Amine **62** was transformed into ethylcarbamate **63**, which is the known synthetic intermediate of morphine reported by Taber in 2002 [52].

The pentacyclic core **63** was converted into codeine by a different approach from that of Taber (Scheme 14). Treatment of **63** with dibromohydantoin generated bromohydrin **64** stereoselectively. In this reaction, the reagent approaches from the less hindered β-face and the resulting β-cyclic bromonium ion was opened with water in *trans*-diaxial manner. Under the reaction conditions, the C-1 position of aromatic ring was concomitantly brominated. Exposure of **64** to KOH/dioxane
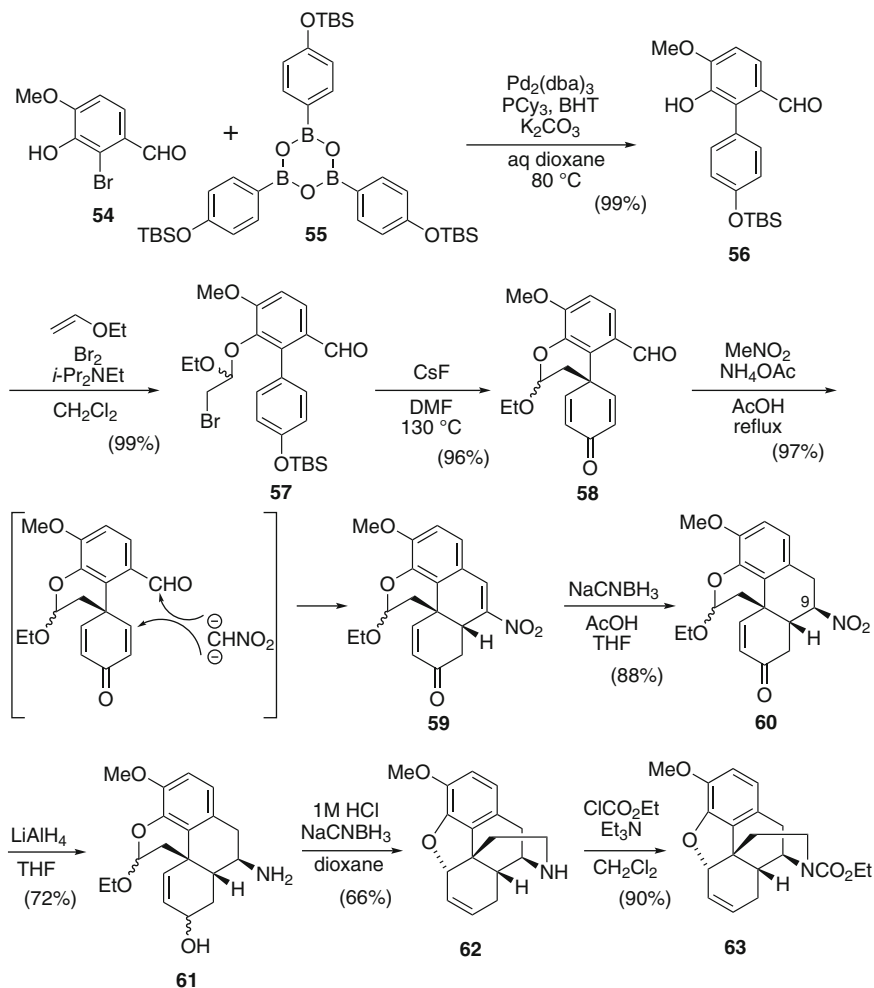
Scheme 13 Synthesis of a tetracyclic core of morphine by the intramolecular S$_N$2 reaction

afforded α-epoxide **65**. Diaxial opening of the epoxide ring in **65** with PhSNa gave **66**, which was oxidized by the action of H$_2$O$_2$ to afford diastereomeric sulfoxides **67**. Without purification, sulfoxides **67** were heated in toluene in the presence of NaHCO$_3$ to give elimination product **68** along with a saturated ketone **69** in 76% and 17% isolated yields, respectively. On the other hand, the same transformation using PhSeNa, instead of PhSNa, provided **68** as the sole product in 72% from **65**. Finally, treatment of **68** with LiAlH$_4$ reduced the ethylcarbamate function and removed the C-1 bromine atom to afford codeine.
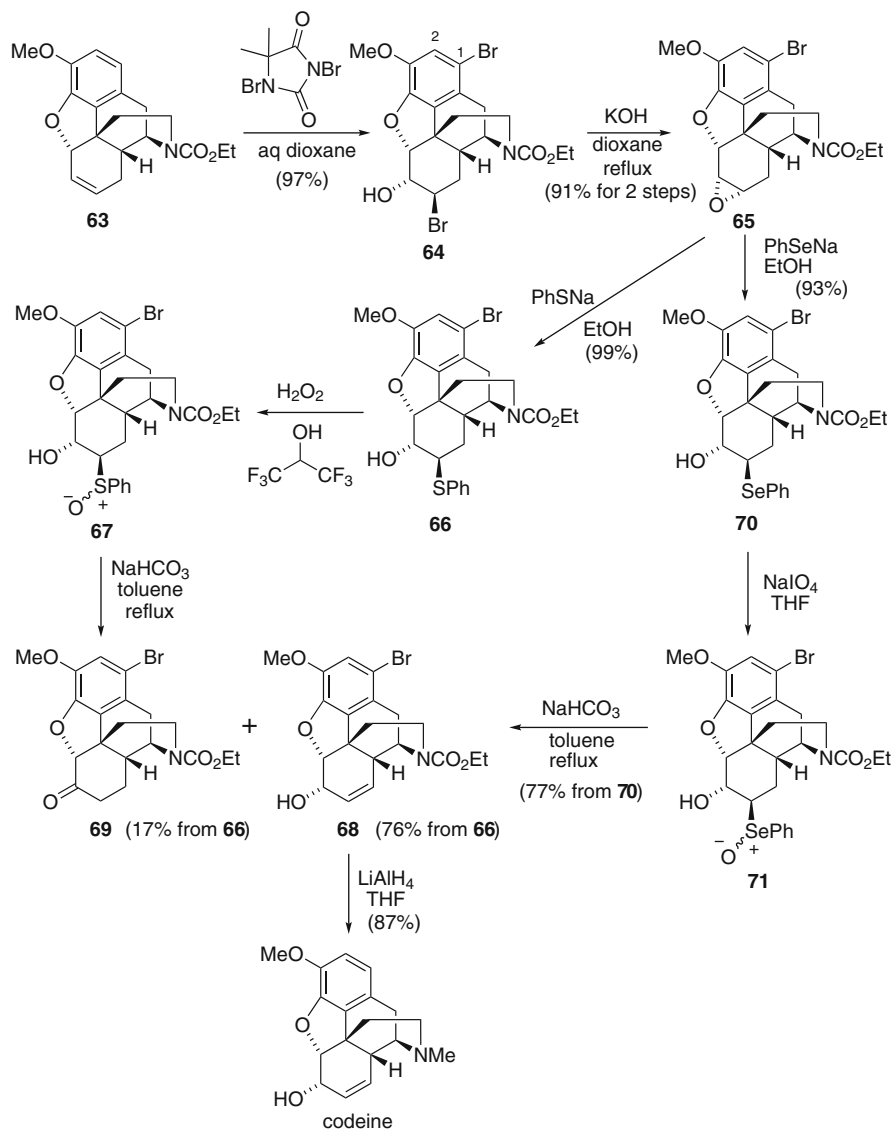
Scheme 14 Synthesis of codeine by Magnus

2.2 Chiral Synthesis

The synthesis of biologically active natural products in optically active form is highly important since, in many cases, enantiomers of natural products show no or different biological activities. In this section, chiral syntheses of morphine-related

compounds reported since 2005 are discussed. Interesting and independent approaches to the target compounds in optically active forms, a Pd-catalyzed asymmetric alkylation by Trost, an asymmetric reduction of ketone carbonyl by Parker, an enzymatic oxidation of benzene derivative by Hudlicky, and a chiral pool approach by Chida have been reported. Earlier works of enantioselective syntheses of morphine-related compounds have been reviewed by Taber [14].

2.2.1 Trost Group

In 2002, Trost and Tang reported the chiral total synthesis of (–)-codeine in short reaction steps using a palladium-catalyzed asymmetric allylic alkylation (AAA) [53] as the key transformation [54]. In 2005, a detailed full account of their synthesis was published [55]. The key features of their synthesis are (1) a preparation of an aryl ether with high optical purity by the Pd-catalyzed AAA reaction, (2) the intramolecular Heck reaction to generate the A–C–E benzofuran skeleton, (3) the second intramolecular Heck reaction of Z-vinyl bromide providing the phenanthrofuran core, and (4) the intramolecular hydroamination for the construction of D-ring by the action of LDA and visible light.

The Pd-catalyzed AAA reaction of bromophenol **54** and allylic carbonate **72** in the presence of chiral bis-phosphine ligand **73** gave aryl ether **74** in 72% yield with 88% ee (Scheme 15). After protection of the aldehyde function in **74** as a dimethyl
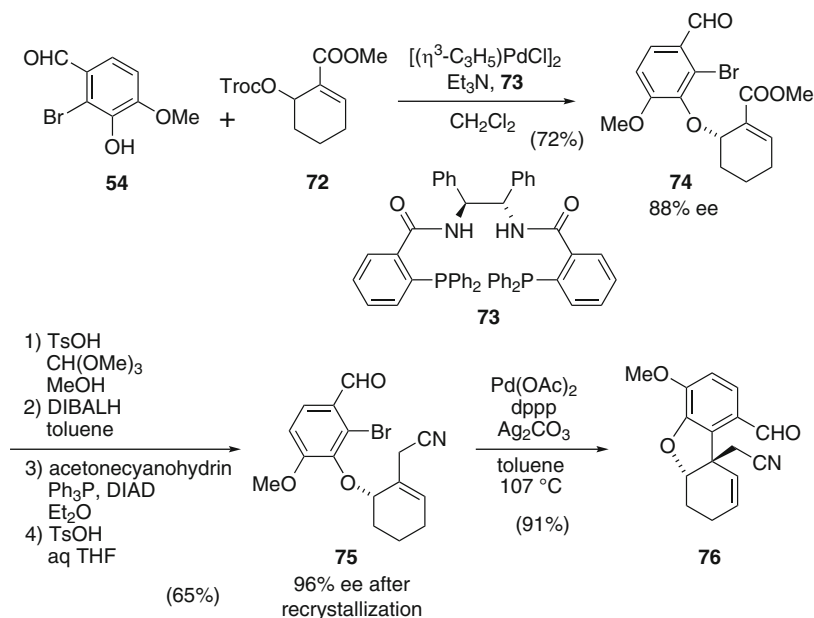
Scheme 15 Preparation of optically active A–C–E ring of codeine by Trost

acetal, the ester function was reduced to a primary alcohol. The β,γ-unsaturated nitrile was synthesized by the Mitsunobu reaction. Acid hydrolysis of the dimethyl acetal followed by recrystallization provided **75** with 96% ee. Intramolecular Heck reaction produced the A–C–E ring system **76** possessing a quaternary carbon with correct stereochemistry in 91% yield (see Sect. 2.1.1).

Corey−Fucus olefination [56] of **76** followed by regioselective debromination [57] afforded Z-vinyl bromide **77** (Scheme 16). The intramolecular Heck vinylation successfully constructed the B-ring to provide phenanthrofuran skeleton **78** in 65% yield. The success in the formation of the tetracyclic core fully revealed the effectiveness of the Heck reaction for the stereoselective preparation of the morphine skeleton. Allylic oxidation of **78** with SeO$_2$ gave a mixture of an allylic alcohol and an α,β-unsaturated ketone. This mixture was treated with DMP to give ketone **79**. The 1,2-reduction of **79** with DIBALH in THF-Et$_2$O gave the desired α-alcohol **80**. Reaction of **80** with DIBALH in CH$_2$Cl$_2$-Et$_2$O reduced the nitrile function to give an imine, which was then treated with NH$_4$Br and excess methylamine in methanol to give a secondary imine. Without isolation, NaBH$_4$ reduction
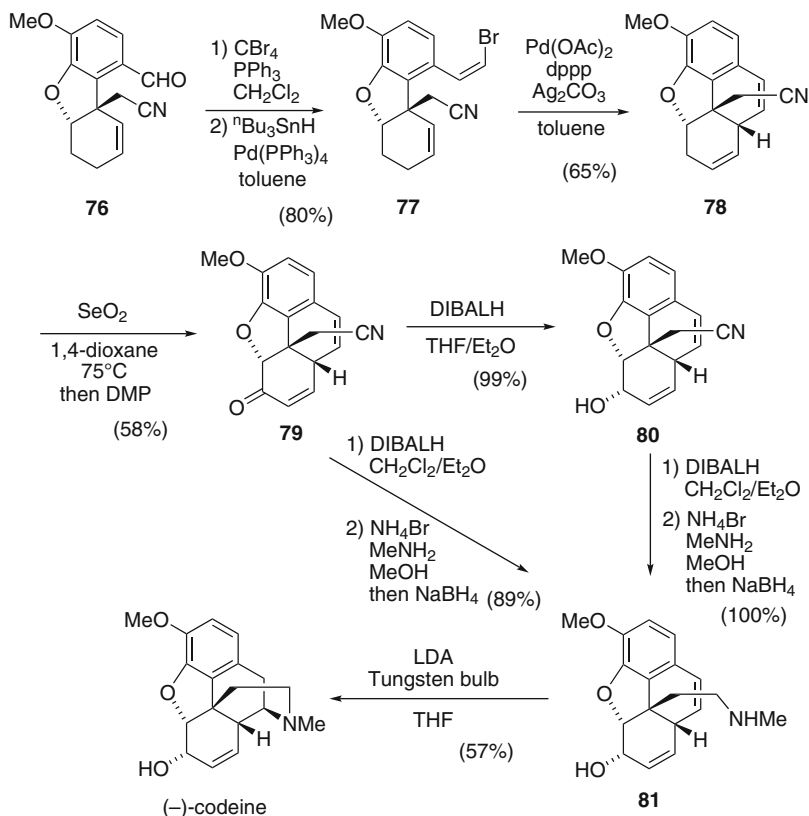
Scheme 16 Synthesis of (−)-codeine

of the mixture afforded amine **81**, quantitatively. Alternatively, reduction of **79** with DIBALH in CH$_2$Cl$_2$-Et$_2$O, followed by the treatment with NH$_4$Br and methyl-amine and subsequent reduction with NaBH$_4$ also afforded **81** in one-pot reaction. Subjecting the solution of **81** and LDA in THF to irradiation with a 150-W tungsten light bulb at room temperature led to the intramolecular hydroamination to afford (−)-codeine in 57% yield. Since the similar reaction without the irradiation gave no cyclized product, the Trost group suggested that the visible light might have promoted the single electron transfer to facilitate the cyclization (see Sect. 2.1.2).

2.2.2 Parker Group

In 1992, Parker and Fokas reported the short step (11 steps) synthesis of racemic dihydroisocodeine, which completes a formal synthesis of codeine and morphine [58]. The key feature of their synthesis are (1) a construction of an aryl ether moiety (connection of the A and C rings) by Mitsunobu reaction, (2) a tandem radical cyclization of aryl bromide possessing the C-ring precursor to generate the A–B–C–E ring of morphine, and (3) a hydroamination for the construction of the D-ring by the reaction of a tosylamide with Li/NH$_3$. In 2006, they reported the chiral version of the synthesis of dihydrocodeinone [59].

m-Methoxyphenethylamine **82** was employed as the starting material (Scheme 17). Birch reduction of **82** gave dienol ether **83**. *N*-Tosylation followed by hydrolysis and subsequent *N*-methylation afforded cyclohexenone **84**. To obtain chiral cyclohexenol **87**, whose racemic compound had been used as the key intermediate in their racemic synthesis of dihydroisocodeine, cyclohexenone **84** was subjected to various asymmetric reduction conditions. Chiral reduction of **84** with Terashima's reagent (LiAlH$_4$/(−)-*N*-methylephedrine/2-ethylaminopyridine) [60] and the Corey−Bakshi−Shibata (CBS) reagent [61] afforded the desired (*R*)-cyclohexenol **87**; however, the optical purity of the product was found to be
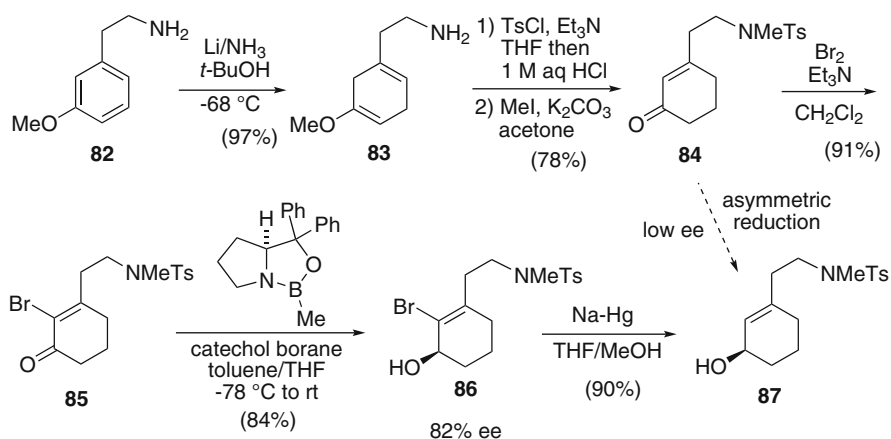
Scheme 17 Preparation of an optically active cyclohexenol by asymmetric reduction

unsatisfactory (5% ee with Terashima's reagent and 35–40% ee with CBS reagent). For improvement of the optical purity of **87**, compound **84** was then converted into 2-bromocyclohexenone derivative **85**, since it has been reported that the CBS reduction of 2-bromocyclohexenone gave the product with high (91%) ee [62]. Indeed, reduction of **85** with the CBS reagent [(*S*)-oxazaborolidine and catechol borane] afforded bromo-cyclohexenol **86** in 84% yield with 82% ee. The similar CBS asymmetric reduction was also employed in the synthesis of optically active dihydroisocodeine by Overman [21]. Treatment of **86** with sodium amalgam provided **87** in 90% yield.

With the chiral cyclohexenol **87** in hand, the synthesis of optically active morphine was carried out based on the similar reaction sequence as employed for their racemic synthesis (Scheme 18). Treatment of **87** with *m*-CPBA gave
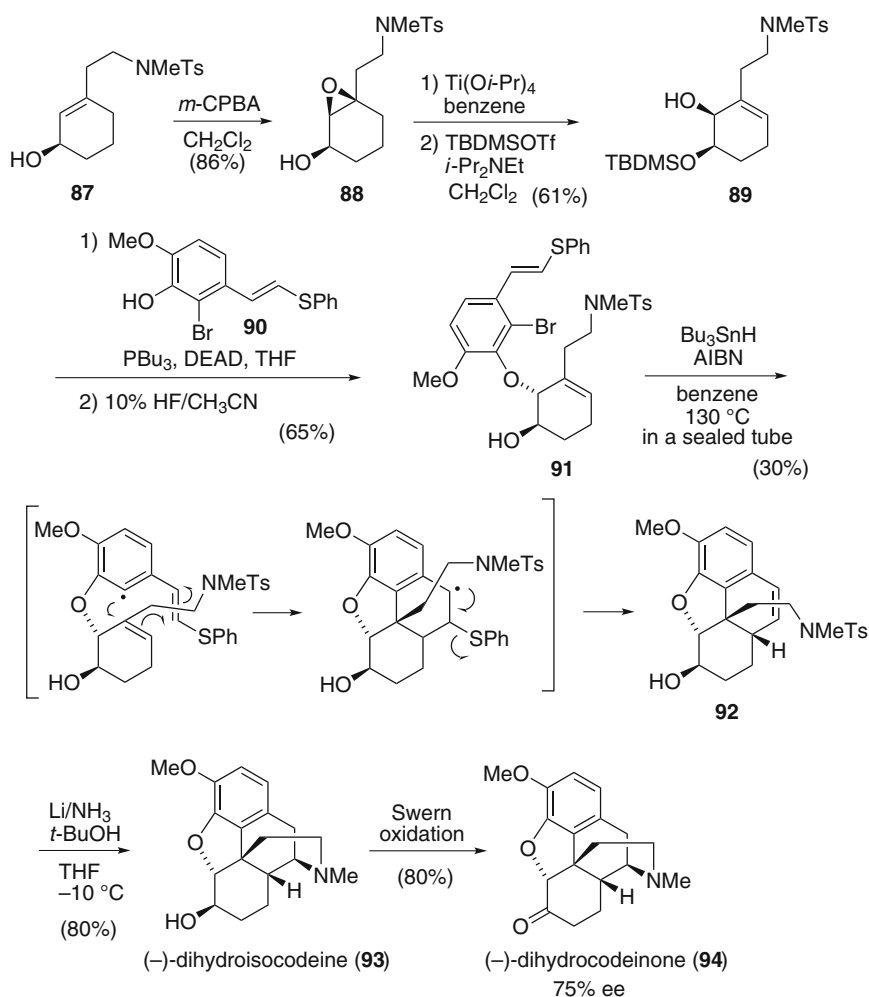
Scheme 18 Synthesis of (−)-dihydrocodeinone by Parker

β-epoxide **88**. Regioselective isomerization of **88** with Ti(O*i*-Pr)$_4$ followed by *O*-silylation afforded **89**. Mitsunobu coupling of **89** with phenol **90** and subsequent deprotection of the silyl group cleanly gave aryl ether **91**. When **91** was reacted with Bu$_3$SnH and AIBN in benzene at 130°C, compound **91** underwent the projected tandem radical cyclization/elimination sequence to give phenanthrofuran compound **92** (A–B–C–E ring system of morphine) in 30% yield in one-pot reaction. Treatment of **92** with Li/NH$_3$ removed the *N*-Ts group to generate the nitrogen radical (or anion), which spontaneously added to the β-carbon of the styrene moiety, affording dihydroisocodeine (**93**) directly in 80% yield (see Sects. 2.1.2 and 2.2.1). Swern oxidation of **93** provided dihydrocodeinone (**94**) in 80% yield. Comparison of $[\alpha]_D$ values of synthetic **94** with that of the authentic sample revealed that dihydrocodeinone obtained in this synthesis had 75% ee. Since dihydroisocodeinone had been successfully converted into morphine [63, 64], synthesis of (–)-morphine in the formal sense has been achieved.

2.2.3 Hudlicky Group

In 2007, the Hudlicky group reported the total synthesis of (+)-codeine (an enantiomer of the natural product) starting from a chiral cyclohexadiene-diol derivative obtained by the enzymatic oxidation of β-bromoethylbenzene [65]. Later, total synthesis of (–)-codeine starting from the same chiral cyclohexadiene-diol was reported in 2009 [66]. The key features of their synthesis involve (1) an enantio-divergent synthesis of (+)- and (−)-codeine starting from the same cyclohexene derivative, (2) the intramolecular Heck reaction to generate the A–C–E tricyclic system including the stereoselective generation of a quaternary carbon center, (3) the second Heck reaction of a vinyl bromide for the construction of a phenanthrofuran core, and (4) the mercury(II)-mediated intramolecular amino-mercuration/demercuration for the final D-ring closure.

Diimide reduction of **96**, obtained by the enzymatic oxidation of **95** (96% ee) [67], followed by *O*-acetylation afforded cyclohexene-diol **97** in 47% yield (Scheme 19). Compound **97** was converted into carbamate **98** by S$_N$2 reaction with methylamine and subsequent urethane formation. Regioselective protection of the diol in **98** with TBSCl afforded **99**, which was coupled with bromoisovanillin **54** under the conditions of Mitsunobu to provide **100** (see Sect. 2.2.2). The intramolecular Heck reaction of **100** constructed the benzofuran ring including a quaternary center to afford **101** in 82% yield. Wittig reaction of **101** with Ph$_3$P=CHBr generated vinyl bromide **102** in 49% yield as a mixture of *E*- and *Z*-isomers (*E*:*Z* = ca. 1:2).

The second Heck reaction of **102** (*E*/*Z* isomers) utilizing the vinyl bromide function, which had been employed in the synthesis of codeine by Trost (see Sect. 2.2.1), afforded phenanthrofuran skeleton **103** in 44% yield (Scheme 20). Since only the *Z*-isomer of **102** can participate in the cyclization reaction, this Heck cyclization resulted in the rather modest yield. After deprotection of the *O*-TBS group in **103**, the stereochemistry at C-6 hydroxy group was inverted by
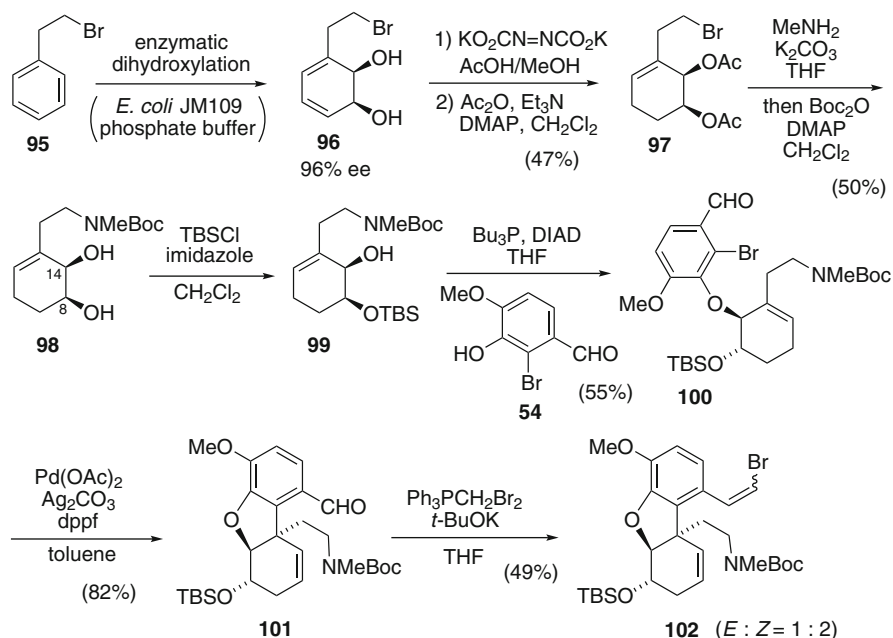
Scheme 19 Preparation of A–C–E ring of (+)-codeine by Hudlicky
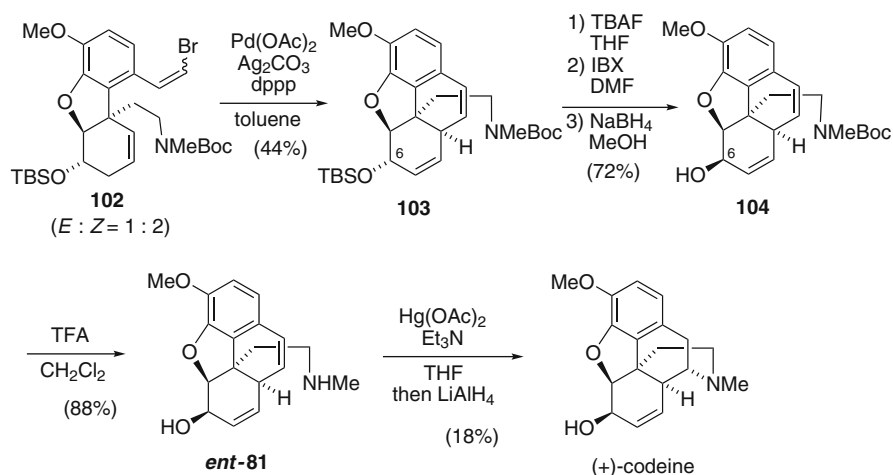
Scheme 20 Synthesis of (+)-codeine

oxidation−reduction procedure to give **104**. Removal of the *N*-Boc protecting group in **104** generated tetracyclic amine ***ent*-81**, which is an enantiomer of the known synthetic intermediate reported by Trost (see Sect. 2.2.1). Following Trost's protocol, ***ent*-81** was treated with LDA with irradiation of visible light. However, the reproducibility of the hydroamination was found to be rather poor. To solve the

problem, the Hudlicky group adopted the intramolecular aminomercuration/demercuration procedure. Thus, treatment of **ent-81** with Hg(OAc)$_2$ followed by reduction with LiAlH$_4$ successfully provided (+)-codeine, an enantiomer of the natural product, in 18% yield.

Starting from diol **98**, total synthesis of (–)-codeine was also accomplished (Scheme 21). Mitsunobu reaction of **98** with *p*-nitrobenzoic acid gave an inverted ester **105** regioselectively. It is interesting to note that the silylation of **98** gave 8-*O*-TBS derivative **99** exclusively (Scheme 17), whereas the Mitsunobu conditions activated another (C-14) hydroxy group. The Hudlicky group suggested that the observed reverse regioselectively might be explained by the anchimeric assistance of the carbamate function. The alcohol in **105** was tosylated to give **106**, which was then treated with base to give α-epoxide **107**. Reaction of **107** with potassium salt of bromoisovanillin afforded aryl ether **ent-100** regioselectively in 46% yield. The intramolecular Heck reaction produced tricycle **ent-101** in 91% yield.

The same reaction sequence as employed for the conversion of **101** to **103** was applied to **ent-101** to give tetracycle **ent-103** in 18% yield (two steps) (Scheme 22). Alternatively, Wittig reaction of **ent-101** with Ph$_3$P=CHI afforded vinyl iodide **108** in better yield (72%, *E:Z* = 1:2). The Heck reaction of **108**, however, resulted in the formation of **ent-103** with lower yield (31%) than that of **ent-102**. The attempted new procedure via vinyl iodide **108** slightly improved the overall yield of **ent-103** from **ent-101** (22% for two steps). Inversion of the C-6 hydroxy group and deprotection of *N*-Boc group gave methylamine **81**. Aminomercuration/demercuration of **81** provided (–)-codeine in 24% yield.

2.2.4 Chida Group

In 2008, the Chida group reported the synthesis of (–)-dihydroisocodeine starting from D-glucal [68]. This report, based on the "chiral pool" approach, would be the
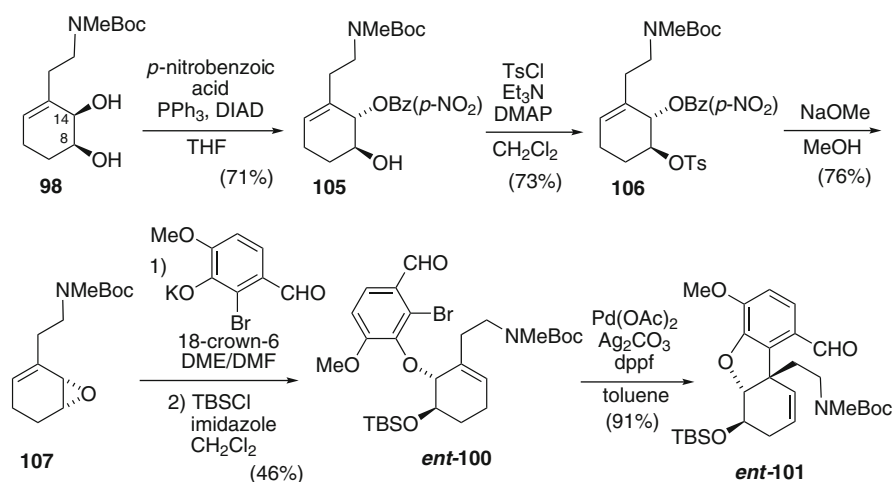
Scheme 21 Preparation of A–C–E ring of (−)-codeine
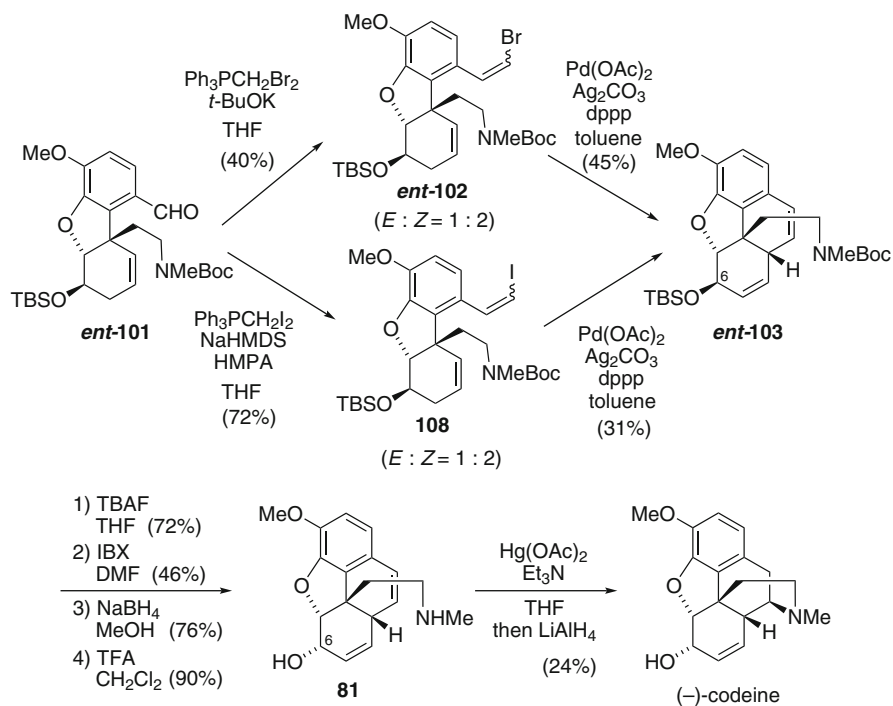
Scheme 22 Synthesis of (−)-codeine

first example of the chemical synthesis of optically pure morphine starting from an enantiomerically pure compound. The key features of their synthesis are (1) a use of carbohydrate as a chiral building block for the C-ring precursor, (2) a construction of A–C ring by way of Suzuki−Miyaura coupling in good yield, (3) the cascade Claisen rearrangement creating the vicinal tertiary and quaternary carbon centers in morphine skeleton stereoselectively in a one-pot reaction, and (4) a construction of B-ring by way of the Friedel−Crafts-type cyclization/dehydration under mild acidic conditions.

Treatment of D-glucal, obtained by methanolysis of commercially available tri-O-acetyl-D-glucal **109**, with p-anisaldehyde dimethylacetal produced a 4,6-O-benzylidene derivative, whose hydroxy group was protected as a TBS ether to give **110** (Scheme 23). Reductive opening of a benzylidene group by DIBALH and subsequent treatment of the product with Ph₃P·HBr in methanol provided methyl glycoside, which was transformed into primary iodide **111**. Elimination of HI provided enopyranoseide **112**. Treatment of **112** with a catalytic amount of Hg (OCOCF₃)₂ in aqueous acetone induced the catalytic Ferrier's carbocyclization [69–71] to give cyclohexenone **113**, which was cleanly converted into cyclohexenone **114** by the action of MsCl and Et₃N. 1,4-Reduction of **114** with L-selectride and subsequent trap of the resulting enolate with Commins reagent gave vinyl triflate **115**. Suzuki−Miyaura coupling of **115** with 2,3-dimethoxyphenyl boronic
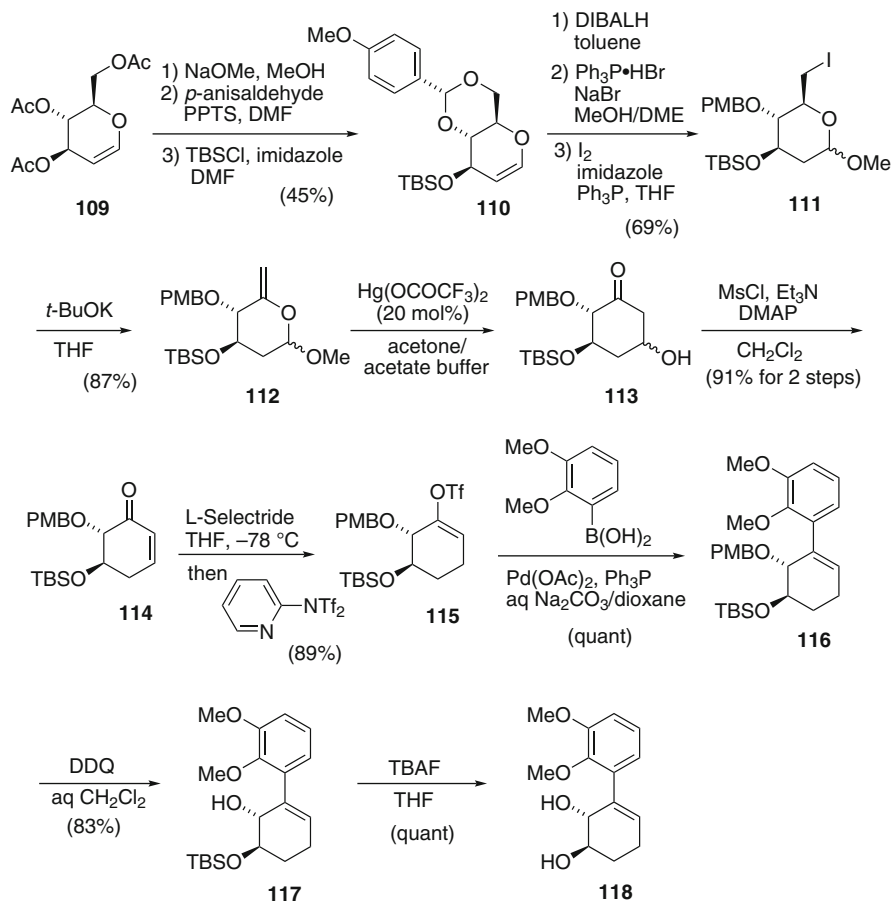
Scheme 23 Preparation of an enantiomerically pure A–C ring from D-glucal

acid afforded coupling product **116**, quantitatively. Deprotection of *O*-PMB group by the action of DDQ afforded cyclohexenol **117**. Further deprotection of **117** with TBAF afforded diol **118**.

When the mixture of **118** with 2-nitrophenol in triethyl orthoacetate was heated at 140°C in a sealed tube, the cascade Claisen rearrangement took place to afford the doubly rearranged product **119** in 36% yield (Scheme 24). By this cascade sigmatropic rearrangement, the vicinal tertiary and quaternary carbon centers in codeine (C-14 and C-13) were stereoselectively constructed via the sequential chirality transfer. On the other hand, Claisen rearrangement of **117** in the presence of propionic acid afforded the rearranged product **120** in 87% yield. Deprotection of the TBS group afforded **121**. The second Claisen rearrangement of **121** in the presence of 2-nitrophenol provided **119** in 48% overall yield (56% overall yield based on the recovered starting material) from **117**. They reported that attempted
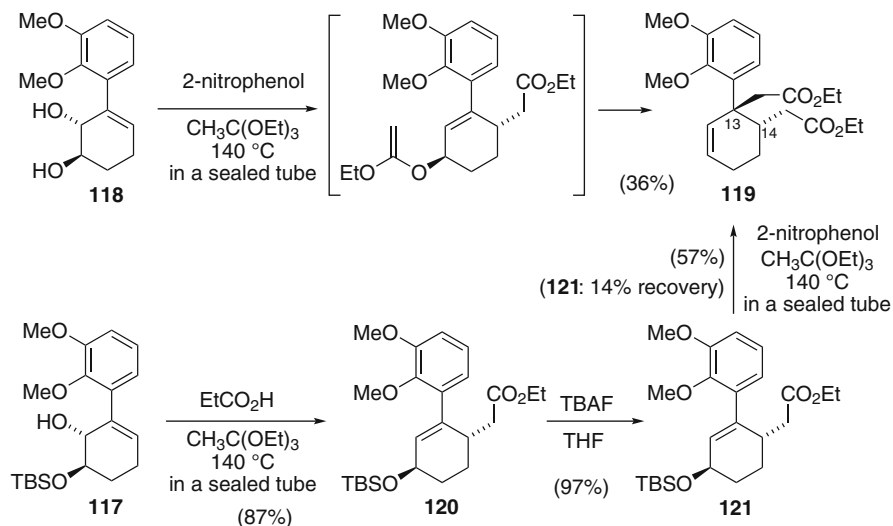
Scheme 24 Cascade Claisen rearrangement installing the vicinal tertiary and quaternary carbons

Eschenmoser Claisen rearrangement and Ireland Claisen rearrangement of **118** produced no doubly rearranged product (see Sect. 2.1.2).

Treatment of **119** with *m*-CPBA induced the dealkylating etherfication to generate dibenzofuran skeleton, and the subsequent protection of a hydroxyl group as a TBS ether provided **122** (Scheme 25). The similar epoxide-mediated dealkylating etherfication has been employed in the synthesis of morphine by Multzer [39]. The ester functions in **122** were reduced with DIBALH to give dialdehyde **123**. When **123** was treated with montmorillonite K-10 clay [72] in dichloroethane at room temperature, Friedel−Crafts-type cyclization took place, and subsequent dehydration of the resulting benzylic alcohol constructed the tetracyclic phenanthrofuran core. Since the TBS protecting group was partially deprotected under these reaction conditions, the reaction mixture was re-silylated to provide **124** in 75% yield from **122**. As mentioned in Sect. 2.1.2, the similar Friedel−Crafts-type cyclization/ dehydration process for the construction of the B-ring has been reported by Ogasawara in 2002 (ethyleneglycol and CSA in benzene, reflux, 50% yield) and Guillou in 2008 (*p*-TsOH, toluene, room temperature, 40% yield) in their synthesis of morphine. It should be noted that the current reaction proceeded under very mild reaction conditions with good yield (75%), and another aldehyde function was intact throughout the reaction. Reductive amination of **124** with methylamine smoothly gave **125**, whose amino group was tosylated and TBS group was deprotected to give the known synthetic intermediate **92** of morphine reported by Parker (see Sect. 2.2.2). The similar reductive hydroamination of **92** as the Parker's method provided (−)-dihydroisocodeine in 92% yield, completing the formal synthesis of (−)-morphine (see Sect. 2.2.2).
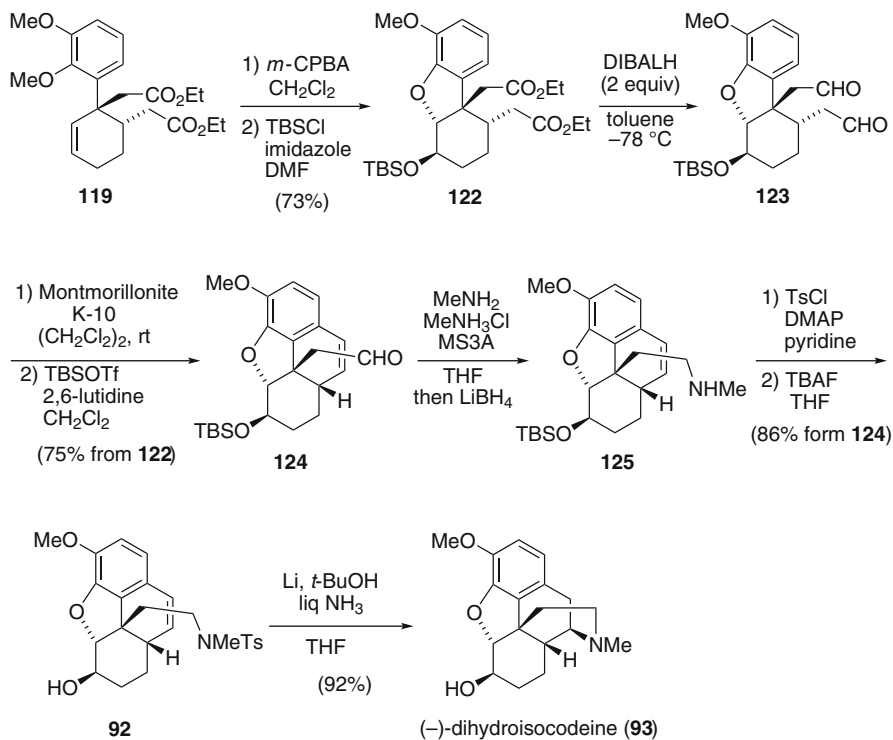
Scheme 25 Synthesis of (−)-dihydroisocodeine by Chida

3   Closing Remarks

The work that culminated in the synthesis of morphine and its related compounds reported from eight research groups during 2004–2009 has been shortly reviewed. It is interesting that each group employed different strategies and key reactions for the construction of a morphine-skeleton. These insightful approaches would be useful and valuable for synthetic organic chemists to plan their own synthetic strategies of morphine-type alkaloids as well as other nitrogen-containing compounds. Morphine, not such a big molecule, but possessing densely functionalized structure with five contiguous chiral centers, has been a good target to test the quality of the strategies and tactics of the synthesis. The synthetic endeavor to such a challenging small but complex molecule based on the imaginative idea sometimes makes a great discovery in organic chemistry. Although the synthetic ways to morphine that have been reported to date may not be truly practical, the more imaginative and creative idea, and most importantly, the enthusiasm for the organic chemistry, surely would give rise to the more efficient synthesis of the alkaloid. There is little doubt that the challenges for organic chemists will continue.

References

1. Booth M (1998) Opium: a history. St. Martin's Press, New York
2. Kapoor LD (1995) Opium poppy: botany, chemistry, and pharmacology. The Haworth, New York
3. Cordell GA (1981) Introduction to alkaloids: a biogenetic approach. Wiley, New York
4. Butora G, Hudlicky T (1998) The story of morphine structure elucidation: one hundred years of deductive reasoning. In: Hudlicky T (ed) Organic synthesis: theory and applications. JAI Press, Stamford, p 1
5. Gates M, Tschudi G (1952) J Am Chem Soc 75:1109
6. Gates M, Tschudi G (1956) J Am Chem Soc 78:1380
7. Maier M (1995) Synthesis of morphine. In: Waldmann H (ed) Organic synthesis highlights II. VCH, Weinheim, p 357
8. Kametani T (1977) The total syntheses of isoquinoline alkaloids. In: ApSimon J (ed) The total synthesis of natural products, vol 3. Wiley, New York, p 1
9. Corey EJ, Cheng XM (1989) The logic of chemical synthesis. Wiley, New York
10. Novak BH, Hudlicky T, Reed JW, Multzer J, Trauner D (2000) Curr Org Chem 4:343
11. Blakemore PR, White JD (2002) Chem Commun 1159
12. Hudlicky T, Butora G, Feamley SP, Gum AG, Stabile MR (1996) A historical perspective of morphine synthesis. In: Atta-ur-Rahman (ed) Natural products chemistry, vol 18. Elsevier, Amsterdam, p 45
13. Zezula J, Hudlicky T (2005) Synlett 388
14. Taber DF, Neubert TD, Schlecht MF (2004) The enantioselective synthesis of morphine. In: Harmata M (ed) Strategies and tactics in organic synthesis, vol 5. Elsevier, London, p 353
15. Mascavage LM, Wilson ML, Dalton DR (2006) Curr Org Synth 3:99
16. Uchida K, Yokoshima S, Kan T, Fukuyama T (2006) Org Lett 8:5311
17. Uchida K, Yokoshima S, Kan T, Fukuyama T (2009) Heterocycles 77:1219
18. Tsuji J (1995) Palladium reagents and catalysis. Wiley, New York
19. Mitsunobu O (1981) Synthesis 1
20. Hughes DL (1992) The Mitsunobu reaction. In: Paquette LE (ed) Organic reactions, vol 42. Wiley, New York, p 335
21. Hong CY, Kado N, Overman LE (1993) J Am Chem Soc 115:11028
22. Cheng CY, Liou JP, Lee MJ (1997) Tetrahedron Lett 38:4571
23. Hsin LW, Chang LT, Chen CW, Hsu CH, Chen HW (2005) Tetrahedron 61:513
24. Hsin, LW, Chang LT, Liou HL (2008) Synlett 2299
25. Omori AT, Finn KL, Leisch H, Carroll RJ, Hudlicky T (2007) Synlett 2859
26. Itoh Y, Hirao T, Saegusa T (1978) J Org Chem 43:1101
27. Barton DHR, Motherwell RSH, Motherwell WB (1981) J Chem Soc Perkin Trans 1:2363
28. Rice KC (1977) J Med Chem 20:164
29. Varin M, Barre E, Iorga B, Guillou C (2008) Chem Eur J 14:6606
30. Wick AE, Steen K, Eschenmoser A (1964) Helv Chim Acta 47:2425
31. Castro AMM (2004) Chem Rev 104:2939
32. Kazmaier U (1994) Angew Chem Int Ed Engl 33:998
33. Ireland RE, Mueller RH (1972) J Am Chem Soc 94:5897
34. Johnson WS, Werthermann L, Barlett WR, Brocksom TJ, Li TT, Faulkner DJ, Petersen MR (1970) J Am Chem Soc 92:741
35. Bower S, Kreutzer KA, Buchwald SL (1996) Angew Chem Int Ed Engl 35:1515
36. Elad D, Ginsburg D (1954) J Chem Soc 3052
37. White DJ, Hrnciar P, Stappenbeck F (1997) J Org Chem 62:5250
38. Mulzer J, Durner G, Trauner D (1996) Angew Chem Int Ed Engl 35:2830
39. Multzer J, Bats JW, List B, Opatz T, Trauner D (1997) Synlett 441
40. Trauner D, Bats JW, Werner A, Mulzer J (1998) J Org Chem 63:5908

41. Evans DA, Mitch CH (1982) Tetrahedron Lett 23:285
42. Nagata H, Miyazawa N, Ogasawara K (2001) Chem Commun 1094
43. Olofson RA, Martz JT, Senet JP, Piteau M, Malfroot T (1984) J Org Chem 49:2081
44. Umbreit MA, Sharpless KB (1977) J Am Chem Soc 99:5526
45. Stork G, Yamashita A, Damu J, Schulte GR, Chesworth R, Miyazaki Y, Farmer JJ (2009) J Am Chem Soc 131:11402
46. Suzuki K (1994) Pure Appl Chem 66:1557
47. France S, Boonsombat J, Leverett CA, Padwa A (2008) J Org Chem 73:8120
48. Tius M, Kerr MA (1992) J Am Chem Soc 114:5959
49. Barber RB, Rapoport H (1975) J Med Chem 18:1074
50. Magnus P, Sane N, Fauber BP, Lynch V (2009) J Am Chem Soc 131:16045
51. Luzzio FA (2001) Tetrahedron 57:915
52. Taber DF, Neubert TD, Rheingold AL (2002) J Am Chem Soc 124:12416
53. Trost BM, Machacek MR, Aponick AA (2006) Acc Chem Res 39:747
54. Trost BM, Tang W (2002) J Am Chem Soc 124:14542
55. Trost BM, Tang W, Toste FD (2005) J Am Chem Soc 127:14785
56. Corey EJ, Fuchs PL (1972) Tetrahedron Lett 13:3769
57. Uenishi J, Kawahama R, Shiga Y, Yonemitus O, Tsuji J (1996) Tetrahedron Lett 37:6759
58. Parker KA, Fokas D (1992) J Am Chem Soc 114:9688
59. Parker KA, Fokas D (2006) J Org Chem 71:449
60. Kawasaki M, Suzuki Y, Terashima S (1985) Chem Pharm Bull 33:52
61. Corey EJ, Bakshi RK, Shibata S (1987) J Am Chem Soc 109:5551
62. Corey EJ, Bakshi RK, Shibata S, Chen CP, Singh VK (1987) J Am Chem Soc 109:7925
63. Weller DD, Rapoport H (1976) J Med Chem 19:1171
64. Iijima I, Rice K, Silverton JV (1977) Heterocycles 6:1157
65. Omori AT, Finn KJ, Leisch H, Carroll RJ, Hudlicky T (2007) Synlett 2859
66. Leisch H, Omori AT, Finn KJ, Gilmet J, Bissett T, Ilceski D, Hudlicky T (2009) Tetrahedron 65:9862
67. Stabile MR, Hudlicky T, Meisels ML (1995) Tetrahedron Asymmetry 6:537
68. Tanimoto H, Saito R, Chida N (2008) Tetrahedron Lett 49:358
69. Ferrier RJ (1979) J Chem Soc Perkin Trans 1:1455
70. Ferrier RJ, Middleton S (2001) Top Curr Chem 215:277
71. Chida N, Ohtsuka M, Ogura K, Ogawa S (1991) Bull Chem Soc Jpn 64:2118
72. Sartori G, Maggi R (2006) Chem Rev 106:1077

Opioids in Preclinical and Clinical Trials

Hiroshi Nagase and Hideaki Fujii

Abstract Since 1952, when Gates determined the stereo structure of morphine, numerous groups have focused on discovering a nonnarcotic opioid drug [1]. Although several natural, semisynthetic, and synthetic opioid ligands (alkaloids and peptides) have been developed in clinical studies, very few were nonnarcotic opioid drugs [2]. One of the most important studies in the opioid field appeared in 1976, when Martin and colleagues [3] established types of opioid receptors (these are now classified into μ, δ, and κ types). Later, Portoghese discovered a highly selective μ type opioid receptor antagonist, β-funaltrexamine [4]. This led to the finding that the μ type opioid receptor was correlated to drug dependence [5]. Consequently, δ, and particularly κ, opioid agonists were expected to lead to ideal opioid drugs. Moreover, opioid antagonists were evaluated for the treatment of symptoms related to undesirable opioid system activation. In this chapter, we provide a short survey of opioid ligands in development and describe the discovery of the two most promising drugs, TRK-851 [6] and TRK-820 (nalfurafine hydrochloride) [7].

Keywords Clinical development · Nonnarcotic · Opioid drug · TRK-820 · TRK-851

Contents

H. Nagase (✉) and H. Fujii
School of Pharmacy, Kitasato University, 5-9-1, Shirokane, Minato-ku, Tokyo, Japan
e-mail: nagaseh@pharm.kitasato-u.ac.jp

Abbreviations

AAW	Acetic acid writhing
ADME	Absorption, distribution, metabolism, and excretion
ADR	Adverse drug reaction
β-FNA	β-Funaltrexamine
BBB	Blood–brain barrier
BNTX	7-Benzylidenenaltrexone
cLog P	Calculated log P
CNS	Central nervous system
CTOP	H-D-Phe-Cys-Tyr-D-Trp-Orn-Thr-Pen-Thr-NH_2
DAMGO	[D-Ala^2, N-Me-Phe^4, Gly-ol^5]enkephalin
DPDPE	[D-Pen^2, D-Pen^5]enkephalin
DSLET	Tyr-D-Ser-Gly-Phe-Leu-Thr
GPI	Guinea pig ileum
HPLC	High-performance liquid chromatography
i.c.	Intracisternal
i.d.	Intradermal
i.p.	Intraperitoneal
i.t.	Intrathecal
MVD	Mouse vas deferens
nor-BNI	nor-Binaltorphimine
NTI	Naltrindole
PBS	Phosphate-buffered saline
p.o.	Peroral
SAR	Structure–activity relationship
s.c.	Subcutaneous
S.E.M.	Standard error of the mean
TF	Tail flick
VAS	Visual analog scale

1 Opioid Ligands in Early Drug Development

Representative opioid agonists and antagonists for μ, δ, and κ opioid receptors are listed in Table 1.

Recent drug development efforts in the opioid field have mainly focused on improving patient compliance by creating new formulations, including slow release, long acting tablets, and transdermal delivery [8–11]. Others have focused on preventing illegal use by combining an opioid agonist with an opioid antagonist, naloxone, in an oral formulation. Naloxone is immediately metabolized in its first pass through the liver clearance process. Therefore, when the combination drug is used orally, the opioid agonist has a normal analgesic effect. However, when the drug is ground to a powder for intravenous injection, the naloxone works to prevent the effect of the opioid agonist [12].

Recently, relatively small numbers of new opioid compounds have been developed. New chemicals for producing an opioid drug can be categorized into four classes:

1. Peripheral antagonists
2. δ Agonists
3. δ Antagonists
4. κ Agonists

We will provide short reviews of these drug candidates in the following subsections.

1.1 Peripheral Antagonists

Patients that take prescription opioid analgesics often experience intolerable side effects, including nausea, emesis, or constipation. Because opioid analgesics act primarily on the central nervous system (CNS), targeting an antagonist outside the CNS might prevent peripheral side effects without affecting the analgesic effects.

Table 1 Representative opioid ligands

Type	Selective		Nonselective		Endogenous
	Agonists	Antagonists	Agonists	Antagonists	
μ	DAMGO	CTOP	Etorphine	Naloxone	Endomorphin
	Morphine	β-FNA	Levorphanol	Naltrexone	Endorphin
	Fentanyl				
δ	DPDPE	NTI			Enkephalin
	DSLET	NTB			
	SNC-80	BNTX			
	TAN-67				
κ	U-50,488H	nor-BNI			Dynorphin
	U-62,066				
	TRK-820				
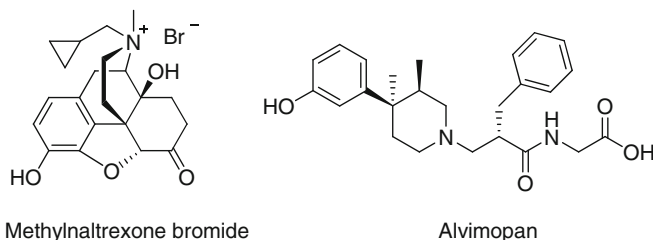
Fig. 1 Structures of methylnaltrexone bromide and alvimopan

This concept proved to be successful with methylnaltrexone bromide (Fig. 1) [13], which was launched in 2008 by Wyeth (originated at the University of Chicago) for the treatment of constipation caused by opioid analgesics. The addition of a quaternary cationic 17-nitrogen moiety prevented the compound from passing through the blood–brain barrier (BBB), but also reduced the antagonistic activity. Other examples of peripheral antagonists include Alvimopan (Fig. 1) [14] and S-297995[1] (in Phase I by Shionogi; chemical structure undetermined). Alvimopan was launched in 2008 by GSK (originated by Adolor) for recovery of normal gastrointestinal function after abdominal surgery and to accelerate upper and lower gastrointestinal recovery after partial large or small bowel resection surgery with primary anastomosis.

1.2 δ Opioid Agonists

Currently, there are no δ opioid pharmaceuticals on the market; moreover, the essential properties of this class of drugs remain unclear. It is unknown whether δ opioid agonists incur the side effects observed with other opioid drugs, like dependency and constipation.

SNC-80 (GSK, NIH) [15] is one of the leading δ opioid agonists in development. SNC-80 has a bisarylmethyl substituted piperazine substructure (Fig. 2). Some SNC-80 derivatives for treating pain or urinary incontinence are in clinical development, including DPI-3290 [16] (δ and μ opioid agonist; GSK, Enhance Biotech), PF-04856880 [17] (ADL-5859; Pfizer, Adolor), PF-04856881 [18] (ADL-5747; Pfizer, Adolor), and a dimethylpiperazine derivative [19] (University of Arizona, NIH) (Fig. 2).

---

[1] Shionogi reports Financial Results for the Third Quarter of Fiscal Year 2009, Shionogi Press Release 2010, February 1.
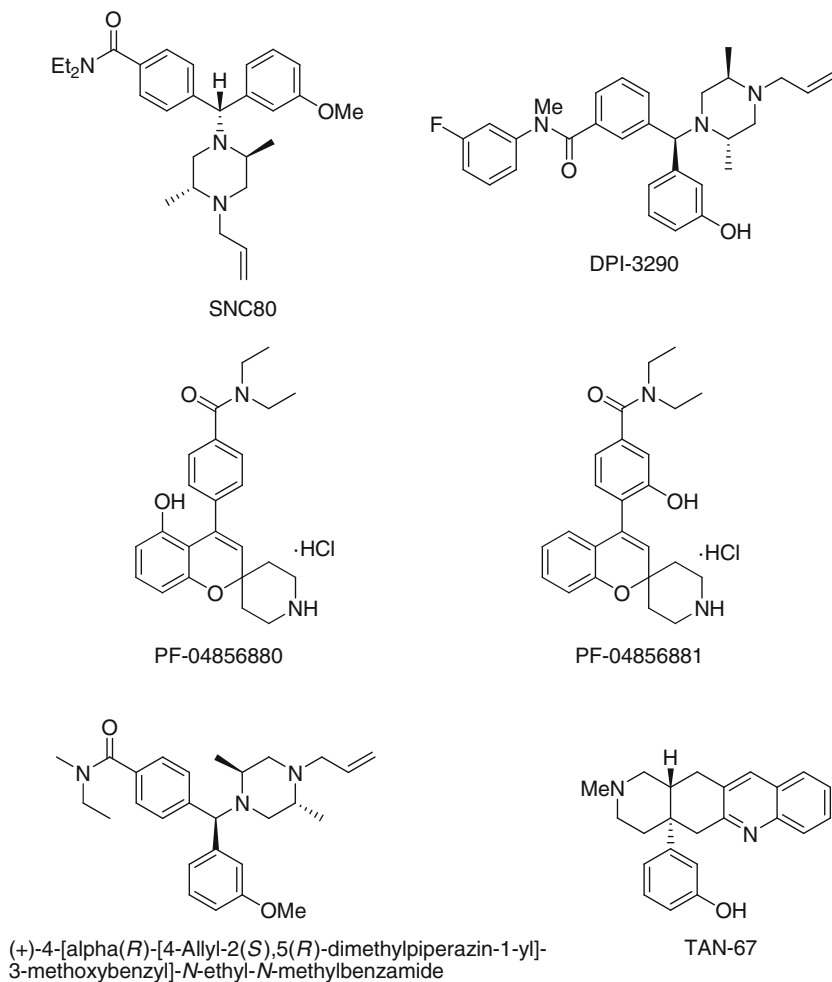
Fig. 2 Structures of δ opioid agonists in clinical development

Our group is currently developing TAN-67 (Toray), another lead δ opioid agonist with a characteristic 4a-aryl-decahydroisoquinoline structure. We previously discussed the design rationale and pharmacology of this compound [20, 21].

1.3 δ Opioid Antagonists

Portoghese and Suzuki have studied the possibility of reducing the undesirable side effects of μ opioid agonists by combining them with a δ opioid antagonist. This concept is based on the cross-talk among all three types of opioid receptors.
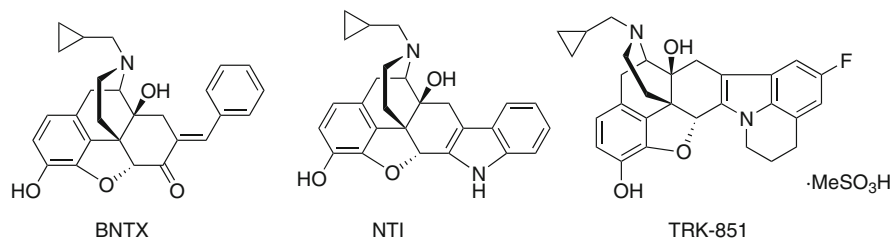
Fig. 3 Structures of δ opioid antagonists BNTX, NTI, and TRK-851

Portoghese and coworkers have shown that the dependency and tolerance induced by morphine could be treated with 7-benzylidenenaltrexone (BNTX), a δ_1 opioid antagonist (Fig. 3) [22]. Suzuki and colleagues also suggested that the psychological dependence induced by morphine could be reduced with naltrindole (NTI), another δ opioid antagonist (Fig. 3) [23, 24]. However, no drugs of this type are currently in clinical development. It has also been suggested that δ opioid antagonists might be potentially useful for immunosuppression [25], but no clinical development has been reported for this indication. The immunosuppressive effect of the δ antagonist NTI was suggested to arise from an alternative mechanism [26].

Kamei and colleagues discovered that an opioid network was involved in the cough reflex. A selective δ antagonist, TRK-851 (Toray, Fig. 3), is a clinical candidate in development as an antitussive agent [6]. This compound will be discussed in detail in Sect. 2.

1.4 κ Opioid Agonists

For the past three decades, considerable effort has been focused on developing an opioid κ selective agonist that could eliminate undesirable side effects of morphine-like drugs. In 1982, Upjohn (currently merged with Pfizer) discovered a highly selective κ agonist known as U-50,488H [27]. Subsequently, several research groups have modified this structure to create more selective and more potent κ agonists (Fig. 4) [29, 30].

In animal models, these κ agonists had potent antinociceptive effects and could eliminate the undesirable side effects of morphine-like drugs. They all had very similar structures that included the [N–C–C–N(sp^2)] pharmacophore sequence (shaded parts in Fig. 4), because they were derived from U-50,488H. Moreover, they lacked the tyrosine moiety that is essential for opioid activity from the viewpoint of endogenous opioid chemistry (Fig. 5).

Currently, the only clinically successful κ agonist drug has been TRK-820 (nalfurafine hydrochloride) (Toray, Fig. 6). Almost all of the U-50,488H derivatives apparently had side effects that were different from that of morphine,
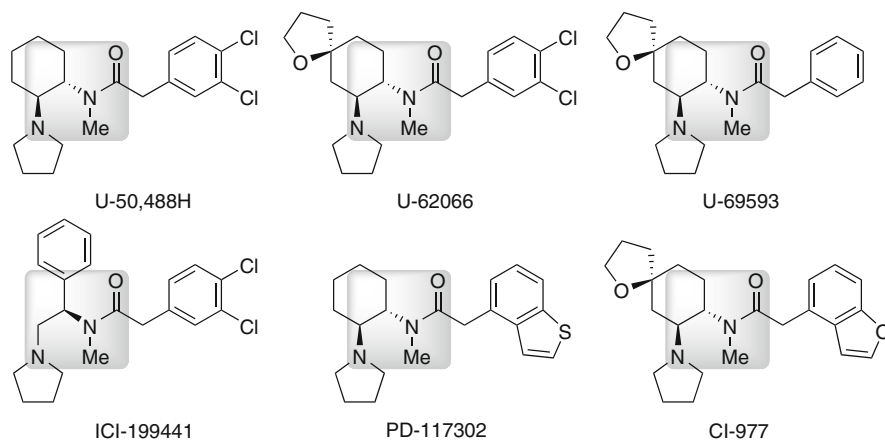
Fig. 4 Structures of κ agonist U-50,488H and its derivatives. Reprinted from [28], with permission from Elsevier. Copyright (2008)

Endomorphin-1(μ) **Tyr**-Pro-Trp-Phe-NH2
Endomorphin-2(μ) **Tyr**-Pro-Phe-Phe-NH2

[Met^5]enkephalin (δ) **Tyr**-Gly-Gly-Phe-Met
[Leu^5]enkephalin(δ) **Tyr**-Gly-Gly-Phe-Leu

Dynorphin A (κ) **Tyr**-Gly-Gly-Phe-Leu-Arg-Arg-Ile-Arg-Pro-Lys-Leu-Lys-Trp-Asp-Asn-Gln
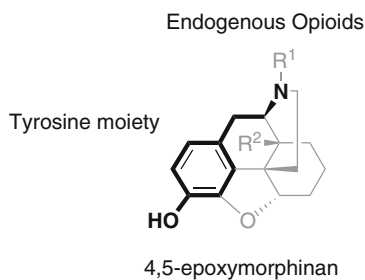
Fig. 5 Structures of 4,5-epoxymorphinan and typical opioid peptides. The tyrosine moiety is shown in *bold*. Reprinted from [28], with permission from Elsevier. Copyright (2008)
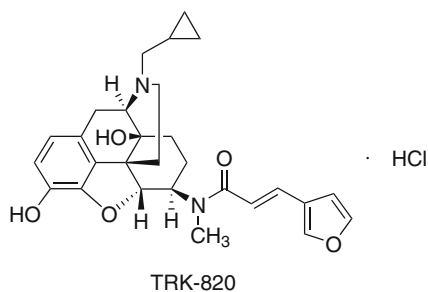
Fig. 6 Structure of κ agonist TRK-820

including dysphoria and psychotomimetic effects. We will describe the design rationale for TRK-820 in Sect. 3.

2 Antitussive δ Opioid Antagonist TRK-851

TRK-851 is a clinical candidate for an antitussive drug; it has a novel, complex morphinan ring system. The development of TRK-851 was motivated by the finding that NTI, a selective δ opioid receptor antagonist, showed antitussive effect. In this section we will describe the process of developing TRK-851, including the structure–activity relationship (SAR) studies on NTI derivatives and the difficulties encountered in overcoming a defect in the metabolism of a prototype clinical candidate, TRK-850.

2.1 *Antitussive Effects of Opioid Ligands*

It was recently recognized that opioid receptor agonists have antitussive effects [31]. Morphine (Fig. 7) is a potent μ opioid receptor agonist that exhibits marked antitussive effect, and it has been used for the treatment of severe coughs. Codeine (Fig. 7) is one of the most reliable centrally acting antitussive agents; its antitussive
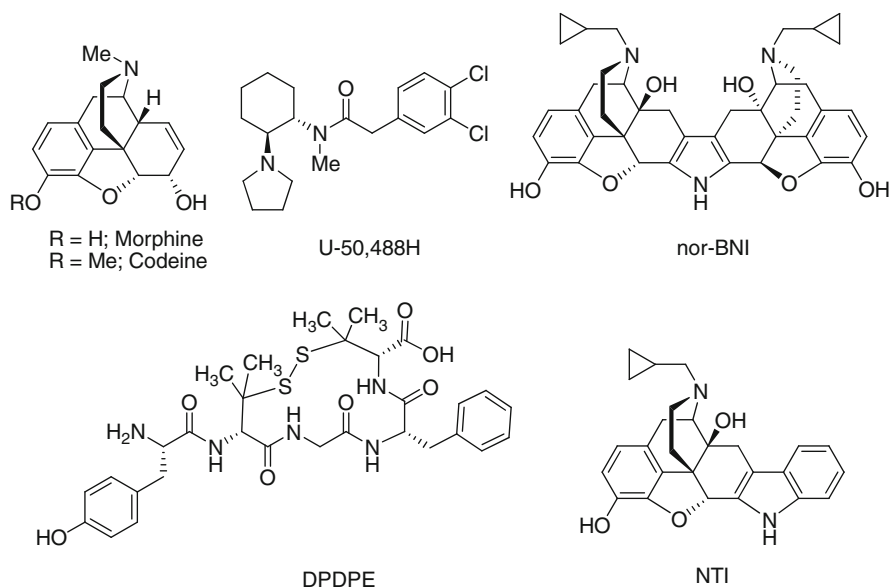
Fig. 7 Structures of opioid receptor ligands that have antitussive effects (agonists: morphine, codeine, U-50,488H; antagonists: NTI), δ opioid agonist DPDPE, and κ opioid antagonist nor-BNI

	Opioid ligand (s)	Antitussive effect
Table 2 Different opioid receptor ligands and their antitussive effects in rats	μ Agonist	++
	κ Agonist	+
	δ Agonist	−
	μ Agonist + δ agonist	−
	κ Agonist + δ agonist	−
	δ Antagonist	+

effect is thought to be derived from the activation of both a codeine specific receptor and the μ opioid receptor, because one of its active metabolites is morphine. Although these narcotic antitussive agents have sufficient therapeutic effects, they also exhibit μ opioid receptor-mediated side effects, *e.g.*, constipation, dependency, and respiratory depression. Therefore, the use of these drugs is limited [31, 32].

The effects of κ and δ opioid receptor activation on the cough reflex have been particularly investigated by Kamei and coworkers. They showed that U-50,488H (Fig. 7), a selective κ opioid receptor agonist, suppressed the cough reflex induced by capsaicin inhalation in rats. This antitussive effect was blocked by coadministration of the κ receptor antagonist, nor-BNI (Fig. 7). This suggested that the κ opioid receptor had mediated the antitussive effects (Table 2) [33].

On the other hand, the δ opioid receptor agonists exhibited activity in contrast to μ and κ agonists. One δ opioid receptor agonist, DPDPE ([D-Pen^2, D-Pen^5]enkephalin) (Fig. 7), hardly induced antitussive effect, but it blocked the antitussive effect of morphine. The blockade could be antagonized by the coadministration of NTI (Fig. 7), a selective δ opioid receptor antagonist (Table 2) [34]. The antitussive activity of U-50,488H was also blocked by DPDPE, and that blockade was also antagonized by the coadministration of NTI [35]. These results suggested that activation of the δ opioid receptor suppressed the antitussive activities of μ and κ opioid agonists.

Furthermore, Kamei *et al.* reported that the administration of NTI alone also produced an antitussive effect (Table 2) [36].

2.2 Mechanism of the Antitussive Effect of NTI

Figure 8 shows the mechanism proposed for the antitussive effect of NTI [36]. When the respiratory tract is stimulated by irritants, *e.g.*, xenobiotics, the cough reflex occurs, and the stress of coughing triggers the secretion of endogenous opioid peptides, which may simultaneously stimulate three types of opioid receptors. In a disease state, the stimulation of the δ opioid receptor could block the μ and κ opioid receptor-mediated suppression of the cough reflex, which would result in continual coughing (Fig. 8a). When a selective δ opioid antagonist, *e.g.*, NTI, is administered,
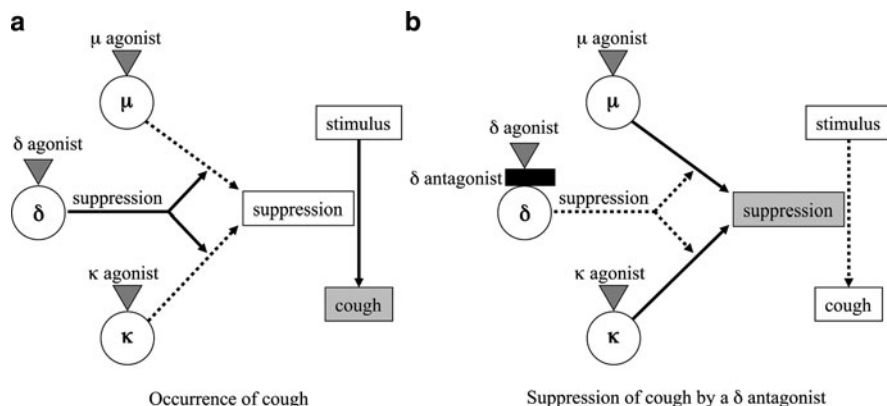
Fig. 8 Possible mechanism of the antitussive effect caused by δ opioid receptor antagonists. *Solid arrows* indicate activated pathways; *dotted lines* indicate inactivated pathways

it blocks the antagonism by δ agonist to cough suppression derived from the μ and κ receptors, and coughing is suppressed (Fig. 8b).

These observations strongly supported the feasibility of δ opioid receptor antagonists as antitussive drugs that did not have μ opioid receptor-mediated side effects.

2.3 Improvement on the Antitussive Activity of NTI

2.3.1 Rat Cough Model

In order to discuss the SARs of opioid ligands, we must first describe the rat cough model. In this model, rats are exposed to a capsaicin aerosol that induces coughing (Fig. 9) [36]. The coughs are detected as changes in air pressure inside the rat chamber, and the number of coughs can be counted as the number of peaks on the polygraph with careful distinction of coughs from wriggles. The ED_{50} values of NTI injected *via* intraperitoneal (i.p.) and peroral (p.o.) routes were 104 μg/kg and 1,840 μg/kg, respectively, comparable to those of codeine.

This cough model was used to determine SARs of NTI derivatives. In addition to the antitussive efficacy of compounds, it is possible to assess not only compounds' intrinsic affinity for the receptor but their absorption, distribution, metabolism, and excretion (ADME) properties.

2.3.2 Design and Rationale of NTI

Improving a drug's permeability through the BBB can enhance its concentration in the CNS. Therefore, improving the BBB permeability of NTI might augment its antitussive activity.
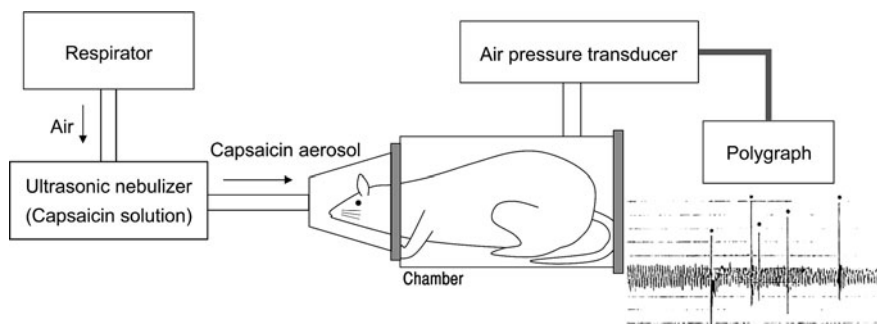
Fig. 9 Rat model of capsaicin-induced coughing

The BBB consists of microcapillary blood vessels that run throughout the brain in close proximity to brain cells [37, 38]. On the inner surface of the capillaries, the endothelial cells are held tightly together to each other to form a monolayer. Centrally acting drugs must permeate through these endothelial cells to penetrate into the brain.

In general, the physicochemical properties of a compound can greatly affect its capacity for passive transcellular BBB permeation. General strategies for modifying drug structures to improve BBB permeability include the following [37, 38]:

1. Reduction of hydrogen bond donors
2. Augmentation of hydrophobicity
3. Reduction of molecular weight

In addition to passive transport, active transport can occur with proteins lodged in the BBB that facilitate uptake and efflux of compounds into and out of the CNS. Therefore, compounds can be modified to enhance their affinity for uptake transporters or reduce their affinity for efflux transporters (*e.g.*, *P*-glycoprotein) to improve BBB permeability [37]. However, these strategies required major structural transformations; thus, we focused on strategies related to changing the physicochemical properties of NTI, as mentioned below.

2.3.3 Introducing Alkyl Substituents into the Indole Ring of NTI

One strategy for improving the BBB permeability of NTI was to augment its hydrophobicity by introducing alkyl substituents into the indole ring. Several NTI derivatives with alkyl substituents were synthesized and tested for potentiation of the antitussive activity. Table 3 presents a comparison of the resulting NTI derivatives. Methylation of the 3-hydroxy group in NTI (compound **1**) slightly increased the antitussive activity [39]. In contrast, *N*-methylation at the 1′ position of NTI (compound **2**) reduced the antitussive activity. However, simultaneous alkylations (compound **3**) at both the 3-hydroxy group and the 1′ position markedly improved the antitussive activity. Moreover, introduction of a third alkyl substituent at the 7′

Table 3 Antitussive effects of alkyl-substituted NTI derivatives in rats (administered i.p.)
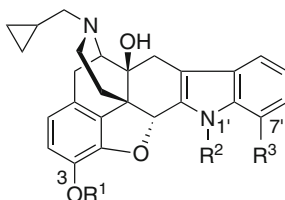
Compound	R^1	R^2	R^3	ED_{50} (μg/kg)[a]	cLog P
NTI	H	H	H	104 (20.3–553)	3.2
1	Me	H	H	63.9 (29.4–139)	3.8
2	H	Me	H	204 (41.8–999)	3.7
3	Me	n-Pr	H	14.8 (4.09–53.8)	5.3
4	Me	Me	Me	6.35 (2.05–19.6)	4.8
5	Me	Et	Me	1.79 (0.67–4.89)	5.3

[a]ED_{50} value; the dose that reduces the number of coughs to 50% vs control, expressed as the mean ($n = 8$). *Figures in parentheses* indicate 95% confidence limits

position in compounds **4** and **5** led to further enhancement of potency by factors of 16 and 58, respectively, compared to the parent compound.

These results suggested that introducing alkyl groups into the indole substructure, especially at the 1′ and 7′ positions, increased the hydrophobicity of these compounds, which is supported by the calculated log P values (cLog P). This enhanced their BBB permeability and, as a result, the antitussive activities were enhanced. Reducing the number of hydrogen bond donors was another strategy for improving BBB permeability; however, although NTI derivatives **1** and **2** lacked a single hydrogen bond donor, they did not show improved antitussive activity compared to NTI.

2.3.4 NTI Derivatives with an Additional Fused Ring

Among the compounds in Table 3, compound **5** showed the highest antitussive activity; however, it showed a markedly reduced δ receptor antagonist activity in the mouse vas deferens (MVD) assay (Table 4). In the MVD assay, the *Ke* value indicated the potency of the test compound antagonist activity for each receptor type. Compound **5** showed a markedly high *Ke* value (low potency) for the δ receptor compared with that of unmodified NTI [39]. Moreover, compound **5** showed a reduced selectivity for the δ receptor over the μ and κ receptors. This suggested that the antitussive activity of compound **5** may be induced by its active metabolites (*e.g.*, 3-OH analog).

We suspected that the bulky substituents in the indole ring of compound **5** might have caused its reduced affinity for the δ receptor, which resulted in a reduction in δ receptor antagonist activity. Thus, to reduce the bulkiness of the indole ring on
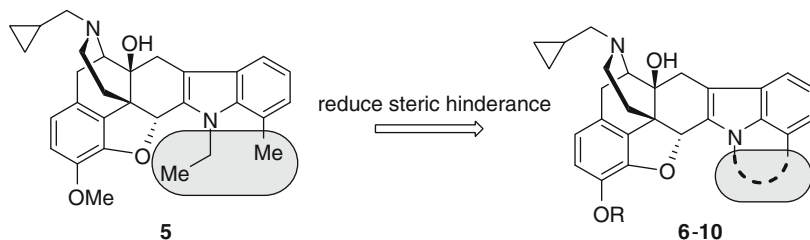
Fig. 10 Additional fused ring design of new NTI derivatives

Table 4 Antagonist effect of NTI and its derivatives (MVD assay)[a]

6-10
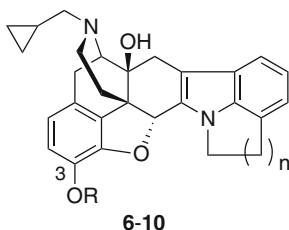
Compound	R	n	Ke (nM)[b]		
			DPDPE (δ)	Morphine (μ)	U-50,488H (κ)
NTI	–	–	0.074	50	2.9
5	Me	–	204	263	213
6	H	1	0.61	17	8.6
7	H	2	0.80	13	28
8	Me	2	6.3	[c]	68
9	H	3	3.1	18	53
10	Me	3	333	[d]	17

[a]DPDPE, morphine, and U-50,488H were used as agonists of δ, μ, and κ opioid receptors, respectively

[b]The Ke values were calculated according to the following equation. Ke = [test compound concentration]/[dose ratio–1]. The dose ratio was the ratio of agonist concentrations that elicited equal responses in the absence and presence of the test compound at increasing concentrations

[c]No antagonism at a test compound concentration of 100 nM

[d]No antagonism at a test compound concentration of 10 nM

compound **5**, we designed and synthesized a new type of NTI derivative, with an additional fused ring system (Fig. 10).

As expected, the fused ring compounds **6–9** exhibited higher δ receptor antagonist activity than compound **5** (Table 4) [39]. In the 3-OMe derivatives, compound **8** (a propylene bridge) showed higher δ antagonist potency than compound **10** (a butylene bridge). In the 3-OH derivatives, the δ antagonist potency order was **6** (an ethylene bridge) $\approx$ **7** (a propylene bridge) > **9** (a butylene bridge). These results strongly suggested that the δ receptor binding affinity was reduced with the

Table 5 Antitussive effects of NTI derivatives that had an additional fused ring structure (administered i.p. in rats)

Compound	ED_{50} (µg/kg)[a]	cLog P
NTI	104 (20.3–553)	3.2
	1,830 (890–3,820)[b]	
6	9.14 (4.23–19.8)	3.8
7	8.58 (2.33–31.7)	4.2
8 (TRK-850)	3.43 (0.93–12.6)	4.8
	6.40 (1.54–26.5)[b]	
9	12.3 (3.92–38.3)	4.8
10	9.68 (1.98–47.4)	5.3

[a]ED_{50} value; the dose that reduces the number of coughs to 50% vs control, expressed as the mean ($n = 8$). *Figures in parentheses* indicate 95% confidence limits
[b]p.o. administration

bulkiness of the indole ring, and a compact fused ring facilitated a higher δ receptor binding affinity.

Table 5 shows the antitussive activities of the fused ring NTI derivatives [39]. All the fused ring compounds **6–10** showed dramatically improved antitussive activity compared to NTI. In particular, the 3-OMe analog **8**, whose methanesulfonic acid salt was selected as a prototype clinical candidate, TRK-850, showed very high antitussive activity; its ED_{50} value was 30-fold lower than that of NTI. Moreover, when administered p.o., TRK-850 also exhibited a highly potent antitussive effect; its ED_{50} value was 6.40 µg/kg, or 280 times lower than that of NTI given p.o. The increased hydrophobicity and lower bulkiness of TRK-850 led to potent antitussive effects.

In summary, the introduction of alkyl chains into NTI resulted in increased antitussive activities of these compounds, but it simultaneously reduced the δ receptor antagonist activity. The introduction of an extra fused ring created a compact-sized hydrophobic moiety attached to the indole ring in NTI. This led to a compound, TRK-850, with both high δ receptor antagonism and potent antitussive effects.

2.4 Improvement of Metabolic Defect of TRK-850

2.4.1 Strategies

As mentioned above, TRK-850 had excellent pharmacological properties (potent δ antagonist activity and antitussive effect by p.o. administration). However, a serious defect in TRK-850 was observed during the ADME study. After p.o. administration of tritiated TRK-850 in a rat, the plasma sample showed only a small parent peak with HPLC [³H]-detection. This indicated that TRK-850 was

Fig. 11 Structure of compound **8** (TRK-850) and its main metabolic pathways. Reprinted from [6] with permission from Elsevier. Copyright (2008)
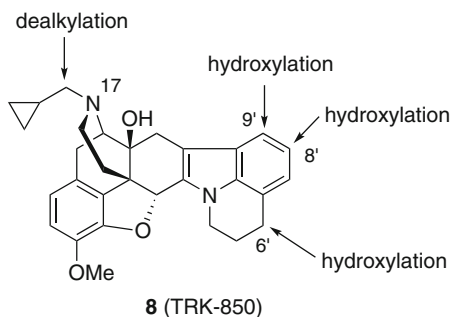
8 (TRK-850)

metabolized at an extremely high rate, which later proved to be caused by cytochrome P450 [6]. Therefore, we concluded that TRK-850 was inadequate as a long-lasting drug. The metabolism of TRK-850 was investigated in detail by isolating the main metabolites in the plasma samples of rats that received oral TRK-850. We identified four primary metabolites: 17-decyclopropylmethyl, 9′-hydroxy, 8′-hydroxy, and 6′-hydroxy derivatives (Fig. 11) [6].

On the basis of the structures of the four metabolites, we designed strategies for improving the oxidative metabolic profile of TRK-850.

In general, oxidative metabolism may be prevented with the following strategies [38]:

1. Incorporating blocking groups at the labile site.
2. Modifying the labile site with bulky substituents, which prohibit the metabolic enzyme from approaching its substrate through steric hindrance.
3. Reducing the lipophilicity of the compound.
4. Introducing electron-withdrawing groups around the labile site to reduce electron density at the labile site and, consequently, prohibit an oxidative metabolic reaction.

2.4.2 Structure–Metabolic Stability Relationships of TRK-850 Derivatives

Several TRK-850 derivatives were synthesized based on the general strategies mentioned above, and their metabolic stabilities were evaluated in the presence of human liver microsomes. Metabolic rates were determined by incubating the compounds with human liver microsomal enzymes and then quantifying the remaining parent peak by HPLC analysis. The data were expressed as the elimination rate constant (K_{EL}) and the relative metabolic rate, or the K_{EL} of the compound compared with the K_{EL} of TRK-850 (K_{EL} ratio).

Replacement of one of the metabolic sites, the 6′-methylene group of TRK-850, with an oxygen atom or dimethylmethylene group improved the metabolic stability (Table 6) [6].

The derivatization that most effectively lowered the metabolic rate was the demethylation of the 3-methoxy group (Table 6). The conversion of the 3-methoxy

Table 6 Metabolic rates of TRK-850 derivatives in the presence of human liver microsomes
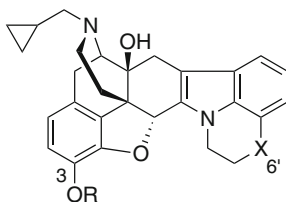
Compound	X	R	Metabolic rate[a]		cLogP
			K_{EL} (min^{-1})	$(K_{EL}$ ratio$)^{-1}$	
8 (TRK-850)	CH$_2$	Me	0.341	1	4.8
11	CMe$_2$	Me	0.0618	5.51	5.8
12	O	Me	0.0627	5.43	4.2
7	CH$_2$	H	0.0249	13.7	4.2
13	CMe$_2$	H	0.0758	4.5	5.2
14	O	H	0.0334	10.2	3.6

[a]K_{EL}, an elimination rate constant calculated from the time course of compound elimination. K_{EL} ratio $= (K_{EL}$ of a given compound$)/(K_{EL}$ of TRK-850)

group of TRK-850 to a hydroxyl group (compound **7**) dramatically improved metabolic stability. This stabilizing effect was also observed in compound **14**. These results might be due to the reduced lipophilicity of these compounds, as suggested by the cLog P values.

Next, we evaluated the metabolic rates of compound **7** derivatives, which had a substituent in the indole benzene ring (**15–28**; Table 7) [6]. Introduction of an electron-withdrawing substituent into the indole moiety tended to suppress the metabolism of a compound (**16**, **18**, **19**, **21–23**, **27**). On the other hand, an electron-donating substituent tended to enhance the metabolism of a compound (**20**, **26**, **28**). These observations suggested that the electron density around the indole moiety was correlated to the cytochrome P450 oxidative metabolic rate. In addition, the position of substitution was important. For example, blocking at the 8′-position suppressed the metabolism more effectively than blocking at the 7′- or 9′-positions.

2.4.3 Antitussive Activities of TRK-850 Derivatives: Journey to TRK-851

The antitussive effects of selected TRK-850 derivatives were evaluated (Table 8) [6]. Incorporation of a substituent into the indole moiety resulted in lower potency than that of compound **7**; nevertheless, some derivatives still exhibited high anti-tussive activity (**19–21**, **24**, **26**). Incorporation of bulky substituents at the 8′-position also tended to reduce potency (**22**, **23**). Incorporation of fluorine, the smallest substituent with the greatest electron-withdrawing capacity, resulted in the

Table 7 Metabolic rates of compound **7** derivatives in the presence of human liver microsomes
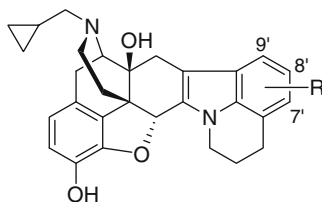
Compound	R	Metabolic rate[a]	
		K_{EL} (min^{-1})	$(K_{EL}$ ratio$)^{-1}$
7	H	0.0249	13.7
15	7'-Cl	0.0290	11.7
16	7'-Br	0.0218	15.6
17	7'-OMe	0.0262	13.0
18	8'-Cl	0.0177	19.2
19	8'-Br	0.0151	22.6
20	8'-OMe	0.0331	10.3
21	8'-F	0.0174	19.6
22	8'-OCF$_3$	0.00909	37.5
23	8'-CF$_3$	0.0162	21.0
24	9'-Cl	0.0270	12.6
25	9'-Br	0.0371	9.20
26	9'-OMe	0.0285	12.0
27	9'-CF$_3$	0.0167	20.4
28	9'-Me	0.0339	10.1

[a]K_{EL}, an elimination rate constant calculated from the time course of compound elimination. K_{EL} ratio = (K_{EL} of a given compound)/(K_{EL} of TRK-850)

minimum loss of potency (**21**). Among these derivatives, compound **21** showed the most potent antitussive activity and had a metabolic rate 20 times lower than that of the parent compound, TRK-850. The methanesulfonic acid salt of compound **21** was called TRK-851. Figure 12 shows that p.o. administration of TRK-851 reduced the number of coughs in a dose-dependent manner with an ED$_{50}$ value of 35.5 μg/kg. Thus, the potency of TRK-851 was over 50-fold higher than that of the starting compound, NTI [6].

The opioid receptor selectivity of TRK-851 was tested in the MVD assay (Table 9). TRK-851 strongly antagonized the agonist activity of DPDPE (δ), and it showed over 200 times greater selectivity for the δ opioid receptor than for μ or κ receptors. These results strongly suggested that the antitussive effect of TRK-851 was derived from its marked antagonism of δ opioid receptors [6].

2.5 Summary

NTI derivatives that possessed hydrophobic substituents were designed and synthesized based on the hypothesis that increased hydrophobicity might improve their

Table 8 Antitussive effects of TRK-850 derivatives in rats (administered s.c.)
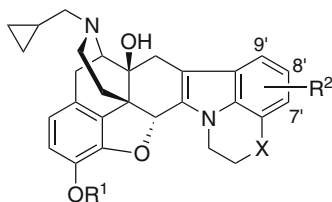
Compound	X	R^1	R^2	ED$_{50}$ (µg/kg)[a]
7	CH$_2$	H	H	0.20 (0.06–0.6)
				8.58 (2.33–31.7)[b]
8 (TRK-850)	CH$_2$	Me	H	3.43 (0.93–12.6)[b]
15	CH$_2$	H	7′-Cl	13.8 (0.62–310)
16	CH$_2$	H	7′-Br	27.4 (8.81–85.1)
17	CH$_2$	H	7′-OMe	54.2 (18.6–158)
18	CH$_2$	H	8′-Cl	78.4 (11.5–538)[b]
19	CH$_2$	H	8′-Br	5.05 (2.58–9.86)
20	CH$_2$	H	8′-OMe	2.0 (0.4–9.4)
21 (TRK-851)	CH$_2$	H	8′-F	1.7 (0.4–7.3)
				15.7 (5.31–46.4)[b]
22	CH$_2$	H	8′-OCF$_3$	>1,000
23	CH$_2$	H	8′-CF$_3$	>1,000
24	CH$_2$	H	9′-Cl	3.5 (1.4–8.7)
25	CH$_2$	H	9′-Br	94.6 (5.11–389)
26	CH$_2$	H	9′-OMe	8.67 (1.02–73.6)

[a]ED$_{50}$ value; the dose that reduces the number of coughs to 50% vs control, expressed as the mean ($n = 8$). *Figures in parentheses* indicate 95% confidence limits
[b]Administered i.p.

permeability through the BBB. This was expected to increase their antitussive activities compared with that of unmodified NTI. Although the introduction of alkyl groups into the NTI skeleton increased the antitussive activities of these derivatives, it simultaneously decreased the δ opioid receptor antagonist activity. Thus, the antitussive activities of these compounds may be affected more potently by brain exposure of the compounds rather than by their δ antagonist activity.

The introduction of an extra fused ring, a compact-sized moiety, into the indole ring of NTI conferred both suitable hydrophobicity and low steric hindrance. Consequently, compound **8** (TRK-850) was identified as a prototype clinical candidate that exhibited both potent antitussive activity and selective δ receptor antagonist activity.

However, TRK-850 was found to be susceptible to oxidative metabolism by cytochrome P450. The results from structure optimization studies suggested that a drug candidate must have sufficiently low hydrophobicity to prevent a high metabolic rate, but also have sufficiently high hydrophobicity to retain potent antitussive activity. Therefore, additional compact indole substituents that were expected to
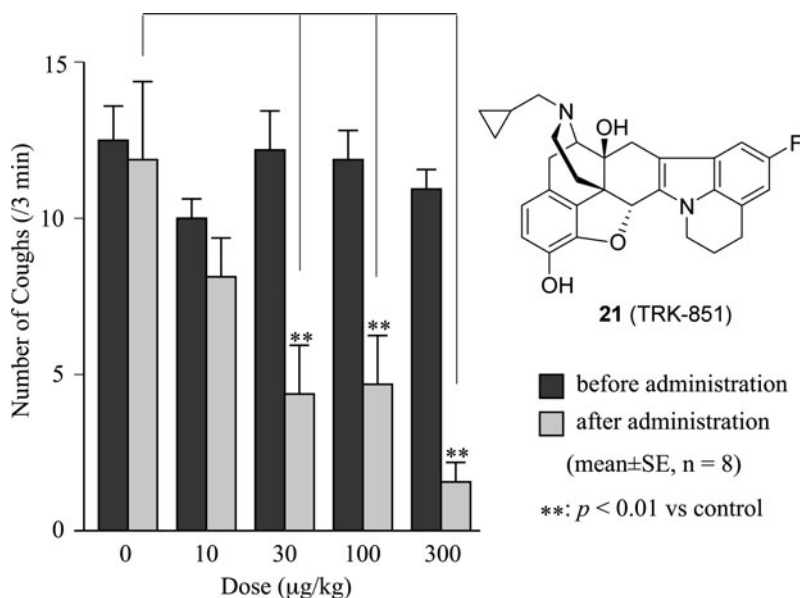
Fig. 12 Antitussive effect of compound **21** (TRK-851) on capsaicin-induced coughing in rats (p.o. administration). The number of coughs over 3 min were counted in the same rats before and 60 min after p.o. administration. The ED_{50} value (the dose that reduced the number of coughs to 50% vs control) for the inhibition of coughing was calculated to be 35.5 µg/kg (95% confidence limits: 16.8–72.9 µg/kg). Reprinted from [6] with permission from Elsevier. Copyright (2008)

Table 9 Compound **21** (TRK-851) antagonism of opioid receptors (MVD assay)[a]

Compound	Ke (nM)[b]		
	DPDPE (δ)	Morphine (μ)	U-50,488H (κ)
21 (TRK-851)	1.46	333	[c]

[a]DPDPE, morphine, and U-50,488H were used as agonists of δ, μ, and κ opioid receptors, respectively
[b]The Ke values were calculated according to the following equation: Ke = [test compound concentration]/[dose ratio–1]. The dose ratio was the ratio of agonist concentrations that elicited equal responses in the absence and presence of the test compound at increasing concentrations
[c]No antagonism at test compound concentration of 10 nM

metabolize slowly were examined for their antitussive activity. Modifications of TRK-850, including demethylation of the 3-methoxy group and introduction of 8′-fluorine, provided the appropriate hydrophobicity and potent δ antagonist activity. Finally, TRK-851, a potent, selective δ receptor antagonist that metabolized slowly, was identified as a highly potent oral antitussive agent, and was chosen for further clinical evaluation.

3 Antipruritic κ Opioid Agonist TRK-820 (Nalfurafine Hydrochloride)

Nalfurafine hydrochloride is a first-in-class, nonaddictive opioid drug that is used as an antipruritic for severe itching associated with hemodialysis. This drug was launched in Japan in 2009. It has a unique morphinan structure that is rarely observed in typical and traditional opioid κ agonists. The design rationale for this characteristic compound was described in a previous study [7, 28], and would be of interest to researchers in the opioid field. We will summarize the rationale in Sect. 4.

3.1 Design Rationale

Since the Upjohn Group first described the synthesis of U-50,488H (Fig. 4) [27], numerous U-50,488H derivatives have been synthesized and examined for pharmacological effects. However, none of these drugs was appropriate for practical indications. We questioned whether U-50,488H derivatives were actually κ opioid agonists. Therefore, we designed and synthesized a new type of nonpeptide κ agonist with a novel chemical structure. This compound retained the tyrosine moiety in order to reduce the side effects of the prototype κ agonists, including dysphoria and psychotomimetic effects [7, 40].

Portoghese and colleagues at Minnesota University proposed the "Message-Address Concept" for designing selective δ and κ antagonists (Fig. 13: NTI and nor-BNI) [41, 42]. They pointed out that the 4,5-epoxymorphinan skeleton, defined as the "message" subsite, which is commonly found in NTI and nor-BNI, was necessary for the intrinsic activity of an opioid. The other part of the structure was defined as the "address" subsite, and it is involved in the receptor type selectivity. As shown in Fig. 13, the receptor type selectivity of these opioid antagonists can be regulated by altering the size of the address structure. Although this concept was suitable for designing a selective opioid antagonist, a further strategy was necessary to design an opioid agonist.

The strategy for designing an opioid agonist included a working hypothesis of an "accessory site". This hypothesis holds that the receptor can change its shape to accommodate the structure of an agonist ("induced fit") and facilitate agonist binding to the receptor. This change would lead to activating the signal transduction pathway that expressed the effects of the agonist. On the other hand, the antagonist might be considered to be a compound with an extra structural part that interferes with the accommodating changes in the receptor. As a result, the antagonist shows no agonistic effects. The structural moiety that could interfere with the induced fit is called an "accessory site" [43], and it comprises a highly hydrophobic moiety and a sterically hindered structure.

Fig. 13 Message-Address Concept proposed for opioid antagonists. Reprinted from [28] with permission from Elsevier. Copyright (2008)

μ: Naltrexone

δ: NTI

κ: nor-BNI

Message subsite   Address subsite
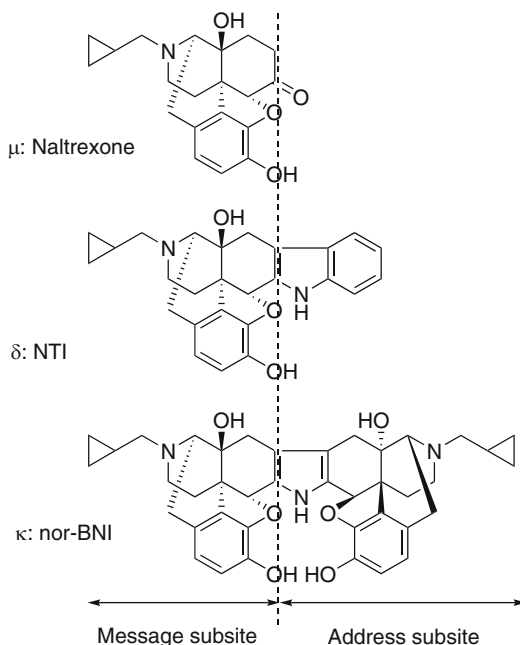
To design a new agonist, we first attempted to remove the accessory site of nor-BNI and maintain the message and address sites. The message site of nor-BNI, a 4,5-epoxymorphinan skeleton with a cyclopropylmethyl substituent, was considered to be indispensable for opioid activity because it corresponded to the tyrosine of endogenous opioid peptides. Therefore, we postulated that the accessory site of nor-BNI was located in the address subsite of this antagonist.

The meso isomer of nor-BNI, **27** (Fig. 14), showed κ selectivity and antagonist activity similar to those of nor-BNI [44]. Compound **28**, which had a nor-BNI address site, but lacked the phenol ring, also maintained high κ receptor selectivity, similar to that of nor-BNI [45]. These facts indicated that neither the phenol ring nor the hydroxyl group of the ring junction in the address site of nor-BNI were required for κ selectivity or antagonist activity. Based on a comparison between the κ antagonist **28**, naltrexone, and NTI, we proposed that the feature of the address subsite that was essential for receptor selectivity was the length of the address site (Fig. 14). From this point of view, the design of a κ selective agonist required the removal of the accessory site from compound **28**, but the length of the address site must be maintained for binding the κ receptor. On the basis of that concept, we designed and synthesized compounds (**A**) that had a C6 (carbon atom in the 6-position) and an X (a hetero atom) with a single bond (Fig. 14). The single bond was expected to give structural flexibility to the ligand, which would facilitate the ability of the receptor to assume an induced fit for binding the agonist. Based on these design principles, a number of compounds were synthesized (**29–33**) with the proper side chain structure, size, and length (address subsite) for a κ agonist activity.
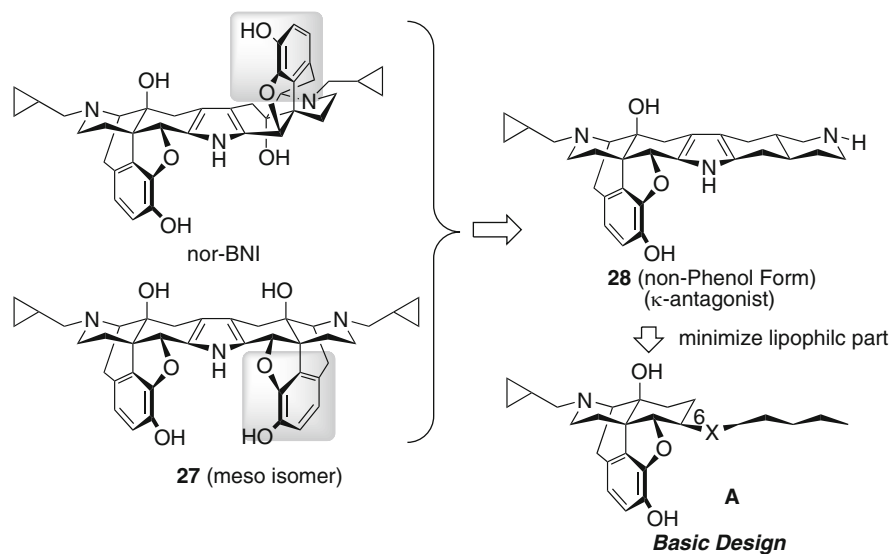
Fig. 14 Basic design of a new chemical class opioid κ agonist. Reprinted from [28] with permission from Elsevier. Copyright (2008)

3.2 Pharmacology and Medicinal Chemistry

Table 10 shows the results of screening for the most appropriate X spacer for κ agonist activity. The side chain was fixed at a 6-carbon length, which is similar to the size of the address site of nor-BNI. Opioid receptor selectivity and agonistic activity were evaluated with the MVD assay [46]. The agonist potencies were expressed as IC_{50} values. The *Ke* value indicated the receptor selectivity of test agonists. After detecting the opioid receptor agonist activity of test compounds *in vitro*, the acetic acid writhing (AAW) test [47] was conducted in mice to estimate the *in vivo* potency. The analgesic effects of test compounds could be effectively antagonized by pretreatment with the opioid κ antagonist, nor-BNI.

Almost all the compounds showed similar agonistic activity in the MVD assay. Although KT-90 and KT-95 (Fig. 15) [48–50] which had thioester structures, reportedly showed opioid κ agonist activity, compound **31**, also with a thioester, showed almost no agonistic activity *in vitro* or *in vivo*. This finding revealed the importance of the chemical structure of the "address" site of the analog. Amide compounds, particularly the *N*-methyl amido compound **32b**, showed the most potent agonistic activity in the AAW test and the highest κ selectivity in the MVD assay.

Table 11 shows that both κ agonistic activity and selectivity were affected by the introduction of an unsaturated bond and a lipophilic moiety into the *N*-methyl amide side chain. Often, the binding affinity or agonistic activity could be increased by introducing an unsaturated bond into the side chain. This might fix a favorable

Table 10 SAR studies on the variation of the spacer X
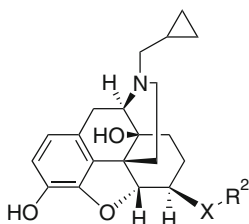
Compound	X-R^2	MVD^a				AAW, ED$_{50}$ (mg/kg)^j		
		IC$_{50}$ (nM)	Ke (nM)^b			s.c.	p.o.	p.o./s.c.
			μ^c	δ^e	κ^h			
29	O-C$_6$H$_{13}$	16	4.5	1.5	0.12	1.8	ND^k	ND^k
30	S-C$_6$H$_{13}$	38% inhibition (1 μM)				16	ND^k	ND^k
31	S(CO)-C$_5$H$_{11}$	Not effective				Not effective		
32a	NH(CO)-C$_5$H$_{11}$	2.0	14	NC^f	0.3	0.29	ND^k	ND^k
33	NH-C$_6$H$_{13}$	25	4.4	2.3	0.26	25% inhibition (10 mg/kg)		
32b	NMe(CO)-C$_5$H$_{11}$	15	UD^d	90^g	0.046^i	0.77	0.63	8.2

^{a}Data were expressed as the mean (n = 4–9)

^{b}The Ke values were calculated from the following equation: Ke = [antagonist]/(IC$_{50}$ ratio–1); [antagonist]: concentration of the antagonist; IC$_{50}$ ratio:the IC$_{50}$ without the antagonist over the IC$_{50}$ with the antagonist. Each preparation was incubated with a selective antagonist for 20 min before the addition of a test compound

^{c}Naloxone (30 nM) was used as a μ selective antagonist

^{d}Undetectable (IC$_{50}$ did not change with up to 100 nM of naltrexone)

^{e}NTI (10 nM) was used as a δ selective antagonist

^{f}Not calculated (the IC$_{50}$ ratio was too small to calculate the Ke value)

^{g}NTI (100 nM) was used

^{h}nor-BNI (10 nM) was used as a κ selective antagonist

^{i}nor-BNI (20 nM) was used

^{j}Data were expressed as the mean (n = 10)

^{k}Not determined

Reprinted from [28] with permission from Elsevier. Copyright (2008)
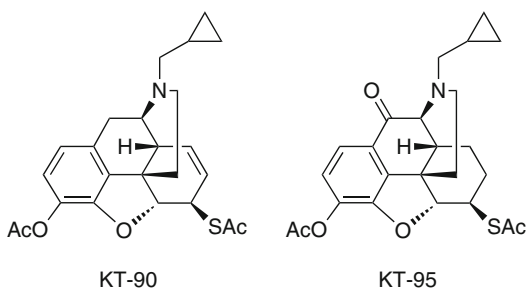
Fig. 15 Structures of KT-90 and KT-95

conformation (Fig. 16) and may contribute to π–π interactions with the receptor. We also attempted to optimize the length of the side chain. In the course of these SAR studies, we found an attractive lead compound, **32f** (Fig. 16; Table 11),
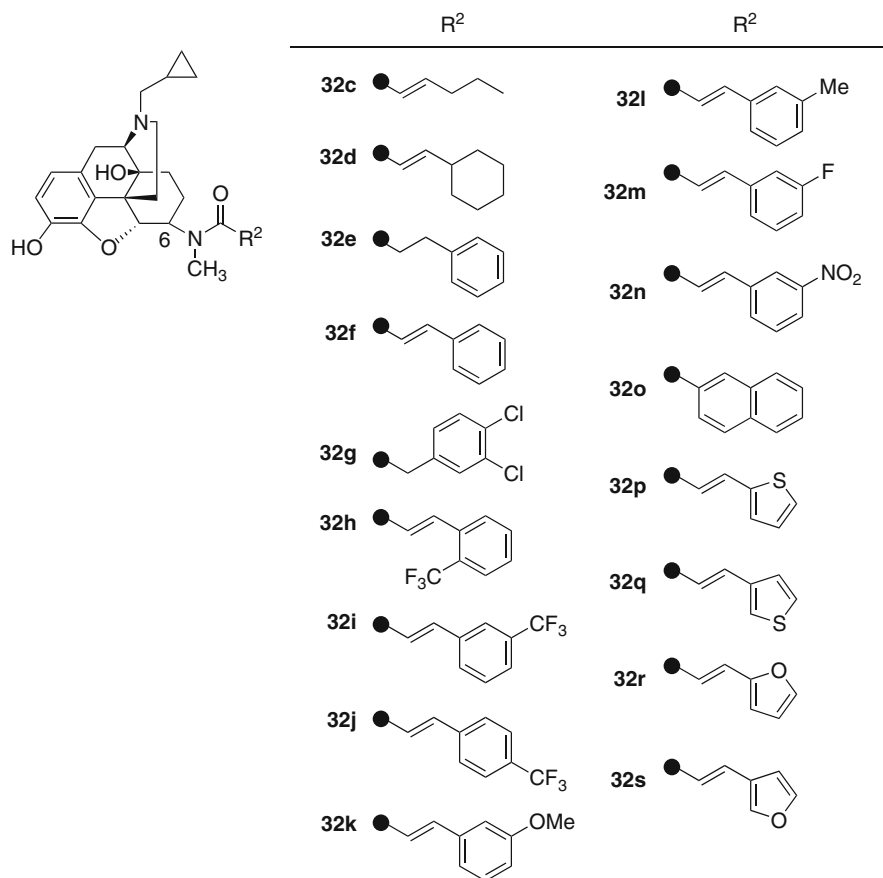
Fig. 16 Potential κ agonist structures: 6-amide derivatives of compound **32b**. Reprinted from [28] with permission from Elsevier. Copyright (2008)

a 6β-cinnamamido derivative. Compound **32f** showed high selectivity for the κ receptor in the MVD assay and significant *in vivo* κ agonist potency in the AAW test, even with p.o. administration. Furthermore, the agonist effect of **32f** showed adequate duration in the *in vivo* test. However, **32f** had significant side effects.

Therefore, a lead optimization study was performed by focusing on the stereo-chemistry, length, and aromatic ring structure of the side chain. A number of **32f** derivatives were synthesized by condensing α- and β-*N*-methylnaltrexamine with various carboxylic acids (Fig. 16; Table 12). Compounds α- and β-**32 g** were considered the simple combination of a morphinan structure with U-50,488H, because U-50,488H had the same side chain (3,4-dichlorophenylacetamido). How-ever, their analgesic activities, especially when administered p.o., were neither potent nor long lasting. Both the compounds that were simple derivations of the

Table 11 SAR study on the variation of the side chain R^2 (structures shown in Fig. [16])

Compound	MVD[a]				AAW, ED_{50} (mg/kg)[i]			
	IC_{50} (nM)	Ke (nM)[b]			s.c.	p.o.	p.o./s.c.	Duration[j]
		μ[c]	δ[e]	κ[g]				
32b	15	UD[d]	89.6[f]	0.046[h]	0.77	0.63	8.2	ND[k]
32c	0.65	1,797	UD[d]	0.072	0.024	0.21	8.8	S
32d	0.46	5,713	143	1.08	0.004	0.071	17.0	L
32e	0.019	UD[d]	188	0.008	0.040	0.29	7.3	S
32f	0.17	922	263	0.861	0.002	0.011	5.5	L

[a]Data were expressed as the mean ($n = 4$–9)

[b]The Ke values were calculated from the following equation: $Ke = $ [antagonist]/(IC_{50} ratio–1); [antagonist]: concentration of the antagonist; IC_{50} ratio: IC_{50} without the antagonist over the IC_{50} with the antagonist. Each preparation was incubated with a selective antagonist for 20 min before the addition of a test compound

[c]Naloxone (30 nM) was used as a μ selective antagonist

[d]Undetectable

[e]NTI (10 nM) was used as a δ selective antagonist

[f]NTI (100 nM) was used

[g]nor-BNI (10 nM) was used as a κ selective antagonist

[h]nor-BNI (20 nM) was used

[i]Data were expressed as the mean ($n = 10$)

[j]Dose that inhibited 90% of the AAW behavior at 30 min after test compound administration (s.c.). AAW test was performed at time points of 60, 120, 180, and 240 min postadministration. S (Short): effect decreased within 120 min; L (Long): effect continued for 180 min or more

[k]Not determined

Reprinted from [28] with permission from Elsevier. Copyright (2008)

U-50,488H chemical structure proved to be unsuccessful. In the course of the lead optimization process, we found the two following tendencies: (1) compounds with a 6β-amido structure showed a low s.c./p.o. potency ratio and a long p.o. duration in the AAW test and (2) the aromatic ring structure in the C6-side chain was one of the most important components for optimizing the pharmacological profile, particularly for attenuating the psychotomimetic effect.

Finally, we found that the compound with a furanacrylamido side chain, β-**32s**, had the best properties. Thus, the pharmacological profile of compound β-**32s**, or TRK-820, was examined in detail. The agonist potency of β-**32s** was 6,000-fold and 1,800-fold stronger than that of morphine in the guinea pig ileum (GPI) and MVD preparations, respectively (Table [13]) [28]. Compared to U-50,488H, TRK-820 was approximately 140 times and 30 times more potent in the GPI and MVD assays, respectively.

We also evaluated TRK-820 for its antinociceptive effects in the AAW and tail flick (TF) tests in mice. TRK-820 showed high antinociceptive activity in both tests (Table [13]) [28], with ED_{50} values of 0.0033 mg/kg (AAW) and 0.062 mg/kg (TF). These activities were 85–175 times more potent than that of morphine and 80–350 times more potent than that of U-50,488H. This analgesic effect was antagonized by nor-BNI (κ antagonist) but not by NTI (δ antagonist) or by low-dose naloxone (μ antagonist). Furthermore, TRK-820 was notable for its low psychotomimetic effects. In contrast, morphine showed a significant preferential (addictive) effect

Table 12 SAR study on the variation of the side chain configuration and R^2 (structures shown in Fig. 16)

Compound	6-α or 6-β	MVD[a]				AAW, ED_{50} (mg/kg)[h]			
		IC_{50} (nM)	Ke (nM)[c]			s.c.	p.o.	p.o./s.c.	Duration[i]
			μ[d]	δ[f]	κ[g]				
32f	β	0.166	922	263	0.861	0.002	0.011	5.5	L
	α	0.12	16.5	0.43	4.90	0.0058	0.23	39.3	L
32g	β	17.0	17,000	1,113	1.37	0.46	17.99	39.1	ND[b]
	α	0.40	53.0	17.1	0.55	0.017	0.83	48.0	S
32h	β	ND[b]	–	–	–	0.18	ND[b]	–	ND[b]
32i	β	0.47	UD[e]	291	3.20	0.0046	0.034	7.4	ND[b]
32j	β	0.07	524	78.0	0.20	0.023	0.026	1.1	L
32k	β	0.75	60.9	96.4	1.60	0.0011	0.0048	4.4	L
32l	β	0.32	1,778	64.5	1.95	0.0049	0.064	9.7	L
32m	β	1.60	UD[e]	276	2.37	0.0019	0.0070	3.7	L
32n	β	0.23	185	89.0	1.40	0.017	0.220	12.9	ND[b]
32o	β	ND[b]	ND[b]	ND[b]	ND[b]	3.6	ND[b]	–	ND[b]
32p	β	0.10	UD[e]	89.6	0.28	0.0027	0.026	9.6	L
32q	β	0.10	UD[e]	UD[e]	1.71	0.0042	0.040	9.5	L
32r	β	0.55	UD[e]	UD[e]	0.20	0.0016	0.015	9.4	L
32s	α	0.049	31.9	245	0.91	0.0081	0.13	16.0	ND[b]
	β	0.42	14,000	41.6	0.16	0.0033	0.032	9.7	L

[a]Data were expressed as the mean ($n = 4$–9)

[b]Not determined

[c]The Ke values were calculated from the following equation: $Ke = $ [antagonist]/(IC_{50} ratio–1). [antagonist]: concentration of the antagonist; IC_{50} ratio:IC_{50} without the antagonist over IC_{50} with the antagonist. Each preparation was incubated with a selective antagonist for 20 min before the addition of a test compound

[d]Naloxone (30 nM) was used as a μ selective antagonist

[e]Undetectable

[f]NTI (10 nM) was used as a δ selective antagonist

[g]nor-BNI (10 nM) was used as a κ selective antagonist

[h]Data were expressed as the mean ($n = 10$)

[i]Dose that could inhibit 90% of the AAW behavior at 30 min after test compound administration (s.c.). AAW test was performed at time points of 60, 120, 180, and 240 min postadministration. S (Short): effect decreased within 120 min; L (Long): effect continued for 180 min or more

Reprinted from [28] with permission from Elsevier. Copyright (2008)

and U-50,488H appeared to induce an aversive (dysphoric) behavior in test animals. It was concluded that TRK-820 had a neutral effect (neither preferential nor aversive effect) on behavior and, thus, it was expected to cause less psychotomimetic side effects [25].

Next, we attempted to clarify which part of the TRK-820 structure was associated with its excellent pharmacological profile. The AAW test (s.c.) in mice was selected to evaluate structure–activity and structure–ADME relationships. Table 14 shows a summary of the results of a SAR study on compound TRK-820 derivatives (**34–42**).

Although the main factor that determined activity on the AAW test remains to be clarified, these data implied the importance of the followings: (1) the tyrosine components (17-nitrogen and the 3-hydroxy group) were indispensable for the

Table 13 Detailed comparison of compound TRK-820 (β-**32s**) with morphine and U-5,0488H

Compound	GPI				MVD						AAW (s.c.)	TF (s.c.)
	IC_{50}[a] (nM)	Ke (nM)[b]		μ/κ	IC_{50}[a] (nM)	Ke (nM)[b]			μ/κ	δ/κ	ED_{50} (mg/kg)[a]	ED_{50} (mg/kg)[a]
		κ	μ			κ	μ	δ				
β-**32s**	0.0081	0.070[c]	5.5[f]	78.6	0.080	0.049[c]	48[f]	NC[i]	980	–	0.0033	0.062
Morphine	49.3	20.5[d]	5.06[g]	0.25	145.1	53.5[d]	3.29[g]	7.35[h]	0.06	0.14	0.58	5.26
U-50,488H	1.12	0.031[c]	12.1[f]	390	2.35	0.031[e]	31.5[f]	41.2[h]	1016	1329	1.16	5.18

[a]Data were expressed as the mean (n = 5–7)

[b]The Ke values were calculated from the following equation: Ke = [antagonist]/(IC50 ratio–1). [antagonist]: concentration of the antagonist; IC$_{50}$ ratio: IC$_{50}$ without the antagonist over IC$_{50}$ with the antagonist. Each preparation was incubated with a selective antagonist for 20 min before the addition of a test compound

[c]nor-BNI (10 nM) was used as a κ selective antagonist

[d]nor-BNI (100 nM) was used as a κ selective antagonist

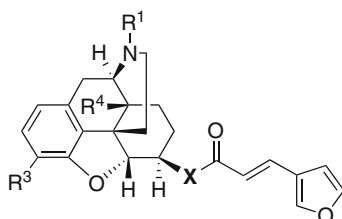[e]nor-BNI (1 nM) was used as a κ selective antagonist

[f]Naloxone (100 nM) was used as a μ selective antagonist

[g]Naloxone (20 nM) was used as a μ selective antagonist

[h]NTI (100 nM) was used as a δ selective antagonist

[i]Not calculated

Reprinted from [40] with permission from Elsevier. Copyright (2008)

Table 14 SAR study on compound TRK-820 derivatives

Compound	R^1	R^3	R^4	X	MVD[a]				AAW, ED_{50} (mg/kg)[h]
					IC_{50} (nM)	Ke (nM)[c]			
						μ[d]	δ[f]	κ[g]	
TRK-820	CPM	OH	OH	NMe	0.42	14,000	41.6	0.16	0.0033
34	Me	OH	OH	NMe	55	8.1	33	6.3	1.03
35	H	OH	OH	NMe	ND[b]	–	–	–	7.07
36	Phenethyl	OH	OH	NMe	ND[b]	–	–	–	1.03
37	CPM	H	OH	NMe	27.2	12.0	8.40	0.07	0.013
38	CPM	NH$_2$	OH	NMe	ND[b]	–	–	–	0.20
39	CPM	NHAc	OH	NMe	ND[b]	–	–	–	>10
40	CPM	OH	H	NMe	0.035	8.04	1.31	0.07	0.02
41	CPM	OH	OH	NH	0.87	UD[e]	8,100	0.44	0.95
42	CPM	OH	OH	S	ND[b]	–	–	–	>10

[a]Data were expressed as the mean ($n = 10$)

[b]Not determined

[c]The Ke values were calculated with the following equation: Ke = [antagonist]/(IC_{50} ratio–1). [antagonist]: concentration of the antagonist; IC_{50} ratio: IC_{50} without the antagonist over IC_{50} with the antagonist. Each preparation was incubated with a selective antagonist for 20 min before the addition of a test compound

[d]Naloxone (30 nM) was used as a μ selective antagonist

[e]Undetectable

[f]NTI (10 nM) was used as a δ selective antagonist

[g]nor-BNI (10 nM) was used as a κ selective antagonist

[h]Data were expressed as the mean ($n = 4$–9)

Reprinted from [28] with permission from Elsevier. Copyright (2008)

in vivo activity of TRK-820 and (2) the 17-cyclopropylmethyl, 14-hydroxy, and *N*-methyl substituents were also important for its agonist activity.

3.3 Clinical Development of TRK-820 in Postoperative Surgery

TRK-820 was first developed as an analgesic for postoperative pain. However, in a Phase II clinical trial, it was concluded that, although the analgesic effect could be sufficiently potent, the safety margin was found to be insufficient. During that study, a physician suggested that patients who received a μ opioid receptor

agonist, like morphine often complained of an intolerable itch; in contrast, patients who were treated with TRK-820 rarely complained of itching. In addition to this pharmacological observation, μ opioid agonists and κ opioid agonists often showed contrary effects; for example, a preference for an aversive stimulus or hyperactivity in response to sedation. These findings led us to estimate the antipruritic effect of TRK-820. After confirming a significant antipruritic effect of TRK-820 in various animal itching models established by Kuraishi *et al.* [51–58], we initiated another clinical development study with the intent to develop an antipruritic agent.

3.4 Clinical Development of TRK-820 as an Antipruritic Agent

3.4.1 Antipruritic Activity of TRK-820 in an Animal Model

Epidural or intrathecal (i.t.) administration of morphine produced an itching sensation in humans [59, 60]. It has been reported that intradermal (i.d.) injections of histamine or substance P and intracisternal (i.c.) injections of morphine induced scratching in mice [61–63]. Scratching behavior in mice is considered to represent the itching sensation observed in humans. The administration of TRK-820 (p.o.) inhibited the scratching behavior in mice induced by histamine (i.d.), with an ED_{50} of 7.3 μg/kg (Fig. 17a) [51, 54, 57]. Moreover, TRK-820 (p.o.) inhibited substance P (i.d.) induced scratching behavior in mice (ED_{50} = 19.6 μg/kg, p.o.), which was resistant to treatment with antihistamine drugs (chlorpheniramine and ketotifen) (Fig. 17b) [51, 54, 57]. The antipruritic effect of TRK-820 was antagonized by nor-BNI (Fig. 18) [51, 54]. Based on these studies, TRK-820 was expected to be a more effective antipruritic than antihistamines. Furthermore, TRK-820 inhibited morphine (i.c.) induced scratching behavior in mice, but ketotifen did not [52, 54, 57]. This indicated that TRK-820 might also have an antipruritic effect on antihistamine-resistant pruritus of CNS origin. In addition, scratching behavior in monkeys induced by morphine (i.v. or i.t. injections) could be attenuated by i.v. or intramuscular injections of TRK-820 [53, 58]. TRK-820 was also reported to exhibit antipruritic effects on scratching induced by compound 48/40 [56] or chloroquine [55], and itching observed in disease models for autoimmune disease [64] or cholestasis induced by chronic ethynylestradiol injections [65].

3.4.2 Clinical Effectiveness on Uremic Pruritus

Patients on hemodialysis often complain of an intractable pruritus (uremic pruritus). Indeed, the consequent sleep disorder can impair the quality of life. Clinical and preclinical data suggested that the μ opioid system induced itching, but not the κ system. The antipruritic efficacy of nalfurafine hydrochloride (general name of TRK-820) was demonstrated for patients on hemodialysis in two multicenter, randomized, double-blind, placebo-controlled, clinical studies in Europe [66].
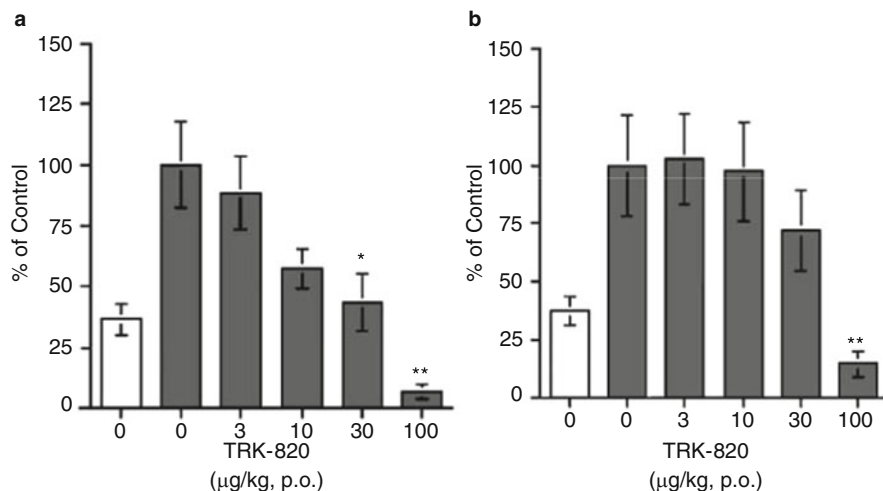
Fig. 17 Effects of TRK-820 on the scratching behavior in mice induced by histamine (**a**) or substance P (**b**). Mice (ICR strain) were given a p.o. administration of vehicle (*open bars*) or TRK-820 (*filled bars*). Then, 30 min later, phosphate-buffered saline, pH 7.4 (PBS), histamine (**a**), or substance P (**b**) was i.d.-injected. Immediately after the injection of PBS, histamine, or substance P, the number of scratching events was recorded and counted over a 30-min period. The numbers of scratching events observed with histamine or substance P injections in the absence of TRK-820 were considered 100% on the vertical axes. Each value represents the mean $\pm$ standard error of the mean (S.E.M.) ($n = 8$). **$P < 0.01$ compared between the PBS and histamine- or substance P-injected groups (Dunnett's test). Reprinted from [51] with permission from Elsevier. Copyright (2002)

Recently, Kumagai and colleagues also published results that clearly showed that nalfurafine hydrochloride was an effective treatment for itching in humans [67, 68]. The effects of the drug on severe itching in patients on hemodialysis was evaluated in a Phase III, randomized, double-blind, placebo-controlled study in Japan. In that study, the efficacy and safety of nalfurafine hydrochloride were prospectively investigated in 337 patients on hemodialysis with itching that was resistant to currently available treatments, *e.g.*, antihistamines. They randomly (1:1:1) administered 5 µg (high dose) or 2.5 µg (low dose) of the drug or a placebo orally for 14 days in a double-blind study design. The primary endpoint was the mean decrease in the visual analog scale (VAS)[2] from baseline. Decreases in the VAS were significantly larger in both the high dose ($n = 114$) and the low dose ($n = 112$) groups compared to the placebo group ($n = 111$, $P = 0.0002$ and $P = 0.0001$, respectively; one-sided test at 2.5% significance level; Fig. 19). The incidence of adverse drug reactions (ADRs) was 35.1%, 25.0%, and 16.2% in the

---

[2] The VAS test consisted of a 100-mm horizontal line without scale markings. The patients were asked to mark the intensity of itching on the scale, where the right end of the line (100 mm) indicated the strongest possible itching and the left end (0 mm) indicated no itching. The VAS has been widely accepted as a quantitative index of subjective sensations like pain and itching.
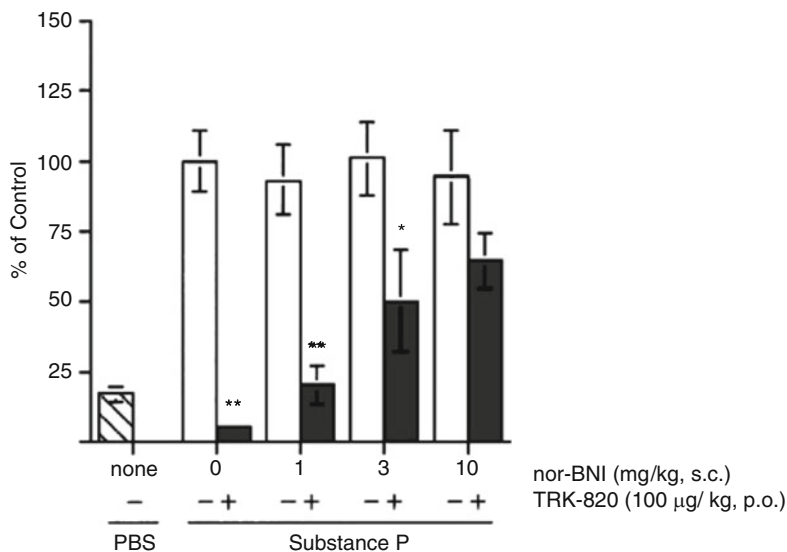
Fig. 18 Effect of nor-BNI on the antipruritic effect of TRK-820. Mice (ICR strain) were given an s.c. injection of nor-BNI or PBS (*hatched bar*). The next day, mice were given a p.o. administration of 100 μg/kg of TRK-820 (*filled bars*) or vehicle (*open bars*), and 30 min later, either PBS (*hatched bar*) or substance P was i.d. injected. Immediately after the latter, the number of scratching events was recorded and counted over a 30-min period. The number of scratching events recorded with substance P in the absence of nor-BNI and TRK-820 was considered to be 100% on the vertical axis. Each value represents the mean ± S.E.M. ($n = 8$). *$P < 0.05$, **$P < 0.01$ when compared with the corresponding vehicle-injected group (unpaired t-test). Reprinted from [51] with permission from Elsevier. Copyright (2002)
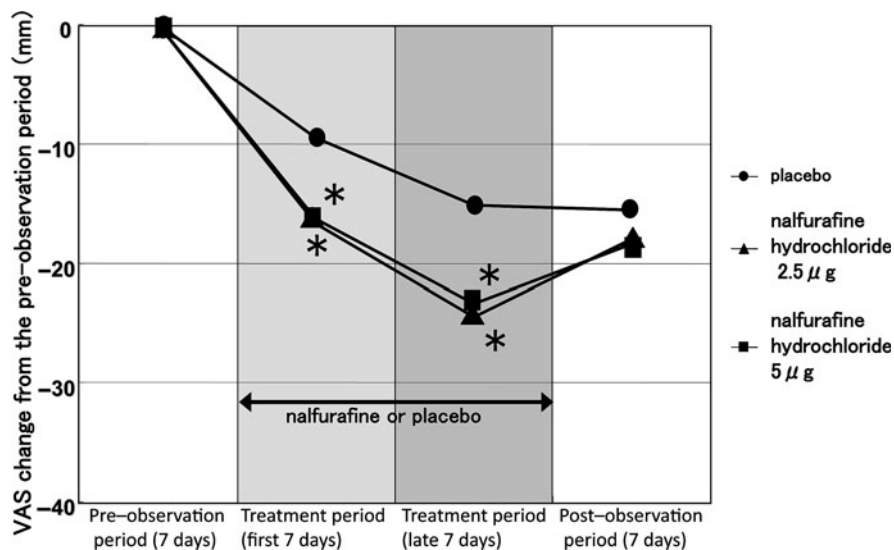
Fig. 19 Changes in VAS values from the preobservation period. All symbols show the mean values of VAS changes. *$P < 0.025$ compared with the placebo group, one-sided ANCOVA

high dose, low dose, and placebo groups, respectively. Mild to moderate ADRs were observed in 10 of the 226 patients, and the most common was insomnia (sleep disturbance), observed in 24 of the 226 patients. However, because all the ADRs were transient and readily resolved, nalfurafine hydrochloride could be considered a safe agent. This Phase III study clearly showed that oral nalfurafine hydrochloride effectively reduced uremic pruritus with few significant ADRs.

After the Phase III study, a 1-year open-label study showed that nalfurafine hydrochloride (5 μg, p.o.) provided antipruritic effects for 211 patients on hemodialysis with itching that was resistant to currently available treatments. These results suggested that tolerance to the antipruritic effect of the agent was not observed, at least after 1 year of treatment. It is noteworthy that nalfurafine hydrochloride exhibited neither physical nor psychological dependency [68].

This novel drug was officially approved for clinical use in January 2009 by the Ministry of Health, Labour, and Welfare of Japan. This is the first pharmaceutical success ever achieved for a selective opioid κ agonist. All the other compounds derived from modifications of U-50,488H have been withdrawn or halted in early clinical phase development. Furthermore, nalfurafine hydrochloride is recognized as the first nonnarcotic opioid drug in history.

3.5   Concluding Remarks

The development of opioid drugs has been considered a high-risk endeavor. Indeed, it was expected to be particularly tough because the goal was to discover an opioid drug without addictive properties. Because opioids have potent analgesic, antitussive, antipruritic, and antiurinary incontinence effects, much more research is expected to be undertaken in order to produce many ideal drugs. The success of TRK-820 will contribute to the initiation of new and creative studies for discovering clinically applicable opioid compounds.

References

1. Gates M, Tschudi G (1952) J Am Chem Soc 74:1109
2. Casy AF, Parfitt RT (1986) Opioid analgesics, chemistry and receptors. Plenum, New York
3. Martin WR, Eades CG, Thompson JA, Huppler RE, Gilbert PE (1976) J Pharmacol Exp Ther 197:517
4. Takemori AE, Larson DL, Portoghese PS (1981) Eur J Pharmacol 70:445
5. DeLander GE, Portoghese PS, Takemori AE (1984) J Pharmacol Exp Ther 231:91
6. Sakami S, Kawai K, Maeda M, Aoki T, Fujii H, Ohno H, Ito T, Saitoh A, Nakao K, Izumimoto N, Matsuura H, Endo T, Ueno S, Natsume K, Nagase H (2008) Bioorg Med Chem 16:7956
7. Nagase H, Hayakawa J, Kawamura K, Kawai K, Takezawa Y, Matsuura H, Tajima C, Endo T (1988) Chem Pharm Bull 46:366

8. Turgeon J, Gröning R, Sathyan G, Thipphawong J, Richarz U (2010) Expert Opin Drug Deliv 7:137
9. Matsumoto AK (2007) Expert Opin Pharmacother 8:1515
10. Nelson L, Schwaner R (2009) J Med Toxicol 5:230
11. Vadivelu N, Hines RL (2008) Clin Interv Aging 3:421
12. Stauffer J, Setnik B, Sokolowska M, Romach M, Johnson F, Sellers E (2009) Clin Drug Investig 29:777
13. Diego L, Atayee R, Helmons P, von Gunten CF (2009) Expert Rev Gastroenterol Hepatol 3:473
14. Bream-Rouwenhorst HR, Cantrell MA (2009) Am J Health Syst Pharm 66:1267
15. Calderon SN, Coop A (2004) Curr Pharm Des 10:733
16. Gengo PJ, Pettit HO, O'Neill SJ, Wei K, McNutt R, Bishop MJ, Chang KJ (2003) J Pharmacol Exp Ther 307:1221
17. Le Bourdonnec B, Windh RT, Ajello CW, Leister LK, Gu M, Chu GH, Tuthill PA, Barker WM, Koblish M, Wiant DD, Graczyk TM, Belanger S, Cassel JA, Feschenko MS, Brogdon BL, Smith SA, Christ DD, Derelanko MJ, Kutz S, Little PJ, DeHaven RN, DeHaven-Hudkins DL, Dolle RE (2008) J Med Chem 51:5893
18. Le Bourdonnec B, Windh RT, Leister LK, Zhou QJ, Ajello CW, Gu M, Chu GH, Tuthill PA, Barker WM, Koblish M, Wiant DD, Graczyk TM, Belanger S, Cassel JA, Feschenko MS, Brogdon BL, Smith SA, Derelanko MJ, Kutz S, Little PJ, DeHaven RN, DeHaven-Hudkins DL, Dolle RE (2009) J Med Chem 52:5685
19. Katsura Y, Zhang X, Homma K, Rice KC, Calderon SN, Rothman RB, Yamamura HI, Davis P, Flippen-Anderson JL, Xu H, Becketts K, Foltz EJ, Porreca F (1997) J Med Chem 40:2936
20. Nagase H, Kawai K, Hayakawa J, Wakita H, Mizusuna A, Matsuura H, Tajima C, Takezawa Y, Endoh T (1998) Chem Pharm Bull 46:1695
21. Nagase H, Yajima Y, Fujii H, Kawamura K, Narita M, Kamei J, Suzuki T (2001) Life Sci 68:2227
22. Portoghese PS, Takemori AE (1994) USP 5,352,680
23. Suzuki T, Tsuji M, Mori T, Misawa M, Nagase H (1995) Life Sci 57:PL247
24. Suzuki T, Tsuji M, Mori T, Misawa M, Nagase H (1997) Pharmacol Biochem Behav 57:293
25. Arakawa K, Akami T, Okamoto M, Akioka K, Nakai I, Oka T, Nagase H (1993) Transplant Proc 25(1 Pt 1):738
26. Gavériaux-Ruff C, Filliol D, Simonin F, Matthes HW, Kieffer BL (2001) J Pharmacol Exp Ther 298:1193
27. Piercey MF, Lahti RA, Schroeder LA, Einspahr FJ, Barsuhn C (1982) Life Sci 31:1197
28. Kawai K, Hayakawa J, Miyamoto T, Imamura Y, Yamane S, Wakita H, Fujii H, Kawamura K, Matsuura H, Izumimoto N, Kobayashi R, Endo T, Nagase H (2008) Bioorg Med Chem 16:9188
29. Costello GF, Main BG, Barlow JJ, Carroll JA, Shaw JS (1988) Eur J Pharmacol 151:475
30. Halfpenny PR, Horwell DC, Hughes J, Hunter JC, Rees DC (1990) J Med Chem 33:286
31. Chang KF, Chang AB (2002) Pulm Pharmacol Ther 15:335
32. Bolser DC (2006) Respir Physiol Neurobiol 152:349
33. Kamei J, Tanihara H, Kasuya Y (1990) Eur J Pharmacol 187:281
34. Kamei J, Tanihara H, Kasuya Y (1991) Eur J Pharmacol 203:153
35. Kamei J, Tanihara H, Kasuya Y (1992) Chem Pathol Pharmacol 76:375
36. Kamei J, Iwamoto Y, Suzuki T, Misawa M, Nagase H, Kasuya Y (1993) Eur J Pharmacol 249:161
37. Hitchcock SA, Pennington LD (2006) J Med Chem 49:7559
38. Kerns E, Di L (2008) Drug-like properties: concepts, structure design and methods from ADME to toxicity optimization. Academic, London
39. Sakami S, Maeda M, Kawai K, Aoki T, Kawamura K, Fujii H, Hasebe K, Nakajima M, Endo T, Ueno S, Ito T, Kamei J, Nagase H (2008) J Med Chem 51:4404
40. Nagase H, Kawai K, Kawamura K, Hayakawa J, Endo T (1993) WO 93/15081

41. Portoghese PS, Lipkowski AW, Takemori AE (1987) J Med Chem 30:238
42. Portoghese PS, Sultana M, Nagase H, Takemori AE (1988) J Med Chem 31:281
43. Nogrady T (1985) Medicinal chemistry, a biochemical approach. Oxford University Press, New York
44. Portoghese PS, Nagase H, Takemori AE (1988) J Med Chem 31:1344
45. Lin CE, Takemori AE, Portoghese PS (1993) J Med Chem 36:2412
46. Shook JE, Pelton JT, Wire WS, Hirning LD, Hruby VJ, Burks TF (1987) J Pharmacol Exp Ther 240:772
47. Endo T, Matsuura H, Tajima A, Izumimoto N, Tajima C, Suzuki T, Saitoh A, Suzuki T, Narita M, Tseng L, Nagase H (1999) Life Sci 65:1685
48. Kanematsu K (1998) Yakugaku Zasshi 118:1
49. Katsumata S, Ienaga Y, Minami M, Nakagawa T, Kanematsu K, Satoh M (1996) Eur J Pharmacol 312:349
50. Hosoki R, Niizawa S, Koike K, Sagara T, Kanematsu K, Takayanagi I (1996) Arch Int Pharmacodyn Ther 331:136
51. Togashi Y, Umeuchi H, Okano K, Ando N, Yoshizawa Y, Honda T, Kawamura K, Endoh T, Utsumi J, Kamei J, Tanaka T, Nagase H (2002) Eur J Pharmacol 435:259
52. Umeuchi H, Togashi Y, Honda T, Nakao K, Okano K, Tanaka T, Nagase H (2003) Eur J Pharmacol 477:29
53. Wakasa Y, Fujiwara A, Umeuchi H, Endoh T, Okano K, Tanaka T, Nagase H (2004) Life Sci 75:2947
54. Utsumi J, Togashi Y, Umeuchi H, Okano K, Tanaka T, Nagase H (2004) In: Yosipovitch G, Greaves MW, Fleischer AB Jr, McGlone F (eds) Itch. Basic mechanisms and therapy. Marcel Dekker, New York, p 107
55. Inan S, Cowan A (2004) Eur J Pharmacol 502:233
56. Wang Y, Tang K, Inan S, Siebert D, Holzgrabe U, Lee DYW, Huang P, Li J-G, Cowan A, Liu-Chen L-Y (2005) J Pharmacol Exp Ther 312:220
57. Nakao K, Mochizuki H (2009) Drugs Today 45:323
58. Ko MC, Husbands SM (2009) J Pharmacol Exp Ther 328:193
59. Cousins MJ, Mather LE (1984) Anesthesiology 61:276
60. Ballantyne JC, Loach AB, Carr DB (1988) Pain 33:149
61. Kuraishi Y, Nagasawa T, Hayashi K, Satoh M (1995) Eur J Pharmacol 275:229
62. Andoh T, Nagasawa T, Satoh M, Kuraishi Y (1998) J Pharmacol Exp Ther 286:1140
63. Tohda C, Yamaguchi T, Kuraishi Y (1997) Jpn J Pharmacol 74:77
64. Umeuchi H, Kawashima Y, Aoki CA, Kurokawa T, Nakao K, Itoh M, Kikuchi K, Kato T, Okano K, Gershwin ME, Miyakawa H (2005) Eur J Pharmacol 518:133
65. Inan S, Cowan A (2006) Pharmacol Biochem Behav 85:39
66. Wikström B, Gellert R, Ladefoged SD, Danda Y, Akai M, Ide K, Ogasawara M, Kawashima Y, Ueno K, Mori A, Ueno Y (2005) J Am Soc Nephrol 16:3742
67. Kumagai H, Ebata T, Takamori K, Muramatsu T, Nakamoto H, Suzuki H (2009) Nephrol Dial Transplant (in press). doi:10.1093/ndt/gfp588
68. Kumagai H, Ebata T, Suzuki H, Takamori K (2008) 10th Souyaku vision symposium, Tokyo, 18–19 Dec 2008, The Pharmaceutical Society of Japan, p 24

Synthesis of 14-Alkoxymorphinan Derivatives and Their Pharmacological Actions

Helmut Schmidhammer and Mariana Spetea

Abstract Among opioids, morphinans play an important role as therapeutically valuable drugs. They include pain relieving agents such as naturally occurring alkaloids (e.g. morphine, codeine), semisynthetic derivatives (e.g. oxycodone, oxymorphone, buprenorphine), and synthetic analogs (e.g. levorphanol). Currently used opioid analgesics also share a number of severe side effects, limiting their clinical usefulness. The antagonist morphinans, naloxone and naltrexone are used to treat opioid overdose, opioid dependence, and alcoholism. All these opioid drugs produce their biological actions through three receptor types, μ, δ, and κ, belonging to the G-protein-coupled receptor family. Considerable effort has been put forward to understand the appropriate use of opioid analgesics, while medicinal chemistry and opioid pharmacology have been continuously engaged in the search for safer, more efficacious and nonaddicting opioid compounds, with the final goal to reduce complications and to improve patient compliance. Toward this goal, recent advances in chemistry, ligand-based structure activity relationships and pharmacology of 14-alkoxymorphinans are reviewed in this chapter. Current developments of different structural patterns of 14-alkoxymorphinans as research tools and their potential therapeutic opportunities are also summarized.

Keywords 14-Alkoxymorphinans · Opioid agonist · Opioid antagonist · Opioid receptors · Opioids

H. Schmidhammer (✉) and M. Spetea
Department of Pharmaceutical Chemistry, Institute of Pharmacy and Center for Molecular Biosciences Innsbruck (CMBI), University of Innsbruck, Innrain 52a, 6020 Innsbruck, Austria
e-mail: Helmut.Schmidhammer@uibk.ac.at

Contents

Abbreviations

$[^{35}S]GTP\gamma S$	Guanosine-5′-O-(3-$[^{35}S]$thio)-triphosphate
AD_{50}	Analgesic dose necessary to elicit a 50% effect
BBB	Blood–brain barrier
CBE	Colonic bead expulsion test
CHO	Chinese hamster ovary
CNS	Central nervous system
DMF	*N,N*-dimethylformamide
ED_{50}	Effective dose necessary to elicit a 50% effect
GPI	Guinea pig ileum bioassay
HP	Hot-plate test
IC_{50}	Concentration necessary to produce a 50% effect
IL-2	Interleukin-2
K_i	Inhibition constant
MeOH	Methanol
MLR	Mixed lymphocyte reaction
MVD	Mouse vas deferens bioassay
NaH	Sodium hydride
NTB	Naltriben
NTI	Naltrindole
PBMC	Peripheral blood mononuclear cells
PPOM	14-Phenylpropoxymetopon
PPQ	Paraphenylquinone writhing test
RVD	Rat vas deferens bioassay
SAR	Structure–activity relationship
s.c.	Subcutaneous
TF	Tail-flick test
TosMIC	Tosylmethylisocyanid

1   Introduction

Although the pain relieving and mood altering effects of extracts of the opium poppy *Papaver Somniferum* have been known for thousands of years, it was only in the twentieth century that there were substantial advances made in understanding the pharmacology of the active constituents of opium, like morphine [1]. Exciting discoveries such as the identification of the endogenous opioid peptides (enkephalins, endorphins, and dynorphins), the existence of specific opioid receptors and cloning of three opioid receptors (μ, δ, and κ) as members of the G-protein coupled receptor (GPCR) family markedly influenced the course of opioid research over the years [2]. Gene cloning and characterization was an important step to evolve the comprehension of opioid receptors, as proteins that operate in the central and peripheral nervous systems (CNS and PNS), and peripheral tissues [3–6] and control nociceptive, hedonic, emotional, autonomic, neuroendocrine, and immune responses [7, 8]. The driving force behind the many years of synthetical efforts in the opioid field has been the search for an alternative to morphine, which would produce powerful analgesia and would be free of undesirable side effects. All the gained knowledge led to viable strategies in exploring the pharmacotherapeutic potential of the opioid system through the discovery of opioid drugs with alternative therapeutic properties. A diversity of opioid ligands was made available through chemical syntheses, which are appraised as valuable research tools or potential therapeutic agents. Such developments resulted in many pharmacologically interesting and clinically useful opioid compounds possessing different degrees of selectivity for each opioid receptor type, agonist or antagonist activity, and central or peripheral site of action [9–19].

Among opioids, morphinans (Fig. 1) play an important role as therapeutically valuable drugs. Representative examples of the morphinan class of compounds (Fig. 2) are μ-opioid analgesic agents for the treatment of moderate-to-severe pain such as naturally occurring alkaloids (e.g. morphine, codeine), semisynthetic derivatives (e.g. oxycodone, oxymorphone, buprenorphine), and synthetic analogs (e.g. levorphanol, butorphanol) [19–21]. Codeine is also an effective antitussive drug. The oxymorphone derivatives naloxone [22] and naltrexone [23] represent
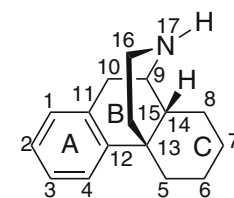
(-)-Morphinan

Morphinans: B/C ring fusion *cis*
Isomorphinans: B/C ring fusion *trans*
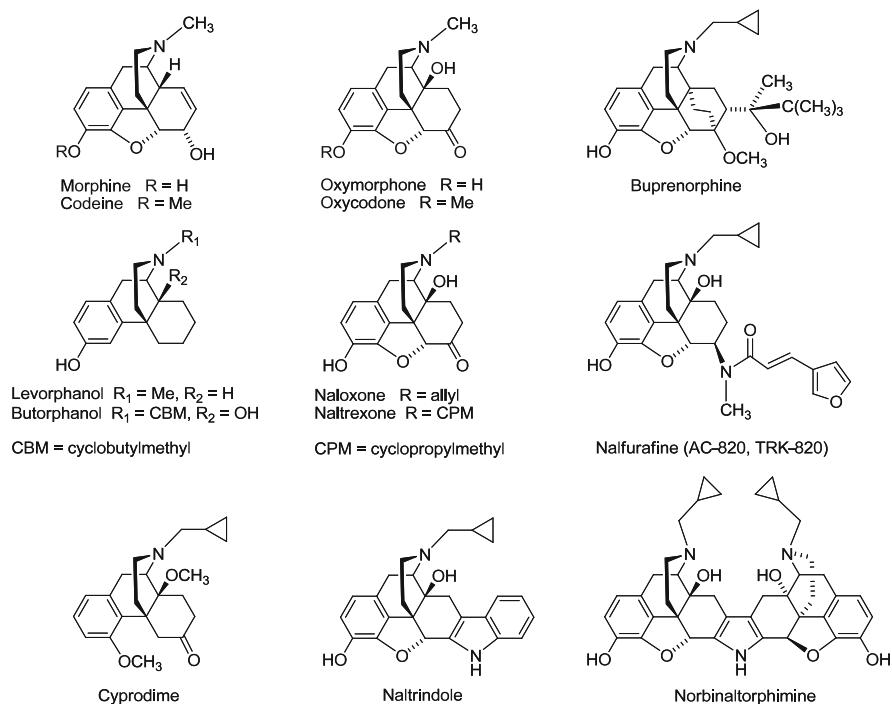
Fig. 1 Morphinan

Fig. 2 Examples of opioid morphinans

two opioid antagonists commonly used as rescue medication to reverse severe side effects (respiratory depression, overdose) induced by opioid agonists [18, 19]. They are also used clinically to treat dependence induced by opioid use and alcoholism [18, 19, 24, 25]. The quaternary derivative of naltrexone, methylnaltrexone [26], was recently introduced for clinical use in the therapy of opioid-induced bowel dysfunction [27]. The κ-opioid receptor agonist nalfurafine (AC-820, TRK-820) [28] (Fig. 2) showed efficacy as an antipruritic agent in uremic pruritus patients [29]. Other potential therapeutic indications of opioid morphinans include addiction, depression, feeding behavior, and Parkinson-induced tardive dyskinesia [12, 16, 18, 30–32]. Also, important research tools to investigate opioid receptor multiplicity and function *in vitro* and *in vivo* have come from the development of morphinans, including opioid antagonists cyprodime (μ) [33], naltrindole (δ) [34], and norbinaltorphimine (κ) [35] (Fig. 2).

During the past decade, 14-alkoxymorphinans have emerged as highly interesting and promising substitution patterns to improve potency and selectivity towards single opioid receptor types affording opioid ligands that besides their scientific value as pharmacological tools, may also have the potential of emerging as novel therapeutic agents. This chapter will cover 14-alkoxymorphinan derivatives including recent chemical developments, pharmacology and ligand-based structure–activity relationships (SAR), with a focus on a number of key findings and selected studies.

2 Synthesis

2.1 Synthesis of 14-Alkoxymorphinan-6-ones

2.1.1 Introduction of a 14-Alkoxy Group

Introduction of a 14-Alkoxy Group into 7,8-Didehydromorphinans

Introduction of a 14-alkoxy group into morphinans was first accomplished by methanolysis of 14-bromocodeinone dimethyl acetale (**1**) to yield 14-methoxycodeinone (**2**) (Scheme 1) [36]. An improved synthesis of 14-methoxycodeinone (**2**) was performed by 14-*O*-methylation of 14-hydroxycodeinone (**3**) using either methyliodide [37] or dimethyl sulfate [38] as the alkylating agent in DMF in the presence of NaH (Scheme 2). 14-Ethoxycodeinone (**4**) was synthesized similarly by alkylation of **2** with diethyl sulfate [38]. Catalytic hydrogenation of **2** and **4** gave the dihydrocodeinones **5** and **6** [38]. Analogously compounds **10** and **11** have been prepared from 7,8-didehydromorphinan **7** via **8** and **9** (using methyliodide or ethyliodide and NaH) (Scheme 3) [39, 40].

Introduction of a 14-Alkoxy Group into Morphinan-6-ones Without
7,8 Double Bond

14-*O*-Alkylation can also be achieved using oxymorphone-derived morphinan-6-ones without a 7,8 double bond employing dimethyl or diethyl sulfate under
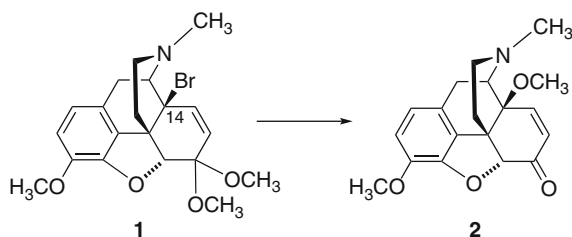
Scheme 1

Scheme 2

Scheme 3

CH$_3$

OH

14

H$_3$CO

7

CH$_3$

OR

H$_3$CO

8 R = Me
9 R = Et

CH$_3$

OR

H$_3$CO

10 R = Me
11 R = Et

Scheme 4

CH$_3$

OH

14

R O O

12 R = H
13 R = OCH$_2$Ph

CH$_3$

OR$_2$

R$_1$ O OR$_2$

14 R$_1$ = H, R$_2$ = Me
15 R$_1$ = OCH$_2$Ph, R$_2$ = Me
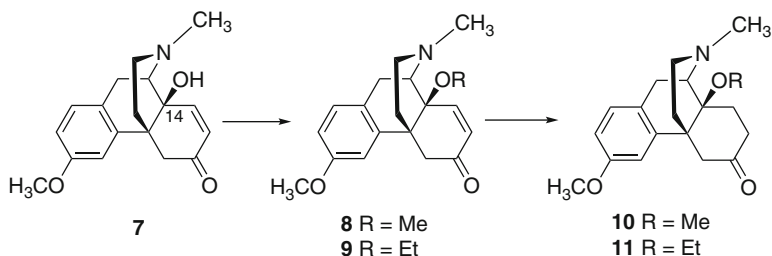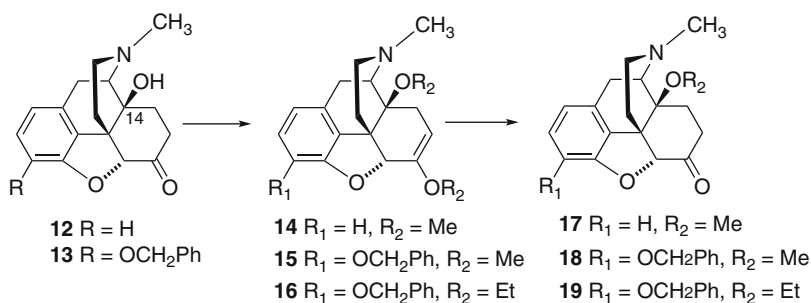**16** R$_1$ = OCH$_2$Ph, R$_2$ = Et

CH$_3$

OR$_2$

R$_1$ O O

17 R$_1$ = H, R$_2$ = Me
18 R$_1$ = OCH$_2$Ph, R$_2$ = Me
19 R$_1$ = OCH$_2$Ph, R$_2$ = Et
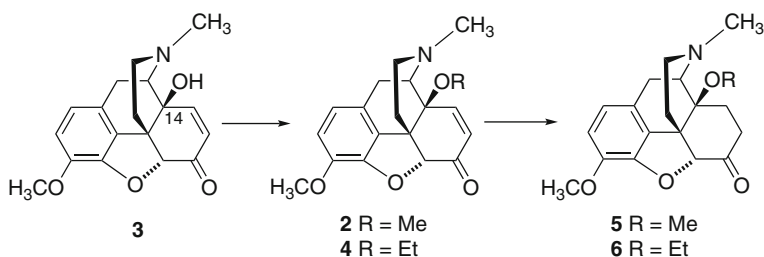
similar conditions as described above. Thus, 3-deoxygenated oxymorphone (**12**) and the 3-*O*-benzyl-substituted oxymorphone derivative **13** yielded 14-alkoxy-substituted enol ethers **14–16**, which were hydrolyzed under mild acidic conditions to give ketones **17–19** (Scheme 4) [41, 42].

Introduction of a 14-Alkoxy Group Using Allylic Halides

Because of the low reactivity of the tertiary alcohol, alkylation of the C14-hydroxyl with alkyl halides such as propyl or isoamyl halides was unsuccessful [Schmidhammer H, unpublished observations]. Therefore, allylic halides were employed to introduce 14-*O*-alkenyl substituents using similar conditions as described above [43–46]. Catalytic hydrogenation afforded the corresponding 14-*O*-alkyl derivatives [43–45]. Thus, 14-hydroxy-5-methylcodeinone (**20**) was treated with 3,3-dimethylallyl bromide in DMF in the presence of NaH to give compound **21**, which underwent catalytic hydrogenation to yield 14-*O*-isoamyl-substituted morphinan **24** (Scheme 5) [43]. Similarly 14-phenylpropoxymorphinans **25** and **26** were prepared from 14-hydroxycodeinone (**3**) and **21**, respectively, via intermediates **22** and **23**, which were obtained by alkenylation using cinnamyl bromide (Scheme 5) [44, 45].

20 R = Me
3 R = H

21 R$_1$ = CH$_2$CH=C(CH$_3$)$_2$, R$_2$ = Me
22 R$_1$ = CH$_2$CH=CHPh, R$_2$ = H
23 R$_1$ = CH$_2$CH=CHPh, R$_2$ = Me

24 R$_1$ = (CH$_2$)$_2$CH(CH3)$_2$, R$_2$ = Me
25 R$_1$ = (CH$_2$)$_3$Ph, R$_2$ = H
26 R$_1$ = (CH$_2$)$_3$Ph, R$_2$ = Me

Scheme 5

3 R$_1$ = H, R$_2$ = Me
27 R$_1$ = Me, R$_2$ = H

28 R$_1$ = CH$_2$Ph, R$_2$ = H, R$_3$ = Me
29 R$_1$ = R$_3$ = CH$_2$Ph, R$_2$ = Me

30 R$_1$ = CH$_2$Ph , R$_2$ = H, R$_3$ = Me
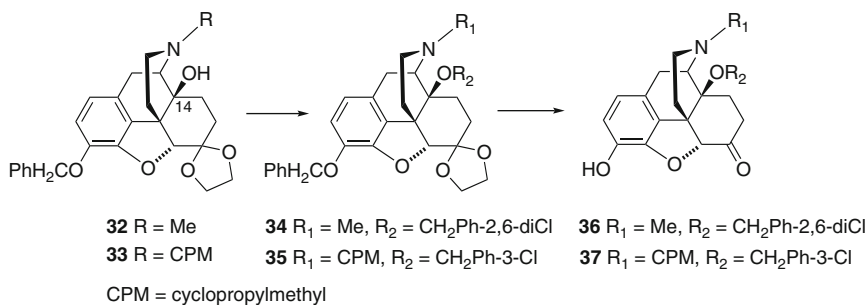**31** R$_1$ = CH$_2$Ph, R$_2$ = Me, R$_3$ = H
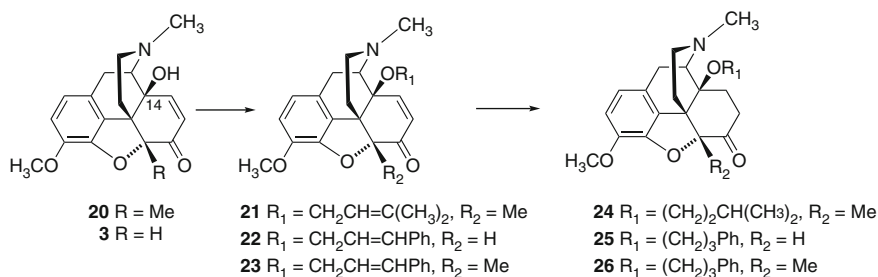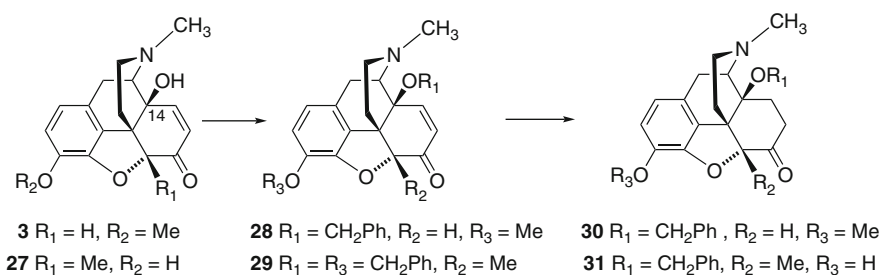
Scheme 6

Introduction of 14-Arylmethoxy Substituents into 7,8-Didehydromorphinans

Introduction of 14-arylmethoxy substituents can be achieved starting from 14-hydroxycodeinones (e.g. **3**) or 14-hydroxymorphinones (e.g. **27**) using aryl-methyl bromides (e.g. benzyl bromide) in DMF in the presence of NaH to yield compounds **28** and **29**, respectively (Scheme 6). Catalytic hydrogenation leads to the desired *N*-methylmorphinan-6-ones **30** and **31**, respectively [47].

Introduction of 14-Benzyloxy Substituents into Morphinan-6-ones Without 7,8 Double Bond

14-*O*-Benzylation can also be achieved using oxymorphone and derivatives thereof (e.g. naltrexone). Since 14-*O*-alkylation of morphinan-6-ones without 7,8 double bond does not proceed as smoothly when other alkylating reagents than dimethyl or diethyl sulfate (see above) are used, the 6-keto function was protected by ketaliza-tion [47, 48]. For instance, 3-*O*-benzyl-protected ketals **32** and **33** were 14-*O*-alkylated with different benzyl bromides in DMF in the presence of NaH to afford compounds **34** and **35**, respectively. Removal of the protecting groups

32 R = Me
33 R = CPM

34 R$_1$ = Me, R$_2$ = CH$_2$Ph-2,6-diCl
35 R$_1$ = CPM, R$_2$ = CH$_2$Ph-3-Cl

36 R$_1$ = Me, R$_2$ = CH$_2$Ph-2,6-diCl
37 R$_1$ = CPM, R$_2$ = CH$_2$Ph-3-Cl

CPM = cyclopropylmethyl

Scheme 7

R$_1$ = Me, allyl, CPM, CBM etc.
R$_2$ = Me, Et, Pr, benzyl etc.
R$_3$ = H, Me

CPM = cyclopropylmethyl
CBM = cyclobutylmethyl

Indolomorphinans: X = NH
Benzofuromorphinans: X = O
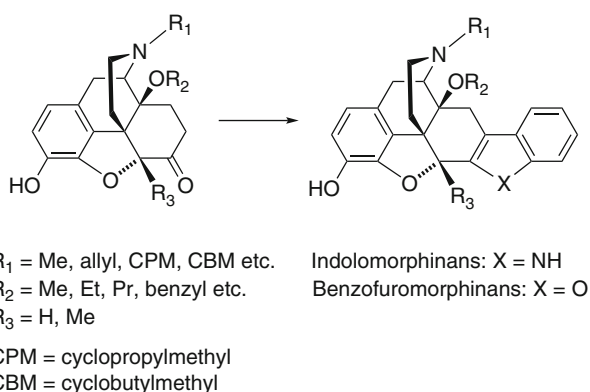
Scheme 8

was accomplished with methanol/HCl to give ketones **36** and **37**, respectively (Scheme 7) [47, 48].

2.2 Synthesis of 14-Alkoxy-Substituted Indolo- and Benzofuromorphinans

2.2.1 Synthesis from 14-Alkoxymorphinan-6-ones

Indolomorphinans can be prepared from their 6-ketomorphinan precursors via Fischer indole synthesis with phenylhydrazine hydrochloride in glacial acetic acid [43, 49, 50], while benzofuromorphinans can be synthesized from the corresponding 6-ketomorphinans using *O*-phenylhydroxylamine hydrochloride and methanesulfonic acid in MeOH (Scheme 8) [43].

NTB: R = H, X = O
NTI: R = H, X = NH
38 R = CH₂OMe, X = O
39 R = CH₂OMe, X = NCH₂OMe

Series A: X = O
Series B: X = NCH₂OMe

Series C: X = O
Series D: X = NH

R = alkyl, arylalkyl
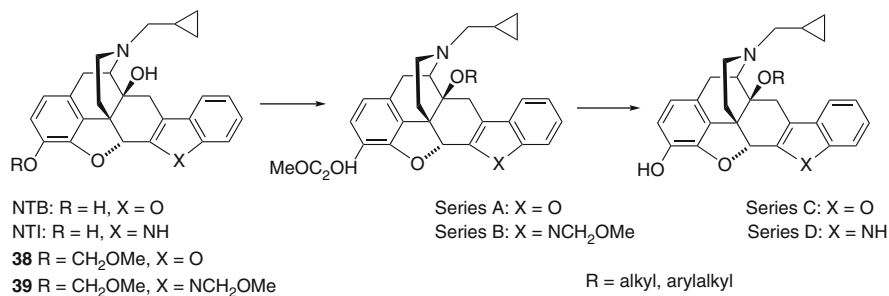
Scheme 9

2.2.2 Synthesis Starting from Naltrindole or Naltriben

Naltrindole (NTI) [34, 51] and naltriben (NTB) [52] are prototype δ-opioid receptor antagonists belonging to the indolo- and benzofuromorphinan series of compounds. Starting either from NTI or NTB, a more efficient synthesis of 14-alkoxy-substituted indolo- and benzofuromorphinans in three steps was reported, whereby the 14-*O*-alkyl group is introduced in the penultimate step of the procedure [53]. Thus, protection of the C3-hydroxyl group of NTB and of both the C3-hydroxyl group and indole nitrogen of NTI with methoxymethyl bromide gave methoxymethyl-protected derivatives **38** and **39**, respectively. Subsequent 14-*O*-alkylation with different alkyl bromides in DMF using NaH as the base afforded 14-*O*-alkylated series A and series B, respectively. Acid hydrolysis (MeOH/1 N HCl) yielded the desired benzofuromorphinans (series C) and indolomorphinans (series D) (Scheme 9). Similarly benzofuromorphinans of series C were prepared using the triisopropyl-silyl protecting group instead of methoxymethyl [53].

2.3 Introduction of New Functionalities to 14-Alkoxymorphinan-6-ones

Among the most indispensable analgesics, morphinan-6-ones such as oxymorphone, oxycodone, and dihydromorphinone have their main importance in clinical use. As earlier shown, hydrazone, oxime, carbazone, and semicarbazone derivatives of these morphinan-6-ones exhibit high affinity at the μ-opioid receptor [54–56] and exhibit high antinociceptive potency in addition to less pronounced side effects [19, 57–60]. Therefore, it remains a promising synthetic task to convert the carbonyl group into various functionalities.

2.3.1 Incorporation of Acrylonitrile Substructures into Morphinans

An interesting approach to incorporate acrylonitrile substructures into morphinans is the van Leusen homologation reaction in which the standard reagent
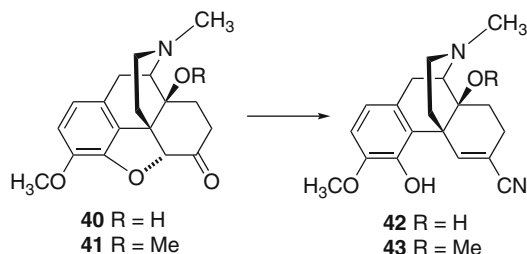
tosylmethylisocyanid (TosMIC) reacts with carbonyl compounds to give the corresponding nitriles with one additional carbon atom [61].

Van Leusen Reaction Applied to Morphinan-6-ones Without 7,8 Double Bond
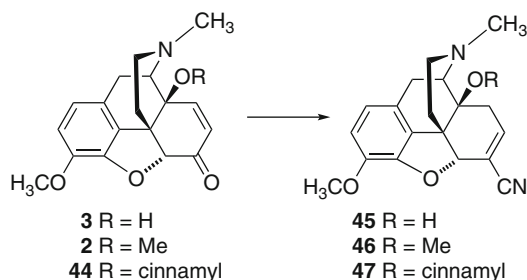
Applying the van Leusen reaction [61] to oxycodone (**40**) and 14-*O*-methyloxyco-done (**41**), the ether bridge between positions 4 and 5 was opened and the respective acrylonitrile derivatives **42** and **43** were formed (Scheme 10) [62].

Van Leusen Reaction Applied to 7,8-Didehydromorphinan-6-ones

In contrast to the cyanation of oxycodone (**40**) and 14-*O*-methyoxycodone (**41**) with TosMIC (Sect. 2.3.1.1), 7,8-didehydromorphinan-6-ones such as 14-hydroxycodei-none (**3**), 14-methoxycodeinone (**2**), and 14-cinnamyloxycodeinone (**44**) were found to yield 6,7-didehydrocarbonitriles **45**–**47** with retainment of the 4,5-epoxy ring under these conditions (Scheme 11) [63].

40 R = H
41 R = Me

42 R = H
43 R = Me

Scheme 10

3 R = H
2 R = Me
44 R = cinnamyl

45 R = H
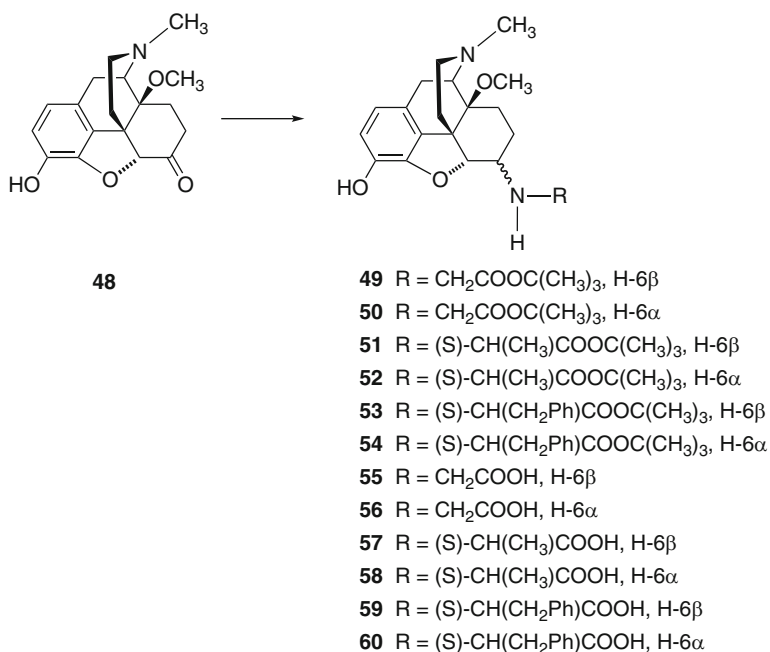**46** R = Me
47 R = cinnamyl

Scheme 11

2.3.2 Synthesis of 6-Amino Acid-Substituted 14-Alkoxymorphinans

Morphinans with zwitterionic moieties show greatly reduced access to the CNS without substantially decreased opioid receptor activity [64, 65]. A series of 6-amino acid conjugates (glycine, alanine, and phenylalanine) of the highly potent opioid analgesic 14-*O*-methyloxymorphone (**48**) [41] has been synthesized in an effort to obtain opioid agonists with high potency that would have reduced ability to cross the blood–brain barrier (BBB) [66] (Scheme 12). A novel synthetic approach for the synthesis of 6-amino acid derivatives in the morphinan series was employed. Thus, the *tert*-butyl ester derivatives **49–54** were prepared from 14-*O*-methyloxymorphone (**48**) by reductive amination with the respective *tert*-butyl ester hydrochlorides and sodium cyanoborohydride in ethanol. After separating the epimers by column chromatography, esters **49–54** were treated with tetrafluoroboric acid to afford compounds **55–60** as bis(tetrafluoroborates).
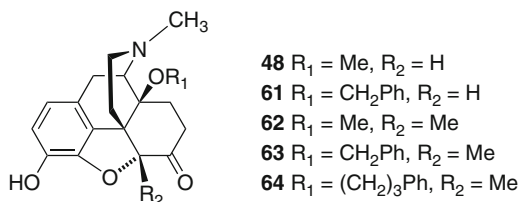
3 Pharmacological Actions

3.1 *14-Alkoxymorphinan-6-ones*

Introduction of a 14-methoxy group in oxymorphone resulted in 14-*O*-methyloxy-morphone (**48**) (Fig. 3) [41] which not only increases affinity to opioid receptors in

48

49 R = CH$_2$COOC(CH$_3$)$_3$, H-6β
50 R = CH$_2$COOC(CH$_3$)$_3$, H-6α
51 R = (S)-CH(CH$_3$)COOC(CH$_3$)$_3$, H-6β
52 R = (S)-CH(CH$_3$)COOC(CH$_3$)$_3$, H-6α
53 R = (S)-CH(CH$_2$Ph)COOC(CH$_3$)$_3$, H-6β
54 R = (S)-CH(CH$_2$Ph)COOC(CH$_3$)$_3$, H-6α
55 R = CH$_2$COOH, H-6β
56 R = CH$_2$COOH, H-6α
57 R = (S)-CH(CH$_3$)COOH, H-6β
58 R = (S)-CH(CH$_3$)COOH, H-6α
59 R = (S)-CH(CH$_2$Ph)COOH, H-6β
60 R = (S)-CH(CH$_2$Ph)COOH, H-6α

Scheme 12

Fig. 3 Oxymorphone
derivatives

48 R_1 = Me, R_2 = H
61 R_1 = CH_2Ph, R_2 = H
62 R_1 = Me, R_2 = Me
63 R_1 = CH_2Ph, R_2 = Me
64 R_1 = $(CH_2)_3Ph$, R_2 = Me

Table 1 Opioid receptor binding affinities of oxymorphone derivatives [45, 47]

Compound	K_i μ (nM)	K_i δ (nM)	K_i κ (nM)	Selectivity ratio	
				δ/μ	κ/μ
48	0.10	4.80	10.2	48	102
61	0.12	2.14	1.18[a]	18	10
62	0.15	13.3	25.2	89	168
63	0.18	3.67	2.46[a]	20	14
64	0.20	0.14	0.40[a]	0.7	2
Oxymorphone	0.97	80.5	61.6[a]	83	63
Morphine	6.55	217	113	33	17

[a]Guinea rat or guinea pig brain membranes were used in binding assays
K_i inhibition constant

Table 2 Antinociceptive potencies of oxymorphone derivatives [45, 47]

Compound	HP AD_{50} (nmol/kg)	HP ED_{50} (μg/kg)	TF ED_{50} (μg/kg)	PPQ ED_{50} (μg/kg)
48	53	–	–	–
61	9.6	–	–	–
62	280	30	30	9.0
63	65			
64	–	0.10	0.08	0.16
Morphine	6,690	850	1,920	400

AD_{50} and ED_{50} analgesic and effective dose, respectively, necessary to elicit a 50% effect in mice after *s.c.* administration; *HP* hot-plate test; *TF* tail-flick test; *PPQ* paraphenylquinone writhing test; – not tested

in vitro opioid binding assays, while retaining the μ-receptor selectivity of oxymorphone (Table 1), but also markedly enhances the antinociceptive potency [41, 47, 67]. The presence of the methoxy group at position 14 resulted in a considerable increase in μ-opioid agonist activity in the mouse vas deferens (MVD) bioassay with derivative **48** having over 800-fold increased potency compared to oxymorphone [67]. 14-*O*-Methyloxymorphone (**48**) was characterized by potent agonist properties in the guinea pig ileum (GPI) and rat vas deferens (RVD) bioassays with IC_{50} values of 2 nM and 143 nM, respectively [47, 67]. It was reported to possess about 40-fold higher antinociceptive potency than its parent compound, and was up to 400-fold more potent than the "golden standard" for pain therapy, morphine, in rodent models of acute nociception i.e. hot-plate test in mice (Table 2) [41, 47] and tail-flick test in rats [67, 68] and mice [67], after subcutaneous (s.c.) administration. Compound **48** induces the classical opioid side effects of the conventional μ-opioid

analgesics including respiratory depression [41], physical dependence [41], and constipation [47] after s.c. administration to mice.

Using 14-*O*-methyloxymorphone (**48**) as the lead structure, a series of novel 14-alkoxy-substituted (i.e. allyloxy, benzyloxy, naphthylmethoxy) morphinan-6-one derivatives was prepared and pharmacologically evaluated [47]. The analog having a benzyl group in position 14 (**61**, Fig. 3) preserved the high affinity at the μ-opioid receptor of the parent compound **48** but had significantly increased interaction with the other opioid receptor types, δ and κ (Table 1), thus resulting in a reduction in μ-receptor selectivity. It was a highly potent μ-opioid agonist in the GPI ($IC_{50} = 0.9$ nM) and MVD bioassays ($IC_{50} = 1.5$ nM), showing 2- and 20-fold, respectively, increased agonist potency in comparison to the 14-*O*-methyl analog **48** [47]. Antinociceptive potency in the hot-plate test after s.c. administration in mice was further augmented through the introduction of a 14-benzyloxy group compared to the methoxy group, by about 5-fold increase when compared to the parent compound **48**, and by about 500-fold increase versus morphine (Table 2). Remarkable was the observation that the 14-benzyloxy substitution gave rise to a μ-opioid agonist eliciting negligible constipative activity at the analgesic dose, using the colonic bead expulsion test (CBE) in mice after s.c. administration. Analog **61** was 7-fold less constipating than 14-*O*-methyloxymorphone (**48**) as assessed by the CBE (ED_{50} CBE/AD_{50} hot-plate test = 2.8 and 0.4, respectively [47]).

A second approach to obtaining μ-opioid analgesics in the *N*-methylmorphinan-6-one class exhibiting more favorable pharmacological features was based on the introduction of a methyl group in position 5 of 14-*O*-methyloxymorphone, leading to 14-methoxymetopon (**62**) (Fig. 3). Following its first description in 1990 [69], a number of reports on *in vitro* and *in vivo* activities of 14-methoxymetopon (**62**) were published in the past years [47, 67, 70–78]. The presence of the 5-methyl substituent had no major effect on affinity to the μ-opioid receptor compared to 14-*O*-methyloxymorphone (**48**), while a slight decrease in binding to δ- and κ-receptors was observed, thus, maintaining the μ-receptor selectivity (Table 1). The 5-methyl-substituted derivative **62** showed high agonist activity and comparable potency to the 5-unsubstituted derivative **48** in the GPI, MVD, and RVD bioassays [47, 67]. The high agonist potency of compound **62** was also established using [^{35}S]GTPγS functional assay in rat brain [74], calf striatum [77], and Chinese hamster ovary (CHO) cells expressing mouse μ-receptor splice variants [77]. A tritium-labeled form of 14-methoxymetopon, [^{3}H]14-methoxymetopon, has also been prepared [74] and possesses high affinity and selectivity for native and recombinant μ-opioid receptors [74, 77].

In vivo, introduction of a methyl group in position 5 in 14-*O*-methyloxymorphone (**48**) resulted in somewhat of a decrease in antinociceptive potency, i.e. 5-fold in the hot-plate test (Table 2) and 2-fold in the tail-flick test in mice after s.c. administration for compound **62** [67]. Pharmacological studies consistently reported on the high antinociceptive activity of the μ-opioid agonist **62** ranging between 24- and 20,000-fold in comparison to morphine in diverse models of acute nociception (i.e. hot-plate test [44, 47, 71], tail-flick test [44, 67, 73, 76, 79] and tail electrical stimulation test [72]), and visceral pain (acetic acid- [69, 79], and

paraphenylquinone (PPQ)-induced writing test [44]) in rodents (mice, rats) after systemic administration. It was equipotent to sufentanil in eliciting analgesia in the skin-twitch test in canines after intravenous administration [70]. Antinociceptive effects of compound **62** after s.c. administration were also reported in inflammatory pain using a rat model of carrageenan-induced hindpaw inflammation [75]. The μ-agonist **62** at a dose of 20 μg/kg showed comparable efficacy to morphine (2 mg/kg) in inhibiting nociceptive behavior in inflamed hindpaws, thus being 100-fold more potent than morphine in experimental inflammatory pain.

Despite its high analgesic potency, 14-methoxymetopon (**62**) was reported to display little respiratory depression, hypotension, bradycardia, or sedation compared to sufentanil in canines [70]. It decreases gastrointestinal transit far less than morphine and reportedly develops lower levels of tolerance [76, 79], physical dependence [79], and a diminished propensity to cause convulsions in mice [79]. Behavioral studies showed that compound **62** is far more effective than morphine in reducing the emotive/affective component of pain and in producing an anxiolytic effect in rats [72]. Therefore, it was depicted as a highly potent μ-opioid analgesic with a pharmacological profile distinct from that of traditional μ-opioid agonists such as morphine.

Physicochemical properties are often an important consideration for understanding the behavior of bioactive molecules and their correlation with pharmacological activities. Experimentally determined liphophilicity of oxymorphone derivatives, 14-*O*-methyloxymorphone (**48**) and 14-methoxymetopon (**62**), have been recently reported [67]. 14-*O*-Methyloxymorphone (**48**) displays comparable lipophilicity to its parent compound oxymorphone (log*P* values of 0.60 and 0.67, respectively), but shows greater μ-opioid receptor affinity (Table 1) and behaves as a more potent agonist *in vitro* and *in vivo* [67]. Introduction of a methyl group in position 5 in 14-*O*-methyloxymorphone (**48**) leads to a more liphophilic molecule **62** (log*P* = 1.12), while showing comparable antinociceptive potency *in vivo* and similar activities i.e. μ-opioid affinity and agonist potency *in vitro*.

Further chemical derivatization having 14-methoxymetopon (**62**) as the lead, resulted in a series of 14-arylalkyloxymetopon derivatives i.e. benzyloxymetopon [47] and phenylpropoxymetopon [45]. Replacement of the 14-methoxy substituent by benzyloxy or phenylpropoxy gave rise to analogs **63** and **64** (Fig. 3) displaying markedly enhanced binding affinities to both δ- and κ-opioid receptors, while the high affinity at the μ-receptor remains unchanged. This resulted in a decrease in selectivity for the μ-receptor of derivative **63** and a complete loss of μ-selectivity for 14-phenylpropoxymetopon (PPOM, **64**) (Table 1). Both analogs were potent antinociceptive agents in mice after s.c. administration (Table 2). The most striking finding was that compound **64** acted as an extremely potent opioid agonist *in vivo*, showing considerable increased antinociceptive potency (60- to 400-fold) compared to 14-methoxymetopon (**62**) in different nociceptive tests (i.e. hot-plate, tail-flick, and PPQ writing tests) in mice after s.c. administration (Table 2). PPOM (**64**) was 8,500- and 24,000-fold more active in the hot-plate and tail-flick tests, respectively, than morphine. It was reported that the 14-phenylpropoxy-substituted analog **64** is even more potent as an antinociceptive agent than etorphine, a well-known

opioid morphinan used in veterinary medicine [80, 81]. The 3-O-methyl ether of PPOM (**26**) showed unexpectedly high antinociceptive potency after s.c. administration in mice although its potency was about 10- to 55-fold lower than that of PPOM (**64**) [45]. On the basis of SAR studies, it was evident that the nature of the substituent at position 14 in N-methylmorphinan-6-ones has a major impact on their abilities to interact with opioid receptors leading to profound alteration in the pharmacological profile in this class of opioid compounds. A 14-phenylpropoxy substituent would also increase liphophilicity of 14-methoxymetopon (**62**) which might broaden the therapeutic scope, for example use in transdermal systems.

Established and generally accepted SAR models have assigned critical importance in defining the pharmacological profile of agonist/antagonist of morphinan-6-ones to the substituent at the morphinan nitrogen [82, 83]. Substituents such as cyclopropylmethyl or allyl at the nitrogen have been commonly associated with an antagonist character. Well-known examples are the nonselective opioid receptor antagonists, naloxone and naltrexone (Fig. 2). The introduction of a 14-O-methyl or ethyl group into naloxone and naltrexone, respectively, did not significantly alter the *in vitro* and *in vivo* potencies of these two antagonists [12, 38]. A 14-phenylpropoxy substitution in naloxone and naltrexone afforded derivatives **65** and **66**, respectively (Fig. 4) [44] having high affinity at all three opioid receptor types, with low K_i values in the subnanomolar range (Table 3). Surprisingly, they acted as opioid agonists *in vivo*, inducing potent antinociceptive effects in different nociceptive tests (i.e. hot-plate, tail-flick and PPQ-writhing tests) in mice after s.c. administration (Table 3). Both 14-phenlypropxy analogs **65** and **66** were several folds more potent than morphine (100- and 300-fold in the hot-plate and tail-flick tests, respectively for compound **65**, and 400-, 600- and 60-fold in the hot-plate, tail-flick and PPQ-writhing tests, respectively, for compound **66**). They even
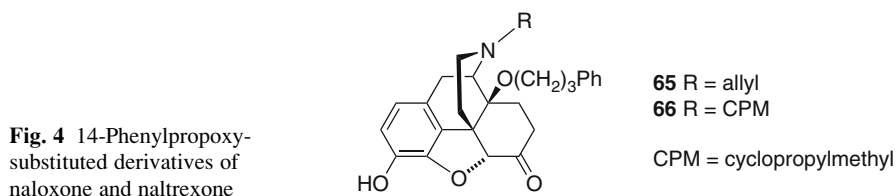

Fig. 4 14-Phenylpropoxy-substituted derivatives of naloxone and naltrexone

65 R = allyl
66 R = CPM

CPM = cyclopropylmethyl

Table 3 *In vitro* and *in vivo* opioid activities of 14-phenylpropoxy derivatives of naloxone and naltrexone [44]

Compound	Receptor binding assay					Antinociception		
	K_i μ (nM)	K_i δ (nM)	K_i κ (nM)	Selectivity ratio		ED$_{50}$ (mg/kg s.c.)		
				δ/μ	κ/μ	HP	TF	PPQ
65	0.20	0.26	0.11	0.55	1.30	0.006	0.006	–
66	0.34[a]	0.48[a]	0.41[a]	1.96	1.84	0.002	0.003	0.006

C6 rat glioma cells or [a]rat brain membranes were used in binding assays
K_i inhibition constant; *ED$_{50}$* effective dose necessary to elicit a 50% effect in mice after s.c. administration; *HP* hot-plate test; *TF* tail-flick test; *PPQ* paraphenylquinone writhing test; – inconsistent dose response

surpassed 14-methoxymetopon (**62**) in analgesic potency and were essentially inactive as antagonists in the tail-flick test in mice versus morphine [44]. This observation is in contrast to the findings upon 14-*O*-methylation and ethylation of naloxone and naltrexone which did not significantly alter binding affinities and agonist potency. These derivatives of naloxone and naltrexone were reported to be essentially devoid of agonist activities in the MVD bioassay and nociceptive assays (i.e. hot-plate and tail-flick tests) in rats and were pure opioid antagonists [12, 38].

Another study [84] reported on the effect of introduction of a 14-phenylpropoxy group in cyprodime and analogs (Fig. 5) on *in vitro* and *in vivo* opioid activities. The presence of a 14-phenylpropoxy substituent in cyprodime, a selective μ-opioid receptor antagonist (Fig. 2) markedly improved the interaction with the μ-receptor, noted as a considerable increase in μ-binding affinity (K_i values of 10.6 nM for cyprodime, 0.34 nM for the analog **67**, and 0.40 nM for analog **68**) and similar or higher μ-receptor selectivity compared to cyprodime (Table 4). In the [^{35}S]GTPγ functional assay, both derivatives **67** and **68** were low efficacy partial agonists at μ- and δ-opioid receptors while at the κ-receptor, antagonist activity was shown by the 14-phenylpropoxy analog **67** and some partial activity by the derivative **68**. Compound **67** was tested for antagonism at human κ-receptors and showed a K_e value of 2.52 nM in the [^{35}S]GTPγS functional assay [84]. *In vivo*, it was found that cyprodime was converted into potent antinociceptive agents through the introduction of a 14-phenylpropoxy group (Table 4). When tested in mice after s.c. administration using hot-plate, tail-flick and PPQ-induced writhing tests, derivatives **67** and **68** were considerably more potent than morphine, with phenol **68** showing the highest antinociceptive potency (21-, 38- and 300-fold in the hot-plate, tail-flick and PPQ-writhing tests, respectively). It also showed similar potency to 14-methoxymetopon (**62**) in all three nociceptive assays. Both 14-phenylpropoxy-

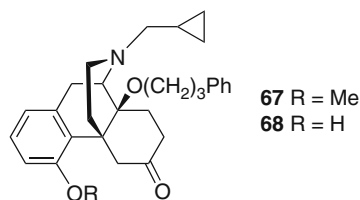**Fig. 5** 14-Phenylpropoxy-substituted derivatives of cyprodime

67 R = Me
68 R = H

Table 4 *In vitro* and *in vivo* opioid activities of 14-phenylpropoxy derivatives of cyprodime [84]

Compound	Receptor binding assay					Antinociception		
	K_i μ (nM)	K_i δ (nM)	K_i κ (nM)	Selectivity ratio		ED$_{50}$ (mg/kg s.c.)		
				δ/μ	κ/μ	HP	TF	PPQ
67	0.34	16.9	7.36	55	20	0.30	0.28	0.06
68	0.40	5.06	5.84	13	15	0.04	0.05	0.0014
Cyprodime	10.6	414	109	39	10	–	–	–

Rat brain membranes were used in binding assays

K_i inhibition constant; *ED$_{50}$* effective dose necessary to elicit a 50% effect in mice after s.c. administration; *HP* hot-plate test; *TF* tail-flick test; *PPQ* paraphenylquinone writhing test; – not applicable

substituted derivatives of cyprodime where inactive as antagonists against morphine in the tail-flick test in mice [84].

The SAR studies and pharmacological findings reported in the two studies [44, 84] provide evidence that not necessarily the nature of the substituent at the nitrogen in morphine-like compounds but rather residues occupying a defined position in the vicinity to the morphinan nitrogen seem to be responsible for the agonist/antagonist action. This observation seems to revise the traditionally established SAR models [82, 83]. In the series of morphinan-6-ones with a 14-phenylpropoxy group, even with N-substituents such as cyclopropylmethyl and allyl that are usually associated with distinct antagonist properties, agonists and highly potent analgesics were obtained.

3.2 6-Cyanomorphinans

The C6 carbonyl group of morphinan-6-ones can be easily chemically modified, and pharmacological studies have shown that such modifications generally do not affect the opioid character of the ligand [54–56], while the resulting compounds have high antinociceptive potencies, together with reduced unwanted side effects such as respiratory depression and gastrointestinal inhibition [57, 58]. These included for example hydrazones, oximes, and semicarbazone derivatives of N-methyl-6-ketomorphinans. On the basis of the pharmacological findings that 4,5-oxygen bridge-opened morphinan-6-ones (N-methyl substituted [41] and N-cycloproplymethyl substituted [84]) have increased affinities at the μ-opioid receptor and higher antinociceptive potency than their 4,5-oxygen-bridged analogs, it was investigated how and to what degree the presence of a 6-cyano group would affect the opioid receptor binding profile and *in vivo* antinociceptive potency compared to their 6-keto analogs.

The report [85] on acrylonitrile incorporated 4,5-oxygen bridge-opened N-methylmorphinans (Fig. 6) described that a 6-cyano substituent leads to compounds (**42**, **43**, and **69**) with high affinity at the μ-opioid receptor and decreased interaction with δ- and κ-receptors, thus being μ-selective (Table 5). Also, the replacement of the 6-keto group by a 6-cyano group did not significantly affect μ-opioid receptor affinity and retained the low binding to the δ- and κ-sites. *In vivo*, the 6-cyanomorphinans (**42**, **43**, and **69**) acted as potent antinociceptive agents in three nociceptive
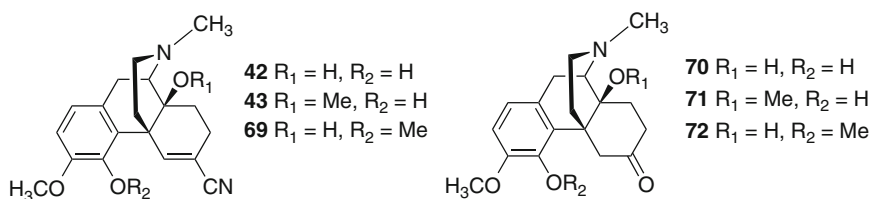

Fig. 6 6-Cyanomorphinans and their 6-keto analogs

Table 5 *In vitro* and *in vivo* opioid activities of 6-cyanomorphinans and their 6-keto analogs [85]

Compound	Receptor binding assay					Antinociception		
	K_i μ (nM)	K_i δ (nM)	K_i κ (nM)	Selectivity ratio		ED_{50} (mg/kg s.c.)		
				δ/μ	κ/μ	HP	TF	PPQ
42	31.7	498	1648	16	52	0.50	1.88	0.18
43	5.38	197	378	37	70	0.25	0.21	0.11
69	2.44	107	364	44	149	0.15	0.018	0.026
70	32.6	881	763	27	23	2.60	–	–
71	4.65	180	592	39	127	0.29	–	–
72	3.88	91.6	693	24	179	0.14	–	–
Oxycodone (**40**)	43.6	1087	2658	25	61	1.37	0.94	0.38

Rat brain membranes were used in binding assays

K_i inhibition constant; ED_{50} effective dose necessary to elicit a 50% effect in mice after s.c. administration; *HP* hot-plate test; *TF* tail-flick test; *PPQ* paraphenylquinone writhing test; – not tested

tests (i.e. hot-plate, tail-flick and PPQ-writing tests) in mice after s.c. administration. They were either more active or equipotent to their 6-keto counterparts (**70**–**72**), and also to oxycodone (**40**) (Table 5). The presence of a 14-methoxy substituent (compound **43**) instead of a hydroxy group in 6-cyanomorphinan **42** not only increases *in vitro* binding affinity at the μ-receptor, but also enhances the antinociceptive potency (Table 5), a similar observation being made for the morphinan-6-ones [44, 47, 84]. The chemically highly versatile acrylonitrile substructure allows for further conversion into various and more polar derivatives, and, therefore bears the potential to open up a new field in morphinan chemistry and opioid pharmacology.

3.3 6-Amino Acid-Substituted 14-Alkoxymorphinans

The important function of opioid receptors outside of the CNS in different pathophysiological conditions has gained considerable attention during the past decades, and nowadays opioid researchers and physicians are beginning to appreciate the new "peripheral" paths for improved and innovative therapy [6, 8, 86]. Medicinal chemistry and opioid pharmacology focuses increasingly on exploring the potential of peripheral opioid receptors through the development of peripherally acting opioid compounds as therapeutic agents in the treatment of disease states such as pain, inflammatory diseases, and gastrointestinal disorders [14, 18, 27, 87–89]. Approaches to limit access to the CNS and as a consequence also to reduce the occurrence of unwanted CNS side effects include chemical modifications at opioid compounds that increase their hydrophilicity such as incorporation of highly polar substituents. Earlier works to develop peripherally selective opioids have primarily focused on the quaternization of the nitrogen in known opioid morphinans such as morphine, oxymorphone, or naloxone [14, 26, 90]. Although quaternary compounds show reduced ability to cross the BBB relative to their tertiary amine

precursors, they have considerably lower affinity to opioid receptors [26, 90]. Quaternization also trends to reduce potency *in vivo*. In order to avoid these limitations, opioids with hydrophilic groups attached at the C6 position of the morphinan skeleton have been synthesized from β-oxymorphamine [64], β-naltrexamine [64], and β-funaltrexamine [91]. Such opioids with zwitterionic moieties showed reduced penetration to the CNS, without substantially decreased opioid receptor activity [64, 65].

The study [66] reported on the incorporation of an amino acid residue into the highly potent centrally acting μ-opioid analgesic 14-*O*-methyloxymorphone leading to zwitterionic 6-amino acid-substituted derivatives (glycine, alanine, and phenylalanine) (**55–60**) of 14-*O*-methyloxymorphone (**48**) (Scheme 12) as potent μ-opioid receptor agonists with limited access to the CNS. In binding studies with rat brain membranes [92], all 6-amino acid conjugates **55–60** displayed high affinities ($K_i = 0.77$–2.58 nM) at the μ-opioid receptor (Table 6). They were potent μ-opioid agonists in the MVD bioassay ($IC_{50} = 5.52$–26.8 nM). While the α-amino acid epimers were favored by μ-opioid receptors, the β-epimers have increased interaction with δ-binding sites (Table 6). Only the 6β-phenylalanine **60** conjugate showed some preference for δ- over μ-opioid receptors, and δ-opioid receptor agonist activity in the MVD bioassay (Table 6). The μ- and δ-receptor affinities remained somewhat similar to the parent compound 14-*O*-methyloxymorphone (**48**), whereas affinities at the κ-receptor were significantly decreased independent of α- or β-substitution (Table 6).

A number of *in vivo* pharmacological studies reported that amino acid substitution in position 6 of 14-*O*-methyloxymorphone (**48**) afforded derivatives **55–60** that produce potent antinociceptive actions via peripheral mechanisms after s.c. administration in different pain models such as acute nociception i.e. tail-flick test [68], inflammatory pain i.e. formalin test [68] and carrageenan-induced hindpaw inflammation [75] and visceral pain i.e. acetic acid-induced writhing test [93]. In the tail-flick test in the rat, the 6-amino acid derivatives were 19- to 209-fold more potent than morphine (Table 7) and showed similar potency to fentanyl after s.c

Table 6 Opioid receptor binding affinities and agonist potencies of 6-amino acid-substituted derivatives of 14-*O*-methyloxymorphone (**48**) [92]

| Compound | Receptor binding assay | | | | | MVD bioassay |
| | K_i μ (nM) | K_i δ (nM) | K_i κ (nM) | Selectivity ratio | | IC_{50} (nM) |
				δ/μ	κ/μ	
55	0.89	15.4	43.2	17	49	26.8
56	0.83	7.86	44.8	9.5	54	7.00
57	0.77	26.9	142	35	184	12.2
58	1.90	7.71	63.7	4.1	34	19.6
59	0.95	3.67	28.5	3.9	30	5.52
60	2.58	1.03	151	0.40	59	6.07
48	0.10	4.80	10.2	48	102	7.76

Rat brain membranes were used in binding assays

K_i inhibition constant; *MVD* mouse vas deferens; *IC_{50}* agonist concentration necessary to produce a 50% effect

Table 7 Antinociceptive potencies of 6-amino acid-substituted derivatives of 14-*O*-methyloxymorphone (**48**) [68]

Compound	ED$_{50}$ (nmol/kg s.c.)		
	Tail-flick test	Formalin test	
		I phase	II phase
55	58.5	72	110
56	29.0	125	204
57	68.9	–	–
58	53.4	–	–
59	315	171	292
60	>3,600	79	107
48	14.9	–	–
Morphine	6,053	1,613	1,472
Fentanyl	38.6	–	–

ED$_{50}$ effective dose necessary to elicit a 50% effect in rats after s.c. administration; – not tested

administration [68]. Both s.c. (Table 7) and local intraplantar administration [94] of the zwitterionic compounds **55**, **56**, **59**, and **60** produced antihyperalgesic effects in the formalin test in the rat showing greater potencies than morphine. Potent and significant antinociceptive behavior was also reported after s.c. administration of the 6β-glycine conjugate **56**, using a rat model of prolonged inflammatory pain, i.e. unilateral carrageenan-induced hindpaw inflammation [75] and a mouse model of abdominal visceral pain [93]. Antihyperalgesic and antiallodynic effects of compounds **55**, **56**, **59**, and **60** were also described in rats with neuropathic pain after local intraplantar administration [94]. Generally, antinociceptive actions of the 6-amino acid-substituted derivatives of 14-*O*-methyloxymorphone **55–60** were considerably longer-lasting (2–3 h in the tail-flick and writhing tests and up to 4 h in carrageenan-induced inflammatory pain) compared to the clinically relevant μ-opioid analgesics, morphine and fentanyl, and the structurally related and centrally acting μ-opioids, 14-*O*-methyloxymorphone (**48**) and 14-methoxymetopon (**62**) (30–60 min) [68, 75, 93]. Also, a significant and long-lasting antinociceptive effect (up to 4 h) was reported after oral administration of the 6β-glycine conjugate **56** (10 mg/kg) to rats with carrageenan-induced inflammatory pain [75]. Opioid analgesics with limited access to the CNS that could be administered systemically or orally are of high relevance for clinical use.

3.4   14-Alkoxy-Substituted Indolo- and Benzofuromorphinans

The δ-opioid receptor was the first opioid receptor type to be cloned in 1992 [2], and its molecular and functional characterization was largely based on the use of the δ-selective indolomorphinan NTI (Fig. 2) and its benzofuran analog naltriben (NTB). SAR studies on series of NTI and NTB analogs focusing on the introduction of alkoxy groups at position 14 were reported [43, 50] (Fig. 7). Further chemical modifications, SAR and biological investigations on 14-alkoxy analogs of NTI and
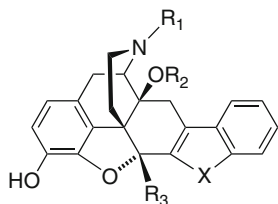
73 R$_1$ = CPM, R$_2$ = Me, R$_3$ = H, X = NH
74 R$_1$ = CPM, R$_2$ = Et, R$_3$ = H, X = NH
75 R$_1$ = allyl, R$_2$ = Me, R$_3$ = H, X = NH
76 R$_1$ = allyl, R$_2$ = Et, R$_3$ = H, X = NH
77 R$_1$ = CPM, R$_2$ = Me, R$_3$ = Me, X = NH
78 R$_1$ = CPM, R$_2$ = Et, R$_3$ = Me, X = NH
79 R$_1$ = CPM, R$_2$ = Pr, R$_3$ = Me, X = NH
80 R$_1$ = allyl, R$_2$ = Me, R$_3$ = H, X = N-Me
81 R$_1$ = allyl, R$_2$ = allyl, R$_3$ = H, X = N-allyl
82 R$_1$ = CPM, R$_2$ = Et, R$_3$ = H, X = O
83 R$_1$ = allyl, R$_2$ = Et, R$_3$ = H, X = O

CPM = cyclopropylmethyl

Fig. 7 14-Alkoxy-substituted indolo- and benzofuromorphinans

Table 8 Opioid receptor binding affinities of 14-alkoxy-substituted indolo- and benzofuromorphinans [43, 50, 95]

Compound	K_i δ (nM)	K_i μ (nM)	K_i κ (nM)	Selectivity ratio	
				μ/δ	κ/δ
73	1.44	68.7	103	48	72
74	0.40	97.0	313	242	783
75	3.8	869	233	229	134
76	2.6	1368	349	526	134
77	1.15	284	421	247	366
78	0.78	340	134	436	172
79	5.3	555	504	105	95
80	1.97	731	149	371	76
81	7.3	1001	763	137	105
82	1.18	185	94	157	80
83	1.20	22.8	68	19	57
NTI	0.14	13.0	15.8	93	113
NTB	0.15	27.1	23.4	180	156

Rat brain membranes were used in μ- and δ-receptor binding assays and guinea pig brain membranes were used in the κ-receptor binding assay
K_i inhibition constant

NTB differently substituted in position 5 and 17 and at the indole nitrogen were described [43, 50, 95–98].

The introduction of a 14-alkoxy instead of the 14-hydroxy group present in NTI resulted in somewhat lower binding affinity at the δ-receptor, while δ-receptor selectivity was considerably increased (compounds **74–81**) (Table 8). The nature of the substituent in position 14 was reported to be an important determinant for the interaction with δ-receptors. A 14-ethoxy group in indolomorphinans seems to be superior to 14-methoxy and 14-propoxy substitution concerning δ-affinity and selectivity. The presence of a 14-ethoxy group (compounds **74**, **76**, and **78**) resulted in higher affinity and selectivity for the δ-receptor compared to their 14-methoxy-substituted derivatives **73**, **75**, and **77**, respectively, and 14-propoxy analog **79**

(Table 8). Arylalkoxy substituents in position 14 reduced δ-affinity and selectivity [50]. The introduction of a 5-methyl group in the 14-methoxy indolomorphinan **73** did not significantly change δ-receptor affinity, but decreased affinities at μ- and κ-receptors, resulting in higher μ/δ and κ/δ selectivity ratios (247 and 366, respectively) for compound **77**. Substitution at the indole nitrogen with methyl (compound **80**) or allyl groups (compounds **81**) does not have much influence on δ-receptor affinity and selectivity when compared to the unsubstituted analogs (Table 8). The nature of X (O-, NH-, or N-substituted) did not largely affect δ-receptor affinity and selectivity. Also, replacement of the 17-cyclopropylmethyl group by an allyl substituent has little influence on binding at the δ-receptor [43, 50].

The higher δ-receptor selectivity of the 14-ethoxy-substituted indolomorphinans **76** and **78** compared to NTI based on opioid receptor binding assays was also reported in [^{35}S]GTPγS functional assays [43, 95]. Potent antagonist activities at the δ-receptor were described for other 14-alkoxy-substituted indolo- and benzo-furomorphinans compared to NTI and NTB [43, 50, 97]. The interesting opioid receptor activity profile of derivative **78** makes this compound a useful tool to selectively antagonize δ-opioid receptor agonist-induced effects or to assess receptor specificity of opioid ligands *in vitro* and *in vivo* [74, 99–101].

Highly interesting was the observation reported in several studies [102–104] that the indolomorphinan δ-opioid receptor antagonist NTI significantly prolongs renal allograft survival in the rat and inhibits allogenic mixed lymphocyte reaction (MLR) *in vitro*, similar to the clinically used immunosuppressant cyclosporin A. This remarkable finding brought attention to this class of δ-opioid antagonists as potential immunosuppressive agents in organ transplantation and inflammatory diseases. The 14-ethoxy-5-methyl-substituted derivative of NTI (**78**), which showed higher selectivity and antagonist potency towards the δ-opioid receptor than NTI, was reported to inhibit rat lymphocyte proliferation *in vitro* (IC$_{50}$ = 0.54 μM), being more active than NTI (IC$_{50}$ = 6.93 μM) [95]. Other structurally related selective δ-opioid antagonists **73**, **75**, **77**, and **83** were also found to possess immunosuppressive activity *in vitro* in human peripheral blood mononuclear cells (PBMC) at a concentration of 10 μM [96]. Similar to NTI, they reduce interleukin-2 (IL-2) production in mouse and human lymphocytes [96]. The immunosuppressive action of NTI and close derivatives was reported not to be mediated through the δ-opioid receptor or any of the other opioid receptor types (μ and κ) using *in vitro* MLR with splenocytes from δ and triple μ/δ/κ opioid receptor knockout mice [105]. These observations have shed new light on the immunoregulatory mode of action of this class of opioids. It has been postulated that structural determinants of the indolo moiety in NTI and derivatives **73**, **75**, **77**, and **78** or the corresponding benzofuran group in **83** (Fig. 7) appear to be required for the immunosuppressive activity, since naltrexone was inactive in the MLR suppression [105]. Recently, NTI and 14-alkoxy-substituted indolomorphinan derivatives **77** and **78** have been reported to suppress tryptophan degradation and neopterin formation (markers for diseases that are associated with inflammation or altered immune function [106]), in mitogen-induced human PBMC, with derivatives **77** and **78** exhibiting slightly higher potency than NTI [98]. Thus, there is evidence that such opioid indolomorphinans

besides their significant scientific value as pharmacological tools might also have potential for therapeutic use in immunopathological disorders.

4 Conclusions

In recent years, numerous amounts of synthetical efforts have resulted in the development of new 14-alkoxymorphinans together with a significant expansion of knowledge on their pharmacology and ligand-based structure–activity relationships. The nature of the substituent at position 14 in this class of compounds has a major impact on the ability of morphinans to interact with opioid receptors, leading to qualitative and quantitative differences in biological and pharmacological activities. Targeting position 14 represents a viable approach for tuning the pharmacological properties of this class of opioids. Additional substitution patterns in positions 5, 6, and 7 in 14-alkoxymorphinans results in compounds with distinct opioid activities and provided further understanding of structural requirements and functional selectivity. Appropriate molecular manipulations of the morphinan template can afford novel opioid ligands, which besides their scientific value as pharmacological tools, may also have the potential of emerging as novel therapeutic agents for the treatment of human disease states. These advances may lead to strategies in investigating the pharmacotherapeutic potential of the opioid system through the discovery of novel and innovative opioid drugs from the 14-alkoxymorphian class. They will provide a continued infusion of new scientific input into the drug discovery process for identification of safer, more efficacious drugs with improved side effect profiles than the conventional therapies.

References

1. Evans CJ (2004) Secrets of opium poppy revealed. Neuropharmacology 47:293–299
2. Kieffer BL, Evans CJ (2009) Opioid receptors: from binding sites to visible molecules *in vivo*. Neuropharmacology 56:205–212
3. Mansour A, Fox CA, Akil H, Watson SJ (1995) Opioid-receptor mRNA expression in the rat CNS: Anatomical and functional implications. Trends Neurosci 18:22–29
4. McCarthy L, Wetzel M, Sliker JK, Eisenstein TK, Rogers TJ (2001) Opioids, opioid receptors, and the immune response. Drug Alcohol Depend 62:111–123
5. Stein C (2003) Opioid receptors on peripheral sensory neurons. Adv Exp Med Biol 521:69–76
6. Holzer P (2009) Opioid receptors in the gastrointestinal tract. Regul Pept 155:11–17
7. Kieffer BL, Gaveriaux-Ruff C (2002) Exploring the opioid system by gene knockout. Prog Neurobiol 66:285–306

8. Bodnar RJ (2009) Endogenous opiates and behavior: 2008. Peptides 30:2432–2479
9. Zimmerman DM, Leander JD (1990) Selective opioid receptor agonists and antagonists: research tools and potential therapeutic agents. J Med Chem 33:895–902
10. Takemori AE, Portoghese PS (1992) Selective naltrexone-derived opioid receptors antagonists. Annu Rev Pharmacol Toxicol 32:239–269
11. Borsodi A, Toth G (1995) Characterization of opioid receptor types and subtypes with new ligands. Ann NY Acad Sci 757:339–352
12. Schmidhammer H (1998) Opioid receptor antagonists. In: Ellis GP, Luscombe DK, Oxford AW (eds) Prog Med Chem 35:83–132
13. Schiller PW, Weltrowska G, Berezowska I, Nguyen TM, Wilkes BC, Lemieux C, Chung NN (1999) The TIPP opioid peptide family: development of δ antagonists, δ agonists, and mixed μ agonist/δ antagonists. Biopolymers 51:411–425
14. DeHaven-Hudkins DL, Dolle RE (2004) Peripherally restricted agonists as novel analgesic agents. Curr Pharm Design 10:743–757
15. Eguchi M (2004) Recent advances in selective opioid receptor agonists and antagonists. Med Res Rev 24:182–212
16. Metcalf MD, Coop A (2005) Kappa opioid antagonists: past successes and future prospects. AAPS J 7:E704–E722
17. Schiller PW (2005) Opioid peptide-derived analgesics. AAPS J 7:E560–E565
18. Goodman AJ, Le Bourdonnec B, Dolle RE (2007) Mu opioid receptor antagonists: recent developments. Chem Med Chem 2:1552–1557
19. Fürst S, Hosztafi S (2008) The chemical and pharmacological importance of morphine analogues. Acta Physiol Hung 95:3–44
20. Trescot AM, Datta S, Lee M, Hansen H (2008) Opioid pharmacology. Pain Physician 11: S133–S153
21. Nicholson B (2009) Benefits of extended-release opioid analgesic formulations in the treatment of chronic pain. Pain Pract 9:71–81
22. Blumberg H, Dayton HB, Wolf PS (1966) Counteraction of narcotic antagonist analgesics by the narcotic antagonist naloxone. Proc Soc Exp Biol Med 123:755–758
23. Resnick RB, Volavka J, Freedman AM, Thomas M (1974) Studies of EN-1639A (naltrexone): a new narcotic antagonist. Am J Psychiatry 131:646–650
24. O'Malley SS (1996) Opioid antagonists in the treatment of alcohol dependence: clinical efficacy and prevention of relapse. Alcohol Alcohol Suppl 1:77–81
25. Morris PL, Hopwood M, Whelan G, Gardiner J, Drummond E (2001) Naltrexone for alcohol dependence: a randomized controlled trial. Addiction 96:1565–1573
26. Brown DR, Goldberg LI (1985) The use of quaternary narcotic antagonists in opiate research. Neuropharmacology 24:181–191
27. Viscusi ER, Gan TJ, Leslie JB, Foss JF, Talon MD, Du W, Owens G (2009) Peripherally acting μ-opioid receptor antagonists and postoperative ileus: mechanisms of action and clinical applicability. Anesth Analg 108:1811–1822
28. Nagase H, Hayakawa J, Kawamura K, Kawai K, Takezawa Y, Matsuura H, Tajima C, Endo T (1998) Discovery of a structurally novel opioid kappa-agonist derived from 4, 5-epoxymorphinan. Chem Pharm Bull 46:366–369
29. Nakao K, Mochizuki H (2009) Nalfurafine hydrochloride: a new drug for the treatment of uremic pruritus in hemodialysis patients. Drugs Today 45:323–329
30. Coop A, Rice KC (2000) Role of δ-opioid receptors in biological processes. Drug News Perspect 13:481–487
31. Sadée W, Wang D, Bilsky EJ (2005) Basal opioid receptor activity, neutral antagonists, and therapeutic opportunities. Life Sci 76:1427–1437
32. Cunningham CW, Coop A (2006) Therapeutic applications of opioid antagonists. Chem Today 24:54–57

33. Schmidhammer H, Burkard WP, Eggstein-Aeppli L, Smith CFC (1989) Synthesis and bio-logical evaluation of 14-alkoxymorphinans. 2. (-)-N-(cyclopropylmethyl)-4, 14-dimethoxy-morphinan-6-one, a selective μ opioid receptor antagonist. J Med Chem 32:418–421

34. Portoghese PS, Sultana M, Takemori AE (1988) Naltrindole, a highly selective and potent non-peptide δ-opioid receptor antagonist. Eur J Pharmacol 146:185–186

35. Portoghese PS, Lipkowski AW, Takemori AE (1987) Binaltorphimine and nor-binaltorphi-mine, potent and selective κ-opioid receptor antagonists. Life Sci 40:1287–1292

36. Heinisch G, Klintz V, Viehböck F (1971) Methanolysis of 14-bromocodeinone dimethyl acetale. Monatsh Chem 102:530–539

37. Razdan RK, Ghosh AC (1980) US Patent No 4,232,028

38. Kobylecki RJ, Carling RW, Lord JAH, Smith CFC, Lane AC (1982) Common anionic receptor site hypothesis: its relevance to the antagonist action of naloxone. J Med Chem 25:116–120

39. Razdan RK, Ghosh AC (1980) UK Patent No 2,045,758

40. Ghosh AC, Razdan RK (1982) US Patent No 4,362,733

41. Schmidhammer H, Aeppli L, Atwell L, Fritsch F, Jacobson AE, Nebuchla M, Sperk G (1984) Synthesis and biological evaluation of 14-alkoxymorphinans. 1. Highly potent opioid agonists in the series of (–)-14-methoxy-N-methylmorphinan-6-ones. J Med Chem 27:1575–1579

42. Schmidhammer H, Jennewein HK, Krassnig R, Traynor JR, Patel D, Bell K, Froschauer G, Mattersberger K, Jachs-Ewinger C, Jura P, Fraser GL, Kalinin VN (1995) Synthesis and biological evaluation of 14-alkoxymorphinans. 11. 3-Hydroxycyprodime and analogues: opioid antagonist profile in comparison to cyprodime. J Med Chem 38:3071–3077

43. Schütz J, Dersch CM, Horel R, Spetea M, Koch M, Meditz R, Greiner E, Rothman RB, Schmidhammer H (2002) Synthesis and biological evaluation of 14-alkoxymorphinans. 17. Highly δ opioid receptor selective 14-alkoxy-substituted indolo- and benzofuromorphinans. J Med Chem 45:5378–5383

44. Greiner E, Spetea M, Krassnig R, Schüllner F, Aceto M, Harris LS, Traynor JR, Woods JH, Coop A, Schmidhammer H (2003) Synthesis and biological evaluation of 14-alkoxymorphi-nans. 18. N-Substituted 14-phenylpropoxymorphinan-6-ones with unanticipated agonist properties: extending the scope of common structure-activity relationships. J Med Chem 46:1758–1763

45. Schütz J, Spetea M, Koch M, Aceto MD, Harris LS, Coop A, Schmidhammer H (2003) Synthesis and biological evaluation of 14-alkoxymorphinans. 20. 14-Phenylpropoxymeto-pon: an extremely powerful analgesic. J Med Chem 46:4182–4187

46. Cami-Kobeci G, Neal AP, Bradbury FA, Purington LC, Aceto MD, Harris LS, Lewis JW, Traynor JR, Husbands SM (2009) Mixed κ/μ opioid receptor agonists: the 6β-naltrexamines. J Med Chem 52:1546–1552

47. Lattanzi R, Spetea M, Schüllner F, Rief SB, Krassnig R, Negri L, Schmidhammer H (2005) Synthesis and biological evaluation of 14-alkoxymorphinans. 22. Influence of the 14-alkoxy group and the substitution in position 5 in 14-alkoxymorphinan-6-ones on *in vitro* and *in vivo* activities. J Med Chem 48:3372–3378

48. Schüllner F, Meditz R, Krassnig R, Morandell G, Kalinin VN, Sandler E, Spetea M, White A, Schmidhammer H, Berzetei-Gurske IP (2003) Synthesis and biological evaluation of 14-alkoxymorphinans. 19. Effect of 14-*O*-benzylation on the opioid receptor affinity and antagonist potency of naltrexone. Helv Chim Acta 86:2335–2341

49. Schmidhammer H, Daurer D, Wieser M, Monory K, Borsodi A, Elliott J, Traynor JR (1997) Synthesis and biological evaluation of 14-alkoxymorphinans. 14. 14-Ethoxy-5-methyl substi-tuted indolomorphinans with δ opioid receptor selectivity. Bioorg Med Chem Lett 7:151–156

50. Biyashev D, Monory K, Benyhe S, Schütz J, Koch M, Schmidhammer H, Borsodi A (2001) Novel delta-opioid-receptor-selective ligands in the 14-alkoxy-substituted indolo- and ben-zofuromorphinan series. Helv Chim Acta 84:2015–2021

51. Portoghese PS, Sultana M, Nagase H, Takemori AE (1988) Application of the message-address concept in the design of highly potent and selective non-peptide δ opioid receptor antagonists. J Med Chem 31:281–282

52. Portoghese PS, Nagase H, Maloney Huss KE, Lin C-E, Takemori AE (1991) Role of spacer and address components in peptidomimetic δ opioid receptor antagonists related to naltrindole. J Med Chem 34:1715–1720

53. Schmidhammer H, Schwarz P, Wei Z-Y (1998) A novel and efficient synthesis of 14-alkoxy-substituted indolo- and benzofuromorphinans in the series of selective δ opioid receptor antagonists. Helv Chim Acta 81:1215–1222

54. Pasternak GW, Hahn EF (1980) Long-acting opiate agonists and antagonists: 14-hydroxy-dihydromorphinone hydrazones. J Med Chem 23:674–676

55. Varga E, Toth G, Benyhe S, Hosztafi S, Borsodi A (1987) Synthesis and binding of ^{3}H-oxymorphazone to rat brain membranes. Life Sci 40:1579–1588

56. Krizsan D, Varga E, Hosztafi S, Benyhe S, Szucs M, Borsodi A (1991) Irreversible blockade of the high and low affinity (^{3}H)naloxone binding sites by C-6 derivatives of morphinan-6-ones. Life Sci 48:439–451

57. Fürst Z, Borsodi A, Friedmann T, Hosztafi S (1992) 6-Substituted oxycodone derivatives have strong antinociceptive effects and block irreversibly the low affinity [^{3}H]-naloxone binding sites in rat brain. Pharm Res 25:31–32

58. Fürst S, Hosztafi S, Friedmann T (1995) Structure-activity relationships of synthetic and semisynthetic opioid agonists and antagonists. Curr Med Chem 1:423–440

59. Monory K, Greiner E, Sartania N, Sallai L, Pouille Y, Schmidhammer H, Hanoune J, Borsodi A (1999) Opioid binding profiles of new hydrazone, oxime, carbazone and semicarbazone derivatives of 14-alkoxymorphinans. Life Sci 64:2011–2020

60. Gergely A, Gyimesi-Forras K, Horvath P, Hosztafi S, Kökösi J, Nagy PI, Szasz G, Szentesi A (2004) 6-Oxo-morphinane oximes: pharmacology, chemistry and analytical application. Curr Med Chem 11:2555–2564

61. Oldenziel OH, van Leusen D, van Leusen AM (1977) Chemistry of solfonylmethyl isocyanides. 13. A general one-step synthesis of nitriles from ketones using tosylmethyl isocyanide. Introduction of a one-carbon unit. J Org Chem 42:3114–3118

62. Greiner E, Schottenberger H, Wurst K, Schmidhammer H (2001) Novel class of morphinans with acrylonitrile incorporated substructures as key intermediates for non-oxygen-bridged opioid ligands. J Am Chem Soc 123:3840–3841

63. Schütz J, Windisch P, Kristeva E, Wurst K, Ongania K-H, Horvath UIE, Schottenberger H, Laus G, Schmidhammer H (2005) Mechanistic diversity of the van Leusen reaction applied to 6-ketomorphinans and synthetic potential of the resulting acrylonitrile substructures. J Org Chem 70:5323–5326

64. Botros S, Lipkowski AW, Larson DL, Stark AP, Takemori AE, Portoghese PS (1989) Opioid agonist and antagonist activities of peripherally selective derivatives of naltrexamine and oxymorphamine. J Med Chem 32:2068–2071

65. Portoghese PS, Farouz-Grant F, Sultana M, Takemori AE (1995) 7′-Substituted amino acid conjugates of naltrindole. Hydrophilic groups as determinants of selective antagonism of δ$_1$ opioid receptor-mediated antinociception in mice. J Med Chem 38:402–407

66. Schütz J, Brandt W, Spetea M, Wurst K, Wunder G, Schmidhammer H (2003) Synthesis of 6-amino acid substituted derivatives of the highly potent analgesic 14-O-methyloxymorphone. Helv Chim Acta 86:2142–2148

67. Riba P, Friedmann T, Király KP, Al-Khrasani M, Sobor M, Asim MF, Spetea M, Schmidhammer H, Fürst S (2010) Novel approach to demonstrate high efficacy of micro opioids in the rat vas deferens: a simple model of predictive value. Brain Res Bull 81:178–184

68. Fürst S, Riba P, Friedmann T, Tímar J, Al-Khrasani M, Obara I, Makuch W, Spetea M, Schütz J, Przewlocki R, Przewlocka B, Schmidhammer H (2005) Peripheral versus central

antinociceptive actions of 6-amino acid-substituted derivatives of 14-*O*-methyloxymorphone in acute and inflammatory pain in the rat. J Pharmacol Exp Ther 312:609–618

69. Schmidhammer H, Schratz A, Mitterdorfer J (1990) Synthesis and biological evaluation of 14-alkoxymorphinans. 8. 14-Methoxymetopon, an extremely potent opioid agonist. Helv Chim Acta 73:1784–1787

70. Freye E, Schmidhammer H, Latasch L (2000) 14-Methoxymetopon, a potent opioid, induces no respiratory depression, less sedation, and less bradycardia than sufentanil in the dog. Anesth Analg 90:1359–1364

71. Zernig G, Saria A, Krassnig R, Schmidhammer H (2000) Signal transduction efficacy of the highly potent μ-opioid agonist 14-methoxymetopon. Life Sci 66:1871–1877

72. Urigüen L, Fernandez B, Romero EM, De Pedro N, Delgado MJ, Guaza C, Schmidhammer H, Viveros MP (2002) Effects of 14-methoxymetopon, a potent opioid agonist, on the responses to the tail electric stimulation test and plus-maze activity in male rats: neuroendocrine correlates. Brain Res Bull 57:661–666

73. King MA, Su W, Nielan C, Chang AH, Schütz J, Schmidhammer H, Pasternak GW (2003) 14-Methoxymetopon, a very potent μ-opioid analgesic with an unusual pharmacological profile. Eur J Pharmacol 459:203–209

74. Spetea M, Tóth F, Schütz J, Ötvös F, Tóth G, Benyhe S, Borsodi A, Schmidhammer H (2003) Binding characteristics of [^{3}H]14-methoxymetopon, a high affinity μ-opioid receptor agonist. Eur J Neurosci 18:290–295

75. Bileviciute-Ljungar I, Spetea M, Guo Y, Schütz J, Windisch P, Schmidhammer H (2006) Peripherally mediated antinociception of the μ-opioid receptor agonist 2-[(4, 5α-epoxy-3-hydroxy-14β-methoxy-17-methylmorphinan-6β-yl)amino]acetic acid (HS-731) after subcutaneous and oral administration in rats with carrageenan-induced hindpaw inflammation. J Pharmacol Exp Ther 317:220–227

76. Király KP, Riba P, D'Addario C, Di Benedetto M, Landuzzi D, Candelotti S, Romualdi P, Fürst S (2006) Alterations in prodynorphin gene expression and dynorphin levels in different brain regions after chronic administration of 14-methoxymetopon and oxycodone-6-oxime. Brain Res Bull 70:233–239

77. Mahurter L, Garceau C, Marino J, Schmidhammer H, Toth G, Pasternak GW (2006) Separation of binding affinity and intrinsic activity of the potent μ-opioid 14-methoxymetopon. J Pharmacol Exp Ther 319:247–253

78. Sabino V, Cottone P, Steardo L, Schmidhammer H, Zorrilla EP (2007) 14-Methoxymetopon, a highly potent μ opioid agonist, biphasically affects ethanol intake in sardinian alcohol-preferring rats. Psychopharmacology 192:537–546

79. Fürst S, Búzás B, Friedmann T, Schmidhammer H, Borsodi A (1993) Highly potent novel opioid receptor agonist in the 14-alkoxymetopon series. Eur J Pharmacol 236:209–215

80. Stegmann GF (1999) Etorphine-halothane anaesthesia in two five-year-old African elephants (*Loxodonta africana*). J S Afr Vet Assoc 70:164–166

81. Sterken J, Troubleyn J, Gasthuys F, Maes V, Diltoer M, Verborgh C (2004) Intentional overdose of large animal immobilon. Eur J Emerg Med 11:298–301

82. Feinberg AP, Creese I, Snyder SH (1976) The opiate receptor: a model explaining structure-activity relationships of opiate agonists ad antagonists. Proc Natl Acad Sci USA 73:4215–4219

83. Casy AF, Parfitt RT (1986) Opioid analgesics: chemistry and receptors. Plenum, New York

84. Spetea M, Schüllner F, Moisa RC, Berzetei-Gurske IP, Schraml B, Dörfler C, Aceto MD, Harris LS, Coop A, Schmidhammer H (2004) Synthesis and biological evaluation of 14-alkoxymorphinans. 21. Novel 4-alkoxy and 14-phenylpropoxy derivatives of the μ opioid receptor antagonist cyprodime. J Med Chem 47:3242–3247

85. Spetea M, Greiner E, Aceto MD, Harris LS, Coop A, Schmidhammer H (2005) Effect of a 6-cyano substituent in 14-oxygenated *N*-methylmorphinans on opioid receptor binding and antinociceptive potency. J Med Chem 48:5052–5055

86. Stein C, Clark JD, Oh U, Vasko MR, Wilcox GL, Overland AC, Vanderah TW, Spencer RH (2009) Peripheral mechanisms of pain and analgesia. Brain Res Rev 60:90–113

87. Stein C, Schäfer M, Machelska H (2003) Attaching pain at its source: new perspectives on opioids. Nat Med 9:1003–1008

88. Walker JS (2003) Anti-inflammatory effects of opioids. Adv Exp Med Biol 521:148–160

89. Smith HS (2008) Peripherally-acting opioids. Pain Physician 11:S121–S132

90. Iorio MA, Frigni V (1984) Narcotic agonist/antagonist properties of quaternary diastereo-isomers derived from oxymorphone and naloxone. Eur J Med Chem 19:301–303

91. Larson DL, Hua M, Takemori AK, Portoghese PS (1993) Possible contribution of a glutathione conjugate to the long-duration action of β-funaltrexamine. J Med Chem 36:3669–3673

92. Spetea M, Friedmann T, Riba P, Schütz J, Wunder G, Langer T, Schmidhammer H, Fürst S (2004) *In vitro* opioid activity profiles of 6-amino acid substituted derivatives of 14-*O*-methyloxymorphone. Eur J Pharmacol 483:301–308

93. Al-Khrasani M, Spetea M, Friedmann T, Riba P, Kiraly K, Schmidhammer H, Fürst S (2007) DAMGO and 6β-glycine substituted 14-*O*-methyloxymorphone but not morphine show peripheral, preemptive antinociception after systemic administration in a mouse visceral pain model and high intrinsic efficacy in the isolated rat vas deferens. Brain Res Bull 74:369–375

94. Obara I, Makuch W, Spetea M, Schütz J, Schmidhammer H, Przewlocki R, Przewlocka B (2007) Local peripheral antinociceptive effects of 14-*O*-methyloxymorphone derivatives in inflammatory and neuropathic pain in the rat. Eur J Pharmacol 558:60–67

95. Spetea M, Erlandsson Harris H, Berzetei-Gurske IP, Klareskog L, Schmidhammer H (2001) Binding, pharmacological and immunological profiles of the δ-selective opioid receptor antagonist HS 378. Life Sci 69:1775–1782

96. D'Ambrosio A, Noviello L, Negri L, Schmidhammer H, Quintieri F (2004) Effect of novel non-peptidic δ opioid receptor antagonists on human T and B cell activation. Life Sci 75:63–75

97. Tryoen-Toth P, Decaillot FM, Filliol D, Befort K, Lazarus LH, Schiller PW, Schmidhammer H, Kieffer BL (2005) Inverse agonism and neutral antagonism at wild type and constitutively active mutant δ opioid receptors. J Pharmacol Exp Ther 313:410–421

98. Jenny M, Winkler C, Spetea M, Schennach H, Schmidhammer H, Fuchs D (2008) Non-peptidic δ-opioid receptor antagonists suppress mitogen-induced tryptophan degradation in peripheral blood mononuclear cells *in vitro*. Immunol Lett 118:82–87

99. Cao CQ, Hong YG, Dray A, Perkins MN (2001) Selective depression of nociceptive responses of dorsal horn neurones by SNC80 in a perfused hindquarter preparation of adult mouse. Neuroscience 107:329–338

100. Cao CQ, Hong YG, Dray A, Perkins MN (2001) Spinal δ opioid receptors mediate suppression of systemic SNC80 on excitability of the flexor reflex in normal and inflamed rat. Eur J Pharmacol 418:79–87

101. Shahbazian A, Heinemann A, Schmidhammer H, Beubler E, Holzer-Petsche U, Holzer P (2002) Involvement of μ- and κ-, but not δ-opioid receptors in the peristaltic motor depression caused by endogenous and exogenous opioids in the guinea-pig intestine. Br J Pharmacol 135:741–750

102. Arakawa K, Akami T, Okamoto M, Nakajima H, Mitsuo M, Nakai I, Oka T, Nagase H, Matsumoto S (1992) Immunosuppressive effects of δ-opioid receptor antagonist on xenogeneic mixed lymphocyte response. Transplant Proc 24:696–697

103. Arakawa K, Akami T, Okamoto M, Akioka K, Akai I, Oka T, Nagase H (1993) Immunosuppression by δ opioid receptor antagonist. Transplant Proc 25:738–740

104. Linner KM, Stickney BJ, Quist HE, Sharp BM, Portoghese PS (1998) The δ_1 opioid receptor antagonist, 7-benzylspiroindanylnaltrexone, prolongs renal allograft survival in a rat model. Eur J Pharmacol 354:R3–R5

105. Gavériaux-Ruff C, Filliol D, Simonin F, Matthes HWD, Kieffer BL (2001) Immunosuppression by δ-opioid antagonist naltrindole: δ- and triple μ/δ/κ-opioid receptor knockout mice reveal a nonopioid activity. J Pharmacol Exp Ther 298:1193–1198
106. Winkler C, Neurauter G, Schroecksnadel K, Wirleitner B, Fuchs D (2006) Immunomodulatory effects of plant extracts. In: Govil JN, Singh VK, Arunachalam C (eds) Recent progress in medicinal plants, vol 11. Studium, Houston, pp 139–158

14-Amino-4,5-Epoxymorphinan Derivatives and Their Pharmacological Actions

John W. Lewis and Stephen M. Husbands

Abstract 14-Hydroxy-7,8-dihydromorphinone (oxymorphone) and its derivatives (oxycodone, naloxone, naltrexone) have become among the most important clinical agents to have been produced from opium. 14-Aminocodeinone and its 7,8-dihydro and morphinone derivatives are of more recent origin thanks to the work of Professor Gordon Kirby and his collaborators. The 14-amino parent compounds have proved of limited interest but their 14-acylamino- and 14-alkylamino derivatives have been extensively studied. The 4′-substituted cinnamoylamino-17-cyclopropylmethyl-7,8-dihydronormorphinones, C-CAM and M-CAM are the best available selective MOR irreversible antagonists and the related dihydrocodeinone MC-CAM, 4′-chloro-cinnamoylamino-17-cyclopropylmethyl-7,8-dihydronorcodeinone, is a long-acting MOR partial agonist with extended MOR-pseudoirreversible antagonist activity that could be a candidate for pharmacotherapy of opiate abuse/dependence.

Keywords Agonist, Antagonist, Epoxymorphinan, MOR, Opioid

Contents

S.M. Husbands (✉) and J.W. Lewis
Department of Pharmacy and Pharmacology, University of Bath, Bath BA2 7AY, UK
e-mail: S.M.Husbands@bath.ac.uk

Abbreviations

CBM   Cyclobutylmethyl
CPM   Cyclopropylmethyl
DOR   Delta opioid receptor
GTPγS   Guanosine 5′-O-[gamma-thio]triphosphate
i.c.v.   Intracerebroventricular
i.p.   Intraperitoneal
KOR   Kappa opioid receptor
MOR   Mu opioid receptor
s.c.   Subcutaneous
TF   Tail flick
TW   Tail withdrawal

1   Introduction

Naturally occurring and semisynthetic epoxymorphinans (**1**, **2**) (Fig. 1) have proved to be of the utmost importance as analgesics for the treatment of moderate to severe pain as a result of their agonist actions at the mu opioid receptor (MOR).

1a: R = Me, codeine   2a: R = Me, R'= H, hydrocodone   3a: R= H, R'= CH₂CH=CH₂, Naloxone
1b: R = H, morphine   2b: R=R'= H, hydromorphone   3b: R= H, R'= CPM, Naltrexone
                         2c: R= Me, R'= OH, oxycodone   3c: R= Me, R'= CH₂CH=CH₂
                         2d: R= H, R'= OH, oxymorphone   3d: R= Me, R'= CPM

4: Methylnaltrexone   5

5-9
a: R= (CH₂)ₙCH₃
b: R= CH=CHC₆H₅

6: R'= CH₂CH=CH₂
7: R'= CH₂CH=C(Me)₂
8: R'= CPM
9: R'= CBM
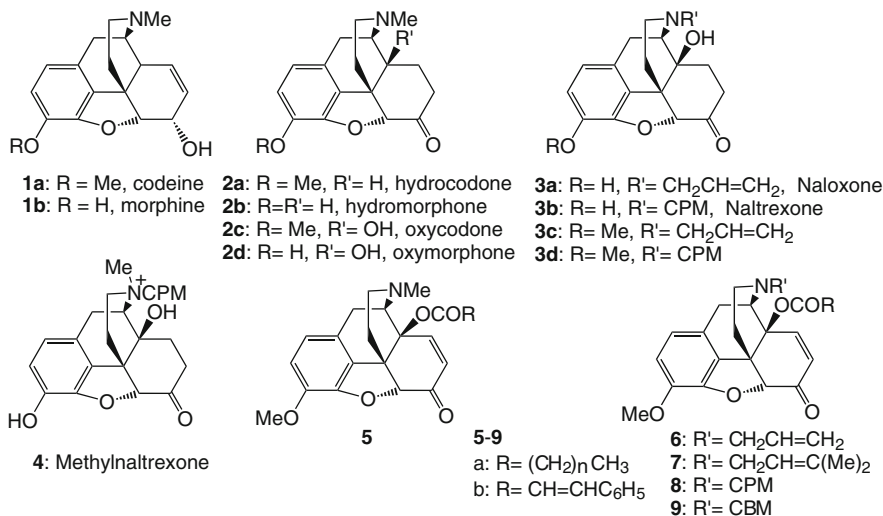
Fig. 1 Epoxymorphinans and epoxymorphinones

The 17-*N*-allyl-(naloxone, **3a**) and 17-*N*-cyclopropylmethyl (naltrexone, **3b**) analogues of oxymorphone (**2d**) are the prototype opioid receptor antagonists with some selectivity for MOR. They have entered clinical practice as treatments for narcotic overdose (naloxone) and alcoholism or opioid abuse/dependence (naltrexone). The 17-quaternary derivative of naltrexone, methylnaltrexone (**4**) has recently been introduced into clinical practice as a treatment for opiate-induced bowel dysfunction [1].

Acylation of the 14-hydroxyl group of 14-hydroxycodeinone gave esters (**5**) (Fig. 1) in which antinociceptive potency increased with the length of the alkyl chain in the acyl group (**5a**) peaking in the heptanoyloxy derivative (**5a**, *n* = 5) which had 60 times the potency of morphine [2], a level of potency that was matched by the cinnamoyloxy derivative (**5b**) [3]; further increases in the chain length reduced potency [2].

A series of 14-*O*-acyl derivatives of 17-allyl-, 17-dimethylallyl-, 17-cyclopropylmethyl- and 17-cyclobutylmethyl-7,8-dihydronorcodeinones (**6–9**) (Fig. 1) were patented as safe analgesics with favourable dependence profiles [4]. The pentanoyloxy and hexanoyloxy derivatives in the 17-cyclopropylmethyl series (**8a**; *n* = 3,4) had the highest potency in the antiwrithing test in mice. Acylation of the 14-hydroxyl group increased the antinociceptive potency of **3d** by two orders of magnitude so that **8a** (*n* = 3,4) were as potent as morphine.

It was at this time that we, at Reckitt and Colman became interested in the work of Professor Gordon Kirby on Diels–Alder reactions of thebaine with nitroso derivatives with the objective of providing a viable synthesis of 14-aminocodeinone. This would allow access to a wide range of 14-acylamino- and 14-alkylamino-codeinones and morphinones which could be improvements on the available derivatives of 14-hydroxycodeinone and oxycodone.

The first indication that derivatives of 14-aminocodeinone and 14-aminomorphinone could be accessible came from the reaction of thebaine with nitrosobenzene to yield a cyclic adduct (**10a**) which yielded 14β-phenylaminodihydrocodeinone (**11a**) on sequential hydrolysis and reduction (Scheme 1) [5]. Schwab then utilised this chemistry for the synthesis of a small series of 14-phenylaminodihydrocodeinones and derivatives (**11**) [6]. Some codeinone derivatives produced by these reactions were evaluated in antinociceptive assays, showing that the *N*-methyl derivatives (**11a,b**) had substantial activity in the writhing assay but only weak

9: R = Me or CPM

10a: R = Me, Aryl = Ph
10b: R = Me, Aryl = 4'-F-Ph
10c: R = CPM, Aryl = Ph
10d: R = CPM, Aryl = 4'-F-Ph

11a: R = Me, Aryl = Ph
11b: R = Me, Aryl = 4'-F-Ph
11c: R = CPM, Aryl = Ph
11d: R = CPM, Aryl = 4'-F-Ph
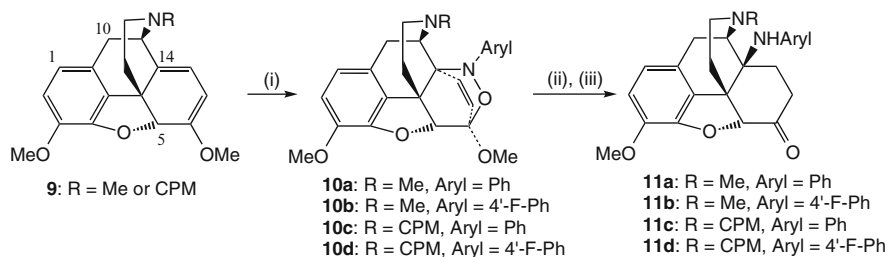
Scheme 1 (i) Nitrosoarene, CHCl$_3$, 57–96%; (ii) 1 N HCl, 86–91%; (iii) H$_2$, 10% Pd/C, 22–57%

activity in the more demanding tail withdrawal (TW) assay (54 °C water). In this assay the 17-cyclopropylmethyl analogues (**11c,d**) displayed modest morphine antagonist activity [6].

2 Synthesis

2.1 Synthesis of 14-Aminocodeinone, 14-Aminomorphinone and Their 7,8-Dihydro Analogues

Utilising the ability of thebaine (**9**) to react with electrophiles, the first viable synthesis of 14-aminocodeinone (**13**) was by initial nitration of thebaine with the mild nitrating agent tetranitromethane (Scheme 2). The reaction produced highest yields, though these are not recorded, in the presence of ammonia, but resulted in the generation of the ammonium salt of trinitromethane which is hazardous due to its thermal instability [7]. Nevertheless, 14β-aminocodeinone (**13**) and its 17-cyclopropylmethyl analogue (**26**) were prepared by this method in sufficient quantity to allow synthesis, characterization and pharmacological evaluation of close
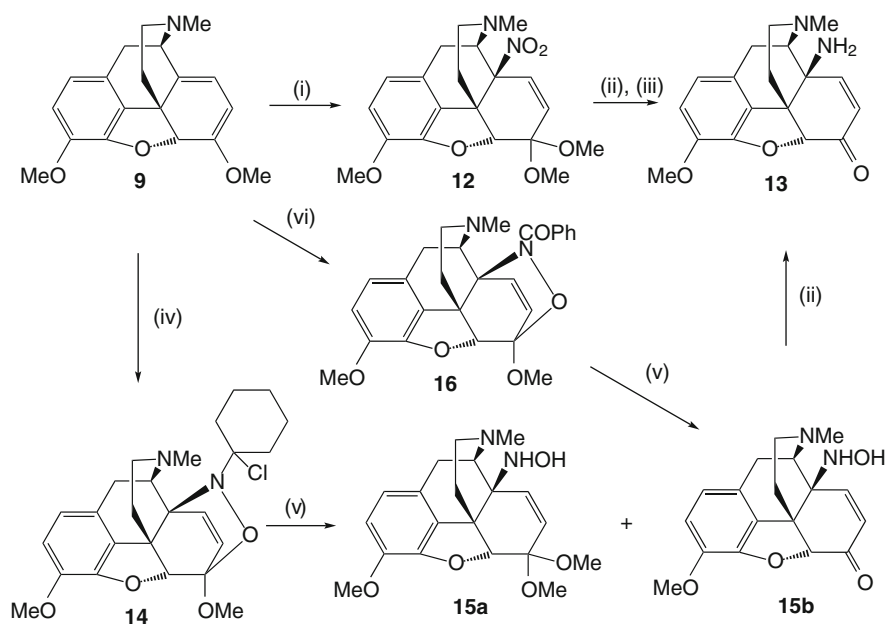
Scheme 2 (i) Tetranitromethane, methanolic ammonia, rt; (ii) Zn, NH$_4$Cl, MeOH, reflux; (iii) 2 N HCl; (iv) 1-chloro-1-nitrosocyclohexane; (v) aqueous methanolic HCl, yield over steps iv, v, ii 35%; (vi) benzohydroxamic acid, tetraethylammonium periodate, 97%

to 300 opioid ligands listed in two patents [8, 9] resulting from the collaboration of Reckitt and Colman with Professor Kirby.

At this time, efforts were also being made to extend the scope of the Diels–Alder chemistry of thebaine. Horsewood and Kirby [10] found that reaction of thebaine with 1-chloro-1-nitrosocyclohexane which, following hydrolysis with methanolic HCl, gave 14-hydroxyaminocodeinone **15b** (Scheme 2), via adduct **14**. This method was never widely adopted, only finding limited use within the medicinal chemistry community [11]. Similarly, **15b** was also obtained through reaction of thebaine with benzohydroxamic acid in the presence of tetraethylammonium periodate, to generate the corresponding nitrosocarbonyl compound *in situ*, and thence the adduct **16**, followed by hydrolysis in methanolic HCl [12].

Further improvements in the synthesis of **13**, using *in situ* generated nitrosoformates, were made by the Kirby group (Scheme 3) [13]. This method has proven both more convenient and higher yielding than the earlier methods. In brief, 2,2,2-trichloroethyl *N*-hydroxycarbamate was oxidised by sodium periodate in the presence of thebaine to yield adduct (**17**) which was converted into (**18**) before zinc powder mediated reduction to an amino acetal and hydrolysis to 14-aminocodeinone (**13**).

Variations on this synthetic route remain the method of choice for accessing derivatives of 14-aminocodeinone. Improvements were made through process research at Reckitt & Colman (now Reckitt Benckiser). In this modification, adduct (**17**) was treated with ethylene glycol and trimethylorthoformate followed by acetyl chloride to yield ethylene ketal (**19**) (Scheme 3). This was reduced using zinc in ammonium carbonate with subsequent hydrolysis to the codeinone (**13**). This remains the current method of choice.

The equivalent 14-aminodihydrocodeinone (**20a**) can be reached by direct hydrogenation of (**13**) (Scheme 4) [11, 14], giving an overall yield for the thebaine to 14β-aminodihydrocodeinone conversion in the range 50–60%. A more direct
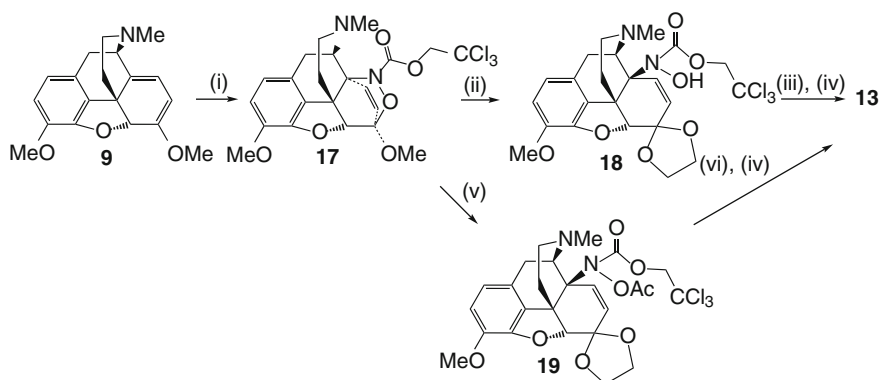
Scheme 3 (i) 2,2,2-Trichloroethyl *N*-hydroxycarbamate, sodium periodate, 0.5 M NaOAc, EtOAc, pH 6, 0 °C, 82%; (ii) ethylene glycol, HCl, CH$_2$Cl$_2$, 95%; (iii) Zn, glycolic NH$_4$Cl, 80%; (iv) HCl(aq), MeOH, 80%; (v) ethylene glycol, trimethylorthoformate, CH$_2$Cl$_2$ then AcCl; (vi) Zn, NH$_4$CO$_3$
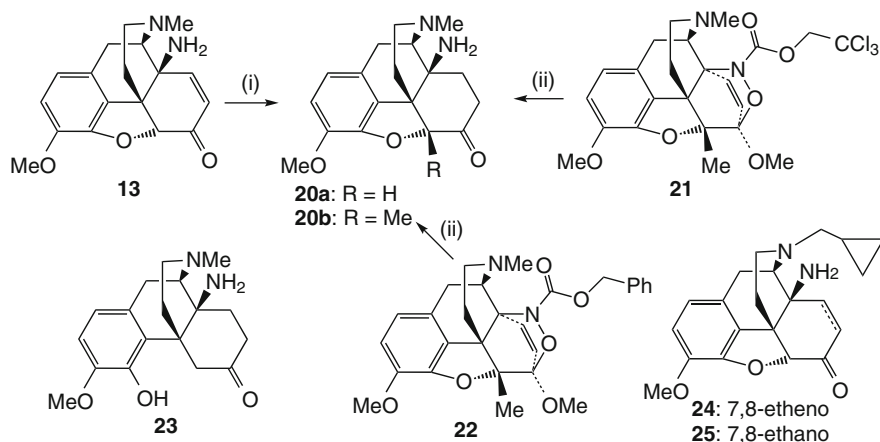
Scheme 4 (i) H$_2$, 10% Pd/C, MeOH; (ii) H$_2$, 10% Pd/C, MeOH, NaOAc/HOAc buffer, 73% (**21** → **20b**), 82% (**22** → **20b**)

method, involving catalytic reduction of the adduct (**21**), is possible with **20b**, having a 5β-methyl group [15]. This latter method has also been updated by Archer and colleagues [16] in which benzyl *N*-hydroxycarbamate replaces the trichloroethyl ester to furnish adduct (**22**), with catalytic reduction giving dihydrocodeinone (**20b**) in excellent yield (76% from thebaine) (Scheme 4). This direct route to **20b** does not work reliably for **20a**, with treatment of **17** under the same conditions leading to hydrogenolysis of the oxide bridge and formation of the C4-phenol (**23**) [17].

Access to the equivalent 17-cyclopropylmethyl compounds (**24**, **25**) uses the same chemistry, but starting from 17-cyclopropylmethylnorthebaine. The yield of around 20% for the synthesis of **25** from 17-cyclopropylmethylnorthebaine using this method is substantially reduced compared to the 17-methyl series where the yield is typically 50–60%. The corresponding morphinones are then reached by boron tribromide mediated 3-O-demethylation [18, 19].

2.2 Synthesis of 14-Acylamino- and 14-Alkylamino-Codeinones and Morphinones

Alkyl and acyl derivatives (**28**, **30**) of 14-aminocodeinones (**13**, **26**) and dihydro-codeinones (**20a**, **27**) are readily prepared; acylation is achieved under standard conditions of acid chloride or acid anhydride in the presence of an organic base, while alkylation can be achieved directly with an alkyl halide or by acylation and then lithium aluminium hydride reduction (Scheme 5). In this latter method the 6-keto group is protected as an acetal [8, 9, 18, 19]. For direct alkylation with unactivated alkyl halides, carrying out the reaction in a sealed tube at 120 °C has
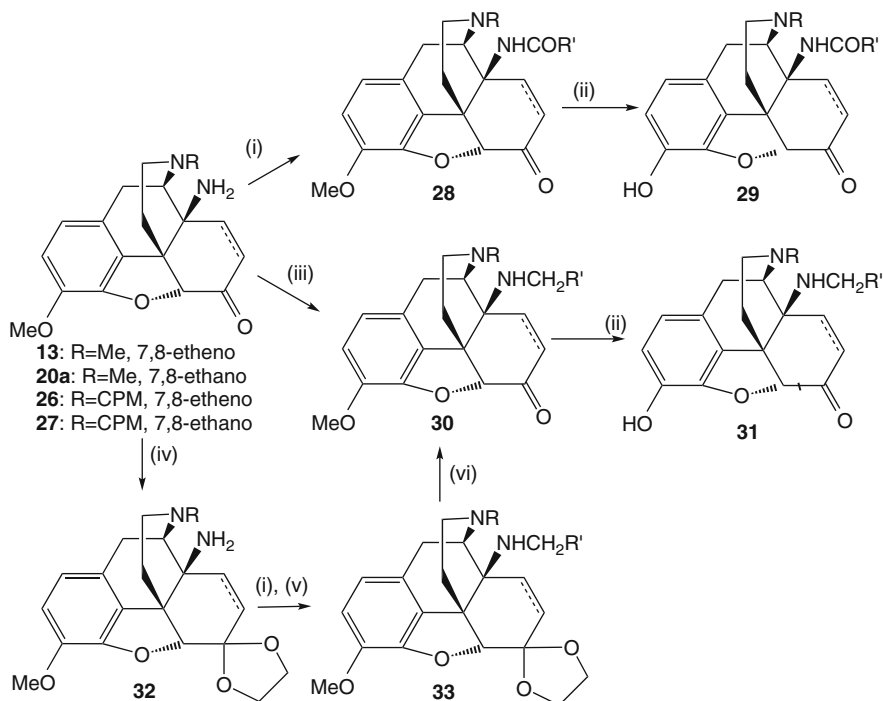
Scheme 5 (i) R′COCl or R′COOCOR′, NEt$_3$, 40–90%; (ii) BBr$_3$, CH$_2$Cl$_2$, 50–80%; (iii) R′CH$_2$X (X = halide), NaHCO$_3$, 35–80%; (iv) ethylene glycol, HCl, CH$_2$Cl$_2$; (v) LiAlH$_4$, THF, 60%
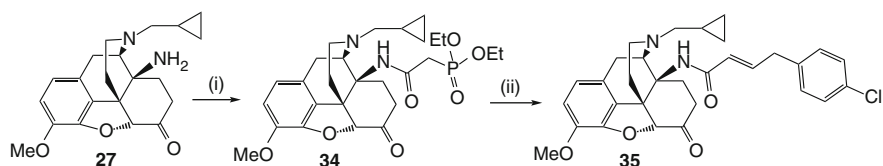
Scheme 6 (i) (EtO)$_2$P(O)CH$_2$COCl, THF, 60%; (ii) LDA, THF then 4-chlorophenylacetaldehyde, 28%

proven beneficial [20]. The corresponding morphinones (**29**, **31**) are then reached by boron tribromide mediated 3-O-demethylation [18, 19]. Morphinones can be converted into alternative 3-*O*-alkyl ethers (**41**), in high yield, through the use of an appropriate alkyl halide, potassium carbonate in wet acetone [21].

The instability of 4-(4′-chlorophenyl)-2-butenoic acid led to an alternative strategy for the preparation of (**35**) (Scheme 6) [18]. The protocol involved Horner–Wadsworth–Emmons-type chemistry, initially acylating with diethoxy-phosphorylacetyl chloride before treatment with lithium diisopropylamide and 4-chlorophenylacetaldehyde.

3   Pharmacology

3.1   *Pharmacological Activities of 14-Acylaminomorphinones, 14-Alkylaminomorphinones, the Equivalent Codeinones and Their 17-Cyclopropylmethyl Analogues*

With the availability of a viable synthesis of 14-aminocodeinone (**13**) and the closely related analogues **20a**, **26** and **27**, Reckitt and Colman in collaboration with Professor Kirby set about the synthesis of a whole range of 14-alkylamino-, 14-arylalkylamino- and 14-acylaminocodeinones and equivalent morphinones as well as the 7,8-dihydro analogues and the *N*-cyclopropylmethyl equivalents. The synthesised compounds were listed in two patents, US 4,241,066 and US 4,241,067 [8, 9]. Many of them were evaluated in a primary screen for MOR activity, *in vitro* in the mouse vas deferens assay and *in vivo* in rat antinociceptive assays (Tables 1 and 2). In the *in vivo* assays tail pressure was the nociceptive stimulus for agonist activity, whereas for morphine antagonism warm water (55 °C) was used with tail withdrawal as the end point.

MOR agonist potency increased in the series of acylaminomorphinones (**36c**) (Fig. 2) peaking at the hexanoylamino derivative [$R'' = (CH_2)_4CH_3$] which was over 4000-times more potent than normorphine *in vitro*, though only 100-fold more potent than morphine *in vivo* (Table 1). This structure–activity relationship closely matches that found in the 14-*O*-acylcodeinones [2]. In the alkylaminomorphinone series (**37c**) the peak of activity was reached with the hexylamino derivative [$R'' = (CH_2)_4CH_3$] which was 1,000 times more potent than normorphine *in vitro* and with the same potency advantage over morphine *in vivo*. When a phenyl group was located at the end of an acylamino side chain, peak activity was reached in the phenylpropiolylamino derivative [**36c**, $R'' = Ph(CH_2)_2$] which was over 700 times more potent *in vitro* and 200 times more potent *in vivo* than normorphine and morphine, respectively (Table 1).

In the 14-acylamino-17-cyclopropylmethylnormorphinone series (**36d**) the lower members (formylamino-, acetylamino- and propanoylamino-) were potent MOR antagonists *in vitro* equal or more potent than naloxone but with much lower activity *in vivo* (Table 2). This may be due to relatively rapid metabolic hydrolysis to the hydrophilic 14-amino parent (**38**) which had a similar loss of *in vivo* activity when compared to its *in vitro* potency. From the 14-butanoylamino derivative through to heptanoylamino- [**36d**: $R'' = (CH_2)_2CH_3$ through $(CH_2)_5CH_3$] the *N*-cyclopropylmethyl derivatives were MOR partial agonists *in vitro* with increasing potency as agonists but retaining potent antagonist potency. MOR agonism *in vivo* peaked at hexanoylamino- but surprisingly none of the ligands had significant MOR antagonism *in vivo* (Table 2).

The 14-alkylamino-17-cyclopropylaminonormorphinone series (**37d**) *in vitro* showed substantial differences from the acylamino equivalents (**36d**). From methylamino- through to hexylamino- they had no agonist activity *in vitro* but were potent

Table 1 *In vitro* and *in vivo* agonist activity of compounds of structures **36** and **37** (Fig. 2)

	R″	*In vitro* potency times normorphine[a]	*In vivo* potency times morphine[b]
36a	Me	0.1	0.17
	n-Pr	2.1	2.8
	n-Bu	3.7	3.8
	n-Pent	77	27
	n-Hex	168	31
	n-Hept	36	8.9
36c	Me	0.4	0.44
	n-Pr	32	12
	n-Bu	191	56
	n-Pent	4000	117
	n-Hex	628	82
	n-Hept	394	61
	Ph	38	18
	CH_2Ph	272	148
	$(CH_2)_2Ph$	744	222
	$(CH_2)_3Ph$	490	7.0
	$(CH_2)_4Ph$	32	11
37a	Me	0.2	0.67
	Et	0.15	0.73
	n-Pr	0.25	2.4
	n-Bu	0.9	2.0
	n-Pent	8.1	6.6
	n-Hex	30	73
	n-Hept	46	9.4
37c	n-Pr	20	65
	n-Bu	39	11
	n-Pent	220	297
	n-Hex	1,000	980
	n-Hept	538	408
	n-Oct	289	153
	CH_2Ph	32	34
	$(CH_2)_2Ph$	3370	2512
	$(CH_2)_3Ph$	1,500	ND
	$(CH_2)_4Ph$	508	ND
	$(CH_2)_5Ph$	329	ND

[a]Determined in the mouse vas deferens
[b]Determined in rat tail pressure test

antagonists. The heptylamino- derivative retained potent antagonism *in vitro* but also had mouse vas deferens agonist activity of greater potency than normorphine. It was also active in the rat tail pressure test of analgesic activity (Table 2).

From the initial evaluation of the large number of 14-acylamino- and 14-alkylamino-codeinones and morphinones synthesised in the Reckitt and Colman programme, it became clear that the C14 side chains of particular interest were those with an aryl group joined to C14 by an alkyl group of two to four carbon atoms with three carbon chain compounds having special qualities. Lewis et al. [14] revealed

Table 2 *In vitro* and *in vivo* activity of compounds of structure **36** and **37** (Fig. 2)

	R″	Agonist *in vitro* potency times normorphine[a]	Antagonist *in vitro* potency times naloxone[b]	Agonist *in vivo* potency times morphine[c]	Antagonist *in vivo* potency times naloxone[d]
36b	H	0.1	0.1	ND	<0.01
	Me	ND	0.3	ND	<0.01
	Et	0.1	<0.1	ND	ND
	n-Pr	1.0	<0.1	1.0	ND
	n-Bu	4.9	<0.1	49	ND
	n-Pent	22	<0.1	11	ND
	n-Hex	33	<0.1	13	ND
	n-Hept	23	<0.1	0.55	ND
36d	H	ND	6.0	ND	0.03
	Me	ND	1.0	ND	ND
	Et	<0.1	3.0	ND	0.07
	n-Pr	0.1	2.0	10	<0.01
	n-Bu	3.7	1.0	30	ND
	n-Pent	23	2.0	136	<0.1
	n-Hex	32	0.5	100	<0.05
37d	H	<0.1	3.0	ND	0.28
	Me	<0.1	1.0	ND	0.28
	n-Bu	ND	1.0	ND	0.09
	n-Pent	<0.1	0.5	ND	0.12
	n-Hex	<0.1	0.7	ND	0.02
	n-Hept	3.0	0.5	0.5	0.05
	n-Oct	ND	1.3	0.5	<0.05
	CH₂Ph	<0.01[e]	1.0	0.33	ND

ND not determined

[a]Determined in mouse vas deferens

[b]Determined in mouse vas deferens vs normorphine

[c]Determined in rat tail pressure assay

[d]Determined in rat tail withdrawal vs morphine

[e]53 times normorphine in guinea pig ileum

36a: R = Me, R′ = Me
36b: R = Me, R′ = CPM
36c: R = H, R′ = Me
36d: R = H, R′ = CPM

37a: R = Me, R′ = Me
37b: R = Me, R′ = CPM
37c: R = H, R′ = Me
37d: R = H, R′ = CPM

38
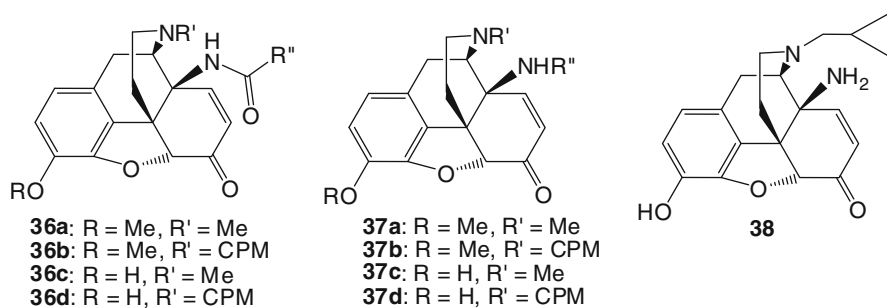
Fig. 2 14-Acyl- and 14-alkylaminomorphinones and codeinones

structure–activity relationships relating to substitution in the aromatic ring of the cinnamoylamino group, the effect of hydrogenation of cinnamoylamino to dihydrocinnamoylamino and morphinone to 7,8-dihydromorphinone as well as the

R = Me or CPM
R' = H or Me
R" = 2'- and 4'-Me, F, Cl, Br

(a) R' = Me, R" = 4'-Cl, MC-CAM
(b) R' = Me, R" = 4'-Br
(c) R' = Me, R" = 4'-Me, MM-CAM
(d) R' = H, R" = 4'-Cl, C-CAM
(e) R' = H, R" = 4'-Br
(f) R' = H, R" = 4'-Me, M-CAM
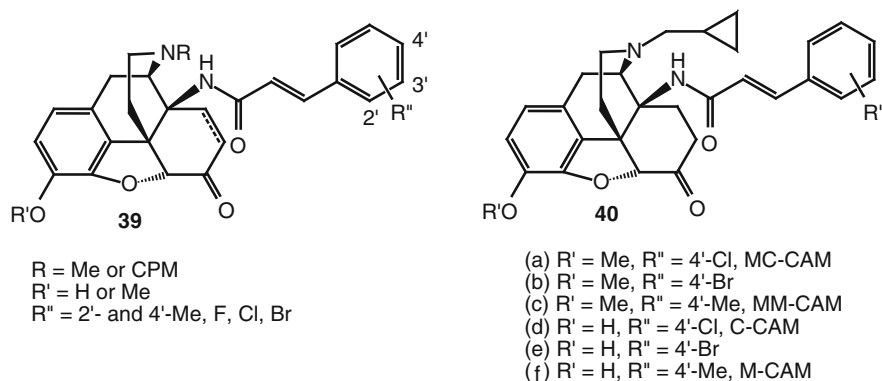
Fig. 3 14-Cinnamoylamino analogues

more usual relationships between codeinones and morphinones and 17-methyl to 17-cyclopropylmethyl groups (**39**) (Fig. 3). There was a clear effect of orientation of chloro and methyl groups, but not fluoro, in the cinnamoyl group; 4′-substitution substantially reduced MOR agonist efficacy whereas 2′- and 3′-substitution appeared to have relatively little effect when compared to the unsubstituted cinnamoylamino group. Thus the cinnamoylaminomorphinone **39** (R = Me, R′ = R″ = H) and its analogues substituted in the aromatic ring with 2′-chloro, 2′-methyl and 4′-fluoro groups had potencies as agonists in the mouse vas deferens assay of between 353 and 585 times that of normorphine. In the rat tail pressure *in vivo* assay they had ED_{50} values between 0.003 mg/kg and 0.014 mg/kg compared to morphine's ED_{50} of 0.66 mg/kg. The effect of hydrogenation of the 7,8-double bond was to reduce opioid receptor efficacy, though not dramatically; hydrogenation of the cinnamoylamino side-chain resulted in a more substantial increase in MOR efficacy [14].

3.2 Pharmacological Actions of 14-Cinnamoylamino-17-Cyclopropylmethyl-7,8-Dihydronormorphinones and Equivalent Codeinones

Attention was drawn to the 4′-substituted 14-cinnamoylamino-17-cyclopropyl-methyl-7,8-dihydronorcodeinones and equivalent morphinones (**40**) (Fig. 3). Of particular interest to Reckitt and Colman's target of buprenorphine-like opioid activity were the dihydrocodeinones (**40a–c**) from which the 4′-chloro derivative, called methoclocinnamox (**40a**, MC-CAM), was selected for detailed study. The Reckitt and Colman group had shown the three 4′-substituted dihydrocodeinones (**40a–c**) to be predominantly MOR partial agonists of long duration *in vivo* [14]. Importantly, MC-CAM showed bell-shaped dose–response curves in both tail withdrawal and tail pressure antinociceptive assays. In this respect and in the inability of naltrexone to reverse its antinociceptive effect, as well as its long-lived morphine antagonism, its similarity to buprenorphine was demonstrated.

The 4′-substituted dihydrocodeinones and morphinones (**40**) were the subject of a detailed study by the Drug Evaluation Committee of the National Institute on Drug Abuse [22]. This study confirmed, in a battery of mouse antinociceptive assays and in morphine-dependent rhesus monkeys, the long-acting MOR partial agonist activity of MC-CAM and its analogous 4′-bromo- and 4′-methylcinnamoylaminodihydrocodeinones. The dihydromorphinone (**40d**, clocinnamox; C-CAM) related to MC-CAM and the related 4′-bromo- (**40e**) and 4′-methylcinnamoylamino- (**40f**, M-CAM) analogues were shown to have little or no antinociceptive activity in mice but to have extremely long duration of morphine antagonism in the tail flick (TF) assay [22].

In withdrawn morphine-dependent rhesus monkeys, the morphinones exacerbated withdrawal at very low doses. Withdrawal effects persisted even after morphine administration (3 mg/kg, 6 hourly) was resumed [23]. Self-administration and drug discrimination studies in rhesus monkeys were also included in this report. In the drug discrimination assay the codeinones all generalised to codeine. The 4′-bromo- and 4′-methylcinnamoylaminodihydrocodeinones (**40b**, **40c**) were also self-administered but at rates that were below those of codeine [22]. These results confirmed the MOR partial agonist character of the codeinones.

Preliminary metabolism studies in rats and cynomolgus monkeys showed that MC-CAM was substantially O-demethylated to C-CAM [14]. Thus the delayed long-term morphine antagonism displayed by MC-CAM could have been caused by its transformation to C-CAM. That this was probably not the case was later shown by i.c.v. administration of MC-CAM which resulted only in MOR antagonist activity [24].

Investigations of the detailed pharmacology of C-CAM were initiated by Woods and collaborators. Comer et al. [25] used the TW test to assess the antinociceptive effects of morphine and fentanyl in the presence of C-CAM. Low doses of C-CAM (e.g. 3.2 mg/kg) produced rightward shifts in the dose–response curves of both morphine and fentanyl whereas high doses (>3.2 mg/kg) substantially depressed the maximum effect of morphine with the highest dose (32 mg/kg) also producing the suggestion of suppression of the effect of fentanyl. This is consistent with the designation of fentanyl as a more efficacious MOR agonist than morphine and suggested an irreversible MOR antagonist effect of C-CAM. The highest dose of C-CAM (32 mg/kg) antagonised the antinociceptive effect of morphine for up to 8 days. The irreversible nature of C-CAM's MOR antagonism was confirmed *in vivo* and in binding experiments by Burke et al. [26]. However, when mouse brain membranes were incubated with [^{3}H]C-CAM followed by precipitation of the protein, no specific radiolabelling of receptor protein was seen, suggesting C-CAM did not bind covalently to MOR. Following the initial evidence of C-CAM's ability to rank efficacy of MOR agonists [25], it was reported that C-CAM could be utilised to give efficacy and apparent affinity estimates for MOR agonists in mice [27], rhesus monkeys [28] and squirrel monkeys [29]. Relative efficacies of MOR agonists in drug discrimination assays using C-CAM have also been reported in pigeons [30] and rats [31].

Though the chloro-substituted 14-cinnamoylamino derivatives were the primary focus of attention during the 1990s, the analogue of C-CAM, 4′-methylcinnamoy-laminodihydromorphinone (M-CAM, **40f**) when compared to C-CAM and β-FNA was an even more impressive MOR irreversible antagonist. This was shown in a direct comparison of the three ligands [32]. Neither C-CAM or M-CAM had significant antinociceptive activity in the acetic acid-induced writhing assay and showed very low levels of stimulation of [^{35}S]GTPγS binding in MOR and delta opioid receptors (DORs) expressed in C6 cells and in kappa opioid receptors (KORs) expressed in CHO cells. β-FNA (32 mg/kg) effectively suppressed writh-ing (90% response) and in CHO-hKOR cells β-FNA stimulated [^{35}S]GTPγS bind-ing as a KOR partial agonist [33, 34]. M-CAM was more effective than C-CAM and β-FNA in suppressing MOR antinociceptive activity in TW (55 °C water) and in the writhing assay the order of potency in shifting the morphine dose–response curve rightwards was M-CAM > C-CAM > β-FNA. In this assay, which has a large receptor reserve, no flattening of the agonist dose–response curves by the irreversible antagonists was observed; M-CAM also demonstrated better selectivity for MOR over DOR and KOR, than C-CAM and β-FNA [32].

Woods et al. wrote a monograph on the pharmacology of methoclocinnamox (MC-CAM, **40a**) with comparison made to buprenorphine to determine whether it too could be of interest as a pharmacotherapy for opioid abuse [35]. MC-CAM and its parent phenol C-CAM had very similar high affinities (IC$_{50}$ 1.0 and 0.6 nM) for tritiated etorphine labelled binding sites. In the mouse vas deferens assay MC-CAM inhibited the electrically stimulated twitch with nanomolar potency, an effect that could be prevented by pre-incubation with naltrexone. In the [^{35}S]GTPγS assay MC-CAM was not an agonist at any of the three opioid receptors, but was an antagonist with approximately tenfold selectivity for MOR over KOR and DOR [19].

In mouse antinociceptive assays MC-CAM was inactive in the TF and the TW assays. It was active in the acetic acid-elicited writhing assay in which it was fully active at a dose of 3.2 mg/kg, the effect of which lasted for at least 8 h. MC-CAM's antiwrithing effect was prevented by naltrexone and β-FNA but not by the KOR antagonist norBNI or by the DOR antagonist naltrindole. However, when naltrex-one was used to reverse the antinociceptive effect of MC-CAM it was found to be effective for only the first hour after naltrexone administration. Thereafter the reversal effect of naltrexone was insignificant, representing conversion of a revers-ible agonist action of MC-CAM into antagonist-resistant agonism [35].

The antagonist actions of MC-CAM in the antinociceptive assays were investi-gated when it was administered 24 h before opioid receptor agonist challenge, i.e. when all agonist effects had dissipated. In TW (50 °C water), a high dose (32 mg/kg) of MC-CAM substantially flattened the morphine dose–response curve and effectively antagonised morphine even 4 days after its administration. In the acetic acid-elicited writhing assay this dose shifted the morphine dose–response curve threefold to the right but had no effect on the curves of the selective KOR agonist U69593 and the selective DOR agonist BW373U86 [35].

The agonist and antagonist effects of MC-CAM were investigated in a TW procedure in rhesus monkeys. Using 55 °C water MC-CAM was inactive but at

50 °C it had slow onset and reached the maximum possible effect after 2 h; this was maintained for 90 min when it declined to reach control levels at the 5th hour. MC-CAM's antagonist effect was studied in a dose of 1 mg/kg against the short-acting MOR agonist alfentanil in 55 °C water over 11 days. The antagonist effect of MC-CAM was demonstrable at 24 h pretreatment when the shift of the alfentanil dose–response curve was tenfold, peaked at 48 h when there was evidence of the flattening of the agonist's dose–response curve and was still evident after a week. After 11 days alfentanil's analgesic actions were fully restored [35].

MC-CAM like other MOR agonists was an effective reinforcer using a self-administration procedure that required relatively low capacity of the reinforcer [35, 36]. A dose of 1 mg/kg of MC-CAM was also able to reduce the reinforcing potency of the high efficacy MOR agonist alfentanil initially by 30-fold but significantly for 72 h. A higher dose (3.2 mg/kg) was also able to reduce cocaine self-administration but this effect was of short duration [35].

In morphine-dependent rhesus monkeys, MC-CAM substituted for morphine in withdrawn animals at a dose of 0.8 mg/kg but in non-withdrawn animals the same dose of MC-CAM produced signs of withdrawal slowly over a 3-day period; these signs were incompletely suppressed by regular morphine injections [35].

Although in the tests that had been applied to MC-CAM, buprenorphine showed close similarity, there were some notable differences. In particular MC-CAM's opioid antagonist effects were MOR-selective whereas buprenorphine also had KOR and DOR antagonism. In rhesus monkeys MC-CAM also appeared to have greater MOR agonist efficacy than buprenorphine in antinociceptive assays and, at least initially, unlike buprenorphine it suppressed morphine abstinence. Based on these similarities to, and differences from, buprenorphine, the ligand deserves consideration as a treatment for opioid abuse.

The Lewis and Husbands group have studied in some detail structure–activity relationships relating to the 14-cinnamoylaminodihydrocodeinones and morphinones [37]. In light of the possibility that the delayed morphine antagonism of MC-CAM could be due to its metabolism to C-CAM, a range of alternative phenolic ethers (**41**) (Fig. 4) of C-CAM were prepared and evaluated [21]. The study showed that, when compared to the methyl ether (**41a**, MC-CAM), the cyclopropylmethyl

41
(a) R' = Me
(b) R' = CPM
(c) R' = CH$_2$CH=CH$_2$
(d) R' = CH$_2$CN
(e) R' = (CH$_2$)$_2$CH$_3$
(f) R' = CH$_2$CCH
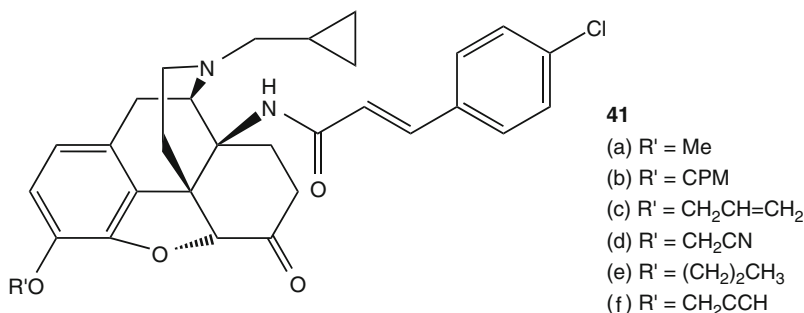
Fig. 4 Ethers of C-CAM

ether (**41b**) was devoid of MOR agonist effects in both mouse tail withdrawal and antiwrithing assays. Conversely, four of the other ethers (**41c–f**) had more agonist effect than MC-CAM since they were active in the TW assay (50 °C water) with the propargyl ether (**41f**) showing greatest activity, with potency at least equal to morphine, which was confirmed in the TF assay. All the new ethers had morphine antagonist activity in TW when they were administered 24 h before morphine and when their agonist effects had waned. The cyclopropylmethyl ether (**41b**) at 32 mg/kg flattened the morphine dose–response curve for more than 48 h and had antagonist effects for greater than 6 days. The overall conclusion from the study was that the results did not support the thesis that the delayed MOR antagonist activity of MC-CAM is due to its metabolism to C-CAM since the metabolic O-demethylation of MC-CAM should be a substantially faster process than other dealkylations and make MC-CAM a better MOR antagonist than the other ethers.

A significant finding was the effect of removal of the 3-phenolic hydroxyl group from C-CAM to give DOC-CAM (**42**, Fig. 5) [38]. In several series of opioids it has been shown that the 3-phenol has higher MOR affinity than the corresponding deoxy (3-*H*) and 3-methoxy analogues. However, in the 14-cinnamoylamino series DOC-CAM, MC-CAM and C-CAM have similar affinity for MOR in binding assays (Kis 0.54 nM, 0.46 nM and 0.25 nM, respectively) and DOC-CAM and C-CAM have similar potencies in antagonising the MOR agonist fentanyl in the [^{35}S]GTPγS assay (Kes 0.28 nM and 0.37 nM, respectively). The major difference between DOC-CAM and C-CAM lies in the lack of irreversible character in DOC-CAM's *in vivo* MOR antagonist activity. Thus it appears that binding of both the 3-oxygen atom and the cinnamoyl group is required for irreversible MOR antagonist activity.

Investigation of the influence of the chain length, position of the alkene group and reduction of the alkene and amide groups in the side chain of analogues of C-CAM was reported by Rennison et al. in compounds of general structure **43** (Fig. 6) [18]. MOR binding affinity for compounds having three carbon chains in the C14 substituent was substantially higher than for equivalent four or two carbon chains. The codeinones (**43**: R′ = Me) showed some selectivity for MOR over KOR

42 : DOC-CAM

Fig. 5 3-Deoxyclocinnamox

43

(a) X = COCH=CH

(b) X = COCH$_2$CH$_2$

(c) X = CH$_2$CH=CH

(d) X = (CH$_2$)$_3$

(e) X = COCH=CHCH$_2$

(f) X = COCH$_2$CH=CH

(g) X = CO(CH$_2$)$_3$

(h) X = CH$_2$CH=CHCH$_2$

(i) X = (CH$_2$)$_4$

(j) X = COCH$_2$

(k) X = (CH$_2$)$_2$
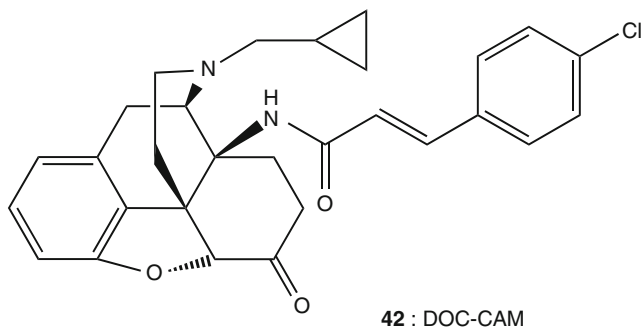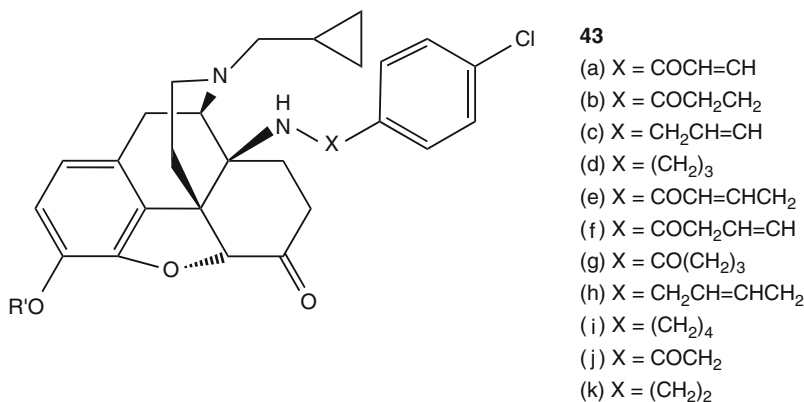
Fig. 6 14-Aminomorphinones with varying C14-side chains

and DOR whereas the morphinones (**43**: R′ = H) had high affinity for all opioid receptors. **43b** and **43d** with saturated C14 side chains had exceptional potency as non-selective opioid antagonists *in vivo* [39]. At a high dose (32 mg/kg s.c.) with 24 h pretreatment, **43b** suppressed morphine's antinociceptive effect in TW to the extent that 320 mg/kg morphine, the highest dose tested, had only 35% of the maximum possible effect whereas the ED$_{100}$ for morphine in this assay was 100 mg/kg. The effect of **43d** was even more dramatic; 32 mg/kg of **43d** administered 24 h before morphine totally suppressed the morphine dose–response curve. The pseudoirreversible MOR antagonist effect of **43b** is equivalent to that of C-CAM (**43a**: R′ = H) whereas that of **43d** is more impressive than C-CAM's and compares with that of M-CAM [32]. Whereas the codeinones and morphinones with three carbon C14 chains (**43a–d**) were all potent antagonists for all three opioid receptors in [^{35}S]GTPγS assays, the four carbon chain analogues (**43e–i**) were MOR antagonists, DOR antagonists or partial agonists and KOR antagonists or partial agonists but with much lower potency. The two carbon chain codeinones and morphinones (**43j–k**) were the only ones to have MOR partial agonist activity; they were also low potency DOR and KOR partial agonists. In a study using the [^{35}S]GTPγS assay and looking at the interaction of DAMGO with ligands having side chains with two and four carbon atoms as well as C-CAM (**43a**, R′ = H), the evidence for irreversible MOR binding showed that all three chain lengths were associated with such binding. However, the phenylacetylmorphinone (**43j**, R′ = H) in the TW assay had substantial MOR agonist activity, greater than was expected from its low efficacy MOR partial agonism *in vitro*. There was no evidence of delayed MOR antagonism in the TW assay. Thus there appears to be inconsistency in the *in vivo* data when compared to the *in vitro* profile [18].

Nieland et al. [19] studied the effect of orientation in the aromatic ring of the cinnamoylamino side chain (**44**, Fig. 7). It was realised early that a 4′-chloro or 4′-methyl substituent as in C-CAM, MC-CAM or M-CAM was associated with powerful irreversible MOR antagonism; the same two substituents when placed in
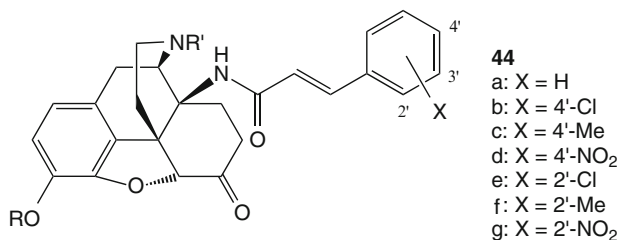
Fig. 7 Substituents in the cinnamoylamino side chain
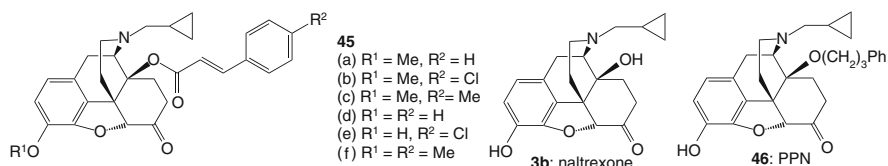
Fig. 8 14-*O*-Substituted derivatives of naltrexone

the 2′-position produced ligands with very much higher MOR efficacy. In [^{35}S] GTPγS assays with the 2′-substituted 17-cyclopropylmethyl ligands (**44**, R′ = CPM) this higher efficacy was more apparent for KOR and DOR activity than for MOR activity, whereas for the 17-methyl ligands (**44**, R′ = Me) it was true for all opioid receptors.

A limited amount of *in vivo* data for the 17-cyclopropylmethyl 2′- and 4′-nitro derivatives (**44d, g**, R′ = CPM) suggested that the effect of orientation of the nitro group was different to that of the chloro and methyl substituents. Thus the 4′-nitrodihydrocodeinone (**44d**, R = Me) had antinociceptive activity in the TW substantially greater than that of the 2′-nitro isomer (**44 g**, R = Me). The 4′-nitrodihydromorphinone (**44d**, R = H) had higher efficacy in TW than any other 17-cyclopropylmethyldihydromorphinone tested, including the unsubstituted derivative (**44a**, R = H) and the 2′-chloro and 2′-methyl (**44e, f**, R = H) analogues. **44d** (R = H, R′ = CPM) was also an impressive delayed morphine antagonist of long duration. The differences between chloro/methyl and nitro substitution seem to reflect the greater lipophilicity of the halo and methyl groups though the reason for this particular differentiation is unclear [19].

4′-Chloro-, 4′-methyl- and unsubstituted 14-*O*-cinnamoyl derivatives of naltrexone (**45**, Fig. 8) have also been evaluated for comparison with the equivalent amides, C-CAM, M-CAM and MC-CAM [40]. In *in vitro* assays only limited efficacy, predominantly at KOR, was observed for the codeinones (**45a–c**), while the morphinones (**45d–f**) were all antagonists of greater potency than their parent, naltrexone (**3b**). *In vivo* the morphinones (**45d–f**) were morphine antagonists with irreversible characteristics, but of shorter duration than their amide counterparts. As in the amides, an unsubstituted cinnamoyloxy ring was associated with higher efficacy than the 4′-substituted analogues. It is interesting to compare the activities

of the unsubstituted morphinone (**45d**) with the phenylpropyloxy derivative (**46**, PPN) as both have a 3-carbon chain linking the aryl ring with the C_{14} oxygen. The ether (**46**, PPN) was a potent agonist, 400–600 times more potent than morphine in the hotplate and TF assays [41], whilst the ester (**46d**) displayed much lower agonist potency and only in the writhing assay where the nociceptive stimulus is of substantially lower intensity than in the thermal assays [40].

The group of Archer and Bidlack produced a substantial body of work on 14β-4′-nitrocinnamoylaminocodeinone (**47a**) and morphinone (**47b**) and the equivalent dihydrocodeinone (**48i**) and dihydromorphinone (**48j**) including analogues with 5β-methyl substitution (**48a–f**) (Fig. 9). Two compounds received special attention. MET-CAMO (**48a**) and *N*-CPM-MET-CAMO (**48b**) having 5β-methyl substitution had high affinity and MOR selectivity in binding assays and when administered i.c.v. antagonised morphine selectively in TW for up to 72 h [42]. Comparisons between equivalent 4′-nitro- and 4′-chlorocinnamoylamino ligands were also made. MET-Cl-CAMO (**48c**) and *N*-CPM-MET-Cl-CAMO (**48d**) were long-term MOR antagonists devoid of agonist properties when administered i.c.v. in TW with 55 °C water [43]. There were only minor differences when compared with MET-CAMO (**48a**) and *N*-CPM-MET-CAMO (**48b**) [42]. The 4′-chlorocinnamoylaminodihydrocodeinones CAM (**48e**) and MC-CAM (**48g**) were compared with the 4′-nitro analogues CACO (**48f**) and *N*-CPM-CACO (**48h**). Again the chloro and nitro derivatives had similar long-term MOR antagonist profiles but whereas the nitro derivatives had short-term agonism when administered i.c.v. in the 55 °C TW assay, CAM and MC-CAM were devoid of agonist activity in this assay [24].

47a: R=Me
47b: R=H

48
(a) R = R² = Me, R¹ = H, R³ = NO₂ MET-CAMO
(b) R = CPM, R¹ = H, R² = Me, R³ = NO₂ N-CPM-MET-CAMO
(c) R = R² = Me, R¹ = H, R³ = Cl MET-Cl-CAMO
(d) R = CPM, R¹= H, R² = Me, R³ = Cl N-CPM-MET-Cl-CAMO
(e) R = R¹ = R² = Me, R³ = Cl CAM
(f) R = R¹ = R² = Me, R³ = NO₂ CACO
(g) R = CPM, R¹ = Me, R² = H, R³ = Cl MC-CAM
(h) R = CPM, R¹ = R² = Me, R³ = NO₂ N-CPM-CACO
(i) R=R¹=Me, R²=H, R³=NO₂
(j) R=Me, R¹=R²=H, R³=NO₂
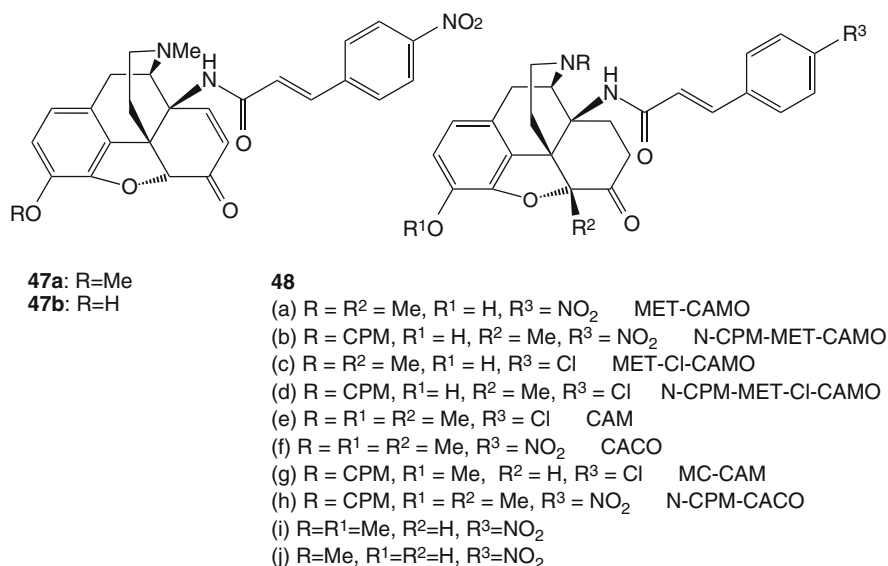
Fig. 9 The CAMO and CACO derivatives

For both CAM and MC-CAM we found MOR agonist activity when they were administered parenterally, though in the case of MC-CAM it was observed only in the antiwrithing assay and not in TW [35]. CAM (**48e**) on the other hand, with parenteral administration in TF, was a powerful antinociceptive agent 50 times more potent than morphine [19]. The disparity between the MOR agonist effects of CAM (**48e**) *in vitro* and *in vivo* when administered peripherally and the agonist-free MOR antagonism when administered i.c.v. strongly suggest that the cinnamoyla-minocodeinones do not owe their delayed MOR antagonist effects to metabolism to the morphinones [14] since direct administration into the brain should minimise the opportunity for extensive metabolism.

Archer et al. also studied 14-thioglycolamidonordihydromorphinone derivatives (Fig. 10). TAMO and *N*-CPM-TAMO were originally given the monomer structure (**49**) [44–47] but it was subsequently realised that the thioglycolamides undergo rapid oxidation in air and on chromatography columns to the dimeric structures (**50**) [48]. Both ligands were shown to have wash-resistant binding to MOR, the nature of which showed that it was due to the formation of a covalent bond to MOR. In the TW assay TAMO (**50a**) produced antinociceptive effects lasting 5 h when given i.p. and 2.5 h when given i.c.v. [45, 49]. These effects were antagonised by β-FNA selectively showing that the antinociceptive actions of TAMO are MOR-mediated. From 8 h to 48 h after i.c.v. administration TAMO selectively antagonised the antinociceptive action of morphine in TW. In a study of the behavioural effects of TAMO, its effects in rhesus monkeys on schedule-controlled behaviour and thermal nociception were investigated [49]. TAMO produced effects typical of MOR agonists in both assays, i.e. decrease in food maintained responding and increase in tail withdrawal latency; both effects were inhibited by the MOR antagonist quadazocine. Pretreatment with TAMO at 24 h failed to inhibit the behavioural effects of the MOR agonist fentanyl but it did produce a small rightward shift in the morphine dose–response curve. This lack of substantial MOR antagonism in monkeys contrasts with the irreversible MOR antagonist effect in mice.
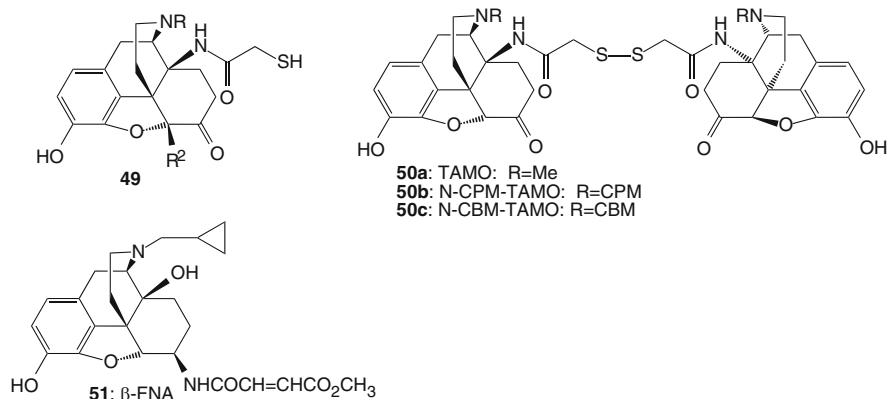
Fig. 10 TAMO and derivatives

The explanation could be simply species differences but is more likely related to the route of administration – i.c.v. in mice, parenteral in monkeys.

N-CPM-TAMO (**50b**) was evaluated in TW assays by i.c.v. administration. It had no antinociceptive activity but was an irreversible MOR antagonist. In the antiwrithing assay *N*-CPM-TAMO had antinociceptive activity mediated by KOR [46]. It was evaluated together with β-FNA (**51**) and *N*-CPM-MET-CAMO (**48b**) to determine whether they had any effect on morphine-induced antinociceptive toler-ance before they showed antagonism of the antinociceptive action of morphine in the tail withdrawal assay (55 °C water); all opioids were administered i.c.v. [50]. In keeping with the rapidly produced wash-resistant binding to MOR, the antagonists inhibited morphine tolerance from 2.3 to 7 h post-administration whereas antago-nism of morphine-induced antinociception was not observed until 8 h post-admi-nistration. It was concluded that long-term antagonism of MOR by irreversible antagonists is more complex than their direct binding to the MOR binding site.

The cyclobutylmethyl derivative *N*-CBM-TAMO (**50c**) has also been reported [51, 52]. It showed wash-resistant binding to MOR and KOR but only to MOR did the binding characteristics indicate that the binding was covalent. In TW (55 °C water) with i.c.v. administration *N*-CBM-TAMO had antinociceptive activity that was partially blocked by both β-FNA (MOR) and norBNI (KOR). It also had long-term antagonism of both MOR and KOR but only the antagonism of morphine (MOR) was irreversible [51]. A dose of *N*-CBM-TAMO (12 mg/kg i.p.) suppressed cocaine and morphine self-administration for 2–3 days with no suppression of water intake [52].

3.3 Pharmacological Actions of 14-Pyridylacryloylaminodihydromorphinones and Codeinones

The effect of orientation of nitro groups in the cinnamoyl aromatic ring was that the para (4′-) substituent was associated with higher MOR efficacy and more pro-nounced long-term MOR antagonism than the ortho (2′-) substituent [19]. In order to throw light on the possible steric effects associated with this difference the isomeric pyridylacryloylamino-dihydrocodeinones (**52a,c–54a,c**) and morphi-nones (**52b,d–54b,d**) were synthesised since they would have electronic character equivalent to the nitrocinnamoylamino derivatives, but not the steric bulk (Fig. 11)

52a: R=R′=Me
52b: R=Me, R′=H
52c: R=CPM, R′=Me
52d: R=CPM, R′=H

53a: R=R′=Me
53b: R=Me, R′=H
53c: R=CPM, R′=Me
53d: R=CPM, R′=H

54a: R=R′=Me
54b: R=Me, R′=H
54c: R=CPM, R′=Me
54d: R=CPM, R′=H
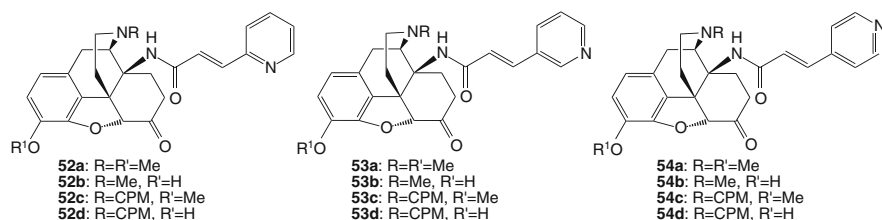
Fig. 11 Pyridylacryloylamino derivatives

[17, 53]. The new ligands were evaluated in receptor binding assays and in the stimulation of [^{35}S]GTPγS binding functional assay, in both cases using recombinant MOR, DOR and KOR transfected into Chinese hamster ovary (CHO) cells (Tables 3 and 4) [33]. All the isomeric pyridylacryloylamino derivatives had high affinity for all three opioid receptors with little selectivity (data not shown). In the functional assays the dihydrocodeinones (**52a–54a**) showed a clear MOR > DOR > KOR pattern of agonist potency. The dihydromorphinones (**52b–54b**) were potent agonists for all three receptor types; the dihydrocodeinones (**52a–54a**) were substantially less potent (Table 3). All of the 17-cyclopropylmethyl compounds (**52c,d–54c,d**) were MOR antagonists in this assay. The dihydrocodeinones (**52c–54c**) were low potency KOR and DOR partial agonists whereas the dihydromorphinones (**52d–54d**) were KOR and DOR antagonists, with the exception of the 4′-isomer (**54d**) which had substantial KOR partial agonist activity (Table 4).

Among the 14-pyridylacryloylaminocodeinones and morphinones there was not a consistent relationship between 2′-, 3′- and 4′-isomers in terms of MOR agonist efficacy; in the 17-methyldihydrocodeinones (**52a–54a**) the relationship was 2′ > 3′ > 4′, whereas with the corresponding dihydromorphinones (**52b–54b**) the reverse was true. It was therefore difficult to draw comparisons with the

Table 3 Agonist activity of 14-pyridylacryloylaminodihydromorphinones and codeinones in the [^{35}S]GTPγS assay

	R	R^1	N-position	MOR EC$_{50}$/nM:% stim'	DOR EC$_{50}$/nM: % stim'	KOR EC$_{50}$/nM: % stim'
52a	Me	Me	2′	4.9:102	12.9:90	132:61
52b	Me	H	2′	0.6:66	3.0:89	1.2:59
53a	Me	Me	3′	5.2:98	32.6:88	147:88
53b	Me	H	3′	0.5:66	3.1:104	5.9:67
54a	Me	Me	4′	19.6:77	29.0:87	68.1:100
54b	Me	H	4′	0.5:104	1.2:122	0.4:104

% stimulation relative to the standard agonists DAMGO (MOR), DPDPE (DOR) and U69593 (KOR)

Table 4 Activity of 17-CPM-14-pyridylacryloylaminodihydronormorphinones and codeinones in the [^{35}S]GTPγS assay

	R	R^1	N-position	MOR EC$_{50}$/nM:% stim' or [Ke/nM]	DOR EC$_{50}$/nM:% stim' or [Ke/nM]	KOR EC$_{50}$/nM:% stim' or [Ke/nM]
52c	CPM	Me	2′	[1.45]	193:39	13.9:57
52d	CPM	H	2′	[0.171]	[0.41]	[0.057]
53c	CPM	Me	3′	[2.86]	102:33	40.1:48
53d	CPM	H	3′	[0.192]	[0.23]	[0.105]
54c	CPM	Me	4′	[2.98]	235:43	13.7:93
54d	CPM	H	4′	[0.18]	[1.42]	0.3:59

% stimulation relative to, or antagonism of, the standard agonists DAMGO (MOR), DPDPE (DOR) and U69593 (KOR)

nitrocinnamoylamino derivatives, to give information on the contribution of steric and electronic effects to structure–activity relationships.

Opioid ligands which exhibit KOR agonism or DOR antagonism have been shown to inhibit some of the behavioural actions of cocaine [54, 55]. A compound with both actions might be expected to have potential as a treatment for cocaine abuse, though a full KOR agonist is unlikely to be acceptable on account of its likely psychomimetic effects. The 17-cyclopropylmethyl-4′-pyridylacrylamino derivative (**54d**), with its *in vitro* profile of KOR partial agonism (EC$_{50}$ 0.3 nM; 59% of efficacy of U69,593) and MOR/DOR antagonism (Ke 0.18 nM vs DAMGO; Ke 1.42 nM vs DPDPE) may be effective against cocaine and be relatively free from unwanted side effects.

4 Pharmacological Actions of 14-Aminomorphindole and Derivatives

14-Amino-7,8-dihydromorphindole (**55a**, Fig. 12) and a selection of its 14-alkylamino (**56**) and 14-acylamino (**57**) derivatives were prepared from **20a** by Fischer indole reaction, followed by acylation or alkylation of the amino group and 3-O-demethylation [20]. Aminomorphindole (**55a**) had high affinity binding to DOR and very much lower binding to KOR and particularly MOR, giving DOR selectivity comparable to oxymorphindole (**58a**) (Table 5). In the [^{35}S]GTPγS functional assay it showed partial agonist activity at DOR and low potency KOR antagonism (Table 5). Alkylation (**56a,b**) of the 14-amino group increased KOR and particularly MOR affinity to reduce sharply DOR selectivity. In the phenethylamino- (**56c**) and phenylpropyl- (**56d**) amino derivatives, though DOR affinity remained high, KOR and MOR affinity were further increased to reduce DOR selectivity even further. In the [^{35}S]GTPγS assays the alkylamino and phenylalkylamino derivatives all had DOR partial agonist activity of similar efficacy but higher potency than the parent aminomorphindole. The alkylamino derivatives (**56a,b**) had good DOR selectivity over KOR and MOR in potency terms. The phenylalkylamino morphindoles (**56c,d**) were still DOR selective but the phenethyl derivative (**56c**) also had high MOR potency and efficacy and could be of interest as an analgesic with

55a: R=Me
55b: R=CPM

56a: R=Me
56b: R=(CH$_2$)$_3$CH$_3$
56c: R=CH$_2$Ph
56d: R=(CH$_2$)$_2$Ph

57a: R=Me
57b: R=(CH$_2$)$_3$CH$_3$
57c: R=CH$_2$Ph
57d: R=(CH$_2$)$_2$Ph

58a: R=Me, OMI
58b: R=CPM, NTI
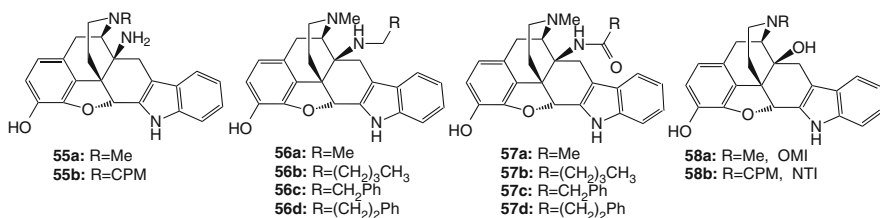
Fig. 12 14-Aminomorphindole and derivatives

Table 5 Activity of 14-aminomorphindole and derivatives in binding and [^{35}S]GTPγS assays

	Binding[a]			DOR[b]	KOR[b]	MOR[b]
	DOR, Ki/nM	Selectivity DOR/ MOR	Selectivity DOR/ KOR	EC$_{50}$/nM:% stim' or [Ke/nM]	EC$_{50}$/nM:% stim' or [Ke/nM]	EC$_{50}$/nM:% stim' or [Ke/nM]
55a	2.9	365	139	8.6:38	[86.8]	–
56a	0.73	105	87	0.33:43	[98.4]	184:50
56b	1.4	27	26	4.71:36	936:33	272:40
56c	1.1	1.5	13	0.95:33	16.4:74	5.33:93
56d	1.9	5	4	0.87:37	27.2:65	45.1:50
57b	2.1	25	349	3.3:74	[56.9]	149:31
57c	6.5	4.5	23	1.2:89	99.6:36	95:53
57d	4.2	2.3	6	1.4:72	[9.5]	5.2:27

[a]Binding assays using [^{3}H]Cl-DPDPE (DOR), [^{3}H]U69,593 (KOR) and [^{3}H]DAMGO (MOR) in recombinant human opioid receptors transfected into Chinese hamster ovary cells
[b]% stimulation of [^{35}S]GTPγS binding relative to, or antagonism of, the standard agonists DAMGO (MOR), DPDPE (DOR) and U69593 (KOR)
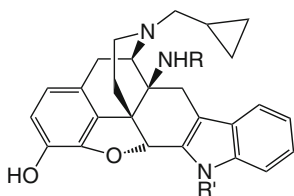
59a R = CH$_2$CH$_3$, R' = H
59b R = (CH$_2$)$_2$CH$_3$, R' = H
59c R = CHO, R' = H
59d R = CHO, R' = (CH$_2$)$_2$F
59e R = CHO, R' = (CH$_2$)$_3$F

Fig. 13 17-Cyclopropylmethylnoraminomorphindole derivatives

reduced tolerance and dependence. In the functional assay the 14-acylaminomorphindoles (**57**) had higher DOR efficacy than the equivalent alkylaminomorphindoles (**56**) but similar potencies. The phenylacetylaminomorphindole (**57c**) had high DOR efficacy and potency and also good selectivity in potency and efficacy over the KOR and MOR partial agonism; thus it was a potent, selective DOR agonist. The SAR for the phenylalkylaminomorphindoles (**56c,d**) and phenacylaminomorphindoles (**57c,d**) showed that MOR efficacy was greater for the derivatives with the shorter two carbon C14 side chain. In this respect it followed the pattern for the phenylalkylamino- and phenacylamino-*N*-cyclopropylmethyldihydronormorphinones where only the side chain derivatives with two carbon atom chains had any MOR agonist effects *in vitro* [18].

Opioid receptor binding data have been reported for a series of 17-cyclopropylmethylnoraminomorphindole derivatives (**59**, Fig. 13) [56]. All but the propylamino derivative (**59b**) had subnanomolar affinity for DOR which reduced its DOR selectivity compared with ethylamino- (**59a**) which was the only new ligand comparable in selectivity with naltrindole (**58b**). The indolic-substituted formylamino- derivatives were investigated as potential PET ligands for imaging studies of DOR. Alkylation of the indolic *N*-atom allowed retention of high affinity for DOR. The fluoroethyl substituent (**59d**) had little effect on selectivity but fluoropropyl (**59e**) lowered selectivity.

5   Conclusions

The groundbreaking work of Professor Gordon Kirby and his collaborators which provided viable synthesis of 14-aminocodeinone and 14-amino-7,8-dihydrocodeinone allowed the preparation of a wide range of derivatives. Among these the 14-cinnamoylaminodihydromorphinones have been most studied as a result of their unrivalled ability to provide MOR-selective irreversible antagonism in clocinnamox (C-CAM) and methcinnamox (M-CAM). The codeinone, methoclocinnamox (MC-CAM), related to C-CAM is a MOR partial agonist and long-term pseudoirreversible MOR antagonist which was considered as a follow-up to buprenorphine as a treatment for opiate abuse and depression. The 14-cinnamoyl derivatives of naltrexone, equivalent to C-CAM and M-CAM, had shorter duration of action and were less effective as pseudoirreversible antagonists. The 14-*O*-cinnamoyldihydrocodeinone derivative related to MC-CAM, *in vivo* had no MOR agonist activity and no pseudoirreversible MOR antagonist activity.

References

1. Viscusi ER, Gan TJ, Leslie JB, Foss JF, Talon MD, Du W, Owens G (2009) Peripherally acting μ-opioid receptor antagonists and postoperative ileus: mechanisms of action and clinical applicability. Anesth Analg 108:1811–1822
2. Buckett WR (1964) The relationship between analgesic activity, acute toxicity and chemical structure in esters of 14-hydroxycodeinone. J Pharm Pharmacol 16:68T–71T
3. Buckett WR (1965) Some pharmacological studies with 14-(cinnamoyloxy)codeinone. J Pharm Pharmacol 17:759–760
4. Buckett WR, Bosman HH (1972) New morphinone derivatives and their preparation. UK Patent 1 300 419
5. Bentley KW, Horsewood P, Kirby GW, Singh S (1969) Diels-Alder adducts from thebaine and nitroso-arenes. J Chem Soc D:1411
6. Schwab L (1980) 14-(Arylhydroxyamino)codeinones and derivatives as analgetics and antagonists. J Med Chem 23:698–702
7. Allen RM, Kirby GW, McDougall DJ (1981) The nitration of thebaine with tetranitromethane. J Chem Soc Perkin Trans I 26:1143–1147
8. Kobylecki RJ, Guest IG, Lewis JW, Kirby GW (1980) 14-Amino derivatives of morphine, methods of making them and analgesic compositions containing them. US Patent 4241066
9. Kobylecki RJ, Guest IG, Lewis JW, Kirby GW (1980) 14-Amino derivatives of morphine, methods of making them and analgesic compositions containing them. US Patent 4241067
10. Horsewood P, Kirby GW (1980) Preparation of 14-beta-hydroxyamino and 14-beta-amino-codeinone from thebaine. J Chem Res (S) 401:(M)4880
11. Archer S, Seyed-Mozaffari A, Osei-Gyimah P, Bidlack JM, Abood LG (1983) 14β-(2-Bromoacetamido)morphine and 14β-(2-bromoacetamido)morphinone. J Med Chem 26:1775–1777
12. Kirby GW, Sweeney JG (1973) Nitrosocarbonyl compounds as intermediates in the oxidative cleavage of hydroxamic acids. J Chem Soc Chem Commun:704–705
13. Kirby GW, McLean D (1985) An efficient synthesis of 14β-aminocodeinone from thebaine. J Chem Soc Perkin Trans I 1443–1445
14. Lewis J, Smith C, McCarthy P, Walter D, Kobylecki R, Myers M, Haynes A, Lewis C, Waltham K (1988) New 14-aminomorphinones and codeinones. NIDA Res Monogr 90:136–143

15. Sebastian A, Bidlack JM, Jiang Q, Deecher D, Teitler M, Glick SD, Archer S (1993) 14β-[(p-Nitrocinnamoyl)amino]morphinones, 14β-[(p-nitrocinnamoyl)amino]-7,8-dihydromorphinones, and their codeinone analogues: synthesis and receptor activity. J Med Chem 36:3154–3160

16. Bidlack JM, Kaplan RA, Sebastian A, Seyed-Mozaffari A, Hutchinson I, Archer S (1995) N-Mmethyl and N-cyclopropylmethyl-14α, 14′β-[dithiobis[(2-oxo-2, 1-ethanediyl)imino]]bis (7,8-dihydro-5β-methyl-morphinone) MET-TAMO and N-CPM-MET-TAMO: synthesis and opioid binding properties. Bioorg Med Chem Lett 5:1695–1700

17. Nieland N (1998) Investigations of derivatives of 14β-amino-7,8-dihydromorphinone. PhD Thesis, University of Bristol

18. Rennison D, Moynihan H, Traynor JR, Lewis JW, Husbands SM (2006) Structural determinants of opioid activity in derivatives of 14-aminomorphinones: effects of changes to the C14-amino to aryl ring linker chain. J Med Chem 49:6104–6110

19. Nieland NPR, Moynihan H, Carrington S, Broadbear J, Woods JH, Traynor JR, Husbands SM, Lewis JW (2006) Structural determinants of opioid activity in derivatives of 14-aminomorphinones: effect of substitution in the aromatic ring of cinnamoylaminomorphinones and codeinones. J Med Chem 49:5333–5338

20. Grundt P, Jales AJ, Traynor JR, Lewis JW, Husbands SM (2003) 14-Amino, 14-alkylamino- and 14-acylamino analogs of oxymorphindole. Differential effects on opioid receptor binding and functional profiles. J Med Chem 43:1563–1566

21. Husbands SM, Sadd J, Broadbear JH, Woods JH, Martin J, Traynor JR, Aceto MD, Bowman ER, Harris LS, Lewis JW (1998) 3-Alkyl ethers of clocinnamox: delayed long-term μ-antagonists with variable μ efficacy. J Med Chem 41:3493–3498

22. Aceto MD, Bowman ER, Harris LS, May EL (1989) Dependence studies of new compounds in the rhesus monkey, rat and mouse. NIDA Res Monogr 95:578

23. Aceto MD, Bowmen ER, May EL, Woods JH, Smith CB, Medzihradsky F, Jacobson AE (1989) Very long-acting narcotic antagonists: the 14β-p-substituted cinnamoylaminomorphinones and their partial mu agonist codeinone relatives. Arzneim-Forsch Drug Res 39:570–575

24. McLaughlin JP, Hill KP, Jiang Q, Sebastian A, Archer S, Bidlack JM (1999) Nitrocinnamoyl and chlorocinnamoyl derivatives of dihydrocodeinone: in vivo and in vitro characterization of μ-selective agonist and antagonist activity. J Pharmacol Exp Ther 289:304–311

25. Comer SD, Burke TF, Lewis JW, Woods JH (1992) Clocinnamox: a novel, systemically active irreversible opioid antagonist. J Pharmacol Exp Ther 262:1051–1056

26. Burke TF, Woods JH, Lewis JW, Medzihradsky F (1994) Irreversible opioid antagonist effects of clocinnamox on opioid analgesia and mu receptor binding in mice. J Pharmacol Exp Ther 271:715–721

27. Zernig G, Issaevitch T, Broadbear JH, Burke TF, Lewis JW, Brine GA, Woods JH (1995) Receptor reserve and affinity of mu-opioid agonists in mouse antinociception – correlation with receptor-binding. Life Sci 57:2113–2125

28. Zernig G, Butelman ER, Lewis JW, Walker EA, Woods JH (1994) In vivo determination of mu opioid receptor turnover in rhesus monkeys after irreversible blockade with clocinnamox. J Pharmacol Exp Ther 269:57–65

29. Pitts RC, Allen RM, Walker EA, Dykstra LA (1998) Clocinnamox antagonism of the antinociceptive effects of mu opioids in squirrel monkeys. J Pharmacol Exp Ther 285:1197–1206

30. Barrett AC, Smith ES, Picker MJ (2003) Use of irreversible antagonists to determine the relative efficacy of mu-opioids in a pigeon drug discrimination procedure: comparison of beta-funaltrexamine and clocinnamox. J Pharmacol Exp Ther 305:1061–1070

31. Walker EA, Young AM (2002) Clocinnamox distinguishes opioid agonists according to relative efficacy in normal and morphine-treated rats trained to discriminate morphine. J Pharmacol Exp Ther 302:101–110

32. Broadbear JH, Sumpter TL, Burke TF, Husbands SM, Lewis JW, Woods JH, Traynor JR (2000) Methcinnamox is a potent, long-lasting and selective antagonist of morphine-mediated

antinociception in the mouse: comparison with clocinnamox, β-FNA and β-chlornaltrexamine. J Pharmacol Exp Ther 294:933–940

33. Zhu J, Lou L-Y, Li J-G, Chen C, Liu-Chen L-Y (1997) Activation of the cloned human *kappa* opioid receptor by agonists enhances [^{35}S]GTPγS binding to membranes: determination of potencies and efficacies of ligands. J Pharmacol Exp Ther 282:676–684

34. Toll L, Berzetei-Gurske IP, Plogar WE, Brandt SR, Adapa ID, Rodriguez L, Schwartz W, Haggart D, O'Brien A, White A, Kennedy JM, Craymer K, Farrington L, Auh JS (1998) Standard binding and functional assays related to medications development division testing for potential cocaine and opiate narcotic treatment medications. NIDA Res Monogr 178:440–445

35. Woods JH, Lewis JW, Winger G, Butelman E, Broadbear J, Zernig G (1995) Methoclocinnamox: a μ partial agonist with pharmacotherapeutic potential for heroin abuse. NIDA Res Monogr 147:195–219

36. Winger G, Palmer RK, Woods JH (1992) Drug-reinforced responding: rapid determination of dose-response functions. Drug Alcohol Depend 24:135–42

37. Husbands SM, Lewis JW (2003) Opioid ligands having delayed long-term antagonist activity: potential pharmacotherapies for opioid abuse. Min Rev Med Chem 3:137–144

38. Derrick I, Neilan CL, Andes J, Husbands SM, Woods JH, Traynor JR, Lewis JW (2000) 3-Deoxyclocinnamox: the first selective, high affinity, non-peptidic, μ-opioid antagonist lacking a phenolic hydroxyl group. J Med Chem 43:3348–3350

39. Lewis JW, Husbands SM, Broadbear J, Woods JH (1995) Opioids – from analgesics to treatment drugs. Franklin M Robinson Memorial Symposium. NIDA Res Monogr 152:67

40. Moynihan H, Jales AR, Greedy BM, Broadbear JH, Purington L, Traynor JR, Woods JH, Lewis JW, Husbands SM (2009) 14β-O-Cinnamoylnaltrexone and related dihydrocodeinones are mu opioid receptor partial agonists with predominant antagonist activity. J Med Chem 52:1553–1557

41. Greiner E, Spetea M, Krassnig R, Schullner F, Aceto M, Harris LS, Traynor JR, Woods JH, Coop A, Schmidhammer H (2003) Synthesis and biological evaluation of 14-alkoxymorphinans. 18. N-Substituted 14-phenylpropyloxymorphinan-6-ones with unanticipated agonist properties: extending the scope of common structure-activity relationships. J Med Chem 46:1758–1763

42. Jiang Q, Sebastian A, Archer S, Bidlack JM (1994) 5β-Methyl-14β-(p-nitrocinnamoylamino)-7,8-dihydromorphinone and its corresponding N-cyclopropylmethyl analogue, N-cyclopropylmethylnor-5β-methyl-14β-(p-nitrocinnamoylamino)-7,8-dihydromorphinone: mu selective irreversible opioid antagonists. J Pharmacol Exp Ther 268:1107–1113

43. McLaughlin JP, Sebastian A, Archer S, Bidlack JM (1997) 14 Beta-chlorocinnamoylamino derivatives of metopon: long-term mu-opioid receptor antagonists. Eur J Pharmacol 320:121–129

44. Bidlack JM, Seyed-Mozaffari A, Archer S (1991) 14β-Thioglycolamido-7, 8-dihydromorphinone, a μ-selective irreversible ligand. Med Chem Res 1:43–46

45. Jiang Q, Seyedmozaffari A, Archer S, Bidlack JM (1992) Antinociceptive properties of 2 alkylating derivatives of morphinone – 14-beta-(thioglycolamido)-7,8-dihydromorphinone (TAMO) and 14-beta-(bromoacetamido)-7,8-dihydromorphinone (H2BAMO). J Pharmacol Exp Ther 262:526–531

46. Jiang Q, Seyedmozaffari A, Archer S, Bidlack JM (1993) Pharmacological study of 14-beta-(thioglycolamido)-7,8-dihydro-n-cyclopropylmethyl-normorphinone (N-CPM-TAMO). J Pharmacol Exp Ther 264:1021–1027

47. Bidlack JM, Frey DK, Kaplan RA, Seyed-Mozaffari A, Archer S (1989) Affinity labelling of mu opioid receptors by sulhydryl alkylating derivatives of morphine and morphinone. Mol Pharmacol 37:50–59

48. Archer S, Seyedmozaffari A, Jiang Q, Bidlack JM (1994) 14-Alpha, 14′beta-[dithiobis [(2-oxo-2, 1-ethanediyl)imino]]bis (7,8-dihydromorphinone) and 14-alpha, 14′beta-

[dithiobis[(2-oxo-2, 1-ethanediyl)imino]]bis[7,8-dihydro-n-(cyclopropylmethyl)normorphi-none] – chemistry and opioid binding-properties. J Med Chem 37:1578–1585

49. Gatch MB, Negus SS, Mello NK, Archer S, Bidlack JM (1996) Effects of the structurally novel opioid 14 alpha, 14′beta-[dithiobis[(2-oxo-2,1-ethanediyl)imino]]bis(7,8-dihydromor-phinone) schedule-controlled behavior and thermal nociception in rhesus monkeys. J Pharmacol Exp Ther 278:1282–1289

50. Jiang Q, Seyedmozaffari A, Sebastian A, Archer S, Bidlack JM (1995) Preventing morphine antinociceptive tolerance by irreversible mu-opioid antagonists before the onset of their antagonism. J Pharmacol Exp Ther 273:680–688

51. Xu JY, SeyedMozaffari A, Archer S, Bidlack JM (1996) N-Cyclobutylmethyl analog of normorphinone, N-CBM-TAMO: a short-term opioid agonist and long-term mu-selective irreversible opioid antagonist. J Pharmacol Exp Ther 279:539–547

52. Archer S, Glick SD, Maisonneuve IM, Bidlack JM, Xu JY, Teitler M, Sebastian A, ElHamouly W, Hutchinson I (1996) Suppression of morphine and cocaine self-administration in rats by a mixed mu antagonist kappa agonist (N-CBM-TAMO) and a long-acting selective D-1 antagonist (AS-300). Bioorg Med Chem Lett 6:1139–1144

53. Lewis JW, Neiland NPR, Traynor JR, Woods JH (2000) Pyridylacryloyl derivatives of 14-β-aminomorphinones. NIDA Res Monogr 180:72

54. Shippenberg TS, Heidbreder C (1995) The delta-opioid receptor antagonist naltrindole prevents sensitization to the conditioned rewarding effects of cocaine. Eur J Pharmacol 280:55–61

55. Mori T, Nomura M, Nagase H, Narita M, Suzuki T (2002) Effects of a newly synthesized kappa-opioid receptor agonist, TRK-820, on the discriminative stimulus and rewarding effects of cocaine in rats. Psychopharmacol 161:17–22

56. Clayson J, Jales A, Tyacke RJ, Hudson AL, Nutt DJ, Lewis JW, Husbands SM (2001) Selective δ-opioid receptor ligands: potential PET ligands based on naltrindole. Bioorg Med Chem Lett 11:939–943

Nonpeptidic Delta (δ) Opioid Agonists and Antagonists of the Diarylmethylpiperazine Class: What Have We Learned?

Silvia N. Calderon

Abstract The discovery of the selective delta (δ) opioid agonists SNC 80 and BW373U86, which possess a diarylmethylpiperazine structure unique among opioids, represented a major advance in the field of δ-opioid ligands. Extensive research has recently been performed to uncover the structure–activity relationships (SAR) of this class of ligands, thereby providing valuable tools for the pharmacological characterization of the δ opioid receptor. This review focuses on the SAR of this unique series of ligands, and provides an overview of the various chemical routes that have been developed and optimized through the years to allow the syntheses of these ligands on a multigram scale. The search for selective δ opioid agonists and antagonists, as well as for those with mixed opioid agonist properties with potential therapeutic value, continues. Several questions regarding the interaction at the molecular level of diphenylmethylpiperazine derivatives and related analogs with opioid receptors and in particular with the δ opioid system still remain unanswered. Indeed, the development and pharmacological characterization of novel nonpeptidic δ opioid ligands remains an active area of research, as it may provide a better understanding of the role of this receptor in multiple disease states and disorders.

Keywords δ Agonists · δ Antagonists · Diphenylmethylpiperazines · Nonpeptidic delta ligands · SNC 80

S.N. Calderon
Center for Drug Evaluation and Research, Food and Drug Administration, 10903 New Hampshire Ave, Silver Spring, MD 20993, USA
e-mail: silvia.calderon@fda.hhs.gov

Contents

Abbreviations

Boc	*tert*-Butoxycarbonyl
Bu	Butyl
Cbz	Benzyloxycarbonyl
ee	Enantiomer excess
Et	Ethyl
Me	Methyl
MeOH	Methanol
Ph	Phenyl
t-Bu	*tert*-Butyl
THF	Tetrahydrofuran
TMEDA	*N*,*N*,*N*′,*N*′-Tetramethyl-1,2-ethylenediamine

1   Introduction

Intensive research over the last 2 decades has provided a better understanding of the structure, distribution, and pharmacology of the opioid receptors. Three types of opioid receptors known as mu (μ), delta (δ), and kappa (κ) receptor types have been identified and the mRNA encoding these receptors has been isolated. It has become clear that each receptor mediates unique pharmacological responses and is differentially distributed in the central nervous system [1–6]. Thus, the design and synthesis of selective ligands that interact with each of these receptors, as well as the characterization of the pharmacological effects that these ligands mediate, remain a very active area of research. The δ opioid receptor has become an attractive target for the development of new drugs with potential therapeutic

benefits in analgesia, addiction, affective disorders, and neurodegenerative and gastrointestinal disorders [7–14]. Work from several research groups indicates that agonists acting at the δ opioid receptor produce analgesia in animal models of pain while appearing to lack the undesirable effects associated with prototypic μ opioid agonist such as morphine [15, 16]. Morphine-like drugs produce analgesia and multiple side effects such as respiratory depression, constipation, miosis, and physical dependence. Three families of endogenous opioid peptides known as β-endorphins, enkephalins, and dynorphins, have been identified. Although most of these endogenous opioids have little selectivity for opioid receptors, in general it is accepted that β-endorphins, enkephalins, and dynorphins displayed greater affinity for μ, δ, and κ receptors respectively [17]. The discovery of endogenous opioid peptide agonists with potent opiate agonist activity at the δ receptor was followed by the synthesis and characterization of many other selective peptidic ligands [18]. However, peptidic ligands are poorly absorbed orally, sensitive to degradation by peptidases, and generally do not cross the blood brain barrier. Thus, to characterize better the pharmacological profile of the δ opioid receptor it was imperative to develop highly selective and potent opioid ligands with good central bioavailability [19]. The understanding of the structure and function of receptors is largely dependent on the discovery of agonist and antagonists. Antagonists have proven to be invaluable tools in pharmacology because they allow the identification of key physiological functions mediated by the receptors through the blockade of their biological responses.

The development and pharmacological characterization of the first nonpeptidic δ opioid selective antagonist, naltrindole (**1**) (Figs. 1 and 2) by Portoghese in 1988 [20] provided the framework for research aimed at understanding the functions mediated by the δ opioids receptors. Naltrindole was designed based on the message–address concept previously introduced by Schwyzer [21], by which a naltrexone-derived recognition unit envisioned as the message component was attached to a benzene moiety that simulated the phenylalanine and considered the address unit of the enkephalins. Another major advance in this area was the discovery of BW373U86 (±)-**2** (Fig. 1) [22, 23], a selective nonpeptidic δ opioid receptor agonist with a new carbon–nitrogen skeleton, followed by the identification and characterization of the highly δ selective SNC 80 (+)-**3** (Fig. 1) [24]. Unlike naltrindole, which has a classical opioid ligand structure, BW373U86 and SNC 80 have a chemical structure not commonly associated with opiates.

Further research led to the characterization of other nonpeptidic agonists and antagonists that belong to other chemical classes. The agonist group includes morphinan derivatives such as SIOM (**4**) (Fig. 1) [25], isoquinoline derivatives like TAN-67 (**5**) (Fig. 1) [26, 27], and the pyrrolooctahydroisoquinolines derivatives. The latter chemical class served as a template for the development of agonists such as SB-219825 (**6**) (Fig. 1) and the antagonists SB-205588 (**7**) and SB-220718 (**8**) (Fig. 2) [28–30]. So far, only one antagonist, DPI2505 (**9**) (Fig. 2) [31], has been identified within the diarylmethylpiperazine series. A series of selective δ opioid antagonists with a biarylpiperidine structure has recently been reported. Compounds **10** and **11** (Fig. 2) exemplify some of the antagonists identified in these series [32].
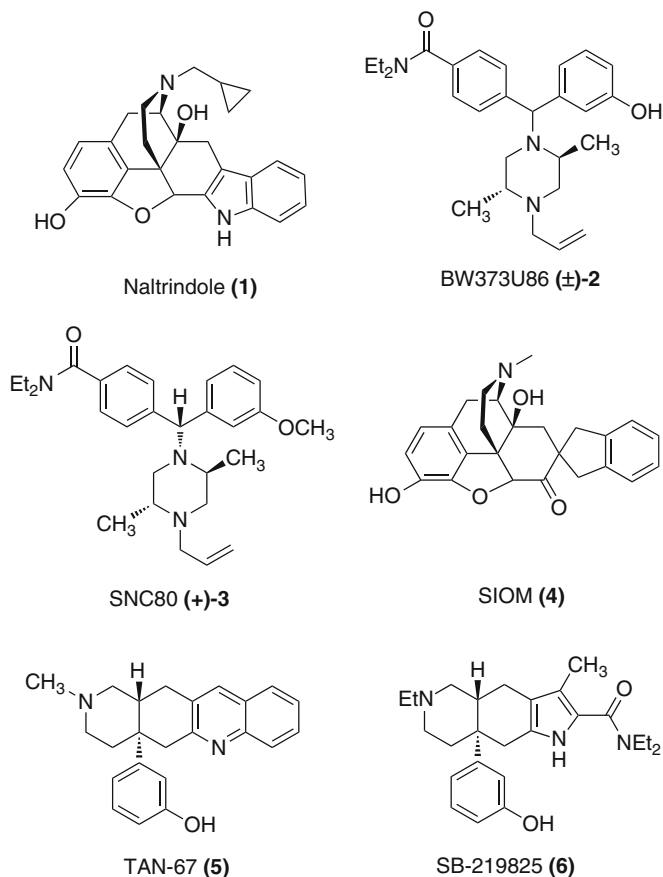
Fig. 1 Structures of the delta opioid antagonist Naltrindole and of prototypic nonpeptidic delta opioid agonists

This review focuses on the advances on the structure–activity relationship (SAR) studies on the diarylmethylpiperazine derivatives of the SNC 80 type, with agonist or antagonist properties at the δ opioid receptors, as well as provides a description of the synthetic procedures used in the synthesis of SNC 80 and its analogs.

2 Structure–Activity Relationship of the Selective Nonpeptidic δ Opioid Agonist SNC 80 and Related Derivatives

2.1 *Diphenylmethylpiperazines and Diarylmethylpiperazines*

As previously captured in other related reviews of the topic [28, 29, 33], the discovery and identification of BW373U86 (±)-**2** [22, 23] with a unique carbon

Naltrindole (1)

SB-205588 (7)

SB-220718 (8)

DPI2505 (9)

(10)

(11)
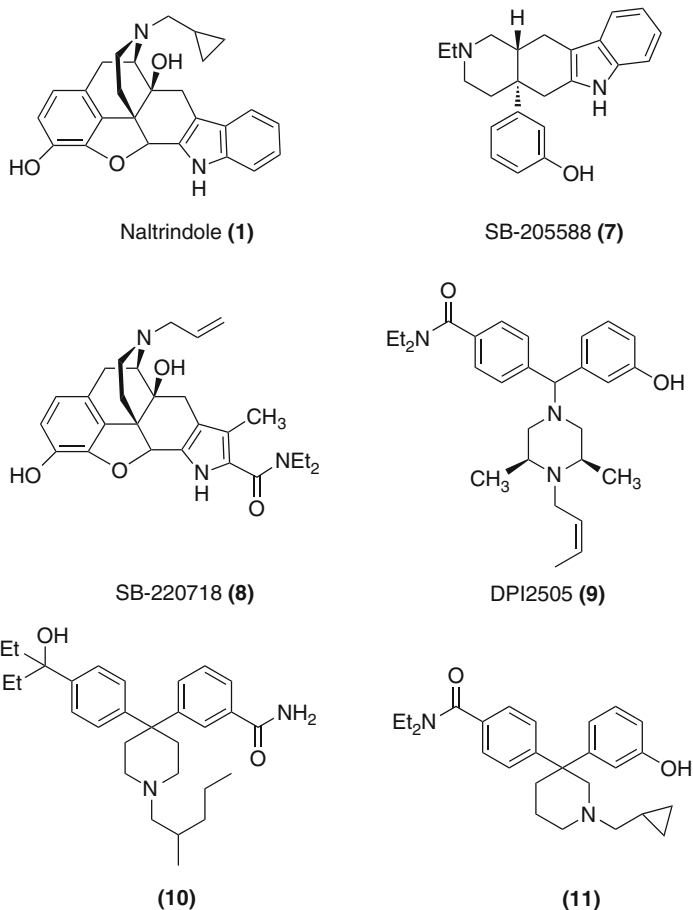
Fig. 2 Structures of nonpeptidic delta antagonists

skeleton, unrelated to other δ agonists, was the starting point of extensive research in the area of nonpeptidic δ ligands. The SAR studies and characterization of (±)-**2** derivatives was reported in the patent literature [34]. Although BW373U86 showed a high degree of selectivity for δ opioid receptors some of its effects proved to be mediated through μ opioid receptors [34, 35]. In an effort to characterize further the structural ligand requirements of the δ opioid receptor, the synthesis and assignment of the absolute configuration of the optical pure enantiomers of BW373U86, its benzylic epimers, and their methyl ethers was later reported [24]. The affinities of these enantiomers and immediate synthetic precursors for μ opioid receptors and δ opioid receptors were determined by inhibition of binding of [3H]-DAMGO to rat brain membranes and [3H]-DADLE to mouse brain membranes depleted of μ binding sites by the pretreatment with the irreversible ligand benzimidazole isothiocyanate (BIT), respectively. In addition, the opioid activity of
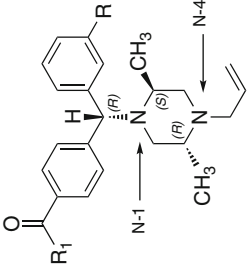
these compounds was next evaluated in the isolated mouse vas deferens (MVD) and in guinea pig ileum (GPI) bioassays. From this first series of compounds the (+)-methoxy precursor of (+)-**2**, known as SNC 80 (+)-**3**, displayed a remarkable μ/δ selectivity in both receptor binding and bioassays and showed opioid agonist activity in the mouse, exerting its effects through both δ_1 and δ_2 receptors [36].

To understand further the interaction of this distinctive diphenylpiperazine structure with the δ opioid receptor, the effect of the replacement of the methoxy group present in SNC 80 template by a hydroxyl function, hydrogen, fluorine, or iodine was evaluated [37]. The pharmacological profile of the most selective enantiomeric precursors of BW373U86 as well as other SNC 80 derivatives is presented in Table 1. These first SAR studies showed that compounds which retained the same spatial orientation at the benzhydryl (α) position as that of SNC 80 displayed higher selectivity than their benzylic epimers. In addition, the replacement of the methoxy group by either hydrogen, (+)-**13,** or fluorine, (+)-**14**, resulted in highly selective analogs of SNC 80. Analysis of the effect of a positional change of the *N,N*-diethylamide function as well as the effect of diverse alkyl substitution at this function followed. A series of *N*-monoalkyl- and dialkylbenzamide derivatives of SNC 80 were synthesized and their pharmacological profile reported [38]. Regarding the binding affinity of the amide positional isomers of the desmethoxy derivative of SNC 80, for δ opioid receptors, both the *meta* and the *ortho* diethylbenzamides displayed lower affinity than the *para* counterpart. The affinity of the *ortho* derivative was in the mM range whereas the *meta* derivatives still retain nM affinity for the δ opioid receptor. Compared to the *para* benzamide analog, the affinity of the *meta* derivative was 90-fold lower [38]. Alkyl substitution at the amide group had a more intense effect in the SNC 80 series, *N*-monoalkylbenzamide derivatives showed lower affinity than the *N,N*-dialkylbenzamide derivatives, and the *N*-unsubstituted benzamide had the lowest affinity for the δ opioid receptors. The *N*-monoalkylbenzamides also showed poor selectivity, while the *N,N*-dialkyl derivatives showed a good μ/δ ratio. From this series, two compounds, the dimethyl substituted, (+)-**15**, and the methyl-ethyl substituted benzamides, (+)-**16**, displayed high affinity and selectivity for δ opioid receptors and proved to be δ agonists in MVD preparations (Table 1).

In the (+)-**2** series, the *meta* diethyl amide derivative retained high affinity for δ as well as for μ opioid receptors. Movement of the diethyl amide from the *para* to the *meta* position resulted in less δ selective ligands with a mixed δ/μ agonist profile in these series. Changing the *meta*-diethylamide to a *meta*-*N*-methylanilide resulted in potent mixed δ and μ agonists [39].

Zwitterionic analogs of SNC 80 designed by replacement of the diethylamide benzamide ring by various 7-yl-3,4-dihydro-2(1*H*)-isoquinoline-carboxylic acids have recently been described in the literature as selective peripheral δ opioid receptor agonists [40].

Analysis of the need of the dimethyl substituted piperazine as well as the role of the two basic nitrogens (N-1 and N-4) and the influence of substituents on N-4 followed [41]. Initially it was noted that the *trans*-dimethyl groups on the piperazine ring were not critical for recognition at the δ receptor [41–43]. Since it was

Table 1 Receptor affinity and agonist activity of selective diphenylmethylpiperazines [24, 37, 38]

Compound	–R; –R₁	Binding (IC₅₀ nM ± SD)			Agonist activity (IC₅₀ nM ± SEM)	
		μ[b]	δ[c]	IC₅₀ ratio μ/δ	MVD (δ)	IC₅₀ ratio GPI/MVD
(±)-**2**, BW373U86	–OH; Et₂N–	46.3 ± 4.42	0.92 ± 0.06[d]	50.3	0.2 ± 0.02	715
(+)-**3**, SNC 80 (αR, 2S, 5R)	–OCH₃; Et₂N–	2,467 ± 200	2.88 ± 0.35	857	2.73 ± 0.50	1,996
(−)-**12** (αR, 2R, 5S)	–OCH₃; Et₂N–	9,138 ± 823	4.88 ± 0.52	1,873	30.9 ± 4.0	49
(+)-**13** (αS, 2S, 5R)[a]	–H; Et₂N–	>2,500	0.94 ± 0.09	>2,660	10.56 ± 0.38	813
(+)-**14** (αR, 2S, 5R)	–F; Et₂N–	1,977 ± 260	2.92 ± 0.36	677	9.77 ± 1.28	265
(+)-**15** (αR, 2S, 5R)	–OCH₃; Me₂N–	3,261 ± 719	4.8 ± 0.69[e]	679	8.92	837
(+)-**16** (αR, 2S, 5R)	–OCH₃; Et(Me)N–	7,373 ± 558	4.2 ± 0.47[e]	1,755	4.45	958

[a]The spatial orientation at the α position of (+)-**13** is the same as in (+)-**3** and the designation of αS-(+)-**13** is arbitrary and results from the application of the Cahn, Ingold, and Prelog nomenclature rules

[b]Binding against [³H]-DAMGO in rat brain membranes [24, 37, 38]

[c]Binding against [³H]-DADLE to rat brain membranes using DAMGO to block μ receptors [37]

[d]Binding inhibition of [³H]-DADLE in mouse brain membranes [24]

[e]Binding of [³H]-DADAL in rat brain membranes [38]

determined that the lack of dimethyl substitution at the piperazine level did not affect the selectivity or affinity of these type of ligands for the δ receptor, and it was known that the desmethoxy derivative of SNC 80, (+)-**13**, retained high affinity and selectivity for the same receptor, a simplified 4-(1-piperazinylbenzhydryl)-*N, N*-diethylbenzamide skeleton was selected as a template to analyze the influence of the N-4 substitution modifications in the affinity and selectivity for the δ receptor. It was shown that the replacement of the *N*-allyl group with an alkyl moiety reduced the affinity at the δ receptor; however, the benzyl derivative retained high affinity and a good agonist profile [41, 44]. The replacement of the N-4 nitrogen with its allyl group by oxygen or a methylene group to give the corresponding morpholino or piperidine analogs, respectively, abolished binding to opioid receptors, indicating that the basic nitrogen N-4 is an important structural element in this series required for the interaction with the δ receptor. In contrast, replacement of the N-1 by a methylene group did not have such a dramatic effect, showing that N-1 could be modified, retaining moderate affinity for the δ receptor. It was also indicated that a cyclic amine was required for recognition at the receptor since diarylmethyl diamines showed low affinity at the δ receptor and did not bind at other opioid receptors. It was then concluded that N-1 was relatively unnecessary for binding to the δ receptor. Later, using the SNC 80 structure as a template, the effect of the N-4 substitution on the affinity and activity of these ligands was studied in more detail. It was found that the 4-crotyl, 2-methylallyl, and benzyl compounds displayed high selectivity and proved to be as efficacious agonists as SNC 80 in the [^{35}S]GTPγS function assay. It was also shown that *N*-cyclopropylmethyl and *N*-allyl substitution in the SNC 80 series did not confer antagonist properties to these ligands, unlike what it is observed in the morphinan series at the μ opioid receptors [45].

The identification and pharmacological evaluation of an SNC 80 simplified structure gave origin to a new series of δ opioid agonists [46]. Initially the structure of SNC 80 was modified to reduce the number of chiral centers to an analog in which the piperazine methyl groups and the *N*-allyl group were eliminated, and in which the aryl methoxy group was replaced by hydrogen (**17**) (Table 2). This template retained strong δ binding affinity, high selectivity, and showed full agonist properties [46]. Substitution of the phenyl ring with a variety of substituted aryl and heteroaryl groups followed. The replacement of the phenyl ring with a cyclohexyl ring (**18**) gave a sharp decrease in affinity and selectivity when compared to the parent compound **17** (Table 2), whereas compounds with a 1-naphthyl or 2-naphthyl substitution had improved binding affinity and agonist potency. In this series the 8-quinolyl derivative (**19**) and the 2,2-dimethyl-2,3-dihydro-1-benzo-furan-7-yl derivative (**20**) had significantly high binding affinity and improved selectivity.

It is of particular interest that another δ opioid selective nonpeptidic piperazine derivative agonist, SL-3111 (1-(4-*tert*-butyl-3′-hydroxy)benzhydryl-4-benzylpiperazine), was designed and synthesized based on the identification of the essential pharmacophores for peptide ligands to interact with δ receptors, and on a model of the proposed bioactive conformation of the potent, conformationally constrained δ-opioid peptide ligand [(2*S*,3*R*)-TMT[1]]DPDPE [47]. This new series used the

Table 2 Receptor affinity and agonist activity of simplified SNC 80 derivatives with a diaryl-methylpiperazine structure [46]
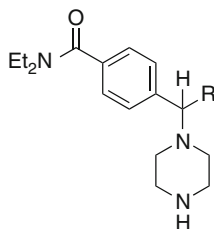
Compound	–R	Binding (IC_{50} nM $\pm$ SD)			Agonist activity[c]	
		μ[a]	δ[b]	IC_{50} ratio μ/δ	(EC_{50} nM $\pm$ SEM)	Emax (%)
17	–Phenyl	8,150 $\pm$ 370	11.3 $\pm$ 2.3	740	36.5 $\pm$ 5.9	104 $\pm$ 5
18	–Cyclohexyl	185 $\pm$ 14	98.4 $\pm$ 11.0	1.9	ND	ND
19	–8-Quinolyl	632 $\pm$ 142	0.51 $\pm$ 0.05	1,239	3.60 $\pm$ 0.24	104 $\pm$ 2
20	–2,2-Dimethyl-2,3-dihydro-1-benzofuran-7-yl	785 $\pm$ 82	1.15 $\pm$ 0.12	682	7.10 $\pm$ 1.05	101 $\pm$ 4

[a]Binding inhibition of [^{125}I]-FK33824 in cloned μ receptors [45]

[b]Binding against [^{125}I]-[D-Ala^2] deltorphin II in cloned δ receptors [46]

[c]Agonist potency (EC_{50}) measured in [^{35}S]GTPγS binding assays in membranes expressing human δ receptors [46]

piperazine template to incorporate relevant pharmacophore groups such as a phenol ring, phenyl groups, and a hydrophobic moiety. The hydrophobic group was design to mimic the hydrophobic character of the D-Pen residues in DPDPE. Racemic SL-3111 showed high affinity and selectivity for δ opioid receptors. Binding studies on the cloned wild-type and mutated human δ opioid receptors suggested that the new nonpeptidic ligand has a binding profile similar to that of DPDPE but different from that of SNC 80 [47]. In this series, the replacement of N-4 by a methylene group have a dramatic effect on the binding to opioids receptors. Similarly to what it was observed in the SNC-80 series, N-4 is essential for binding at the opioids receptors [48].

2.2 Diarylalkenyl Derivatives

The simplified SNC 80 structure **17** was further modified by replacement of the N-1 of the piperazine with carbon double bond, leading to a new series of diarylalk-enylpiperidines [49]. These new compounds were evaluated for their affinity for all three human opioid receptors and their agonist activity was determined using the

[^{35}S]GTPγS binding assays. These new series of compounds resulted in the most selective δ ligands so far described and from the chemistry point of view they have the advantages of not having chiral centers and being easily synthesized.

The simplified structure **21** shows higher affinity for δ receptors in binding studies and higher selectivity than **17** and SNC 80 under the same conditions of the study (Table 3). In this series it was also shown that the aryl ring could accommodate a 3-OMe group (**22**) or a 3-F substituent (**23**) without affecting the selectivity and affinity for the δ receptor. The position of the substituent on the phenyl ring had a greater influence in both the binding affinity and agonist activity. It was observed that substitution at the *para*-position of the phenyl ring as well as di-*ortho*-substitution appeared to be detrimental.

As was observed in the diarylmethylpiperazine series [46], the replacement of the phenyl ring by other aryl or heteroaryl groups did not affect affinity and selectivity. Unlike what was observed in the SNC 80 series, *N*-allyl substitution (**24** and **25**) resulted in compounds with lower affinity than the unsubstituted parent compound **21**.

Table 3 Receptor affinity and agonist activity of *N*,*N*-diethyl-4-(phenylpiperidin-4-ylidene-methyl)benzamide [49]
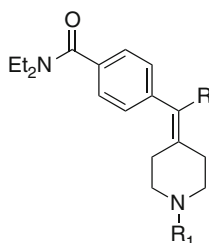
Compound	–R; –R$_1$	Binding (IC$_{50}$ nM ± SD)			Agonist activity[c]	
		μ[a]	δ[b]	IC$_{50}$ ratio μ/δ	(EC$_{50}$ nM ± SEM)	Emax (%)
(+)-**3**, SNC80	–	320 ± 58	1.31 ± 0.17	245	3.67 ± 0.70	100[d]
17	–	8,150 ± 370	11.3 ± 2.3	740	36.5 ± 5.9	104 ± 5
21	–Phenyl; –H	3,800 ± 172	0.87 ± 0.23	4,370	7.2 ± 0.9	110 ± 3
22	–3-MeO-Phenyl;–H	5,250 ± 445	1.56 ± 0.26	3,370	13.7 ± 3.2	109 ± 7
23	–3-F-Phenyl; –H	3,570 ± 444	0.74 ± 0.14	4,820	4.6 ± 0.5	112 ± 6
24	–Phenyl; –Allyl	3,330 ± 275	3.00 ± 0.69	1,110	28.3 ± 2.1	98 ± 3
25	–Phenyl; –3,3-Dimethyl allyl	1,030 ± 100	2.09 ± 0.11	493	14.1 ± 1.8	106 ± 3

[a]Binding inhibition of [^{125}I]-FK33824 in cloned μ receptors [49]
[b]Binding against [^{125}I]-[D-Ala^2] deltorphin II in cloned δ receptors [49]
[c]Agonist potency (EC$_{50}$) measured in [^{35}S]GTP[γS] binding assays in membranes expressing human δ receptors
[d]Reference compound [49]

2.3 4-Diarylaminopiperidines and 4-Diarylaminotropanes

Transposition of the piperazyl N-1 and the benzylic carbon of SNC 80 gave origin to a new series of derivatives known as 4-diarylaminopiperidines. The synthesis of the first analogs with this structure was reported in the patent literature [50]. In this series, replacement of the aryl ring that bears the –OCH₃ group in SNC 80 with other aromatic rings or with substituted phenyl rings as well as piperazine ring contraction was explored, but no biological information was provided. Later, the racemic *cis-* and *trans*-4-[N-allyl-3-methyl-4 piperidinyl) phenylamino]-*N,N*-diethylbenzamides **26** and **27** [51] were synthesized. The *cis* racemate was found to have good affinity and selectivity for the δ receptor in radioligand binding assays (Table 4). In addition, the *cis* racemate was found to stimulate [^{35}S]GTPγS binding at the δ receptor with no measurable stimulation of either the μ or κ receptors. Optical resolution of **26** revealed that the (−)-**26** isomer was responsible for the δ opioid activity of the racemate and behaved as a full agonist. Further information on SAR studies on compounds of the general structure **26** has been reported [52, 53]. These studies have shown that in general these 4-diarylaminopiperidines are less selective relative to their piperazine analogs due to lower δ affinity and an increased affinity for μ receptors. Data available from the *N*-substitution indicates that, in accord with the findings reported in the piperazine series [41, 45], electron rich substituents provide compounds of higher affinity and selectivity (**29, 30**) for the δ opioid receptor. It was also noted that unsubstituted or hydroxyl aryl derivatives in this series were less selective than their methoxy counterparts, possessing greater affinity for both μ and δ receptors (**27, 28**). In these series the *N*-(4-diethylcarboxamidophenyl) group was found to be essential for the interaction at the δ receptor. In addition the *cis* relative stereochemistry between the 3- and 4-substituents in the piperidine ring, a *trans*-crotyl or allyl substituent on the basic nitrogen, and either no substitution or hydroxyl substitution in the aryl ring were features that enhanced the affinity of these ligands for δ receptor receptors. In contrast, binding to the μ receptor appeared to be enhanced by a hydroxyl substitution in the aryl ring, the presence of an additional methyl group in the 2-position of the piperidine ring in a relative *cis* relationship to the 4-amino group, and by *N*-substitution with groups such as cyclopropylmethyl.

In a different series, the effect of replacing the piperidine by a tropane ring was explored [54]. This new class of 4-diarylaminotropanes exhibited high affinity for δ receptors with Kis in the nanomolar range. Affinity was measured by inhibition of [^{3}H]-DPDPE and [^{3}H]-DAMGO to δ opioid and μ opioid receptors from rat brain membranes, respectively. The *endo* isomers were in general more potent and selective than their nonbridged 4-diarylaminopiperidine counterparts and also more selective that the *exo* isomers. The SAR of the endo isomers parallels other series [41, 45, 51, 52].

Table 4 Receptor affinity and agonist activity of 4-[(*N*-substituted-4-piperidinyl)arylamino]-*N,N*-diethylbenzamides [53]
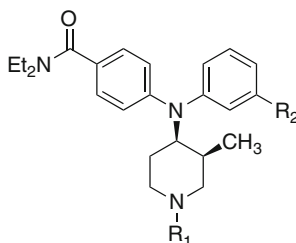
Compound	−R$_1$; −R$_2$	Binding (IC$_{50}$ nM ± SD)			Agonist activity[c]	
		μ[a]	δ[b]	IC$_{50}$ ratio μ/δ	(ED$_{50}$ nM ± SEM)	Emax (%)
(+)-**3**, SNC 80	–	1,614 ± 131	1.57 ± 0.19	1,030	317 ± 54	142 ± 6
(±)-**26** *cis*	−Allyl; −H	1,212 ± 132	11.9 ± 0.9	102	3,500 ± 500	63 ± 5
(+)-**26** *cis*, (3*R*,4*S*)	−Allyl; −H	>4,854	139 ± 11.4	>35	NS[d]	–
(−)-**26** *cis*, (3*S*,4*R*)	−Allyl; −H	2,623 ± 307	5.58 ± 0.31	470	2,508 ± 248	126 ± 5
(±)-**27** *trans*	−Allyl; −OCH$_3$	4,872 ± 541	379 ± 23	13	–	–
(±)-**28** *cis*	−Allyl; −OH	126 ± 9	1.85 ± 0.24	68	90.6 ± 32.4	98 ± 7
(±)-**29** *cis*	*trans*-Crotyl; −H	3,590 ± 285	7.0 ± 0.6	510	–	–
(−)-**29** *cis*	*trans*-Crotyl; −H	938 ± 71	2.72 ± 0.62	345	1,129 ± 230	121 ± 7
(±)-**30** *cis*	*trans*-Crotyl; −OH	40.8 ± 7.8	2.00 ± 0.12	20	28.6 ± 12.5	121 ± 9

[a]Binding inhibition of [^{3}H]-DAMGO in rat brain membranes [53]
[b]Binding against [^{3}H]-[DADLE] in rat brain membranes [53]
[c]Agonist potency, ED$_{50}$ and E$_{max}$, measured in [^{35}S]GTP[γS] binding assays in guinea pig caudate membranes
[d]No simulation [53]

2.4 Diphenylmethyl Bridged Piperazine Derivatives

The replacement of the piperazine ring of SNC 80 with a 6,8-diazabicyclo[3.2.2] nonane scaffold with its trimethylene bridge corresponding to the methyl piperazine substituents in SNC80 gave a series of compounds with high affinity for the δ opioid receptors [55], though relatively lower when compared to SNC80. The analog with the same spatial distribution at the benzhydryl position as SNC80 displayed higher affinity than its diastereomer. Relative to SNC80 these compounds had lower affinity than SNC80.

3 Nonpeptidic δ Opioid Antagonists of the Diarylmethylpiperazine Type

As stated above, alterations in the *N*-substituent to those which tend to confer μ antagonism in the morphinan series (e.g., cyclopropylmethyl) resulted in δ agonists [44]. Indeed, δ antagonists have proved quite elusive in the diarylmethylpiperazine series, and the only antagonist reported to date with a structure of the SNC 80 type is DPI2505 (**9**) (Fig. 2) [31]. The shift of a methyl group in the piperazine ring from the 2-position to the 3-position in the piperazine ring in conjunction with one carbon homologation of the *N*-4-allyl substituent dramatically changed the pharmacological profile of the compounds in these series.

More recently, a series of novel 4,4-diphenylpiperidine and 3,3-diphenyl piperidine derivatives has been characterized as selective antagonists [32]. Compounds **10** and **11** (Fig. 2) are examples of selective antagonists identified in these series. These compounds expand on the SAR of the simplified piperidine analogs of SNC 80 and BW373U86. In these series, the effect of modifications at the amide group, as well as the effect of substitution of the *meta*-phenol group present in BW373U86 by other groups such as low molecular amides, and the effect of the substitution at the piperidine nitrogen were evaluated. In both series, alkyl group modifications were broadly tolerated, and the replacement of the amide with tertiary carbinols was also well tolerated. Primary carboxamides were well tolerated at the *meta*-position, giving compounds with high affinity and selectivity for the δ opioid receptor. Regarding the substitution at the piperidine nitrogen, within the 4,4-biaryl piperidine, long aliphatic and branched alkyl chains resulted in good and selective antagonists. Within the 3,3-diphenyl series, small and medium size alkyl groups at the piperazine nitrogen seems to confer good selectivity and antagonist properties [32].

4 Synthesis of SNC 80 and Related Diphenylarylpiperazines

Several strategies currently exist for the preparation of diphenylmethylpiperazines in optically pure form [24, 44, 56]. SNC 80 and its analogs were initially synthesized by displacing the appropriate benzhydryl chloride with the corresponding enantiomers of the *trans*-1-allyl-2,5-dimethylpiperazine [24]. This initial approach offered the dual advantage of requiring one optical resolution, that of the *trans*-1-allyl-2,5-dimethylpiperazine, and that both optically pure, readily separable, benzylic epimers were obtained in a single step. Though this synthetic route seemed to be adequate to evaluate the effect of the stereochemistry on the δ receptor selectivity, a more efficient stereoselective synthesis of the diarylmethylpiperazine type derivatives that allowed the synthesis of larger quantities of these derivatives was developed by Bishop and McNutt [56]. This synthetic approach involves the stereoselective addition of an organometallic nucleophile to a "masked iminium"

salt to avoid the isolation of the desired iminium salt. The α-benzotriazolylamine was chosen, due to its ability to undergo nucleophilic displacement of the benzotriazole [57, 58]. This adaptation of the Katritzky method for forming tertiary amines provided high yields of the desired diarymethylpiperazine diastereomers with a high diastereomeric excess. Following this approach, compound (+)-2 was synthesized with an 86% diastereomeric excess and 60% yield. Compound (+)-2 was synthesized from the 4-N,N-diethyl-4-formylbenzamide, benzotriazole and the (−)-(2R,5S)-1-allyl-2,5-dimethylpiperazine (Scheme 1). These reagents were heated under reflux in toluene with a Dean–Stark trap attached to remove water. The intermediate benzotriazole was not isolated, and the entire toluene solution was added at room temperature directly to a solution of 3-(tert-butyldimethylsilyloxy) phenylmagnesium bromide in THF at room temperature. Subsequent acidic removal of the silyl protecting group gave (+)-2 in 60% yield in a 93:7 ratio, in favor of the desired diastereomer [56].

The third approach to obtain diarylmethylpiperazine derivatives uses the highly stereospecific chiral oxazaborolidine-catalyzed reduction, using catecholborane as the reductant of the 4-bromobenzophenone chromium tricarbonyl complex, as described by Corey and Helal [59], followed by the stereospecific displacement of the hydroxyl benzyl group by the N-substituted-piperazine [44]. As outlined in Scheme 2, Delorme et al. [44] used this approach for the enantioselective synthesis of compound 31, (+)-4-[(αS)-α-(4-benzyl-1-piperazinyl)benzyl]-N,N-diethylbenzamide. Lithiation of the readily available benzene chromium tricarbonyl with n-BuLi in the presence of TMEDA in THF at −78 °C, followed by addition of
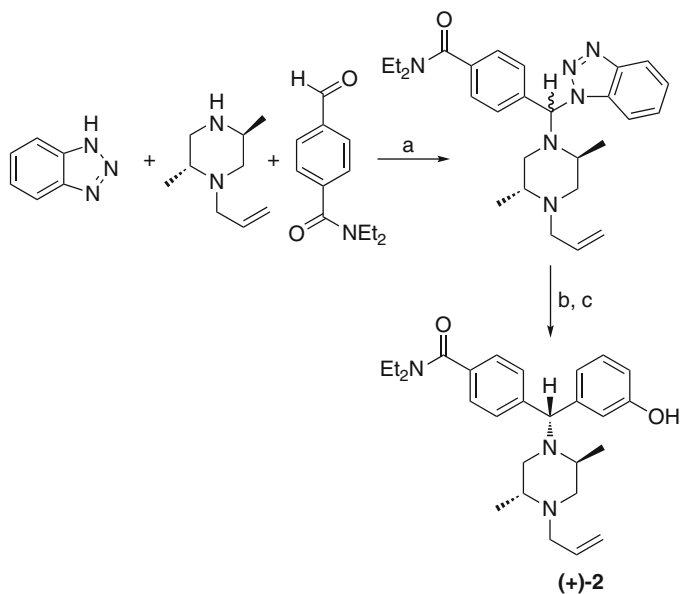
Scheme 1 Reagents. (a) Toluene, 111oC, (-H2O); (b) 3(3-tert-Butylmethylsilyloxy)phenylmagnesium bromide, THF, 25 oC; (c) 3N HCl [56]
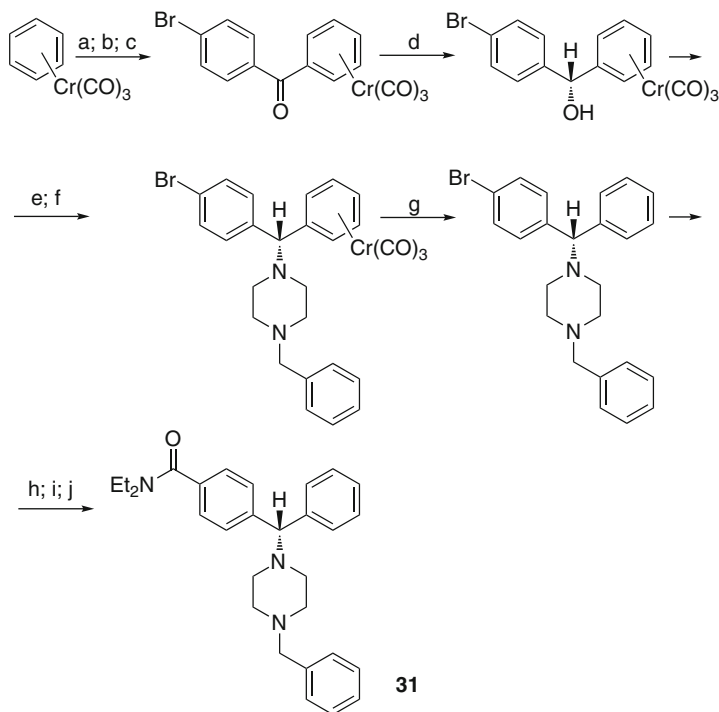
Scheme 2 Reagents. (a) n-BuLi, TMEDA, THF, -78 oC; (b) CuBr. Me2S, THF, -78 oC; (c) p-BrC6H5COCl (74%); (d) , catecholborane, toluene, -78 oC to - 40oC (91%); (e) HBF4-OEt2, CH2Cl2, -60 oC; (f) N-Benzylpiperazine, CH2Cl2 (75%); (g) (NH4)2Ce(NO3)6, MeOH (95%); (h) n-BuLi, CO2, THF, -78 oC; (i) SOCl2, CH2Cl2; (j) Et2NH, CH2Cl2 (34% overall) [44]

copper(I) bromide dimethylsulfide complex (CuBr-Me$_2$S) in THF at $-78\ ^\circ$C, and by reaction with p-bromobenzoyl chloride in THF at $-78\ ^\circ$C, gave the desired 4-bromobenzophenone chromium tricarbonyl complex (74% yield). Addition of a solution of the ketone in toluene to the oxazaborolidine catalyst, formed as described by Corey and Halal [59] by refluxing a solution of (S)-(−)-α,α-diphenyl-2-pyrrolidinemethanol in toluene and n-butyl-boronic acid (n-BuB(OH)$_2$), and catecholborane in toluene at $-78\ ^\circ$C followed by warming of the solution to $-40\ ^\circ$C, afforded the desired benzhydryl alcohol in 91% ee (91% yield). This alcohol was treated with tetrafluoroboric acid–diethyl ether complex (HBF$_4$.OEt$_2$) in CH$_2$C1$_2$ at $-60\ ^\circ$C followed by the addition of N-benzylpiperazine. Decomplexation using ammonium cerium(IV) nitrate ((NH$_4$)$_2$Ce(NO$_3$)$_6$) in MeOH gave the 4-[(αS)-α-(4-benzyl-1-piperazinyl)benzyl]-bromobenzene derivative (95% yield). Transmetallation in dry THF at $-78\ ^\circ$C with n-BuLi, followed by bubbling with carbon dioxide, afforded the corresponding acid, which was treated with thionyl chloride followed by the addition of diethylamine to give compound **31** in 91% ee (34% overall yield).

The synthesis of (+)-**2** and that of SNC 80 requires the enantiopure dimethylpi-perazine derivative, (−)-(2*R*,5*S*)-1-allyl-2,5-dimethylpiperazine. Initially this enantiomer was obtained through a classical resolution of the racemic piperazine. Though practical, this resolution required the use of the unnatural and expensive (−)-camphoric acid to obtain the desired piperazine enantiomer. Janetka et al. [60] described a new, nonchromatogenic, enantioconvergent, synthetic approach that allows the large scale synthesis of the required piperazine enantiomer. This proce-dure involves an efficient optical resolution using relatively inexpensive resolving agents, followed by interconversion of the unwanted (+)-enantiomer to the desired (−)-enantiomer. Allylation of the *trans*-dimethylpiperazine gives a mixture of
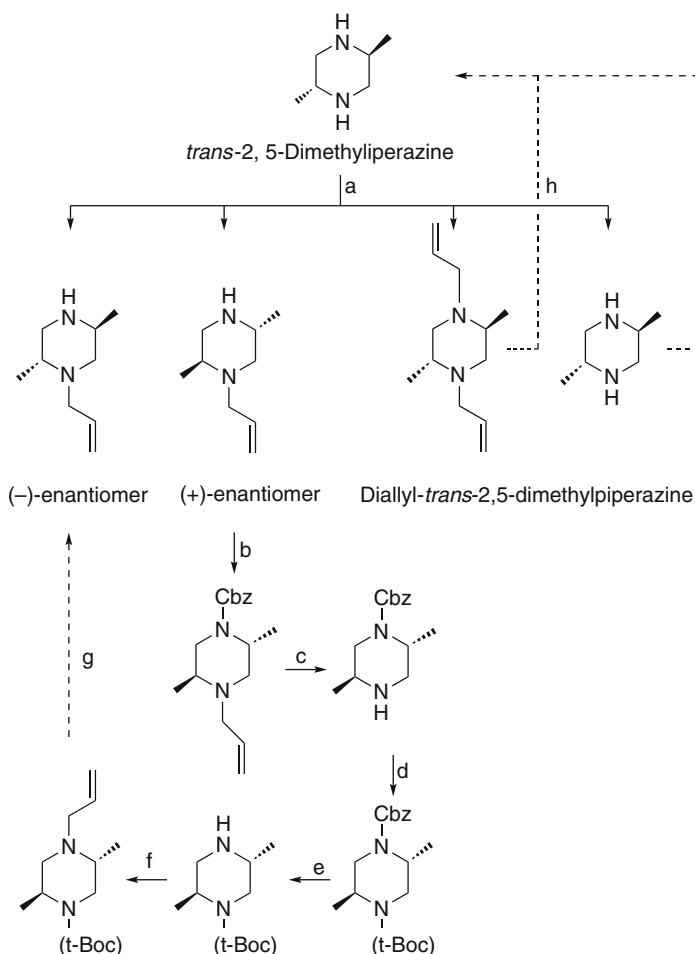
Scheme 3 Reagents. (a) Allyl bromide/Acetone followed by optical resolution; (b) Benzyl chloroformate, NaHCO3 (aq), CHCl3(98%);(c) Pd/C, H2O, AcOH (100%); (d) di-tert-butyl dicarbonate, CH2Cl2 (98%); (e) Pd/C, Ammonium formate, MeOH (97%); (f) Allyl bromide, K2CO3, Acetone (98%); (g) TFA, Triethylsilane, CH2Cl2(89%); (h) Pd/C, H2O, AcOH [60]

unchanged piperazine, (±)-*trans*-2,5-dimethylpiperazine, and 1,4-diallyl-*trans*-2,5-dimethylpiperazine (Scheme 3) [24]. The unchanged piperazine was removed through the hydrobromide salt. The mixture of bases from the filtrate was then treated with succinic acid to give the disuccinate salt of the (±)-monoallylpiperazine. The (+)-enantiomer was removed as its salt with the readily available (+)-camphoric acid and the mixed bases then resolved with (+)-tartaric acid to provide about 40% (of the theoretical 50%) of the desired (−)-enantiomer of >99% optical purity. This procedure proved to be reproducible and satisfactory, using amounts up to 300 g of the (±)-*trans*-2,5-dimethylpiperazine [60]. To increase the efficiency of the resolution a procedure to convert the undesired (+)-enantiomer to the desired one was developed. The goal was to interconvert the (+)-enantiomer to the (−)-enantiomer by moving the allyl group from the N-1 to the N-4 position of the undesired enantiomer This was accomplished by the differential protection of the piperazine's nitrogens as carbamates. To this end, the secondary amine of the (+)-enantiomer was protected as a benzylcarbamate, followed by catalytic *N*-deallylation [61] by one-pot palladium-mediated isomerization and hydrolysis of the resultant enamine. Carbamylation of the benzylcarbamate amine with dibutyl carbamate gave the di-*tert*-butylcarbonate derivative [(2*R*,5*S*)-1-benzyloxycarbonyl-4-*tert*-butoxycarbonyl-2,5-dimethylpiperazine]. Removal of the benzyloxycarbonyl protective group, followed by introduction of the allyl group, and removal of the *tert*-butoxycarbonyl group with trifluoroacetic acid, gave the desired (−)-enantiomer in 79% yield from the (+)-enantiomer (Scheme 3). While the interconversion of enantiomers represented an improvement, the procedure was optimized even further by the recycling of the 1,4-diallyl-2,5-dimethypiperazine, formed in the initial alkylation step, to the *trans*-2,5-dimethylpiperazine by catalytic deallylation (Scheme 3) [61].

5 Conclusions

The discovery of BW373U86 and SNC 80 represented a major development in the search for selective δ opioid agonists, and led to a greater understanding of the pharmacology and to the potential role of the δ opioid system in therapeutics. Structural manipulation has uncovered a unique SAR for these series of ligands, and led to the identification of selective δ opioid agonists and antagonist, as well as of compounds with mixed μ and δ agonist properties. In the last decade, most of the attention has been given to the identification of selective δ opioid ligands. However, research efforts seem to have shifted to the identification of compounds that activate both the δ and the μ receptor systems because this dual receptor modulation may offer a therapeutic advantage in certain disease conditions such as pain management and analgesia [39]. Regarding the chemistry of the diphenylmethylpiperazines, high yield enantioselective synthetic procedures that allow the multigram synthesis of these compounds have been developed [56, 60].

References

1. Pasternak GW (1993) Pharmacological mechanisms of opioid analgesics. Clin Neuropharmacol 16:1–18
2. Quock RM, Burkey TH, Varga E et al (1999) The delta-opioid receptor: molecular pharmacology, signal transduction, and the determination of drug efficacy. Pharmacol Rev 51:503–532
3. Kieffer BL, Befort K, Gavriaux-Ruff C, Hirth CG (1992) The delta-opioid receptor: isolation of a cDNA by expression cloning and pharmacological characterization. Proc Natl Acad Sci USA 89:12048–12052
4. Evans CJ, Keith DE, Morrison H et al (1992) Cloning of a delta opioid receptor by functional expression. Science 258:1952–1955
5. Mansson E, Bare L, Yang D (1994) Isolation of a human kappa opioid receptor cDNA from placenta. Biochem Biophys Res Commun 202:1431–1437
6. Raynor K, Kong H, Chen Y et al (1994) Pharmacological characterization of the cloned kappa-, delta-, and mu-opioid receptors. Mol Pharmacol 45:330–334
7. Brandt MR, Furness MS, Mello NK et al (2001) Antinociceptive effects of delta opioid agonists in rhesus monkeys: effects on chemically induced thermal hypersensitivity. J Pharmacol Exp Ther 296:939–946
8. Mika J, Przewlocki R, Przewlocka B (2001) The role of delta opioid receptor subtypes in neuropathic pain. Eur J Pharmacol 415:31–37
9. Craft RM, Henley SR, Haaseth RC et al (1995) Opioid antinociception in a rat model of visceral pain: systemic versus local drug administration. J Pharmacol Exp Ther 275:1535–1542
10. Broom DC, Jutkiewicz EM, Rice KC et al (2002) Behavioral effects of δ-opioid receptor agonists: potential antidepressants? Jpn J Pharmacol 90:1–6
11. Jutkiewicz EM (2006) The antidepressant-like effects of delta-opioid receptor agonists. Mol Interv 6:162–169
12. Hallet PJ, Brotchie JM (2007) Striatal delta opioid receptor binding in experimental models of Parkinson's disease and dyskinesia. Mov Disord 22:28–40
13. Shippenberg TS, LeFevour A, Chefer VI (2008) Targeting endogenous mu- and delta-opioid receptor systems for the treatment of drug addiction. CNS Neurol Disord Drug Targets 7:442–453
14. Corazziari E (1999) Role of opioid ligands in the irritable syndrome. Can J Gastroenterol 13(Suppl A):71A–75A
15. Rapaka RS, Porreca F (1991) Development of delta opioid peptides as non-addicting analgesics. Pharm Res 8:1–8
16. Galligan JJ, Mosberg HI, Hurst R et al (1984) Cerebral delta opioid receptors mediate analgesia but not the intestinal motility effects of intracerebroventricularly administered opioids. J Pharmacol Exp Ther 229:641–648
17. Reisine T, Pasternak G (1996) Opioid analgesics and antagonists. In: Hardman JG, Limbird LE, Molinoff PB, Ruddon RW, Gila AG (eds) Goodman & Gilman's the pharmacological basis of therapeutics, 9th edn. McGraw-Hill, New York
18. Heyl DL, Schullery SE (1997) Developments in the structure-activity relationships for the delta-selective opioid peptides of amphibian skin. Curr Med Chem 4:117–150
19. Egleton RD, Davis TP (1997) Bioavailability and transport of peptides and peptide drugs into the brain. Peptides 18:1431–1439
20. Portoghese PS, Sultana M, Nagase H (1988) Application of message-address concept in the design of highly potent and selective non-peptide δ opioid receptor antagonists. J Med Chem 31:281–282
21. Schwyzer R (1977) ACTH: a short introductory review. Ann NY Acad Sci 297:3–26
22. Lee PHK, McNutt RW, Chang K-J. In: Abstracts of the 1992 college on problems of drug dependence- international narcotics research conference, Abstract 34

23. Chang KJ, Rigdon GC, Howard JL, McNutt RW (1993) A novel, potent and selective nonpeptidic delta opioid receptor agonist BW373U86. J Pharmacol Exp Ther 267:852–857
24. Calderon SN, Rothman RB, Porreca F et al (1994) Probes for narcotic receptor mediated phenomena. 19. Synthesis of (+)-4-[(αR)-α-((2 S,5R)-4-allyl-2,5-dimethyl-1-piperazinyl)-3-methoxybenzyl]-N,N-diethylbenzamide (SNC 80): a highly selective, nonpeptide delta opioid receptor agonist. J Med Chem 37:2125–2128
25. Portoghese PS, Moe ST, Takemori AE (1993) A selective δ1 opioid receptor agonist derivative from oxymorphone. Evidence for separate recognition sites for δ1 opioid receptor agonists and antagonists. J Med Chem 36:2572–2574
26. Kamei J, Saitoh A, Ohsawa M et al (1995) Antinociceptive effects of the selective non-peptidic delta-opioid receptor agonist TAN-67 in diabetic mice. Eur J Pharmacol 276:131–135
27. Nagase H, Kawai K, Hayakawa J et al (1998) Rational drug design and synthesis of a highly selective nonpeptide δ-opioid agonist, (4aS*,12aR*)-4a-(3-hydroxyphenyl)-2-methyl-1,2,3,44a,12,12a-octahydropyrido[3,4-b]acridine (TAN-67). Chem Pharm Bull 46:1695–1702
28. Dondio G, Ronzoni S, Petrillo P (1997) Non-peptide delta opioid agonists and antagonists. Exp Opin Ther Pat 7:1075–1098
29. Dondio G, Ronzoni S, Petrillo P (1999) Non-peptide delta opioid agonists and antagonists (part II). Exp Opin Ther Pat 9:353–374
30. Dondio G, Ronzoni S, Eggleson DS et al (1997) Discovery of a novel class of substituted pyrrolooctahydroisoquinolines as potent and selective delta opioid agonists, based on an extension of the message-address concept. J Med Chem 40:3192–3198
31. Su YF, McNutt RW, Chang KJ (1998) Delta-opioid ligands reverse alfentanil-induced respiratory depression but not antinociception. J Pharmacol Exp Ther 287:815–823
32. Liras S, McHardy SF, Allen MP et al (2010) Biaryl piperidines as potent and selective delta opioid receptor ligands. Bioorg Med Chem Lett 20:503–507
33. Calderon SN, Coop A (2004) SNC 80 and related agonists. Curr Pharm Des 10:733–742
34. Chang K-J, Boswell GE, Bubacz DG, Collins MA, Davis AO, McNutt RW (1993) International Patent Application WO93/15062
35. Wild KD, McCormick J, Bilsky EJ et al (1993) Antinociceptive actions of BW373U86 in the mouse. J Pharmacol Exp Ther 267:858–865
36. Bilsky EJ, Calderon SN, Wang T et al (1995) SNC 80, a selective, nonpeptidic and systemically active opioid delta agonist. J Pharmacol Exp Ther 273:359–366
37. Calderon SN, Rice KC, Rothman RB et al (1997) Probes for narcotic receptor mediated phenomena. 23. Synthesis, opioid receptor binding, and bioassay of the highly selective delta agonist (+)-4-[(αR)-α-((2 S,5R)-4-allyl-2,5-dimethyl-1-piperazinyl)-3-methoxybenzyl]-N,N-diethylbenzamide (SNC 80) and related novel nonpeptide delta opioid receptor ligands. J Med Chem 40:695–704
38. Katsura Y, Zhang X, Homma K et al (1997) Probes for narcotic receptor-mediated phenomena. 25. Synthesis and evaluation of N-alkyl-substituted (α-piperazinylbenzyl)benzamides as novel, highly selective delta opioid receptor agonists. J Med Chem 40:2936–2947
39. Bishop MJ, Garrido DM, Boswll GE et al (2003) 3-(αR)-α((2S,5R)-4-Allyl-2,5-dimethyl-1-piperazinyl)-3-hydroxybenzyl)-N-alkyl-N-arylbenzamides: potent, non-peptidic agonists of both the μ and δ opioid receptors. J Med Chem 46:623–633
40. Middleton DS, Maw GN, Challenger C et al (2006) Highly potent and selective zwitterionic agonists of the delta-opioid receptor. Part 1. Bioorg Med Chem Lett 16:905–910
41. Zhang X, Rice KC, Calderon SN et al (1999) Probes for narcotic receptor mediated phenomena. 26. Synthesis and biological evaluation of diarylmethylpiperazines and diarylmethylpiperidines as novel, nonpeptidic delta opioid receptor ligands. J Med Chem 42:5455–5463
42. Cottney J, Rankovic Z, Morphy JR (1999) Synthesis of novel analogues of the delta opioid ligand SNC-80 using REM resin. Bioorg Med Chem Lett 9:1323–1328
43. Barn DR, Bom A, Cottney J et al (1999) Synthesis of novel analogues of the delta opioid ligand SNC-80 using AlCl3-promoted aminolysis. Bioorg Med Chem Lett 9:1329–1334

44. Delorme D, Berthelette C, Lavoie R, Roberts E (1998) Asymmetric synthesis of diarylmethy-lamines: preparation of selective opioid delta receptor ligands. Tetrahedron Asymmetry 9:3963–3966
45. Furness SC, Zhang X, Coop A et al (2000) Probes for narcotic receptor-mediated phenomena. 27. Synthesis and pharmacological evaluation of selective delta-opioid receptor agonists from 4-[(αR)-alpha-(2S,5R)-4-substituted-2,5-dimethyl-1-piperazinyl-3-methoxybenzyl]-N,N-diethylbenzamides and their enantiomers. J Med Chem 43:3193–3196
46. Pobleck N, Delorme D, Wei Z-Y et al (2000) New diarylmethylpiperazines as potent and selective nonpeptidic delta opioid receptor agonists with increased in vitro metabolic stability. J Med Chem 43:3878–3894
47. Liao S, Alfaro-Lopez J, Shenderovich MD et al (1998) De novo design, synthesis, and biological activities of high-affinity and selective non-peptide agonists of the delta-opioid receptor. J Med Chem 41:4767–4776
48. Alfaro-Lopez J, Okayama T, Hosohata K et al (1999) Exploring the structure-activity relationships of [1-(4-tert-butyl-3'-hydroxy)benzhydryl-4-benzylpiperazine] (SL-3111), a high-affinity and selective δ-opioid receptor nonpeptide agonist ligand. J Med Chem 42:5359–5368
49. Wei Z-Y, Brown W, Takasaki B et al (2000) N,N-Diethyl-4-(phenylpiperidin-4-ylidene-methyl)benzamide: a novel, exceptionally selective, potent delta opioid receptor agonist with oral bioavailability and its analogues. J Med Chem 43:3895–3905
50. Pelcman B, Roberts E (1998) International Patent Application WO 98/28270
51. Thomas JB, Herault XM, Rothman RB et al (1999) (+/−)-4-[(N-Allyl-cis-3-methyl-4-piperidinyl)phenylamino]-N,N-diethylbenzamide displays selective binding for the delta opioid receptor. Bioorg Med Chem Lett 9:3053–3056
52. Thomas JB, Atkinson RN, Herault XM et al (1999) Optically pure (−)-4-[(N-allyl-3-methyl-4-piperidinyl)phenyl-amino]-N,N-diethylbenzamide displays selective binding and full ago-nist activity for the delta opioid receptor. Bioorg Med Chem Lett 9:3347–3350
53. Thomas JB, Herault XM, Rothman RB et al (2001) Factors influencing agonist potency and selectivity for the opioid delta receptor are revealed in structure-activity relationship studies of the 4-[(N-substituted-4-piperidinyl)arylamino]-N,N-diethylbenzamides. J Med Chem 44:972–987
54. Boyd RE, Carson JR, Codd EE et al (2000) Synthesis and binding affinities of 4-diarylamino-tropanes, a new class of delta opioid agonists. Bioorg Med Chem Lett 10:1109–1111
55. Holl R, Jung B, Schepmann D et al (2009) Synthesis and pharmacological evaluation of SNC80 analogues with bridged piperazine ring. ChemMedChem 4:2111–2122
56. Bishop MJ, McNutt RW (1995) An efficient synthesis of the benzhydrylpiperazine delta opioid agonist (+)-BW373U86. Bioorg Med Chem Lett 5:1311–1314
57. Katritzky AR, Rachwal S, Rachwal B (1987) The chemistry of N-substituted benzotriazoles. Part 4. A novel and versatile method for the mono-N-alkylation of aromatic and heteroaro-matic amines. J Chem Soc Perkin Trans I:805–809
58. Katritzky AR, Yannakopoulou K, Lue P et al (1989) The chemistry of N-substituted benzo-triazoles. Part 14. Novel routes to secondary and tertiary amines and N,N-disubstituted hydroxylamines. J Chem Soc Perkin Trans I:225–233
59. Corey EJ, Helal CJ (1996) Catalytic enantioselective synthesis of the second generation histamine agonist cetirizine hydrochloride. Tetrahedron Lett 37:4837–4840
60. Janetka JW, Furness MS, Zhang X et al (2003) Enantioconvergent synthesis of (−)-(2R,5 S)-1-allyl-2,5-dimethylpiperazine, an intermediate to δ-opioid receptor ligands (2003). J Org Chem 68:3976–3980
61. Tomori H, Shibutami K, Ogura K (1997) Practical synthesis of (S)-3-(p-nitrobenzyloxycar-bonylamino)pyrrolidine and its related compounds from -aspartic acid. Heterocycles 44:213–225

Synthesis of Neoclerodane Diterpenes and Their Pharmacological Effects

Kimberly M. Lovell, Katherine M. Prevatt-Smith, Anthony Lozama, and Thomas E. Prisinzano

Abstract Salvinorin A is a neoclerodane diterpene that has been shown to be an agonist at kappa opioid receptors. Its unique structure makes it an attractive target for synthetic organic chemists due to its seven chiral centers and diterpene scaffold. This molecule is also interesting to pharmacologists because it is a non-serotonergic hallucinogen, and the first opioid ligand discovered that lacks a basic nitrogen. There have been several total synthesis approaches to salvinorin A, and these will be detailed within this chapter. Additionally, research efforts have concentrated on structure modification of the salvinorin A scaffold through semi-synthetic methods. Most modifications have focused on the manipulation of the acetate at C-2 and the furan ring. However, chemistry has also been developed to generate analogs at the C-1 ketone, the C-4 methyl ester, and the C-17 lactone. The synthetic methodologies developed for the salvinorin A scaffold will be described, as well as specific analogs with interesting biological activities.

Keywords Neoclerodane diterpene · Salvinorin A · κ Opioid

Contents

K.M. Lovell and K.M. Prevatt-Smith contributed equally to this work.

K.M. Lovell, K.M. Prevatt-Smith, and T.E. Prisinzano (✉)
Department of Medicinal Chemistry, The University of Kansas, Lawrence, KS 66045-7582, USA
e-mail: prisinza@ku.edu

A. Lozama
Division of Medicinal and Natural Products Chemistry, College of Pharmacy, The University of Iowa, Iowa City, IA 52242-1112, USA

Abbreviations

Ac	Acetyl
acac	Acetylacetonate
AIBN	2,2′-Azobisisobutyronitrile
Ar	Aryl
BINAP	2,2′-Bis(diphenylphosphino)-1,1′-binaphthalene
Bn	Benzyl
Boc	*tert*-Butoxycarbonyl
BOM	Benzyloxymethyl
Bu	Butyl
Bz	Benzoyl
cat	Catalyst
CC	cis-cis
CDMT	2-Chloro-4,6-dimethoxy-1,3,5-triazine
CNS	Central nervous system
Cp	Cyclopentadienyl
CT	cis-trans
d	Day(s)
dba	Dibenzylideneacetone
DBAD	Di-*tert*-butylazodicarboxylate
DBU	1,8-Diazabicyclo[5.4.0]undec-7-ene
DCC	*N,N*-Dicyclohexylcarbodiimide
DDQ	2,3-Dichloro-5,6-dicyano-1,4-benzoquinone
DEAD	Diethyl azodicarboxylate
DIAD	Diisopropyl azodicarboxylate
DIBALH	Diisobutylaluminum hydride
DMAP	4-(Dimethylamino)pyridine
DMF	Dimethylformamide
DMPU	1,3-Dimethyl-3,4,5,6-tetrahydro-2(1H)-pyrimidinone
DMSO	Dimethylsulfoxide
DOB	4-Bromo-2,5-dimethoxyamphetamine
DOP	δ Opioid receptor
dppf	1,1′-Bis(diphenylphosphino)ferrocene
EDCI	*N*-(3-Dimethylaminopropyl)-*N*′-ethylcarbodiimide
eq.	Equivalent(s)

Et	Ethyl
Fmoc	9-Fluorenylmethoxycarbonyl
h	Hour(s)
HOBt	1-Hydroxybenzotriazole
HPLC	High pressure liquid chromatography
Im	Imidazole
i-Pr	Isopropyl
KHMDS	Potassium hexamethyldisilazide, potassium bis(trimethylsilyl)amide
KOP	κ Opioid receptor
L	Liter(s)
LAH	Lithium aluminum hydride
LHMDS	Lithium hexamethyldisilazide, lithium bis(trimethylsilyl)amide
LSD	Lysergic acid diethylamide
m-CPBA	*m*-Chloroperoxybenzoic acid
Me	Methyl
MEM	(2-Methoxyethoxy)methyl
Me-WMK	(*R*)-(−)-Wieland–Miescher ketone
min	Minute(s)
MNBA	2-Methyl-6-nitrobenzoic anhydride
mol	Mole(s)
MOM	Methoxymethyl
MOP	μ Opioid receptor
Ms	Methanesulfonyl (mesyl)
NaHMDS	Sodium hexamethyldisilazide
NBS	*N*-Bromosuccinimide
n-bu	*n*-Butyl
NCS	*N*-Chlorosuccinimide
NMM	4-Methylmorpholine
NMO	4-Methylmorpholine *N*-oxide
PCC	Pyridinium chlorochromate
PDC	Pyridinium dichromate
Ph	Phenyl
PPTS	Pyridinium *p*-toluenesulfonate
Pr	Propyl
PTSA	*p*-Toluene sulfonic acid
Pv	Pivaloyl
py	Pyridine
rt	Room temperature
s	Second(s)
SAR	Structure-activity relationship
s-Bu	*sec*-Butyl
TBAF	Tetrabutylammonium fluoride
TBS	*tert*-Butyldimethylsilyl
TBSOTf	*tert*-Butyldimethylsilyl trifluoromethaneulfonate

t-Bu	*tert*-Butyl
TC	trans-cis
TES	Triethylsilyl
Tf	Trifluoromethanesulfonyl (triflyl)
TFA	Trifluoroacetic acid
TFAA	Trifluoroacetic anhydride
THF	Tetrahydrofuran
THP	Tetrahydropyran-2-yl
TIPS	Triisopropylsilyl
TLC	Thin layer chromatography
TMS	Trimethylsilyl
Tol	4-Methylphenyl
Ts	Tosyl, 4-toluenesulfonyl
TT	trans-trans

1 Introduction

Salvinorin A (**1**), a neoclerodane diterpene, is the active component of *Salvia divinorum* Epling & Jativa (Lamiaceae), a widely available psychoactive plant (Fig. 1) [1]. *S. divinorum* is a member of the sage family and is indigenous to Oaxaca, Mexico [1, 2]. It has been used for centuries by the Mazatec Indians in divination ceremonies as well as for headaches, rheumatism, and *panzón de barrego*, a semi-magical disease [2]. Diterpene **1** was isolated from *S. divinorum* and determined to be a potent hallucinogen with an active dose in humans of 200–1,000 μg when smoked, rivaling the potency of other classical hallucinogens such as lysergic acid diethylamide (LSD) and 4-bromo-2,5-dimethoxyamphetamine (DOB) [1, 3–6]. However, unlike LSD and DOB, **1** does not have activity at the serotonin $5HT_{2A}$ receptor [5, 7]. Instead, **1** was found to be a selective κ opioid (KOP) receptor agonist [4].

Salvinorin A (**1**) is the first non-nitrogenous natural product having high affinity and efficacy at KOP receptors [4]. Its unique structure has little structural similarity to other known opioid receptor ligands such as morphine (**2**), cyclazocine (**3**), fentanyl (**4**), SNC 80 (**5**), U50,488 (**6**), 3FLB (**7**), dynorphin A (**8**) (Fig. 2) [8–11]. All of these known opioid receptor ligands have a basic amino group, which was thought to be required for affinity. It was accepted that the positively charged nitrogen of the ligand interacts with an aspartate residue in the third transmembrane region of the opioid receptor, which is a G-protein coupled receptor [9, 12, 13]. Diterpene **1** lacks a basic amino group, which consequently led to reevaluation of the necessity of a basic nitrogen for opioid receptor affinity and efficacy [14]. In fact, recent work has found that other opioid ligands retain some affinity and efficacy at opioid receptors, even when the basic nitrogen is removed.
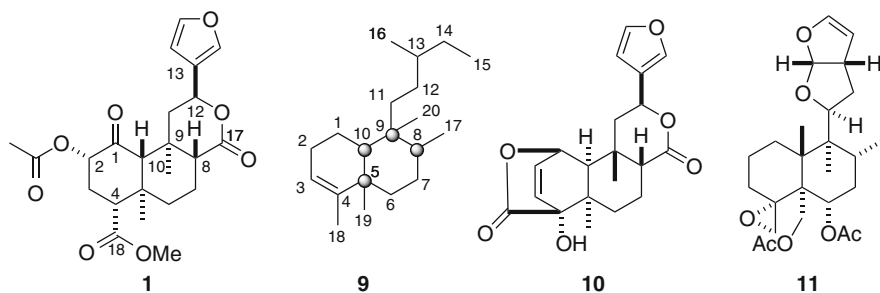
Fig. 1 Salvinorin A (**1**), clerodane skeleton (**9**), columbin (**10**), and clerodin (**11**)
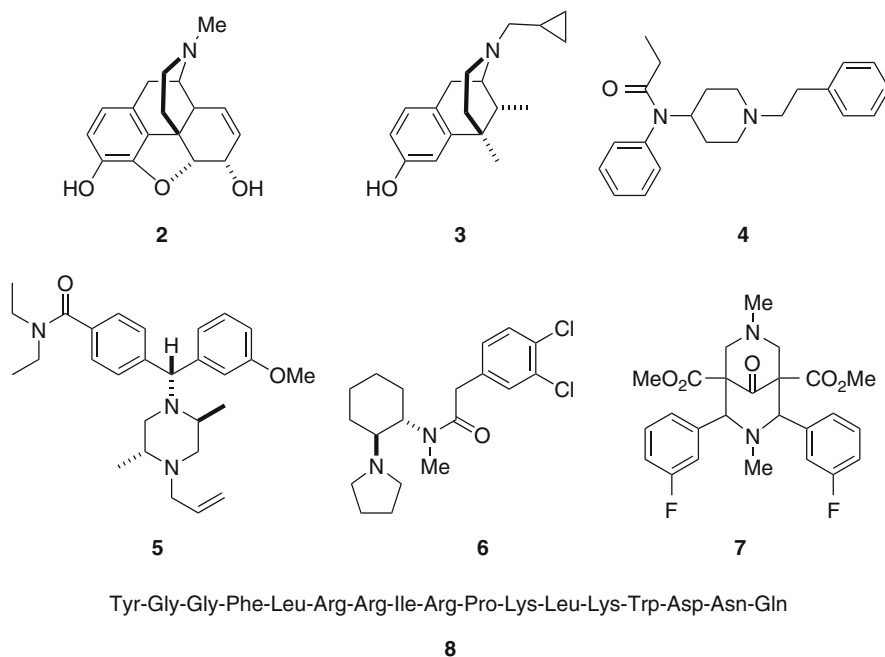
Fig. 2 Morphine (**2**), cyclazocine (**3**), fentanyl (**4**), SNC 80 (**5**), U50,488 (**6**), 3FLB (**7**), and dynorphin A (**8**)

Neoclerodane diterpenes are members of the terpene class of natural products. Terpenes provide interesting chemical targets for organic chemists and pharmacologists. Their structural complexity and diversity, along with their unique pharmacological profiles, result in attractive structural scaffolds for investigation. Terpenes are secondary metabolites and are thus found in very low concentrations in living organisms [15]. They are biosynthesized from units of isoprene and are classified based on the varying number of isoprene units present in their carbon skeleton [15].

Isoprene has the chemical formula of C_5H_8, therefore, each isoprene unit correlates to five carbons present in the skeleton. Terpene classification includes hemiterpenes, monoterpenes, sesquiterpenes, diterpenes, sesterterpenes, and triterpenes, each consisting of one through six isoprene units, respectively [16]. Additional terpene classifications include tetraterpenes, containing eight isoprene units, and polyterpenes, which include isoprene chains. The classification system is further divided into subclasses [15].

Specifically focusing on diterpenes, there are over 50 different subclasses of skeletons and many of these subclasses include compounds with biological activity [16]. Some of the most recognized diterpene subclasses include labdanes, kauranes, gibberlins, beyeranes, aphidicolins, cembranes, and abietanes. The clerodanes are another subclass of diterpenes that are known to have biological activity. Clerodanes (**9**) are ubiquitous throughout nature and are found in a variety of plants, fungi, and microorganisms (Fig. 1) [17]. A secondary metabolite is deemed a clerodane if it contains four isoprene units and four contiguous stereocenters on a *cis* or *trans* decalin ring system [17]. Approximately 25% of clerodanes contain the *cis* ring fusion and an example of this is columbin. Columbin (**10**), a diterpenoid furanolactone, has been isolated from several plants including *Sphenocentrum jollyanum* Pierre (Menispermaceae) and *Jateorhiza columba* Miers (Menispermacea) [18, 19]. It is sold in a crude drug preparation called Calumbae Radix or Tinosporae Radix [18]. Columbin itself has been shown to have dose dependent anti-inflammatory activity and chemopreventative activity against colorectal cancer [18–20]. The other 75% of clerodanes contain the *trans* ring fusion resembling clerodin. Clerodin (**11**) was originally isolated from *Clerodendrum infortunatum* L. (Lamiaceae) and is an insect antifeedant with potential as a natural pesticide [21–23]. Along with the relative configuration of the *trans* or *cis* junctions of the fused rings, clerodanes are further classified by their relative configuration at C-8 and C-9 [17]. This extra clarification results in four types of clerodane skeletons as defined with respect to configuration of ring fusion and substitution pattern at C-8 and C-9: *trans-cis* (TC), *trans-trans* (TT), *cis-cis* (CC) and *cis-trans* (CT) [17]. Clerodanes are further classified by their absolute stereochemistry. Compounds that have the same absolute stereochemistry as clerodin are termed neoclerodanes and compounds that are enantiomers of clerodin are referred to as *ent*-neoclerodanes [24, 25].

The biological activity and structural complexity of neoclerodane diterpenes have driven their study through total synthesis efforts and pharmacological investigation through biological and structure-activity relationship (SAR) studies. However, difficulties in conducting these studies result from the structural complexity, sensitivity to conditions of many typical organic reactions, potential problems in acquiring the natural product or plant material for extraction, and the unknown sites of action of neoclerodane diterpenes. The lack of precedent for chemical methodology required to transform neoclerodanes contributes to the limited SAR studies to date. Furthermore, developing reactions that are chemoselective for molecules that are often polyfunctionalized and contain multiple chiral centers is an extremely difficult undertaking. Determination of the molecular basis of activity through semi-synthetic means requires access to the natural product in substantial quantities,

which can be difficult or impossible to obtain. Additionally, the site of action of neoclerodane diterpenes is often unknown, increasing the difficulty in SAR development. Despite these challenges, several neoclerodane diterpenes, including salvinorin A (**1**), have been investigated through total synthesis, semi-synthetic, and pharmacological studies.

Salvinorin A is a tricyclic *trans-cis* neoclerodane diterpene containing seven chiral centers. Additionally, **1** contains multiple functional groups, which include four carbonyls at C-1, C-17, C-18, and C-21. Two of the carbonyls are esters off of the C-2 and C-4 positions of the decalin core, and the C-17 carbonyl is part of a δ-lactone ring system. Additionally, **1** contains a furan ring off C-12. Along with the functionality present on **1**, C-8 has been shown to undergo epimerization readily in acidic or basic conditions. Despite the molecular complexity, total syntheses of **1** have been accomplished and structural modifications have been completed. This chapter will address total synthetic attempts towards the molecule itself and synthetic methodologies developed and applied to modify the salvinorin A scaffold.

2 Total Synthesis Efforts

The first published attempt at the total synthesis of **1** was by Lingham and coworkers [26]. They envisioned **1** being derived from highly functionalized ketone **12** and lactone **13** (Fig. 3). They believed that these two pieces could converge to form **1** through a Michael-type addition. The synthesis of **13** began with the reaction of 3-furylaldehyde with acetone and NaOH to give the racemic alcohol **14** in 97% yield (Scheme 1). Compound **14** was reacted with (Z)-2-bromobut-2-enoyl chloride to produce **15** in 92% yield. Treatment of this compound with Rieke zinc and acid afforded **13** as a 1:1 mixture of isomers in 92% yield. There are no additional reports towards the synthesis of **1** by this group to date.

In 2007, the first successful total synthesis of **1** was reported by Evans and coworkers in 33 steps with 4.5% overall yield [27]. Evans envisioned **1** being derived from macrolactone **16** through a transannular Michael cascade (Fig. 4). Compound **16** would be derived from the fusion of vinyl iodine **17** and the highly functionalized aldehyde **18**. The synthesis began when 3-furylaldehyde was reacted with propyne and oxidized with MnO_2 to afford ketone **19** in 70% yield (Scheme 2). Reduction of **19** with (R)-β-methyl-oxazaborolidene gave the α-alcohol **20** in 85% yield. Using KH and $H_2N(CH_2)_3NH_2$, alkyne **20** was isomerized and followed with carboalumination and protection of the alcohol to give **17** in 68% yield. Compound **22** was produced in 85% yield from a Claisen condensation between **21** and ethyl hydrogen malonate. Lithium hexamethyldisilazide (LHMDS) and $ClPO(OEt)_2$ followed by Fe-catalyzed cross-coupling produced **23** in 92% yield [28]. Compound **23** was involved in an aldol addition, alcohol protection, and acetylide addition to afford propargylic alcohol **24** in 83% yield. Compound **24** went through a series of reactions including protection, semi-hydrogenation, dihydroxylation, and ultimately oxidative cleavage to give **18** in 92% yield. A Grignard of **17** was

Fig. 3 Retrosynthetic
analysis of salvinorin A
proposed by Lingham and
co-workers
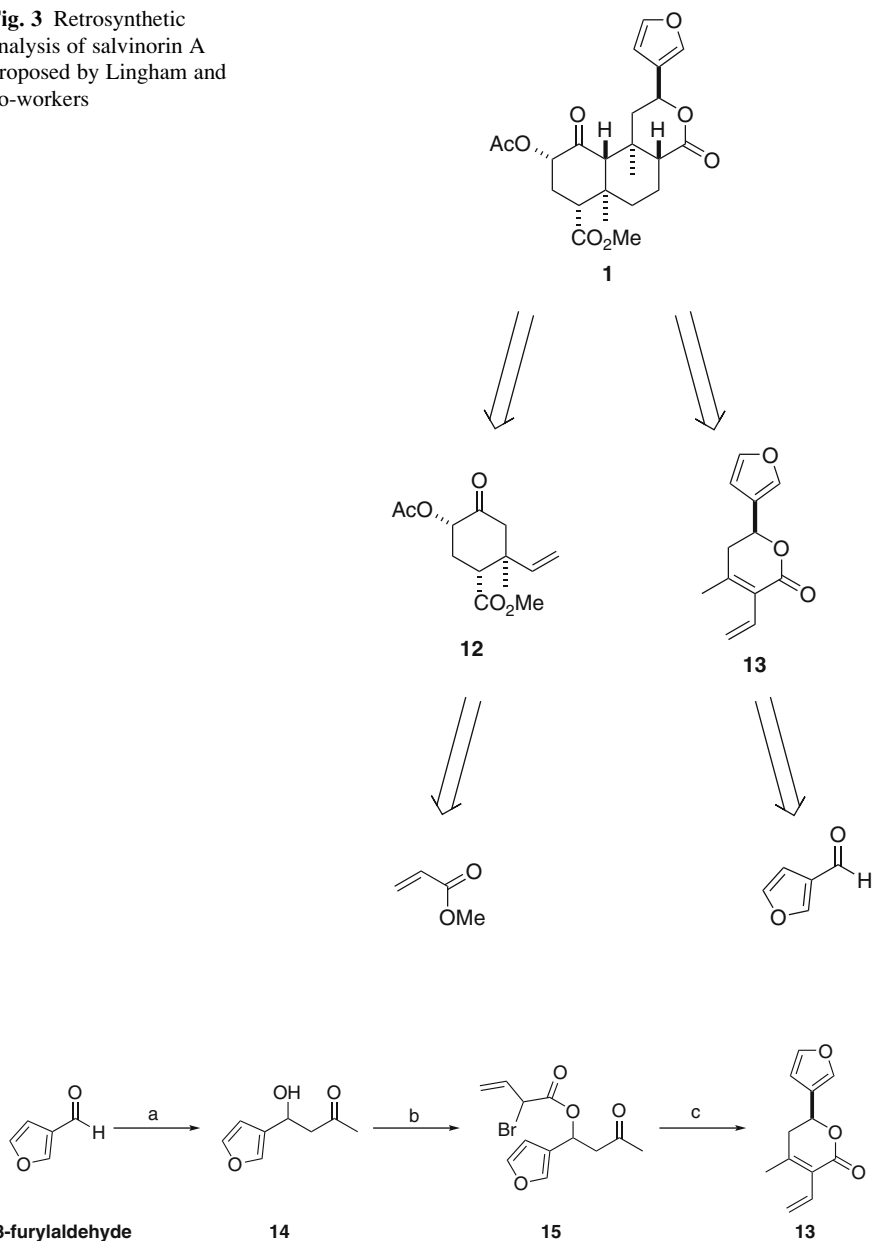
Scheme 1 (a) Acetone, NaOH; (b) (Z)-2-bromobut-2-enoyl chloride, Et$_3$N, Et$_2$O; (c) Rieke zinc in THF/H$_3$O$^+$

then reacted with **18** to give alcohol in **25** 75% yield. Alcohol **25** was then silated with *tert*-butyldimethylsilyl trifluoromethaneulfonate (TBSOTf), and subsequently deprotected and hydrolyzed with LiOH to give **26** in 93% yield. Shiina
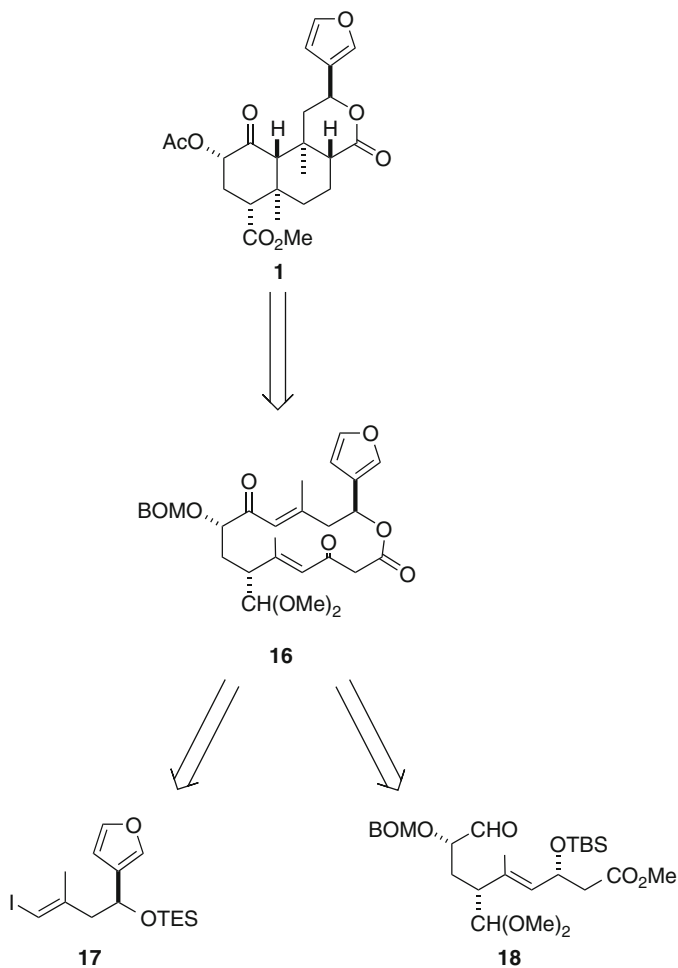
Fig. 4 Retrosynthetic analysis of salvinorin A proposed by Evans and co-workers

macrolactonization followed by removal of a silyl group and oxidation gave **16** in 95% yield [29, 30]. Treating **16** with tetrabutylammonium fluoride (TBAF) at −78 °C, followed by warming to 5 °C triggered the transannular cascade to give the tricyclic compound **27** as a single diastereomer in 95% yield. The enol of compound **27** was deoxygenated utilizing triflate formation followed by catalytic and conjugate reduction to give **28** in 78% yield. Compound **28** was subjected to deprotection, oxidation, and esterification to give **29** in 95% yield. K_2CO_3 in MeOH was used to epimerize C-8 and subsequent acylation afforded **1** in 78% yield.

Many neoclerodanes, including **1** contain a *trans*-decalin core. In their attempt to synthesize **1**, Burns and Forsyth have developed a synthetic strategy to establish the core through an intramolecular Diels–Alder/Tsuji allylation sequential sequence
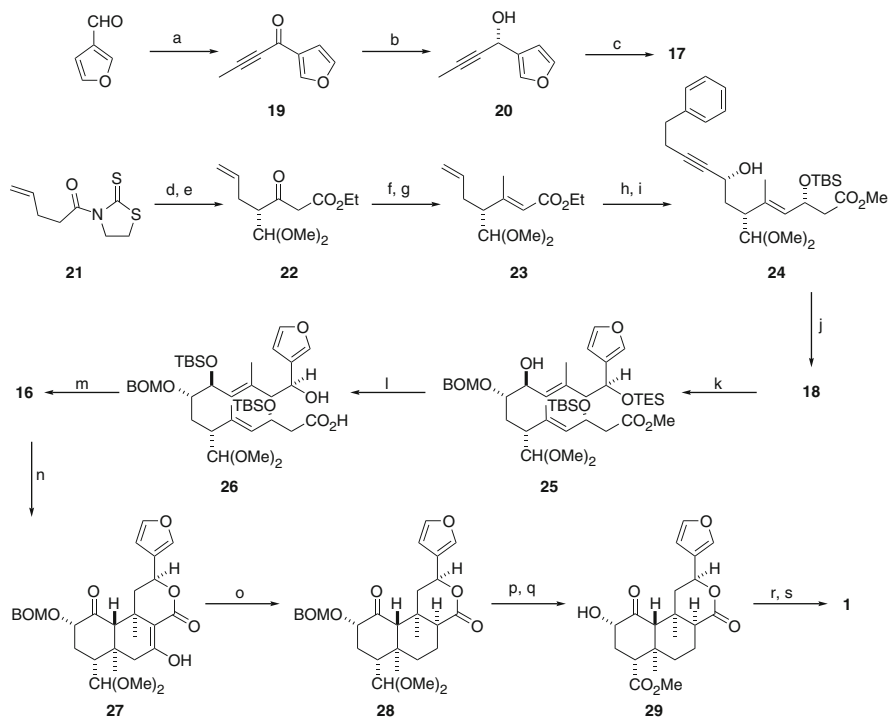
Scheme 2 (a): (1) Propyne, *n*-BuLi, Et$_2$O, -78 °C, (2) MnO$_2$; (b) (*R*)-*B*-Methyl-CBS catalyst, BH$_3$•Me$_2$S, -30 °C; (c): (1) KH, H$_2$N(CH$_2$)$_3$NH$_2$, 0 °C; (2) Me$_3$Al, Cp-2ZrCl$_2$, I$_2$, -45° C; (3) TESCl, imidazole; (d) Ni-(*R*)-BINAP(OTf)$_2$, 2,6-lutidine, BF$_3$•OEt$_2$, HC(OMe)$_3$; (e) HO$_2$CCH$_2$-CO$_2$Et, *i*-PrMgCl, 65 °C; (f) LHMDS, ClPO(OEt)$_2$; (g) Fe(acac)$_3$, MeMgCl, -20 °C; (h): (1) DIBALH, -78 °C; (2) MnO$_2$; (3) Sn(OTf)$_2$, *N*-ethylpiperidine, (*S*)-3-acetyl-4-isopropylthiazoli-dine-2-thione, -78 °C; (i): (1) TBSOTf, 2,6-lutidine; (2) K$_2$CO$_3$, MeOH; (3) OsO$_4$, NMO, NaIO$_4$; (4) Zn(OTf)$_2$, (−)-*N*-methyl-ephedrine, Et$_3$N, 4-phenyl-1-butyne; (j): (1) BOMCl, NaHMDS, -78 °C; (2) Lindlar catalyst, H$_2$; (3) K$_2$OsO$_4$, NMO, citric acid, 50°C, Pb(OAc)$_4$, K$_2$CO$_3$; (k) **17**, *n*-BuLi, MgBr•OEt$_2$, CH$_2$Cl$_2$, -78 to 0 °C; (l): (1) TBSOTf, 2,6-lutidine; (2) PPTS, MeOH; (3) LiOH, *i*-PrOH, H$_2$O; (m): (1) MNBA, DMAP, [0.0015 M]; (2) TBAF; (3) Dess–Martin periodinane; (n) TBAF, -78 to 5 °C; (o): (1) NaH, Comins' reagent; (2) Pd(OAc)$_2$, dppf, Et$_3$SiH; (3) L-selectride, *t*-BuOH, -78 to -55 °C; (p) LiBF$_4$, CH$_3$CN/H$_2$O; (q) NaClO$_2$, TMSCHN$_2$; (r) K$_2$CO$_3$, MeOH; (s) Ac$_2$O, pyridine, DMAP

(Fig. 5) [31]. They believed that **1** could be derived from **30** through a series of protection, deprotections, and functionalizations. Intermediate **30** could result from highly functionalized ketone **31** through cyclization and Tsuji allyation. Reaction of the highly functionalized alkene **32** with Hg(ClO$_4$)$_2$, CaCO$_3$ in a mixture of tetrahydrofuran (THF) and H$_2$O at 0 °C afforded **31** in 33% yield (Scheme 3). Heating **31** with toluene and butylated hydroxybenzene initiated an intramolecular Diels–Alder reaction to afford cyclic compounds **33** and **34** in 77% yield. Intramolecular Tsuji allyation was carried out using Pd$_2$(dba)$_3$ and PPh$_3$ in toluene to give **30** in 86% yield and **35** in 61% yield, respectively. To date, Burns and Forsyth have
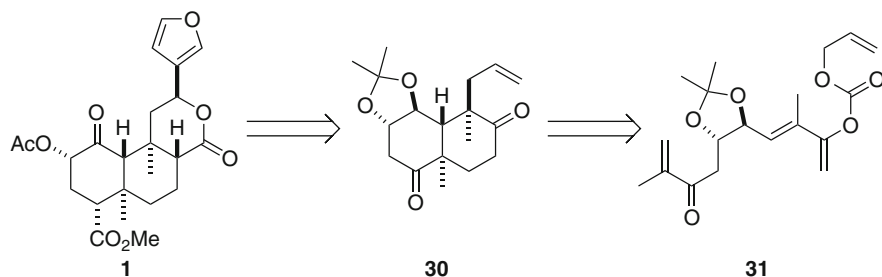
Fig. 5 Retrosynthetic analysis of salvinorin A by Burns and Forsyth
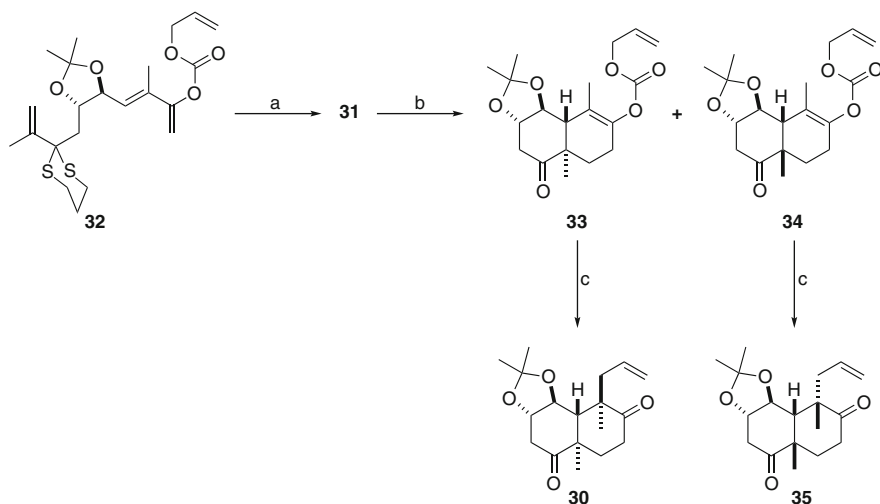
Scheme 3 (a) $Hg(ClO_4)_2$, $CaCO_3$, THF/H_2O; (b) toluene, butylated hydroxyl benzene; (c) $Pd_2(dba)_3$, PPh_3, toluene

not published any further progress towards **1**; however, their strategy does provide a way to achieve both *cis* and *trans* decalin cores which may have utility towards the synthesis of **1** or the synthesis of other neoclerodanes/natural products.

In 2008, Hagiwara and co-workers reported the total synthesis of **1** [32]. They were able to achieve **1** in 20 steps with 0.95% yield employing a similar strategy they also used for the synthesis of (−)-methyl barbascoate [33]. They envisioned that **1** could be achieved from enone **36** through a linear series of functionalizations beginning with the methyl analog of (*R*)-(−)-Wieland–Miescher ketone (Me-WMK) (Fig. 6). Starting with Me-WMK, protection, followed by reaction with NH_4Cl in a mixture of KOH and MeOH gave **36** (Scheme 4). Compound **36** was then subjected to reductive alkylation and this afforded **37** and **38** in 25 and 51% yield, respectively. Compound **38** was carried forward and deprotected to afford
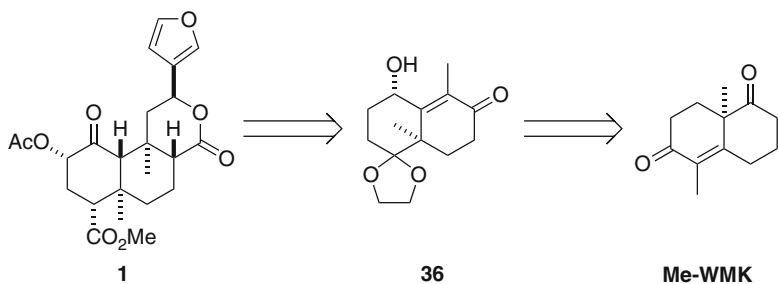
Fig. 6 Retrosynthetic analysis of salvinorin A proposed by Hagiwara and co-workers
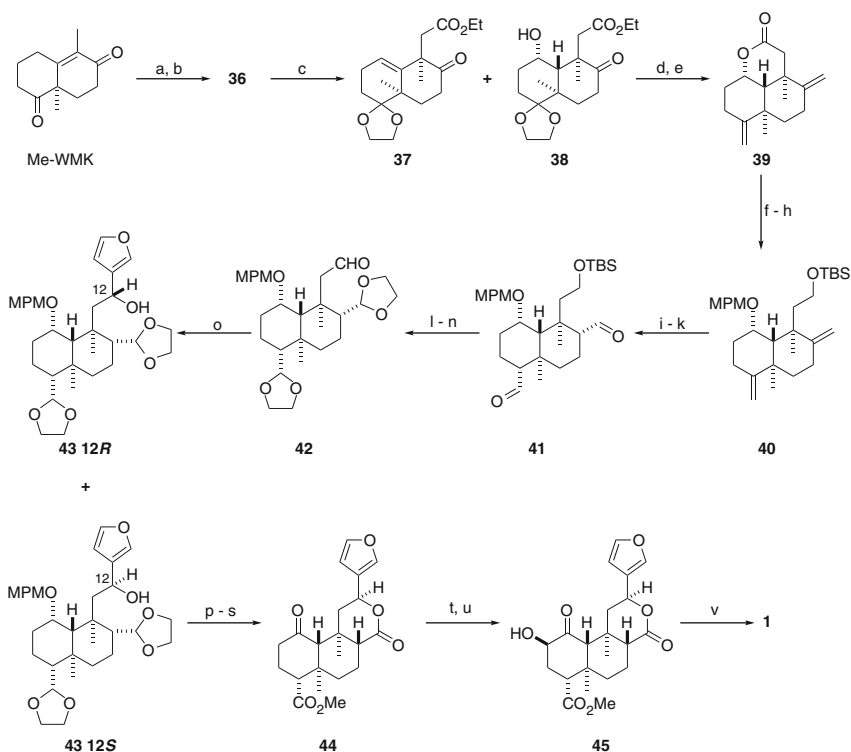
Scheme 4 (a) $(CH_2)_2(OTMS)_2$, Me_3SiOTf, 15 Kbar, 40 °C; (b) KOH, MeOH/H_2O, O_2, 65 °C; (c) Li/NH_3, THF, −78 °C, alkyl iodide; (d) 3M HCl aqueous EtOH; (e) NaHMDS, Ph_3PCH_3Br, THF; (f) LAH, Et_2O, 0 °C; (g) TBSCl, DMAP, Et_3N, CH_2Cl_2 (h) NaH, MPMCl, DMF; (i) BH_3, THF, 3M NaOH, H_2O_2; (j) PDC, NaOAc, MS-4 Å, CH_2Cl_2; (k) NaOMe, MeOH; (l) ethylene glycol, PTSA, 40 °C; (m) TBAF, THF; (n) PDC, NaOAc, MS-4 Å, CH_2Cl_2; (o) 3-bromofuran, t-BuLi, THF, −78 °C; (p) PTSA, acetone, H_2O, reflux; (q) DDQ, H_2O, CH_2Cl_2, 0 °C; (r) PDC, 2-methyl-2-butene, DMF; (s) DCC, DMAP, MeOH, CH_2Cl_2; (t) NaHMDS, TESCl, THF; (u) m-CPBA, NaHCO_3, toluene, H_2O, 0 °C, AcOH; (v) PPh_3, DIAD, AcOH, CH_2Cl_2

the diketone and subsequently underwent double Wittig methylenation with sodium hexamethyldisilazide (NaHMDS) and Ph₃PCH₃Br to yield **39**. Upon isolation of **39**, it was immediately treated with lithium aluminum hydride (LAH) to afford the diol, which was itself protected, to produce **40** in 54% yield. Compound **40** was converted to the di-aldehyde **41** through hydroboration followed by oxidation in 94% yield. After protection of the formyl groups, deprotection of the silyl ether, and subsequent oxidation, **42** was converted to **43** in 78% yield. A 2:3 mixture of both the 12*R* and 12*S* isomer of **43** was achieved in 66% yield from the reaction of **42** with 3-lithiofuran. The 12*S* isomer of **43** underwent deprotection, oxidation and esterification to afford 2-desacetoxysalvinorin A (**44**) in 90% yield. Compound **44** was treated with NaHMDS and chlorotriethylsilane (TESCl) in THF at −78 °C to give the silyl enol ether, which itself underwent Rubottom oxidation to yield **45** in 70% yield. Mitsunobu conditions were then employed to invert the C-2 stereochemistry and acetylate the hydroxyl to afford **1** in 86% yield [34, 35].

Recently, Hagiwara and co-workers have developed a second-generation total synthesis of **1** [36]. The first few steps are similar to the previous synthesis of **1**, but they have been able to optimize their approach using a different strategy to complete the synthesis. Compound **38**, the intermediate used in the previous generation synthesis, went through protection and deprotection steps followed by conversion of the carbonyls to enol triflates with Comins' reagent and NaHMDS in THF to afford **46** in 66% yield (Scheme 5). The ester group of **46** was converted to the Weinreb amide and reacted with 3-furyllithium to give **47** in 70% yield. Treatment of **47** with Pd(PPh₃)₄, dppf, carbon monoxide and triethylamine (Et₃N) at 60 °C in a 3:1 mixture of MeOH and dimethylformamide (DMF) afforded the bis-ester **48** in 84% yield. Treating **48** with K-selectride resulted in reduction and concomitant ring closure to give **49** in 95% yield with the 12(*S*) configuration as the sole diastereomer. The two alkenes present in **49** were reduced using samarium iodide in the presence of Et₃N, acetic acid, and toluene followed by an O₂ quench to produce **50** in 64% yield. Deprotection, C-8 epimerization, and Dess–Martin oxidation produced **44**, which was transformed to **1** in similar fashion as the first generation synthesis. Overall, the second generation synthesis of **1** by Hagiwara reduced the number of steps from 20 to 13 steps and increased the overall yield from 0.95 to 2.8%.

In the attempt to synthesized 20-norsalvinorin A (**51**) Perlmutter and co-workers prepared a tricyclic intermediate (**52**) [37]. They chose to synthesize this analog to determine the importance of the methyl group at C-20. They envisioned that **51** could be achieved from modification of this advanced intermediate (Fig. 7). Compound **52** was thought to be derived from **53**. The synthesis begins with complexion of **54** with TiCl₄ at −78 °C, which was followed by the addition of **53** (derived from Snapper's protocol in three steps from 3-furylaldehyde) [38] to afford **55** in 37% yield (Scheme 6). Compound **55** was treated with 1,8-diazabicyclo-[5.4.0]undec-7-ene (DBU) at room temperature in CH₂Cl₂ to give **56** in 87% yield. This transformation was carried out in order to induce the correct stereochemistry at C-10 of the tricyclic core. The alkene at the 2,3 position of **56** was reduced selectively using Na₂S₂O₄ and
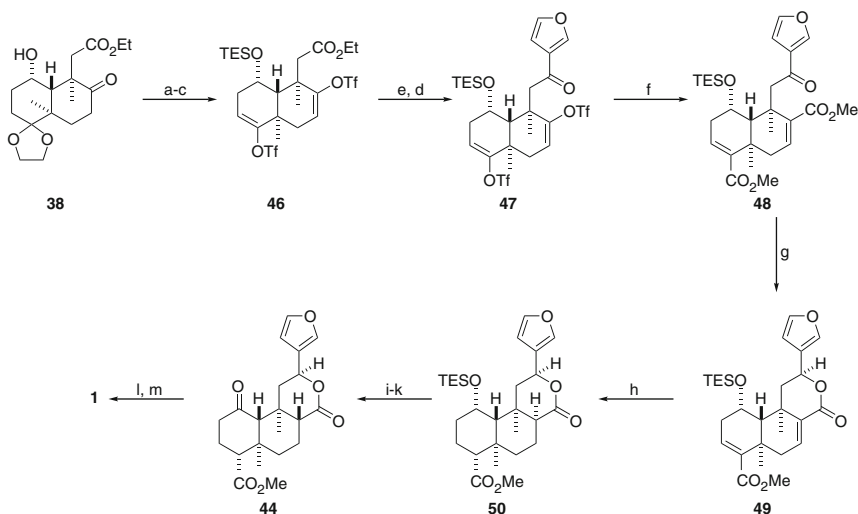
Scheme 5 (a) 3M HCl aqueous EtOH; (b) TESOTf, pyridine, DMAP, DMF, 100 °C; (c) Comins' reagent, NaHMDS, THF; (d): (1) *i*-PrMgBr, THF; (2) MeN$^+$(OMe)H$_2$Cl$^-$; (e) 3-bromofuran, *t*-BuLi, THF; (f) Pd(PPh$_3$)$_4$, CO, dppf, MeOH/DMF; (g) K-selectride, *t*-BuOH, THF; (h) (1) SmI$_2$, Et$_3$N, AcOH; (2) toluene, O$_2$ quench; (i) TBAF, THF; (j) K$_2$CO$_3$, MeOH (k) Dess–Martin, CH$_2$Cl$_2$; (l) (1) NaHMDS, TESCl, THF; (2) *m*-CPBA, NaHCO$_3$, toluene, H$_2$O, 0 °C, AcOH; (m) PPh$_3$, DIAD, AcOH, CH$_2$Cl$_2$
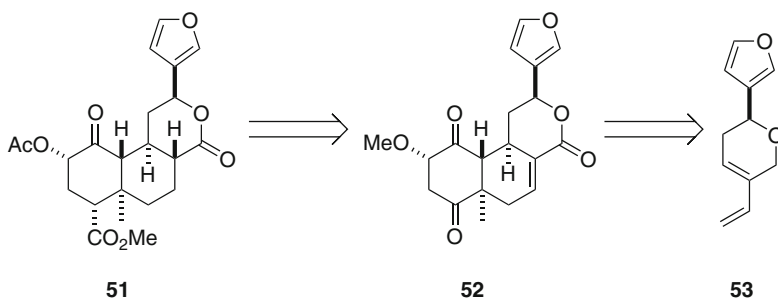
Fig. 7 Retrosynthetic analysis of 20-nor-salvinorin A proposed by Perlmutter and co-workers

NaHCO$_3$ in a mixture of toluene and H$_2$O, without the loss of the methoxy group at C-2 to afford the desired intermediate **52** in 73% yield. While having successfully synthesized their desired intermediate, to date Bergman and co-workers have not reported any further progress towards the synthesis of **51** or **1**.
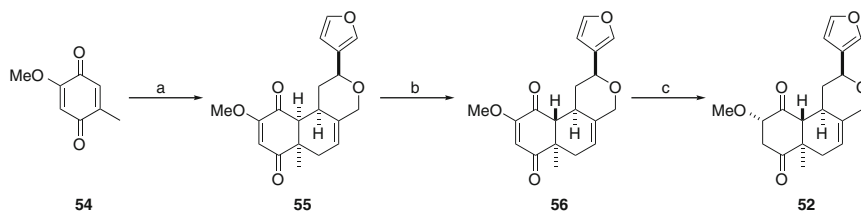
Scheme 6 (a): (1) TiCl$_4$, toluene, $-78\,^{\circ}$C; (2) **53**, $-45\,^{\circ}$C; (b) 10% DBU, CH$_2$Cl$_2$; (c) Na$_2$S$_2$O$_4$, NaHCO$_3$, toluene/H$_2$O, Adogen 464

3 Semisynthetic Modifications of Salvinorin A

3.1 C2 Modifications

In addition to the total syntheses of salvinorin A (**1**), semi-synthetic structural modifications to **1** have been performed to establish SAR. The most extensively studied position on the salvinorin A core is the C-2 ester followed closely by the furan ring. Further investigations have been performed at C-1, C-4, and C-17 as well. The quantity and diversity of analogs synthesized at C-2 is partly due to the ability to hydrolyze selectively the C-2 ester to the C-2 hydroxyl intermediate, salvinorin B (**57**). While retaining the stereochemistry of the stereocenters of **1**, selective removal of the C-2 acetate has been achieved by treating **1** with Na$_2$CO$_3$ in MeOH to give salvinorin B (**57**) in 77% yield (Scheme 7) [39, 40]. Several other attempts have been made to achieve this intermediate such as ammonolysis at 0 $^{\circ}$C in MeOH. These conditions also resulted in the synthesis of **57** but this method resulted in low yields and significant epimerization of C-8 [39]. The epimerization of C-8 is thought to occur readily during deacetylation of C-2 due to breaking the C-8/C-9 bond via base-promoted cleavage [41, 42]. A number of diverse organic and inorganic bases have been tried but have resulted in no overall improvement in the synthesis of **57** [41]. KOH in MeOH under O$_2$ resulted in the oxidation of **1** and gave products **58** and **59** in 53% and 37% yield, respectively [43]. However, refluxing **1** in 5% aqueous KOH resulted in **60** in 95% yield [44, 45]. When Ba(OH)$_2$ was used as the base in MeOH, the oxidative-elimination product **61** was formed in 75% yield [41]. Also attempted was refluxing KCN in MeOH/THF to achieve the deacetylated product; this resulted in a 51% yield of the **8-epi-57** [46].

The C-2 hydroxyl derivative with the unnatural configuration (**2-Epi-57** or **62**) was synthesized using Mitsunobu conditions of triphenylphosphine (PPh$_3$), diisopropyl azodicarboxylate (DIAD), and 4-nitrobenzoic acid as the nucleophile, which was subsequently hydrolyzed with K$_2$CO$_3$ in MeOH to afford **62** in 64% yield over two steps [34]. Compounds **57** and **2-epi-57** have been exploited as common intermediates in diversification of the C-2 position. Hydroxyl **57** has been utilized
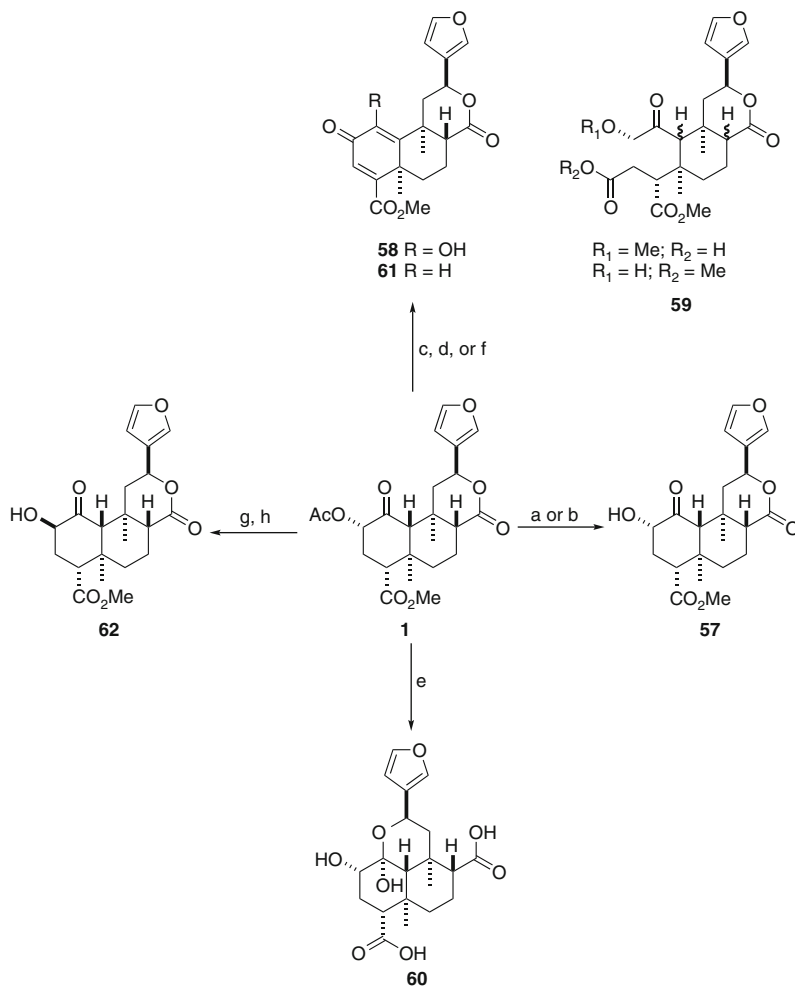
Scheme 7 (a) Na$_2$CO$_3$, MeOH; (b) NH$_3$, MeOH, 0 °C; (c) KOH, MeOH, O$_2$; (d) Me$_3$SiCHN$_2$ (e) 5% aqueous KOH, 80 °C; (f) Ba(OH)$_2$, MeOH; (g) 4-nitrobenzoic acid, PPh$_3$, DIAD, CH$_2$Cl$_2$; (h) K$_2$CO$_3$, MeOH

in the synthesis of esters, carbamates and carbonates, ethers and amines, amides and thioesters, and sulfonyl esters and sulfonamides.

Preparation of C-2 esters was performed by subjecting **57** to a number of standard acylating procedures with slight deviation in the base used (Scheme 8) [34, 41]. Common procedures include the use of the appropriate acid chloride or anhydride with a catalytic amount of 4-(dimethylamino)pyridine (DMAP) in CH$_2$Cl$_2$ to yield a number of aryl and alkyl esters (**63**) [34, 39, 41, 47]. Furthermore, **57** has been exposed to conditions coupling in appropriate carboxylic acids with
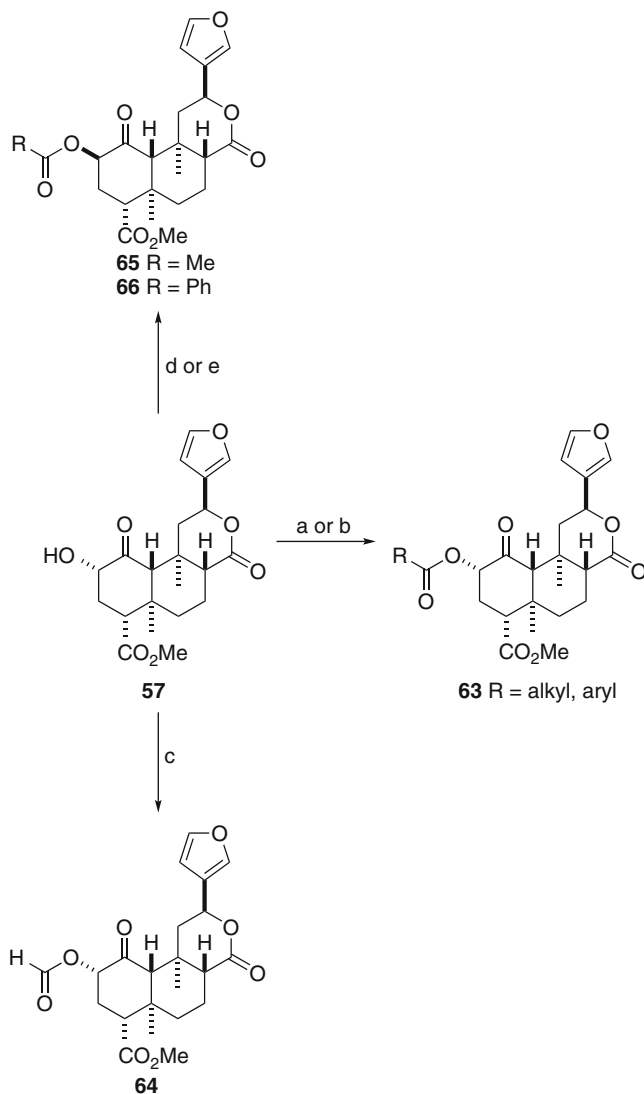
Scheme 8 (a) Appropriate alkyl chloride or anhydride, DMAP, CH_2Cl_2; (b) appropriate acid, EDCI, HOBt, CH_2Cl_2; (c) formic acid, acetic anhydride; (d) AcOH, PPh_3, DIAD, CH_2Cl_2; (e) appropriate acid, (2-Py)PPh$_2$, DBAD, THF, 60 °C

N-(3-dimethylaminopropyl)-N'-ethylcarbodiimide (EDCI) and 1-hydroxybenzo-triazole (HOBt) in CH_2Cl_2 (**63**) [48]. Ester derivatives were also prepared from **2-epi-57** by alkylating with appropriate acid chloride or anhydrides and Et$_3$N in CH_2Cl_2 [34]. In addition, **57** was treated with a mixture of formic acid and acetic anhydride (Ac$_2$O) to yield the C-2 formate (**64**) [49].

The C-2 epimer of **1** was synthesized from **57** using Mitsunobu conditions of PPh$_3$, DIAD, and acetic acid in a 38% yield (**65**) [34]. However, the C-2 acetyl and benzyl C-2 epimers of **1** also have been prepared using modified Mitsunobu conditions [50]. Diphenyl-2-pyridylphosphine and either acetic acid or benzoic acid were dissolved in THF followed by the addition of di-*tert*-butylazodicarboxylate (DBAD) at 60 °C to yield analogs **65** and **66** in 80% and 75% yield, respectively [50].

Alkyl carbonates were synthesized by treating **57** with methyl or ethyl chloroformate and a catalytic amount of DMAP in CH$_2$Cl$_2$ to afford **67** and **68**, respectively (Scheme 9) [41]. Compound **69** was generated from **57** and trichloroacetyl isocyanate in CH$_2$Cl$_2$ followed by in situ hydrolysis with aluminum oxide in 91% yield over two steps [51]. Additional carbamates were synthesized by treating **57** with methyl isocyanate or ethyl isocyanate, pyridine, and a catalytic amount of DMAP in CH$_2$Cl$_2$ in 68% (**70**) and 53% (**71**) yield, respectively [51]. Compounds **72** and **73** were obtained by treating **57** with phenylisocyanate or allylisocyanate in CH$_2$Cl$_2$ resulting in a 14% yield and 17% yield, respectively [39].

69 R = H   **72** R = Ph
70 R = Me **73** R = allyl
71 R = Et

57

67 R = Me
68 R = Et
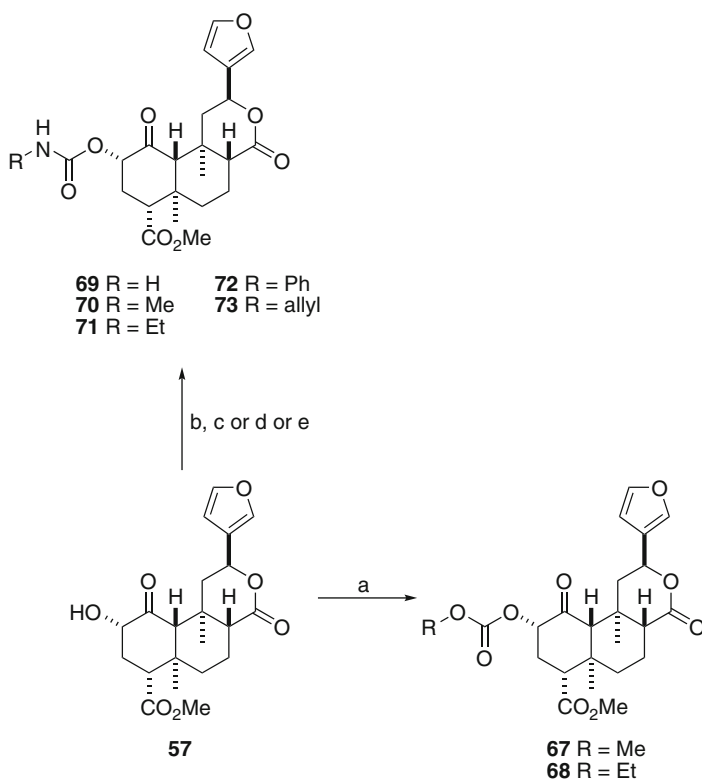
Scheme 9 (a) Chloroformate, DMAP, CH$_2$Cl$_2$; (b) Cl$_3$C(O)NCO, CH$_2$Cl$_2$; (c) Al$_2$O$_3$; (d) appropriate isocyanate, DMAP, pyridine; (e) appropriate isocyanate, TMSCl, CH$_2$Cl$_2$

Appropriate alkyl iodides or bromides were reacted with **57** and **2-epi-57** in the presence of Ag_2O in CH_3CN with yields ranging from 36 to 77% (**74**, Scheme 10) [34, 51]. However, with these conditions preparation of branched alkyl ethers was unsuccessful [51]. Reacting **57** with chloromethyl methyl ether, diisopropylethylamine, and catalytic DMAP in CH_2Cl_2 afforded **75** in a 72% yield and was the first **1** derivative reported to have increased affinity at the KOP receptor relative to **1**. [41, 52]. Based on the successful increase in affinity of derivative **75**, additional simple alkoxymethyl ethers were obtained using appropriate alkyoxymethyl chloride with diisopropylethylamine in DMF (**76–78**). However, more complex alkoxymethyl derivatives were synthesized from the common methylthiomethyl ether intermediate (**79**), which was obtained from reaction of **57** with acetic acid, acetic anhydride, and dimethylsulfoxide (DMSO) [52]. Compound **79** was then
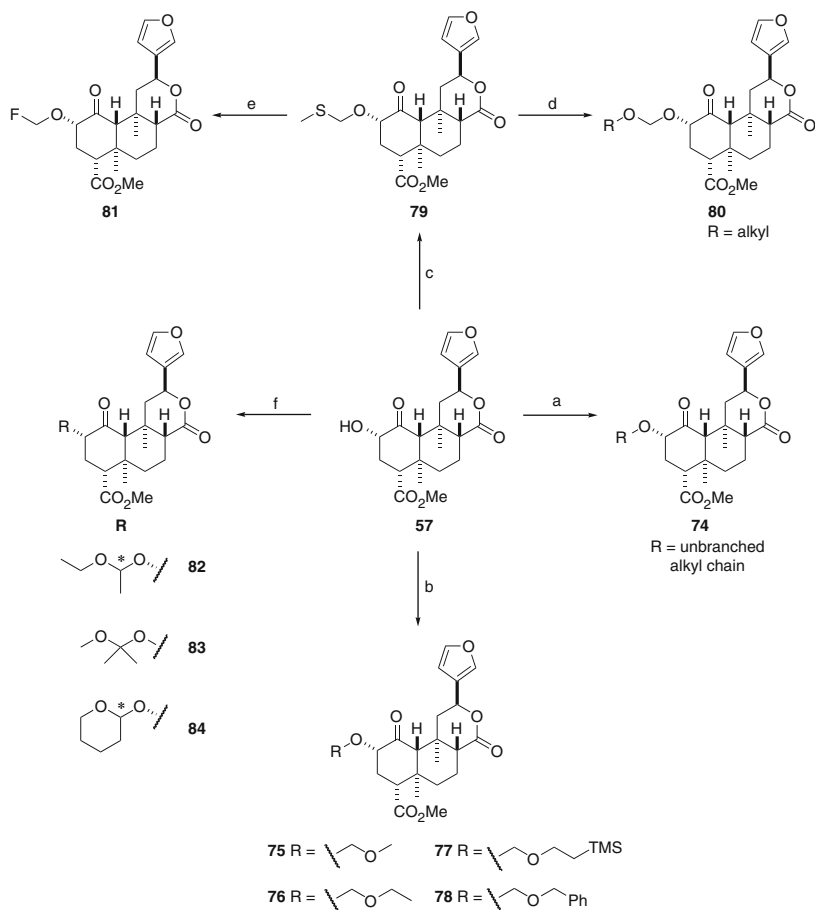
Scheme 10 (a) RX, Ag_2O, CH_3CN; (b) $ROCH_2Cl$, i-Pr_2NEt, DMF; (c) Ac_2O, AcOH, Me_2SO; (d) NIS, ROH, TfOH, 4-Å sieves; (e) NIS, Et_2NSF_3, 4-Å sieves; (f) PPTS or PTSA, CH_2Cl_2

exposed to alcoholysis in the presence of *N*-iodosuccinimide (NIS) and catalytic trifluoromethanesulfonic acid (TfOH) to afford the desired ethers (**80**) [52]. These conditions were ineffective for the synthesis of the fluoromethyl ether analog **81**, and conditions were modified to include NIS and Et$_2$NSF$_3$ [52]. Additional alkoxyalkyl ethers were synthesized using ethoxyethene (**82**), 2-methoxypropene (**83**), and 3,4-dihydro-2*H*-pyran (**84**) with catalytic pyridinium *p*-toluenesulfonate (PPTS) in CH$_2$Cl$_2$ [52].

Substituted amines with the unnatural configuration at C-2 were obtained by activation of the C-2 alcohol of **57** with trifluoromethanesulfonic anhydride and nucleophilic displacement with desired amine (**85**, Scheme 11) [34, 51]. Amines that retained the C-2 configuration were synthesized using the same methodology starting with **2-*epi*-57** to yield **86** [34]. The synthesis of the primary amine at C-2 began with **57** which was treated with the desired thionyl halide to yield the C-2 halogen (**87**, Scheme 12) [34, 53, 54]. The C-2 halogen was then displaced by
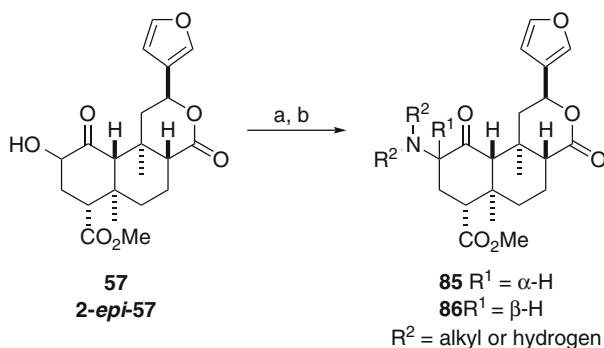
Scheme 11 (a) (CF$_3$SO$_2$)$_2$O, pyridine, CH$_2$Cl$_2$; (b) R^{2}NH, THF
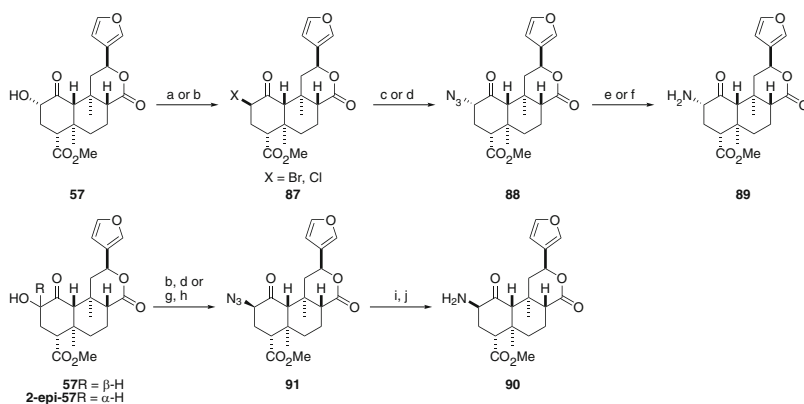
Scheme 12 (a) SOX$_2$, Et$_3$N, ClCH$_2$CH$_2$Cl; (b) CBr$_4$, PPh$_3$, CH$_2$Cl$_2$; (c) NaN$_3$, DMSO; (d) NaN$_3$, DMF, AcOH; (e) TMSCl, NaI, CH$_3$CN; (f) Zn, NH$_4$Cl, MeOH, CH$_2$Cl$_2$; (g) (CF$_3$SO$_2$)$_2$O, pyridine, CH$_2$Cl$_2$; (h) NaNH$_3$, DMF; (i) PPh$_3$; (j) H$_2$O, THF

nucleophilic attack of sodium azide to yield azide **88** [34, 53]. Azide **88** was then reduced with TMSCl and sodium iodide in CH_3CN to give the primary amine (**89**) in 5% yield over three steps [34]. Improvement of the procedure to obtain the primary amine was achieved by using CBr_4, PPh_3, and CH_2Cl_2 to afford the brominated product **87** in 59% yield [48]. Yield of the nucleophilic displacement of bromide with sodium azide was increased to 86% by modifying the solvent to a mixture of DMF and acetic acid (**88**) [48]. Reduction of azide **88** was then carried out with Zn metal and NH_4Cl and yielded amine **89** in 36% yield, an 18% yield over three steps [48]. Additionally, **2-epi-57** was submitted to identical conditions, leading to the generation of azide **91** [48]. Finally, **57** has been activated with trifluoromethanesulfonic anhydride and displaced with nucleophilic attack of sodium azide to afford **91**, which was reduced by Staudinger conditions to afford amine **90** in a 35% yield over three steps [34]. Secondary and tertiary amides were synthesized by subjecting previously prepared primary and secondary amines (**86** and **89**) to appropriate acid chloride or anhydride with Et_3N and optional DMAP in CH_2Cl_2 (**92** and **93**) (Scheme 13) [34, 48]. C-2-*Epi*-amides were also synthesized using C-2 epimerized amines **85** and **90** under the same conditions (**94** and **95**) [34].

To synthesize thioester derivatives, the C-2 halogen (**87**) was treated with the potassium salt of thiobenzoic acid or thioacetic acid in CH_3CN or acetone to yield
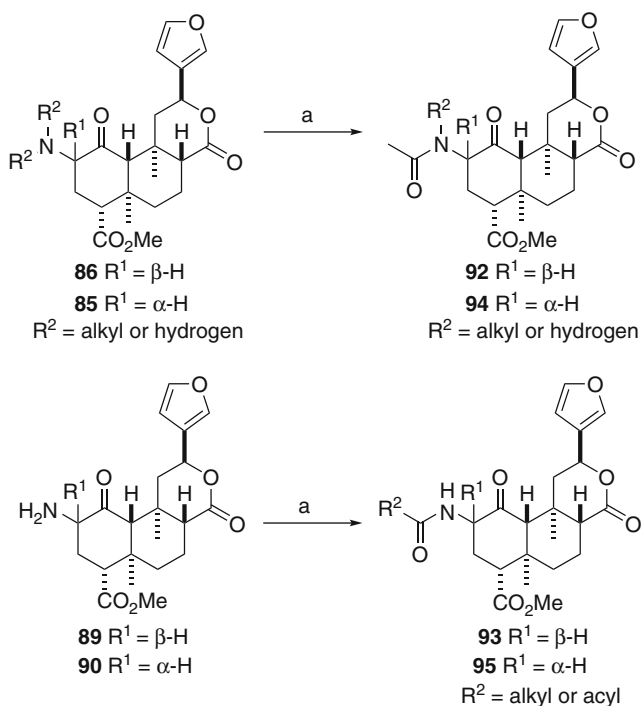
Scheme 13 (a) Appropriate acid chloride or anhydride, DMAP, NEt_3, CH_2Cl_2

thioesters **96** and **97**, respectively (Scheme 14) [48, 53]. In addition, the reaction of the C-2 chloride with sodium hydrogen sulfide (NaSH) in MeOH and DMF afforded compound **98** [54]. However, low yield and formation of side products resulted in amendments to proceed through thioacetate **96** and then deacetylate with sodium thiomethoxide in MeOH and CH_2Cl_2 to afford **98** [54]. Finally, **2-*epi*-96** can be achieved by triflating **57** and subsequent treatment with potassium thioacetate in acetone at $-20\,^{\circ}C$ [54].

Sulfonyl esters were synthesized by treating **57** with appropriate sulfonyl chlorides with a catalytic amount of DMAP in CH_2Cl_2 to afford the desired sulfonyl
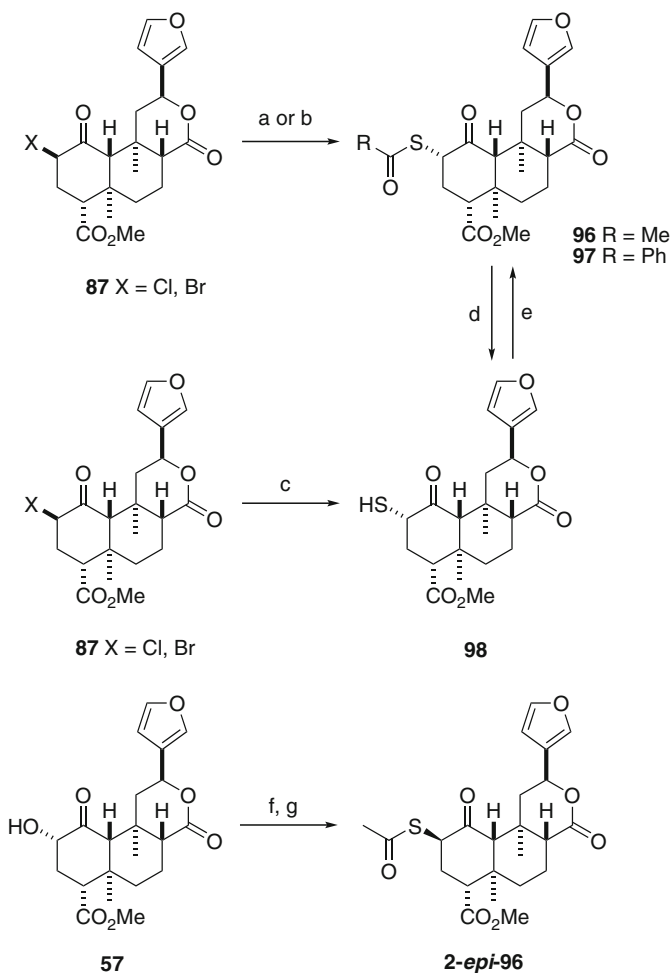
Scheme 14 (a) RCOSK, CH_3CN; (b) potassium thioacetate, acetone; (c) NaSH, MeOH, DMF; (d) NaSMe, MeOH, CH_2Cl_2, $-20\,^{\circ}C$; (e) Ac_2O, DMAP, CH_2Cl_2; (f) $(CF_3SO_2)_2O$, pyridine, CH_2Cl_2, $-20\,^{\circ}C$; (g) potassium thioacetate, acetone, $-20\,^{\circ}C$
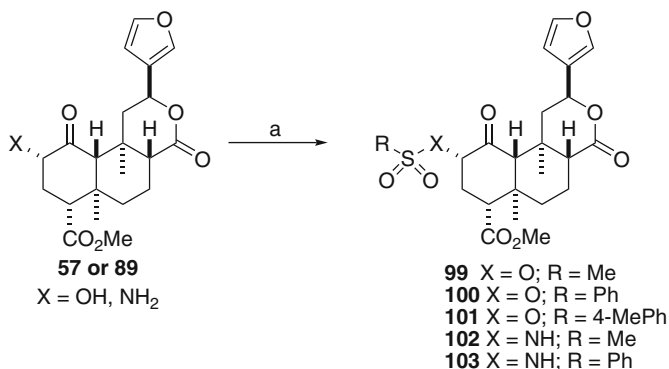
Scheme 15 (a) Appropriate sulfonyl chloride, DMAP, CH_2Cl_2

esters (**99–101**) in 32–86% yield (Scheme 15) [39, 47]. Along with sulfonyl esters, sulfonamides were synthesized by utilizing previously prepared amine **89** and subjecting it to methanesulfonyl chloride or benzenesulfonyl chloride with a catalytic amount of DMAP in CH_2Cl_2 to provide sulfonamides **102** and **103** in 56% and 97% yields, respectively [48].

Another modification made off the C-2 position of **1** is the trichloroacetimidate derivate (**104**), which was prepared by treating **57** with trichloroacetonitrile and DBU in $ClCH_2CH_2Cl$ at 0 °C to yield product **104** in a 37% yield (Scheme 16) [39]. Efforts were also made to remove the C-2 hydroxyl of **57** entirely. Hydroxyl **57** was treated with 1,1-thiocarbonyldiimidazole and catalytic DMAP in CH_2Cl_2 to afford imidazole **105** in 64% yield [50]. Imidazole **105** was then refluxed with 2,2′-azobis (2-methylpropionitrile) (AIBN) and tributyltin hydride in toluene to bestow C-2 dehydroxylated **57** in a C-8 epimeric mixture of C-8 α-H and β-H in 13 and 27% yield (**106** and **107**), respectively [50]. Additionally, dilactone **108** was obtained by treating **57** with a mixture of chromium trioxide and pyridine in CH_2Cl_2 in a 37% yield [50].

3.2 Furan Ring Modifications

It has been shown that natural products containing a furan ring are potentially hepatotoxic [55]. This toxicity is thought to arise from oxidation of the furan ring to an enedial by cytochrome P450 enzymes. The enedial can subsequently react with biological nucleophiles and form stable conjugates. Thus, there has been a relatively large amount of research interest concentrated on elucidating replacements for the furan ring in the salvinorin A scaffold that will not only allow for exploration of SAR, but also result in the production of compounds with reduced potential for hepatotoxicity.
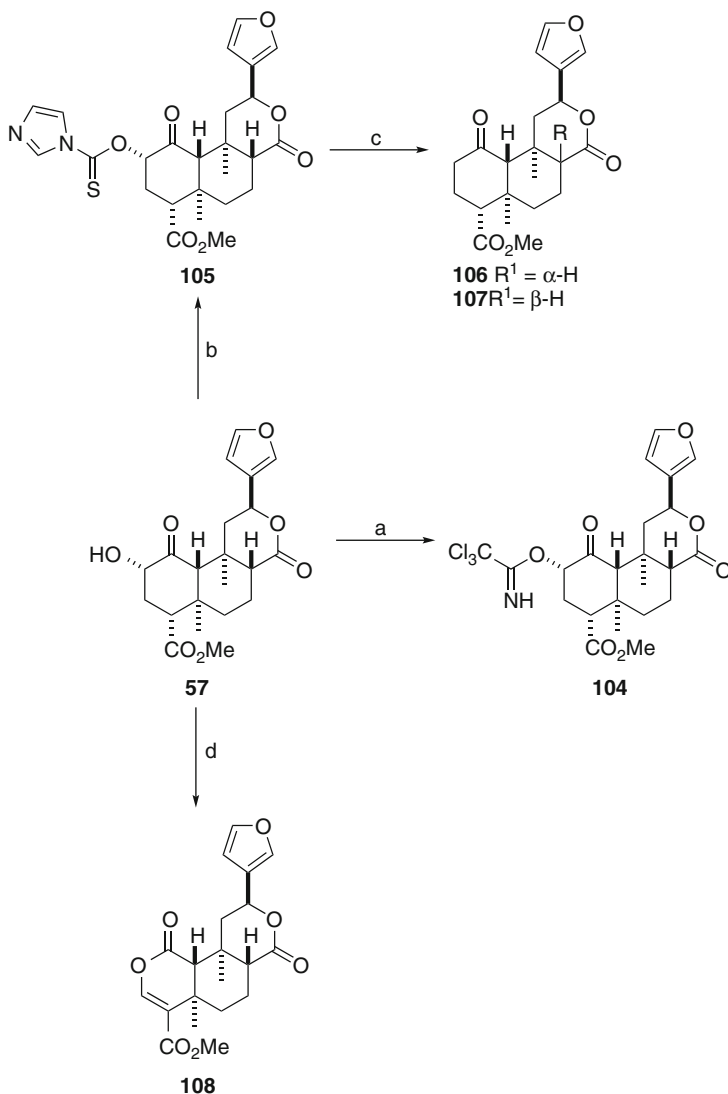
Scheme 16 (a) Trichloroacetonitrile, DBU, ClCH$_2$CH$_2$Cl, 0 °C; (b) (Im)$_2$CS, DMAP, CH$_2$Cl$_2$; (c) AIBN, Bu$_3$SnH, toluene; (d) CrO$_3$, pyridine

Catalytic hydrogenation of salvinorin A (**1**) in MeOH over 5% Pd/C quantitatively afforded a stereoisomeric mixture (at C-13) of products resulting from hydrogenolysis of the lactone (**109**, Scheme 17) [1]. Carboxylic acid **109** was esterified with diazomethane to yield methyl ester **110** [42]. While treatment of **1** with sodium borohydride has been found to lead to extensive epimerization at C-8, it was found that methyl ester **110** was relatively stable towards epimerization at
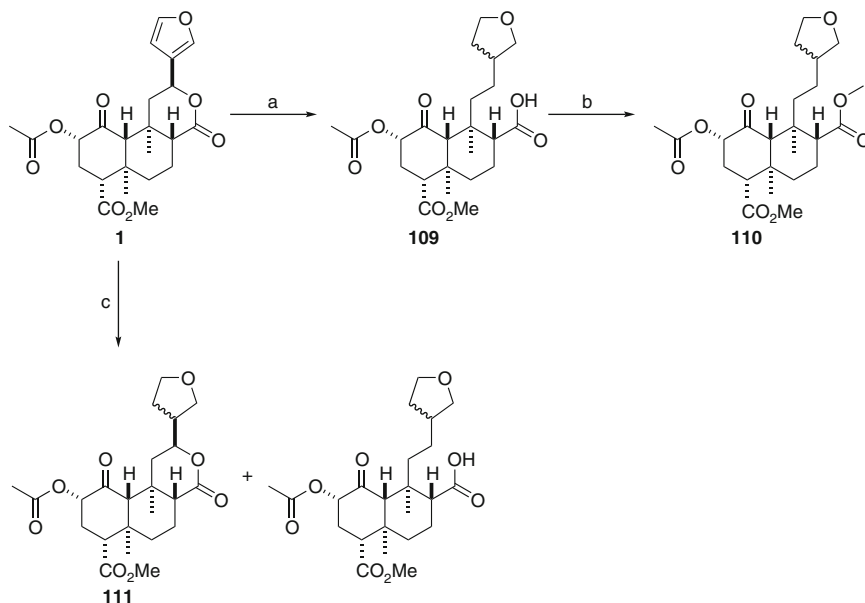
Scheme 17 (a) H$_2$, Pd/C, MeOH; (b) CH$_2$N$_2$/MeOH, 0 °C; (c) H$_2$, Rh/C, CH$_2$Cl$_2$/MeOH
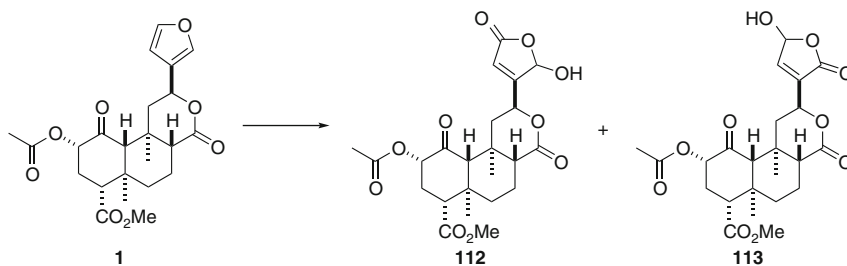
Scheme 18 Photoxidation in the presence of light

C-8, allowing the use of sodium borohydride for the reduction of the C-1 ketone. The use of rhodium catalyst in place of palladium was found to minimize the hydrogenolysis of the lactone and allowed access to tetrahydrosalvinorin A (**111**) [49]. The C-13*R* epimer of **111** was separable by HPLC [49, 56]. Exposure of **1** to sunlight in CH$_2$Cl$_2$ and MeOH yielded the natural products salvidivin A (**112**) and salvidivin B (**113**) in 6.7 and 18.2% yield, respectively (Scheme 18) [56].

The treatment of **1** with bromine in a mixture of CH$_2$Cl$_2$ and MeOH at −30 °C gave the 2,5-dimethoxydihydrofuran product (**114**) in 93% yield as a mix of *cis* and *trans* isomers, which were separable by HPLC (Scheme 19) [50, 56]. As a mixture,
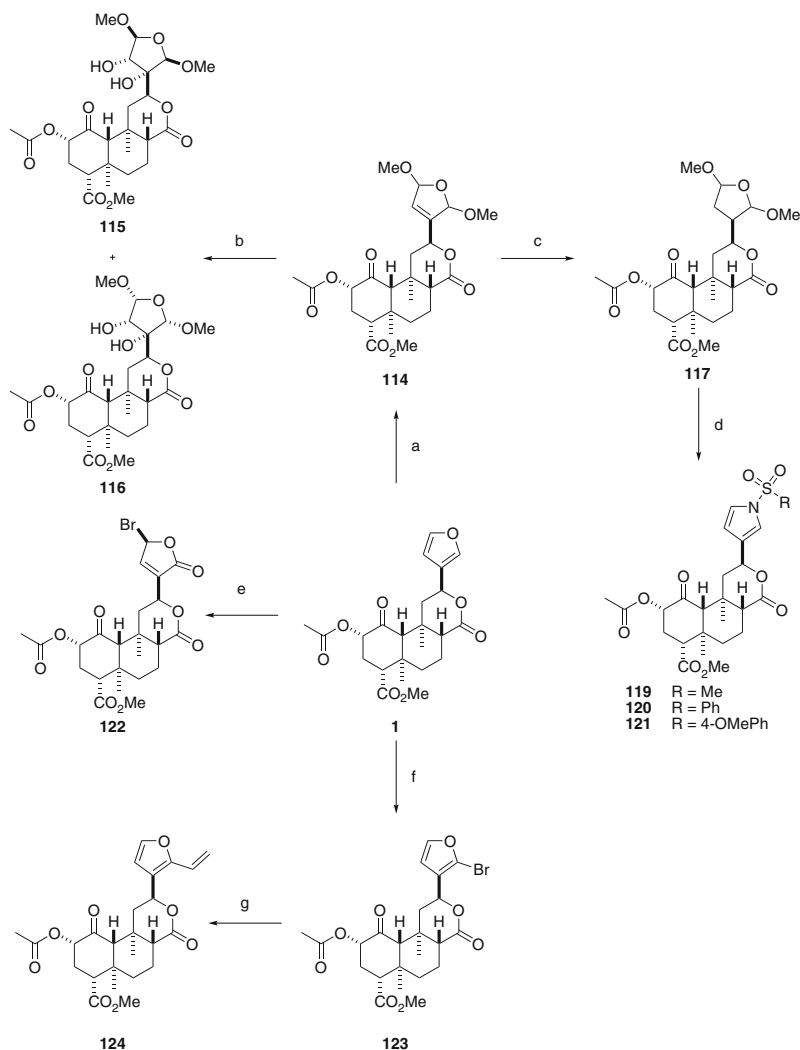
Scheme 19 (a) Br$_2$, MeOH, CH$_2$Cl$_2$, -30 °C; (b) KMnO$_4$, THF/H$_2$O, -10 °C; (c) H$_2$, Rh/C, MeOH; (d) appropriate sulfonamide, HOAc, 95 °C; (e) Br$_2$, DMF; (f) NBS, CH$_3$CN; (g) tributylvinyltin, Pd(PPh$_3$)$_4$, toluene, 80 °C

the *cis* isomer of **114** was selectively oxidized over the *trans* isomer with KMnO$_4$ in THF in H$_2$O at -10 °C to afford a mixture of the natural products salvinicin A (**115**) and salvinicin B (**116**) in an approximate 3:2 ratio, respectively. These were readily separable from each other and from the unreacted *trans* isomer by flash column chromatography. Dimethoxydihydrofuran **114** was also catalytically reduced with hydrogen and 5% Rh/C to give dimethoxytetrahydrofuran **117** in 92% yield as a mixture of compounds containing the 2,5-dimethoxy *cis* and *trans* isomers [57].

The purification of this mixture has been accomplished by HPLC [56]. As a mixture, the treatment of **117** with methanesulfonamide at 95 °C in acetic acid afforded a mixture of the methanesulfonylpyrrole (**119**, 30% yield) and its C-8 epimer (25% yield) [57]. Using this methodology, alkyl- and arylsulfonamides (**119–121**) have been prepared in 23–30% yield, but with significant amounts of the C-8 epimers also formed (18–20% yield).

The treatment of **1** with bromine in DMF at 0 °C afforded a dihydrofuran product (**122**) as a mixture of C-15 α and β isomers instead of the expected 2-bromofuran product (Scheme 19) [50]. However, treatment of **1** with *N*-bromosuccinimide (NBS) in acetonitrile gave the desired 2-bromofuran product (**123**) in 38% yield. From **123**, Stille coupling with tributylvinyl tin in the presence of Pd(PPh$_3$)$_4$ afforded the 2-vinylfuran product (**124**) in 58% yield [44].

The reaction of **1** with NaIO$_4$ and a catalytic amount of RuCl$_3$•3H$_2$O in a mixture of CCl$_4$, CH$_3$CN, and H$_2$O resulted in oxidative degradation of the furan ring, providing the carboxylic acid at C-13 (**125**) in 74% yield (Scheme 20) [50]. Carboxylic acid **125** was converted to the thioester in 88% yield by treatment with 2-chloro-4,6-dimethoxy-1,3,5-triazine (CDMT) and *N*-methylmorpholine, followed by ethanethiol [58]. The thioester derivative was reduced with triethylsilane and Pd/C to afford the aldehyde at C-13 (**126**) in 82% yield [58].

Generation of the carboxylic acid and aldehyde at the C-13 position of the salvinorin A scaffold has granted access to a variety of chemical methods for the development of salvinorin A analogs with a C-13 carbonyl moiety. From carboxylic acid **125**, alcohols and ethers at C-13 have been synthesized [44]. The primary alcohol at C-13 (**127**) was produced in 46% yield by reducing carboxylic acid **125** using BH$_3$•THF (Scheme 21). Alcohol **127** was then alkylated using alkyl iodides in the presence of Ag$_2$O to afford alkyl ethers (**128** and **129**) in 12–15% yield. The primary alcohol was also acetylated (**130**) in 11% yield with acetic anhydride and Et$_3$N.

Different conditions have been used to access a variety of esters at the C-13 position (Scheme 21). The methyl ester of carboxylic acid **125** was prepared in 48% yield by treatment of **125** with (trimethylsilyl)diazomethane (TMSCHN$_2$) [44]. Further alkyl esters (**131**) have been produced in 26–54% yield using appropriate alcohols in the presence of EDCI and DMAP, or in 40–72% yield using appropriate alcohols in the presence of EDCI, HOBt, and Et$_3$N [44, 58]. A large variety of
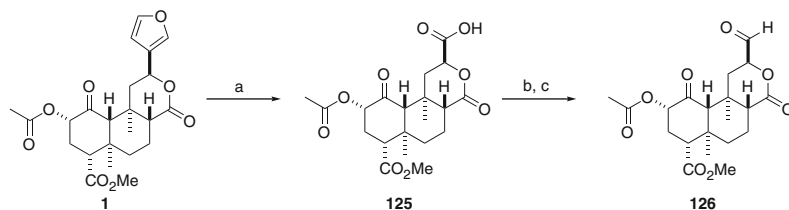
Scheme 20 (a) RuCl$_3$, NaIO$_4$, CCl$_4$/CH$_3$CN/H$_2$O; (b) CDMT, NMM, EtSH, CH$_2$Cl$_2$; (c) Pd/C, Et$_3$SiH, CH$_2$Cl$_2$
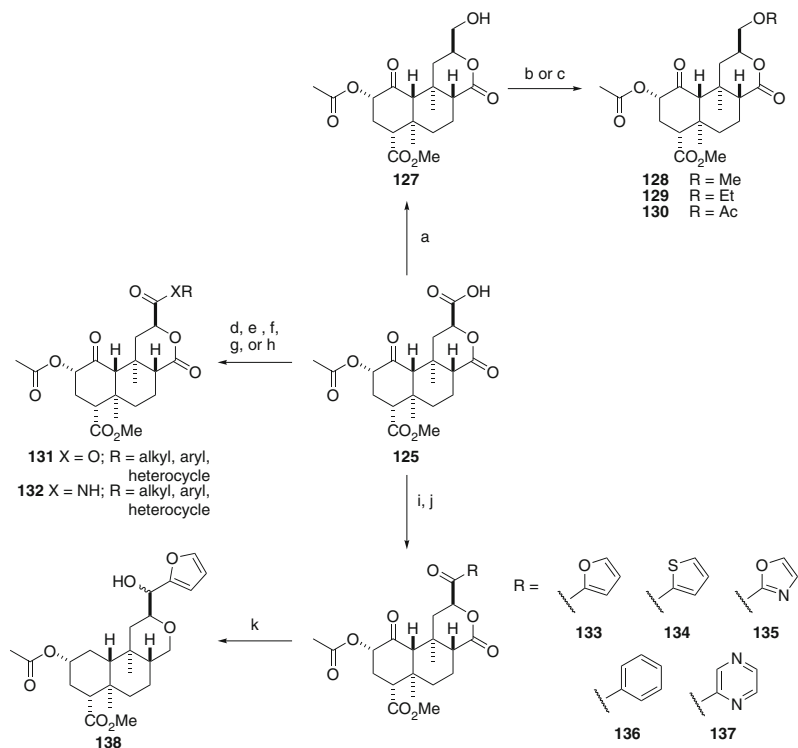
Scheme 21 (a) BH$_3 \bullet$THF, THF, 55 °C; (b) R-I, Ag$_2$O, CH$_3$CN, 60 °C; (c) Ac$_2$O, Et$_3$N, CH$_2$Cl$_2$; (d) TMSHN$_2$, MeOH, toluene; (e) R-OH, EDCI, DMAP, CH$_2$Cl$_2$; (f) R-OH, EDCI, HOBt, Et$_3$N, CH$_2$Cl$_2$; (g) R-NH$_2$, EDCI, HOBt, CH$_2$Cl$_2$; (h) R-NH$_2$, EDCI, HOBt, Et$_3$N, CH$_2$Cl$_2$; (i) (COCl)$_2$, CH$_2$Cl$_2$; (j) Bu$_3$SnR, Pd(PPh$_3$)$_4$, toluene, 80–100 °C; (k) NaBH$_4$, MeOH, 0 °C

amides (**132**) have been produced from carboxylic acid **125** in 45–72% yield using appropriate amines in the presence of EDCI and HOBt [44], or in 18–75% yield using appropriate amines in the presence of EDCI and HOBt with the addition of Et$_3$N (Scheme 21) [58].

Carboxylic acid **125** has also been useful for the generation of ketones at the C-13 position. Conversion of carboxylic acid **125** to the acyl chloride was achieved using oxalyl chloride (Scheme 21) [44]. The crude product was carried through and coupled to appropriate aryltributyl tin reagents under Stille conditions to afford a variety of arylketones (**133–137**) in 7–57% yield [44, 59]. The 2-furylketone compound (**133**) produced with this methodology was subsequently reduced using sodium borohydride to afford the corresponding alcohol (**138**) as a mixture of C-13 epimers in 19% yield.

B-Allyl-(10*S*)-(trimethylsilyl)-9-borabicyclo[3.3.2]decane (prepared in situ from commercially available 9-[(1*R*,2*R*)-pseudoephedrinyl]-(10*S*)-(trimethylsilyl)-9-borabicyclo[3.3.2]decane and allylmagnesium bromide) achieved the asymmetric
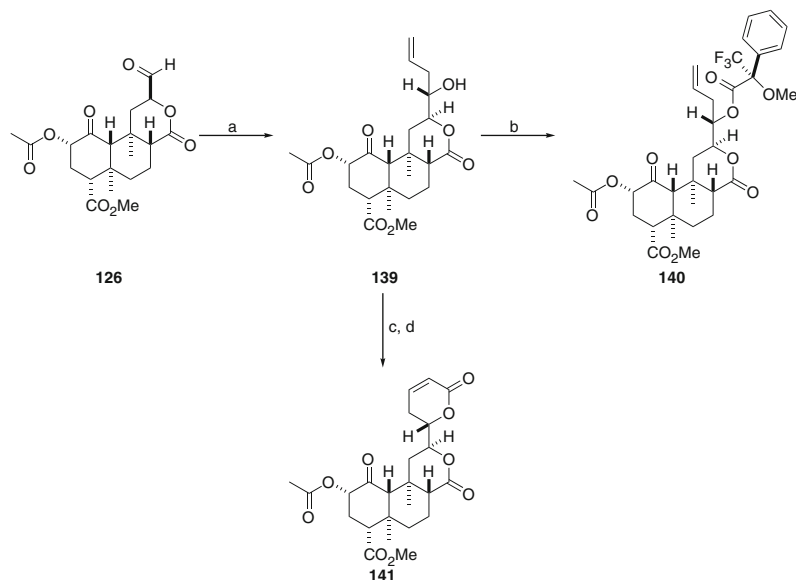
Scheme 22 (a) 9-(1*R*,2*R*-Pseudoephedrinyl)-(10*S*)-(trimethylsilyl)-9-borabicyclo[3.3.2]decane, allylMgBr, Et$_2$O; (b): (1) (*R*)-(+)-α-methoxy-α-trifluoromethylphenylacetic acid, oxalyl chloride, benzene; (2) DMAP, Et$_3$N, CH$_2$Cl$_2$; (c) acryloyl chloride, DMAP, Et$_3$N, CH$_2$Cl$_2$; (d) Grubbs II, CH$_2$Cl$_2$

allylation (**139**) of the C-13 aldehyde (**126**) in 82% yield (Scheme 22) [58]. In order to determine the stereochemistry of the allylic alcohol product, the Mosher ester (**140**) was prepared in 82% yield using oxalyl chloride and (*R*)-(+)-α-methoxy-α-trifluoromethylphenylacetic acid. Allylic alcohol **139** was acylated with acryloyl chloride in the presence of Et$_3$N and DMAP, and the subsequent ester was subjected to ring closing metathesis using second generation Grubb's catalyst to afford the 5,6-dihydro-2*H*-pyran-2-one product (**141**) in 23% yield over two steps.

Aldehyde **126** was converted to the terminal alkyne (**142**) in 61% yield by Seyferth–Gilbert homologation (Scheme 23) [60]. These basic conditions were well tolerated and no C-8 epimerization or C-2 deacetylation was observed. Alkyne **142** was coupled with various azides under copper(I)-catalyzed click reaction conditions to afford 1,4-disubstituted-1,2,3-triazoles (**143–145**) in 88% yield. Similar conditions were used to generate unsubstituted 1,2,3-triazoles. Alkyne **142** was coupled to azidomethyl pivalate under click reaction conditions to give the pivalyl triazole (**146**) in 88% yield. The pivalyl triazole was then treated with 1N NaOH to remove both the pivalyl group and the C-2 acetyl group. These conditions also led to C-8 epimerization. Acetylation of the epimeric mixture under standard conditions (Ac$_2$O, pyridine) and preparative scale separation by TLC furnished the C-8 epimeric N-unsubstituted triazoles (**147**) in 54% yield over three steps in a ratio of 4:6 (C-8:epi-C-8).
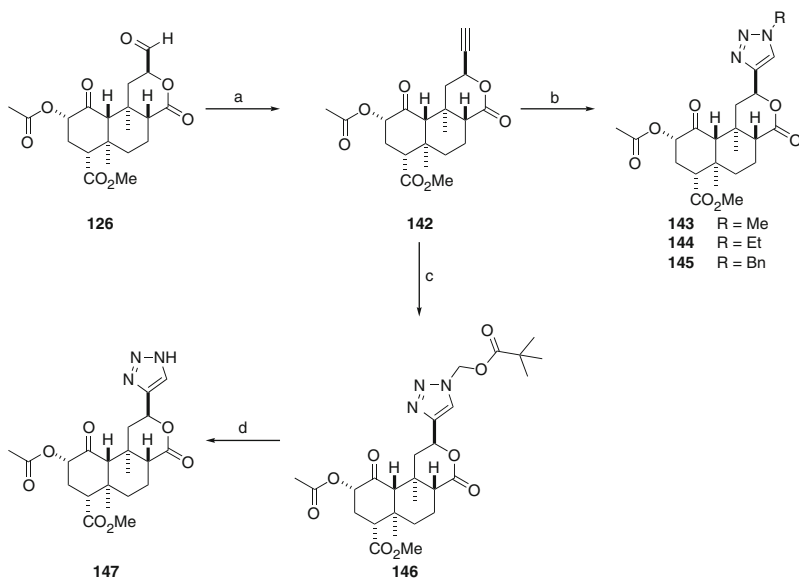
Scheme 23 (a) Ohira-Bestmann reagent; (b) RN_3CuSO_4 (cat.), sodium asorbate, t-BuOH/H_2O; (c) azidomethyl pivalate, $CuSO_4$ (cat.), sodium asorbate, t-BuOH/H_2O; (d): (1) 1M NaOH (2.2 eq.), MeOH/H_2O, (2) 1M HCl (2.2 eq.), (3) Ac_2O, pyridine

Removal of the furan ring (**148**) was accomplished in two steps in 45% overall yield from carboxylic acid **125** (Scheme 24) [57]. Carboxylic acid **125** was coupled with selenophenol via the mixed anhydride using phenyl dichlorophosphate to give the phenyl seleno ester. Decarbonylation of the phenyl seleno ester was accomplished with tributyltin hydride and AIBN in toluene.

Carboxylic acid **125** was coupled with ethanolamine or L-serine methyl ester hydrochloride in the presence of EDCI, HOBt, and Et_3N to afford the corresponding β-hydroxy amides, which were cyclized using bis(2-methoxyethyl)aminosulfur trifluoride (Deoxo-Fluor) to afford oxazolines (**149** and **150**, Scheme 24) [56, 57]. Oxazoline **150** was converted to oxazole **151** in 80% yield by treatment with bromotrichloromethane and DBU, conditions which did not lead to epimerization at C-8 [57]. A variety of oxadiazoles (**152–158**) have been produced in 10–56% yield by treating carboxylic acid **125** with appropriate amidoximes in the presence of EDCI and HOBt followed by heating in toluene (Scheme 24) [44, 57, 58]. These conditions led to some epimerization at C-8, necessitating purification by HPLC. Carboxylic acid **125** was treated with either (2-hydroxybenzyl)triphenyl- or (2-thiobenzyl)triphenyl phosphonium bromide in the presence of CDMT and Et_3N to afford the benzofuran (**159**) and benzothiophene (**160**) products in 26 and 35% yield, respectively (Scheme 24) [58].

In addition to the large variety of replacements for the furan ring, the stereochemistry of C-12 has been inverted. Heating **1** in 5% aqueous KOH afforded the diacid in 95% yield (**161**, Scheme 25) [44]. The free hydroxyl at C-2 was
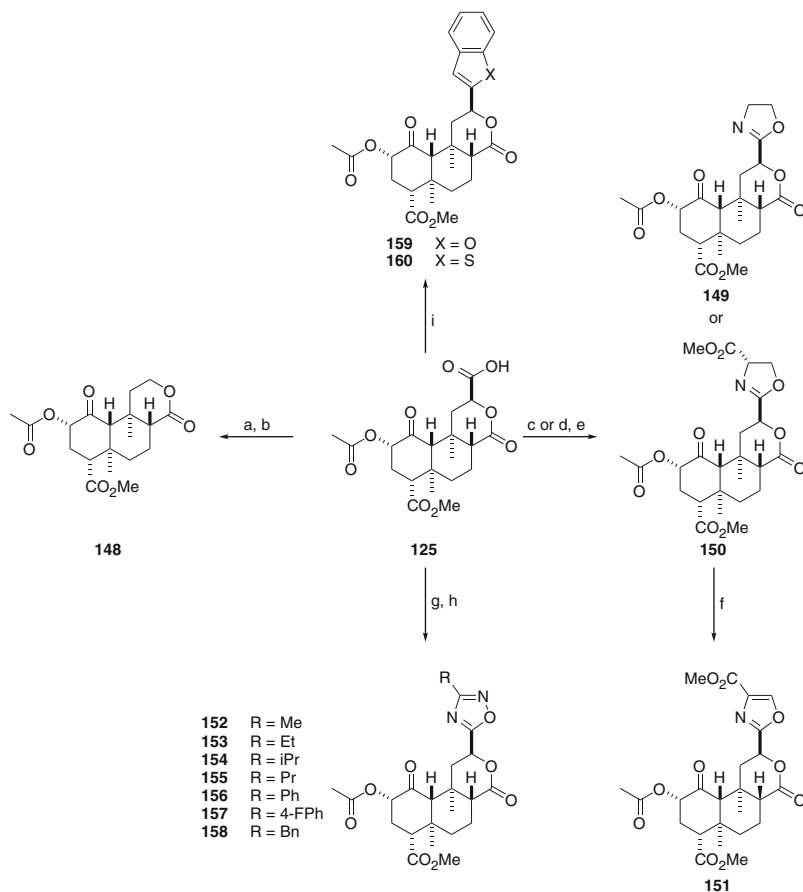
Scheme 24 (a) PhOPOCl$_2$, PhSeH, Et$_3$N, THF; (b) Bu$_3$SnH, AIBN, toluene; (c) EDCI, HOBt, ethanolamine, Et$_3$N, CH$_2$Cl$_2$; (d) EDCI, HOBt, L-serine methyl ester hydrochloride, Et$_3$N, CH$_2$Cl$_2$; (e) deoxo-fluor, CH$_2$Cl$_2$; (f) BrCCl$_3$, DBU, CH$_2$Cl$_2$; (g) EDCI, R(NH$_2$)=NOH, CH$_2$Cl$_2$; (h) toluene, heat; (i) CDMT, Et$_3$N, appropriate Wittig reagent, CH$_2$Cl$_2$/toluene, reflux

re-acetylated (**162**) with Ac$_2$O and pyridine in 48% yield. Refluxing in acetic acid promoted cleavage at C-1 and lactonization to afford the inverted center at C-12, and subsequent methylation of the acid at C-4 using TMSCHN$_2$ provided 12-epi-salvinorin A (**163**) in 19% yield over two steps.

3.3 C1 Modifications

Synthetic methodologies have been explored and developed for selective access to the C-1 ketone for the production of analogs. When **1** was treated with
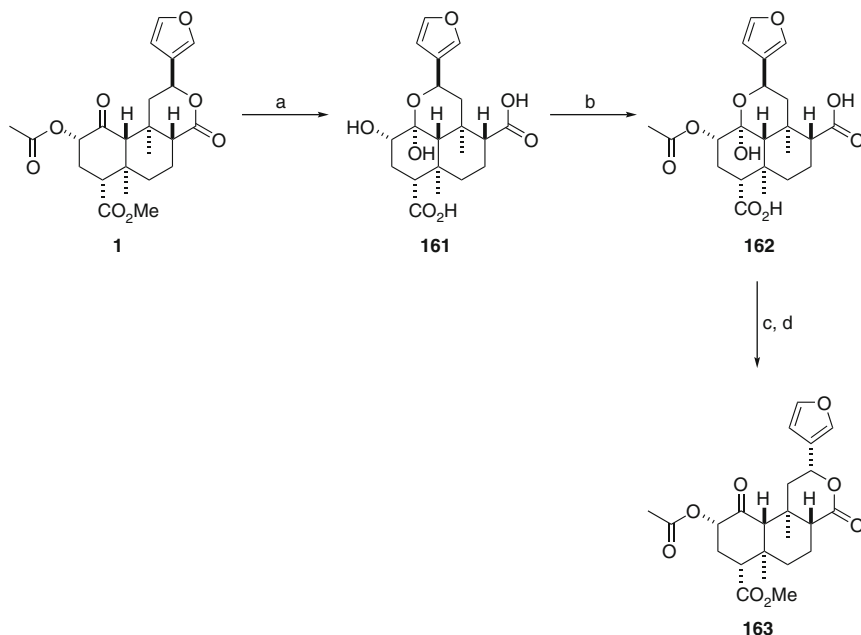
Scheme 25 (a) 5% KOH (aq.), 80 °C; (b) Ac$_2$O, pyridine; (c) AcOH, 118 °C; (d) TMSCHN$_2$, CH$_3$CN

sodium borohydride, the *cis*-1,2-diol (**164**) was produced in 40% yield (Scheme 26) [1, 61]. Unfortunately, these conditions also led to significant epimerization at C-8, also producing the stereoisomeric diol in 40% yield. Using standard conditions (Ac$_2$O, pyridine), the C-2 hydroxyl was selectively acetylated to give the C-2 monoacetate (**165**). The C-1 hydroxyl was selectively acetylated in 83% yield with trimethyl orthoacetate in the presence of catalytic acetic acid at 100 °C to afford the C-1 monoacetate (**166**) [61]. Subsequent acetylation of monoacetate **166** under standard conditions yielded the 1, 2-diacetate (**167**) in 94% yield.

Diol **164** was treated with 1,1′-thiocarbonyldiimidazole to produce the cyclic thiocarbonate (**168**) product in 67% yield over two steps from salvinorin A (Scheme 26) [49]. Unfortunately, these conditions were found to cause epimerization at C-8, the products of which were inseparable on silica gel. However, this meant that initial separation of the C-8 epimers of the *cis*-diol starting material was not necessary. Radical reduction (tributyltin hydride, AIBN, toluene, 80 °C) of the epimeric thiocarbonate mixture afforded the separable C-1 deoxy products in 47% combined yield. Subsequent acetylation of the C-2 hydroxyl under standard conditions (Ac$_2$O, pyridine) gave 1-deoxysalvinorin A (**169**) in 82% yield.
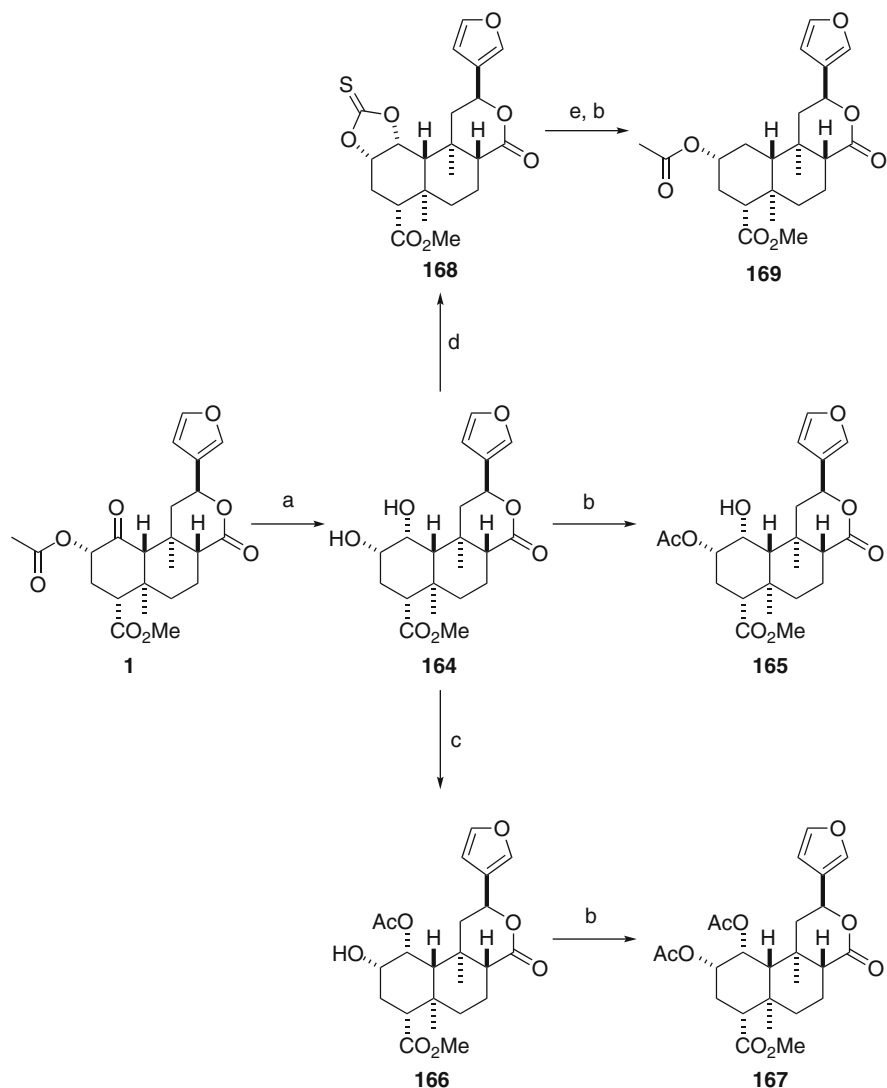
Scheme 26 (a) NaBH$_4$, *i*-PrOH; (b) Ac$_2$O, pyridine; (c) trimethyl orthoacetate, AcOH (cat.), 100 °C; (d) thiocarbonyldiimidazole, DMF, 90 °C; (e) Bu$_3$SnH, AIBN, toluene, 80 °C

Recently, the conditions for the hydride reduction of the C-1 ketone were improved (Scheme 27). Treating **1** or herkinorin (**170**, for synthetic conditions see Scheme 8) with an aqueous solution of sodium borohydride in THF selectively reduced the C-1 ketone (**171** and **172**) in 77 or 45% yield respectively, with no evidence of C-8 epimerization [62]. Treatment of 1α-hydroxysalvinorin A (**171**)
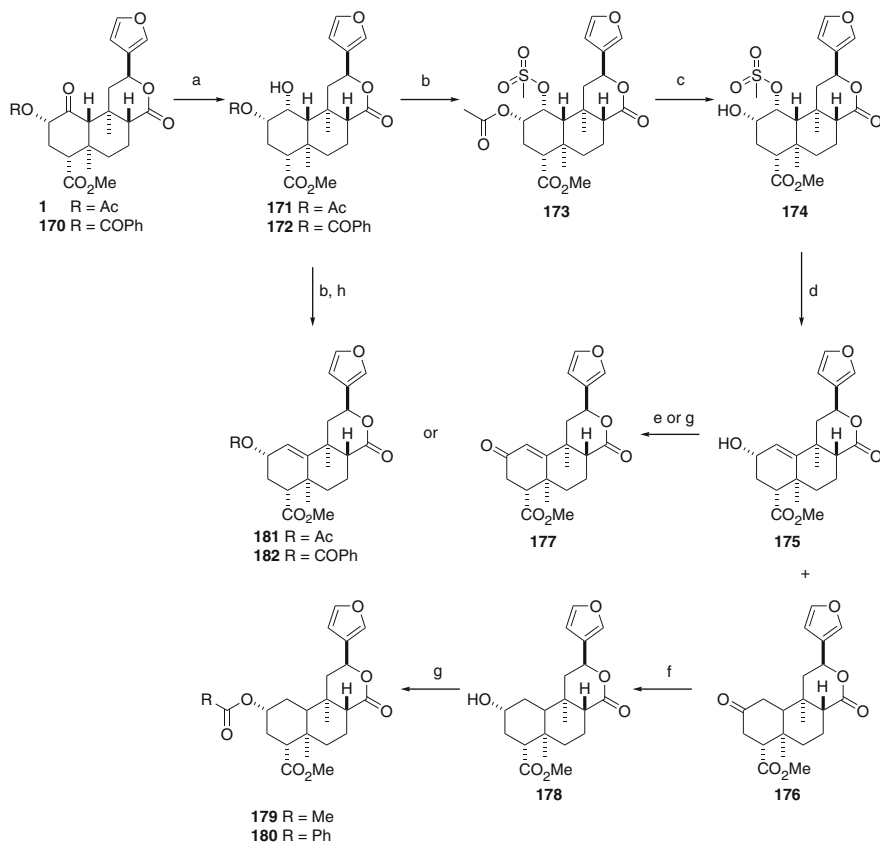
Scheme 27 (a) NaBH$_4$, THF/H$_2$O; (b) (CH$_3$SO$_2$)$_2$O, DMAP, CH$_3$CN; (c) NaOH, MeOH, CH$_2$Cl$_2$, $-10\,^{\circ}$C; (d) DMAP, DMSO, $170\,^{\circ}$C; (e) MnO$_2$, toluene; (f) NaBH$_4$, CH$_3$CN; (g) Ac$_2$O or benzoyl chloride, DMAP, CH$_2$Cl$_2$; (h) trimethylphenylammonium chloride, CH$_3$CN

with methansulfonic anhydride and DMAP afforded 1α-mesyloxysalvinorin A (**173**) in 99% crude yield. Mesylate **173** was hydrolyzed at C-2 by NaOH in MeOH/CH$_2$Cl$_2$ at $-10\,^{\circ}$C to give crystalline 1α-mesyloxysalvinorin B (**174**) in 70% overall yield from 1α-hydroxysalvinorin A (**171**). 1α-Mesyloxysalvinorin B (**174**) was then treated with DMAP in DMSO at $170\,^{\circ}$C to give a mixture of 1-deoxo-1,10-dehydrosalvinorin B (**175**, 76% yield) and 2-keto-1-deoxosalvinorin A (**176**, 22% yield). Allylic alcohol **175** was oxidized with MnO$_2$ in toluene to afford the α,β-unsaturated ketone (**177**) in 78% yield. The reduction of 2-keto-1-deoxosalvinorin A (**176**) with sodium borohydride gave 1-deoxosalvinorin B (**178**) in 41% yield. Acylation of 1-deoxosalvinorin B (**178**) was accomplished through treatment with acetic anhydride or benzoyl chloride in the presence of DMAP to afford 1-deoxosalvinorin A (**179**) and 1-deoxoherkinorin (**180**), respectively. Treatment of 1α-hydroxysalvinorin A (**171**) with methanesulfonic anhydride followed

by heating with trimethylphenylammonium chloride furnished the dehydrated product (**181**) in 76% yield. Finally, 1-deoxo-1,10-dehydrosalvinorin B (**175**) was treated with benzoyl chloride in the presence of DMAP to give 1-deoxo-1, 10-dehydroherkinorin (**182**).

3.4 C4 Modifications

Modifications of **1** have also been performed to modify the methyl ester off C-4 (Scheme 28). Diterpene **1** was treated with lithium ethanethiolate in 1,3-dimethyl-3,4,5,6-tetrahydro-2(1*H*)-pyrimidinone (DMPU); however, in addition to nucleophilic cleavage of the C-4 methyl ester, these conditions cleaved the C-2 acetate. Therefore, standard acetylating conditions were employed to yield acids **183** and **184** due to the mixture of C-8 epimers [49]. Conditions were then modified to selectively cleave the C-4 acid by treating **1** with lithium iodide in pyridine (**183** and **184**) resulting in a 1:1 mixture of the C-8 epimer [63]. The C-8 epimeric mixture of acids **183** and **184** were subjected to standard esterification conditions such as *N*,*N*′-dicyclohexylcarbodiimide (DCC), catalytic DMAP in CH_2Cl_2 with desired alcohols including alkyl, alkenyl, and terminal alkynes (**185** and **186**) [63, 64]. After esterification, the C-8 epimers were separated by chromatography. Additionally, the C-18 methoxyethoxymethyl (**187** and **188**) and methoxymethyl (**189** and **190**) derivatives were synthesized with chloromethoxyethoxymethyl ether (MEMCl), iPr_2NEt in CH_2Cl_2 or MOMCl and Et_3N in CH_2Cl_2, respectively [63, 64]. C-4 Amides were prepared by using EDCI, DMAP, and DMF or EDCI, HOBt, Et_3N, and DMF (**191** and **192**) [34, 63]. Amides synthesized include the addition of alkyl, alkenyl, benzyl, amino acid, and terminal hydroxyl residues to the C-18 position [63]. Specifically, the C-4 acid with natural C-8 configuration was treated with 3-aminopropanenitrile to yield amide **193** [64]. Amide **193** was then treated with PPh_3, azidotrimethylsilane ($TMSN_3$), and DIAD in THF to afford the rearranged product and C-4 salvinorin A acid isostere **194** in a 29% yield over two steps [64].

The C-4 acids (**183** and **184**) have also been subjected to borane reduction conditions to afford alcohol **195** in 23–50% yield or 64% yield as the C-8 epimeric mixture (**195** and **196**, Scheme 29) [34, 49, 64]. The C-8 alcohol epimers **195** and **196** have been treated separately as a common intermediate for a number of C-4 derivatives including esters, ethers, and amines [34, 49, 64]. Alcohols **195** and **196** was subjected to DCC, DMAP, and desired acid chloride or carboxylic acid in CH_2Cl_2 affording ester analogs in 50–92% yield [64]. Esters prepared include alkyl, aryl, and fluorenylmethyloxycarbonyl (Fmoc) protected amino acid derivatives (**197** and **198**) [64]. Ethers were prepared with various alkyl halides and Ag_2O in CH_3CN at 40 °C. Alkyl, allyl, and benzyl ethers were prepared in 45–80% yield (**199** and **200**) [34, 64]. Alcohols **195** and **196** were then activated to the triflates and displaced by a variety of amines by treatment with trifluoromethanesulfonic anhydride and desired amine in 22% – quantitative yield over two steps (**201** and **202**)

	R^1	R^2
185	β-H	alkyl, alkenyl, terminal alkynes
186	α-H	
187	β-H	
188	α-H	
189	β-H	
190	α-H	

183 R = β-H
184 R = α-H

191 R^1 = β-H
192 R^1 = α-H
R^2 = alkyl, alkenyl, benzyl

1

193

194
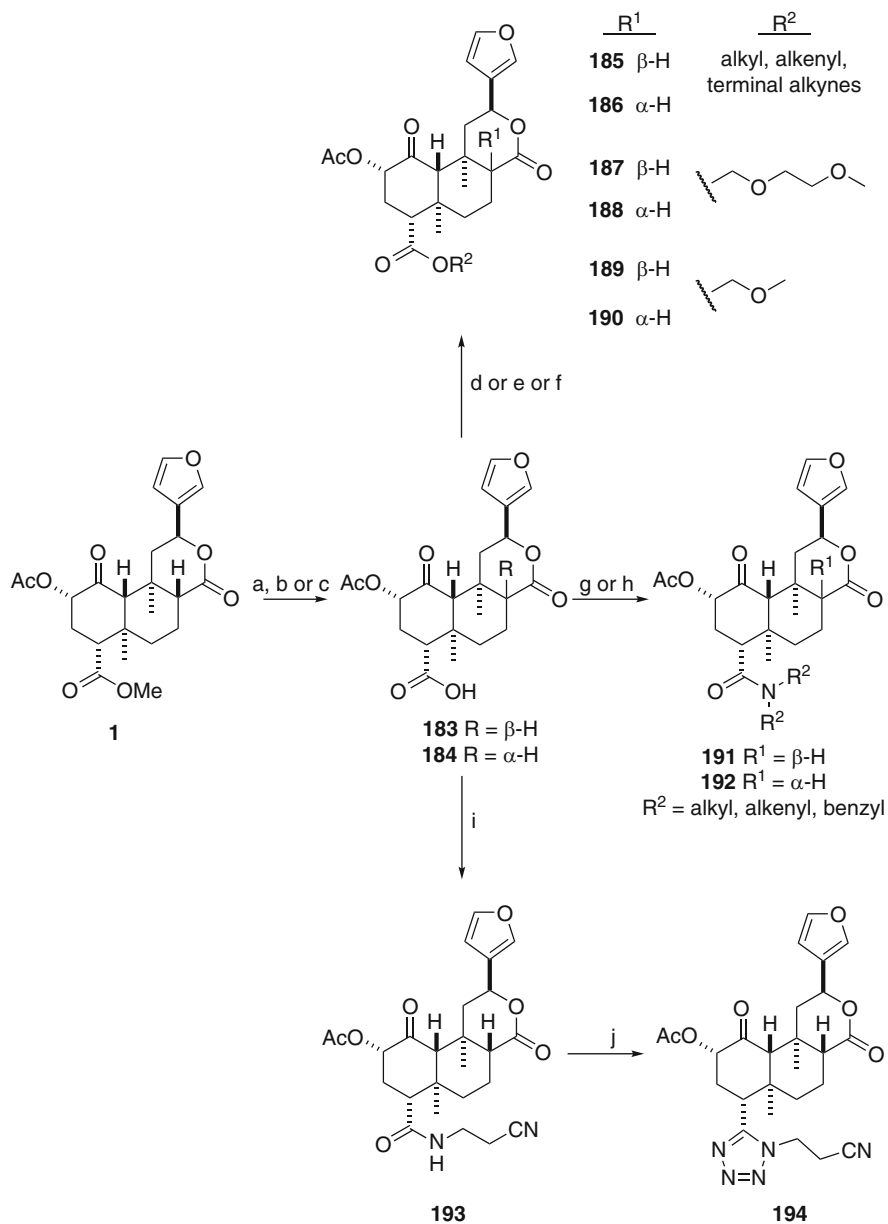
Scheme 28 (a) LiSEt, DMPU, 55 °C; (b) Ac₂O, DMAP, pyridine; (c) LiI, pyridine, 120 °C; (d) ROH, DCC, DMAP, CH₂Cl₂; (e) MEMCl, *i*-Pr₂NEt, CH₂Cl₂; (f) MOMCl, Et₃N, CH₂Cl₂; (g) EDCI, HOBt, Et₃N, DMF; (h) EDCI, DMAP, DMF; (i) 3-aminopropanenitrile, EDCI, HOBt, DMF; (j) PPh₃, TMSN₃, DIAD, THF

Scheme 29 (a) BH$_3$-THF, 55 °C; (b) appropriate acid, DCC, DMAP, CH$_2$Cl$_2$; (c) appropriate acyl chloride, DMAP, CH$_2$Cl$_2$; (d) RX, Ag$_2$O, MeCN, rt or 40 °C; (e) (CF$_3$SO$_2$)$_2$O, pyridine, CH$_2$Cl$_2$, 0 °C; (f) appropriate amine, THF; (g) Et$_3$N, DMSO, (COCl)$_2$, −60 °C
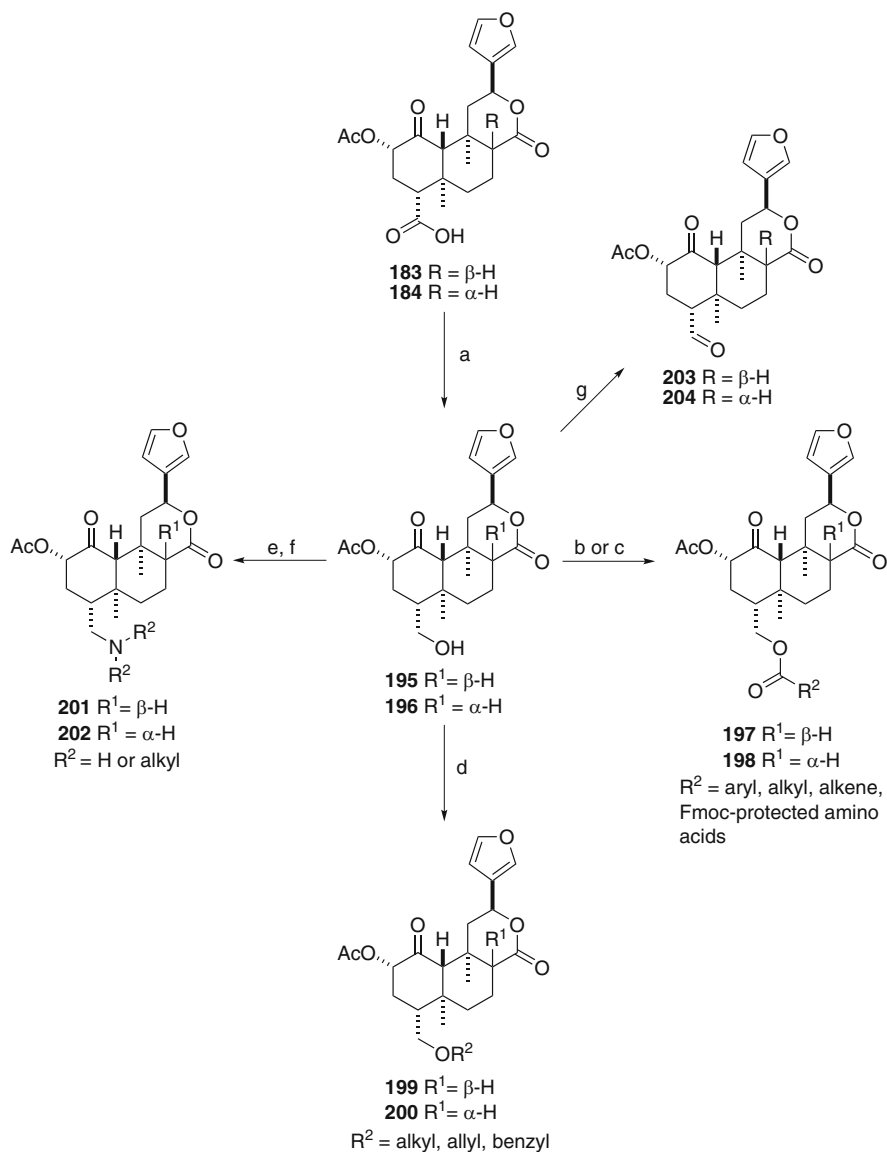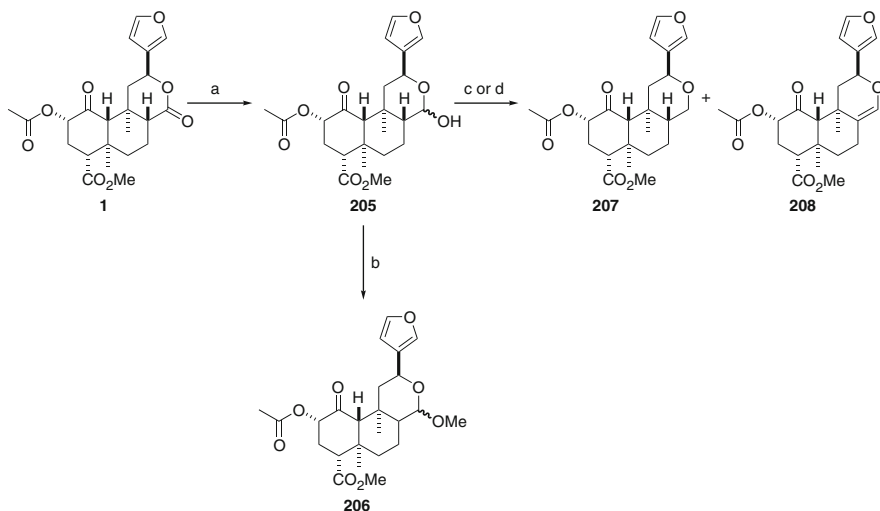
Scheme 30 (a) DIBALH, THF, $-78\ °C$; (b) PPTS, MeOH; (c) Et_3SiH, $BF_3\bullet Et_2O$, CH_2Cl_2, $0\ °C$; (d) Et_3SiH, Amberlyst 15 resin, CH_2Cl_2

[34]. Additionally, alcohols **195** and **196** were oxidized to the aldehydes in 75% yield (**203** and **204**) [64].

3.5 C17 Modifications

Few analogs have been generated at the C-17 position. Salvinorin A (**1**) was converted to the C-17 lactol (**205**) in 65% yield by treatment with diisobutylaluminum hydride (DIBALH) (Scheme 30) [49]. Treatment of the lactol **205** with PPTS in MeOH afforded the methoxy derivatives (**206**) as an epimeric mixture that was separable by silica gel column chromatography [65]. 17-Deoxysalvinorin A (**207**) was synthesized in 48% yield by deoxygenation of lactol **205** using Et_3SiH and $BF_3\bullet Et_2O$ [49]. The C-8 – C-17 enol ether (**208**) was formed in 23% yield as a byproduct of these reaction conditions. The substitution of Amberlyst 15 resin for $BF_3\bullet Et_2O$ in the reaction conditions provided the enol ether (**208**) as the sole product in 76% yield.

4 Bioactivity

Salvinorin A is an agonist at KOP receptors [4]. Medicinal chemistry efforts have explored the SAR of salvinorin A, and have generally focused on improving the affinity and selectivity for KOP receptors. The SAR known at this time is

summarized in Fig. 8. At the C-1 position, reduction (**165**) or removal (**169**) of the carbonyl is tolerated (Fig. 9, Table 1). Interestingly, replacement of the acetyl group in **169** with a benzoyl group (**180**) resulted in an antagonist at μ opioid receptors (MOP), KOP receptors, and δ opioid receptors (DOP) (Fig. 9, Table 2). Introduction of an alkene at C-1 – C-10, exemplified by **181** (Fig. 9, Table 2), is also likely to impart antagonist activity. At the C-2 position, bioisosteric replacements of the ester functionality, such as amides, carbonates, and carbamates, are tolerated. In general, small alkyl groups favor affinity at KOP receptors. The methoxymethyl (**75**) and ethoxymethyl (**76**) ethers at this position are among the most potent salvinorin A derived KOP agonists reported to date (Fig. 9, Table 1). Aromatic groups at C-2 tend to favor affinity at MOP receptors. Examples of this change in
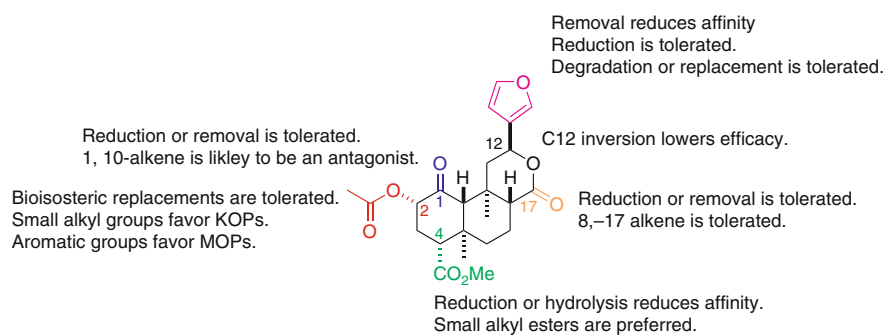
Fig. 8 Summary of the structure-activity relationships of salvinorin A analogs
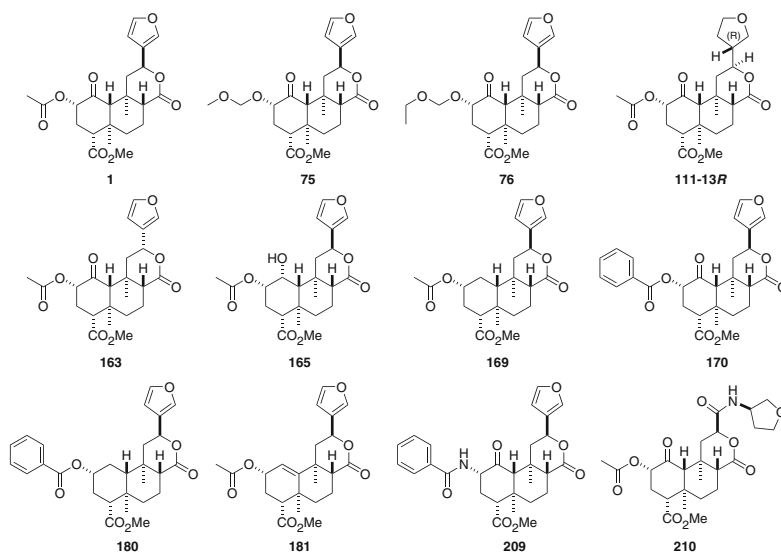
Fig. 9 Structures of interesting biologically active salvinorin A derivatives

Table 1 Opioid receptor affinity, potency, and efficacy of salvinorin A analogs

Compound	MOP K_i ± SD (nM)	DOP K_i ± SD (nM)	KOP K_i ± SD (nM)	EC_{50} ± SEM (nM)	E_{max} ± SEM (%)	Refs.
1	>1,000	>5,970 ± 980	1.9 ± 0.2	(κ) 40 ± 10	(κ) 120 ± 2	[39]
75	ND	ND	0.4 ± 0.02	(κ) 0.6 ± 0.2	(κ) 98	[41]
76	ND	ND	0.32 ± 0.02	(κ) 0.14 ± 0.01	ND	[52]
111 13R	9,790 ± 1,090	>10,000	3.7 ± 0.2	(κ) 750 ± 60	(κ) 81 ± 7	[56]
163	ND	ND	41 ± 5	(κ) 84 ± 8	(κ) 67 ± 5	[44]
165	ND	ND	1,125 ± 365	ND	ND	[49]
169	ND	ND	18 ± 2	(κ) 141 ± 43	(κ) 122 ± 27	[49]
170	12 ± 1	1,170 ± 60	90 ± 2	(μ) 500 ± 140	(μ) 130 ± 4	[47, 48]
209	3.1 ± 0.4	810 ± 30	7,430 ± 880	(μ) 360 ± 60	(μ) 134 ± 5	[48]
210	>10,000	3,090 ± 220	>10,000	ND	ND	[58]

Table 2 Inhibition of agonist stimulated [^{35}S]GTP-γ-S binding

Compound	–	$K_e \pm SD$ (nM)	–	Refs.
–	μ, DAMGO	δ, DPDPE	κ, U69,593	–
180	$4,700 \pm 910$	$8,780 \pm 2,130$	580 ± 30	[62]
181	200 ± 30	400 ± 90	570 ± 140	[62]

affinity are herkinorin (**170**), the first non-nitrogenous selective MOP receptor agonist described, and the related benzamido herkinorin (**209**, Fig. 9, Table 1). At the C-4 position, reduction or hydrolysis of the ester reduces affinity. Replacement of the methyl ester with small alkyl groups is tolerated, whereas replacement with larger groups reduces affinity. At the C-17 position, reduction or removal of the lactone is tolerated. Subsequent methylation of the lactol after reduction of the lactone has little effect on affinity at KOP receptors. Additionally, introduction of a C-8 – C-17 alkene was tolerated. For the furan ring, removal reduces affinity. However, reduction to the tetrahydrofuran (**111–13R**, Fig. 9, Table 1) is tolerated. Inversion of the stereochemistry at the C-12 position (**163**, Fig. 9, Table 1) produces a partial agonist at KOP receptors. Finally, degradation of the furan ring and/or replacement with other heterocycles is tolerated. In fact, exploration at this point in the molecule has produced the first DOP selective ligand derived from the salvinorin A scaffold (**210**, Fig. 9, Table 1).

5 Future Directions

Future research involving salvinorin A will uncover more high affinity, selective ligands for opioid receptors. Even with the wealth of currently available SAR information, there are still some significant gaps in the literature. Collective research has produced a large variety of salvinorin A-based selective KOP receptor agonists. However, there are comparatively few selective KOP receptor antagonists. Further, although herkinorin (**170**, Fig. 9) has been identified as a high affinity, selective MOP receptor agonist, there are no salvinorin A-based selective MOP receptor antagonists, nor are there any high affinity ligands selective for the DOP receptor. Identification of these currently missing salvinorin A-based opioid receptor ligands would not only provide interesting biological probes, but would also potentially lead to the discovery of new opioids for therapeutic use in the clinic.

Currently, the C-2 position and the furan ring (C-13) of salvinorin A are still the most manipulated sites on the scaffold. At the C-2 position, much research has focused on bioisosteric replacements of the ester moiety. However, given the identification of the high affinity and potency methoxymethyl (**75**) and ethoxymethyl (**76**) ether analogs (Scheme 10), the C-2 position merits an investigation of conformational constraint. At the C-13 position, the only synthetic methodology developed to date for the formation of direct carbon-carbon bonds is Stille coupling conditions (Scheme 21). Future methodologies directed at this position would

benefit from improving upon these conditions by eliminating the need for tin reagents. Finally, very little research has been conducted to scrutinize the core ring structure of the salvinorin A scaffold. Total synthesis efforts have provided several ways to arrive at the neoclerodane core ring structure, but there have been no SAR investigations to probe, for example, the necessity of the B-ring, or of the methyl group off C-9. Further explorations of the SAR of salvinorin A would benefit from the systematic introduction of flexibility into this relatively highly constrained scaffold, and new synthetic methodologies are needed in order to achieve this.

Over the past decade, we have witnessed unparalleled advances in our understanding of the basic biological processes that contribute to many human diseases. However, lack of detailed understanding of the underlying etiologies of many central nervous system (CNS) disorders offers a unique opportunity for chemists working on opioids in collaboration with pharmacologists. Expanding the exploration of molecules with opioid receptor activity is likely to identify novel active agents that may serve as drug leads and new chemical tools to understand better the etiology of complex CNS disorders.

References

1. Valdes LJ, Butler WM, Hatfield GM et al (1984) Divinorin A, a psychotropic terpenoid, and divinorin B from the hallucinogenic Mexican mint, *Salvia divinorum*. J Org Chem 49:4716–4720
2. Valdes LJ III, Diaz JL, Paul AG (1983) Ethnopharmacology of ska Maria Pastora (*Salvia divinorum*, Epling and Jativa-M.). J Ethnopharmacol 7:287–312
3. Ortega A, Blount JF, Manchand PS (1982) Salvinorin, a new trans-neoclerodane diterpene from *Salvia divinorum* (Labiatae). J Chem Soc Perkin Trans 1:2505–2508
4. Roth BL, Baner K, Westkaemper R et al (2002) Salvinorin A: a potent naturally occurring nonnitrogenous kappa opioid selective agonist. Proc Natl Acad Sci USA 99:11934–11939
5. Siebert DJ (1994) *Salvia divinorum* and salvinorin A: new pharmacologic findings. J Ethnopharmacol 43:53–56
6. Valdes LJ III (1994) *Salvia divinorum* and the unique diterpene hallucinogen, Salvinorin (divinorin) A. J Psychoactive Drugs 26:277–283
7. Prisinzano TE (2005) Psychopharmacology of the hallucinogenic sage *Salvia divinorum*. Life Sci 78:527–531
8. Aldrich J, Vigil-Cruz S (2003) Narcotic analgesics. In: Abraham DA (ed) Burger's medicinal chemistry and drug discovery, 6th edn. John Wiley, New York
9. Eguchi M (2004) Recent advances in selective opioid receptor agonists and antagonists. Med Res Rev 24:182–212
10. Kaczor A, Matosiuk D (2002) Non-peptide opioid receptor ligands – recent advances. Part II. Antagonists. Curr Med Chem 9:1591–1603

11. Kaczor A, Matosiuk D (2002) Non-peptide opioid receptor ligands – recent advances. Part I. Agonists. Curr Med Chem 9:1567–1589

12. Lu Y, Weltrowska G, Lemieux C et al (2001) Stereospecific synthesis of (2S)-2-methyl-3-(2′, 6′-dimethyl-4′-hydroxyphenyl)propionic acid (Mdp) and its incorporation into an opioid peptide. Bioorg Med Chem Lett 11:323–325

13. Surratt CK, Johnson PS, Moriwaki A et al (1994) μ-Opiate receptor. Charged transmembrane domain amino acids are critical for agonist recognition and intrinsic activity. J Biol Chem 269:20548–20553

14. Weltrowska G, Chung NN, Lemieux C et al (2010) "Carba"-analogues of fentanyl are opioid receptor agonists. J Med Chem 53:2875–2881

15. Ruzicka L (1953) Isoprene rule and the biogenesis of terpenic compounds. Experientia 9:357–367

16. Breitmaier E (2006) Terpenes: flavors, fragrances, pharmaca, pheromones. Wiley-VCH, Weinheim

17. Tokoroyama T (2000) Synthesis of clerodane diterpenoids and related compounds – stereoselective construction of the decalin skeleton with multiple contiguous stereogenic centers. Synthesis 611–633

18. Kohno H, Maeda M, Tanino M et al (2002) A bitter diterpenoid furanolactone columbin from Calumbae Radix inhibits azoxymethane-induced rat colon carcinogenesis. Cancer Lett 183:131–139

19. Moody JO, Robert VA, Connolly JD et al (2006) Anti-inflammatory activities of the methanol extracts and an isolated furanoditerpene constituent of Sphenocentrum jollyanum Pierre (Menispermaceae). J Ethnopharmacol 104:87–91

20. Shi Q, Liang M, Zhang W et al (2007) Quantitative LC/MS/MS method and pharmacokinetic studies of columbin, an anti-inflammation furanoditerpen isolated from Radix Tinosporae. Biomed Chromatogr 21:642–648

21. Bruno M, Fazio C, Arnold NA (1996) Neo-clerodane diterpenoids from Scutellaria cypria. Phytochemistry 42:555–557

22. Lallemand J-Y, Six Y, Ricard L (2002) A concise synthesis of an advanced clerodin intermediate through a Vaultier tandem reaction. Eur J Org Chem 503–513

23. Ley SV, Denholm AA, Wood A (1993) The chemistry of azadirachtin. Nat Prod Rep 10:109–157

24. Merritt AT, Ley SV (1992) Clerodane diterpenoids. Nat Prod Rep 9:243–287

25. Rogers D, Unal GG, Williams DJ et al. (1979) The crystal structure of 3-epicaryoptin and the reversal of the currently accepted absolute configuration of clerodin. J Chem Soc Chem Commun 97–99

26. Lingham AR, Huegel HM, Rook TJ (2006) Studies towards the synthesis of salvinorin A. Aus J Chem 59:340–348

27. Scheerer JR, Lawrence JF, Wang GC et al (2007) Asymmetric synthesis of salvinorin A, a potent kappa opioid receptor agonist. J Am Chem Soc 129:8968–8969

28. Satoh T, Kokubo K, Miura M et al (1994) Effect of copper and iron cocatalysts on the palladium-catalyzed carbonylation reaction of iodobenzene. Organometallics 13:4431–4436

29. Shiina I (2004) An effective method for the synthesis of carboxylic esters and lactones using substituted benzoic anhydrides with Lewis acid catalysts. Tetrahedron 60:1587–1599

30. Shiina I, Kawakita Y-i (2004) The effective use of substituted benzoic anhydrides for the synthesis of carboxamides. Tetrahedron 60:4729–4733

31. Burns A, Forsyth C (2008) Intramolecular Diels–Alder/Tsuji allylation assembly of the functionalized trans-decalin of salvinorin A. Org Lett 10:97–100

32. Nozawa M, Suka Y, Hoshi T et al (2008) Total synthesis of the hallucinogenic neoclerodane diterpenoid salvinorin A. Org Lett 10:1365–1368

33. Hagiwara H, Hamano K, Nozawa M et al (2005) The first total synthesis of (−)-methyl barbascoate. J Org Chem 70:2250–2255

34. Béguin C, Richards MR, Li J-G et al (2006) Synthesis and in vitro evaluation of salvinorin A analogues: effect of configuration at C(2) and substitution at C(18). Bioorg Med Chem Lett 16:4679–4685
35. Harding Wayne W, Schmidt M, Tidgewell K et al (2006) Synthetic studies of neoclerodane diterpenes from *Salvia divinorum*: semisynthesis of salvinicins A and B and other chemical transformations of salvinorin A. J Nat Prod 69:107–112
36. Hagiwara H, Suka Y, Nojima T et al (2009) Second-generation synthesis of salvinorin A. Tetrahedron 65:4820–4825
37. Bergman YE, Mulder R, Perlmutter P (2009) Total synthesis of 20-norsalvinorin A. 1. Preparation of a key intermediate. J Org Chem 74:2589–2591
38. Cheung AK, Murelli R, Snapper ML (2004) Total syntheses of (+)- and (−)-cacospongionolide B, cacospongionolide E, and related analogues. Preliminary study of structural features required for phospholipase A2 inhibition. J Org Chem 69:5712–5719
39. Harding WW, Tidgewell K, Byrd N et al (2005) Neoclerodane diterpenes as a novel scaffold for micro opioid receptor ligands. J Med Chem 48:4765–4771
40. Tidgewell K, Harding WW, Schmidt M et al (2004) A facile method for the preparation of deuterium labeled salvinorin A: synthesis of [2, 2, 2–2H3]-salvinorin A. Bioorg Med Chem Lett 14:5099–5102
41. Lee DYW, Karnati VVR, He M et al (2005) Synthesis and in vitro pharmacological studies of new C(2) modified salvinorin A analogues. Bioorg Med Chem Lett 15:3744–3747
42. Koreeda M, Brown L, Valdes LJ (1990) The absolute stereochemistry of salvinorins. Chem Lett 19:2015–2018
43. Munro TA, Goetchius GW, Roth BL et al (2005) Autoxidation of salvinorin A under basic conditions. J Org Chem 70:10057–10061
44. Béguin C, Duncan K, Munro T et al (2009) Modification of the furan ring of salvinorin A: identification of a selective partial agonist at the kappa opioid receptor. Bioorg Med Chem 17:1370–1380
45. Bikbulatov RV, Stewart J, Jin W et al (2008) Short synthesis of a novel class of salvinorin A analogs with hemiacetalic structure. Tetrahedron Lett 49:937–940
46. Lozama A, Prisinzano TE (2009) Chemical methods for the synthesis and modification of neoclerodane diterpenes. Bioorg Med Chem Lett 19:5490–5495
47. Tidgewell K, Harding WW, Lozama A et al (2006) Synthesis of salvinorin A analogues as opioid receptor probes. J Nat Prod 69:914–918
48. Tidgewell K, Groer CE, Harding WW et al (2008) Herkinorin analogues with differential beta-arrestin-2 interactions. J Med Chem 51:2421–2431
49. Munro TA, Rizzacasa MA, Roth BL et al (2005) Studies toward the pharmacophore of salvinorin A, a potent kappa opioid receptor agonist. J Med Chem 48:345–348
50. Harding WW, Schmidt M, Tidgewell K et al (2006) Synthetic studies of neoclerodane diterpenes from *Salvia divinorum*: semisynthesis of salvinicins A and B and other chemical transformations of salvinorin. J Nat Prod 69:107–112
51. Béguin C, Richards MR, Wang Y et al (2005) Synthesis and in vitro pharmacological evaluation of salvinorin A analogues modified at C(2). Bioorg Med Chem Lett 15:2761–2765
52. Munro TA, Duncan KK, Xu W et al (2008) Standard protecting groups create potent and selective κ opioids: salvinorin B alkoxymethyl ethers. Bioorg Med Chem 16:1279–1286
53. Stewart DJ, Fahmy H, Roth BL et al (2006) Bioisosteric modification of salvinorin A, a potent and selective kappa-opioid receptor agonist. Arzneim Forsch 56:269–275
54. Bikbulatov RV, Yan F, Roth BL et al (2007) Convenient synthesis and in vitro pharmacological activity of 2-thioanalogs of salvinorins A and B. Bioorg Med Chem Lett 17:2229–2232
55. Kouzi SA, McMurtry RJ, Nelson SD (1994) Hepatotoxicity of germander (*Teucrium chamaedrys* L.) and one of its constituent neoclerodane diterpenes teucrin A in the mouse. Chem Res Toxicol 7:850–856

56. Simpson DS, Katavic PL, Lozama A et al (2007) Synthetic studies of neoclerodane diterpenes from *Salvia divinorum*: preparation and opioid receptor activity of salvinicin analogues. J Med Chem 50:3596–3603
57. Harding WW, Schmidt M, Tidgewell K et al (2006) Synthetic studies of neoclerodane diterpenes from *Salvia divinorum*: selective modification of the furan ring. Bioorg Med Chem Lett 16:3170–3174
58. Simpson DS, Lovell KM, Lozama A et al (2009) Synthetic studies of neoclerodane diterpenes from *Salvia divinorum*: role of the furan in affinity for opioid receptors. Org Biomol Chem 7:3748–3756
59. Stille JK (1986) The palladium-catalyzed cross-coupling reactions of organotin reagents with organic electrophiles [New Synthetic Methods (58)]. Angew Chem Int Ed 25:508–524
60. Yang L, Xu W, Chen F et al (2009) Synthesis and biological evaluation of C-12 triazole and oxadiazole analogs of salvinorin A. Bioorg Med Chem Lett 19:1301–1304
61. Valdes LJ, Chang H-M, Visger DC et al (2001) Salvinorin C, a new neoclerodane diterpene from a bioactive fraction of the hallucinogenic Mexican mint *Salvia divinorum*. Org Lett 3:3935–3937
62. Holden KG, Tidgewell K, Marquam A et al (2007) Synthetic studies of neoclerodane diterpenes from *Salvia divinorum*: exploration of the 1-position. Bioorg Med Chem Lett 17:6111–6115
63. Lee DYW, He M, Kondaveti L et al (2005) Synthesis and in vitro pharmacological studies of C(4) modified salvinorin A analogues. Bioorg Med Chem Lett 15:4169–4173
64. Lee DYW, He M, Liu-Chen L-Y et al (2006) Synthesis and in vitro pharmacological studies of new C(4)-modified salvinorin A analogs. Bioorg Med Chem Lett 16:5498–5502
65. Prisinzano TE, Rothman RB (2008) Salvinorin A analogs as probes in opioid pharmacology. Chem Rev 108:1732–1743

Synthesis of Novel Basic Skeletons Derived from Naltrexone

Hiroshi Nagase and Hideaki Fujii

Abstract We will describe eight interesting reactions using naltrexone derivatives. Almost all these reactions are characteristic of naltrexone derivatives, and can lead to the synthesis of many novel skeletons that provide new interesting pharmacological data. Some of the new reactions that were found with naltrexone derivatives were expanded into general reactions. For example, the reaction of 6α-hydroxyaldehyde derived from naltrexone led to the oxazoline dimer and the 1,3,5-trioxaza-triquinane skeleton (triplet drug); this reaction was applied to general ketones which were converted to α-hydroxyaldehydes, followed by conversion to dimers and trimers, as described in Sect. 7.

Keywords Intramolecular reaction · Naltrexone · Oligomerization · Opioid · Rearrangement reaction

Contents

H. Nagase (✉) and H. Fujii
School of Pharmacy, Kitasato University, 5-9-1, Shirokane, Minato-ku, Tokyo, Japan
e-mail: nagaseh@pharm.kitasato-u.ac.jp

Abbreviations

ACE   1-Chloroethoxycarbonyl
COSY   Correlation spectroscopy
CPM   Cyclopropylmethyl
GPCR   G-protein-coupled receptor
HMBC   Heteronuclear multiple bond coherence
HSQC   Heteronuclear single quantum correlation
MVD   Mouse vas deferens
NBO   Natural bond orbital
NOE   Nuclear Overhauser effect
NTI   Naltrindole
TCE   1,1,2,2-Tetrachloroethane
Troc   2,2,2-Trichloroethoxycarbonyl

1 Introduction

Since morphine was first isolated by the German pharmacist Sertürner [1] and its structure was independently determined by Gulland and Robinson [2, 3] and Schöpf [4], many research groups have studied its skeleton, its conversion, and its total synthesis. Morphine has a unique 4,5-epoxymorphinan skeleton that comprises some sequential asymmetric centers and a phenolic hydroxy group, a 4,5-epoxy ring, and a basic nitrogen. This structure has given rise to many complex and novel reactions. Many of the early reactions were described in detail in two books published in 1986, entitled Opioid Analgesics; Chemistry and Receptors [5] and Opiates [6]. After that, only a few studies focused on 14-hydroxy-4,5-epoxymorphinan represented by naloxone and naltrexone (**1**), and those were mostly limited to *intermolecular* reactions, although Portoghese *et al*. described many interesting reactions [7–12] with naltrexone (**1**).

Naltrexone (**1**) has a 14-OH group in addition to the 4,5-epoxymorphinan structure, which comprises four sequential asymmetric centers with two OH groups, and a basic nitrogen. This structure has led to many complex *intramolecular* reactions. In fact, in 1989 and 1990, we showed that the 14-OH group participated in several characteristic intramolecular reactions [13, 14].
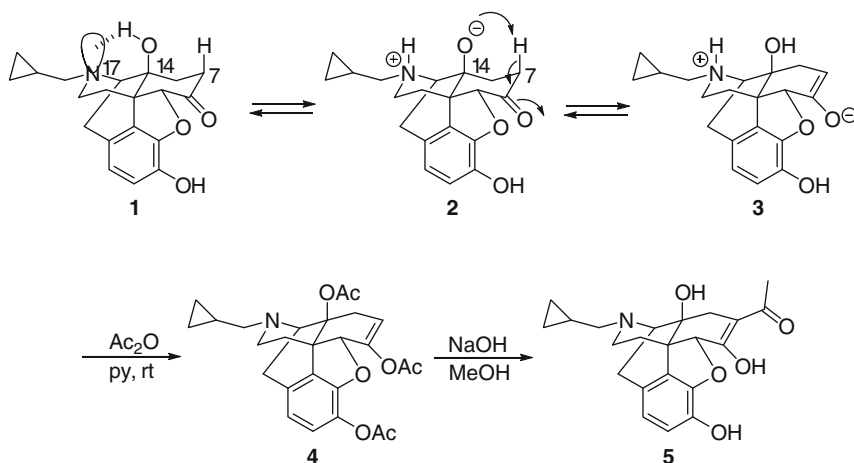
Scheme 1 The 14-OH group of naltrexone (**1**) participates in a reaction that facilitates the enolization of 6-ketone
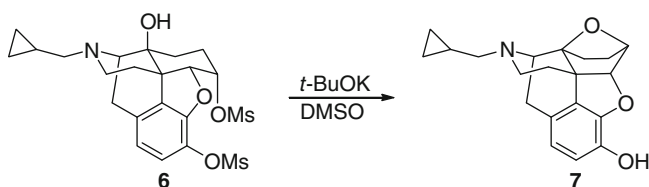
Scheme 2 Intramolecular S$_N$2 reaction between the 14-OH group and the 6α-mesylate of naltrexone derivative **6**

Naltrexone (**1**) is less polar than 14-H naltrexone due to the hydrogen bond between the 14-hydroxy group and the 17-nitrogen (Scheme 1). The basic nitrogen readily extracts the 14-OH proton to give an alkoxide ion **2**, which accelerates the enolization of 6-ketone to give enolate **3**. The enolate **3** reacts with acetic anhydride-pyridine at room temperature to afford triacetate **4**. Furthermore, when **4** is treated with a base, an intramolecular acetyl migration reaction occurs that produces β-diketone (enol form) **5** [14]. Another example of an intramolecular S$_N$2 reaction with the 14-OH group is shown in Scheme 2 [15].

Thus, the reactivity of naltrexone (**1**) is different from that of 14-H morphinans. More recently, we described several other intramolecular reactions of naltrexone (**1**).

The focus of this chapter is on our recent studies on naltrexone (**1**), including intramolecular reactions with the 14-OH group and oligomerization reactions.

Figure 1 shows several structures derived from naltrexone (**1**) with various types of reactions, including bond scission, cyclization, and rearrangements. Some reactions occur due to intramolecular interactions with the 14-OH group. First, we will describe the reactions that involve 14-OH participation, then we will describe other reactions. We will also describe some oligomerization reactions that produce two
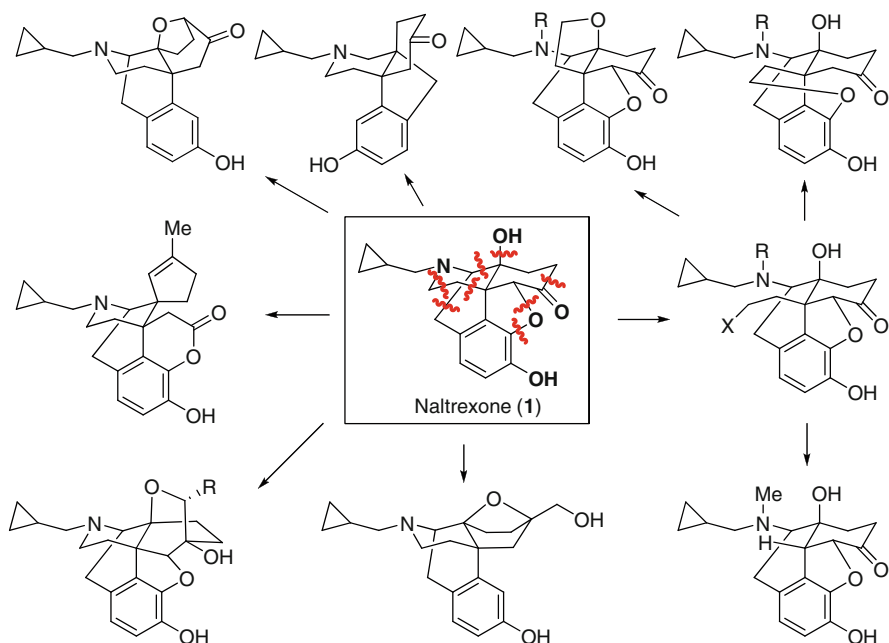
Fig. 1 Novel basic structural skeletons of naltrexone (**1**) derivatives

types of dimers and one trimer (Fig. 2). These products are converted to various derivatives that have interesting pharmacological effects on opioid receptors. Unfortunately, due to the limitation of space, we cannot describe all the reactions and their pharmacological effects. Therefore, we will discuss eight characteristic reactions of naltrexone (**1**).

2   Synthesis of a Novel Ortho Ester [16]

Buprenorphine and etorphine are potent μ and ε opioid analgesics. Like opioid analgesics in general, they are capable of causing serious respiratory depression. Moreover, the side effects produced by these two particular analgesics are particularly dangerous because they cannot be reversed with the μ opioid antagonist, naloxone [17]. This resistance to naloxone antagonism is generally attributed to their high affinity for the μ receptor and their high lipophilicity [18]. TAN-821 is a potent, selective ε opioid receptor agonist that produces strong analgesia *in vivo* [19]. However, it is not highly selective for the ε receptor; in fact, it has been found to bind to the μ opioid receptor *in vitro* (mouse vas deferens (MVD) assay). These three compounds all have a skeleton that comprises 6,14-endoethanotetrahydrothebaine with a 7,8-ethylene bridge. We hypothesized that their strong affinity for the
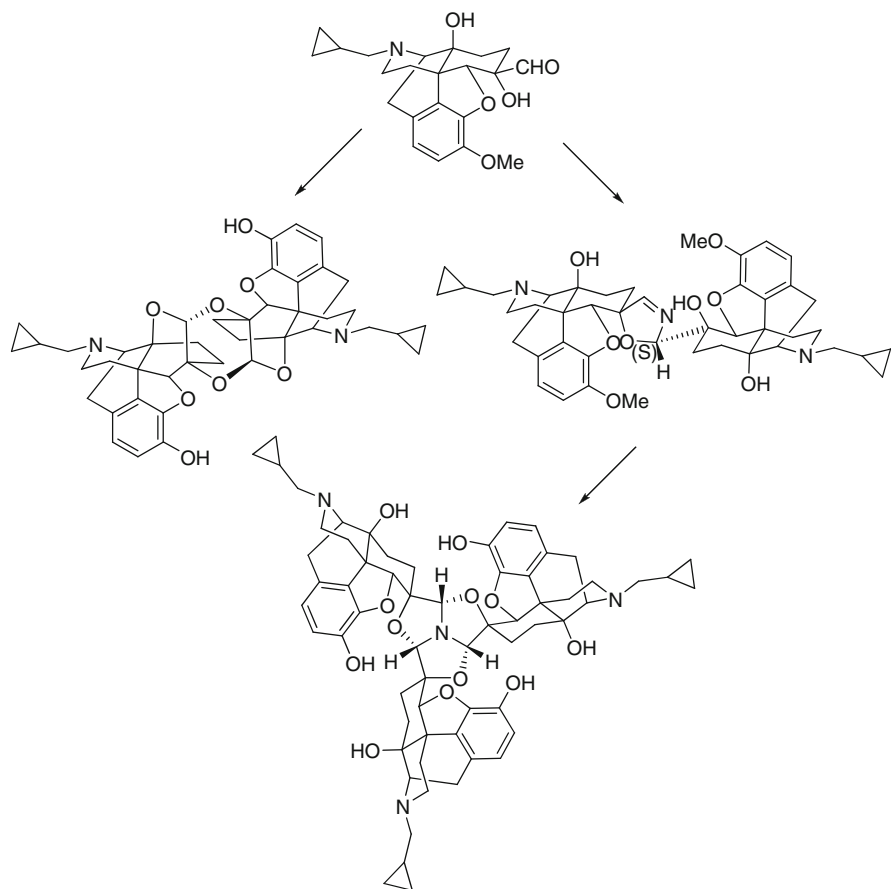
Fig. 2 Synthesis of two dimers and a trimer from naltrexone 6-hydroxy-6-aldehyde

μ opioid receptor may derive, in part, from the high lipophilicity conferred by this bridge. If true, it should be possible to reduce their affinity for the μ opioid receptor by introducing a hydrophilic group. To test this hypothesis, we designed a novel-compound **8a** with a hydrophilic bridge. This compound **8a** was called 17-(cyclo-propylmethyl)-4,5-epoxy-3,6-dihydroxy-8-oxa-6,14-endoethnomorphinan (Fig. 3). We expected compounds derived from **8a** to show improved ε selectivity compared to TAN-821 *in vitro*.

Initially, we planned to synthesize the hemiacetal **8b** or acetal **8c** with an intramolecular cyclization between the 14-OH and 6-aldehyde groups in α-hydro-xyaldehyde **9**. We reasoned that **9** could be obtained by reacting naltrexone methyl ether with a carbanion of 1,3-dithiane, followed by oxidative hydrolysis of thioa-cetal **10** (Fig. 4). However, when we attempted to obtain **9** from the hydrolysis of **10** with CuCl₂/CuO or HgCl₂/CdCO₃ in aqueous MeCN or CH₃COCH₃ [20, 21], we
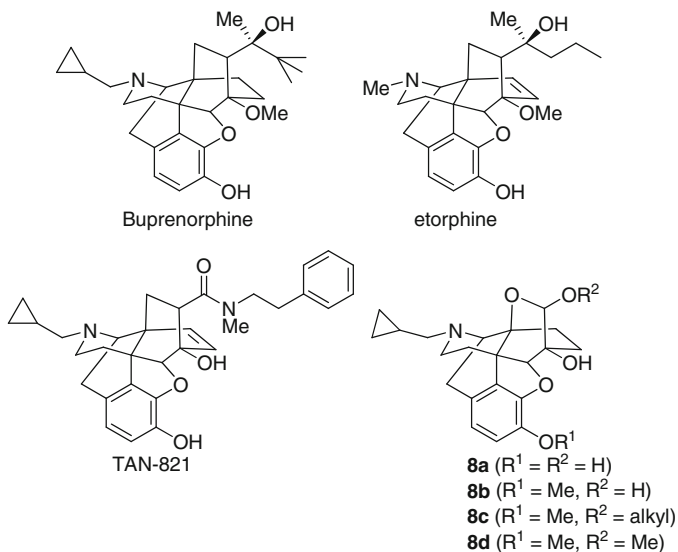
Fig. 3 Structures of buprenorphine, etorphine, TAN-821, and derivatives of compound **8**
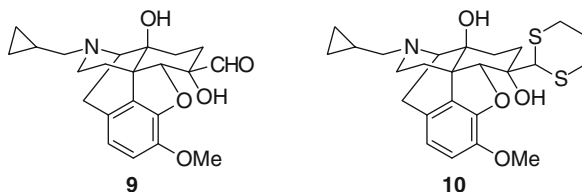
Fig. 4 The structures of α-hydroxyaldehyde **9** and thioacetal **10**

were unsuccessful. We next tried subjecting **10** to an acetal exchange reaction with $CuCl_2$/CuO (2 and 4 equiv.) and $CH(OMe)_3$ in MeOH at 50 °C; from this we expected to obtain the dimethyl acetal **11**. Instead, surprisingly, we obtained a substantial yield (55%) of the ortho ester **12**. This was the first time that an oxidation method succeeded in introducing a 6β-carboxylic acid functional group into naltrexone (**1**) without the oxidation of any other functional groups (*e.g.*, N or OH). Moreover, this approach produced the first 8-oxabicyclo[2.2.2]octane derivative **12** to be described in opioid chemistry. We therefore sought to find conditions that optimized this reaction (Fig. 5).

   We first ran the reaction with metals commonly used to catalyze the hydrolysis of thioacetal, including $HgCl_2$/$CdCO_3$, $AgNO_3$/AgO, and $FeCl_3$/CuO. We found that the hydrolysis (oxidation) proceeded with $FeCl_3$/CuO and, alternatively, with $CuCl_2$/CuO, but not with $HgCl_2$/$CdCO_3$ or $AgNO_3$/AgO. Between $FeCl_3$/CuO and $CuCl_2$/CuO, the latter exhibited a shorter reaction time; thus, we focused on

Fig. 5 Structures of acetal **11** and ortho ester **12**

11

12
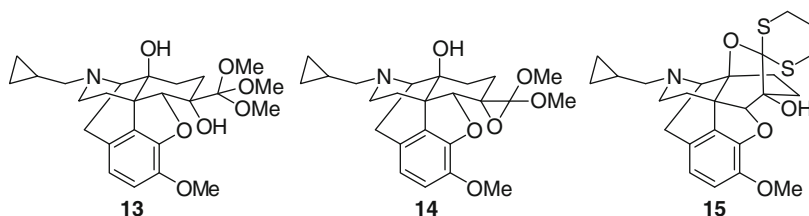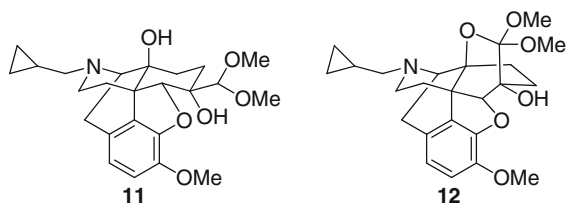
Fig. 6 Structures of compound **13–15**

13

14

15

CuCl₂/CuO in our subsequent optimization efforts. Next, we examined the effects of varying the amount of catalyst. When the level of $CuCl_2$ was less than 0.25 equiv., no ortho ester **12** was obtained. However, when 1 equiv. of $CuCl_2$ was used, good yields were obtained. When less than 0.5 equiv. of CuO was used, a remarkably low yield was obtained, and varying the ratio of $CuCl_2$ to CuO led to the synthesis of other novel compounds **13–15** in addition to **12** (Fig. 6). The best yield of **12** (78%) was obtained when $CuCl_2$ and CuO were included in equal amounts (1 equiv.).

Substitution of K_2CO_3 for CuO resulted in a high yield of **12** (80%), which was the only product. In contrast, when CSA was substituted for CuO, little or no **12** was produced; however, this produced a good yield of **11** (65%) and a small amount of the cyclic acetal **8d** (18%). In summary, the substitution of K_2CO_3 for CuO was a good approach for obtaining **12** without the related compounds **8d**, **11**, **13–15**, and **19**; substitution of CSA for CuO was a good approach for obtaining the dimethylacetal **11**.

We proposed that the synthesis of **12** proceeded *via* the mechanistic sequence depicted in Scheme 3. A key step in this sequence was the abstraction of the proton in the 2′-position by the alkoxide ion derived from the 14-hydroxide of the dithiane derivative **10**. Previous reports have described the participation of this 14-OH group in the formation of naltrexone derivatives [13]. In our scheme, the 14-OH group of naltrexone (**1**) is activated intramolecularly by the lone electron pair on the 17-nitrogen; then the resulting 14-OH extracts the axial hydrogen from the 7-position of naltrexone (**1**). This facilitates enolization, and enol acetate is produced with Ac_2O in pyridine at room temperature (Scheme 1). Consistent with this proposal, we found that the key intermediate **15** was isolated
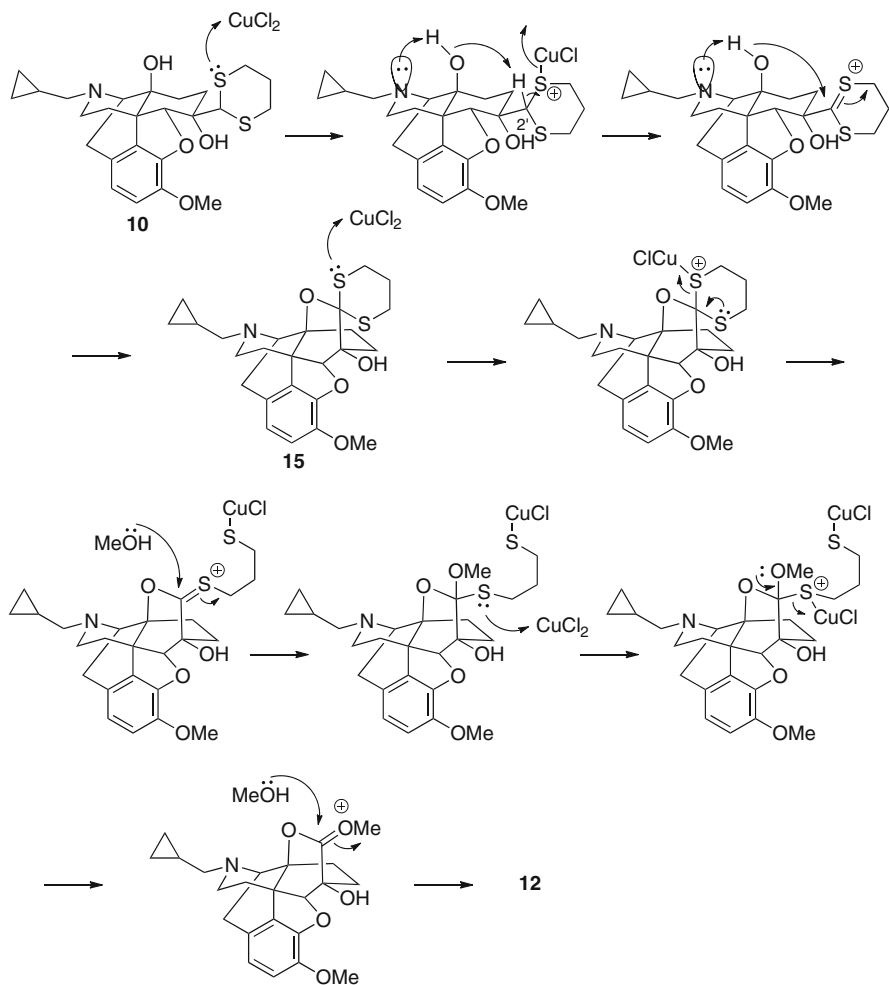
Scheme 3 Proposed reaction mechanism for formation of the ortho ester **12**

and readily hydrolyzed to **12** under the same conditions that enabled the acetal exchange reaction in **10**.

As a further test, we attempted to convert the 14-OH group to hydrogen in **10**, to confirm that the 14-OH group participated in the abstraction of the 2′-hydrogen of dithiane **10**. Compound **16** was synthesized from naltrexone methyl ether [22] and then subjected to the same acetal exchange reaction as above. Under the same conditions, acetal **18** was obtained instead of the objective ortho ester (Scheme 4), consistent with our hypothesis that the 14-OH group participated in the ortho ester formation. Subsequently, the obtained ortho ester **12** was readily hydrolyzed with acid to give ester **19** (Scheme 5).
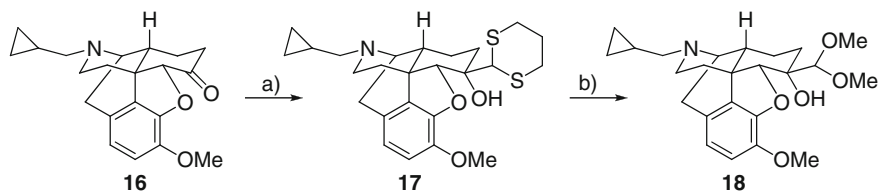
Scheme 4 Acetal exchange reaction of the 14-H compound **16**. Reagents and conditions: (a) *n*-BuLi, 1,3-dithiane, DME, −70 °C, 49%; (b) CuCl$_2$·2H$_2$O, CuO, CH(OMe)$_3$, MeOH, 50 °C, 63%
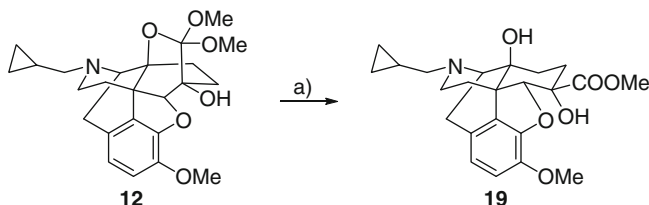
Scheme 5 Hydrolysis reaction of ortho ester **12**. Reagents and conditions: (a) AcOH, 80 °C, 67%

3 Synthesis of Opioid Ligands with Oxabicyclo[2.2.2]octane and Oxabicyclo[2.2.1]heptane Skeletons [23]

As mentioned above, we synthesized the novel ortho ester **12** with an oxabicyclo [2.2.2]octane skeleton. However, this compound was not stable. The facile opening of the ether ring produced the corresponding hydroxy ester **19** (Scheme 5). Therefore, we sought to synthesize a stable basic skeleton **20**. In the course of these studies, we developed new synthetic methods for an oxabicyclo[2.2.2]octane skeleton **20** and an oxabicyclo[2.2.1]heptane skeleton **21** (Fig. 7).

The 6-keto group of naltrexone (**1**) is accessible to nucleophilic attack from the β-side to provide 6α-alcohol derivatives. Therefore, we attempted to synthesize a 6α-epoxide derivative **24** of naltrexone with a stable sulfur ylide derived from trimethylsulfoxonium iodide [24]. The 6α-epoxide **24** was expected to convert to the objective oxabicyclo[2.2.2]octane derivative **20**. Instead, the 6β-epoxide **23** was obtained in 67% yield, but not the objective 6α-epoxide **24** (Scheme 6). The structure of **23** was determined by X-ray crystallographic analysis (Fig. 8).

Although nucleophilic attack occurred on the β-side of naltrexone methyl ether (**22**), we postulated that the kinetically formed α-hydroxy intermediate **A** had returned to the original ketone (**22**) due to the strong dipole-dipole interaction between the 4,5-epoxy ring and the resulting hydroxide ion (Scheme 7). Ultimately, nucleophilic attack of the reagent occurred on the α-side due to a reversible reaction with the stable ylide to afford the stable β-alcohol **B** without the dipole-dipole interaction (Scheme 7).

If this postulation was correct, the 4,5-epoxy open-ring compound **25** [25] could yield the objective 6α-epoxide **26** by reacting with the stable ylide. Although
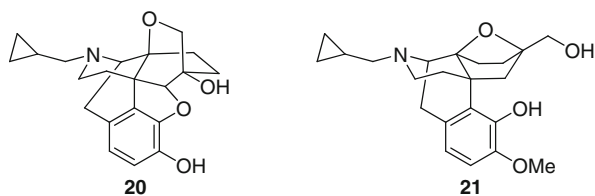
Fig. 7 Structures of oxabicyclo[2.2.2]octane **20** and oxabicyclo[2.2.1]heptane derivative **21**
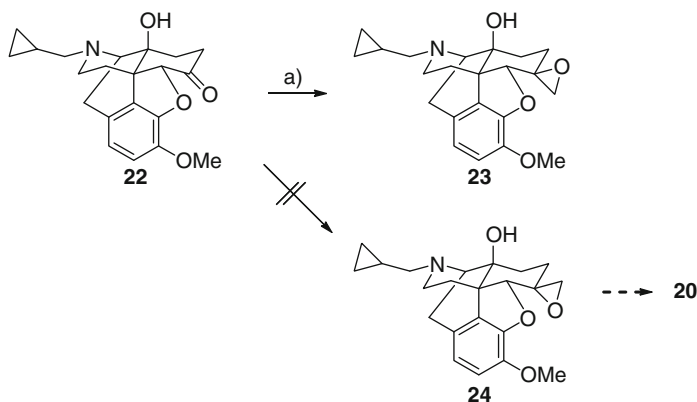
Scheme 6 Reaction of naltrexone methyl ether (**22**) with a stable sulfur ylide. Reagents and conditions: (a) trimethylsulfoxonium iodide, NaH, THF, 55 °C to rt, 67%
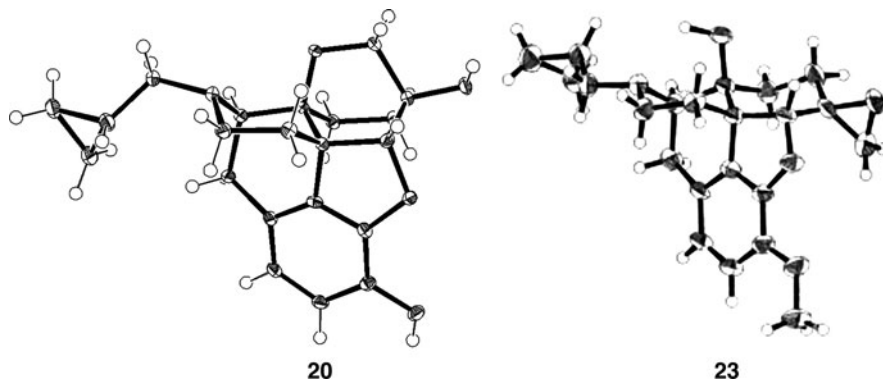
Fig. 8 X-ray crystallographic analyses of **20** and **23**

compound **25** has a 4-OH group and not a 4,5-epoxy ring, the 4-OH group may be flexible enough to move into a position that avoids a dipole-dipole interaction with the α-OH group at the 6 position. Thus, the 6α-epoxide **26** might be expected to convert to the objective compound **27**. However, surprisingly, when the open-ring
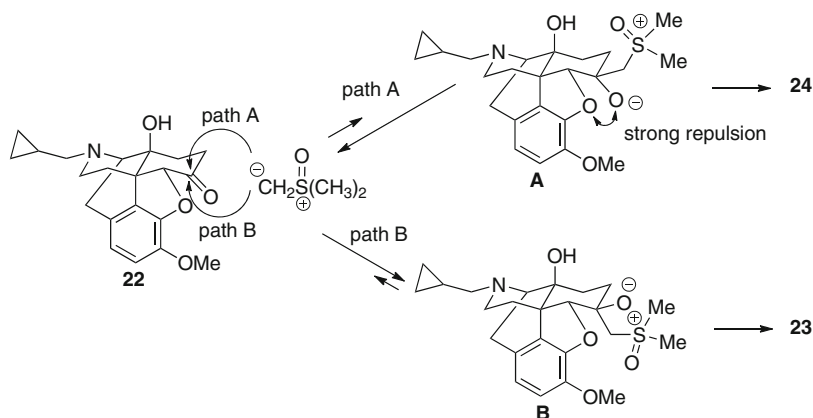
Scheme 7 Reaction mechanism of naltrexone methyl ether (**22**) with stable sulfur ylide to afford 6β-epoxide **23**
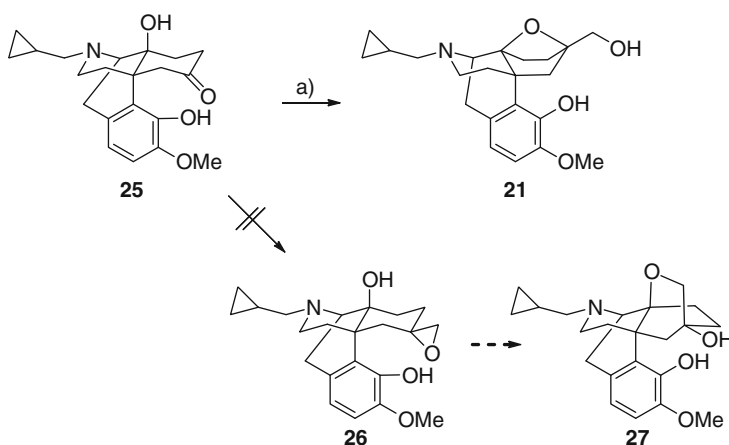
Scheme 8 Reaction of 4-hydroxy morphinan **25** with stable sulfur ylide. Reagents and conditions: (a) trimethylsulfoxonium iodide, NaH, THF, 55 °C to rt, 58%

compound **25** was treated with the stable ylide at 55 °C, an unexpected product **21** was obtained in 58% yield (Scheme 8).

To investigate the source of the unexpected cyclization, we combined a precursor **28** that did not have a 4-hydroxy group with the same stable ylide. This produced compound **29** with an oxabicyclo[2.2.1]heptane skeleton *via* the epoxide **30**. Alternatively, the morphinan methyl ether **28** could also react with the stable sulfur ylide derived from trimethylsulfoxonium iodide at room temperature. The definitive intermediate, 6α-epoxide **30**, was isolated, and then treated with NaH in DMF at 80 °C to produce the objective bicyclic compound **29** (Scheme 9).
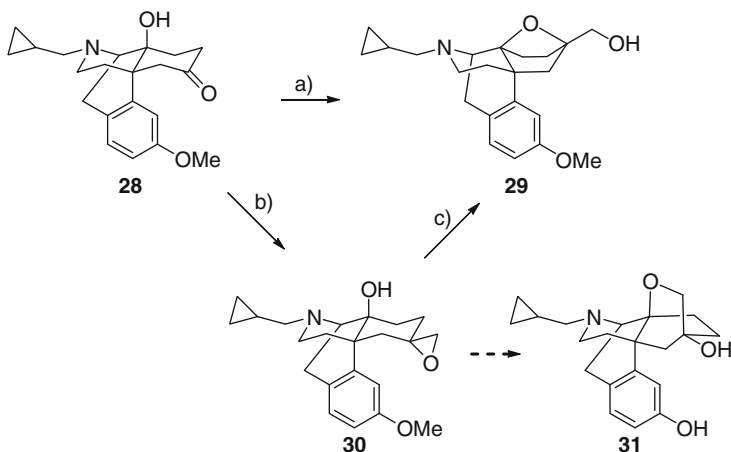
Scheme 9 Reaction of morphinan **28** with stable sulfur ylide to produce oxabicyclo[2.2.1]heptane derivative **29**. Reagents and conditions: (a) trimethylsulfoxonium iodide, NaH, THF, 55 °C, 80%; (b) trimethylsulfoxonium iodide, NaH, THF, rt; (c) NaH, DMF 80 °C, 61%
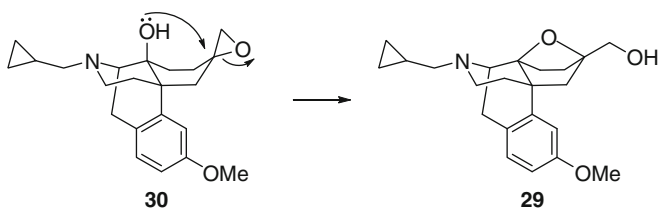
Scheme 10 Intramolecular cyclization reaction of epoxide **30** to produce **29**

The cyclization of **30** may proceed *via* the boat conformation. The distance between the 14-OH group and the 6-quarternary carbon would be closer than the distance between the 14-OH group and methylene carbon of the α-epoxide; thus, cyclization might occur and give **29**, as shown in Scheme 10. On the other hand, Baldwin's rule could explain this selective cyclization.

This reaction was also conducted with the unstable ylide derived from trimethyl-sulfonium iodide to provide an epoxide **30** in 65% yield. Then treatment with NaH in DMF at 80 °C afforded the objective compound **29** (Scheme 11).

On the other hand, when naltrexone methyl ether (**22**) was treated with the unstable ylide at 0 °C in THF-DMSO, the initial objective product **31** was obtained in 62% concomitantly with the methyl ether derivative **32** (Scheme 12).

In this case, once the unstable ylide attacked the β-side of the 6-ketone, the ylide cannot be displaced, because it is an irreversible reaction. The presence of the 4,5-epoxy ring might disturb the formation of an ideal boat form in the resulting compound **33**. This may bring the 14-hydroxy group and methylene group of the
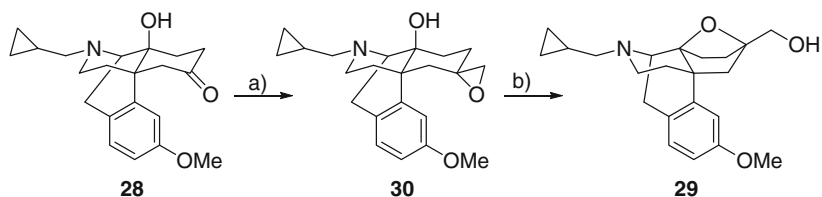
Scheme 11 Reaction of morphinan **28** with unstable sulfur ylide to give **29**. Reagents and conditions: (a) trimethylsulfonium iodide, NaH, THF-DMSO, rt, 65%; (b) NaH, DMF, 80 °C, 61%
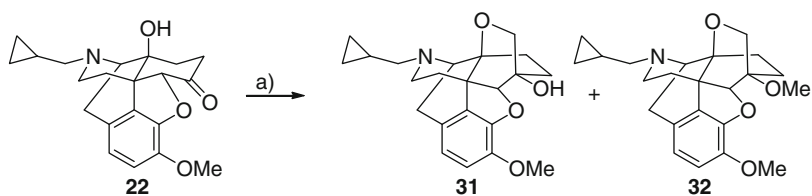
Scheme 12 Reaction of naltrexone methyl ether (**22**) with unstable sulfur ylide to afford **31** and **32**. Reagents and conditions: (a) trimethylsulfonium iodide, NaH, THF-DMSO, 0 °C, **31**: 62%, **32**: 26%
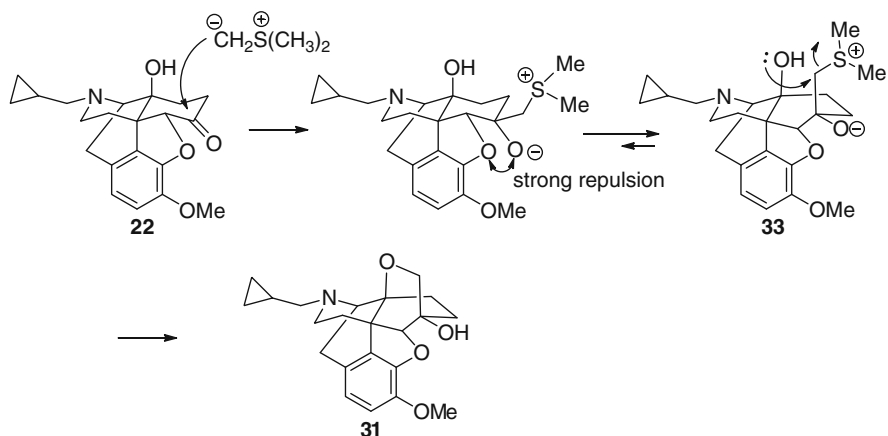
Scheme 13 Reaction mechanism for obtaining **31**

methyl sulfonium moiety into closer proximity than the corresponding 6-carbon of **33**; this would produce the oxabicyclo[2.2.2]octane skeleton **31** (Scheme 13).

Demethylation of **31** with 1-propanethiol and *t*-BuOK afforded **20** (Scheme 14). The structure of **20** was also confirmed by X-ray crystallographic analysis (Fig. 8).

Scheme 14 Demethylation
reaction of **31** to give **20**.
Reagents and conditions: (a)
t-BuOK, 1-PrSH, DMF,
150 °C, 96%
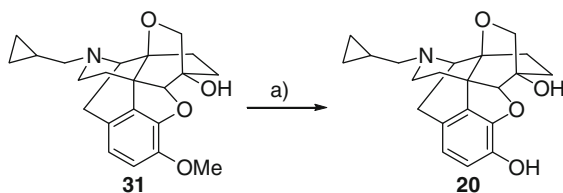
4 Novel Cleavage Reaction of the C16–N17 Bond in Naltrexone Derivatives [26]

The 17-substituent of morphinans is believed to influence its agonistic or antagonistic activity towards the opioid receptor [5]. For example, 17-methyl morphinans, morphine, and oxymorphone are agonists. On the other hand, 17-allyl and 17-cyclopropylmethyl (CPM) morphinans, naloxone and naltrexone (**1**) are antagonists [5]. Therefore, a dealkylation, especially demethylation reaction of 17-substituents has been widely used to synthesize morphinan derivatives that possess various 17-substituents [27–33]. However, the reaction with chloroformates has only been applied to 14-H-morphinans. Therefore, we were interested in the 17-dealkylation reaction in 14-OH-morphinans, like naltrexone (**1**). In the course of the study, we found a novel reaction that cleaved the C16–N17 bond in a naltrexone derivative **35** that produced oxazolidinone **36**, which lacked a D-ring (Scheme 15).

This novel cleavage reaction is interesting from the viewpoints of both organic chemistry and medicinal chemistry, because this reaction could open the door for the synthesis of morphinan derivatives without a piperidine ring (D-ring). This reaction may be useful for converting a partial μ opioid receptor agonist, morphine[1] [34–38] into a full agonist derivative. In this section, we describe a novel reaction that cleaves the C16–N17 bond in the naltrexone derivative **35** and produces the oxazolidinone derivative **36**.

We first attempted to dealkylate the CPM group in naltrexone derivative **35** with 1-chloroethyl chloroformate (ACE-Cl) under the original reaction conditions [33]; however, the reaction hardly proceeded. After extensive investigation, we found that the piperidine ring of naltrexone derivative **35** could be cleaved with ACE-Cl (9 equiv.) in pyridine to give, surprisingly, oxazolidinone **36** in 60% yield concomitantly with the starting material **35**. However, that reaction did not produce the objective carbamate derivative **37** (Scheme 15, condition (a); Fig. 9 shows the structure of compound **37**). Therefore, we focused on the abnormal reaction that

---

[1]Although morphine is a classical μ opioid receptor agonist, its intrinsic activity is known to be lower than that of a representative full μ opioid receptor agonist, DAMGO. Moreover, recent reports showed that morphine was a partial agonist for the opioid μ receptor in some pharmacological assays. See [34–38].
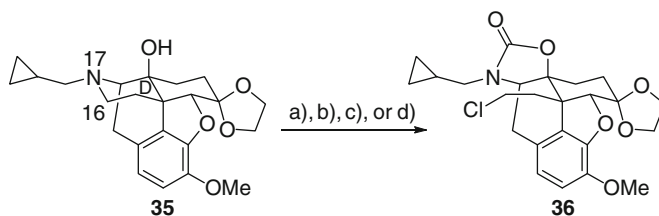
Scheme 15 Novel C16-N17 cleavage reaction with ACE-Cl. Reagents and conditions: (a) ACE-Cl (9 equiv.), pyridine, 100 °C, 60%; (b) ACE-Cl (22 equiv.), pyridine, 100 °C, 80%; (c) ACE-Cl (5.6 equiv.), K_2CO_3, TCE, reflux, 93%; (d) Troc-Cl (5.6 equiv.), K_2CO_3, TCE, reflux, 70%
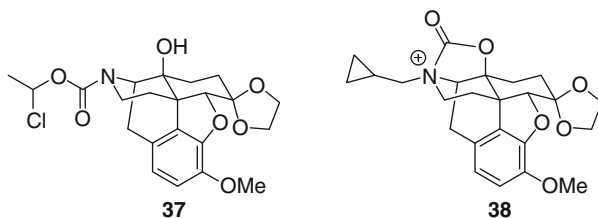
Fig. 9 Structures of carbamate **37** and the oxazolidinium intermediate **38**

caused cleavage of the C16–N17 bond and produced oxazolidinone **36**; we attempted to improve the yield of compound **36**, and we also examined the reaction mechanism.

We developed the working hypothesis that, first, a reaction intermediate, oxazolidinium **38** (Figs. 9 and 10) would be formed, and then chloride ion would attack C16. Sufficient chloride ions in the reaction system could facilitate an attack on C16 to cleave the C16–N17 bond. Insufficient free chloride ions would cause the cleavage reaction to proceed too slowly, and the remaining intermediate **38** would be hydrolyzed to give the starting material **35** during workup. Although pyridine might neutralize any HCl derived from the reaction of **35** with ACE-Cl, the resulting pyridinium chloride may limit the available free chloride ion in solution, because pyridine is a weak base and pyridinium chloride cannot dissociate effectively into free chloride ion and pyridine. On the basis of the above working hypothesis, we used a large excess of ACE-Cl (22 equiv.) in pyridine to facilitate production of the objective compound **36** (80% yield) (Scheme 15, condition (b)). We next attempted to use K_2CO_3 as a base. The K_2CO_3 reacts with HCl to produce KCl and H_2CO_3, which will decompose into CO_2 and water. Thus, the starting naltrexone derivative **35** was treated with ACE-Cl (5.6 equiv.) in the presence of K_2CO_3 (9 equiv.) in 1,1,2,2-tetrachloroethane (TCE). We obtained the objective oxazolidinone **36** in 93% yield (Scheme 15, condition (c)). Finally, the reaction of **35** with 2,2,2-trichloroethyl chloroformate (Troc-Cl) also afforded **36** in 70% yield (Scheme 15, condition (d)).

Next, we examined how the C16–N17 bond cleavage could occur without removing the CPM group. Figure 10 shows the respective intermediates **38**
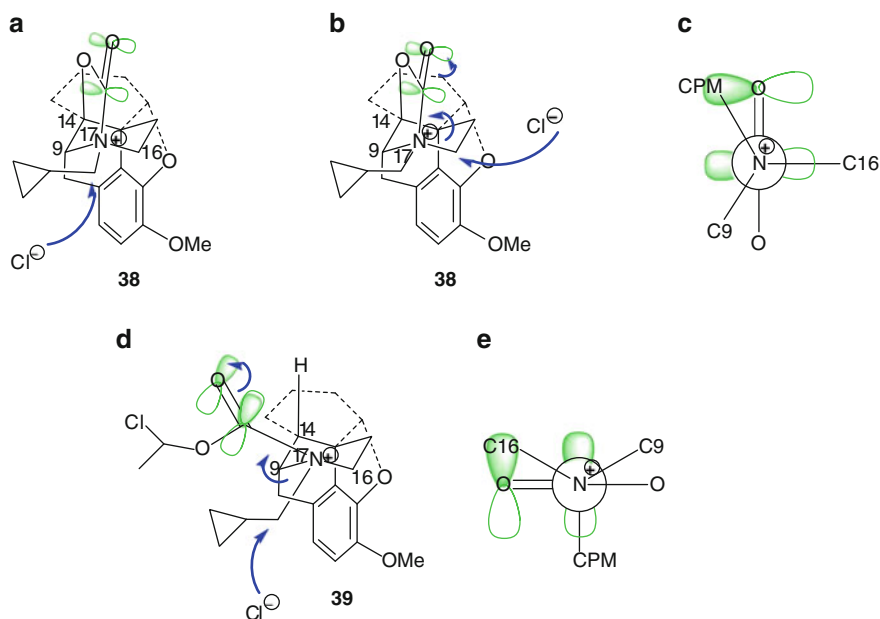
Fig. 10 The postulated reaction mechanisms for bond cleavage in the respective intermediates **38** (**a**, **b**) and **39** (**d**) of 14-OH and 14-H-morphinan, with their Newman projection formulas (**c**, **e**). In intermediate **38**, the CPM–N17 bond appears to be nearly orthogonal to the π-orbital (*green*) of the carbonyl group (**a**, **c**). However, the C16–N17 bond appears to be parallel to the π-orbital (*green*) (**b**, **c**). The CPM–N17 bond in intermediate **39** could be parallel to the π-orbital (*green*) (**d**, **e**)

(Fig. 10a, b) and **39** (Fig. 10d) of 14-OH and 14-H-morphinan with their Newman projection formulas (Fig. 10c, e). The figure includes a postulated reaction mechanism for bond cleavage. In Fig. 10a, the carbamate moiety of intermediate **38** would be fixed by the rigid ring structure. Therefore, the σ-bond between the 17-nitrogen and the CPM group in **38** would be fixed nearly orthogonal to the π-orbital of the carbonyl group in the oxazolidinone ring; thus, it may not be conjugated with the carbonyl group of the oxazolidinone ring and, consequently, may not be activated by the carbonyl group. In contrast, the C16–N17 bond of **38** would be parallel to the π-orbital of the carbonyl group in the oxazolidinone ring (Fig. 10b). Thus, the σ-orbital of the C16–N17 bond could be effectively conjugated with the carbonyl π-orbital, which would accelerate the cleavage of the C16–N17 bond in the reaction with a chloride ion. As a result, the C16–N17 bond would be stereoelectronically preferred for cleavage compared with the bond between the 17-nitrogen and the CPM group. The Newman projection formula of intermediate **38** (Fig. 10c) indicates the definitive difference between the position of the carbonyl π-orbital relative to the CPM–N17 bond and the C16–N17 bond. On the other hand, in intermediate **39** of 14-H-morphinan, the CPM group would be preferentially cleaved, because the N–C bond of the carbamate moiety could rotate freely and the σ-bond between the 17-nitrogen and the CPM group could be activated (Fig. 10d, e).
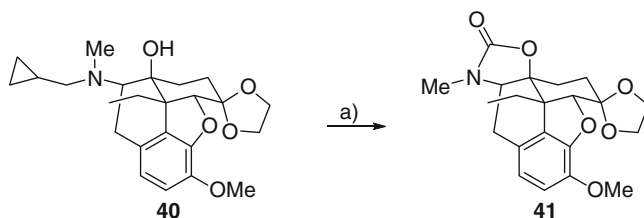
Scheme 16 Reaction of 16,17-*seco*-naltrexone derivative **40** with Troc-Cl. Reagents and conditions: (a) Troc-Cl (10 equiv.), K$_2$CO$_3$, TCE, reflux, 65%

Fig. 11 Structure of
oxazolizinium
intermediate **42**
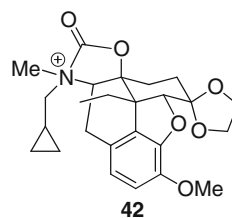
The reaction of acyclic amine **40** with Troc-Cl afforded the oxazolidinone derivative **41** without a CPM group in 65% yield (Scheme 16). In this case, the Me group is less hindered than the CPM group; therefore, Me group was predicted to be preferred for attack in a bimolecular nucleophilic substitution reaction. Nevertheless, the CPM group was preferentially removed over the Me group to give oxazolidinone **41**. The conformation of reaction intermediate **42** (Fig. 11), was more flexible than that of **38**; thus, both the N17–Me and N17–CPM bonds could be oriented parallel to the carbonyl π-orbital for activation. Therefore, the stereoelectronic effect could not explain the preferential cleavage of the CPM group. Alternatively, it may be explained by postulating the extreme stability of the cyclopropylcarbinyl cation [39–42]. Generally speaking, CPM tosylate can be solvolyzed 10^6 times faster than isobutyl tosylate because the tosylate ion could be solvolitically eliminated from the CPM tosylate to afford a stable cyclopropylcarbinyl cation [41]. The polarization of the CPM–N17 bond, probably due to the stability of the tentatively formed cyclopropylcarbinyl cation, may give the carbon of the CPM group a partial positive charge [43, 44] and, as a result, a nucleophile could easily attack on the carbon of the CPM group.

5 A Double Decarboxylation Reaction of an Oxazolidinone and a Carboxylic Acid: Its Application to the Synthesis of a New Opioid Lead Compound [45]

In the above section, we described the C16–N17 bond cleavage reaction of naltrexone derivative **35** that gave oxazolidinone derivative **36** without a D-ring (Scheme 15). This cleavage reaction prompted us to reinvestigate the Beckett-Casy

opioid receptor – ligand binding model [46–48], using 4,5-epoxymorphinan deri-
vatives cleaved in their D-rings [49]. In the course of the investigation, we found a
novel double decarboxylation reaction. One of the resulting derivatives showed
stronger affinity for the μ receptor than morphine, the classical and clinically
applied μ agonist. In this section, we describe a novel double decarboxylation
reaction and its application to the synthesis of opioid derivatives with a novel
skeleton.

Naltrexone acetal **35** was treated with ACE-Cl in the presence of K_2CO_3 in TCE
to give oxazolidinone chloride **36** (Scheme 15) [26], followed by treatment with
NaI to afford iodide **43** in 94% yield (Scheme 17). Ozonolysis of compound **44**,
prepared from iodide **43** by an elimination reaction, gave aldehyde **45**. The result-
ing aldehyde **45** was oxidized with $NaClO_2$ (Pinnick oxidation) [50] to afford
carboxylic acid **46**. Surprisingly, when carboxylic acid **46** was treated with
K_2CO_3 in DMF, two carbon dioxide units (a carboxyl group and an oxazolidinone
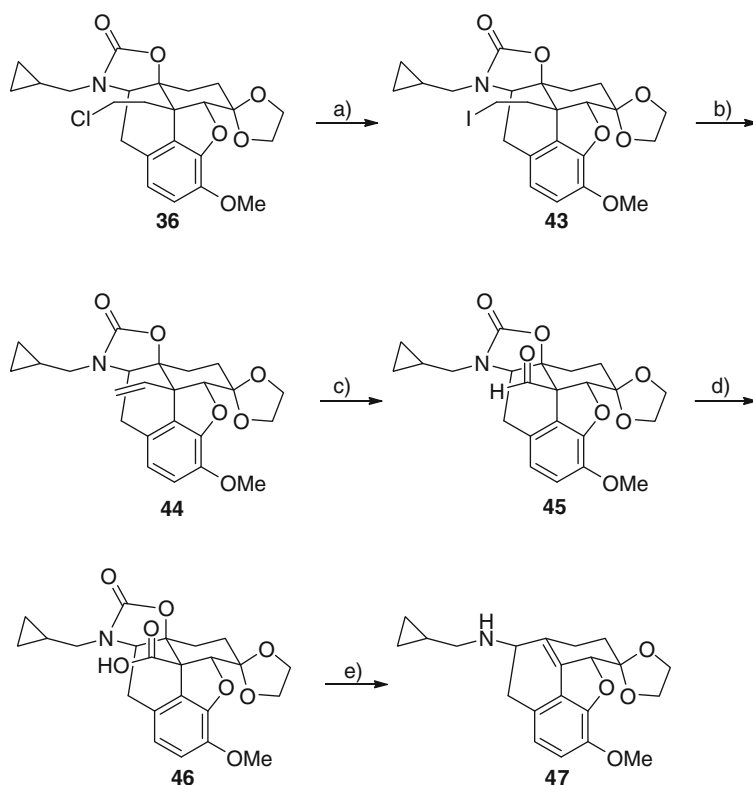
Scheme 17 Elimination of the C15, C16 moiety of oxazolidinone chloride **36**. Reagents and
conditions: (a) NaI, DMF, 130 °C, 94%; (b) *t*-BuOK, THF, 0 °C, 99%; (c) O₃, then Me₂S, CH₂Cl₂,
−78 °C, 86%; (d) NaClO₂, NaH₂PO₄, 2-methyl-2-butene, *t*-BuOH/H₂O, rt, 84%; (e) K₂CO₃,
DMF, 60 °C, 93%
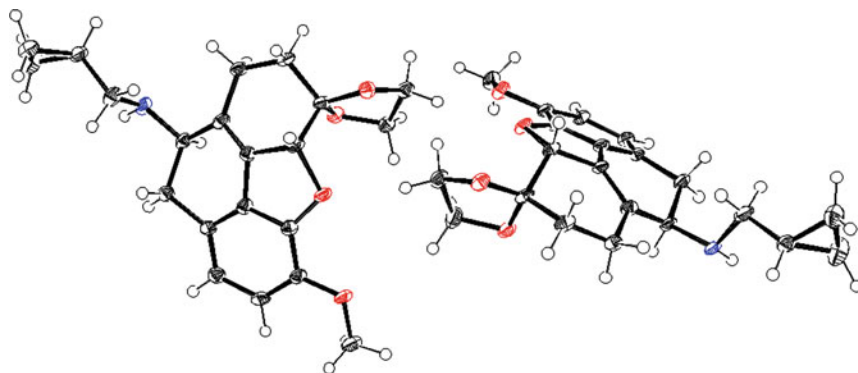
Fig. 12 ORTEP plot of **47**

unit) were simultaneously eliminated to give olefin **47** in 93% yield. The structure of compound **47** was determined by X-ray crystallography (Fig. 12).

The double decarboxylation of **46** was assumed to proceed *via* a four-membered ring intermediate **C** (β-lactone; Scheme 18)[2] [51–58]. However, the treatment of compound **48**, which lacks a carboxyl group, with K_2CO_3 in MeOH and water also produced the same decarboxylated compound **47** in 87% yield (Scheme 19), while the same treatment in DMF furnished the recovery of compound **48**. This result may suggest an E2 or E1cB elimination mechanism[3] rather than a mechanism that proceeds *via* a β-lactone. The E2 elimination usually proceeds *via* an antiperiplanar transition state. However, the C–O bond of the oxazolidinone ring lies in synclinal conformations with the carboxyl group in **46** and the hydrogen in **48**. This suggested that the elimination reaction would not be likely to occur *via* an E2 fashion (some examples of *syn* eliminations have been described for molecules in which β-hydrogen and a leaving group could not achieve an antiperiplanar conformation; [62])[4]. Therefore, the double decarboxylation reaction was more likely to proceed *via* the E1cB mechanism. In that scenario, a carbanion **D** (Fig. 13), arising from the first decarboxylation of compound **46** or the deprotonation in compound **48** by K_2CO_3, might be stabilized by the phenyl ring and/or the carbonyl group in the oxazolidinone ring (Fig. 13).

The decarboxylation of oxazolidinones **46** and **48** is seemingly similar to removal of the well-known amino protective group, the Fmoc group. Fmoc

---

[2]The thermal decarboxylation of a β-lactone has been widely used for preparation of an olefin. See [51, 52]. Recent examples of the thermal decarboxylation of β-lactones are described in [53–57].

[3]Olefins have been prepared by elimination reactions, in which oxazolidinone functioned as a leaving group. See [59–61].

[4]In cyclic systems, the extent of *anti* and *syn* elimination depends on ring size. Cyclohexyl systems have a very strong preference for *anti* elimination. See [62, 63].
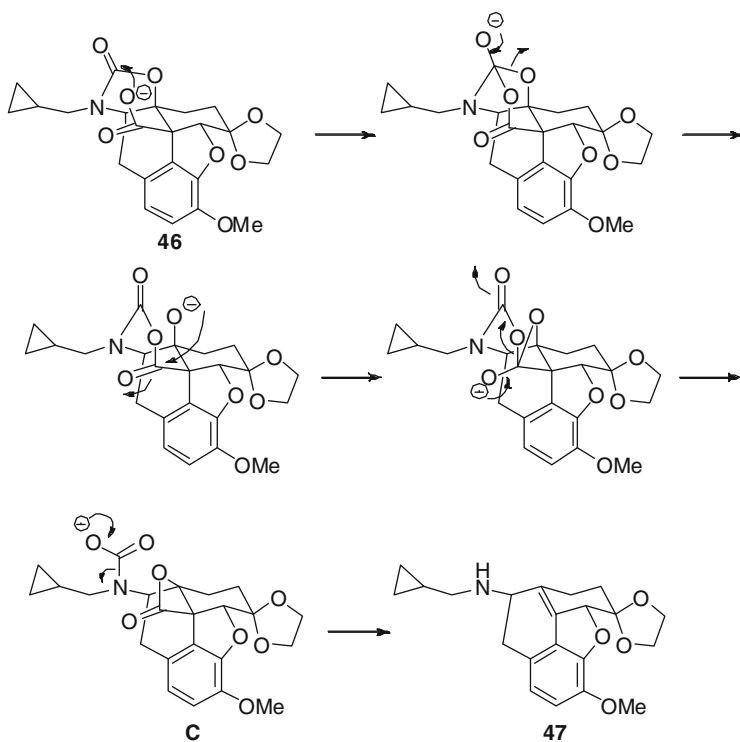
Scheme 18 Proposed decarboxylation mechanism of **46** *via* the four-membered ring intermediate **C** (β-lactone)
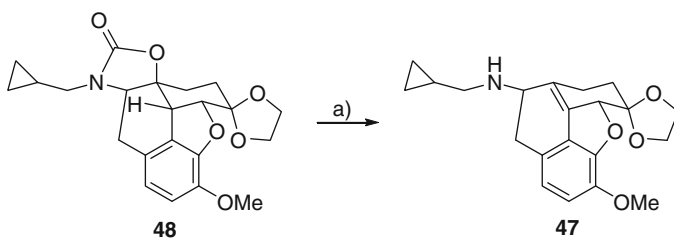
Scheme 19 Decarboxylation of oxazolidinone **48**. Reagents and conditions: (a) K$_2$CO$_3$, MeOH/H$_2$O, 80 °C, 87%
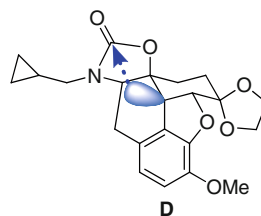
Fig. 13 The carbonyl group in the oxazolidinone ring may stabilize carbanion **D**
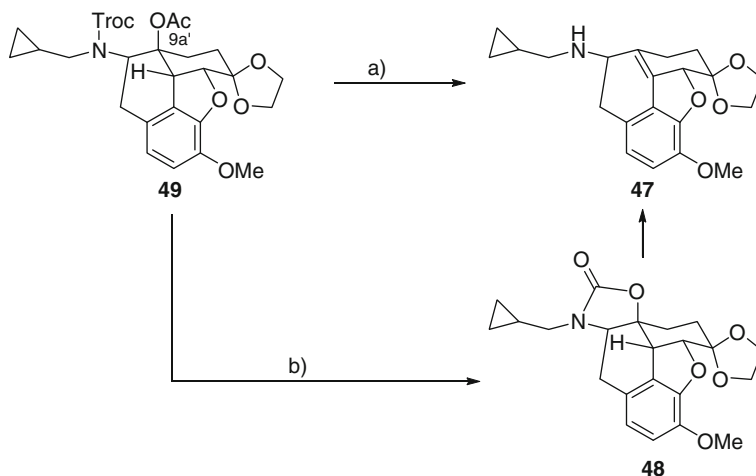
Scheme 20 Elimination reaction of compound **49**. Reagents and conditions: (a) K$_2$CO$_3$, MeOH/H$_2$O, 80 °C, 80%; (b) K$_2$CO$_3$, MeOH/H$_2$O, rt, 94%

deprotection occurs through cleavage by a weak base, like an amine, *via* elimination and simultaneous decarboxylation [64].

Compound **47** was also obtained in 80% yield when 9a′-acetyl-*N*-Troc derivative **49** was treated with K$_2$CO$_3$ in MeOH and water at 80 °C (Scheme 20). It was proposed that compound **47** was produced by decarboxylation of **48** (Scheme 21, path A), because the treatment of compound **49** with K$_2$CO$_3$ at room temperature gave oxazolidinone **48** (Scheme 20); then **48** could be converted into compound **47** by the same treatment at 80 °C (Scheme 19). An alternative route for the production of **47** could be *via* the sequential hydrolysis of carbamate and elimination of acetate (Scheme 21, path B). However, path B can be ruled out by the following results. First, hydrolysis of the carbamate required harsher reaction conditions and longer reaction time [26]. Second, when 9a′-acetate **50** was hydrolyzed under basic conditions, only compound **52** was obtained (Scheme 22). Finally, treatment of compound **49** with Zn in AcOH afforded acetamide **54** by migration of the acetyl group (Scheme 23), but acetamide **54** was not converted into olefin **47** with basic treatment. Taken together, these results strongly suggest that compound **47** could be obtained *via* oxazolidinone **48** (path A), but not by path B (Scheme 21). Thus, the oxazolidinone structure may play an important role in the second decarboxylation reaction. Moreover, treatment of acyclic carbamate **51** with K$_2$CO$_3$ produced only compound **52** by hydrolysis (Scheme 22). This result supported the importance of the cyclic carbamate, oxazolidinone structure, in the second decarboxylation reaction.

Compound **47** has a novel structure that lacks the D-ring in the 4,5-epoxymorphinan skeleton. Therefore, we next evaluated the affinity of 15-16 nornaltrexone derivative **57**, derived from **47**, for the opioid receptor. Compound **57** was prepared from **47** as shown in Scheme 24. The secondary amino group in olefin **47** was
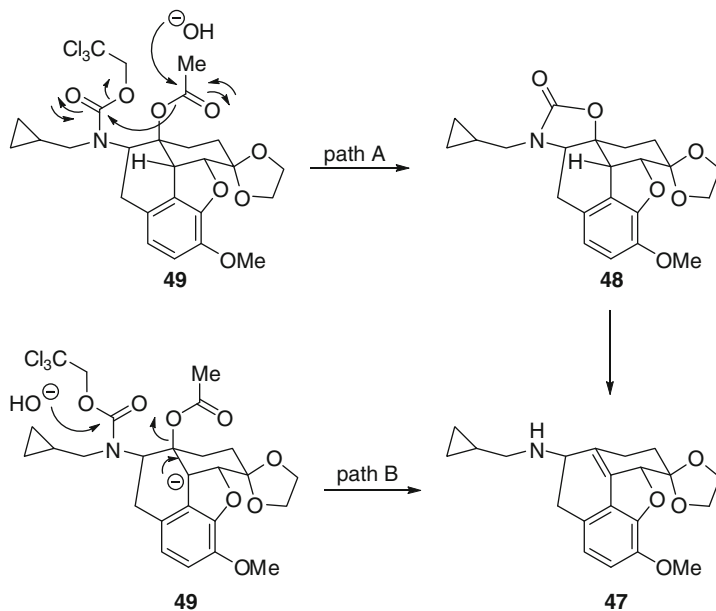
Scheme 21 Proposed decarboxylation mechanisms of **49** *via* oxazolidinone **48** (path A) or *via* sequential hydrolysis of carbamate and elimination of acetate (path B)
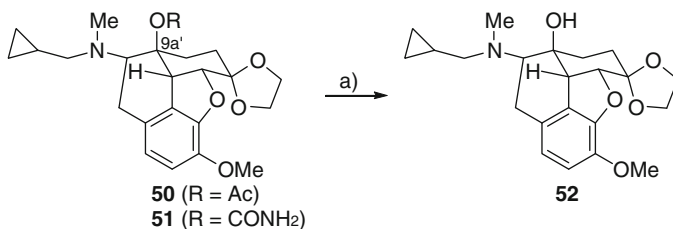
Scheme 22 Hydrolysis of 9a′-acetate **50** and 9a′-carbamate **51**. Reagents and conditions: (a) K$_2$CO$_3$, MeOH/H$_2$O, 80 °C, quant. from **50**, 69% from **51**

protected with a Cbz group followed by oxidation with *m*CPBA and subsequent hydrogenation of **55** to provide compound **56**. The stereochemistries of compounds **55** and **56** were determined by 2D NMR analyses of their analogs. Compound **56** was converted into compound **52** by reductive alkylation, followed by acidic deprotection of the acetal and subsequent demethylation with BBr$_3$ to produce the objective compound **57**. In the competitive binding assay, compound **57** showed stronger binding affinity ($K_i = 1.17$ nM) for the μ receptor than morphine ($K_i = 1.98$ nM). This indicated that compound **57** could be a new lead for designing receptor type-selective opioid ligands.
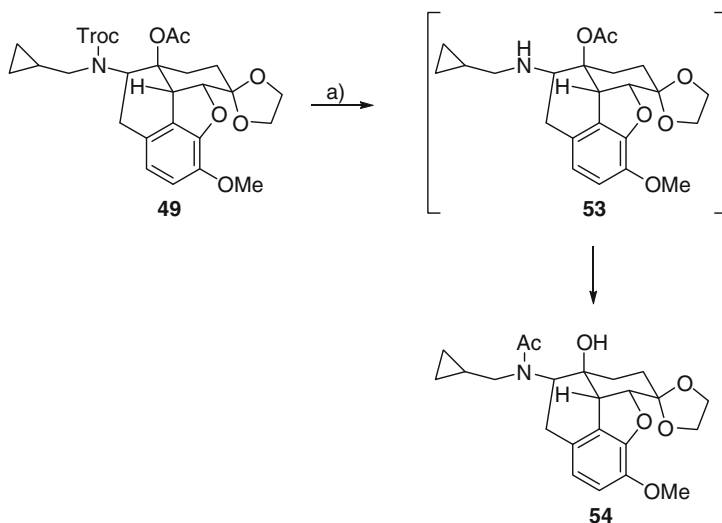
Scheme 23 Removal of the Troc protective group and migration of the acetyl group. Reagents and conditions: (a) Zn, AcOH, rt, 80%
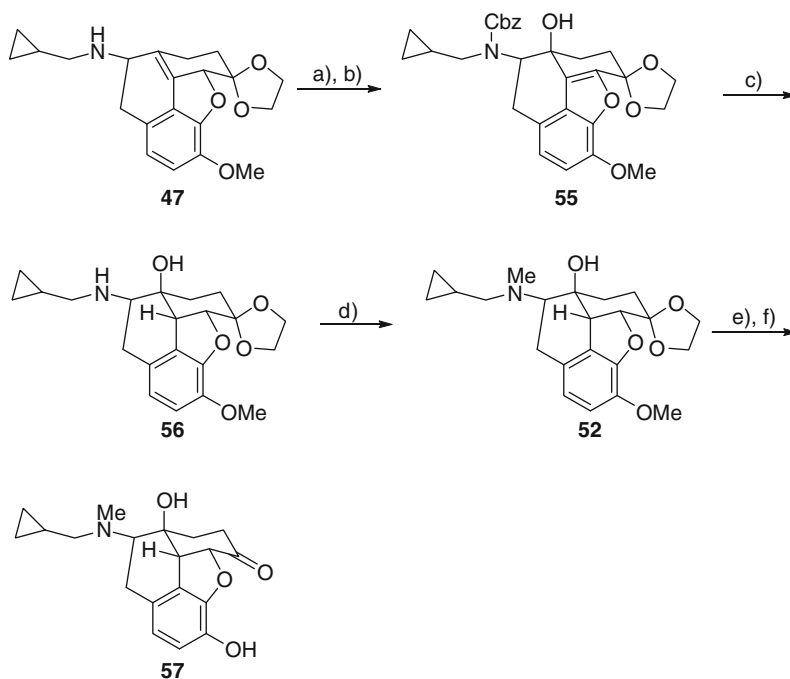
Scheme 24 Synthesis of 15–16 nornaltrexone derivative **57**. Reagents and conditions: (a) Cbz-Cl, proton-sponge, CH$_2$Cl$_2$, rt; (b) mCPBA, CH$_2$Cl$_2$, 0 °C, 68% from **47**; (c) H$_2$, 10% Pd/C, MeOH, rt, 69%; (d) (CH$_2$O)$_n$, NaBH$_3$CN, AcOH, rt, 88%; (e) 2 M HCl, MeOH, reflux, quant.; (f) BBr$_3$, CH$_2$Cl$_2$, rt, 19%

6   Synthesis of a Stable Iminium Salt and Propellane Derivatives [43]

The 4,5-epoxymorphinan skeleton is believed to influence the intrinsic activity of the opioid receptor [10, 11, 65], and it is thought to contribute to three points of association between the drug molecule and the receptor site. These include an ionic interaction with the 17-nitrogen, a $\pi-\pi$ interaction with the phenol ring, and a hydrogen bond between the phenol hydroxy and the opioid receptor [46, 47]. However, the role of the 14-OH group in receptor binding has not been clarified. We attempted to remove the 14-OH group in order to compare the pharmacological profiles of 14-OH derivatives and 14-H variants. In the course of these investigations, we obtained iminium salt **59**, which has a propellane skeleton. Surprisingly, the iminium salt **59** was stable and could be purified by silica gel column chromatography. In this section, we describe the synthesis of this stable iminium ion bearing a propellane skeleton.

Morphinan derivative **58a**, which was synthesized from naltrexone (**1**) [25, 66, 67], was dehydrated with $SOCl_2$ in pyridine to afford the dehydrated product **60** and an abnormal rearrangement product **59** (iminium salt) (Scheme 25). The reaction mixture was separated by silica gel column chromatography with a $CHCl_3$/MeOH eluent to isolate pure iminium ion **59** in 28% yield, together with the dehydrated product **60** in 71% yield. In ^{1}H NMR analysis, a vinyl proton of iminium chloride **59** was observed at 10.13 ppm; this suggested that **59** was an iminium compound, not an α-chloroamine. In contrast, when 4,5-epoxymorphinan **35** was subjected to the same reaction conditions, only the dehydrated product **61** was obtained (Scheme 25) [22]. We became interested in the abnormal stability of the iminium salt and attempted to improve its yield. A plausible mechanism for the rearrangement reaction that produced the iminium chloride **59** is shown in Scheme 26.

The lone electron pair of the 17-nitrogen might play a crucial role in facilitating the rearrangement necessary for obtaining **59**. We hypothesized that a proton acquired during this reaction could protonate the 17-nitrogen, and interrupt the rearrangement reaction. Conversely, we postulated that reaction conditions in the absence of protons would facilitate the rearrangement and promote the production of the iminium salt **59**. After extensive investigation of our working hypothesis, the reaction of morphinan **58a** with MsCl and NaH provided the objective iminium **63a** in 93% yield without the dehydrated product **60** (Table 1, entry 1).

The rearrangement reactions of morphinans **58a–e** with various 17-substituents produced moderate to excellent yields, except in the case of morphinan **58f**. The morphinan **58f** had a strong electron-withdrawing CF_3CH_2 group [68] at the 17-position, and we only recovered the starting material **58f** (entry 6). These results suggested that the 14-OH group may not be directly mesylated. Instead, the results shown in Table 1 could be reasonably explained by hypothesizing that the lone electron pair on the 17-nitrogen initially attacked the sulfene prepared *in situ*, and this was followed by migration of the Ms group from the 17-nitrogen to the 14-OH
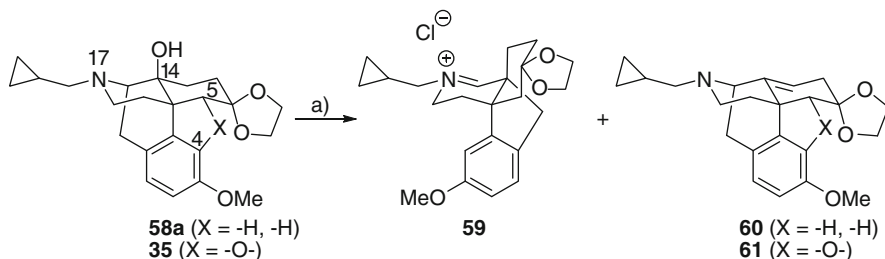
Scheme 25 Dehydration of morphinan **58a** and 4,5-epoxymorphinan **35**. Reagents and conditions: (a) SOCl$_2$, py
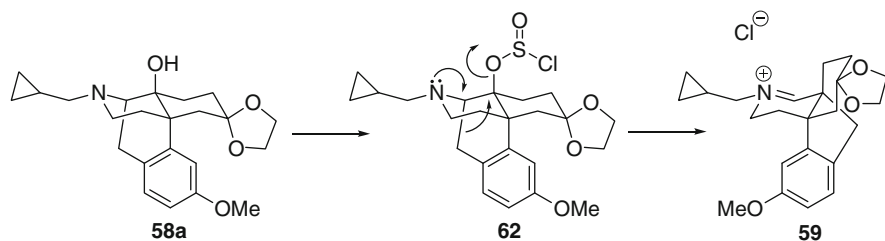
Scheme 26 A plausible mechanism for the rearrangement of morphinan derivative **58a** to produce the iminium salt **59**

Table 1 Substituent effect on rearrangement reaction[a]
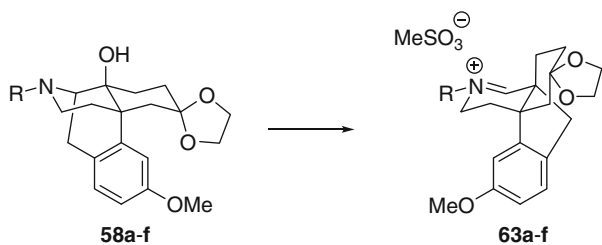
Entry	Morphinan	Product	R	Yield (%)	Reaction time (h)
1	**58a**	**63a**	CPM	93	1
2	**58b**	**63b**	i-Bu	39	2
3	**58c**	**63c**	Me	95[b]	1.25
4	**58d**	**63d**	Et	93	1.25
5	**58e**	**63e**	Allyl	92	3.5
6	**58f**	**63f**	CF$_3$CH$_2$	0[c]	31.5

[a]Morphinan **58** was treated with NaH and MsCl in THF
[b]Including some amounts of inseparable impurities
[c]Only the morphinan **58f** was recovered
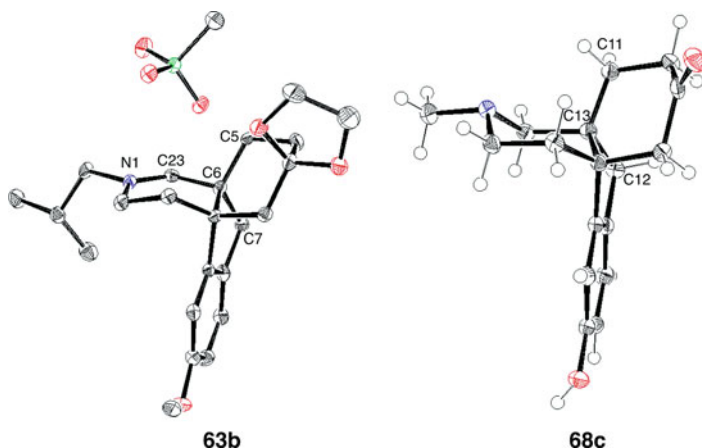
Fig. 14 ORTEP plots of **63b** and **68c**

group.[5] The strong electron-withdrawing CF_3CH_2 group [68] would drastically reduce the electron density on the 17-nitrogen and decrease its nucleophilicity, which would result in recovery of the starting material **58f**. All the synthesized iminium **63** were purified by silica gel column chromatography. In ^{1}H NMR analyses, a vinyl proton was observed at approximately 9.5 ppm for each iminium mesylate **63**. Finally, compound **63b** with a 17-*i*-Bu group was isolated as a crystalline product and its structure was determined by X-ray crystallography (Fig. 14).

To the best of our knowledge, X-ray crystallographic analyses of iminium ions are very rare,[6] except in the case of conjugated iminium ions.[7] An example that most resembled iminiums **59** and **63** was the $Fe(CO)_3$ complex of iminium tetra-fluoroborate **64** (Fig. 15) [70, 83, 84]. In the case of iminium **64**, anchimeric participation of the double bond derived from a homoallylic system and an inert counter anion, tetrafluoroborate, could stabilize the iminium ion. Moreover, the bulky $Fe(CO)_3$ group may contribute to the stability of iminium ion **64**. The other examples of nonconjugated iminium ions **65**–**67** (Fig. 15), whose structures were determined by X-ray crystallography, also had inert counter anions [69–71] and would be stabilized by an intramolecular interaction with an olefin moiety (iminium **65**) [71] or by an intermolecular interaction with the phenyl groups of a counter anion (iminium **66**). In contrast, iminium compounds **59** and **63** had neither an olefin moiety nor a $Fe(CO)_3$ group to participate in the stabilization of the iminium ion. Furthermore, iminium ion **59** had a reactive counter anion, the chloride ion.

---

[5]The reaction of **58a** with the CPM group seemed to proceed most rapidly. This observation might be explained by considering the very stable cyclopropylcabinyl cation (see Sect. 4 and [39–42]).

[6]For X-ray crystallography of nonconjugated iminium salts, see [69–71].

[7]For X-ray crystallography of conjugated iminium salts, see [72–82].

Fig. 15 Iminium ions whose structures were determined by X-ray crystallography

$[Me_2C=NHMe]^+BPh_4^-$ (**66a**)

$[Me_2C=NMe_2]^+BPh_4^-$ (**66b**)

$[Me_2C=NHEt]^+BPh_4^-$ (**66c**)

$[MeEtC=NHMe]^+BPh_4^-$ (**66d**)

$[Me_2C=NMe_2]^+ClO_4^-$ (**67**)
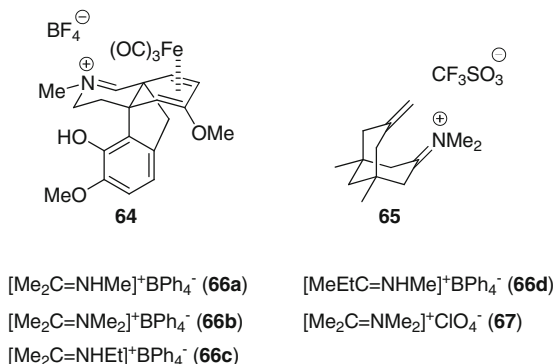
Fig. 16 Structures of compounds **63b** and **68c**
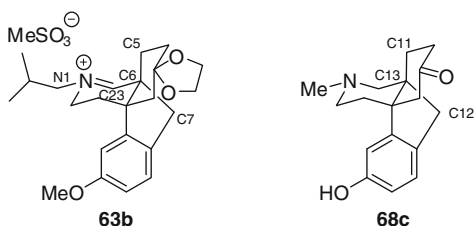
The X-ray crystallography indicated that the length of C5–C6 (1.545 Å) in iminium **63b**, which was parallel to the π-orbital of the N1–C23 double bond, was longer than that of the corresponding bond C11–C13 in the saturated compound **68c** (1.532 Å), derived from iminium **63c** (Fig. 16). Parallel bonds can easily overlap each other. This observation suggested that the σ bond C5–C6 would interact with the π* bond of the iminium and that the electronic interaction (hyperconjugation) may play a crucial role in stabilizing the iminium ion. To investigate hyperconjugative stabilization of the iminium, we performed natural bond orbital (NBO) analysis [85] with the ab initio molecular orbital calculation at the HF/6-31G* level. This analysis used the second order perturbation theory of the Fock operator with the NBO basis. It indicated that there was substantial interaction from σ (C5–C6) to π* (N1–C23) (interaction energy: 6.31 kcal/mol). The optimal bond length of C5–C6 was 0.011 Å longer than that of the corresponding bond in **68c**.[8] Taken together, the stereoelectronic effects (hyperconjugation) attributed to the structures of iminiums **59** and **63b** could play an important role in the extreme stabilization of these iminium ions.

---

[8]The NBO analysis showed that the optimal bond length of C6–C7 was also 0.007 Å longer than that of the corresponding bond in **68c**, with an interaction energy between σ (C6–C7) and π* (N1–C23) of 4.98 kcal/mol. However, in X-ray crystallography, the C6–C7 in **63b** showed the same bond length (1.551 Å) as the C13–C12 in **68c**. This result suggested that the C5–C6 might also partially participate in the stabilization of the iminium ion.
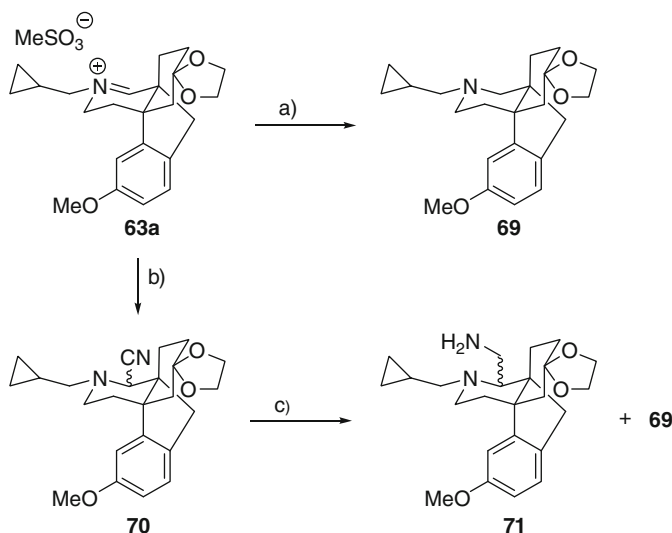
Scheme 27 Reaction of iminium **63a**. Reagents and conditions: (a) NaBH$_4$, MeOH, 0 °C, 81%; (b) NaCN, H$_2$O, rt; (c) LiAlH$_4$, THF, 0 °C, **71**: 26% from **63a**, **69**: 74% from **63a**

Fig. 17 Structure of iminium **63a**. The hyperconjugation is shown with *dotted lines*
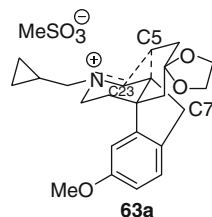
We next examined the reactivity of the stable iminium ion **63a** (Scheme 27). When the iminium **63a** was treated with NaOAc or NaN$_3$, only the starting material was recovered. The reaction of **63a** with *n*-BuLi or lithiated dithiane gave complex mixtures. The stronger basic nucleophiles, like *n*-BuLi and lithiated dithiane, may attack both the iminium carbon (C23) and the hyperconjugated carbons (C5) to give complex mixtures (Fig. 17). However, the reduction of iminium **63a** with NaBH$_4$[9] afforded the saturated propellane derivative **69**. The reaction of iminium **63a** with NaCN[10] provided nitrile **70**; then reduction of the nitrile **70** produced amine **71** in a

---

[9]In the case of the Fe(CO)$_3$ complex **64**, the reduction was reported to take 20 min (see [84]). On the other hand, the reduction of **63a** was completed within 5 min.

[10]The reaction of the Fe(CO)$_3$ complex **64** with NaCN was reported to proceed in acetone under reflux for 5 min (see [83]). In contrast, the reaction of **63a** was completed at room temperature within 5 min.

Fig. 18 Structures of propellane derivatives **68c** and **68a** and their K_i values for the μ and κ opioid receptors

68c

K_i (μ) = 3.6 nM

68a

K_i (κ) = 17.4 nM
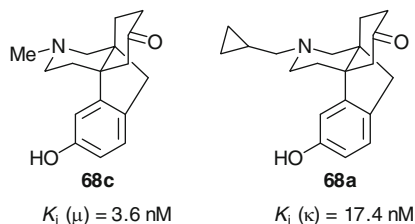
mixture of diastereomers along with compound **69**. Compound **69** may be obtained by reduction of the iminium derived from nitrile **70** *via* elimination of the cyanide ion. These observations suggested that the adduct **70** could be easily returned to the starting iminium ion **63a** due to its extreme stability.

In a preliminary pharmacological evaluation, saturated propellane **68c** and its 17-CPM derivative **68a**, which were synthesized from propellane **69**, selectively bound to the μ (K_i = 3.6 nM) and κ opioid receptors (K_i = 17.4 nM), respectively (Fig. 18). These results suggested that propellane **68c**, which was readily prepared from stable iminium ion **63c**, might be a fundamental skeleton for novel opioid ligands. Birch *et al*. described synthesis of a propellane derivative from a $Fe(CO)_3$ complex of the iminium ion **64** and its application as an opioid ligand. Nevertheless, they did not show the yield of iminium ion **64** with $Fe(CO)_3$ or demonstrate the propellane derivative as an opioid ligand [83, 84]. Furthermore, their synthesis of the propellane derivative required flammable, toxic $Fe(CO)_5$ as a crucial reagent and thebaine (narcotic) as a starting material, which is not readily available. In distinct contrast, our practical synthesis of a propellane derivative started with the readily available naltrexone and required no toxic reagents.

Recently, researchers in China also published a description of propellane derivatives; however, their pharmacological data were limited to the indole derivatives [86].

7 Novel Synthesis of a 1,3,5-Trioxazatriquinan Skeleton Using a Nitrogen Clamp [87]

As mentioned above, the twin drug **72** (Fig. 19) was also prepared from naltrexone (**1**) and showed ε receptor antagonist activity [88]. In the course of the synthetic investigation of **72**, we unexpectedly obtained a triplet drug **73** with a 1,3,5-trioxazatriquinane skeleton (red color in Fig. 19).

In this molecule, nitrogen plays an important role in the formation of the novel skeleton. Nitrogen is a trivalent atom that gathers the three molecular units through their keto moieties and fixes them in a precise rigid trimer. Thus, nitrogen acts like a three-pronged clamp, and we have termed this phenomenon a "*nitrogen clamp*". The *nitrogen clamp* may be expected to apply to the general synthesis of triplet
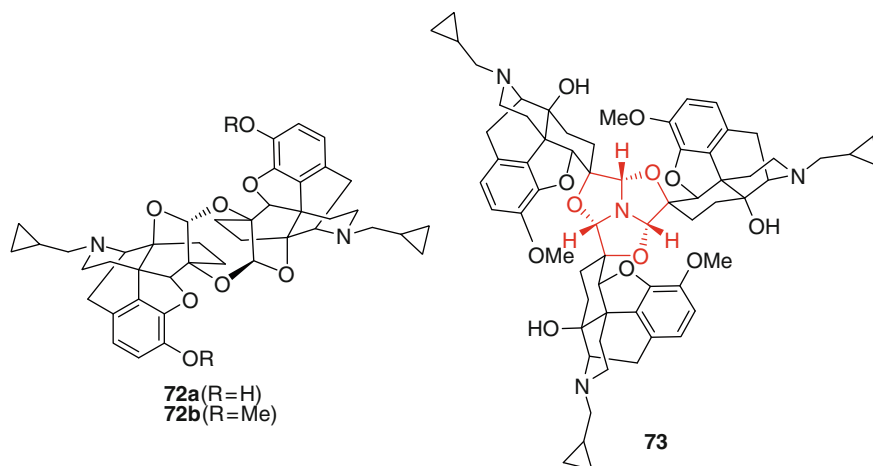
Fig. 19 Structures of the twin drugs **72** and the triplet drug **73**
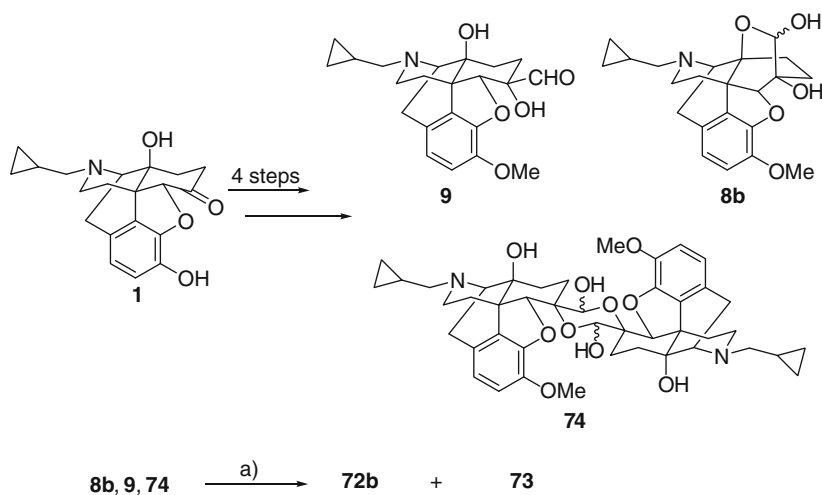
Scheme 28 Syntheses of acetal dimer **72b** and trimer **73**. Reagents and conditions: (a) CSA, toluene, reflux

drugs from various ketones that would show unique pharmacological effects. In this section, we describe a novel synthetic method for synthesizing triplet drugs with a rigid 1,3,5-trioxazatriquinane skeleton and a *nitrogen clamp*.

We recently reported that the acetal dimer **72b**, a precursor of the twin drug **72a**, was obtained from a mixture of α-hydroxyaldehyde **9**, hemiacetal **8b**, and the hemiacetal dimer **74**, derived from naltrexone (**1**) in four steps [88]. Examination of the synthesized products revealed that a novel trimer **73** with the 1,3,5-trioxaza-triquinane skeleton was produced in 10% yield, concomitantly with acetal dimer **72b** in 13% yield (Scheme 28). Initially, the nitrogen source was not clear but, after

a precise analysis, we determined that the nitrogen was derived from the solvent (saturated ammonia–CHCl$_3$) that was used in the silica gel column chromatography for separation of the objective dimer **72b**. The structure of trimer **73** was determined by X-ray crystallography (Fig. 20). We were interested in the novel structure of **73**; therefore, we attempted to improve the yield of **73** and clarify the reaction mechanism. When the mixture of compounds **8b**, **9**, and **74** was treated with NH$_4$Cl and AcONa in MeOH under reflux, the oxazoline dimer **75a** (46%) and its isomer **75b** (9%) were obtained (Scheme 29). Moreover, acetal **11**, a precursor of compounds
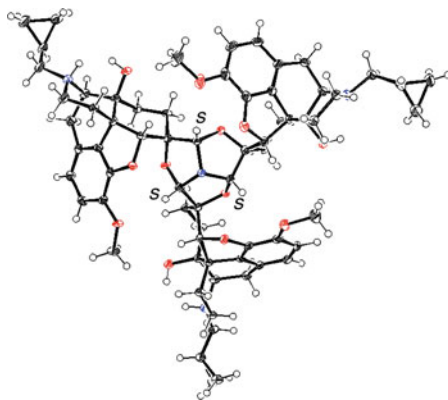
Fig. 20 X-ray crystallography of trimer **73**
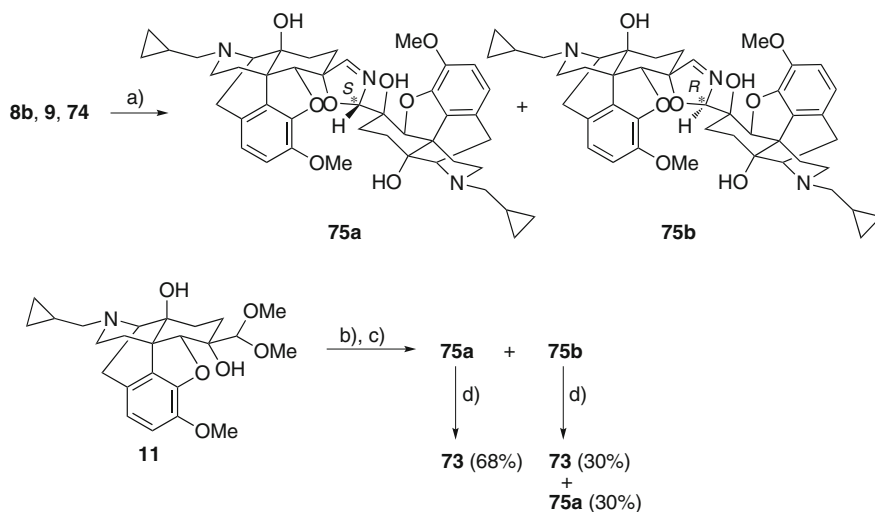
Scheme 29 Synthesis of the trimer **73** *via* the dimers **75**. Reagents and conditions: (a) NH$_4$Cl, AcONa, MeOH, reflux, **75a**: 46%, **75b**: 9%; (b) 2 M HCl, reflux, (c) NH$_4$Cl, AcONa, MeOH, reflux, **75a**: 45%, **75b**: 43%; (d) CSA, CHCl$_3$, reflux
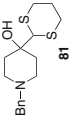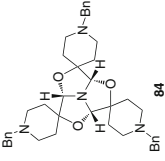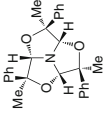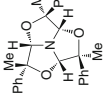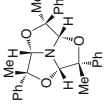
8b, **9**, and **74**, was hydrolyzed with 2 M HCl under reflux, and the resulting mixture (without purification) was also treated with NH$_4$Cl and AcONa in MeOH under reflux. This produced a mixture of oxazoline **75a** (45%) and isomer **75b** (43%) (Scheme 29). The dimer **75b** was treated with CSA in CHCl$_3$ under reflux to give a mixture of dimer **75a** (30%) and the trimer **73** (30%). On the other hand, the dimer **75a** could be converted to the trimer **73** in 68% yield under the same conditions (Scheme 29). These observations supported the notion that the dimer **75a** was the stable isomer and **75b** was unstable one, but could be converted to the trimer **73** *via* its stable isomer **75a**. Interestingly, X-ray analysis showed that the absolute configuration of the three newly formed asymmetric centers of the 1,3,5-trioxazatriquinane moiety in trimer **73** were all in *S* configurations (Fig. 20). The selective formation of the asymmetric centers may be attributed to asymmetric induction by the natural naltrexone skeleton. We also assigned the configurations of the * positions in dimers **75a** and **75b** as *S* and *R* (Scheme 29), respectively, based on 2D NMR spectroscopy. Eventually, the *R* configuration isomer **75b** would be the kinetically controlled product and the *S* isomer **75a** would be the thermodynamically controlled product. Based on the above considerations, a series of reactions was performed without purification to convert acetal **11** into trimer **73** in 79% yield. Oxycodone (**76**) also provided trimer **77b** in 6% total yield (Scheme 30).

Next, we examined the application of this reaction to model compounds to investigate the generality of the reaction (Table 2). *N*-Benzylpiperidone (**78**) was converted to trimer **84** in 18% total yield. Acetophenone (**79**) was converted to a mixture of trimers **85a**–**85c** in 35% total yield. Thioacetals **83a** and **83b**, obtained from 4-phenylcyclohexanone (**80**), were converted to trimers **86a** (35%) and **86b**
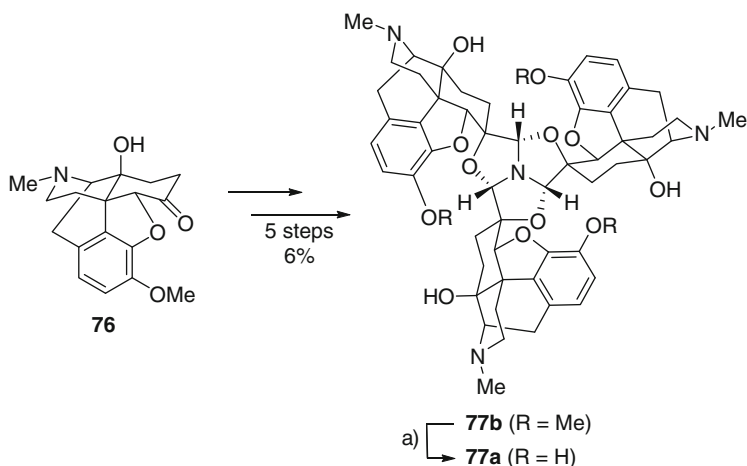
Scheme 30 Synthesis of the *N*-methyl trimer **77**. Reagents and conditions: (a) BBr$_3$, CH$_2$Cl$_2$, rt, 48%

Table 2 General synthesis of trimers

Run	Starting material	Intermediate	Product	Total yield (%)
1	N-Benzylpiperidone (**78**)	**81**	**84**	18
2	Acetophenone (**79**)	**82**	**85a** 11%, **85b** 14%, **85c** 10%	35

(*continued*)

Table 2 (continued)

Run	Starting material	Intermediate	Product	Total yield (%)
3	4-Phenylcyclohexanone (**80**)	**83a**, **83b**	**86a** 35%, **86b** 13%	48

(13%), respectively. We also attempted to apply this reaction to the synthesis of a nonsymmetric trimer (Scheme 31). The dimer **87**, prepared from 4-phenylcyclo-hexanone (**80**), was reacted with α-hydroxyaldehyde **93** (CSA/CHCl$_3$, reflux) to produce the nonsymmetrical trimer **88** in 91% yield. The dimer **87** was also reacted with the glycolaldehyde dimer (**94**) (CSA/CHCl$_3$, rt) to give the nonsymmetric trimer **89** in 98% yield. Furthermore, dimers **75a** and **75b**, obtained from a mixture of **8b**, **9**, and **74**, were reacted with **96** (derived from haloperidol), the glycolalde-hyde dimer (**94**), and α-hydroxyaldehyde **95** to produce the nonsymmetric trimers **90**, **91**, and **92** in yields of 23, 75, and 50%, respectively.

The symmetrical trimer **77a** (Scheme 30), obtained from oxycodone (**76**), showed potent analgesic action in the acetic acid writhing assay (ED$_{50}$ = 0.037 mg/kg). The antinociceptive effect was approximately 20 times more potent than that of morphine (ED$_{50}$ = 0.6 mg/kg). This strong analgesic potency may derive from the binding with oligomeric receptor sites [89, 90].

In conclusion, we have established the first general method for synthesizing a trimer with a 1,3,5-trioxazatriquinane skeleton fixed with a nitrogen clamp that can be applied to the synthesis of both symmetrical and nonsymmetrical trimers. Recent studies have reported that G-protein-coupled receptors (GPCRs) exist as dimers, but may be present as either homo- or hetero-dimers/oligomers. Although the existence of GPCR dimers/oligomers was predicted from early pharmacological and biochemical studies [89, 90], further evaluations of this phenomenon have been impeded by the lack of appropriate reagents [91]. Twin drugs that combined two structural components into a single molecule have been described in numerous domains of medicinal chemistry. Symmetrical twin drugs can bind simultaneously to symmetrical binding sites of a protein complex for increased activity. In contrast,
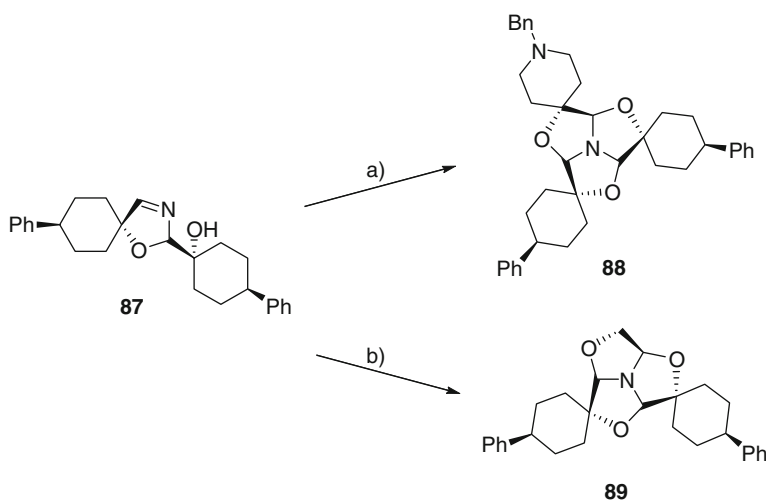
Scheme 31 Syntheses of nonsymmetric trimers **88–92**. Reagents and conditions: (a) **93**, CSA, CHCl$_3$, reflux, 91%; (b) **94**, CSA, CHCl$_3$, rt, 98%; (c) **96**, CSA, CHCl$_3$, reflux, 23% from mixture of **8b**, **9**, **74**; (d) **94**, CSA, CHCl$_3$, rt, 75% from mixture of **8b**, **9**, **74**; (e) **95**, CSA, CHCl$_3$, reflux, 50% from mixture of **8b**, **9**, **74**
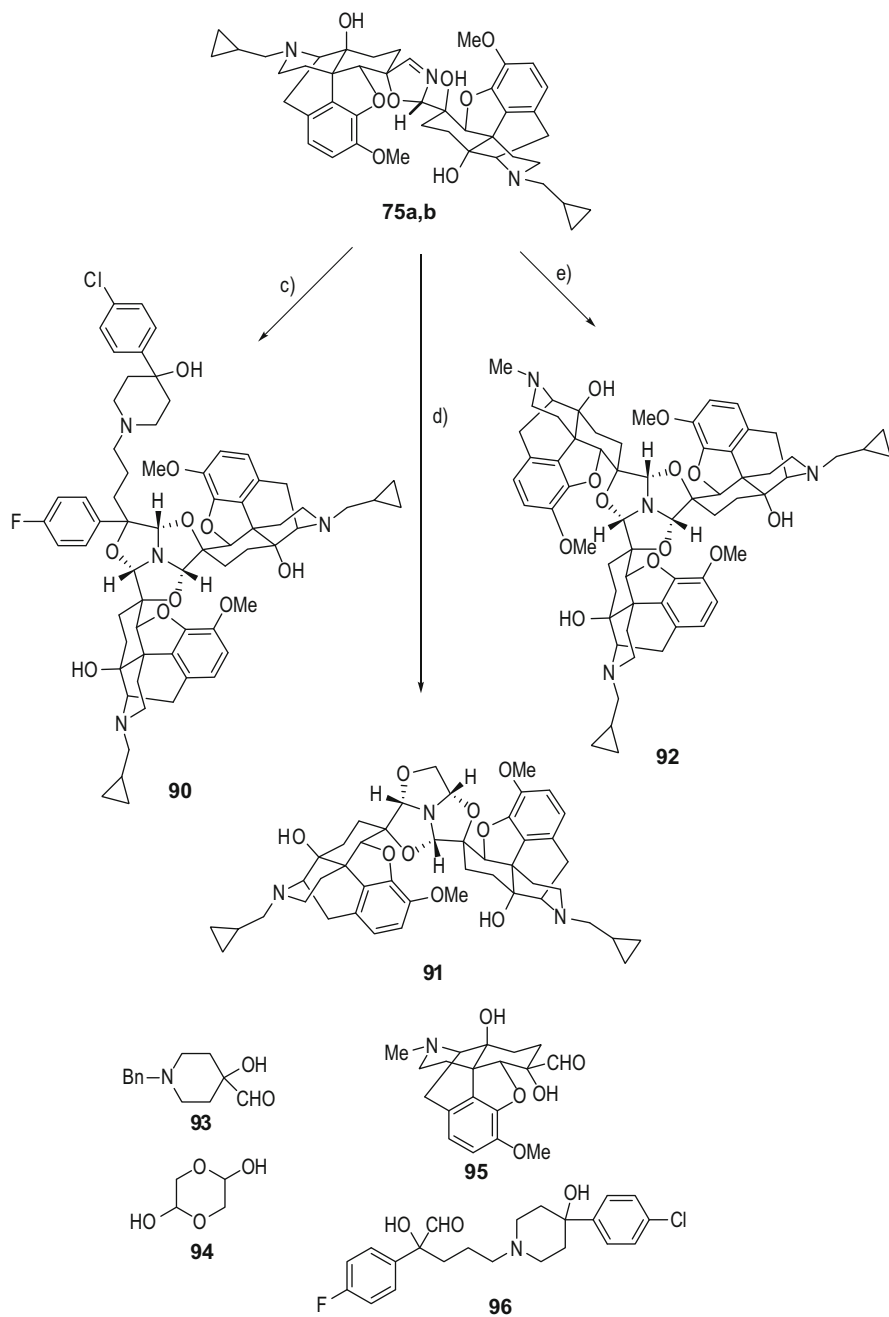
Scheme 31 (Continued)

nonsymmetrical twin drugs may bind to the individual relevant binding sites to provide dual actions. However, twin drugs can play only one role, either an increase in activity or dual actions. On the other hand, nonsymmetric triplet drugs with two identical moieties and one different moiety may exhibit both increased pharmacological activity and dual actions, because the two identical portions could bind identical receptor sites simultaneously, and the third portion could bind a different receptor site or enzyme. Moreover, a symmetrical triplet drug **77a** showed 20 times stronger analgesic activity than the monomeric compound morphine. This suggested that symmetrical triplet drugs could provide extremely potent activities. Therefore, the thus obtained trimers with a rigid 1,3,5-trioxazatriquinane skeleton fixed with a nitrogen clamp may be a very useful tool for investigation of oligomeric receptors and enzymes.

8 New Rearrangement Reaction for the Synthesis of a New Opioid Ligand with an Oxabicyclo[3.2.1]octane Skeleton [92]

In Sect. 7, we described a method for the synthesis of the rigid triplet drug **73** with a 1,3,5-trioxazatriquinane skeleton and three naltrexone units with 4,5-epoxy rings [87]. This synthetic method could be applied to three general ketones (*N*-benzylpiperidone (**78**), acetophenone (**79**), and 4-phenylcyclohexanone (**80**)) [87]. However, this method could not be applied to dimethyl acetal **98**, which was synthesized from morphinan derivative **28** [23, 93] in two steps. When **98** was subjected to the same reaction conditions as those applied to the naltrexone derivative (4,5-epoxymorphinan), the monomer **102** was obtained in 21% yield instead of the objective trimer **101** (Scheme 32). The structure of the monomer was identified as the novel oxabicyclo[3.2.1]octane derivative **102** by 2D NMR, MS, and IR spectroscopy (Fig. 21). We were interested in the novel compound **102** and examined the reaction mechanism (Scheme 33). We hypothesized that a dimer **100**, derived from α-hydroxyaldehyde **99**, would be more flexible than **75**, derived from naltrexone methyl ether (**22**). Thus, the 14-OH group may readily participate in the double bond of the oxazoline ring of **100** to produce the cyclic ether **103**. Moreover, the oxonium intermediate **104** may also be more flexible than a structure with a 4,5-epoxy ring; thus, the C6–C7′ σ-bond in **104** may be readily rearranged to the oxonium double bond to afford the rearrangement product **102**.

If our hypothesis was correct, the oxonium ion **99′**, derived from dimethyl acetal **98**, would rearrange more readily than oxazoline **100** to give **102**. The bond between the 6-carbon and 6′-oxonium carbon in **99′** can rotate freely around the axis; this would facilitate the approach of the 14-OH group and its overlap with the π orbital of the carbonyl carbon in **99′** to produce the cyclic acetal intermediate **105**. Then **105** could rearrange to **102** *via* the oxonium **106** (Scheme 34). Furthermore, we had shown that the three aforementioned general ketones (*N*-benzylpiperidone (**78**), acetophenone (**79**), and 4-phenylcyclohexanone (**80**)) without OH groups
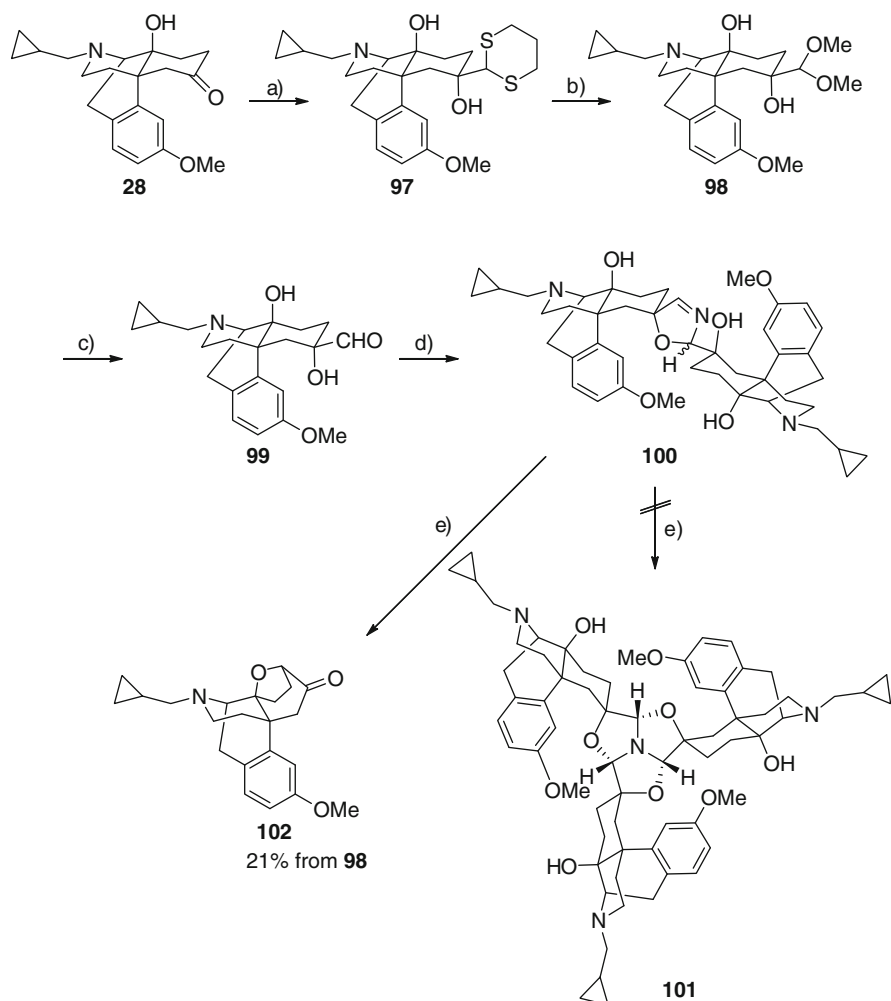
Scheme 32 Synthesis of oxabicyclo[3.2.1]octane derivative **102**. Reagents and conditions: (a) *n*-BuLi, 1,3-dithiane, DME, −70 °C, 69%; (b) CuCl$_2$·2H$_2$O, CSA, CH(OMe)$_3$, MeOH, 50 °C, 37%; (c) 2 M HCl, reflux; (d) NH$_4$Cl, AcONa, MeOH, reflux,; (e) CSA, CHCl$_3$, reflux

Fig. 21 Observed nuclear Overhauser effect (NOE) spectra of compound **102**
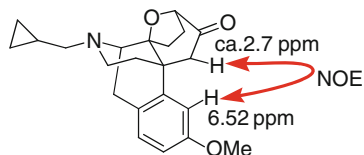
were converted to the corresponding trimers. Therefore, the 14-OH group could be expected to participate in the rearrangement reaction. To test our hypothesis, dimethyl acetal **98** was treated with CSA in toluene under reflux to give the
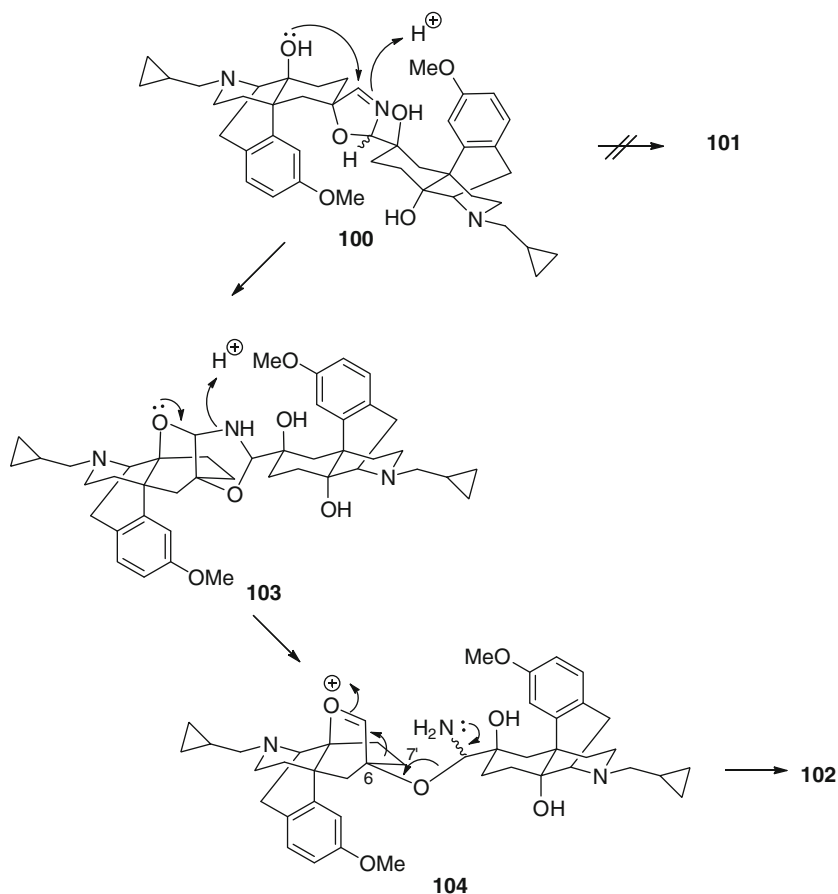
Scheme 33 Reaction mechanism for producing compound **102**

expected compound **102** in 90% yield (Scheme 35). In contrast, the dimethyl acetal **11** with a 4,5-epoxy ring could not be converted to the corresponding rearrangement product **108**. The existence of the 4,5-epoxy ring in **109** may have fixed the morphinan skeleton and thus, prevented the 7′-carbon from rearranging to the oxonium carbon (Scheme 35).

   To evaluate the opioid receptor binding affinities of the rearranged compounds, compound **102** was demethylated with BBr$_3$ in CH$_2$Cl$_2$ to produce phenol **107** in 87% yield (Scheme 35). Compound **107** showed strong affinity for both the μ and κ opioid receptors, comparable to that of naltrexone (**1**) (Table 3). We previously reported the synthesis of compound **110** with an oxabicyclo[2.2.1]heptanes skeleton and a C-ring in a fixed boat conformation, and the synthesis of its derivative (Fig. 22) [94]. At that time, we postulated that the potent κ agonist TRK-820 also had a C-ring in the boat conformation [95, 96]. Subsequently, we showed that the amide derivative **110** had strong κ agonist activity (Fig. 22) [94]. This result
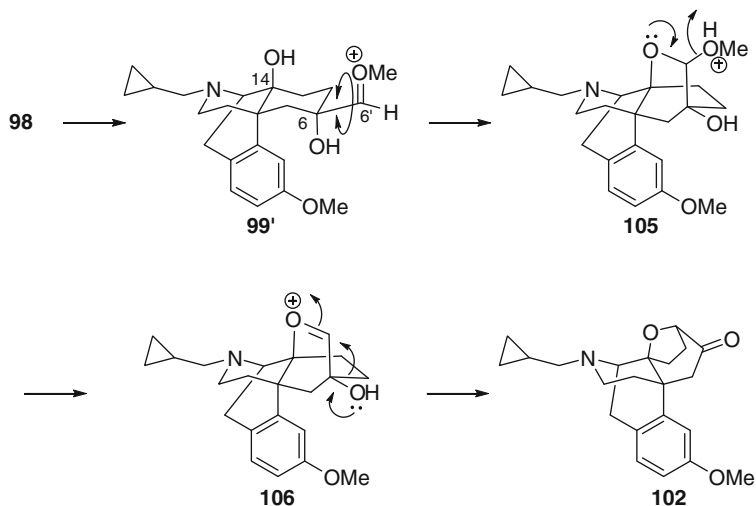
Scheme 34 Plausible mechanism for the rearrangement reaction for providing **102** from **98**
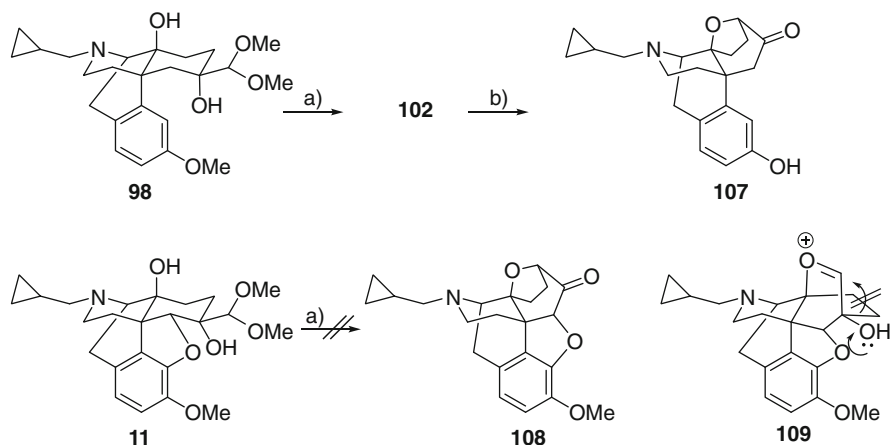
Scheme 35 Comparison between the reactivities of dimethyl acetals **98** and **11**. Reagents and conditions: (a) CSA, toluene, reflux, 90%; (b) BBr$_3$, CH$_2$Cl$_2$, rt, 87%

supported our prediction. Compound **107** also has a C-ring in the fixed boat conformation, i.e., a novel oxabicyclo[3.2.1]octane skeleton. Compound **111**, which is the fundamental skeleton of **110**, also had κ type selectivity (μ/κ K_i ratio = 1.42). Compound **107** showed a rather improved selectivity (μ/κ K_i ratio = 1.70) over that of **111**; however, **107** had reduced affinities for each opioid receptor type compared to **111**. We expected to improve both the affinity and κ selectivity of compound **107** by introducing a C6 side chain, similar to that present in TRK-820 [95, 96].

Table 3 Opioid receptor binding affinities of compound **107**, compound **111**, and naltrexone (**1**)[a]

Compound	K_i (κ)[b]	K_i (μ)[c]	K_i (δ)[d]
107	0.233 nM	0.397 nM	6.84 nM
111	0.102 nM	0.145 nM	3.50 nM
Naltrexone (**1**)	0.373 nM	0.335 nM	20.7 nM

[a]Binding assay was carried out in duplicate using homogenate of guinea-pig brain (κ: cerebellum, μ and δ: forebrain)
[b][^{3}H]U-69,593 was used
[c][^{3}H]DAMGO was used
[d][^{3}H]NTI was used
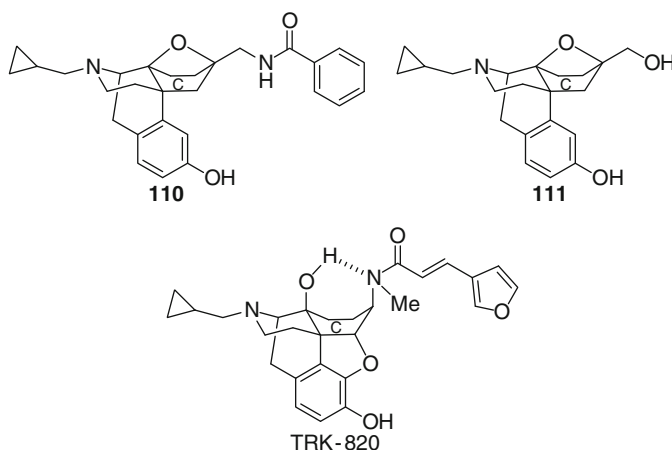
Fig. 22 Structure of TRK-820 with the C-ring fixed in boat conformation *via* an intramolecular interaction between the 14-OH and amide nitrogen; morphinan derivatives **110** and **111** with oxabicyclo[2.2.1]heptane skeletons

9 Novel Rearrangement Reaction for Converting a 6,14-Endoethanomorphinan Derivative to a Benzomorphan Derivative [97]

As mentioned in Sect. 2, we hypothesized that the strong affinity of TAN-821 for the μ opioid receptor may derive, in part, from the high lipophilicity conferred by the 7,8-ethylene bridge. Therefore, we attempted to modify the endoethenotetrahydrothebaine skeleton to improve the ε selectivity of TAN-821 *in vitro*. The ethylene bridge of TAN-821 is on the C-ring [19]. We hypothesized that the substituent above the C ring contributed to the ε receptor selectivity [19]. Based on this hypothesis, we designed a naltrexone derivative **113** with a 14-allyl group to which appropriate substituents could be introduced. We planned to synthesize **113** from the primary alcohol **112** by fragmentation (Scheme 36). In the course of our attempts to convert the alcohol **112** to the 14-allyl derivative **113**, we found a
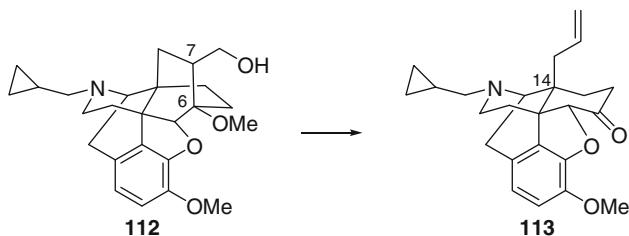
Scheme 36 Planned synthesis of compound **113** from compound **112**
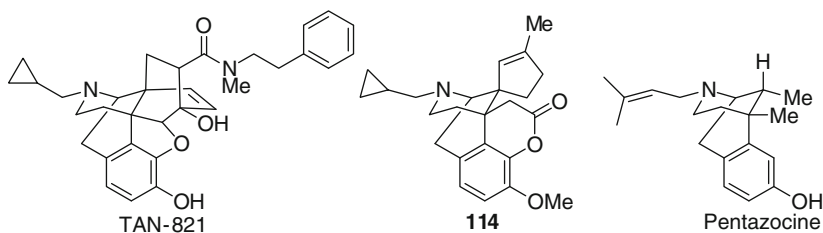
Fig. 23 Structures of TAN-821, rearrangement product **114**, and pentazocine
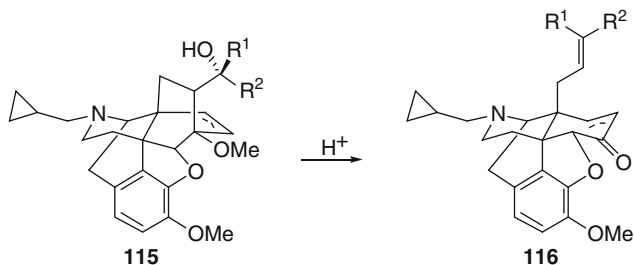
Scheme 37 Formation of the 14-alkenyl derivatives **116** from *sec-* or *tert*-alcohols **115** after treatment with acid

novel rearrangement reaction of the compound **112** that afforded the benzomorphan derivative **114**, which can be converted to the representative benzomorphan, pentazocine (Fig. 23). We became interested in this novel reaction and attempted to clarify the reaction mechanism.

The endoethano- or endoethenotetrahydrothebaine derivatives **115** with either a tertiary or secondary alcohol moiety were reported to undergo fragmentation under acidic conditions to give 14-alkenyl derivatives **116** (Scheme 37)[11] [98–102].

---

[11]The fragmentation of a 7-acyl-6,14-endoethenotetrahydrothebaine derivative was also reported. See [99].
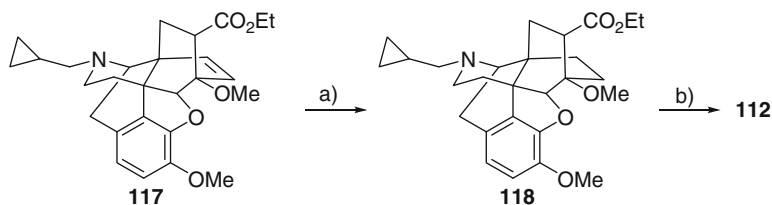
Scheme 38 Preparation of primary alcohol **112** from ester **117**. Reagents and conditions: (a) H_2 (0.4 MPa), Pd/C, EtOH, 50 °C, 93%; (b) LiAlH$_4$, THF, 0 °C to rt, 95%
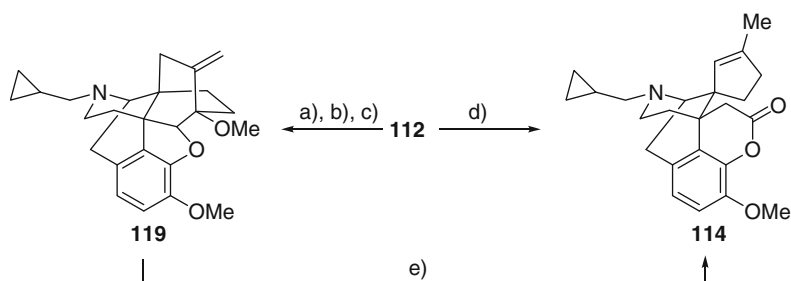
Scheme 39 Preparation of rearrangement product **114** from compound **112** or **119**. Reagents and conditions: (a) Tf$_2$O, CH$_2$Cl$_2$, rt; (b) washing with sat. NaHCO$_3$ aq., (c) toluene, reflux, 91%; (d) Tf$_2$O CH$_2$Cl$_2$, rt, then toluene, reflux, 77%; (e) TfOH, toluene, reflux, quant

We attempted to cleave the C6–C7 bond of alcohol **112**, which possessed a primary alcohol, to afford a naltrexone derivative **113** with a 14-allyl group (Scheme 36). Alcohol **112** was synthesized from compound **117** [19] by hydrogenation and subsequent reduction of the ester group (Scheme 38). We treated **112** with Tf$_2$O in CH$_2$Cl$_2$ at room temperature. After the reaction mixture was washed with a saturated NaHCO$_3$ solution and concentrated under reduced pressure, the resulting residue was dissolved in toluene and refluxed under argon to produce the olefin **119** (the 7-methylidene derivative has been prepared by other methods; for example, a Hofmann degradation of a 7-dimethylaminomethyl derivative, or treatment of the tosylate of the corresponding primary alcohol with *t*-BuOK [103]) in 91% yield. On the other hand, when **112** was treated with Tf$_2$O in CH$_2$Cl$_2$, but not washed with NaHCO$_3$ solution, and then the concentrated reaction mixture was refluxed in toluene under argon, the unexpected rearrangement compound **114** was obtained in 77% yield (Scheme 39). The structure of lactone **114** was determined by IR, mass, and NMR spectra (^{1}H, ^{13}C, COSY, HSQC, and HMBC) (Fig. 24).

We then attempted to clarify the reaction mechanism of this novel rearrangement. When the olefin **119** was treated with TfOH (2.2 equiv.) in toluene under reflux, the objective lactone **114** was obtained in quantitative yield (when the 7-methylidene derivative with a 6,14-etheno bridge was treated with perchloric acid, another product was obtained [104]). Next, treatment of the olefin **119** with a

Fig. 24 Structure
determination of **114**, **120**,
and **121**, and observed HMBC
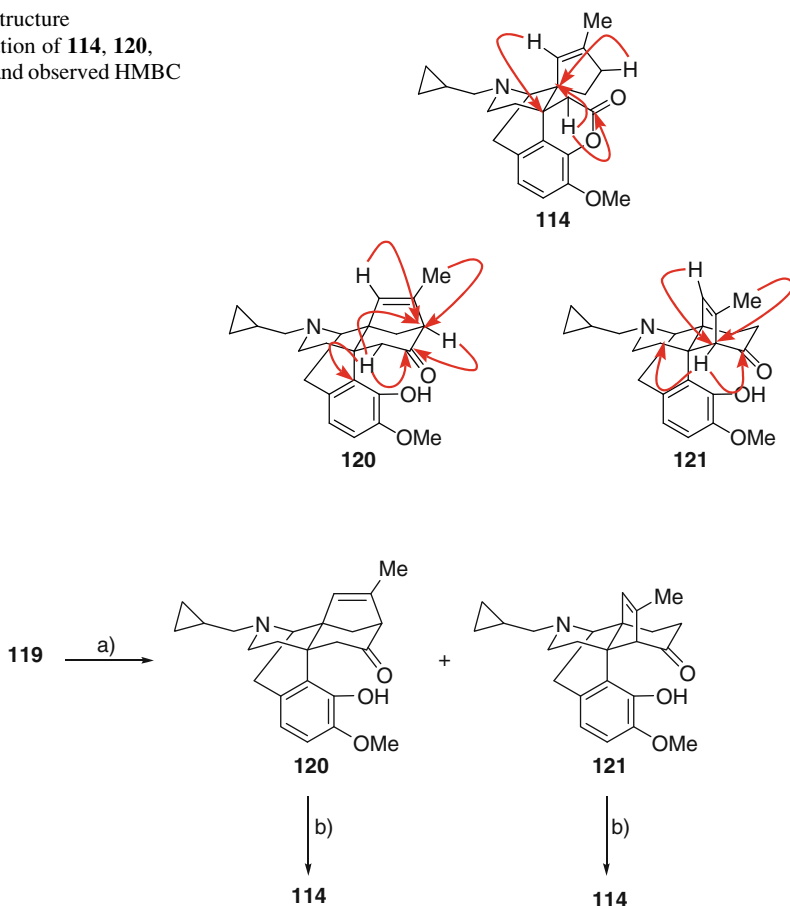
Scheme 40 Preparation of **114** from **120** or **121**. Reagents and conditions: (a) CSA, toluene, reflux, **120**: 34%, **121**: 35%; (b) TfOH, toluene, reflux, quant

weaker acid CSA in toluene under reflux gave ketones **120** and **121** (Scheme 40), whose structures were also determined by IR, mass, and NMR spectra (Fig. 24). Both ketones **120** and **121** were converted into lactone **114** after treatment with TfOH in toluene under reflux. Taken together, these outcomes indicated that the three compounds **119**–**121** are intermediates in the production of lactone **114**.

On the basis of the structures of the three isolated important intermediates **119**–**121**, we proposed a reaction mechanism for the production of lactone **114** (Scheme 41). In this mechanism, catalytic amounts of water or TfOH would play an important role. Oxonium **120′** may be obtained by an intramolecular aldol reaction of the intermediate **122**. Compound **122** may be derived from olefin **119** by acidic hydration, subsequent fragmentation, and isomerization. Oxonium **120′** may undergo intramolecular cyclization to give acetal **123**; then fragmentation
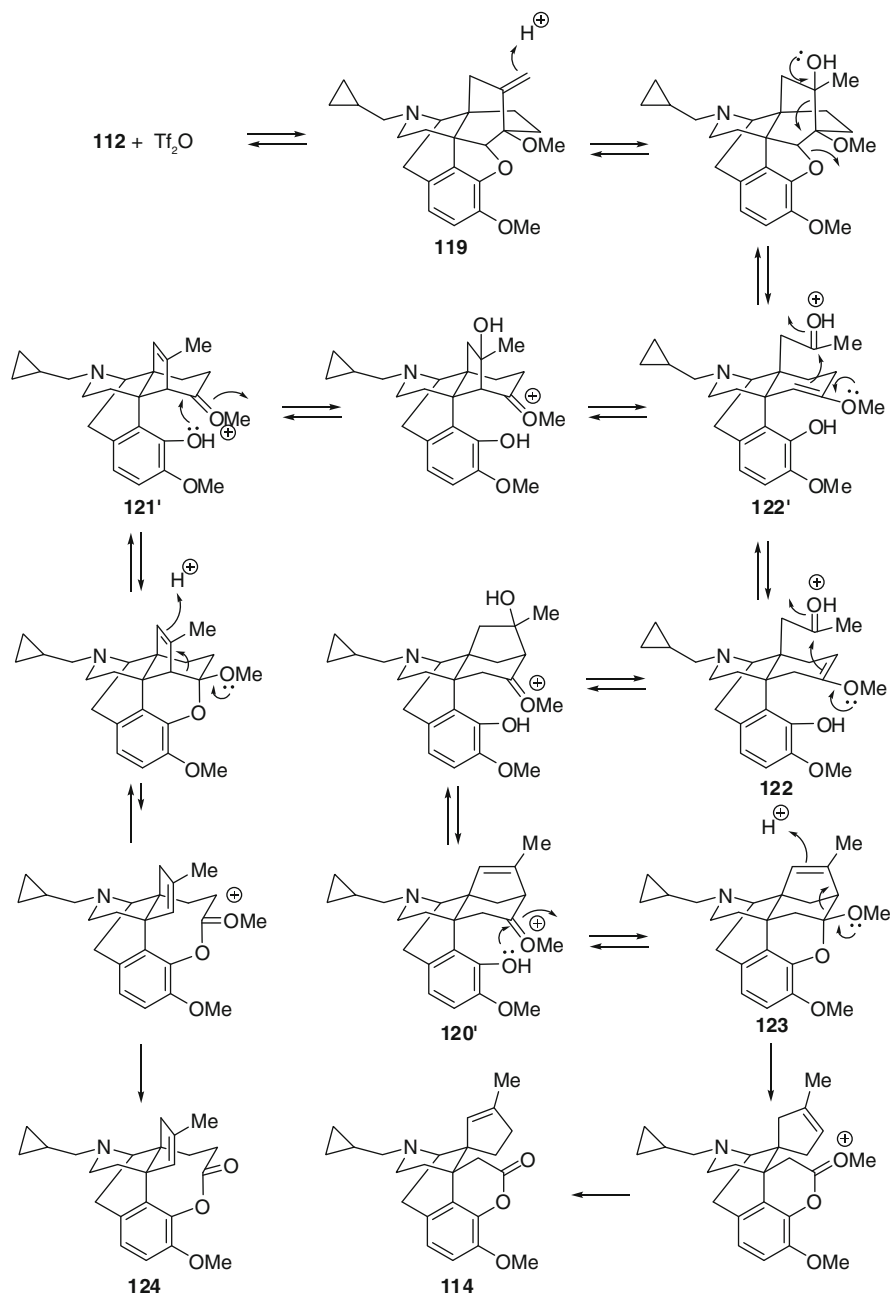
Scheme 41 Reaction mechanism to lactone **114**

and subsequent isomerization would provide lactone **114**. Alternatively, oxonium **120′** may be hydrated and undergo fragmentation to afford carboxylic acid; then esterification of the resulting carboxylic acid may lead to the production of lactone **114**. However, we believe the former route would predominate because intramolecular reactions generally proceed faster than intermolecular reactions. Oxonium **121′** may be obtained from **122′** (regioisomer of **122**) by an intramolecular aldol reaction. Both oxoniums **120′** and **121′** would be converted to lactone **114** due to the equilibrium between **120′** and **121′** under the reaction conditions. The equilibrium was confirmed by the observation that treatment of either pure compound **120** or **121** in the presence of CSA under reflux gave mixture of ketones **120** and **121**. Moreover, although oxonium **121′** could be readily converted to lactone **114** *via* the isomeric oxonium **120′**, lactone **124** was not detected at all. This was surprising, because lactone **124** was expected be obtained directly from **121′** by a reaction sequence comparable to that which converts **120′** to **114** (Scheme 41) Thus, lactones **114** and **124** may have very different reactivities. The olefin moiety and the carbonyl group in lactone **124** may be sufficiently close in space that the reaction rapidly reversed to give ketone **121** (Fig. 25). That is, the equilibrium for the formation of lactone **124** would favor the reversal to ketone **121**. On the other hand, the distance between the olefin moiety and the carbonyl group in lactone **114** may be sufficiently large that the reverse reaction may not occur. Therefore, formation of lactone **114** may be irreversible (Fig. 25). As a result, only lactone **114** would be obtained in high yield, regardless of the ratio of **120** and **121** at equilibrium.

The structure of the rearranged product **114** is very similar to that of the benzomorphan, like pentazocine (Fig. 23) [105, 106], a useful analgesic. Although several papers have previously described the total synthesis of pentazocine, many
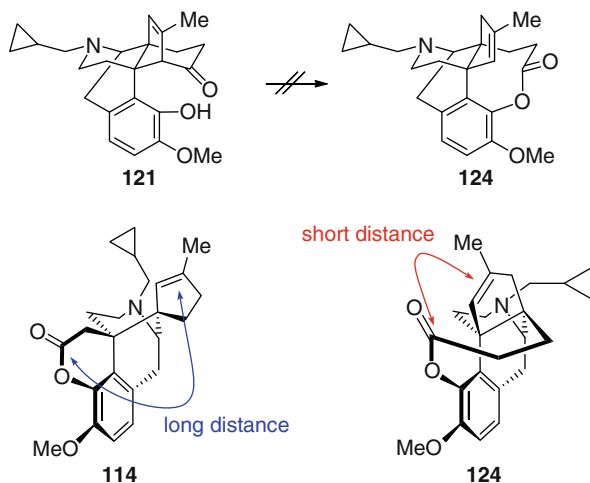
Fig. 25 Backside views of lactone **114** and **124**

were syntheses of a racemic form, but there are several exceptions[12] [107–115, 117–121]. Lactone **114** is a chiral compound with the desirable absolute configuration because it was derived from the commercially available semi-synthetic opioid (−)-naltrexone *via* alcohol **112**. Therefore, the conversion of lactone **114** to the pharmacologically active enantiomer (−)-pentazocine would be expected [116]. We are currently investigating the conversion of **114** to pentazocine and plan to publish our report in the future.

10   Concluding Remarks

In this chapter we have described eight interesting reactions using naltrexone derivatives. Although almost all these reactions are characteristic of naltrexone derivatives, they could lead to many novel skeletons and provide new interesting pharmacological data. Some new reactions found using naltrexone derivatives were expanded to general reactions. For example, the 6α-hydroxy-6-aldehyde derivation from naltrexone that led to the oxazoline dimer and the 1,3,5-trioxaza-triquinane skeleton (triplet drug) was applied to general ketones. These ketones were converted to α-hydroxyaldehydes, followed by conversion to the dimers and trimers (Sect. 7). Furthermore, the reaction in which the 17-nitrogen moiety of naltrexone derivatives interacted with osmium tetroxide to give amide derivatives could apply to general tertiary amines [122]. The ring opening reaction of the cyclopropane ring in the 17-CPM group in naltrexone derivatives with PtO_2 in HBr-MeOH to provide an *i*-Bu group could also be applied to general cyclopropylalkyl derivatives for the exclusive production of branched alkyl derivatives [44, 123]. Finally, there are many other interesting reactions and pharmacological data that could not be described in this chapter due to space limitations. We hope that interested readers will refer to the reference list below [19, 22, 49, 66, 88, 93, 94, 124–128].

---

[12]For synthesis of pentazocine, see [107–111]. For synthesis of (–)-pentazocine with optical resolution, see [112, 113]. For the asymmetric synthesis of (–)-pentazocine, see the asymmetric synthesis of (–)-metazocine (an *N*-methyl derivative of (–)-pentazocine) has also been reported, [114]; very recently, the asymmetric synthesis of (–)-9-*epi*-pentazocine was also reported [115]; it has been shown that (–)-pentazocine is more potent than its antipode [116].

References

1. Sertürner FW (1805) Tommsdrof's J Pharmazie 13:234
2. Gulland JM, Robinson R (1923) J Chem Soc 980
3. Gulland JM, Robinson R (1925) Mem Proc Manchester Lit Phil Soc 69:79
4. Schöpf C (1927) Justus Liebigs Ann Chem 452:411
5. Casy AF, Parfitt RT (1986) Opioid analgesics, chemistry and receptor. Plenum, New York
6. Lenz GR, Evans SM, Walters DE, Hopfinger AJ, Hammond DL (1986) Opiates. Academic, Orlando
7. Portoghese PS, Nagase H, Lipkowski AW, Larson DL, Takemori AE (1988) J Med Chem 31:836
8. Portoghese PS, Sultana M, Nagase H, Takemori AE (1988) J Med Chem 31:281
9. Lipkowski AW, Nagase H, Portoghese PS (1986) Tetrahedron Lett 27:4257
10. Portoghese PS (1989) Trends Pharmacol Sci 10:230
11. Portoghese PS (1991) J Med Chem 34:1757
12. Portoghese PS, Garzon-Aburbeth A, Nagase H, Lin CE, Takemori AE (1991) J Med Chem 34:1792
13. Nagase H, Abe A, Portoghese PS (1989) J Org Chem 54:4120
14. Nagase H, Portoghese PS (1990) J Org Chem 55:365
15. MaloneyHuss KE, Portoghese PS (1990) J Org Chem 55:2957
16. Watanabe A, Kai T, Nagase H (2006) Org Lett 8:523
17. Reisine T, Pasternak G (1995) Opioid analgesics and antagonists. In: Hardman JG, Limbird LE, Molinof PE, Ruddon RW, Gilman AG (eds) Pharmaceutical basis of therapeutics, 9th edn. Mcgraw-Hill, New York, p 521
18. Burkey TH, Ehlert FJ, Hosohata Y, Quack RM, Cowell S, Hosohata K, Varga E, Stropova D, Li X, Slate C, Nagase H, Porreca F, Hruby VJ, Roeske WR, Yamamura HI (1998) Life Sci 62:1531
19. Fujii H, Narita M, Mizoguchi H, Murachi M, Tanaka T, Kawai K, Tseng LF, Nagase H (2004) Bioorg Med Chem 12:4133
20. Corey EJ, Erickson BW (1971) J Org Chem 36:3553
21. Mori K, Hashimoto H, Takenaka Y, Takigawa T (1975) Synthesis 720
22. Osa Y, Ida Y, Yano Y, Furuhata K, Nagase H (2006) Heterocycles 69:271
23. Nagase H, Watanabe A, Nemoto T, Yamamoto N, Osa Y, Sato N, Yoza K, Kai T (2007) Tetrahedron Lett 48:2547
24. Trost BM, Melvin LS (1975) Sulfur ylides: emerging synthetic intermediates. Academic, New York
25. Sawa YK, Tada H (1968) Tetrahedon 24:6185
26. Fujii H, Imaide S, Watanabe A, Nemoto T, Nagase H (2008) Tetrahedron Lett 49:6293
27. Hagemen HA (1953) Org React 7:198
28. von Braun J (1914) Ber 47:2312
29. Bentley KW, Hardy DG (1967) J Am Chem Soc 89:3281
30. Cooley JH, Evain EJ (1989) Synthesis 1
31. Montzka TA, Matiskella JD, Partyka RA (1974) Tetrahedron Lett 15:1325
32. Olofson AR, Schnur RC, Bunes L, Pepe JP (1977) Tetrahedron Lett 18:1567
33. Olofson AR, Martz JT, Senet JP, Piteau M, Malfroot T (1984) J Org Chem 49:2081
34. Selley DE, Sim LJ, Xiao R, Liu Q, Childers SR (1997) Mol Pharmacol 51:87
35. Brown GP, Yang K, Ouerfelli O, Standifer KM, Byrd D, Pasternak GW (1997) J Pharmacol Exp Ther 282:1291
36. Traynor JR, Clark MJ, Remmers AE (2002) J Pharmacol Exp Ther 300:157
37. Schulz S, Mayer D, Pfeiffer M, Stumm R, Koch T, Höllt V (2004) EMBO J 23:3282
38. Johnson EA, Oldfield S, Braksator E, Gonzalez-Cuello A, Couch D, Hall KJ, Mundell SJ, Bailey CP, Kelly E, Henderson G (2006) Mol Pharmacol 70:676

39. Gould ES (1959) Mechanism and structure in organic chemistry. Henry Holt and Company, New York, pp 561–617
40. Richey HG Jr (1972) In: Olah GA, Schleyer PR (eds) Carbonium ions, vol III. Wiley, Canada, pp 1201–1294
41. Lowry TH, Richardson KS (1987) Mechanism and theory in organic chemistry, 3rd edn. Harper & Row Publishers, New York, pp 425–515
42. Olah GA, Prakash Reddy V, Surya Prakash GK (1992) Chem Rev 92:69
43. Nagase H, Yamamoto N, Nemoto T, Yoza K, Kamiya K, Hirono S, Momen S, Izumimoto N, Hasebe K, Mochizuki H, Fujii H (2008) J Org Chem 73:8093
44. Fujii H, Osa Y, Ishihara M, Hanamura S, Nemoto T, Nakajima M, Hasebe K, Mochizuki H, Nagase H (2008) Bioorg Med Chem Lett 18:4978
45. Fujii H, Imaide S, Watanabe A, Yoza K, Nakajima M, Nakao K, Mochizuki H, Sato N, Nemoto T, Nagase H (2010) J Org Chem 75:995
46. Beckett AH, Casy AF (1954) J Pharm Pharmacol 6:986
47. Beckett AH, Casy AF (1956) J Pharm Pharmacol 8:848
48. Casy AF, Parfitt RT (1986) Opioid analgesics, chemistry and receptors. Plenum, New York, pp 473–475
49. Imaide S, Fujii H, Watanabe A, Nemoto T, Nakajima M, Nakao K, Mochizuki H, Nagase H (2010) Bioorg Med Chem Lett 20:1055
50. Bal BS, Childers WE Jr, Pinnick HW (1981) Tetrahedron 37:2091
51. Pommier A, Pons J-M (1993) Synthesis 441
52. Rayner CM (1995) In: Katritzky AR, Meth-Cohn O, Rees CW (eds) Comprehensive organic functional group transformations, vol 1. Pergamon, Oxford, pp 673–718
53. Braun NA, Meier M, Schmaus G, Holscher B, Pickenhangen W (2003) Helv Chim Acta 86:2698
54. Merlic CA, Doroh BC (2003) J Org Chem 68:6056
55. Buckle MJC, Fleming I, Gil S, Pang KLC (2004) Org Biomol Chem 2:749
56. Shindo M, Matsumoto K, Shishido K (2005) Chem Commun 2477
57. Shindo M, Matsumoto K, Shishido K (2007) Tetrahedron 63:4271
58. Hara S, Taguchi H, Yamamoto H, Nozaki H (1975) Tetrahedron Lett 16:1545
59. Danishefsky SJ, Panek JS (1987) J Am Chem Soc 109:917
60. Gates KS, Silverman RB (1989) J Am Chem Soc 111:8891
61. Padwa A, Brodney MA, Lynch SM, Rashatasakhon P, Wang Q, Zhang H (2004) J Org Chem 69:3735
62. Smith MB, March J (2007) March's advanced organic chemistry, 6th edn. John Wiley, New York, pp 1482–1483, and references therein
63. Carey FA, Sundberg RJ (2007) Advanced organic chemistry, part A: structure and mechanisms, 5th edn. Springer, New York, p 559
64. Clayden J, Greeves N, Warren S, Wother P (2001) Organic chemistry. Oxford University Press, New York, pp 496–497
65. Portoghese PS, Sultana M, Takemori AE (1990) J Med Chem 33:1714
66. Nemoto T, Fujii H, Nagase H (2007) Tetrahedron Lett 48:7413
67. Nemoto T, Fujii H, Narita M, Miyoshi K, Nakamura A, Suzuki T, Nagase H (2008) Bioorg Med Chem 16:4304
68. Morgenthaler M, Schweizer E, Hoffmann-Röder A, Benini F, Martin RE, Jaeschke G, Wager B, Fischer H, Bendels S, Zimmerli D, Schneider J, Diederich F, Kansy M, Müller K (2007) Chem Med Chem 2:1100
69. Trefonas LM, Flurry RL Jr, Meyers EA, Copeland RF (1966) J Am Chem Soc 88:2145
70. Birch AJ, Fitton H, McPartlin M, Mason MR (1968) Chem Commun 531
71. Hollenstein S, Laube T (1990) Angew Chem Int Ed Engl 29:188
72. Childs RF, Dickie BD, Faggiani R, Fyfe CA, Lock CJL, Wasylishen RE (1985) J Crystallogr Spectrosc Res 15:73
73. Childs RF, Shaw GS, Lock CJL (1989) J Am Chem Soc 111:5424

74. Santarsiero BD, James MNG, Mahendran M, Childs RF (1990) Am Chem Soc 112:9416
75. Mass G, Rahm R, Mayer D, Baumann W (1995) Organometallics 14:1061
76. Elia GR, Childs RF, Britten JF, Yang DSC, Santasiero BD (1996) Can J Chem 74:591
77. Greci L, Rossetti M, Galeazzi R, Stipa P, Sgarabotto P, Cozzini PJ (1998) J Chem Soc Perkin Trans 2:2683
78. Herz H-G, Schatz J, Maas G (2001) J Org Chem 66:3176
79. Nikolai J, Schlegel J, Regitz M, Maas G (2002) Synthesis 497
80. Reisser M, Maier A, Maas G (2003) Eur J Org Chem 2071
81. Levin VV, Dilman AD, Belyakov PA, Korlyukov AA, Struchkova MI, Tartakovsky VA (2005) Tetrahedron Lett 46:3729
82. Espenlaub S, Gerster H, Maas G (2007) ARKIVOC 114
83. Birch AJ, Fitton H (1969) Aust J Chem 22:971
84. Birch AJ, Kelly LF, Liepa AJ (1985) Tetrahedron Lett 26:501
85. Reed AE, Curtiss LA, Weinhold F (1988) Chem Rev 88:899
86. Fuying L, Linghuan G, Chenlei Y, Jie C, Jinggen L, Xin X, Ao Z (2009) Bioorg Med Chem Lett 19:4603
87. Nagase H, Watanabe A, Harada M, Nakajima M, Hasebe K, Mochizuki H, Yoza K, Fujii H (2009) Org Lett 11:539
88. Fujii H, Watanabe A, Nemoto T, Narita M, Miyoshi K, Nakamura A, Suzuki T, Nagase H (2009) Bioorg Med Chem Lett 19:438
89. Rios CD, Joran BA, Gomes I, Devi LA (2001) Pharmacol Ther 92:71
90. Levac BAR, O'Dowd BF, George SR (2002) Curr Opin Pharmacol 2:76
91. Contreras JM, Bourguignon JJ (2003) In: Wermuth CG (ed) The practice of medicinal chemistry, 2nd edn. Academic, London, p 251
92. Watanabe A, Fujii H, Nakajima M, Hasebe K, Mochizuki H, Nagase H (2009) Bioorg Med Chem Lett 19:2416
93. Osa Y, Ida Y, Fujii H, Nemoto T, Hasebe K, Momen S, Mochizuki H, Nagase H (2007) Chem Pharm Bull 55:1489
94. Nemoto T, Fujii H, Narita M, Miyoshi K, Nakayama A, Suzuki T, Nagase H (2008) Bioorg Med Chem Lett 18:6398
95. Nagase H, Hayakawa J, Kawamura K, Kawai K, Takezawa Y, Matsuura H, Tajima C, Endo T (1998) Chem Pharm Bull 46:366
96. Kawai K, Hayakawa J, Miyamoto T, Imamura Y, Yamane S, Wakita H, Fujii H, Kawamura K, Matsuura H, Izumimoto N, Kobayashi R, Endo T, Nagase H (2008) Bioorg Med Chem 16:9188
97. Fujii H, Watanabe Y, Osa Y, Nemoto T, Sato N, Nagase H (2009) Tetrahedron 65:4808
98. Bentley KW, Hardy DG, Meek B, Taylor JB, Brown JJ, Morton GO (1969) J Chem Soc (C) 2229
99. Bentley KW, Ball JC (1958) J Org Chem 23:1720
100. Bentley KW, Hardy DG, Meek BJ (1967) J Am Chem Soc 89:3293
101. Bentley KW, Hardy DG, Howell CF, Fulmor W, Lancaster JE, Brown JJ, Morton GO, Hardy RA (1967) J Am Chem Soc 89:3303
102. Bentley KW, Bower JD, Lewis JW (1969) J Chem Soc (C) 2569
103. Bentley KW, Hardy DG, Lewis JW, Readhead MJ, Rushworth WI (1969) J Chem Soc (C) 826
104. Lewis JW, Readhead MJ (1972) J Chem Soc (C) 881
105. Clarke EGC (1959) Nature 184:451
106. Archer S, Albertson NF, Harris LP, Pierson AK, Bird JG (1964) J Med Chem 7:123
107. Kametani T, Huang S, Ihara M, Fukumoto K (1976) J Org Chem 41:2545
108. Kametani T, Kigasawa K, Hiiragi M, Wakisaka K, Uryu T, Sugi H, Saitoh S, Ishimaru H, Haga S (1976) Chem Pharm Bull 24:1246
109. Kametani T, Seto H, Nemoto H, Fukumoto K (1977) J Org Chem 42:3605
110. Rice KC, Jacobson AE (1976) J Med Chem 19:430

111. Brine GA, Berrang B, Hayes JP, Carroll FI (1990) J Heterocycl Chem 27:2139
112. Kitamura M, Hsiao Y, Ohta M, Tsukamoto M, Ohta T, Takaya H, Noyori R (1994) J Org Chem 59:297
113. Kitamura M, Hsiao Y, Noyori R, Takaya H (1987) Tetrahedron Lett 28:4829
114. Meyers AI, Dickman DA, Bailey TR (1985) J Am Chem Soc 107:7974
115. Yang X, Zhai H, Li Z (2008) Org Lett 10:2457
116. Tullar BF, Harris LS, Perry RL, Pierson AK, Soria AE, Wetterau WF, Albertson NF (1967) J Med Chem 10:383
117. Kametani T, Kigasawa K, Hiiragi M, Wagatsuma N (1974) Heterocycles 2:79 and references therein
118. Kametani T, Huang S, Ihara M, Fukumoto K (1975) Chem Pharm Bull 23:2010
119. Kametani T, Honda T, Huang S, Fukumoto K (1975) Can J Chem 53:3820
120. Boulanger WA (1999) Synth Commun 29:2201
121. Trost BM, Weiping T (2003) J Am Chem Soc 125:8744
122. Fujii H, Ogawa R, Jinbo E, Tsumura S, Nemoto T, Nagase H (2009) Synlett 2341
123. Fujii H, Okada K, Ishihara M, Hanamura S, Osa Y, Nemoto T, Nagase H (2009) Tetrahedron 65:10623
124. Fujii H, Hirano N, Uchiro H, Kawamura K, Nagase H (2004) Chem Pharm Bull 52:747
125. Fujii H, Narita M, Mizoguchi H, Hirokawa J, Kawai K, Tanaka T, Tseng LF, Nagase H (2004) Bioorg Med Chem Lett 14:4241
126. Nagase H, Oso Y, Nemoto T, Fujii H, Imai M, Nakamura T, Kanemasa T, Kato A, Gouda H, Hirono S (2009) Bioorg Med Chem Lett 19:2792
127. Fujii H, Ogawa R, Ohata K, Nemoto T, Nakajima M, Hasebe K, Mochizuki H, Nagase H (2009) Bioorg Med Chem 17:5983
128. Nagase H, Watanabe A, Nemoto T, Yamaotsu N, Hayashida K, Nakajima M, Hasebe K, Nakao K, Mochizuki H, Hirono S, Fujii H (2010) Bioorg Med Chem Lett 20:121

Twin and Triplet Drugs in Opioid Research

Hideaki Fujii

Abstract Twin and triplet drugs are defined as compounds that contain respectively two and three pharmacophore components exerting pharmacological effects in a molecule. The twin drug bearing the same pharmacophores is a "symmetrical twin drug", whereas that possessing different pharmacophores is a "nonsymmetrical twin drug." In general, the symmetrical twin drug is expected to produce more potent and/or selective pharmacological effects, whereas the nonsymmetrical twin drug is anticipated to show both pharmacological activities stemming from the individual pharmacophores (dual action). On the other hand, nonsymmetrical triplet drugs, which have two of the same pharmacophores and one different moiety, are expected to elicit both increased pharmacological action and dual action. The two identical portions could bind the same receptor sites simultaneously while the third portion could bind a different receptor site or enzyme. This review will mainly focus on the twin and triplet drugs with an evaluation of their *in vivo* pharmacological effects, and will also include a description of their pharmacology and synthesis.

Contents

H. Fujii
School of Pharmacy, Kitasato University, 5-9-1, Shirokane, Minato-ku, Tokyo 108-8641, Japan
e-mail: fujiih@pharm.kitasato-u.ac.jp

Abbreviations

A	Adenosine
ADME	Absorption, distribution, metabolism, and excretion
β-FNA	β-Funaltrexamine
BNTX	7-Benzylidenenaltrexone
BRET	Bioluminescence resonance energy transfer
CBM	Cyclobutylmethyl
CCK	Cholecystokinin
COS	CV-1 origin SV40 cell
CPM	Cyclopropylmethyl
CPP	Conditioned place preference
DAMGO	[D-Ala^2, N-Me-Phe^4, Gly-ol]enkephalin
DCC	Dicyclohexylcarbodiimide
DML	Designed multiple ligand
Dmt	2′,6′-Dimethyltyrosine
DPDPE	Cyclic[D-Pen^2, D-Pen^5]enkephalin
EC$_{50}$	50% Effective concentration
ED$_{50}$	50% Effective dose
EDC	1-Ethyl-3-(3-dimethylaminopropyl)carbodiimide
E$_{max}$	% Maximal stimulation
GNTI	Guanidinonaltrindole
GPI	Guinea pig ileum
GTP	Guanosine triphosphate
HOBt	N-Hydroxybenzotriazole
5-HT	5-Hydroxytryptamine (serotonin)
IBS	Imidazoline binding site
IC$_{50}$	50% Inhibitory concentration
i.c.v.	Intracerebroventricular
i.m.	Intramuscular
I$_{max}$	% Maximal inhibition
i.p.	Intraperitoneal or intraperitoneally
i.t.	Intrathecal

i.v.   Intravenous
MAPK   Mitogen-activated protein kinase
MS 3A   Molecular sieves 3Å
NMM   *N*-Methylmorpholine
nor-BNI   nor-Binaltorphimine
NSAID   Nonsteroidal anti-inflammatory drug
NTB   Naltriben
NTI   Naltrindole
s.c.   Subcutaneous
SP   Substance P
Tic   1,2,3,4-Tetrahydroisoquinoline-3-carboxylic acid

1 Introduction

Twin drugs are defined as compounds that contain two components exerting pharmacological effects, that is, pharmacophores in a molecule. The twin drug having the same pharmacophores is a "symmetrical twin drug", whereas one possessing two different pharmacophores is a "nonsymmetrical twin drug", Although several terms have been used such as bivalent ligands, chimeric compounds, hybrid compounds, conjugated ligands, and so on, in this chapter the term "twin drugs" will mainly be used to describe these drugs. In general, the symmetrical twin drug is expected to produce more potent and/or selective pharmacological effects, whereas the nonsymmetrical twin drug is anticipated to show two different pharmacological activities arising from the individual pharmacophores (dual action) [1].

The report that an enkephalin analog induced clustering of opioid receptors on the surface of neuroblastoma cells [2] prompted Portoghese and his colleagues to design and to synthesize symmetric twin drugs **1–3** (Fig. 1) consisting of two 6-oxymorphamines (R = Me) or 6-naltrexamines (R = CPM (cyclopropylmethyl)) to investigate the receptor clustering [3, 4]. The investigation using the

1: 6β, R = Me
2: 6α, R = Me
3: 6β, R = CPM (cyclopropylmethyl)
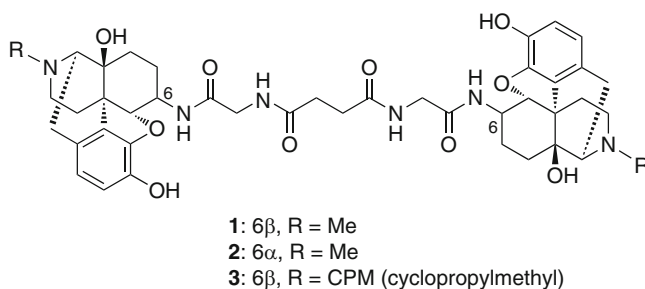
Fig. 1 Structures of twin drugs **1–3**
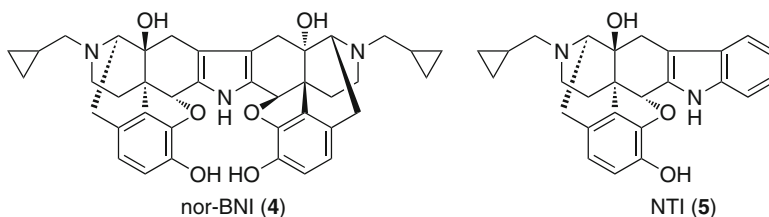
Fig. 2 Structures of nor-BNI (**4**) and NTI (**5**)

twin drugs led to the establishment of the "message-address" concept [5, 6], which is a useful guideline for designing selective ligands for an opioid receptor type, and contributed to the development of the first highly selective and potent κ and δ opioid antagonists, nor-binaltorphimine (**4**, nor-BNI) [7, 8] and naltrindole (**5**, NTI) [9–11], respectively (Fig. 2). This work was a landmark achievement in opioid research.

   Twin drugs are mainly utilized for two aims. One is the investigation of receptor dimerization; the other is the development of medicines with no or fewer adverse side effects. First, since the first evidence that κ and δ receptors must organize as heterodimers to be fully functional [12], numerous reports of hetero- and homo-dimerization of opioid receptors and other receptors have appeared [13–19]. Although opioid receptors have been historically classified into three types (μ, δ, and κ types) and further divided into several subtypes from the pharmacological viewpoint [20], only the three major types have been cloned [21]. Receptor dimerization has been invoked to explain the discrepancy between widely varied pharmacologies and the identification of only three opioid receptor types. Twin drugs are expected to be useful tools for investigation of receptor dimerization and pharmacology derived from receptor dimers, because two pharmacophores in an appropriate twin drug would simultaneously bind to two identical or different binding sites in receptor dimers. Second, drug discovery has been based on the principle of "one molecule-one target-one disease," but many diseases remained inadequately treated by such an approach and gradually it was recognized that simultaneous modulation of multiple targets would be more effective. The designed multiple ligand (DML) strategy is one of the methodologies to modulate multiple targets simultaneously [22–24]. As the DML has two pharmacophores interacting at respective targets, the DML and the twin drug represent the same thing. The DML is categorized into three types: conjugate, fused, and merged DML (Fig. 3). The difference among these DMLs is the distance between the two pharmacophores. The conjugate DML consisting of two pharmacophores linked to each other by a spacer has the longest distance between the two pharmacophores. The fused DML whose pharmacophores are linked with each other directly or *via* a short spacer possesses the middle distance between the two pharmacophores. The merged DML, sharing some part of each pharmacophore, has the shortest distance between the two pharmacophores. Many twin drugs belong to the conjugate or fused DML categories.

Excellent reviews about twin drugs with opioid pharmacophores have been published [25–27], including those that discuss peptidic twin drugs [27–29]. The following chapter will mainly focus on the twin and triplet drugs whose *in vivo* pharmacological effects have been evaluated, and will include a description of their pharmacology and synthesis.

2 Twin Drugs Consisting of Two Opioid Pharmacophores

Many twin drugs consisting of two opioid pharmacophores have been designed and synthesized for investigation of receptor dimerization and/or as DMLs. Some investigations using twin drugs have given insight into receptor subtype.

2.1 μ and κ Pharmacophores

Behavioral studies showed that κ agonists with various activity at the μ receptor more effectively reduced cocaine self-administration in nonhuman primates with fewer undesirable side effects than the highly selective κ agonists [30–32], and thus symmetrical twin drugs possessing two cyclorphans (**6**) [33] or butorphans (**7**) [34], which are full κ agonists and partial μ agonists, were synthesized (Fig. 4) [35–38]. Compounds **8–11** bridged at the 2- or 17-position had low binding affinities for opioid receptors. These results are in agreement with reported structure-activity relationship: introduction of substituents at the 2-position lowers opioid activities [39]; 17-substituents influence the opioid activities and some bulky substituents decrease the affinities [39, 40]. Compounds **12** with an ether linker at the 3-hydroxy position of butorphan (**7**) also bound to opioid receptors with low affinities (Table 1). However, twin drugs **13** linked by ester functions at the 3-hydroxy position of cyclorphan (**6**) or butorphan (**7**) exhibited good binding affinities (Table 1). Twin drugs **14**, which replaced the ester spacer with an amide one, more strongly bound to the opioid receptors than the compounds **12** which were linked by ether functionalities, but showed about 20- to 60-fold weaker binding affinities than twin drugs **13** with the ester linker. Thus, the affinity was very sensitive not only to the bridged position but also to the functionality of the linker. Very recently, twin drugs **15** and **16** with ether linkages containing hydroxy groups were reported to show high binding affinity (Table 1) [41]. This result again
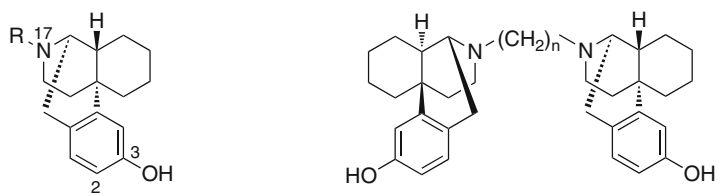
Cyclorphan (**6**): R = CPM
Butorphan (**7**): R = CBM (cyclobutylmethyl)

8

9

10

11

12
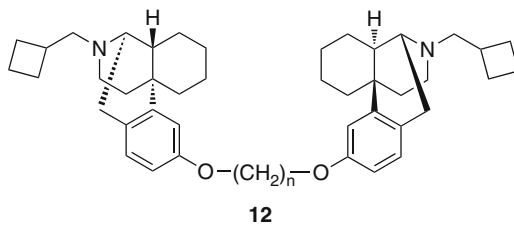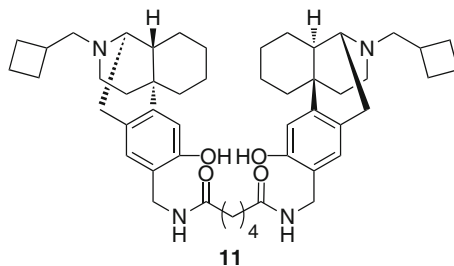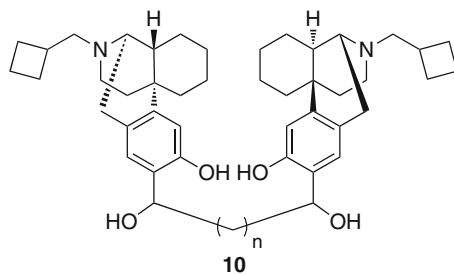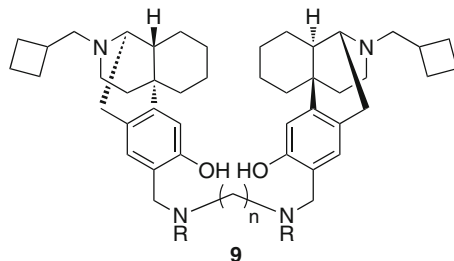
Fig. 4 Structures of cyclorphan (**6**), butorphan (**7**), and twin drugs **8–17**

13 R = CPM, CBM
MCL-139 (R = CBM, n = 2) (**13a**)
MCL-144 (R = CBM, n = 8) (**13b**)

14

15

16

MCL-145 (**17**)
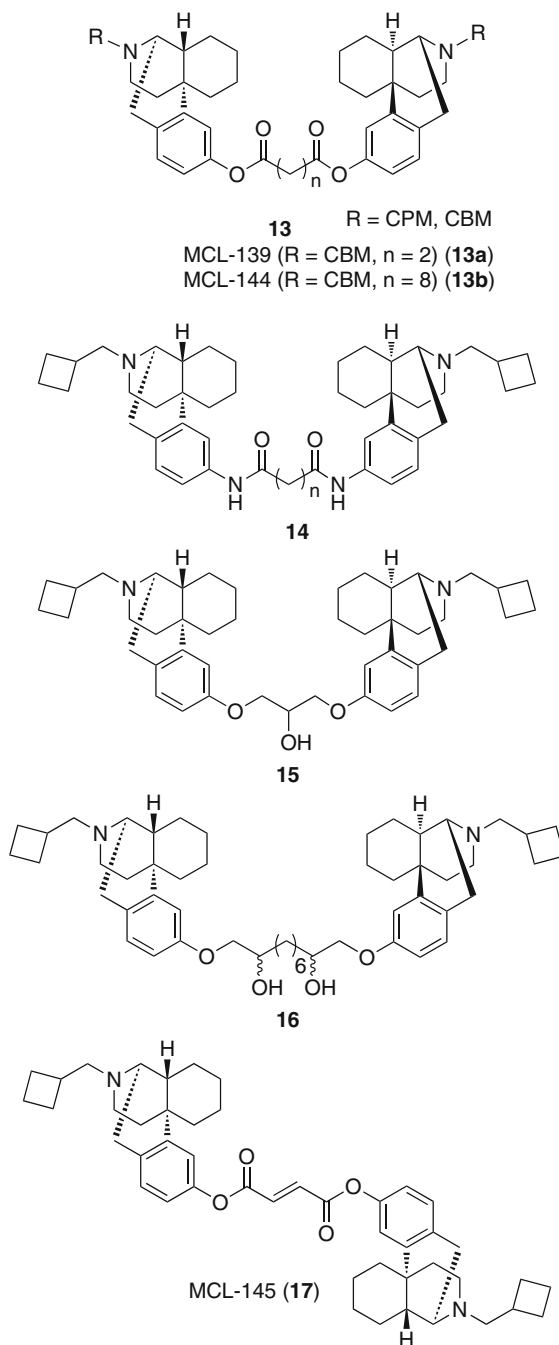
Fig. 4 (Continued)

Table 1 Binding affinities of cyclorphan (**6**), butorphan (**7**), twin drugs **12**, **13**, and **15–17** to the opioid receptors

Compound	$K_i (\mu)$ (nM)	$K_i (\delta)$ (nM)	$K_i (\kappa)$ (nM)
Cyclorphan (**6**)	0.062	1.9	0.034
Butorphan (**7**)	0.23	5.9	0.079
12a ($n = 3$)	7.1	180	6.2
12b ($n = 10$)	66	2,500	120
MCL-139 (**13a**)	0.16	9.4	0.076
MCL-144 (**13b**)	0.09	4.2	0.049
13c (R = CPM, $n = 2$)	0.14	3.8	0.10
13d (R = CPM, $n = 8$)	0.93	32	0.41
15	0.95	37	0.99
16	2.4	27	1.4
MCL-145 (**17**)	0.20	9.4	0.078

emphasizes the importance of linker functionality for binding ability. The phenolic 3-hydroxy group is also known to be one of the crucial functional groups for binding to the opioid receptors [39–41] and intensive searches for bioisosteres of the phenolic hydroxy group have been carried out [42–58]. Notably, some twin drugs substituted at the 3-hydroxy group displayed sufficient binding to the opioid receptors. Among the twin drugs with ester spacers, MCL-139 (**13a**, R = CBM (cyclobutylmethyl), $n = 2$), MCL-144 (**13b**, R = CBM, $n = 8$), and MCL-145 (**17**) strongly bound to the opioid receptors and their affinities were comparable to or higher than the parent compound **7** (Table 1).

Twin drug MCL-144 derivatives having (+) butorphan were also synthesized (Fig. 5). (+)(−)-MCL-144 (**13b′**) had 30- to 108-fold stronger binding affinities than (+)(+)-MCL-144 (**13b″**) but 5- to 24-fold weaker binding than (−)(−)-MCL-144 (**13b**), agreeing with a previous report [59]. A good relationship between the affinities and the number of methylene units in the ester linker was observed and compound **13b** with eight methylene units showed the highest affinity among analogs with two to ten methylene units except for compound **13a** with an ethylene unit or **17** with a vinylene unit. In the functional assay ([^{35}S]GTPγS binding assay), compounds **13a** and **13b** were partial μ agonists and full κ agonists (Table 2) [35]. On the other hand, compound **17** showed bell-shaped agonist activities at μ and κ receptors with a maximum [^{35}S]GTPγS binding at around 10^{-7} M [60]. Intracerebroventricular (i.c.v.) administration of compound **17** produced dose-dependent antinociception (ED$_{50}$ = 0.27 nmol) in the mouse warm-water-tail-flick test, and its activities were more potent than butorphan (**6**) itself (ED$_{50}$ = 7.3 nmol) and equipotent to morphine. Antinociceptive effects induced by **17** were blocked by an i.c.v. treatment of μ antagonist β-funaltrexamine (β-FNA) or κ antagonist nor-BNI, but not by δ antagonist NTI. Moreover, compound **17** at a low dose (0.05 nmol, i.c.v.) inhibited the morphine-induced antinociception [60]. *In vivo* pharmacological effects of the most potent agonist **13b** were also evaluated. The twin drug **13b** bridged with an ester linker with eight methylene units exhibited analgesic effects in a dose-dependent manner. Its potency (ED$_{50}$ = 3.0 nmol, i.c.v.) was about twice that of butorphan (**7**). Antinociception induced by i.c.v. administration of **13b** was

Fig. 5 Structures of twin drugs **13b–13b″**

(-)(-)-MCL-144 (**13b**)

(+)(-)-MCL-144 (**13b'**)
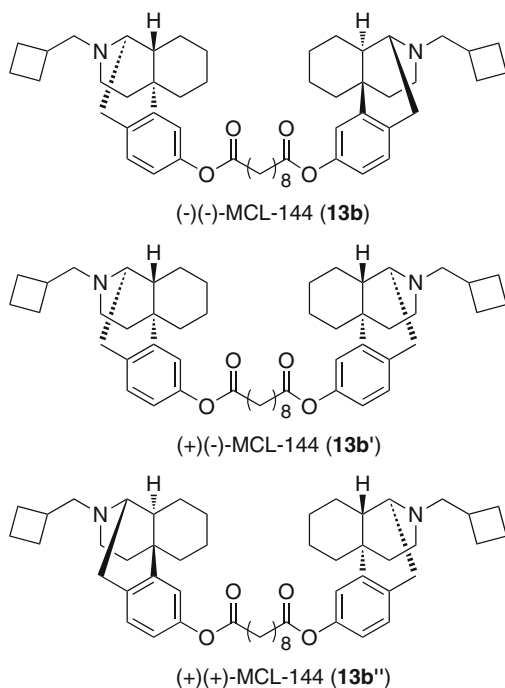
(+)(+)-MCL-144 (**13b''**)

Table 2 Pharmacological properties of compounds MCL-139 (**13a**) and MCL-144 (**13b**) for μ and κ opioid receptors in [^{35}S]GTPγS binding assay

Compound	Receptor type	Pharmacological properties	E_{max} (%)	EC_{50} (nM)	I_{max} (%)	IC_{50} (nM)
MCL-139	μ	Partial agonist	50	7.4	50	170
(**13a**)	κ	Agonist	70	4.5	NI[a]	NI[a]
MCL-144	μ	Partial agonist	50	1.3	60	16
(**13b**)	κ	Agonist	60	0.85	NI[a]	NI[a]

[a]No inhibition

antagonized by an i.c.v. treatment of β-FNA or nor-BNI, but not by δ antagonist ICI 174,864 [61]. On the other hand, intraperitoneally (i.p.) administered compound **13b** produced antinociceptive effects lasting no more than 2 h, but its analgesia was not blocked by i.p. treatment of nor-BNI. Moreover, pretreatment with **13b** 150 min prior to administration of a κ agonist U50,488 attenuated antinociception induced by the κ agonist, suggesting that compound **13b** would not be a κ agonist, but rather a κ antagonist when it was administered by the i.p. route [62]. These outcomes from i.c.v. or i.p. injection of **13b** may result from a metabolite of **13b**. It is worth noting that i.p. injection of compound **13b** dose-dependently attenuated immobility in the forced-swim test, suggesting that the compound **13b** may have antidepressant effects [61]. This observation is consistent with recent studies that activation of the κ receptor would induce depression-like behaviors [63, 64] and vice versa [65–67].
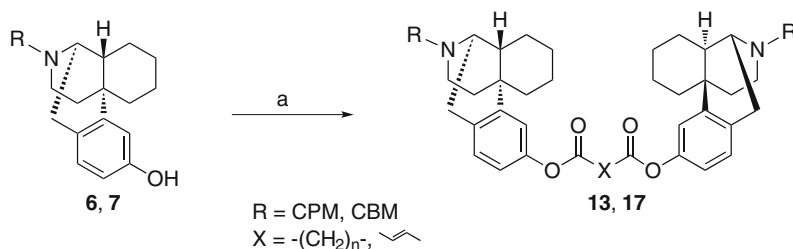
Scheme 1 Synthesis of compounds **13** and **17**. Reagents and conditions: (a) Et$_3$N, ClCOXCOCl, CH$_2$Cl$_2$

There are no reports of the detailed pharmacological effects of compound **13a**. In general, ester moieties are labile to chemical and enzymatic hydrolysis. Therefore, it is not clear that the observed pharmacological effects of these twin drugs with ester spacers were derived from the twin drugs themselves or from their metabolites. Since the half-life of compound **13b** was 46 min in a phosphate buffer (pH 7.4) at 37 °C[1] [37], it was unlikely that metabolites of the twin drugs, at least compound **13b**, were mainly responsible for in their *in vitro* pharmacological effects. Although the half-life of **13b** was 70 min in the rat brain homogenate [61], further investigation would be needed to understand its *in vitro* pharmacological effects. Twin drugs **13** and **17** with ester spacers were synthesized by coupling reaction of compounds **6** or **7** with the appropriate diacyl chloride (Scheme 1).

Twin drug MCL 450 (**19**) consisting of butorphan (**7**) and the δ selective peptidic antagonist Dmt-Tic (**18**) [68] has also been reported (Fig. 6) [69]. MCL 450 (**19**) was synthesized by coupling reaction of butorphan (**7**) with Boc-β-Ala-OH and subsequent deprotection followed by coupling reaction with protected Dmt-Tic using EDC and HOBt (Scheme 2). MCL 450 (**19**) inherited the *in vitro* pharmacological features of each pharmacophore **7** and **18** to bind strongly with all three opioid receptors (Table 3) and to be a μ and κ agonist and a δ antagonist (Table 4).

Twin drugs **25–27** including butorphan (**7**) and the other pharmacophore nalbuphine (**22**: μ agonist/antagonist, κ agonist,), naltrexone (**23**: μ antagonist, κ antagonist), or naloxone (**24**: μ antagonist, κ agonist/antagonist) were also synthesized (Fig. 7) and their *in vitro* pharmacological profiles were evaluated (Tables 5–7). However, their *in vivo* pharmacological effects were not reported [70].

Very recently, the KMN series of twin drugs **30** tethering the μ antagonist β-naltrexamine (**28**) [71] pharmacophore to the selective κ antagonist 5′-guanidinonaltrindole (5′-GNTI, **29**) [72, 73] pharmacophore were designed for investigation of κ–μ heterodimerization (Fig. 8) [74]. While KMN twin drugs **30** with spacers of various length, including KMN-21 (**30a**, $n = 3$) itself, inhibited DAMGO (μ agonist) and U69,593 (κ agonist) induced Ca^{2+} release in preparations

---

[1]It is generally accepted that the rate of a reaction doubles with increase in temperature of 10 °C. Therefore, the rate of hydrolysis of the twin drugs at 25 °C (incubating temperature applied in *in vitro* assays) is predicted to be approximately one-half of that at 37 °C.
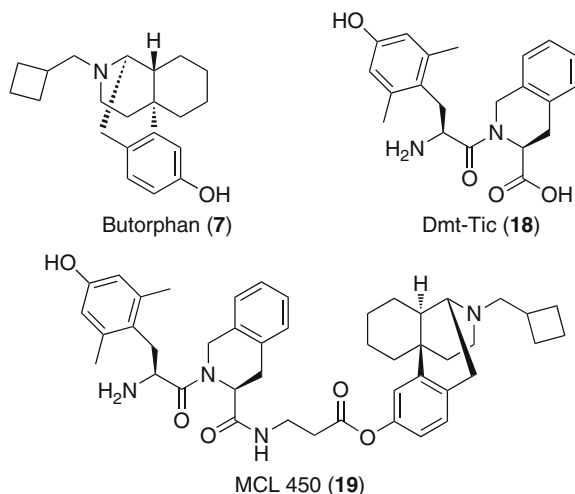
Fig. 6 Structures of Butorphan (7), Dmt-Tic (18), and MCL 450 (19)
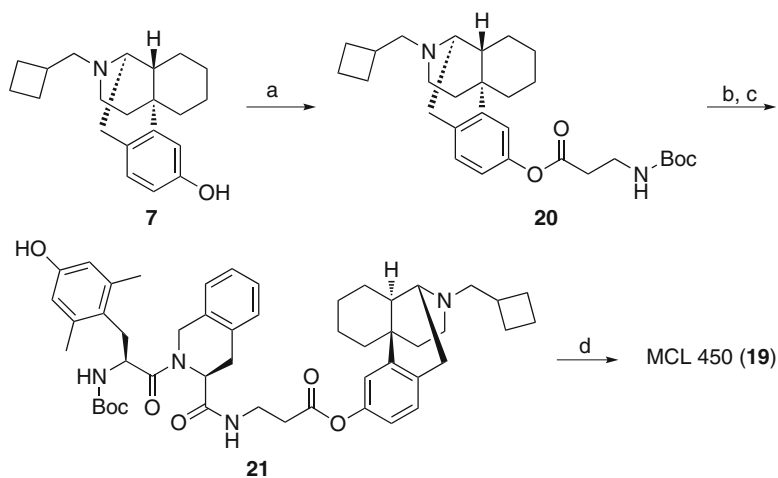
Scheme 2 Synthesis of MCL 450 (19). Reagents and conditions: (a) Boc-β-Ala-OH, EDC, DMAP, CH₂Cl₂, rt, overnight, 50%; (b) TFA, CH₂Cl₂, rt, 2 h, 90%; (c) Boc-Dmt-Tic, EDC, HOBt, NMM, DMF, 0 °C to rt, 27 h, 83%; (d) TFA, CH₂Cl₂, rt, 2 h, 92%

Table 3 Binding affinities of butorphan (7), Dmt-Tic (18), and MCL 450 (19) to the opioid receptors

Compound	K_i (μ) (nM)	K_i (δ) (nM)	K_i (κ) (nM)
Butorphan (7)	0.23	5.9	0.079
Dim-Tic (18)	894	1.6	37,500
MCL 450 (19)	0.69	1.5	0.28

Table 4 Pharmacological properties of MCL 450 (**19**) for the μ, δ, and κ opioid receptors in [^{35}S] GTPγS binding assay

Receptor type	Pharmacological properties	E_{max} (%)	EC_{50} (nM)	I_{max} (%)	IC_{50} (nM)
μ	Agonist/antagonist	79	8.9	47	97
δ	Antagonist	18	2.8	84	3.9
κ	Agonist	130	6.0	NI[a]	NI[a]

[a]No inhibition

nalbuphine (**22**)   naltrexone (**23**)   naloxone (**24**)

25: R = **22**-3-yl
26: R = **23**-3-yl
27: R = **24**-3-yl
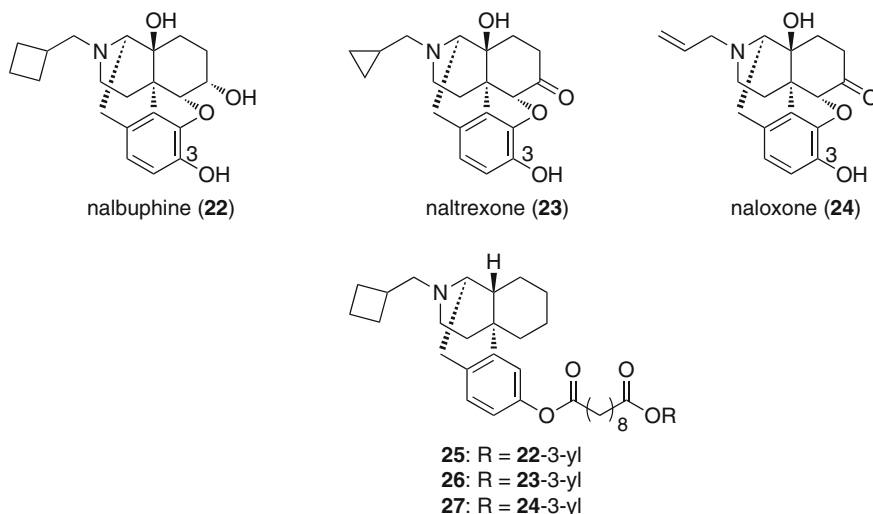
Fig. 7 Structures of nalbuphine (**22**), naltrexone (**23**), naloxone (**24**), and twin drugs **25–27**

Table 5 Binding affinities of compounds **22–27** to the opioid receptors

Compound	K_i (μ) (nM)	K_i (δ) (nM)	K_i (κ) (nM)
Nalbuphine (**22**)	0.89	240	2.2
Naltrexone (**23**)	0.23	38	0.25
Naloxone (**24**)	0.79	76	1.1
25	0.46	28	0.34
26	0.29	15	0.12
27	0.43	39	0.13

Table 6 Pharmacological properties of compound **22–27** for the μ opioid receptor in [^{35}S]GTPγS binding assay

Compound	Pharmacological properties	E_{max} (%)	EC_{50} (nM)	I_{max} (%)	IC_{50} (nM)
Nalbuphine (**22**)	Agonist/antagonist	47	14	74	110
Naltrexone (**23**)	Antagonist	6.7	NA[a]	79	17
Naloxone (**24**)	Antagonist	13	NA[a]	92	23
25	Antagonist	5.1	NA[a]	94	18
26	Agonist/antagonist	43	4.4	50	160
27	Agonist/antagonist	34	2.0	73	25

[a]Not applicable

Table 7 Pharmacological properties of compounds **22–27** for the κ opioid receptor in [^{35}S]GTPγS binding assay

Compound	Pharmacological properties	E_{max} (%)	EC_{50} (nM)	I_{max} (%)	IC_{50} (nM)
Nalbuphine (**22**)	Agonist	81	27	NI[a]	NI[a]
Naltrexone (**23**)	Antagonist	10	NA[b]	67	200
Naloxone (**24**)	Agonist/antagonist	25	10	55	320
25	Agonist/antagonist	67	3.2	39	600
26	Agonist	76	3.4	NI[a]	NI[a]
27	Agonist	86	1.6	NI[a]	NI[a]

[a]No inhibition
[b]Not applicable
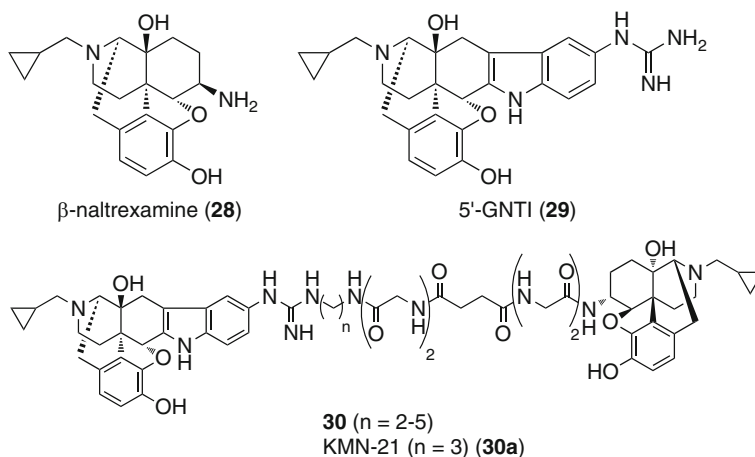
Fig. 8 Structures of β-naltrexamine (**28**), 5′-GNTI (**29**), and KMN twin drugs **30**

of cells singly expressing μ and κ receptors, only KMN-21 (**30a**) antagonized both DAMGO and U69,593 induced Ca^{2+} release in the cells that expressed both the μ and κ receptors together (μ and κ receptors coexpressing cells). These results suggest that KMN-21 (**30a**) with a linker containing 21 atoms would selectively antagonize the activation of κ–μ heterodimers. Compounds **30** were synthesized by coupling compound **32**, having the oligoglycine unit, with N-aminoalkyl 5′-GNTI **35** in a reaction mediated by DCC and HOBt, which was prepared by guanidylation of 5′-amino-NTI **36** [75] with thiourea **34** in the presence of HgCl$_2$ [76, 77] (Scheme 3).

2.2 δ and κ Pharmacophores

To investigate the δ – κ heterodimerization in the spinal cord [78–80], the KDN series of twin drugs **37** incorporating the selective δ antagonist NTI (**5**) [9–11] and
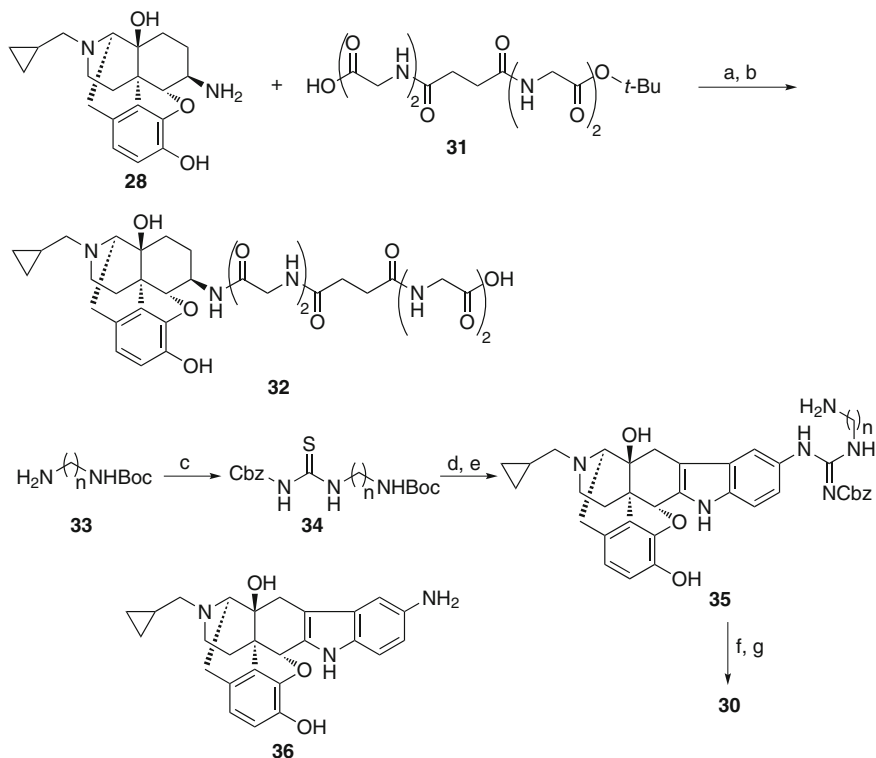
Scheme 3 Synthesis of compounds **30**. Reagents and conditions: (a) DCC, HOBt, DMF; (b) TFA, CH$_2$Cl$_2$; (c) Cbz-Cl, KSCN; (d) **36**, HgCl$_2$, Et$_3$N; (e) HCl/Et$_2$O; (f) **32**, DCC, HOBt, DMF; (g) cyclohexadiene, Pd/C

the selective κ antagonist 5′-GNTI (**29**) [72, 73] were designed (Fig. 9) [81]. The spacer consisted of glycine units and the alkyldiamine moiety. The former maintains a favorable balance between hydrophilicity and lipophilicity, and the latter adjusts the length of the spacer by one atom unit. Twin drugs **37** were synthesized in the manner similar to the synthesis of compounds **30** (Scheme 4). Among the synthesized twin drugs, KDN-21 (**37a**, $n = 2$, $m = 3$) showed 200-fold stronger binding affinity in the δ and κ receptors coexpressing cells than in the mixed preparation of cells expressing the δ and κ receptors singly. Moreover, NTI and 5′-GNTI derivatives **38** and **39** having a spacer whose length corresponds to that of **37a** exhibited very weak binding affinities in the δ and κ receptors coexpressing cells (Table 8). These outcomes suggested that the influence of the spacer had negligible effects on binding and that KDN-21 (**37a**) would bridge the δ and κ binding sites, that is, the δ – κ heterodimer. In the mouse tail flick test, intrathecal (i.t.) administration of **37a** effectively attenuated the antinociceptive effects induced by i.t. injection of DPDPE (δ$_1$ agonist) [82] or bremazocine (κ$_2$ agonist)

NTI (**5**)

5'-GNTI (**29**)

37 (n = 1, 2; m = 2-5)
KDN-21 (n = 2, m = 3) (**37a**)

38

39
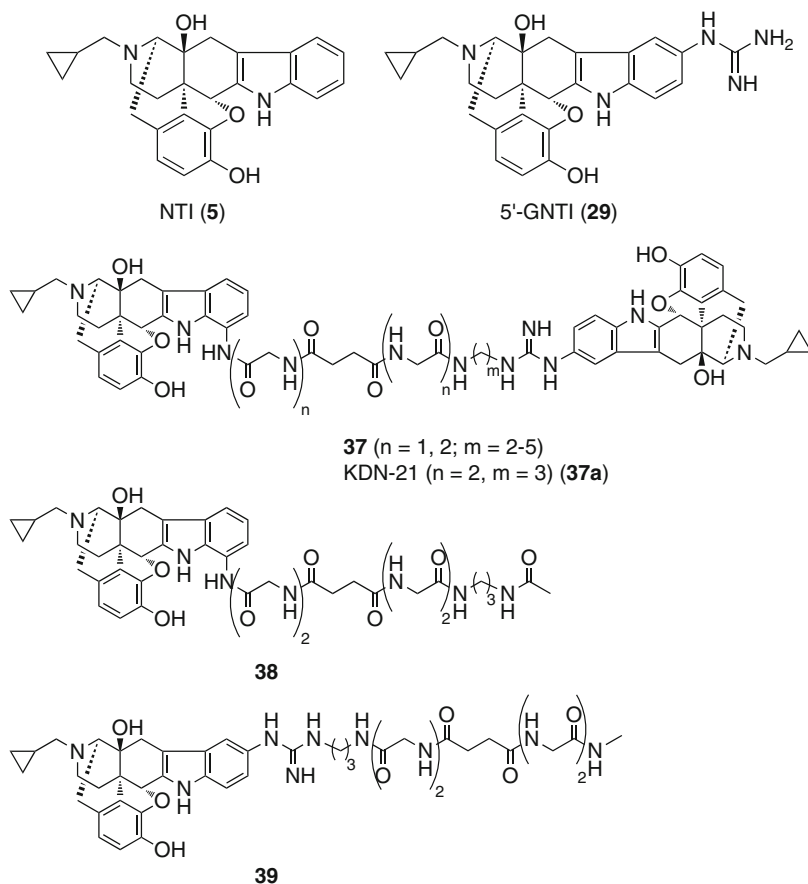
Fig. 9 Structures of NTI (**5**), 5′-GNTI (**29**), KDN twin drugs **37**, and compounds **38** and **39**

[83, 84], but was almost ineffective against deltorphin II (δ_2 agonist) [85] or U50,488 (κ_1 agonist) [83, 86]. In contrast, i.c.v. administered **37a** produced analgesic effects ($ED_{50} = 31$ pmol) but the low dose of **37a**, which showed no analgesia, exhibited antagonism whose profile was different from that obtained by the i.t. route: DPDPE induced antinociception was antagonized but analgesia produced by bremazocine, U50,488, or deltorphin II was not. Taken together, this outcome suggested that KDN-21 (**37a**) bound the $\delta - \kappa$ heterodimer in the spinal cord but not in the brain and that the $\delta - \kappa$ heterodimer seemed to correspond to the δ_1 and κ_2 subtypes. The receptor subtype selectivity of **37a** was also confirmed by mitogen-activated protein kinase (MAPK) activity assay [87].

Tethering the selective δ antagonist NTI (**5**) [9–11] with the κ_1 agonist ICI 199,441 (**43**) [88] gave the KDAN series of twin drugs **44** (Fig. 10) [89]. Twin drugs **44** were synthesized in a similar manner to the synthesis of compound **30**. In the
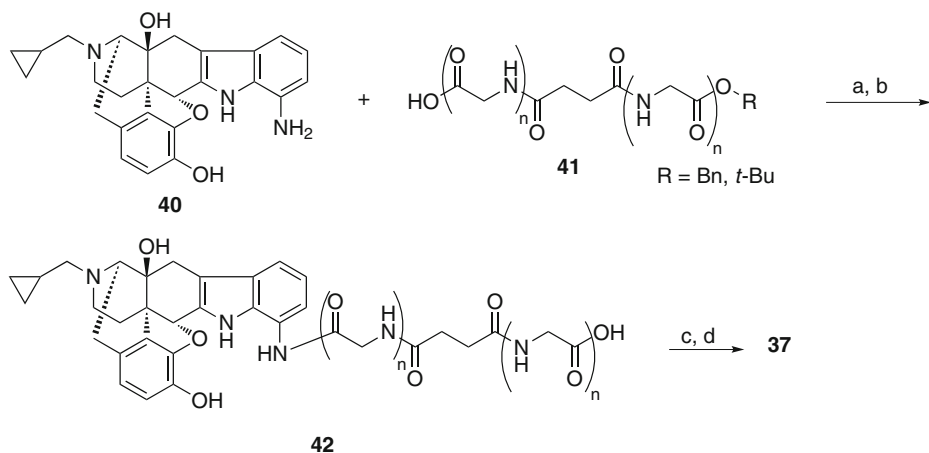
Scheme 4 Synthesis of compounds **37**. Reagents and conditions: (a) DCC, HOBt; (b) 1 M HCl, AcOH, or H₂ (80 psi), Pd/C; (c) **35**, DCC, HOBt; (d) H₂ (85 psi), Pd/C

Table 8 Binding affinities of KDN-21 (**37a**) and compounds **38** and **39** to the δ and κ receptors coexpressing cell or the mixed cells expressing the δ and κ receptors singly

Compound	K_i (coexpressed δ − κ) (nM)	K_i (mixed δ + κ) (nM)
KDN-21 (**37a**)	0.3	63
38	>1,000	199
39	>1,000	54.8
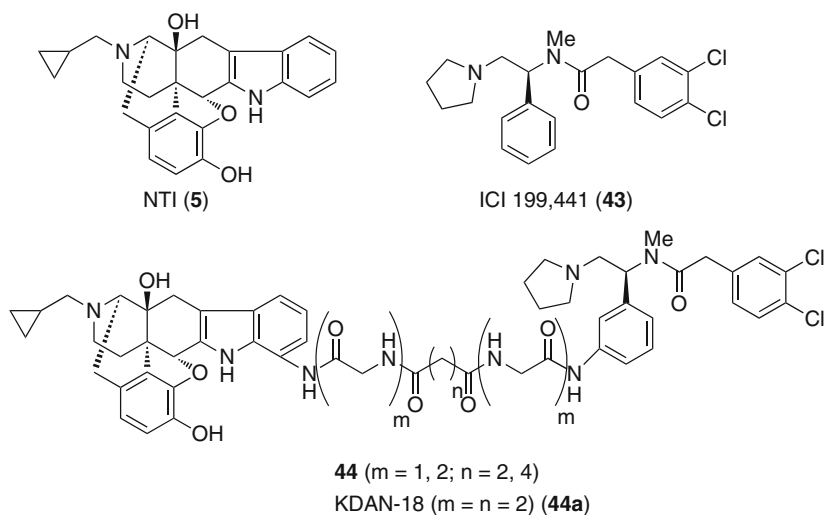
Fig. 10 Structures of NTI (**5**), ICI 199,441 (**43**), and KDAN twin drugs **44**

Table 9 Binding affinities[a] of KDAN-18 (**44a**) to the δ and κ receptors coexpressing cell or the preparation of mixed cells separately expressing the δ and κ receptors singly in the presence or absence of δ antagonists

Antagonist	K_i (coexpressed δ – κ) (nM)	K_i (mixed δ + κ) (nM)
None	0.06	2.51
BNTX	0.19	1.14
NTB	2.34	1.94

[a][^{3}H] U69,593 was used

binding assay using [^{3}H] deltorphin II (δ$_2$ agonist) or [^{3}H] U69,593 (κ$_1$ agonist) [83], KDAN-18 (**44a**, $m = n = 2$) showed respective 65- or 42-fold higher affinities in the δ and κ receptors coexpressing cell as compared to the mixed cells singly expressing the δ and κ receptors ([^{3}H] deltorphin II: K_i (coexpressed δ – κ) = 0.008 nM, K_i (mixed δ + κ) = 0.52 nM; [^{3}H] U69,593: K_i (coexpressed δ – κ) = 0.06 nM, K_i (mixed δ + κ) = 2.51 nM). The binding affinity of **44a**, as evaluated by [^{3}H] U69,593 in the δ and κ receptors coexpressing cells, significantly decreased in the presence of NTB (δ$_2$ antagonist) [90, 91], but not with BNTX (δ$_1$ antagonist) [92, 93] (Table 9). Moreover, the antinociceptive effects induced by i.t. administered **44a** were attenuated by i.t. treatment of NTB or nor-BNI (κ$_1$ antagonist) [94] but not by i.t. injection of BNTX. Based on these results, it was proposed that KDAN-18 (**44a**) would bridge neighboring δ and κ homodimer, giving rise to δ$_2$ and κ$_1$ subtypes. This proposal was supported by the observation that KDN-21 (**37a**), which bound to the δ – κ heterodimer that would give rise to δ$_1$ and κ$_2$ subtypes, did not affect the antinociception induced by KDAN-18 (**44a**) [89].

2.3 μ and δ Pharmacophores

The μ and δ receptors interact with each other to potentiate morphine-induced antinociception [95] and to reduce morphine tolerance and physical dependence [96–100]. To investigate the participation of direct association between the μ and δ receptors in the pharmacological phenomena mentioned above, the MDAN series of twin drugs including the μ agonist oxymorphone (**45**) [71] and the selective δ antagonist NTI (**5**) [9–11] pharmacophores were designed (Fig. 11) [101]. These twin drugs were synthesized by a process similar to the synthesis of compound **30**. In the mouse tail-flick test, i.c.v. administration of MDAN-19 (**46a**, $n = 5$) and MDAN-21 (**46b**, $n = 7$) produced antinociception and their antinociceptive effects (**46a**: ED$_{50}$ = 0.43 nmol; **46b**: ED$_{50}$ = 0.08 nmol) were less potent than oxymorphone (ED$_{50}$ = 0.043 nmol), but more potent than morphine (ED$_{50}$ = 4.1 nmol). Notably, the twin drugs **46a** and **46b** showed analgesic effects by not only i.c.v., but also intravenous (i.v.) administration [102]. Although i.c.v. pretreatment with δ antagonist NTI profoundly increased the
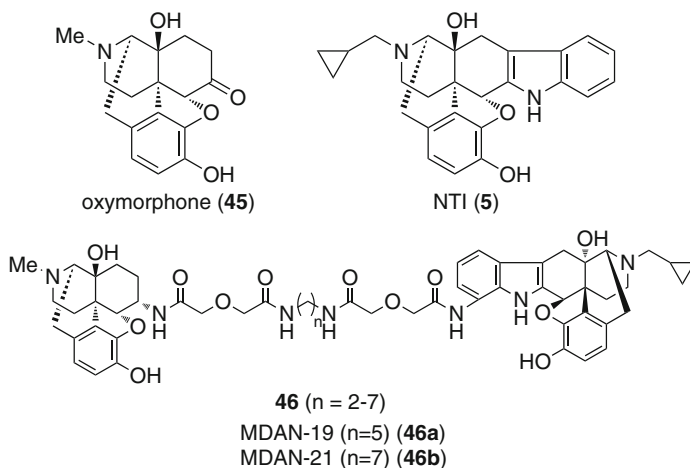
Fig. 11 Structures of oxymorphone (**45**), NTI (**5**), and MDAN twin drugs **46**

acute analgesic potency induced by i.c.v. injection of **46a** or other twin drugs having a shorter spacer length, the effect of i.c.v. pretreatment with NTI on the acute antinociceptive potency produced by i.c.v. administration of **46b** was marginal, suggesting that **46b** would more effectively interact with the μ–δ heterodimer.[2] Chronic effects were also evaluated using mice to which test compounds were i.c.v. infused for 3 days (chronic treatment). The potency of morphine-induced antinociception revealed a sixfold decrease (tolerance) and subcutaneous (s.c.) treatment with the opioid universal antagonist naloxone induced jumping (a sign of drug dependence) in the mice chronically treated with morphine. On the other hand, the antinociceptive potency of the twin drugs **46a** and **46b** did not change and almost no naloxone-induced jumping was observed in the mice chronically treated with **46a** or **46b**, respectively. Moreover, compounds **46a** and **46b** exhibited neither place preference nor place aversion in the conditioned place preference (CPP) test [77]. These results strongly suggest that the twin drugs **46a** and **46b** would be novel and potent analgesics without side effects of tolerance and dependence.

In the patent literature [103], i.v. administration of twin drug **47** consisting of the μ antagonist β-naltrexamine (**28**) [71] and the selective δ antagonist NTI (**5**) [9–11] pharmacophores was reported to reduce plasma glucose levels. Unfortunately, there have been no descriptions of the *in vitro* pharmacological profiles (Fig. 12).

---

[2]The authors proposed that MDAN-21 (**46b**) having a longer spacer could bridge the μ and δ receptors in multiple modes and that binding by MDAN-19 (**46a**) with a shorter linker would be less efficient than that by MDAN-21 (**46b**). As a result, the acute analgesic potency of **46a** would be affected by treatment with NTI.
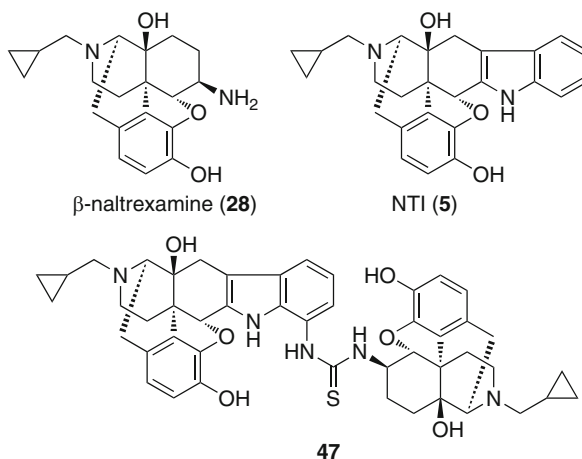
Fig. 12 Structures of β-naltrexamine (**28**), NTI (**5**), and twin drug **47**
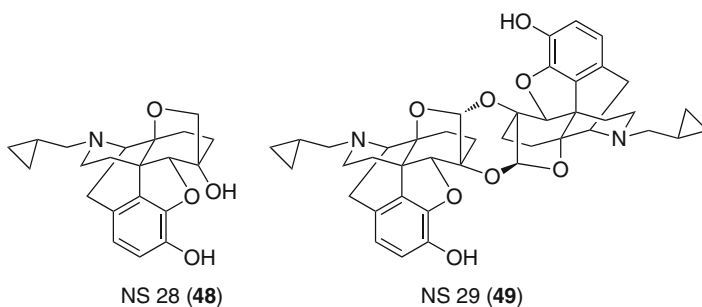
Fig. 13 Structures of NS 28 (**48**) and NS 29 (**49**)

2.4 Symmetrical Twin Drug

Although most of recently reported twin drugs are nonsymmetrical, symmetrical versions have also been reported.

Twin drug NS 29 (**49**) (Fig. 13) [104] consisting of two NS 28 (**48**) units (μ antagonist) [105] with a 1,4-dioxane spacer was synthesized as shown in Scheme 5. The key reaction was conversion of the inseparable mixture of compounds **54–56** into compound **57** under azeotropic reflux conditions. The structure of **57** was determined by X-ray crystallography. NS 28 (**48**) blocked only the morphine-induced [^{35}S]GTPγS binding, while twin drug NS 29 (**49**) attenuated the [^{35}S]GTPγS binding induced by morphine (μ agonist), U50,488 (κ agonist), and β-endorphin (putative ε agonist [106]), but not by SNC-80 (δ agonist), suggesting that dimerization of ligands could affect the selectivity of the monomer pharmacophores for different types of receptors.
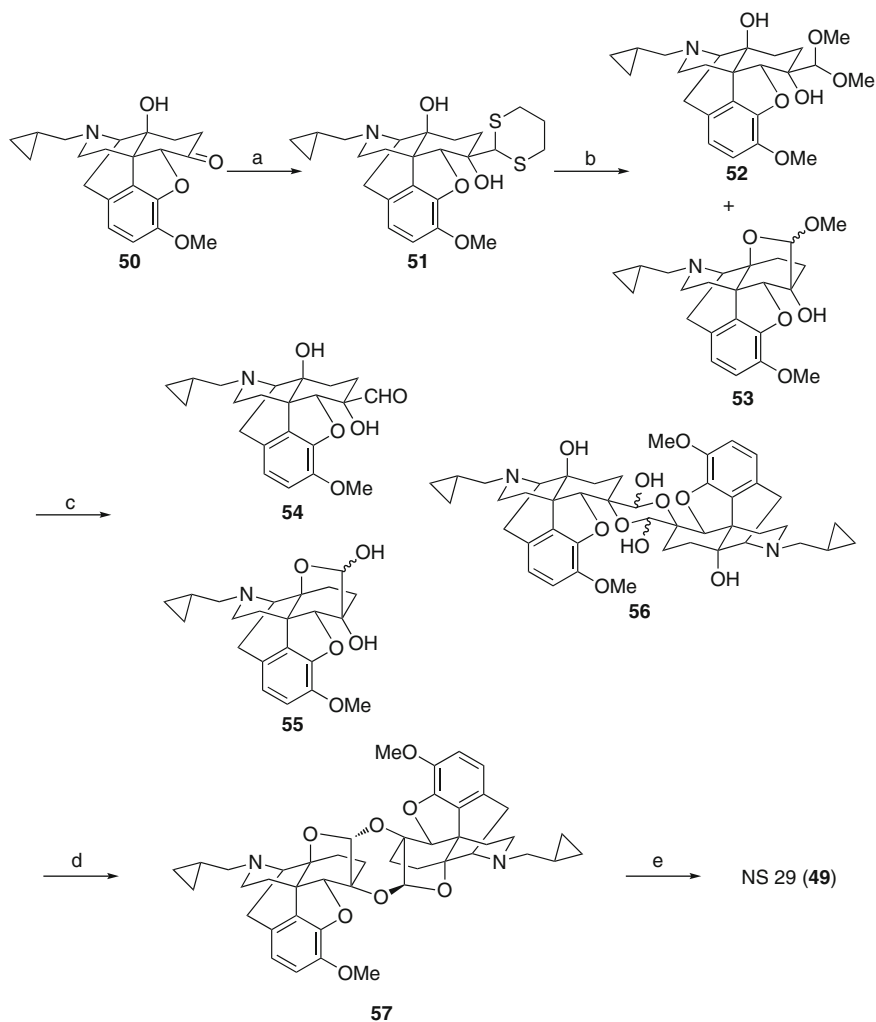
Scheme 5 Synthesis of NS 29 (**49**). Reagents and conditions: (a) 1,3-dithian, *n*-BuLi, THF, −70 °C to −60 ∼ −40 °C, 85%; (b) CH(OMe)$_3$, CuCl$_2$/CSA, MeOH, 50 °C, **52**: 65%, **53**: 18%; (c) 1 M HCl, reflux; (d) CSA, toluene, reflux, 23%; (e) *t*-BuOK, *n*-PrSH, DMF, 150 °C, 82%

3 Twin Drugs Consisting of Opioid and the Other Pharmacophores

Twin drugs consisting of opioid and the other pharmacophores have also been designed. Although many of the twin drugs belonging to this category are peptidic [107–119], non-peptidic twin drugs and non-peptide–peptide hybrids will be featured in this section.

3.1 Opioid and Imidazoline Binding Site Pharmacophores

The imidazoline binding site (IBS) was discovered as an imidazoline preferring binding site of the well-known antihypertensive drug clonidine in 1984 and classified into two types (I_1 and I_2) [120]. IBS ligands were reported to modulate antinociception [121, 122], tolerance [123–125], and dependence [126–128] induced by opioids. In a preliminary study [129], fentanyl (**58**) and the guanidine moiety, which mimics an endogenous I_2–IBS ligand agmatine (**59**) [130], were chosen as the opioid and I_2–IBS pharmacophores, respectively, to provide twin drugs **61** and **62**. Compounds **61** and **62** decreased the binding affinities for IBS, while **61b** and **62b**, having an acyclic guanidine moiety, maintained the affinities for opioid receptors (Fig. 14, Table 10). Compounds **61b** and **62b** showed opioid agonistic activities in the guinea pig ileum (GPI) assay, but their respective potencies were 9- and 31-fold weaker than that of morphine. I.p. administration of compounds **61b** or **62b** exhibited dose-dependent and naloxone-reversible antinociception in the mouse acetic acid writhing assay (**61b**: 50.7% inhibition of writhes at 20 mg/kg, **62b**: 47.4% inhibition of writhes at 25 mg/kg). Although the
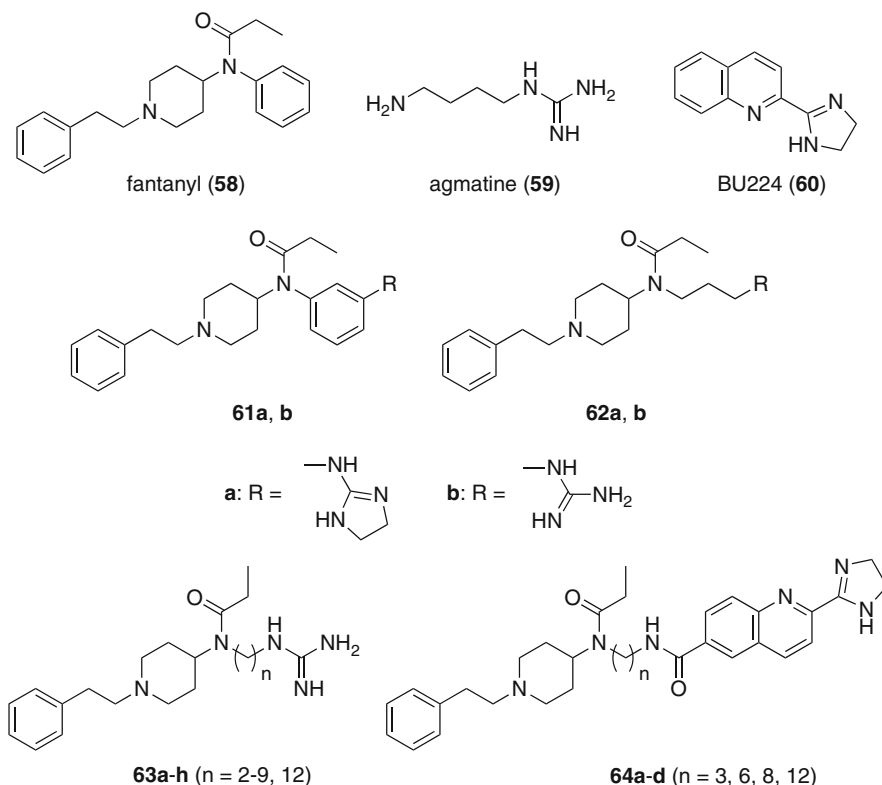
Fig. 14 Structures of fentanyl (**58**), agmatine (**59**), BU224 (**60**), and twin drugs **61–64**

Table 10 Binding affinities of compounds **61** and **62**, idazoxan, and fentanyl (**58**) to the opioid and I$_2$-imidazoline receptors

Compound	K_i (μ) (nM)	K_i (δ) (nM)	K_i (κ) (nM)	K_i (I$_2$) (nM)
Idazoxan[a]	ND[b]	ND[b]	ND[b]	307
Fentanyl (**58**)[c]	6	663	298	5,462
61a	7,119	12,078	11,551	9,630
61b	7.8	181	841	1,890
62a	1,751	24,955	5,043	2,327
62b	37	1,744	355	2,022

[a]Idazoxan was used as a control compound for the I$_2$ ligand
[b]Not determined
[c]Fentanyl was used a control compound for the opioid ligand

Table 11 Binding affinities of compounds **63** and **64**, idazoxan, and fentanyl (**58**) to the μ opioid and I$_2$-imidazoline receptors

Compound	n	K_i (μ) (nM)	K_i (I$_2$) (nM)
Idazoxan[a]	–	ND[b]	28
Fentanyl (**58**)[c]	–	2.9	8,593
63a	2	433	437
63b (=**62b**)	3	23	1,920
63c	4	0.59	>10,000
63d	6	1.04	409
63e	7	0.37	6,627
63f	8	37	126
63g	9	26	58
63h	12	477	6.5
64a	3	6,142	875
64b	6	2,168	323
64c	8	339	>10,000
64d	12	545	547

[a]Idazoxan was used as a control compound for the I$_2$ ligand
[b]Not determined
[c]Fentanyl was used a control compound for the μ opioid ligand

outcome seems to indicate that compound **61b** was superior to compound **62b** as a lead compound for an analgesic, further investigation of compound **62** derivatives was carried out [131, 132]. Twin drugs **63** having various chain lengths were synthesized and evaluated for their binding affinities (Fig. 14, Table 11). The optimal chain length was four to seven carbon units for the μ opioid receptor, while the best binding affinity for I$_2$-IBS was observed in compound **63h** with the longest spacer. Although the twin drugs **64** incorporating the BU224 (**60**, I$_2$-IBS ligand) structure [133] were also prepared (Fig. 14), their binding affinities for both receptors were comparable to or weaker than those of compounds **63**. Compound **63d**, which showed the highest μ opioid receptor along with an acceptable I$_2$-IBS affinity, induced [^{35}S]GTPγS binding and its [^{35}S]GTPγS binding was attenuated by naloxone. However, the maximum binding (E_{max}) of **63d** was about half the value of that of DAMGO (μ full agonist), indicating that **63d** would have a partial
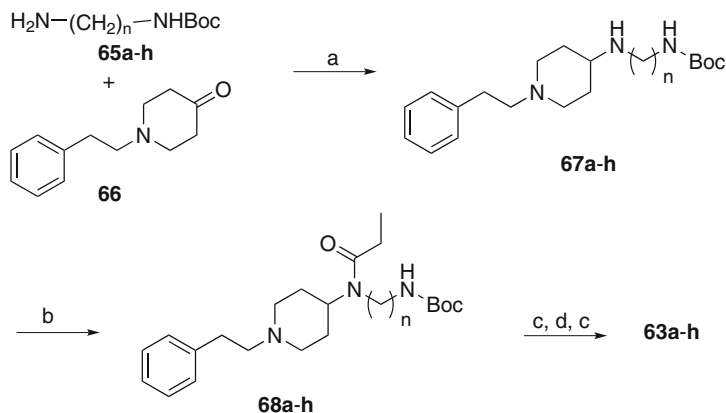
Scheme 6 Synthesis of twin drugs **63**. Reagents and conditions: (a) NaBH$_3$CN, MS 3A, MeOH, rt, 50–82%; (b) (EtCO)$_2$O, DMAP, py, CH$_2$Cl$_2$, rt, 53–86%; (c) TFA, CH$_2$Cl$_2$, 60–99%; (d) BocNH (C=S)NHBoc, HgCl$_2$, Et$_3$N, CH$_2$Cl$_2$, rt, 50–95%

μ agonist activity. Unfortunately, **63d** produced no antinociception in both the acetic acid writhing and the hot-plate tests. These outcomes may stem from low efficacy for the μ opioid receptor, poor permeability of the blood-brain barrier, or both. Synthesis of twin drugs **63** commenced with reductive amination of *N*-phenethylpiperidone (**66**) with mono-Boc-protected alkyldiamines **65** (Scheme 6). Introduction of the guanidine moiety was completed by the reaction of the amine derived from Boc-protected amine **68** with Boc-protected thiourea in the presence of HgCl$_2$ [76, 77].

3.2 Opioid and Substance P Pharmacophores

The neuropeptide substance P (SP) and endogenous opioid peptides are intimately involved in the regulation and modulation of pain transmission [134–139]. SP is known to enhance analgesia and to inhibit tolerance induced by opioids [108, 140, 141]. Based on such background information, several peptidic twin drugs with opioid and SP pharmacophores have been reported [108–112]. Recently a chimeric twin drug MPS9 (**69**) containing morphine and *N*-acetyl SP3–11 ((α-NHAc)Lys-Pro-Gln-Gln-Phe-Phe-Gly-Leu-Met-NH$_2$) pharmacophores with a succinate linker have been synthesized (Fig. 15) and showed moderate to strong binding affinities (approximate affinity: 10^{-7} M (μ and κ receptors), 10^{-6} M (δ receptor), 10^{-9} M (SP receptor)) [142]. Intramuscular (i.m.) administration of compound **69** elicited bell-shaped antinociceptive effects with maximum efficacy at 0.2 mg/kg. This phenomenon was also observed when peptidic twin drugs [107, 108] or coadministration of both morphine and SP [140, 141] were applied. The analgesic effects
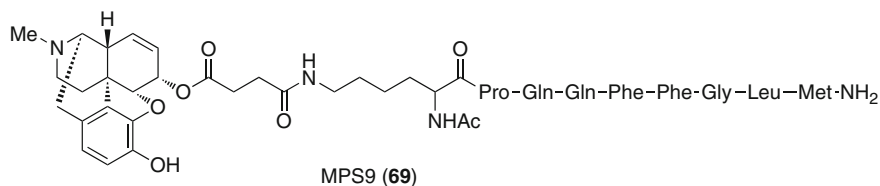
Fig. 15 Structure of MPS9 (69)

produced by **69** were attenuated by L733060 (SP antagonist) or nor-BNI (κ antagonist). Interestingly, twin drug **69** exhibited antinociception in morphine-tolerant rats. Compound **69** was prepared by reaction of morphine with succinic anhydride to give morphine 6-hemisuccinate [143] and subsequent coupling reaction with the SP3–11 fragment using *N*-hydroxysuccinimide.

3.3 Opioid and Cholecystokinin Pharmacophores

Cholecystokinin (CCK) is known to have anti-opioid effects [144–146] and CCK antagonists potentiate opioid-induced antinociception and prevent tolerance and dependence by opioids [147–149]. Based on this information, several peptidic twin drugs consisting of an opioid and CCK pharmacophores have been reported [113–118]. Recently, to investigate the possible existence of heterodimeric μ opioid/ CCK_2 receptors, which may be responsible for the pharmacological observations mentioned above, the twin drugs **71** and **72** possessing the μ agonist oxymorphone (**45**) [71] and the CCK_2 antagonist L-365,260 (**70**) [150] with spacers of various lengths were designed (Fig. 16) [151]. From the bioluminescence resonance energy transfer (BRET) studies [152], it is suggested that the μ opioid receptor and the CCK_2 receptor would form homodimers in the COS cells. Whereas compound **71a**, possessing an 18 atom unit spacer, increased the BRET ratio in COS cells expressing both tagged μ opioid and CCK_2 receptor constructs, compound **72**, having a shorter spacer, did not influence the BRET ratio. The increment of the BRET ratio induced by **71a** was significantly attenuated by the CCK_2 antagonist **73** with a linker. These results suggest that compound **71a** can simultaneously bind to both receptors but compound **72** cannot. On the basis of the results obtained, it was proposed that the μ opioid and CCK_2 receptors coexpressed in COS cell would be present as more stable homodimers composed of the individual receptors and that an appropriate twin drug which can spontaneously bind to each type of receptor would induce heterodimerization of these receptors.

Moreover, in a tolerance study using the mouse tail-flick test, μ agonist **74** with a spacer produced tolerance but twin drugs **71a** and **72** induced no significant tolerance. Taken together, these results suggest that the heterodimerization of μ opioid and CCK_2 receptors would not be relevant to blockade of tolerance. The twin
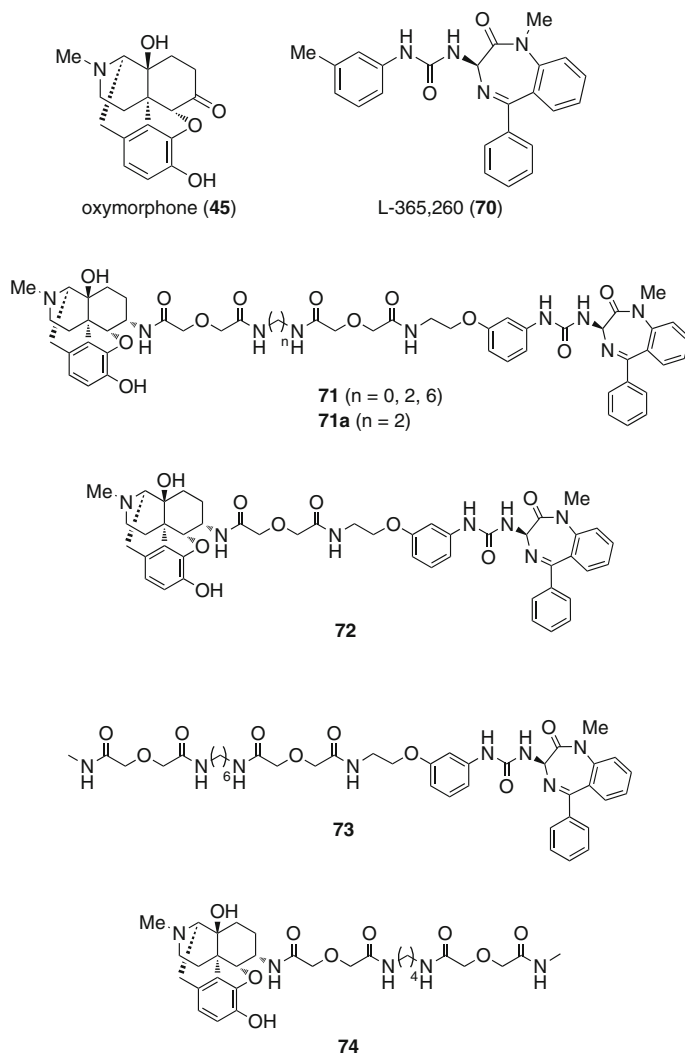
Fig. 16 Structures of oxymorphone (**45**), L-365,260 (**70**), twin drugs **71** and **72**, and compounds **73** and **74**

drugs **71a** and **72** were synthesized as shown in Scheme 7. Chiral (−)-**75** obtained by optical resolution [153] of racemic **75** [154] was converted into isocyanate **76** by treatment with triphosgene. Oxymorphamine derivatives **80** and **81** having the corresponding spacer were prepared by a procedure similar to the synthesis of **30** followed by reduction of the nitro group in precursors of **80** and **81** using Pd/C catalyst. The reaction of the amino group in the resulting compounds **80** and **81** with isocyanate **76** provided twin drugs **71** and **72**.
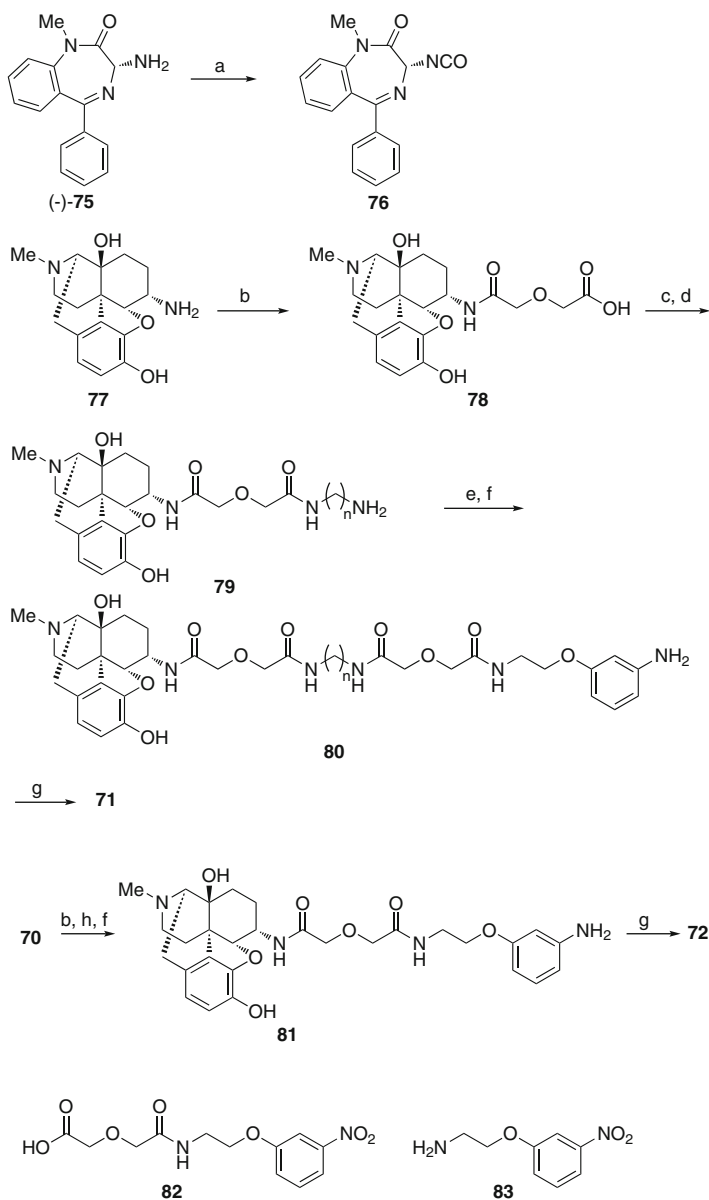
Scheme 7 Synthesis of twin drugs **71** and **72**. Reagents and conditions: (a) CO(OCCl$_3$)$_2$, sat. Na$_2$CO$_3$aq/CH$_2$Cl$_2$, 0 °C; (b) diglycolic anhydride, CH$_2$Cl$_2$, rt; (c) mono-Boc-diamines, DCC, HOBt, DMF; (d) TFA, CH$_2$Cl$_2$; (e) **82**, DCC, HOBt; (f) H$_2$ (50 psi), Pd/C, MeOH; (g) **76**, DMF; (h) **83**, DCC, HOBt, DMF

3.4 Miscellaneous

Twin drug **85** consisting of fentanyl (**58**) (μ agonist) and indomethacin (**84**) (NSAID) pharmacophores [155], twin drugs **89** and **90** containing tramadol (**86**) (μ agonist) and metoclopramide (**87**) (5-HT$_4$ agonist) or cisapride (**88**) (5-HT$_4$ agonist) pharmacophores [156], and twin drug **91** including fentanyl (**58**) (μ agonist) and adenosine (**92**) (A$_1$ agonist) pharmacophores [157] were synthesized (Fig. 17). Only the *in vitro* pharmacological properties have been reported for
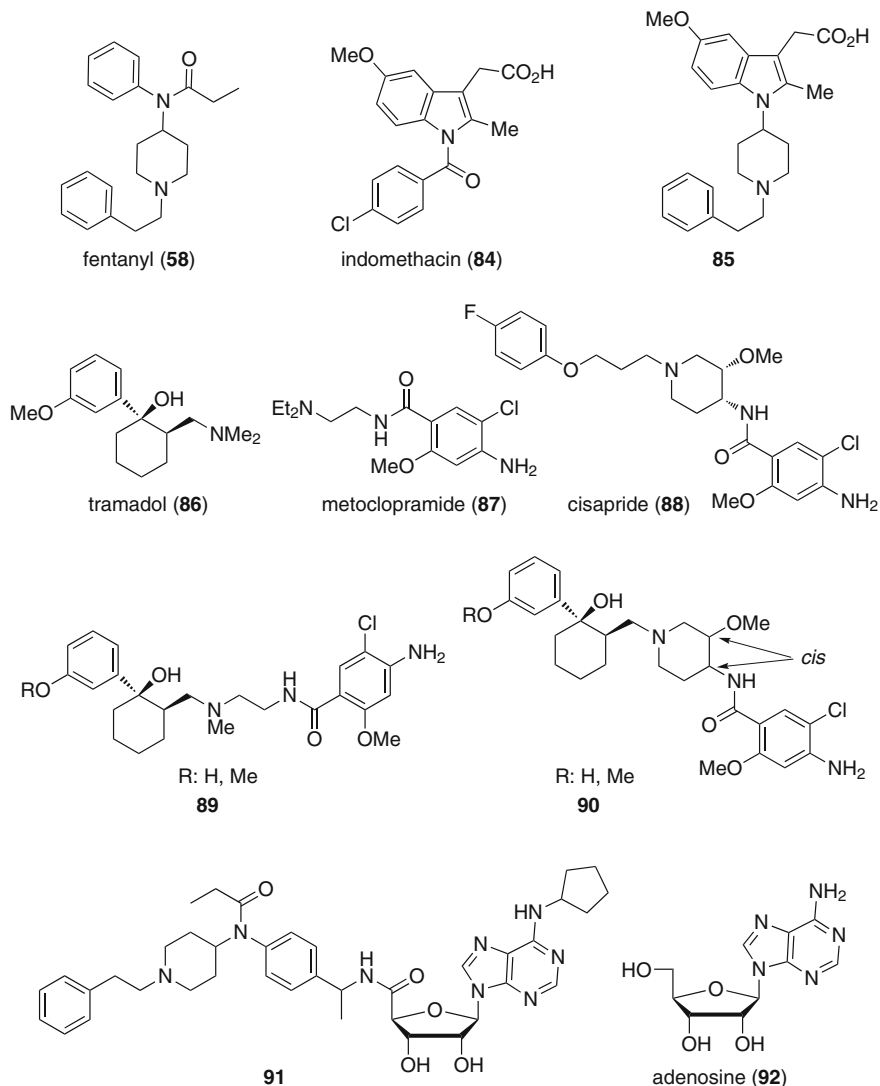
Fig. 17 Structures of compounds **58** and **84–92**

compounds **85**, **89**, and **90**, whereas compound **91** was shown to attenuate the antinociception induced by DAMGO (μ agonist), CPA (A_1 agonist), or coadministration of DAMGO and CPA in the rat tail-flick and hot-plate tests (*in vivo* tests).

4 Triplet Drugs

Triplet drugs are defined as compounds that contain three pharmacophores in a single molecule. As mentioned earlier, although twin drugs can only play one role, either by an increase of activity (symmetrical twin drug) or by a dual action (nonsymmetrical twin drug), triplet drugs are expected to elicit both roles. That is, nonsymmetrical triplet drugs with two of the same pharmacophores and one different moiety may exhibit both increased pharmacological action and dual action because the two identical portions could bind the same receptor sites simultaneously while the third portion could bind a different receptor site or enzyme. Although triplet drugs are predicted to be useful pharmacological tools and to serve as lead compounds for developing novel drugs, there have been no reports of the triplet drugs except for natural products such as valinomycin (**93**) [158, 159] and enterobactin (**94**) [160] (Fig. 18). Recently, novel triplet drugs having 1,3,5-trioxazatriquinane cores were synthesized [161]. S.c. administration of symmetrical triplet drug **95** having three oxymorphone (μ agonist) units exhibited profound antinociceptive effects in the acetic acid writhing test ($ED_{50} = 0.037$ mg/kg) that were 16- and 4-fold more potent than that of morphine ($ED_{50} = 0.6$ mg/kg) and symmetrical twin drug **96** with a capped structure ($ED_{50} = 0.14$ mg/kg), respectively. Given that their ED_{50} values are converted from gram units to molar units, the potency of triplet drug **95** for its antinociception ($ED_{50} = 0.039$ μmol/kg) was 54- and 5-fold higher than that of morphine ($ED_{50} = 2.1$ μmol/kg) and symmetrical twin drug **96** ($ED_{50} = 0.20$ μmol/kg), respectively (Fig. 19). Compounds **95** and its *N*-CPM derivative **99** were synthesized as shown in Scheme 8. Isolation of the intermediates **97** is significant for synthesis of symmetrical twin drugs with a capped structure like **96** or nonsymmetrical triplet drugs **102** (Scheme 9). According to this method, nonsymmetrical triplet drug **103** possessing two opioid pharmacophores and one haloperidol (antipsychotic) moiety has been prepared. However, its pharmacological effects were not reported (Fig. 20).

Attempts to prepare triplet drugs **104** having morphinan structures without a 4,5-epoxy bridge gave not the desired compound **104** but the unexpected rearrangement product **105** [162] (Fig. 21).

5 Conclusion and Perspectives

Many twin drugs and triplet drugs have been synthesized and evaluated for their pharmacological effects including *in vivo* pharmacological effects. Some compounds, such as MCL-144 (**13b**), MCL-145 (**17**), and triplet drug **95**, showed

more potent antinociceptive effects than the corresponding monomeric agonists. Some compounds were designed with the purpose of reducing morphine-induced side effects such as tolerance and dependence. When MDAN-19 (**46a**) and MDAN-21 (**46b**) with μ agonist and δ antagonist pharmacophores were chronically administered, naloxone-induced dependence signs (jumping) were not observed. Compounds **46a** and **46b** also exhibited neither place preference nor place aversion in CPP tests. MPS9 (**69**) with μ agonist and SP pharmacophores produced antinociceptive effects in morphine tolerant rats. These outcomes would give impact to development of novel analgesics with few or no side effects. However, accumulation of further investigations of pharmacological properties, especially *in vivo*

valinomycin (**93**)
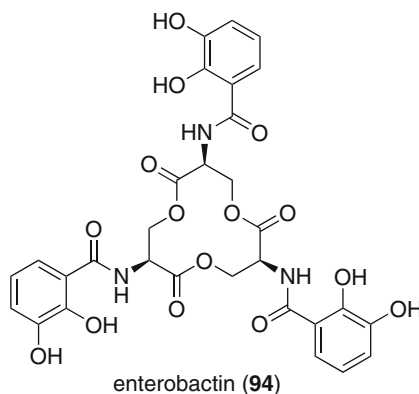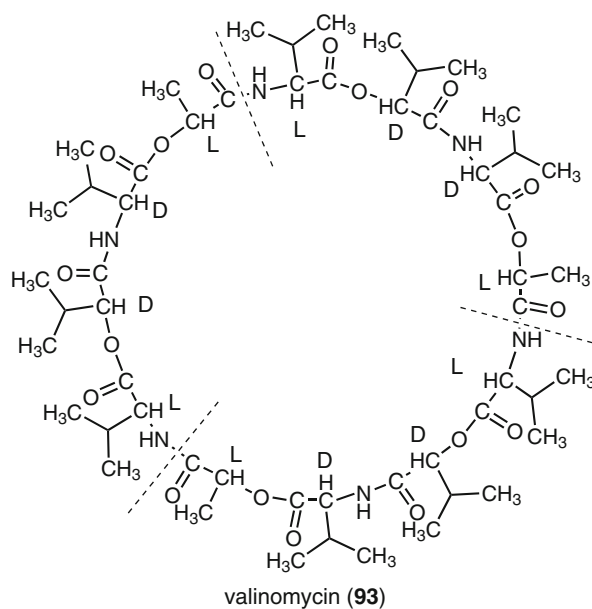
enterobactin (**94**)

Fig. 18 Structures of valinomycin (**93**) and enterobactin (**94**)
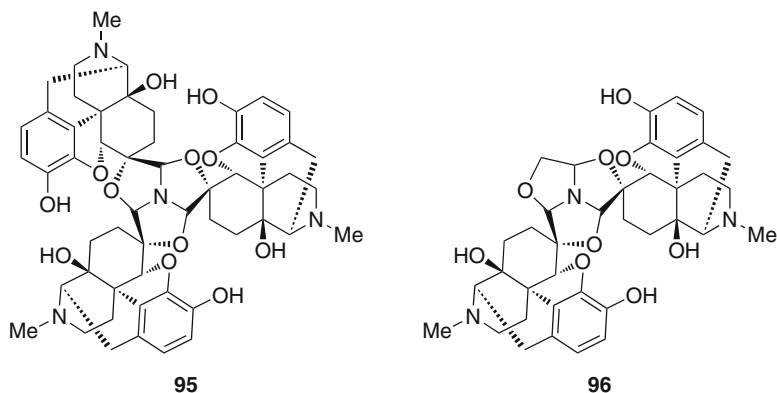
Fig. 19 Structures of triplet drug **95** and twin drug **96** with a capped structure
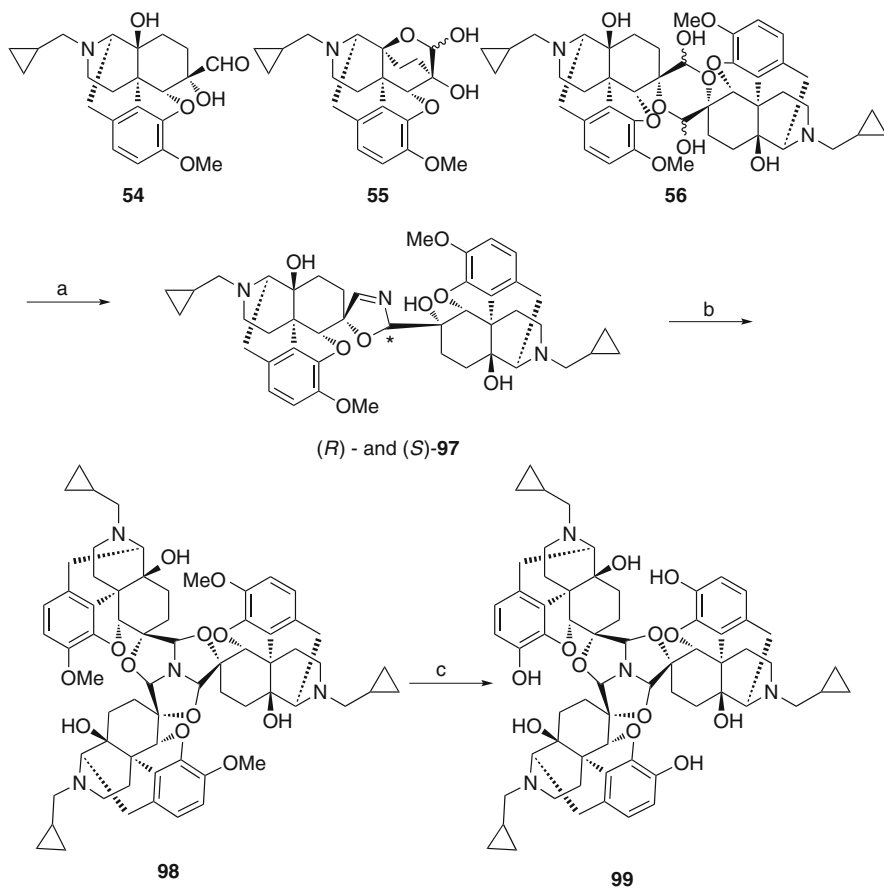
Scheme 8 Synthesis of triplet drug **99**. Reagents and conditions: (a) NH₄Cl, AcONa, MeOH, reflux, (R)-**97**: 46%, (S)-**97**: 9%; (b) CSA, CHCl₃, reflux, 68% from (R)-**97**; (c) BBr₃, CH₂Cl₂, rt, 80%
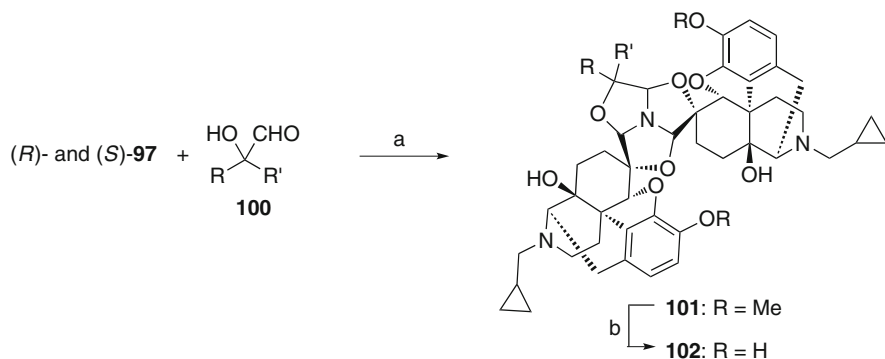
Scheme 9 Synthesis of twin drug **102**. Reagents and conditions: (a) CSA, CHCl₃, rt; (b) BBr₃, CH₂Cl₂, rt

Fig. 20 Structure of nonsymmetrical triplet drug **103**
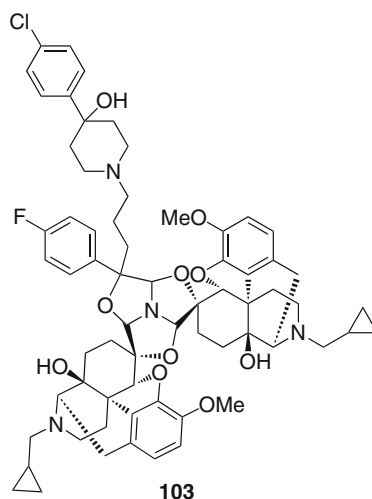
pharmacological ones, as well as absorption, distribution, metabolism, and excretion (ADME), toxicological, and physicochemical evaluation would be required in order to validate the possibilities of twin or triplet drugs for novel medicines. The ester or amide moieties, which are included in most of reported twin drugs, are potentially labile to enzymatic and chemical hydrolysis of the moieties, although stability of compound MCL-144 (**13b**) for hydrolysis was estimated. The ester functionality was a crucial structure for elicitation of binding affinities in twin drugs with two butorphan (**7**) pharmacophores. Therefore, for interpretation of the pharmacological results obtained using twin drugs with ester or amide moieties, it may be important to take metabolites derived from hydrolysis into account. In general,
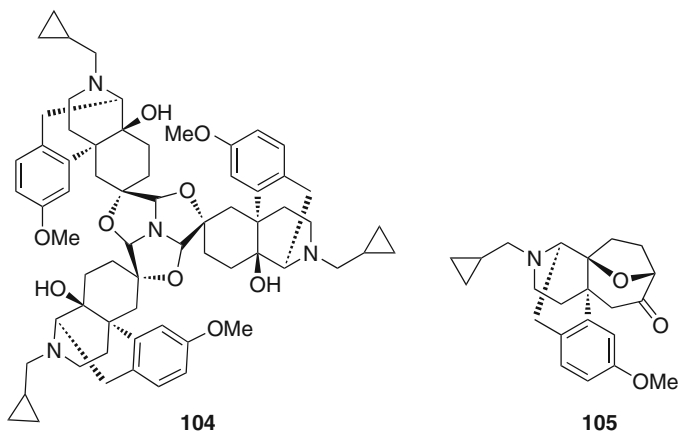
Fig. 21 Structures of expected triplet drug **104** and compound **105**

twin and triplet drugs have high molecular weights, many functional groups, and many rotatable bonds. These properties seem to be inadequate from the viewpoints of drug-likeness [163] and blood-brain barrier permeability [164]. However, it is noteworthy that many compounds showed their pharmacological effects not only by i.c.v or i.t administration but also by systemic routes (i.p., i.v., i.m., or s.c. routes).

Some twin drugs were utilized to investigate receptor dimerization. Based on the results obtained using twin drugs KDN-21 (**37a**) with δ and κ antagonist pharmacophores and KDAN-18 (**44a**) with δ antagonist and κ_1 agonist pharmacophores, the δ – κ heterodimer is proposed to correspond to δ_1 and κ_2 subtypes while the δ_2 and κ_1 subtypes would correspond to δ and κ homodimers, respectively. There are both reports for and against this conclusion [12, 80, 84, 165], and further investigations would be required to obtain definitive agreement.

Twin drugs showing significant effects can be divided into two categories by the spacer length: those with longer chains (at least ten atom units although the length depended on the structure of the pharmacophores and/or the linked positions) and those with shorter linking spacers. It is believed that the twin drugs with longer and appropriate length spacers can bind two active sites simultaneously to exert their effects. On the other hand, although the twin drugs with shorter linker do not seem to bridge two active sites, their binding affinities and/ or potencies of antinociception are greater. Compounds in this category may interact with their target molecules by another mode of action. A representative peptidic twin drug, biphalin (**106**) (Tyr-D-Ala-Gly-Phe-NH-)$_2$ [166], belongs to this category and showed more potent and longer lasting analgesia than the monomeric peptide. Why biphalin (**106**) exhibited such pharmacological profiles remains poorly understood. Elucidation of the mode of action of such compounds with shorter spacers may lead to innovation of novel concepts in drug design.

References

1. Contreras J-M, Sippl W (2008) In: Wermuth CG (ed) The practice of medicinal chemistry, 3rd edn. Academic, Amsterdam, pp 380–414
2. Hazum E, Chang K-J, Cuatrecasas P (1979) Science 206:1077
3. Portoghese PS, Larson DL, Sayre LM, Yim CB, Ronsisvalle G, Tam SW, Takemori AE (1986) J Med Chem 29:1855
4. Portoghese PS (2001) J Med Chem 44:2259
5. Portoghese PS (1989) Trends Pharmacol Sci 10:230
6. Poetoghese PS (1991) J Med Chem 34:1757
7. Portoghese PS, Lipkowski AW, Takemori AE (1987) J Med Chem 30:238
8. Portoghese PS, Nagase H, Lipkowski AW, Larson DL, Takemori AE (1988) J Med Chem 31:836
9. Portoghese PS, Sultana M, Nagase H, Takemori AE (1988) J Med Chem 31:281
10. Portoghese PS, Sultana M, Takemori AE (1988) Eur J Pharmacol 146:185
11. Portoghese PS, Sultana M, Takemori AE (1990) J Med Chem 33:1714
12. Jordan BA, Devi LA (1999) Nature 399:697
13. Lavac BAR, O'Dowd BF, George SR (2007) Curr Opin Pharmacol 2:76
14. Gomes I, Jordan BA, Gupta A, Trapaidze N, Nagy V, Devi LA (2000) J Neurosci 20:RC110
15. George SR, Fan T, Xie Z, Tse R, Tam V, Varghese G, O'Dowd BF (2000) J Biol Chem 275:26128
16. Gomes I, Gupta A, Filipovska J, Szeto HH, Pintar JE, Devi LA (2004) Proc Nat Acad Sci USA 101:5135
17. Wang D, Sun X, Bohn LM, Sadée W (2005) Mol Pharmacol 67:2173
18. Devi LA (2001) Trends Pharmacol Sci 22:532 and references cited therein
19. George SR, O'Dowd BF, Lee SP (2002) Nature Rev Drug Discov 1:808 and references cited therein
20. Dhawan BN, Cesselin F, Raghubir R, Reisine T, Bradley PB, Portoghese PS, Hamon M (1996) Pharmacol Rev 48:567 and references cited therein
21. Sato M, Minami M (1995) Pharmacol Ther 68:343 and references cited therein
22. Morphy R, Kay C, Rankovic Z (2004) Drug Discov Today 9:641
23. Morphy R, Rankovic Z (2005) J Med Chem 48:6523
24. Morphy R, Rankovic Z (2008) In: Wermuth CG (ed) The practice of medicinal chemistry, 3rd edn. Academic, Amsterdam, pp 549–571 and references cited therein
25. Halazy S (1999) Exp Opin Ther Patents 9:431
26. Peng X, Neumeyer JL (2007) Curr Top Med Chem 7:363
27. Dietis N, Guerrini R, Calo G, Salvadori S, Rowbotham DJ, Lambert DG (2009) Br J Anaesth 103:38
28. Ballet S, Pietsch M, Abell AD (2008) Protein Peptide Lett 15:668
29. Schiller PW (2010) Life Sci 86:598
30. Negus SS, Mello NK, Portoghese PS, Lin C-E (1997) J Pharmacol Exp Ther 282:44
31. Mello NK, Negus SS (1998) J Pharmacol Exp Ther 286:812
32. Bowen CA, Negus SS, Zong R, Neumeyer JL, Bidlack JM, Mello NK (2003) Neuropsycho-pharmacology 28:1125
33. Gates M, Montzak TA (1964) J Med Chem 7:129
34. Neumeyer JL, Bidlack JM, Zong R (2000) J Med Chem 43:114
35. Neumeyer JL, Zhang A, Xiong W, Gu X-H, Hilbert JE, Knapp BI, Negus S, Mello NK, Bidlack JM (2003) J Med Chem 46:5162
36. Peng X, Knapp BI, Bidlack JM, Neumeyer JL (2006) J Med Chem 49:256
37. Decker M, Fulton BS, Zhang B, Knapp BI, Bidlack JM, Neumeyer JL (2009) J Med Chem 52:7389
38. Decker M, Si Y-G, Knapp BI, Bidlack JM, Neumeyer JL (2010) J Med Chem 53:402

39. Casy AF, Parfitt RT (1986) Opioid analgesics, chemistry and receptors. Plenum, New York
40. Fries DS (1995) In: Lemke TL, Williams DA (eds) Foye's principles of medicinal chemistry, 6th edn. Williams & Wilkins, Philadelphia, pp 652–678
41. Fulton BS, Knapp BL, Bidlack JM, Neumeyer JL (2010) Bioorg Med Chem Lett 20:1507
42. Wentland MP, Albertson NF, Pierson AK (1980) J Med Chem 23:71
43. Hedberg MH, Johansson AM, Fowler CJ, Terenius L, Hacksell U (1994) Bioorg Med Chem Lett 4:2527
44. Kubota H, Rothman RB, Dersch C, McCullough K, Pinto J, Rice KC (1999) Bioorg Med Chem Lett 8:799
45. Wentland MP, Xu G, Cioffi CL, Ye Y, Duan W, Cohen DJ, Colasurdo AM, Bidlack JM (2000) Bioorg Med Chem Lett 10:183
46. McCurdy CR, Jones RM, Portogese PS (2000) Org Lett 2:819
47. Wentland MP, Duan W, Cohen DJ, Bidlack JM (2000) J Med Chem 46:3558
48. Wentland MP, Lou R, Ye Y, Cohen DJ, Richardson GP, Bidlack JM (2001) Bioorg Med Chem Lett 11:623
49. Wentland MP, Lou R, Dehnhardt CM, Duan W, Cohen DJ, Bidlack JM (2001) Bioorg Med Chem Lett 11:1717
50. Wentland MP, Ye Y, Cioffi CL, Lou R, Zhou Q, Xu G, Duan W, Dehnhardt CM, Sun X, Cohen DJ, Bidlack JM (2003) J Med Chem 46:838
51. Zhang A, Xiong W, Bidlack JM, Hilbert JE, Knapp BI, Wentland MP, Neumeyer JL (2004) J Med Chem 47:165
52. Wentland MP, VanAlstine M, Kucejki R, Lou R, Cohen DJ, Parkhill AL, Bidlack JM (2006) J Med Chem 49:5635
53. Peng X, Knapp BI, Bidlack JM, Neumeyer JL (2007) Bioorg Med Chem Lett 17:1508
54. Peng X, Knapp BI, Bidlack JM, Neumeyer JL (2007) Bioorg Med Chem 15:4106
55. Reden J, Reich MF, Rice KC, Jacobson AE, Brossi A (1979) J Med Chem 22:256
56. Wentland MP, Lu Q, Lou R, Bu Y, Knapp BI, Bidlack JM (2005) Bioorg Med Chem Lett 15:2107
57. Wentland MP, Lou R, Lu Q, Bu Y, VanAlstine MA, Cohen DJ, Bidlack JM (2009) Bioorg Med Chem Lett 19:203
58. Wentland MP, Lou R, Lu Q, Bu Y, Denhardt C, Jin J, Ganorkar R, VanAlstine MA, Guo C, Cohen DJ, Bidlack JM (2009) Bioorg Med Chem Lett 19:2289
59. Portoghese PS, Larson DL, Yim CB, Sayre LM, Ronsisvalle G, Lipkowski AW, Takemori AE, Rice KC, Tam SW (1985) J Med Chem 28:1140
60. Mathews JL, Peng X, Xiong W, Zhang A, Negus SS, Neumeyer JL, Bidlack JM (2005) J Pharmacol Exp Ther 315:821
61. Mathews JL, Fulton BS, Negus SS, Neumeyer JL, Bidlack JM (2008) Neurochem Res 33:2142
62. Reindl JD, Rowan K, Carey AN, Peng X, Neumeyer JL, McLaughlin JP (2008) Pharmacology 81:229
63. Carlezon WA Jr, Béguin C, DiNieri JA, Baumann MH, Richards MR, Todtenkopf MS, Rothman RB, Ma Z, Lee DY-W, Cohen BM (2006) J Pharmacol Exp Ther 316:440
64. McLaughlin JP, Land BB, Li S, Pintar JE, Chavkin C (2006) Neuropsychopharmacology 31:787
65. McLaughlin JP, Marton-Popovici M, Chavkin C (2003) J Neurosci 23:5674
66. Mague SD, Pliakas AM, Todtenkopf MS, Tomasiewicz HC, Zhang Y, Stevens WC Jr, Jones RM, Portoghese PS, Carlezon WA Jr (2003) J Pharmacol Exp Ther 305:323
67. Beardsley PM, Howard JL, Shelton KL, Carroll FI (2005) Psychopharmacology 183:118
68. Salvadori S, Guerrini R, Balboni G, Bianchi C, Bryant SD, Cooper PS, Lazarus LH (1999) J Med Chem 42:5010
69. Neumeyer JL, Peng X, Knapp BI, Bidlack JM, Lazarus LH, Salvadori S, Trapella C, Balboni G (2006) J Med Chem 49:5640
70. Peng X, Knapp BI, Bidlack JM, Neumeyer JL (2007) J Med Chem 50:2254

71. Sayre LM, Portoghese PS (1980) J Org Chem 45:3366
72. Jones RM, Hjorth JRM, Schwartz TW SA, Portoghese PS (1998) J Med Chem 41:4911
73. Jones RM, Portoghese PS (2000) Eur J Pharmacol 396:49
74. Zhang S, Yekkirala A, Tang Y, Portoghese PS (2009) Bioorg Med Chem Lett 19:6978
75. Portoghese PS, Sultana M, Nelson WL, Klein P, Takemori AE (1992) J Med Chem 35:4086
76. Poss MA, Iwanowicz E, Reid JA, Lin J, Gu Z (1992) Tetrahedron Lett 33:5933
77. Kim KY, Qian L (1993) Tetrahedron Lett 34:7677
78. Garzon J, Juarros JL, Castro MA, Sanchez-Blazquez P (1995) Mol Pharmacol 47:738
79. Wessendorf MW, Dooyema J (2001) Neurosci Lett 298:151
80. Portoghese PS, Lunzer MM (2003) Eur J Pharmacol 467:233
81. Bhushan RG, Sharma SK, Xie Z, Daniels DJ, Portoghese PS (2004) J Med Chem 47:2969
82. Mosberg HI, Hurst R, Hurby VJ, Gee K, Yamamura HI, Galligan JJ, Burks TF (1983) Proc Natl Acad Sci USA 80:5871
83. Nock B (1995) In: Tseng LF (ed) The pharmacology of opioid peptides. Harwood Academic Publishers, Singapore, pp 29–56
84. Simonin F, Slowe S, Becker JAJ, Matthes HWD, Filliol D, Chluba J, Kitchen I, Kieffer BL (2001) Eur J Pharmacol 414:189
85. Erspamer V, Melchiorri P, Falconieri-Erspamer G, Negri L, Corsi R, Severini C, Barra D, Simmaco M, Kreil G (1989) Proc Natl Acad Sci USA 86:5188
86. Szmuszkovicz J, Von Voigtlander PF (1982) J Med Chem 25:1125
87. Xie Z, Bhushan RG, Daniels DJ, Portoghese PS (2005) Mol Pharmacol 68:1079
88. Barlow JJ, Blackburn TP, Costello GF, James J, Le Count DJ, Main BG, Pearce RJ, Russel K, Shaw JS (1991) J Med Chem 34:3149
89. Daniels DJ, Kulkarni A, Xie Z, Bhushan RG, Portoghese PS (2005) J Med Chem 48:1713
90. Sofuoglu M, Portoghese PS, Takemori AE (1991) J Pharmacol Exp Ther 257:676
91. Portoghese PS, Nagase H, MaloneyHuss KE, Lin C-E, Takemori AE (1991) J Med Chem 34:1715
92. Portoghese PS, Sultana M, Nagase H, Takemori AE (1992) Eur J Pharmacol 218:195
93. Ohkawa S, Portoghese PS (1998) J Med Chem 41:4177
94. Nock B, Giordano AL, Cicero TJ, O'Connor LH (1990) J Pharmacol Exp Ther 254:412
95. Vaught JL, Takemori A (1979) J Pharmacol Exp Ther 208:86
96. Vaught JL, Rothman RB, Westfall TC (1982) Life Sci 30:1443
97. Miyamoto Y, Portoghese PS, Takemori AE (1993) J Pharmacol Exp Ther 264:1141
98. Abdelhamid EE, Sultana M, Portoghese PS, Takemori AE (1991) J Pharmacol Exp Ther 258:299
99. Miyamoto Y, Brown WD, Portoghese PS, Takemori AE (1994) J Pharmacol Exp Ther 270:37
100. Fundytus ME, Schiller PW, Shapiro M, Weltrowska G, Coderre TJ (1995) Eur J Pharmacol 286:105
101. Daniels DJ, Lenard NR, Etienne CL, Law P-Y, Roerig SC, Portoghese PS (2005) Proc Natl Acad Sci USA 102:19208
102. Lenard NR, Daniels DJ, Portoghese PS, Roerig SC (2007) Eur J Pharmacol 566:75
103. Nagase H, Kawamura K, Mizusuna A, Fujii H, Nakatani I (2002) JP 2002332284A
104. Fujii H, Watanabe A, Nemoto T, Narita M, Miyoshi K, Nakamura A, Suzuki T, Nagase H (2009) Bioorg Med Chem Lett 19:438
105. Nagase H, Watanabe A, Nemoto T, Yamamoto N, Osa Y, Sato N, Yoza K, Kai T (2007) Tetrahedron Lett 48:2547
106. Fujii H, Nagase H (2006) Curr Med Chem 13:1109 and references cited therein
107. Foran SE, Carr DB, Lipkowski AW, Maszczynska I, Marchand JE, Misicka A, Beinborn M, Kopin AS, Kream RM (2000) J Pharmacol Exp Ther 295:1142
108. Foran SE, Carr DB, Lipkowski AW, Maszczynska I, Marchand JE, Misicka A, Beinborn M, Kopin AS, Kream RM (2000) Proc Natl Acad Sci USA 97:7621

109. Bonney IM, Foran SE, Marchand JE, Lipkowski AW, Carr DB (2004) Eur J Pharmacol 488:91
110. Yamamoto T, Nair P, Davis P, Ma S-W, Navratilova E, Moye S, Tumati S (2007) J Med Chem 50:2779
111. Yamamoto T, Nair P, Vagner J, Largent-Milnes T, Davis P, Ma S-W, Navratilova E (2008) J Med Chem 51:1369
112. Yamamoto T, Nair P, Jacobsen NE, Davis P, Ma S-W, Navratilova E, Moye S (2008) J Med Chem 51:6334
113. Hurby VJ, Agnes RS, Davis P, Ma S-W, Lee YS, Vanderah TW, Lai J, Porreca F (2003) Life Sci 73:699
114. Lee YS, Agnes RS, Badghisi H, Davis P, Ma S-W, Lai J, Porreca F, Hruby VJ (2006) J Med Chem 49:1773
115. Ndungu JM, Cain JP, Davis P, Ma S-W, Vanderah TW, Lai J, Porreca F, Hruby VJ (2006) Tetrahedron Lett 47:2233
116. Agnes RS, Lee YS, Davis P, Ma S-W, Badghisi H, Porreca F, Lai J, Hruby VJ (2006) J Med Chem 49:2868
117. Lee YS, Agnes RS, Davis P, Ma S-W, Badghisi H, Lai J, Porreca F, Hruby VJ (2007) J Med Chem 50:165
118. Anges RS, Ying J, Kövér KE, Lee YS, Davis P, Ma S-W, Badghisi H, Porreca F, Lai J, Hruby VJ (2008) Peptides 29:1413
119. Vagner J, Xu L, Handl HL, Josan JS, Morse DL, Mash EA, Gillies RJ, Hruby VJ (2008) Angew Chem Int Ed 47:1685
120. Dardonville C, Rozas I (2004) Med Res Rev 24:639 and references cited therein
121. Sánchez-Blázquez P, Boronat MA, Olmos G, García-Sevilla JA, Garzón J (2000) Br J Pharmacol 130:146
122. Fairbanks CA, Posthumus IJ, Kitto KF, Stone LS, Wilcox GL (2000) Pain 84:13
123. Boronat MA, Olmos G, García-Sevilla JA (1998) Br J Pharmacol 125:175
124. Boronat MA, Olmos G, García-Sevilla JA (1999) Ann NY Acad Sci 881:359
125. Ruiz-Durántez E, Torrecilla M, Pineda J, Ugedo L (2003) Br J Pharmacol 138:494
126. Morgan AD, Campbell UC, Fons RD, Carroll ME (2002) Pharmacol Biochem Behav 72:873
127. Rui-Bin SU, Jin LI, Bo-Yi QIN (2003) Acta Pharmacol Sin 24:631
128. Miralles A, Esteban S, Sastre-Coll A, Moranta D, Asensio VJ, García-Sevilla JA (2005) Eur J Pharmacol 518:234
129. Montero A, Goya P, Jagerovic N, Callado LF, Meana JJ, Girón R, Goicoechea C, Martín MI (2002) Bioorg Med Chem 10:1009
130. Li G, Regunathan S, Barrow CJ, Eshraghi J, Cooper R, Reis DJ (1994) Science 263:966
131. Dardonville C, Jagerovic N, Callado LF, Meana JJ (2004) Bioorg Med Chem Lett 14:491
132. Dardonville C, Fernandez-Fernandez C, Gibbons S-L, Ryan GJ, Jagerovic N, Gabilondo AM, Meana JJ, Callado LF (2006) Bioorg Med Chem 14:6570
133. Diaz A, Mayet S, Dickenson AH (1997) Eur J Pharmacol 333:9
134. Lamotte C, Pert CB, Snyder SH (1976) Brain Res 112:407
135. Hökfelt T, Elde R, Johansson O, Terenius L, Stein L (1977) Neurosci Lett 5:25
136. Go VL, Yaksh TL (1987) J Physiol 391:141
137. Duggan AW, Hendry IA, Morton CR, Hutchinson WD, Zhao ZQ (1988) Brain Res 451:261
138. Kar S, Quirion R (1995) J Comp Neurol 354:253
139. Minami M, Maekawa K, Yabuuchi K, Satoh M (1995) Mol Brain Res 30:203
140. Kream RM, Kato T, Shimonaka H, Marchand JE, Wurm WH (1993) Proc Natl Acad Sci USA 90:3564
141. Maszczynska I, Lipkowski AW, Carr DB, Kream RM (1998) Analgesia 3:1
142. Kream RM, Liu N-J, Zhuang M, Esposito PL, Esposito TR, Stefano GB, Witmeyer JJ III (2007) Med Sci Monit 13:BR25
143. Akbarzadeh A, Mehraby M, Zarbakhsh M, Farzaneh H (1999) Biotechnol Appl Biochem 30:139

144. Itoh S, Katsuura G, Maeda Y (1982) Eur J Pharmacol 80:421
145. Faris PL, Komisaruk BP, Watkins LR, Mayer DJ (1983) Science 219:310
146. Wiesinfeld-Hallin Z, Lucas GA, Alster P, Xu X-J, Hokfelt T (1999) Brain Res 848:78
147. Watkins LR, Kinscheck IB, Mayer DJ (1984) Science 224:395
148. Suberg SN, Culhane ES, Carstens E, Watkins LR (1985) Ann NY Acad Sci 448:660
149. Lu L, Huang M, Liu A, Ma L (2000) Neuroreport 11:829
150. Bock MG, DiPardo RM, Evans BE, Rittle KE, Whitter WL, Garsky VM, Gilbert KF, Leighton JL, Carson KL, Mellin EC, Veber DF, Chang RSL, Lotti VJ, Freedman SB, Smith AJ, Patel S, Anderson PS, Freidiner RM (1993) J Med Chem 36:4276
151. Zheng Y, Akgün E, Harikumar KG, Hopson J, Powers MD, Lunzer MM, Miller LJ, Portoghese PS (2009) J Med Chem 52:247
152. Gomes I, Filipovska J, Devi LA (2003) In: Pan ZZ (ed) Opioid research, methods and protocols. Humana, Totowa, pp 165–170
153. Reider PJ, Davis P, Huges DL, Grabowski EJJ (1987) J Org Chem 52:955
154. Bock MG, Dipardo RM, Evans BE, Rittle KE, Veber DF, Freidinger RM, Hirshfield J, Sringer JP (1987) J Org Chem 52:3232
155. Vardanyan R, Vijay G, Nichol GS, Liu L, Kumarasinghe I, Davis P, Vanderah T, Porreca F, Lai J, Hruby VJ (2009) Bioorg Med Chem 17:5044
156. Shao L, Wang F, Hewitt MC, Barberich TJ (2009) Bioorg Med Chem Lett 19:5679
157. Mathew SC, Ghosh N, By Y, Berthault A, Virolleaud M-A, Carrega L, Chouraqui G, Commeiras L, Condo J, Attolini M, Gaudel-Siri A, Ruf J, Parrain J-L, Rodriguez J, Guieu R (2009) Bioorg Med Chem Lett 19:6736
158. O'Brien JG, Gibson F (1970) Biochim Biophys Acta 215:393
159. Pollack JR, Neilands JB (1970) Biochem Biophys Res Commun 38:989
160. Brockmann H, Schmidt-Kastner G (1955) Chem Ber 88:57
161. Nagase H, Watanabe A, Harada M, Nakajima M, Hasebe K, Mochizuki H, Yoza K, Fujii H (2009) Org Lett 11:539
162. Watanabe A, Fujii H, Nakajima M, Hasebe K, Mochizuki H, Nagase H (2009) Bioorg Med Chem Lett 19:2416
163. Kerns EH, Di L (2008) Drug-like properties: concepts, structure design and methods: from ADME to toxicity optimization. Academic, New York, pp 37–42
164. Kerns EH, Di L (2008) Drug-like properties: concepts, structure design and methods: from ADME to toxicity optimization. Academic, New York, pp 122–136
165. van Rijn RM, Whistler JL (2009) Biol Psychiatry 66:777
166. Lipkowski AW, Konecka AM, Sroczyńska I (1982) Peptides 3:697

3D-Pharmacophore Identification for κ-Opioid Agonists Using Ligand-Based Drug-Design Techniques

Noriyuki Yamaotsu and Shuichi Hirono

Abstract A selective κ-opioid receptor (KOR) agonist might act as a powerful analgesic without the side effects of μ-opioid receptor-selective drugs such as morphine. The eight classes of known KOR agonists have different chemical structures, making it difficult to construct a pharmacophore model that takes them all into account. Here, we summarize previous efforts to identify the pharmacophore for κ-opioid agonists and propose a new three-dimensional pharmacophore model that encompasses the κ-activities of all classes. This utilizes conformational sampling of agonists by high-temperature molecular dynamics and pharmacophore extraction through a series of molecular superpositions.

Contents

N. Yamaotsu (✉) and S. Hirono
School of Pharmacy, Kitasato University, 5-9-1 Shirokane, Minato-ku, Tokyo 108-8641, Japan
e-mail: yamaotsun@pharm.kitasato-u.ac.jp

Abbreviations

2D	Two-dimensional
3D	Three-dimensional
δ/κ	$K_i(\delta)/K_i(\kappa)$
μ/κ	$K_i(\mu)/K_i(\kappa)$
BCG	Bicyclic guanidine
CCK	Cholecystokinin
DOR	δ-Opioid receptor
GPCR	G-protein-coupled receptor
K_i	Inhibition constant
KOR	κ-Opioid receptor
MD	Molecular dynamics
MMFF	Merck molecular force field
MOR	μ-Opioid receptor
ORL1	Opioid receptor-like 1 receptor
pK_a	Negative logarithm of acid dissociation constant
QSAR	Quantitative structure–activity relationship
SAR	Structure–activity relationship

1   Introduction

Opioid receptors belong to the superfamily of G-protein-coupled receptors (GPCRs), and interact with morphine (Fig. 1) and related opiate alkaloids, as well as the various endogenous opioid peptides [1, 2]. They are divided into at least three types: μ-opioid receptors (MORs), κ-opioid receptors (KORs), and δ-opioid receptors (DORs) [2]. A selective KOR agonist could be a powerful analgesic drug without the clinically limiting side effects (such as dependence, respiratory depression, and constipation) of MOR-selective drugs like morphine [3, 4].

Fig. 1 Morphine rings and positions
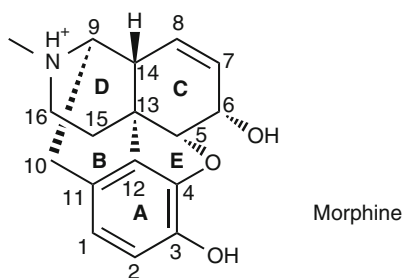
Morphine

The known KOR agonists belong to the following eight classes: peptides (such as dynorphin A) [5–8]; benzomorphan derivatives (such as bremazocine) [9–13]; morphinan derivatives (such as TRK-820) [14–16]; arylacetamide derivatives (such as U-50488H) [17–22]; diazabicyclononanone derivatives (such as HZ2) [23–25]; bicyclic guanidine (BCG) derivatives (such as TPI 614-1) [8, 26, 27]; benzodiazepine derivatives (such as tifluadom) [28–31]; and neoclerodane diterpene derivatives (such as salvinorin A) [32–35].

Because these classes have different chemical structures, many computational studies have attempted to determine the pharmacophore for κ-selective agonists. These studies have been divided into ligand-based methods [16, 36–38] and docking-based methods [7, 13, 29, 31–36, 39–42]. With the former approach, it is difficult to superpose different skeletons onto one another, so ligand-based methods have been applied to congeneric compounds or the charged NH^+ moiety corresponding to the amino (N)-terminus of peptides. The latter approach is powerful when the crystal structure of a target protein is known [43]; however, X-ray structures of opioid receptors are not available. All docking studies of opioid ligands have therefore been based on homology models derived from other GPCRs. Homology modeling is a well-established method, and the main chain of a target protein is predictable [44, 45]. However, many problems remain to be overcome prior to docking, including the induced fit and the difference between agonist/antagonist binding modes [45–47]. Hence, different docking protocols against KOR tend to result in different models [32–35]. Here, we propose a new ligand-based model that can account for the κ-activities of all classes, and utilizes conformational sampling of agonists by high-temperature molecular dynamics (MD) and pharmacophore extraction through a series of molecular superpositions.

2 Skeleton Classes for KOR Agonists

We surveyed the features of each of the eight KOR agonist skeleton classes.

a

Dynorphin A ^+H_3N-Try^1-Gly^2-Gly^3-Phe^4-Leu^5-Arg^6-Arg^7-IIe^8-Arg^9-Pro^{10}-Lys^{11}
-Leu^{12}-Lys-^{13}-Trp^{14}-Asp^{15}-Asn^{16}-Gln^{17}-COO$^-$

b

Dynorphin B ^+H_3N-Try^1-Gly^2-Gly^3-Phe^4-Leu^5-Arg^6-Arg^7-Gln^8-Phe^9-Lys^{10}-Val^{11}
-Val^{12}-Thr^{13}-Arg^{14}-Ser^{15}-Gln^{16}-Glu^{17}-Asp^{18}-Pro^{19}-Asn^{20}-Ala^{21}-Tyr^{22}
-Glu^{23}-Glu^{24}-Leu^{25}-Phe^{26}-Asp^{27}-Val^{28}-COO$^-$
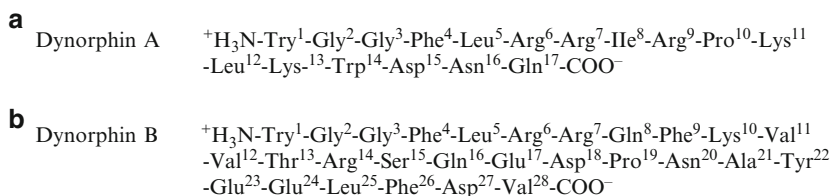
Fig. 2 Sequences of (**a**) dynorphin A and (**b**) dynorphin B

2.1 Peptides

All endogenous μ-opioid, κ-opioid, and δ-opioid peptides have ^+H_3N-Tyr^1-Gly^2-Gly^3-Phe^4 as the common message domain [2]. The endogenous agonists of KORs are dynorphins (Fig. 2). Dynorphin A has high affinity, with a binding constant $K_i(κ)$ of 0.17–0.5 nM and a κ-selectivity of $K_i(μ)/K_i(κ) = μ/κ = 64$ [5, 48, 49]. Various structural modifications have been made to dynorphin molecules in attempts to identify the relevant pharmacophore. Chavkin and Goldstein carried out successive removal of carboxyl (C)-terminal amino acids from dynorphin A-(1-13) [5]. Their experiment indicated important contributions of Arg^7, Lys^{11}, and Lys^{13} to κ-activity. Moreover, the removal of Tyr^1 led to loss of biological activity. Lapalu et al. studied chimeric peptides between dynorphin A and nociceptin, which is the endogenous agonist of the opioid receptor-like 1 (ORL1) receptor [49], and found that Leu^5-Arg^6 of dynorphin A is important for κ-activity. Thus, Leu^5-Arg^6-Arg^7 is thought to be the address domain responsible for κ-specificity.

In an attempt to obtain shorter peptides using combinatorial libraries, Houghten and colleagues identified the highly selective tetrapeptide, D-Phe-D-Phe-D-Nle-D-Arg-NH$_2$ ($K_i(κ) = 1$ nM, μ/κ > 10,000) [6, 8]. Przydzial et al. studied cyclic tetrapeptides and obtained MP-16 (Tyr-C[D-Cys-Phe-D-Cys]-NH$_2$) with an intermediate binding affinity ($K_i(κ) = 38.7$ nM) [7].

2.2 Benzomorphans

Benzomorphans lack the C ring of morphine (Fig. 3). The κ-activities of benzomorphans were originally identified by the unique in vivo pattern of ketazocine (ketocyclazocine) agonist activity [2], so ketazocine is the first synthetic κ-selective agonist. Other benzomorphans include bremazocine, MPCB, pentazocine, and eptazocine [9–13]. These were synthesized in an effort to maximize κ-selectivity and to minimize morphine-like side effects. For example, the selectivity of bremazocine is μ/κ = 3.8–15 [12, 20, 50]. Bremazocine, pentazocine, and eptazocine are KOR agonists and MOR antagonists [9, 10, 51], while pentazocine and eptazocine are drugs that are used clinically.
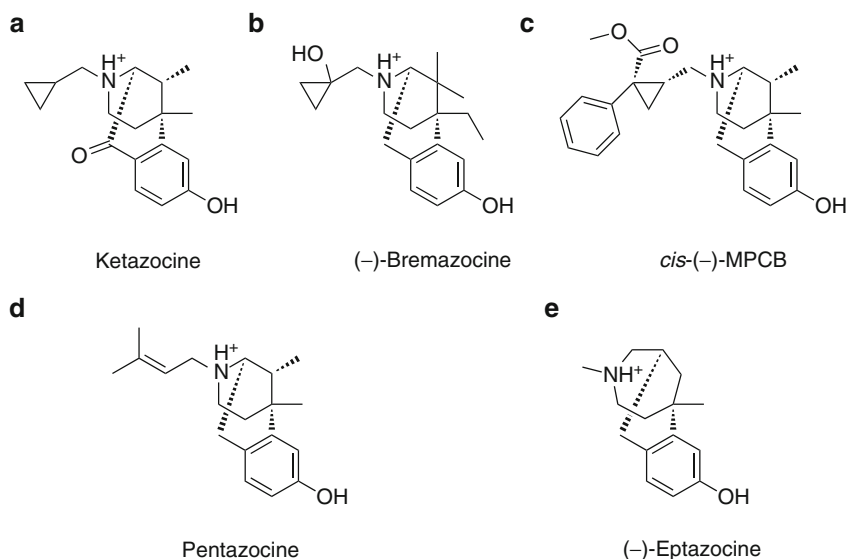
Fig. 3 Chemical structures of benzomorphans: (**a**) ketazocine, (**b**) bremazocine, (**c**) MPCB, (**d**) pentazocine, and (**e**) eptazocine

2.3 Morphinans

Morphine is classified as a 4,5-epoxymorphinan but a μ-selective agonist (μ/κ = 0.02–0.08) [31, 50]. However, butorphanol, which belongs to the morphinan group (Fig. 4), induces analgesia by acting predominantly at the KOR. The novel κ-selective agonist TRK-820 (μ/κ = 2.6) is also a 4,5-epoxymorphinan, but has sedative activity with no adverse effects [14, 16]. The C ring of morphine is cyclohexene, while that of butorphanol and TRK-820 is cyclohexane. Moreover, TRK-820 has a side chain corresponding to the address domain at the 6-position. Butorphanol and TRK-820 (nalfurafine) are approved drugs.

NS-22 and KNT-63 are known to be TRK-820-related compounds. NS-22 is a 6,14-epoxymorphinan with equal μ- and κ-affinities [15, 16]. KNT-63 is a 4,5-epoxymorphinan with an oxabicyclo[2.2.2]octane moiety instead of a cyclohexane moiety of the C ring [16]. It is interesting to note that the chirality of the KNT-62 (7R) side chain is opposite to that of KNT-63 (7S). The selectivities of KNT-63 and KNT-62 are 1.9 and 1.3, respectively [16].

2.4 Arylacetamides

The first arylacetamide to be identified, U-50488H, showed very high κ-selectivity (μ/κ = 630–845) [17, 20, 50]. Its skeleton is different from that of morphine, and
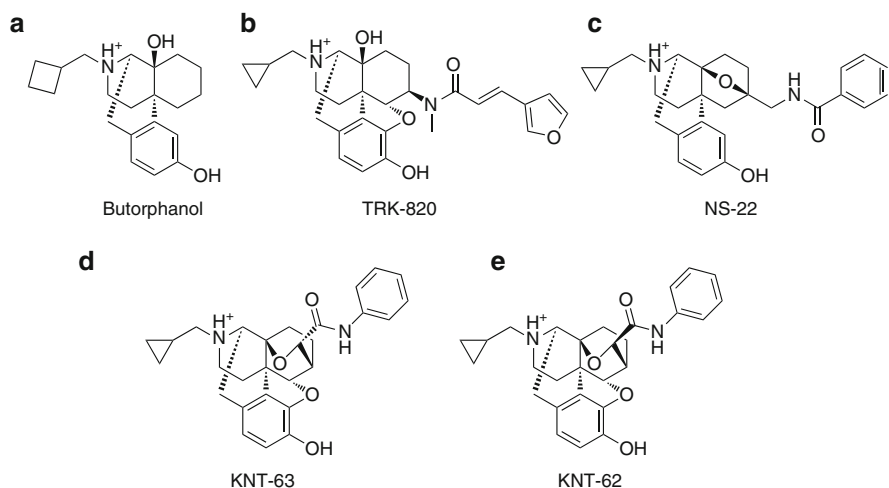
Fig. 4 Chemical structures of morphinans: (**a**) butorphanol, (**b**) TRK-820, (**c**) NS-22, (**d**) KNT-63, and (**e**) KNT-62
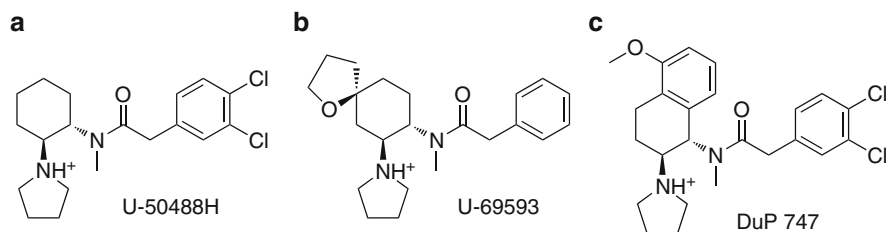
Fig. 5 Chemical structures of arylacetamides: (**a**) U-50488H, (**b**) U-69593, and (**c**) DuP 747

is comparatively simple (Fig. 5). Benzeneacetamido-piperizines have a related skeleton [52]. The identification of U-50488H was followed by compounds such as U-69593, DuP 747, PD117302, and CI-977 [18–22]. Arylacetamides do not produce morphine-like side effects such as respiratory depression and constipation. However, they do possess dysphoric and psychotomimetic properties which are thought to be common to κ-agonists [3].

2.5 Diazabicyclononanones

The diazabicyclononanone (3,7-diazabicyclo[3.3.1]nonan-9-one) skeleton is placed in a relatively new class [23–25], having two positively charged groups, which is also common to peptides (Fig. 6). Diazabicyclononanones include HZ1, 3FLB, and HZ2 [23, 53], the last of which exhibits the next highest κ-selectivity (μ/κ > 66.7) after
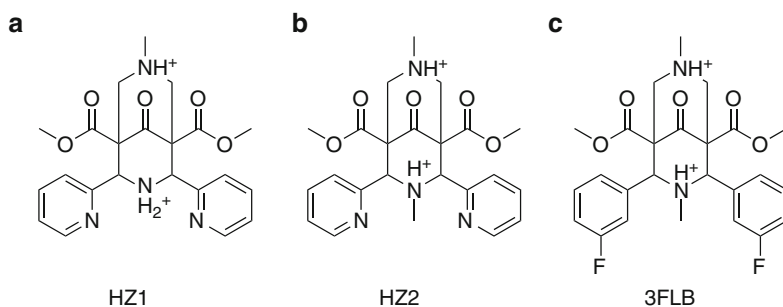
Fig. 6 Chemical structures of diazabicyclononanones: (**a**) HZ1, (**b**) HZ2, and (**c**) 3FLB
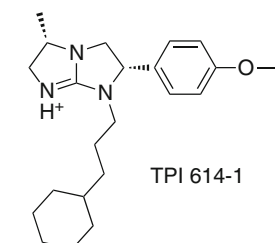
Fig. 7 Chemical structure of a bicyclic guanidine, TPI 614-1

arylacetamides [23]. HZ2 also showed a strong and long-lasting antinociceptive effect in mouse tail-flick tests. In contrast to HZ1 and 3FLB, HZ2 offers a high oral availability in different animal species [23, 53].

2.6 Bicyclic Guanidines

Houghten and colleagues obtained a new trisubstituted bicyclic guanidine (BCG) skeleton following cyclization of reduced *N*-acylated dipeptides [54]. The BCGs were selected after screening of a positional scanning-synthetic combinatorial library, and were evaluated in a KOR-binding assay [8, 26, 27]. BCGs show intermediate-to-low binding affinities for KOR, with the best compound, TPI 614-1 (Fig. 7), having a κ-affinity of 39 nM [8, 27]. Selectivity and agonist activity have not yet been reported.

2.7 Benzodiazepines

Tifluadom is a 2-[(acylamino)methyl]-1,4-benzodiazepine (Fig. 8), with κ-agonist and cholecystokinin-A (CCK-A) antagonist abilities [29]. Cappelli and colleagues successfully discriminated KORs from CCKs, and KORs from MORs using the 2-[(acylamino)ethyl] derivatives [29, 31]. Although tifluadom is a racemic

Fig. 8 Chemical structure of
a benzodiazepine, tifluadom
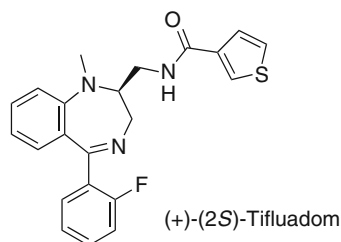
(+)-(2S)-Tifluadom

Fig. 9 Chemical structure of
a neoclerodane diterpene,
salvinorin A

Salvinorin A
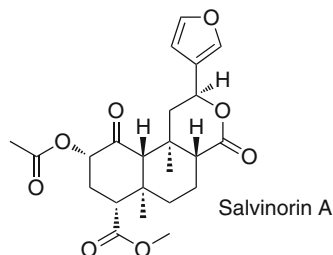
mixture, both enantiomers can bind to the KOR. The affinity and selectivity of (+)-(2S)-tifluadom are $K_i(\kappa) = 0.17$ nM and $\mu/\kappa = 8.8$, and those of (−)-(2R) isomer are $K_i(\kappa) = 0.71$ nM and $\mu/\kappa = 35$ [30]. However, (+)-(2S) isomer induces KOR-related reactions in vivo, whereas (−)-(2R) is related to the benzodiazepine receptor [28].

2.8 Neoclerodane Diterpenes

A neoclerodane diterpene skeleton for the KOR was recently elucidated and shown to be notably different as it does not possess a positively charged group. Salvinorin A is an example of a neoclerodane diterpene isolated from *Salvia divinorum* (Fig. 9), which shows very high κ-selectivity ($\mu/\kappa > 526$) [32, 55]. Salvinorin A is a KOR agonist both in vivo and in vivo [53, 56], but demonstrates little anti-scratching activity and no antinociception in mice. It has been reported as a hallucinogenic, and Harding and colleagues were able to convert it into a new μ-agonist, herkinorin, using chemical modifications [55, 57]. Thus, it is possible for a neoclerodane diterpene skeleton to be a template for other opioid agonists.

3 Previous Efforts to Identify the Pharmacophore for KOR

Biochemists, medicinal chemists, and computer chemists have previously tried to identify the pharmacophore for KOR. Their efforts include the following: schematic models based on structure–activity relationship (SAR) studies; ligand-based

models with molecular superposing; and docking models based on homology modeling and ligand docking. Here, we outline the history and summarize the results.

3.1 Schematic Models Based on SAR Studies

Studies of endogenous dynorphins clarified that $^{+}H_3N$-Tyr^1-Gly^2-Gly^3-Phe^4 is the common message domain for all μ-opioid, κ-opioid, and δ-opioid peptides, whereas Leu^5-Arg^6-Arg^7 is the address domain responsible for κ-specificity [5, 49]. In studies of the synthetic κ-selective antagonists norbinaltorphimine (norBNI) and 5′-guanidinonaltrindole (GNTI) (Fig. 10), a second positively charged group was considered to be the address domain of morphinans [58–60]. However, all selective κ-agonists, with the exception of peptides and diazabicyclononanones, lack a second positively charged group, while neoclerodane diterpenes lack any positively charged group.

The first model for KOR was proposed by Martin and consisted of an anionic subsite corresponding to the N-terminal charged NH$^+$ moiety of the peptide agonist, the benzene subsite for Tyr, and the ketonic oxygen site for ketazocine (at the 10-position of morphine) [61]. Feinberg et al. attempted to explain differences between agonists and antagonists at opioid receptors [62], and outlined a model composed of the amine binding subsite, the lipophilic subsite for Tyr, the agonist binding subsite corresponding to the address domain, and the specific antagonist binding subsite corresponding to large side chains at the 17-position of morphine.

With the conversion of binding modes, Protoghese et al. observed substitution-effect differences on the same positions between morphine and the related skeletons, phenylpiperidines and allylprodines, with the MOR [63, 64]. They suggested that different skeletons might adopt different binding modes. According to this model, the binding site of opioid receptors might consist of the anionic (A) subsite, the Tyr (T) subsite, and the Phe (P) subsite (Fig. 11). The binding mode of phenylpiperidines and allylprodines is thought to be the A–P orientation, whereas that of morphine is the A–T orientation. However, these models only took into account morphine-related skeletons such as benzomorphans and morphinans for the KOR.
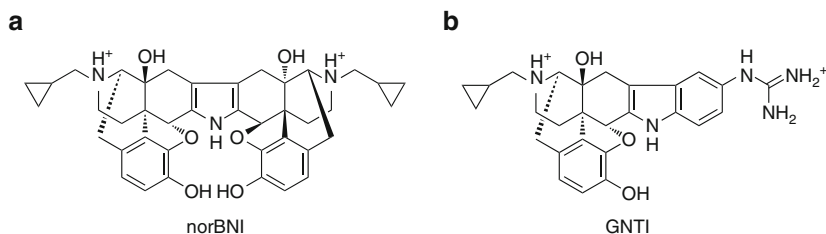
Fig. 10 Structures of κ-antagonists: (**a**) norBNI and (**b**) GNTI
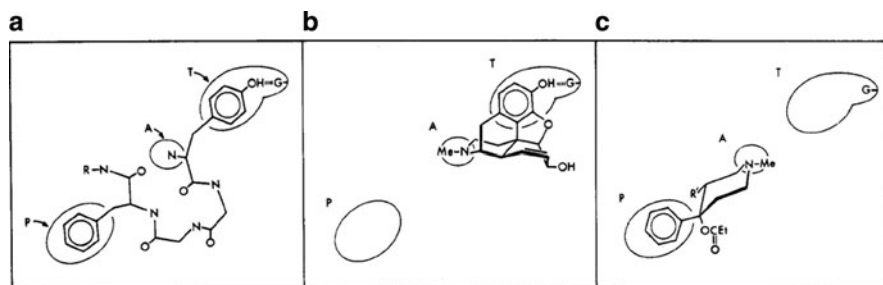
Fig. 11 Schematic models proposed by Protoghese et al. [64]: (**a**) peptide, (**b**) morphine, and (**c**) allylprodine. The anionic (A) subsite interacts with the charged N-terminus of the opioid peptide. The T and P subsites recognize the aromatic residues of Tyr[1] and Phe[4] of the opioid peptide. Reprinted from [64] with permission from American Chemical Society. Copyright (1981)

In addition, traditional quantitative structure–activity relationship (QSAR) models were reported. Gozalbes et al. attempted to predict the blood–brain barrier permeabilities of four arylacetamides using linear discriminant analysis [65], while Medina-Franco et al. discriminated between active and inactive BCG compounds using two-dimensional (2D) and three-dimensional (3D) structural-similarity methods [66].

3.2 Ligand-Based Models Using Molecular Superposing Methods

It is difficult to superpose different skeletons onto one another. Therefore, these methods have required congeneric compounds or the charged NH$^+$ moiety as a matching point. Lavecchia et al. constructed a ligand-based model for eight arylacetamides in which the charged NH$^+$, amide carbonyl, and benzene ring moieties were used as overlapping points [36]. The reported distances among the pharmacophoric points, and the root-mean-square distances from the reference arylacetamide U-50488H, were relatively small.

Filizola et al. proposed each δ, μ, and κ-pharmacophore model using morphinans, fentanyl, and so on [37, 38]. Their κ-model was made up of one κ-specific moiety and five common recognition moieties: the charged NH$^+$ moiety, two hydrophobic moieties of the C and D-rings (corresponding to the 8 and 15-positions of morphine), the aromatic ring, and the phenolic hydroxyl group. The one κ-specific hydrophobic moiety is a long side chain at the positive amine.

In our previous study using the SUPERPOSE program, which does not require an anchor point, the arylacetamide U-50488H was superposed on the morphinan TRK-820 [16]. This model indicated a basic amine and an amide side chain as overlapping points (Fig. 12).
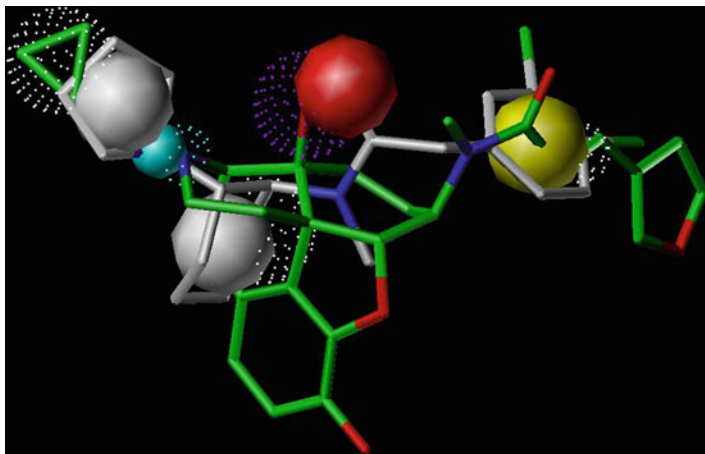
Fig. 12 Our previous superimposition of U-50488H (arylacetamide) on TRK-820 (morphinan) [16]. TRK-820 is shown in *green*, and U-50488H is shown in *white*. Sphere colors indicate the following properties (see Sect. 4.3): hydrophobic (HP, *white*); aromatic (AR, *green*); hydrogen-bond donors (HD, *blue*); hydrogen-bond acceptors (HA, *red*); and hydrogen-bond donors/acceptor (DA, *violet*). *Large and small spheres* represent radii of 1 and 0.5 Å, respectively. The TRK-820 and U-50488H spheres are represented by *dotted and solid spheres*, respectively. Only matched spheres are indicated

3.3 Docking Models Based on Homology Modeling and Ligand Docking Methods

As the X-ray structures of opioid receptors are not yet available, all docking models of κ-agonists have been based on homology models derived from other GPCRs. Subramanian et al. docked arylacetamides to a homology model of KOR, and showed that a salt bridge between the amino proton of the ligands and Asp138, which is the conserved residue in opioid receptors, is important for the agonist association [39]. Lavecchia et al. reported docking models of arylacetamides and a benzomorphan (Fig. 13), and also found that the salt bridge with Asp138 is important for the ligand-receptor recognition process [36]. A hydrogen bond between the amide oxygen of the arylacetamide and the hydroxyl group of Tyr312, and a π-stacking between the dichlorobenzene ring of the arylacetamide and the phenol ring of Try312 were observed, while a hydrogen bond between the phenolic hydroxyl group of the benzomorphan and the imidazole ring of His291 was indicated.

In a docking model of benzodiazepines reported by Anzini and colleagues, these residues were also indicated as key [29, 31]. Kane et al. reported docking models of an arylacetamide, the analog of DuP 747, and listed Asp138, His291, and Tyr312 as important residues [42]. Pogozheva et al. docked the cyclic peptide MP-16, and
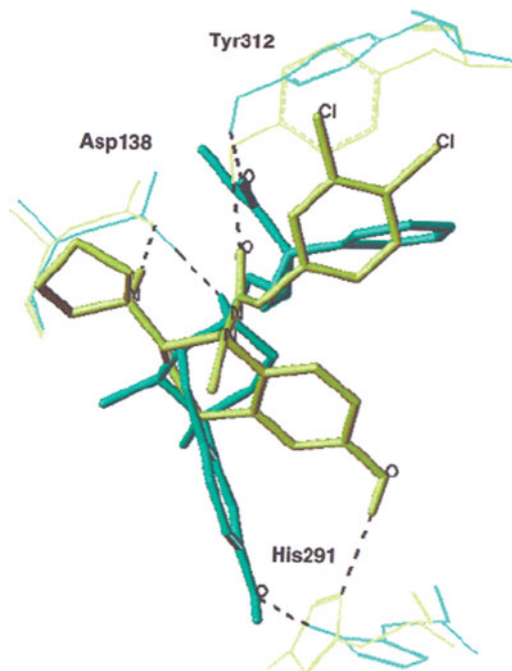
showed that the N-terminus, the hydroxyl group of Tyr, and the benzene ring of Phe in the peptide interacted with Asp138, His291, and Tyr312 on the KOR, respectively [41]. In addition, both Pogozheva et al. [41] and Kane et al. [42] docked antagonists norBNI and GNTI, showing that the second positive charge corresponding to the address domain interacted with Glu297. In the model reported by Holzgrabe and Brandt, in which HZ2 was docked, the two charged NH^+ groups interacted with Glu209 and Glu297 instead of the conserved Asp138. A π-stacking was also observed between Tyr312 and the pyridine ring of HZ2, while a covalent bond between the side chain of Lys200 and the ketocarbonyl carbon atom of HZ2 was predicted, resulting in the long duration of action [40].

Two different docking models have been proposed for salvinorin A. The first (Fig. 14a), put forward by Roth and colleagues, involves the furan ring of salvinorin A interacting with Tyr119 and Tyr320 by a branched hydrogen bond, and a CH-π interaction between the acetyl group of salvinorin A and Tyr313 [32, 33]. In the second model (Fig. 14b), put forward by Kane et al., only Tyr320 is stacked with the furan ring. A CH-π interaction is predicted between Tyr119 and the acetyl group, with another interaction predicted between Tyr313 and the methyl ester group [34, 35]. As described above, docking models strongly depend on homology models of KORs and docking protocols. The state-of-the-art in modeling and ligand docking for GPCRs, to which opioid receptors belong, will be given by [44–47].
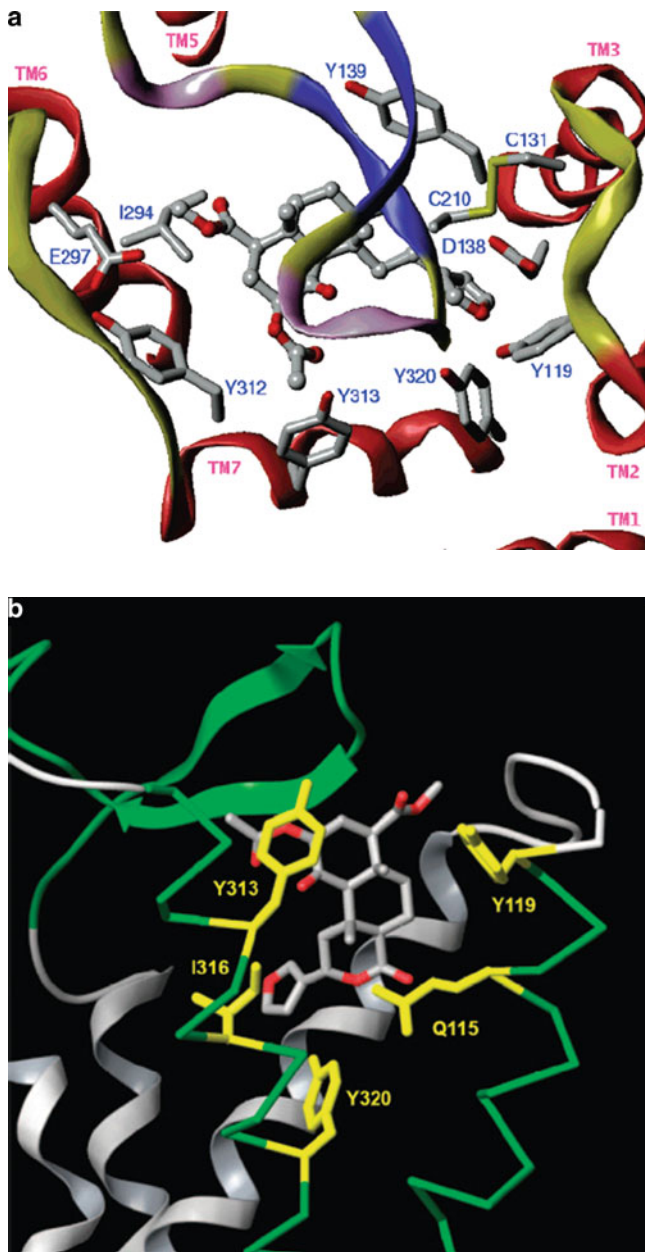
Fig. 14 Two different docking models for salvinorin A, reported by Roth and colleagues [33] (**a**) and Kane et al. [35] (**b**). Reprinted from [33] [Copyright (2005)] and [35] [Copyright (2008)] with permission from American Chemical Society

4 Universal Pharmacophore Model Accounting for All Known Skeletons of κ-Agonists

A universal pharmacophore model taking into account all skeletons remains elusive, because of the differences in their chemical structures. We therefore tried to construct such a 3D-pharmacophore model using the superposing method, which does not require a predefined anchor point [67].

4.1 Preparation of Data Sets

In order to identify the 3D-pharmacophore for κ-agonists, we prepared two data sets: the training set (Fig. 15) and the test set (Fig. 16). Ligands with high affinities and high to intermediate selectivities were used as the training set, which consisted of four morphinans (TRK-820, KNT-63, KNT-62, and NS-22) [14–16], two arylacetamides (U-69593 and U-50488H) [17, 18], and one neoclerodane diterpene (salvinorin A) [32]. In the test set, the affinities ranged from high to intermediate, and the selectivities ranged from high to low. The test set comprised two morphinans (TAN-821 [68] and morphine), one benzomorphan (bremazocine) [9, 12], one diazabicyclononanone (HZ2) [23, 24, 69], one BCG (TPI 614-1) [8, 26, 27], one benzodiazepine (tifluadom) [28–31], and one peptide (MP-16) [7]. Binding assays of the following compounds (TRK-820, KNT-63, KNT-62, NS-22, TAN-821, morphine, and U-69593) were carried out in duplicate using guinea pig brain homogenates (the cerebellum for κ and the forebrain for μ). The ability of each compound was evaluated by displacement of [³H]-U-69593 (κ) and [³H]-DAMGO (μ). Data for other compounds were taken from [7, 16, 20, 23, 24, 27, 30–32, 50, 55]. All agonists were prepared by SYBYL 6.9.1 (Tripos Inc.). The ionization states of molecules were determined according to references or pK_a calculations (ADMET Predictor 4.0, Simulations Plus, Inc.).

4.2 Conformational Sampling of κ-Agonists

Conformational analyses of all compounds were performed on an Apple Power Mac G5 (PowerPC G5; 2.5 GHz; two central processing units [CPUs]) using the Conformational Analyzer with Molecular Dynamics And Sampling (CAMDAS) 2.1 program [70]. Ten MD calculations were simultaneously performed using different initial structures. Each of the MD calculations was carried for 1 ns with an integral time step of 1 fs. The lengths of the covalent bonds were fixed. The temperature of the system was maintained at 1,200 K in order to enhance the sampling efficiency. Conformers were sampled at every 100 steps, and then each conformer was minimized until the root-mean-square of the gradients of the

Training Set
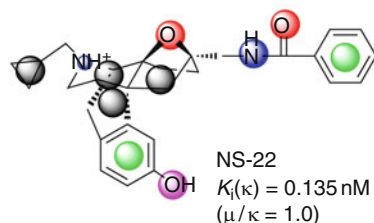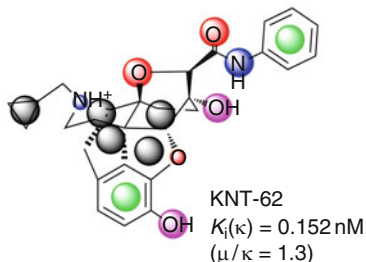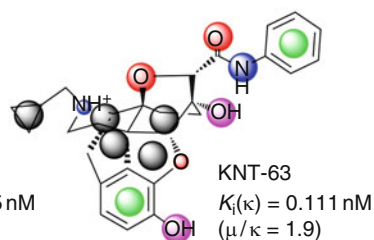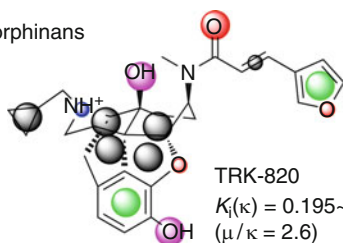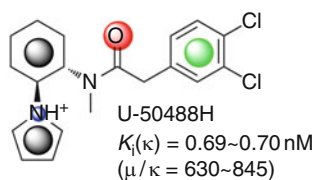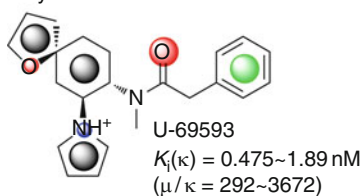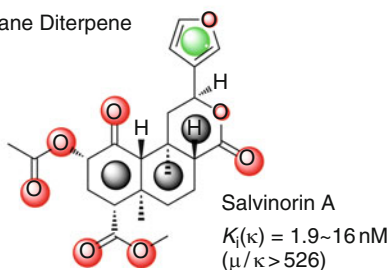
Fig. 15 κ-Agonists in training set and their property spheres. Training set comprising four morphinans (TRK-820, KNT-63, KNT-62, and NS-22), two arylacetamides (U-69593 and U-50488H), and one neoclerodane diterpene (salvinorin A). The spheres on each molecule are property spheres for molecular superposition. The colors of the spheres indicate the following properties: hydrophobic (HP, *black*); aromatic (AR, *green*); hydrogen-bond donors (HD, *blue*); hydrogen-bond acceptors (HA, *red*); and hydrogen-bond donors/acceptor (DA, *violet*). *Large and small spheres* indicate radii of 1 and 0.5 Å, respectively. μ/κ = $K_i(\mu)/K_i(\kappa)$
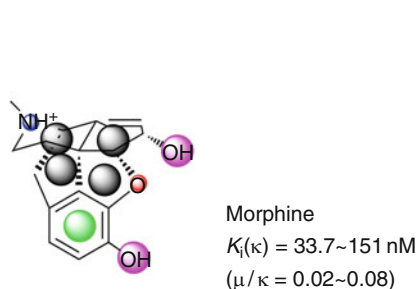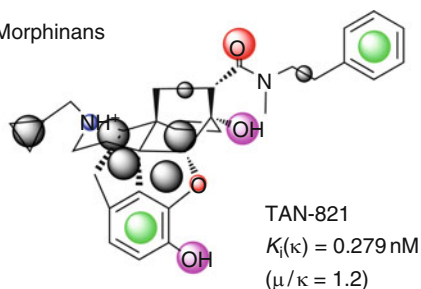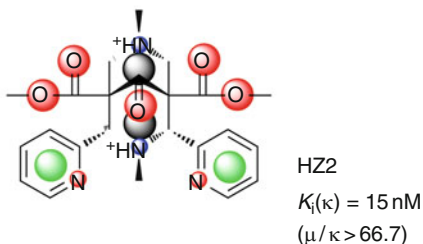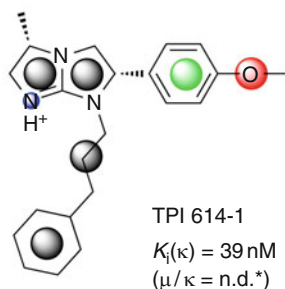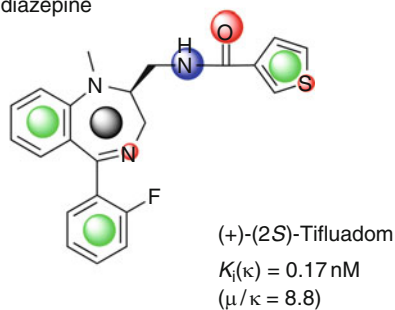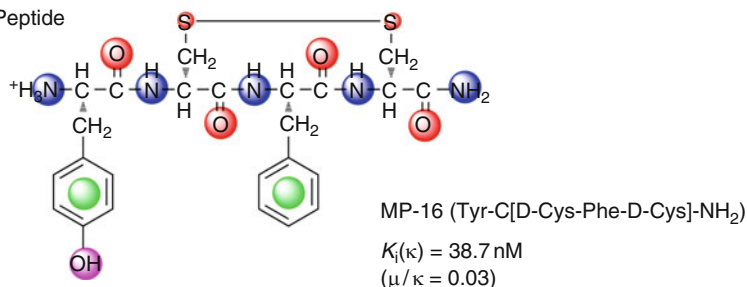
Test Set

Fig. 16 κ-Agonists in test set and their property spheres. Test set comprising two morphinans (TAN-821 and morphine), one benzomorphan (bremazocine), one diazabicyclononanone (HZ2),

potential energy was below 0.001 kcal mol^{-1} Å^{-1}. All conformations were clustered with torsion angles of heavy atoms using a threshold of ±30°. The Merck molecular force field (MMFF) 94s was used to evaluate the potential energy surface of the molecule [71, 72]. The dielectric constant was 80, but no cut-off distance for non-bonded interactions was used. The conformers within 15 kcal mol^{-1} of the minimum energy of the molecule were adopted for superposition because of the low probability of the existence of conformers with higher energies.

4.3 Pharmacophore Extraction Through a Series of Molecular Superpositions

All agonist molecule conformations were superposed onto each another using the parallel version of the SUPERPOSE program [73]. This superposes two molecules based on the physicochemical properties of the atomic groups, which is useful for elucidating the 3D-pharmacophore and estimating the binding conformation of each molecule by distinguishing it from the many conformations that are generated by CAMDAS. The program considers five types of physicochemical property: hydrophobic (HP), aromatic (AR), hydrogen-bond donors (HD), hydrogen-bond acceptors (HA), and hydrogen-bond donors/acceptors (DA). Each type is represented as a sphere with a predefined radius (1.0 Å or 0.5 Å) and is assigned to a functional group in a molecule (Fig. 15). After molecular superposition, the overlaps of the spheres are scored using the scoring matrix (Table 1). One set of agonist conformations was chosen for the binding conformations based on the sum of the scores, and the 3D-pharmacophore was represented as one set of matched spheres on the binding conformations. For the training set we used a series of superpositions to determine the binding conformations. The binding conformations of the test set were extracted using those of the training set. The superposition calculations were performed using 28 nodes of a Dell PowerEdge 1950III (Quad Core Xeon X5460; 3.16 GHz; 56 CPUs in total).

4.4 Determined 3D-Pharmacophore for All κ-Agonists

The alignment of training set KOR agonists in estimated binding conformations and the 3D-pharmacophore of TRK-820 are shown in Fig. 17. The 3D-pharmacophore

---

Fig. 16 (continued) one bicyclic guanidine (TPI 614-1), one benzodiazepine (tifluadom), and one peptide (MP-16). The spheres on each molecule are property spheres for molecular superposition. The colors of the spheres indicate the following properties: hydrophobic (HP, *black*); aromatic (AR, *green*); hydrogen-bond donors (HD, *blue*); hydrogen-bond acceptors (HA, *red*); and hydrogen-bond donors/acceptor (DA, *violet*). *Large and small spheres* indicate radii of 1 and 0.5 Å, respectively. μ/κ = $K_i(μ)/K_i(κ)$. *n.d.* no data

Table 1 Scoring matrix for SUPERPOSE program

	HP	AR	HD	HA	DA
HP	+3	+3	–2	–2	–2
AR	+3	+4[a]	–2	–2	–2
HD	–2	–2	+2	–2	+1
HA	–2	–2	–2	+2	+1
DA	–2	–2	+1	+1	+1

[a]If the planes of two rings cannot be superposed upon each other, a score of +3 is given

of the κ-agonists required three hydrophobic groups (AR1, HP2, and HP3), one hydrogen-bond donor (HD1), and three hydrogen-bond acceptors (DA1, HA2, and HA3). For TRK-820, these corresponded to the following: HD1 as the charged NH^+ group, AR1 as the A ring, and DA1 as the oxygen atom of the phenolic hydroxyl group; HP2 as the C ring and HA2 as the oxygen atom of the amide; and HP3 as the E ring and HA3 as the oxygen atom of the 4,5-epoxy moiety. The κ-agonists in the test set overlapped with the 3D-pharmacophore determined by the training set (Fig. 18).

The estimated binding orientations of κ-agonists are classified into four types (Fig. 19): type I comprises the T-shape orientations of morphinans, peptides, and BCGs; type II comprises the left-to-bottom orientations of arylacetamides and diazabicyclononanones; type III comprises the left-to-right orientations of benzomorphans; and type IV comprises the bottom-to-right orientations of neoclerodane diterpenes and benzodiazepines.

On the MP-16 peptide, HD1 is the charged N-terminus, AR1 and DA1 the side chain of Tyr, and HP2 and HA2 the side chain and amide oxygen atom of the main chain of Phe (Fig. 20). According to the model described by Protoghese et al. (Fig. 11), HD1 corresponds to the anionic (A) subsite on the receptor, AR1 and DA1 correspond to the Tyr (T) subsite, and HP2 and HA2 correspond to the Phe (P) subsite [63, 64]. Type I occupies all of the subsites, types II and III use the A–T and A–P subsites, respectively, while type IV has a unique binding orientation as the ligands lack the charged NH^+ group. Therefore, the A subsite on the receptor is not used, and type IV ligands extend from the T subsite to the P subsite.

The matched property spheres of each κ-agonist are shown in Table 2. All κ-ligands include at least four of the seven spheres. The higher κ-selective ligands contain HP3 and HA3, but lack two or more of HD1, HP1, DA1, HP2, and HA2. Ligand affinities to the μ-receptor might have been weakened through lacking part of the message domain; however, affinities to the κ-receptor might be compensated for by interactions of HP3 and HA3. Therefore, HP3 and HA3 appear to contribute to κ-selectivity. Ligands with acceptor atoms corresponding to HA2 show relatively high affinities. If a ligand has all property spheres, its activity might be high but its selectivity intermediate.

Moreover, when a ligand has a hydrophobic moiety beyond HA2, such as TRK-820, salvinorin A, and tifluadom, the κ-selectivity might be relatively high (Figs. 25 and 26). The hydrophobic moiety might correspond to the Leu or aliphatic part of Arg in the κ-address domain. The κ-selective antagonists norBNI and GNTI have
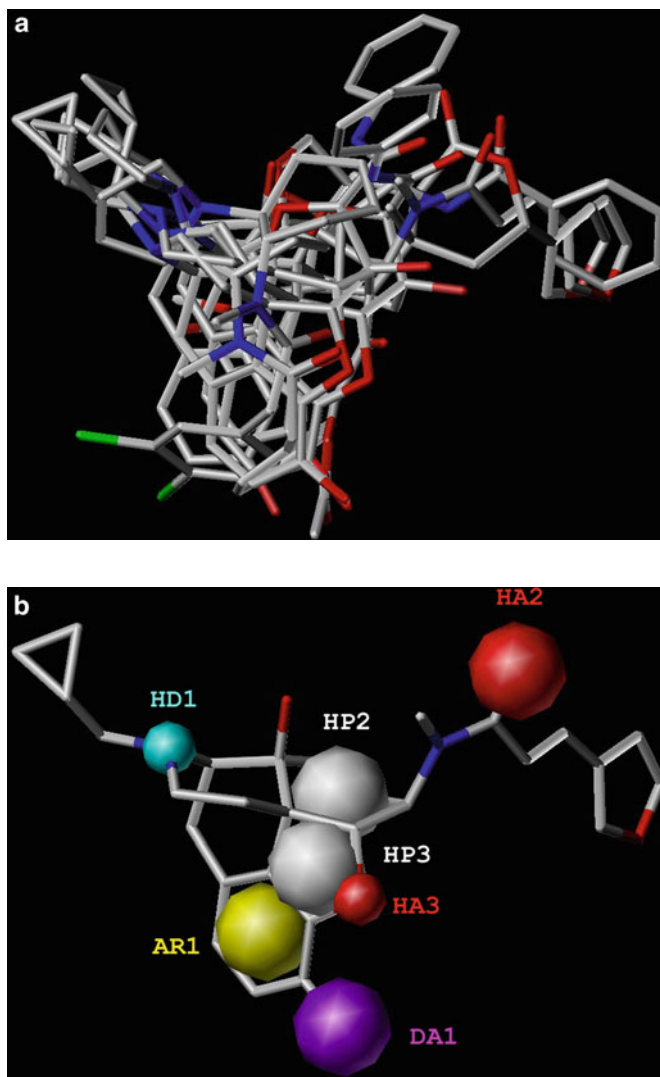
Fig. 17 Alignment of estimated binding conformations of training set and 3D-pharmacophore for κ-agonists. (**a**) Alignment of training set. (**b**) 3D-pharmacophore represented by property spheres on TRK-820. The colors of the spheres indicate the following properties: hydrophobic (HP, *white*); aromatic (AR, *green*); hydrogen-bond donors (HD, *blue*); hydrogen-bond acceptors (HA, *red*); and hydrogen-bond donors/acceptor (DA, *violet*). *Large and small spheres* represent radii of 1 and 0.5 Å, respectively

larger and positively charged moieties corresponding to Leu-Arg-Arg (Fig. 10) [58–60]. Hence, if a longer but thinner positive moiety is introduced into a ligand, it might become a κ-selective agonist.
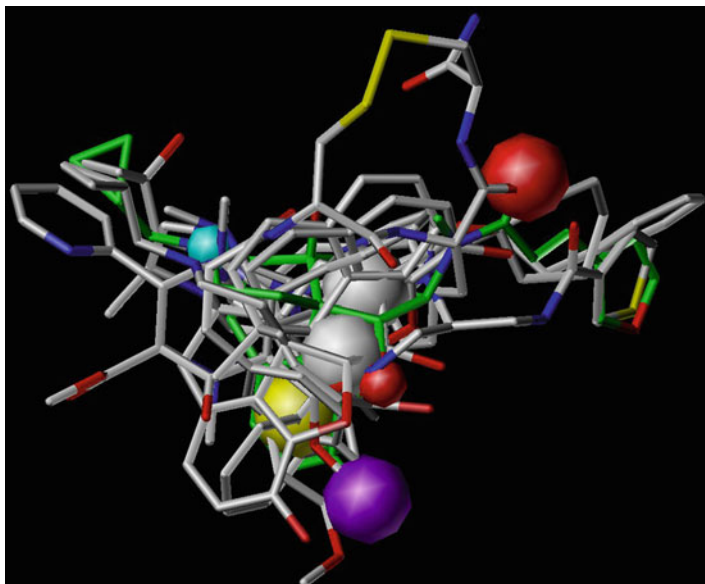
Fig. 18 Alignment of estimated binding conformations of the test set. TRK-820 is shown in *green*, and the compounds in the test set are shown in *white*. The 3D-pharmacophore on TRK-820 is shown as *solid spheres*
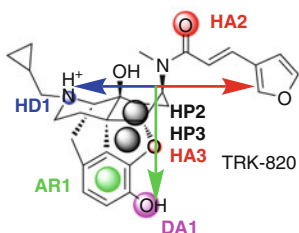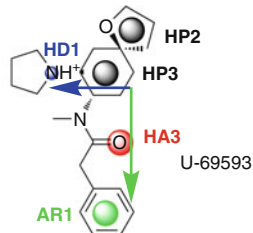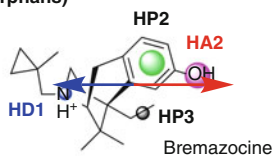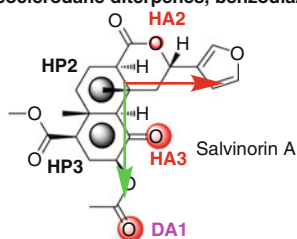
Fig. 19 Classification of binding orientations for κ-agonists. The binding orientations are divided into four classes: type I with a T-shape orientation; type II with a left-to-bottom orientation; type III with a left-to-right orientation; and type IV with a bottom-to-right orientation
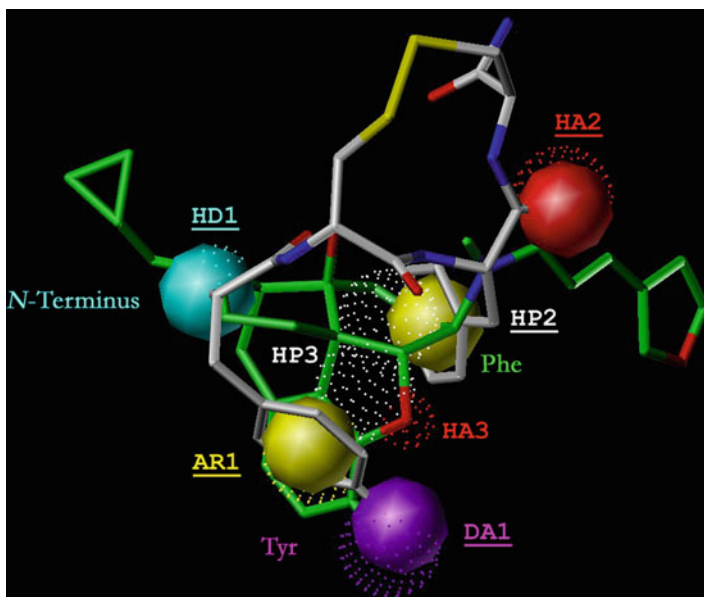
Fig. 20 Superimposition of MP-16 (peptide) on TRK-820 (morphinan) and their 3D-pharmacophores. TRK-820 is shown in *green*, and MP-16 is shown in *white*. The 3D-pharmacophores of TRK-820 and MP-16 are represented by *dotted and solid spheres*, respectively. Matched spheres are indicated by *underlined labels*

In the case of HP3 and HA3, one of the effects of the 4,5-epoxy (E) ring introduced into the morphinan skeleton might have been to maintain the binding conformation with the κ-receptor. A similar effect was observed upon the introduction of the 10-methylene bridge (B ring) to the δ-agonist TAN-67 [74]. The κ-affinity and κ-selectivity of the 10-methylene-bridged SN-28 were 72 and three times greater than those of TAN-67, respectively (Fig. 21). The oxygen atom (HA3) of the epoxy is adjacent to the hydroxyl group (DA1) of the phenol moiety. A hydroxyl group of the protein, such as Tyr, Thr, or Ser, could potentially bind to both by a branched hydrogen bond.

Although bremazocine was expected to adopt the type II binding orientation, type III was chosen by the SUPERPOSE program (Fig. 22). This suggests that the type II orientation might be favorable for the μ-receptor, whereas the type III orientation might be preferable for the κ-receptor. Although compounds from all classes were used to construct our model, the type II orientations for arylacetamides (Fig. 23) were in agreement with the model reported by Lavecchia et al. that used eight arylacetamides and one benzomorphan, MPCB [36]. In this model, the phenol moiety of MPCB was not matched with the dichlorobenzene moiety of arylacetamides (Fig. 13), which supports the type III orientation for bremazocine (benzomorphan) in our current model. This could show similarities to the binding of phenylpiperidines and allylprodines (thin, morphine-like compounds) to the

Table 2 Matching table of property spheres sorted by κ-selectivities

Agonists	μ/κ[a]	HD1	AR1	DA1	HP2	HA2	HP3	HA3
U-69593	292–3,672	HD	AR	–	HP	–	HP	HA
U-50488H	630–845	HD	AR	–	HP	–	–	HA
Salvinorin A	>526	–	–	HA	HP	HA	HP	HA
HZ2	>66.7	HD	–	HA	HP	–	–	HA
Bremazocine	3.8–15.0	HD	–	–	AR	DA	HP	–
Tifluadom	8.8	–	AR	–	–	HA	HP	HA
TRK-820	2.6	HD	AR	DA	HP	HA	HP	HA
KNT-63	1.9	HD	AR	DA	HP	HA	HP	HA
KNT-62	1.3	HD	AR	DA	HP	HA	HP	HA
TAN-821	1.2	HD	HP	–	HP	HA	HP	DA
NS-22	1.0	HD	AR	DA	HP	HA	–	–
Morphine	0.02–0.08	HD	HP	–	AR	DA	HP	DA
MP-16	0.03	HD	AR	DA	AR	HA	–	–
TPI 614-1	n.d.[b]	HD	AR	HA	HP	–	–	–

[a]μ/κ = $K_i(μ)/K_i(κ)$
[b]No data

Fig. 21 The effect of bridging on κ-affinity of the δ-agonist TAN-67. (**a**) TAN-67 ($K_i(κ)$ = 732.45 nM, μ/κ = 0.388, δ/κ = 0.197×10^{-2}). (**b**) The 10-methylene-bridged SN-28 ($K_i(κ)$ = 10.2 nM, μ/κ = 1.13, δ/κ = 1.4×10^{-2})
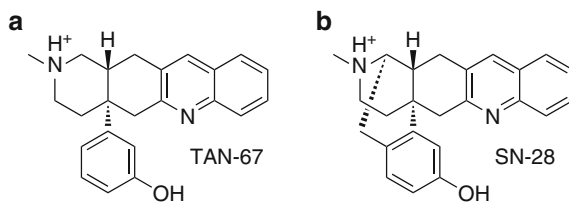
μ-receptor (see Sect. 3.1 and Fig. 11) [63, 64]. The μ-binding mode of these ligands is thought to be the A–P orientation (type III), whereas that of morphine is the A–T orientation (type II).

In our model, the κ-binding mode of morphine was predicted to be type III (Fig. 24). However, the binding site of the κ-receptor could not accept morphine, because it is larger than bremazocine. In addition, the conformation of the C ring of TRK-820 determined by our calculation was the boat form, which is important for the κ-activity to maintain the binding conformation. By contrast, the C ring of morphine is the cyclohexene ring. In a previous study, we reported the type III orientation for arylacetamides by superimposing them on TRK-820 (Fig. 12) [16]. In the current study using all κ-selective classes, the type II orientation was found to be the most likely (Fig. 23), followed by type III. However, it is possible that arylacetamides adopt both in the κ-receptor.

The orientation of type IV for salvinorin A in our model differs from the docking models reported by Roth and colleagues [32, 33] and by Kane et al. [34, 35] (Fig. 14). In our model, salvinorin A avoided the position of the charged NH⁺ group (HD1), that is, the vicinity of the conserved Asp138 in all opioid receptors,
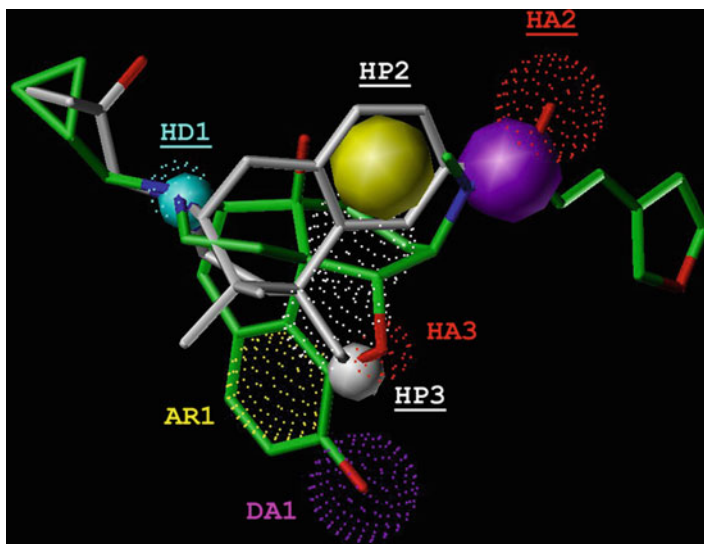
Fig. 22 Superimposition of bremazocine (benzomorphan) on TRK-820 (morphinan) and their 3D-pharmacophores. TRK-820 is shown in *green*, and bremazocine is shown in *white*. The 3D-pharmacophores of TRK-820 and bremazocine are represented by *dotted and solid spheres*, respectively. Matched spheres are indicated by *underlined labels*
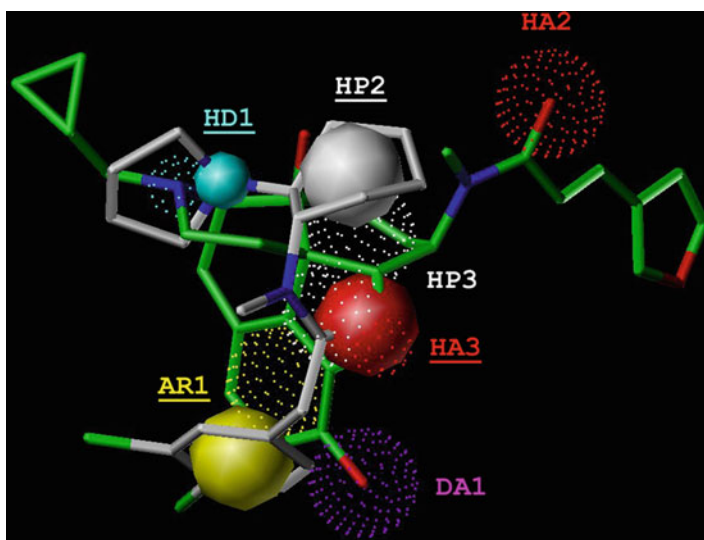
Fig. 23 Superimposition of U-50488H (arylacetamide) on TRK-820 (morphinan) and their 3D-pharmacophores. TRK-820 is shown in *green*, and U-50488H is shown in *white*. The 3D-pharmacophores of TRK-820 and U-50488H are represented by *dotted and solid spheres*, respectively. Matched spheres are indicated by *underlined labels*
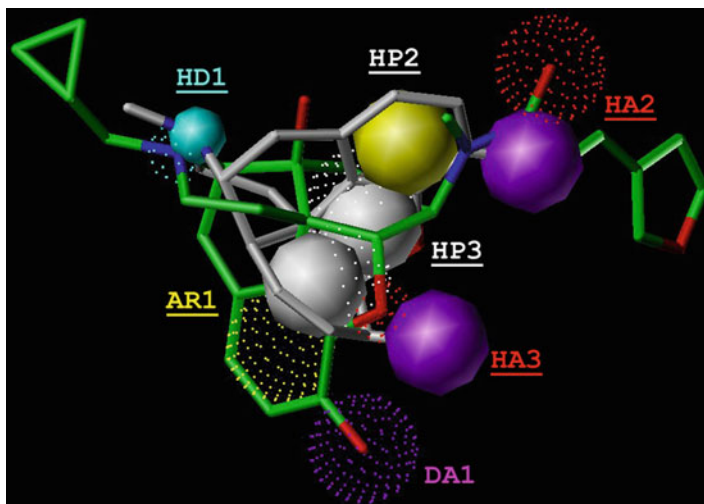
Fig. 24 Superimposition of morphine (morphinan) on TRK-820 (morphinan) and their 3D-pharmacophores. TRK-820 is shown in *green*, and morphine is shown in *white*. The 3D-pharmacophores of TRK-820 and morphine are represented by *dotted and solid spheres*, respectively. Matched spheres are indicated by *underlined labels*
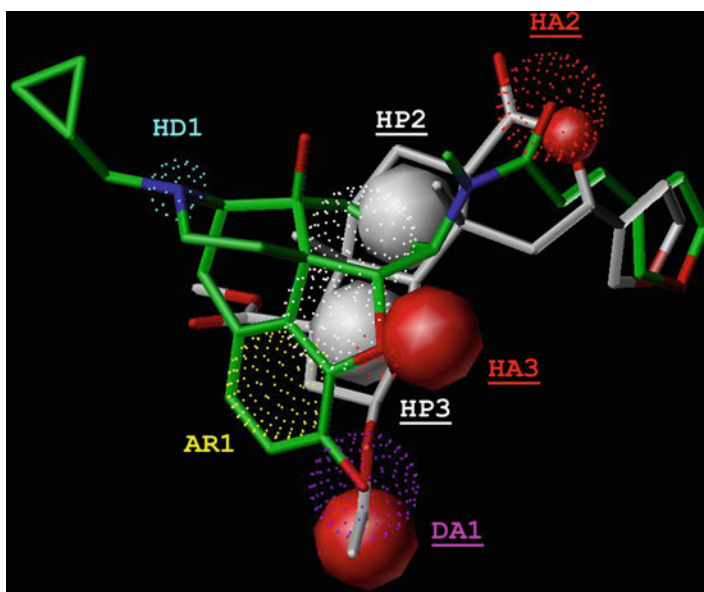
Fig. 25 Superimposition of salvinorin A (neoclerodane diterpene) on TRK-820 (morphinan) and their 3D-pharmacophores. TRK-820 is shown in *green*, and salvinorin A is shown in *white*. The 3D-pharmacophores of TRK-820 and salvinorin A are represented by *dotted and solid spheres*, respectively. Matched spheres are indicated by *underlined labels*
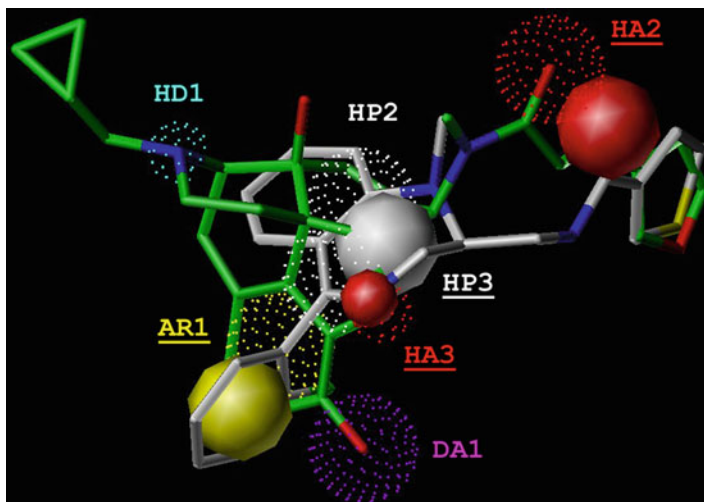
Fig. 26 Superimposition of tifluadom (benzodiazepine) on TRK-820 (morphinan) and their 3D-pharmacophores. TRK-820 is shown in *green*, and tifluadom is shown in *white*. The 3D-pharmacophores of TRK-820 and tifluadom are represented by *dotted and solid spheres*, respectively. Matched spheres are indicated by *underlined labels*
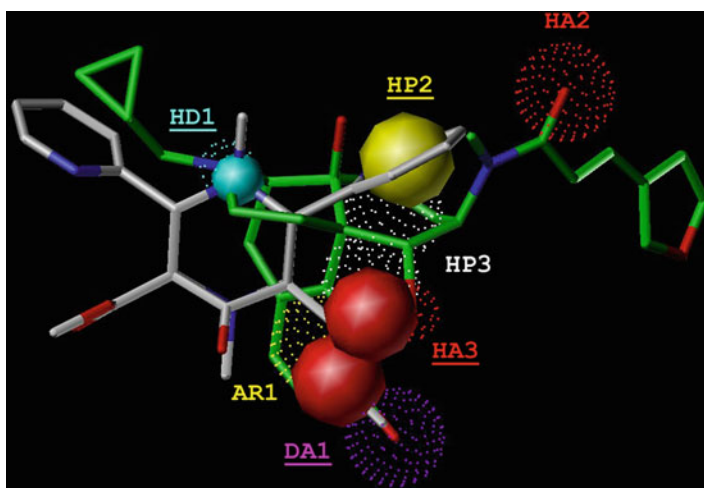
Fig. 27 Superimposition of HZ2 (diazabicyclononanone) on TRK-820 (morphinan) and their 3D-pharmacophores. TRK-820 is shown in *green*, and HZ2 is shown in *white*. The 3D-pharmacophores of TRK-820 and HZ2 are represented by *dotted and solid spheres*, respectively. Matched spheres are indicated by *underlined labels*
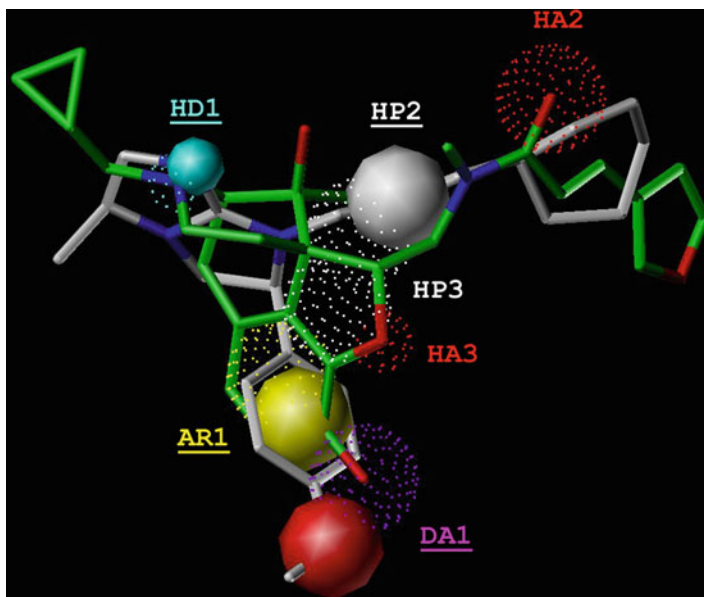
Fig. 28 Superimposition of TPI 614-1 (bicyclic guanidine) on TRK-820 (morphinan) and their 3D-pharmacophores. TRK-820 is shown in *green*, and TPI 614-1 is shown in *white*. The 3D-pharmacophores of TRK-820 and TPI 614-1 are represented by *dotted and solid spheres*, respectively. Matched spheres are indicated by *underlined labels*

because it only has acceptor atoms (Fig. 25). Moreover, the furan ring of salvinorin A overlapped with that of TRK-820. It was therefore assumed that our model was reliable.

Similarly, the docking model of tifluadom reported by Anzini and colleagues differed from our model [29, 31]. In the latter, the position of HD1 was not occupied by tifluadom because the imine nitrogen atom was not thought to be protonated based on our acid dissociation constant (pK_a) calculation (Fig. 26). As the thiophene ring of tifluadom in our model was matched to the furan ring of TRK-820, we considered our model to be acceptable.

Holzgrabe and Brandt proposed a docking model of HZ2, in which the two charged NH$^+$ groups interacted with Glu209 and Glu297 instead of the conserved Asp138 [40]. In our model, one of the two NH$^+$ groups occupied the HD1 position corresponding to Asp138 and the binding orientation was type II as in arylacetamides (Fig. 27). This can explain the high κ-selectivity of HZ2.

The κ-selectivities and κ-agonist activities of BCGs are unknown. In our proposed model for BCGs, the T-shape orientation of TPI 614-1 was similar to that of TRK-820, except for the amide oxygen of HA2 (Fig. 28). Therefore, BCGs might be promising as κ-selective agonists.

5   Conclusion

In conclusion, we constructed a 3D-pharmacophore model for κ-agonists which can account for all known skeletons. This model can provide a rationale for the activities of existing κ-agonists and for designing new κ-selective agonists.

References

1. Kieffer BL (1995) Recent advances in molecular recognition and signal transduction of active peptides: receptors for opioid peptides. Cell Mol Neurobiol 15:615–635
2. Dhawan BN, Cesselin F, Raghubir R, Reisine T, Bradley PB, Portoghese PS, Hamon M (1996) International Union of Pharmacology. XII. Classification of opioid receptors. Pharmacol Rev 48:567–592
3. Millan MJ (1990) κ-Opioid receptors and analgesia. Trends Pharmacol Sci 11:70–76
4. Williams M, Kowaluk EA, Arneric SP (1999) Emerging molecular approaches to pain therapy. J Med Chem 42:1481–1500
5. Chavkin C, Goldstein A (1981) Specific receptor for the opioid peptide dynorphin: structure–activity relationships. Proc Natl Acad Sci U S A 78:6543–6547
6. Dooley CT, Ny P, Bidlack JM, Houghten RA (1998) Selective ligands for the μ, δ, and κ opioid receptors identified from a single mixture based tetrapeptide positional scanning combinatorial library. J Biol Chem 273:18848–18856
7. Przydzial MJ, Pogozheva ID, Bosse KE, Andrews SM, Tharp TA, Traynor JR, Mosberg HI (2005) Roles of residues 3 and 4 in cyclic tetrapeptide ligand recognition by the κ-opioid receptor. J Pept Res 65:333–342
8. Houghten RA, Dooley CT, Appel JR (2006) In vitro and direct in vivo testing of mixture-based combinatorial libraries for the identification of highly active and specific opiate ligands. AAPS J 8:E371–E382
9. Corbett AD, Kosterlitz HW (1986) Bremazocine is an agonist at kappa-opioid receptors and an antagonist at mu-opioid receptors in the guinea-pig myenteric plexus. Br J Pharmacol 89:245–249
10. Tamura T, Ogawa J, Taniguchi T, Waki I (1990) Preferential action of eptazocine, a novel analgesic, with opioid receptors in isolated guinea pig ileum and mouse vas deferens preparations. Folia Pharmacol Japon 95:41–46
11. Ronsisvalle G, Pasquinucci L, Pappalardo MS, Vittorio F, Fronza G, Romagnoli C, Pistacchio E, Spampinato S, Ferri S (1993) Non-peptide ligands for opioid receptors. Design of κ-specific agonists. J Med Chem 36:1860–1865
12. Dortch-Carnes J, Potter DE (2005) Bremazocine: a κ-opioid agonist with potent analgesic and other pharmacologic properties. CNS Drug Rev 11:195–212
13. Pasquinucci L, Iadanza M, Marrazzo A, Prezzavento O, Ronsisvalle S, Scoto GM, Parenti C, De Luca L, Ronsisvalle G (2007) New benzomorphan derivatives of MPCB as MOP and KOP receptor ligands. Pharmazie 62:813–824
14. Kawai K, Hayakawa J, Miyamoto T, Imamura Y, Yamane S, Wakita H, Fujii H, Kawamura K, Matsuura H, Izumimoto N, Kobayashi R, Endo T, Nagase H (2008) Design, synthesis, and structure–activity relationship of novel opioid κ-agonists. Bioorg Med Chem 16:9188–9201
15. Nemoto T, Fujii H, Narita M, Miyoshi K, Nakamura A, Suzuki T, Nagase H (2008) Synthesis of a novel 6,14-epoxymorphinan derivative and its pharmacology. Bioorg Med Chem Lett 18:6398–6401

16. Nagase H, Watanabe A, Nemoto T, Yamaotsu N, Hayashida K, Nakajima M, Hasebe K, Nakao K, Mochizuki H, Hirono S, Fujii H (2010) Drug design and synthesis of a novel κ opioid receptor agonist with an oxabicyclo[2.2.2]octane skeleton and its pharmacology. Bioorg Med Chem Lett 20:121–124

17. Szmuszkovicz J, Von Voigtlander PF (1982) Benzeneacetamide amines: structurally novel non-mμ opioids. J Med Chem 25:1125–1126

18. Lahti RA, Mickelson MM, McCall JM, Von Voigtlander PF (1985) [3H]U-69593 a highly selective ligand for the opioid κ receptor. Eur J Pharmacol 109:281–284

19. Halfpenny PR, Horwell DC, Hughes J, Hunter JC, Rees DC (1990) Highly selective κ-opioid analgesics. 3. Synthesis and structure-activity relationships of novel N-[2-(1-pyrrolidinyl)-4- or -5-substituted cyclohexyl]arylacetamide derivatives. J Med Chem 33:286–291

20. Hunter JC, Leighton GE, Meecham KG, Boyle SJ, Horwell DC, Rees DC, Hughes J (1990) CI-977, a novel and selective agonist for the kappa-opioid receptor. Br J Pharmacol 101:183–189

21. Rajagopalan P, Scribner RM, Pennev P, Schmidt WK, Tam SW, Steinfels GF, Cook L (1992) DuP 747: a new, potent, kappa opioid analgesic. Synthesis and pharmacology1. Bioorg Med Chem Lett 2:715–720

22. Rajagopalan P, Scribner RM, Pennev P, Mattei PL, Kezar HS, Cheng CY, Cheeseman RS, Ganti VR, Johnson AL, Wuonola MA, Schmidt WK, Tam SW, Steinfels GF, Cook L (1992) DuP 747: sar study. Bioorg Med Chem Lett 2:721–726

23. Kögel B, Christoph T, Friderichs E, Hennies H-H, Matthiesen T, Schneider J, Holzgrabe U (1998) HZ2, a selective kappa-opioid agonist. CNS Drug Rev 4:54–70

24. Siener T, Cambareri A, Kuhl U, Englberger W, Haurand M, Kögel B, Holzgrabe U (2000) Synthesis and opioid receptor affinity of a series of 2,4-diaryl-substituted 3,7-diazabicyclono-nanones. J Med Chem 43:3746–3751

25. Benyhe S, Márki Á, Nachtsheim C, Holzgrabe U, Borsodi A (2003) Kappa-receptor selective binding of opioid ligands with a heterocyclic bicyclo[3.3.1]nonan-9-one structure. Acta Biol Hung 54:147–155

26. Houghten RA, Pinilla C, Appel JR, Blondelle SE, Dooley CT, Eichler J, Nefzi A, Ostresh JM (1999) Mixture-based synthetic combinatorial libraries. J Med Chem 42:3743–3778

27. Houghten RA, Pinilla C, Giulianotti MA, Appel JR, Dooley CT, Nefzi A, Ostresh JM, Yu Y, Maggiora GM, Medina-Franco JL, Brunner D, Schneider J (2008) Strategies for the use of mixture-based synthetic combinatorial libraries: scaffold ranking, direct testing in vivo, and enhanced deconvolution by computational methods. J Comb Chem 10:3–19

28. Freye E, Boeck G, Schaal M, Ciaramelli F (1986) The benzodiazepine (+)-tifluadom (KC-6128), but not its optical isomer (KC-5911) induces opioid kappa receptor-related EEG power spectra and evoked potential changes. Pharmacology 33:241–248

29. Cappelli A, Anzini M, Vomero S, Menziani MC, De Benedetti PG, Sbacchi M, Clarke GD, Mennuni L (1996) Synthesis, biological evaluation, and quantitative receptor docking simulations of 2-[(acylamino)ethyl]-1,4-benzodiazepines as novel tifluadom-like ligands with high affinity and selectivity for κ-opioid receptors. J Med Chem 39:860–872

30. Azzolina O, Collina S, Linati L, Anzini M, Cappelli A, Scheideler MA, Sbacchi M (2001) Enantiomers of 2-[(acylamino)ethyl]-1,4-benzodiazepines, potent ligands of κ-opioid receptor: chiral chromatographic resolution, configurational assignment, and biological activity. Chirality 13:606–612

31. Anzini M, Canullo L, Braile C, Cappelli A, Gallelli A, Vomero S, Menziani MC, De Benedetti PG, Rizzo M, Collina S, Azzolina O, Sbacchi M, Ghelardini C, Galeotti N (2003) Synthesis, biological evaluation, and receptor docking simulations of 2-[(acylamino)ethyl]-1,4-benzodiazepines as κ-opioid receptor agonists endowed with antinociceptive and anti-amnesic activity. J Med Chem 46:3853–3864

32. Roth BL, Baner K, Westkaemper R, Siebert D, Rice KC, Steinberg S, Ernsberger P, Rothman RB (2002) Salvinorin A: a potent naturally occurring nonnitrogenous κ opioid selective agonist. Proc Natl Acad Sci U S A 99:11934–11939

33. Yan F, Mosier PD, Westkaemper RB, Stewart J, Zjawiony JK, Vortherms TA, Sheffler DJ, Roth BL (2005) Identification of the molecular mechanisms by which the diterpenoid salvinorin A binds to κ-opioid receptors. Biochemistry 44:8643–8651

34. Kane BE, Nieto MJ, McCurdy CR, Ferguson DM (2006) A unique binding epitope for salvinorin A, a non-nitrogenous kappa opioid receptor agonist. FEBS J 273:1966–1974

35. Kane BE, McCurdy CR, Ferguson DM (2008) Toward a structure-based model of salvinorin A recognition of the κ-opioid receptor. J Med Chem 51:1824–1830

36. Lavecchia A, Greco G, Novellino E, Vittorio F, Ronsisvalle G (2000) Modeling of κ-opioid receptor/agonists interactions using pharmacophore-based and docking simulations. J Med Chem 43:2124–2134

37. Filizola M, Villar HO, Loew GH (2001) Molecular determinants of non-specific recognition of δ, μ, and κ opioid receptors. Bioorg Med Chem 9:69–76

38. Filizola M, Villar HO, Loew GH (2001) Differentiation of δ, μ, and κ opioid receptor agonists based on pharmacophore development and computed physicochemical properties. J Comput Aided Mol Des 15:297–307

39. Subramanian G, Paterlini MG, Larson DL, Portoghese PS, Ferguson DM (1998) Conformational analysis and automated receptor docking of selective arylacetamide-based κ-opioid agonists. J Med Chem 41:4777–4789

40. Holzgrabe U, Brandt W (2003) Mechanism of action of the diazabicyclononanone-type κ-agonists. J Med Chem 46:1383–1389

41. Pogozheva ID, Przydzial MJ, Mosberg HI (2005) Homology modeling of opioid receptor-ligand complexes using experimental constraints. AAPS J 07:E434–E448

42. Kane BE, Svensson B, Ferguson DM (2006) Molecular recognition of opioid receptor ligands. AAPS J 8:E126–E137

43. Kolb P, Ferreira RS, Irwin JJ, Shoichet BK (2009) Docking and chemoinformatic screens for new ligands and targets. Curr Opin Biotechnol 20:429–436

44. Michino M, Brooks CL III (2009) Predicting structurally conserved contacts for homologous proteins using sequence conservation filters. Proteins 77:448–453

45. Michino M, Abola E, GPCR Dock 2008 participants, Brooks CL III, Dixon JS, Moult J, Stevens RC (2009) Community-wide assessment of GPCR structure modelling and ligand docking: GPCR Dock 2008. Nat Rev Drug Discov 8:455–463

46. de Graaf C, Rognan D (2009) Customizing G protein-coupled receptor models for structure-based virtual screening. Curr Pharm Des 15:4026–4048

47. Katritch V, Rueda M, Lam PC-H, Yeager M, Abagyan R (2010) GPCR 3D homology models for ligand screening: lessons learned from blind predictions of adenosine A2a receptor complex. Proteins 78:197–211

48. Raynor K, Kong H, Chen Y, Yasuda K, Yu L, Bell GI, Reisine T (1994) Pharmacological characterization of the cloned κ-, δ-, and μ-opioid receptors. Mol Pharmacol 45:330–334

49. Lapalu S, Moisand C, Mazarguil H, Cambois G, Mollereau C, Meunier J-C (1997) Comparison of the structure-activity relationships of nociceptin and dynorphin A using chimeric peptides. FEBS Lett 417:333–336

50. Emmerson PJ, Liu MR, Woods JH, Medzihradsky F (1994) Binding affinity and selectivity of opioids at mu, delta and kappa receptors in monkey brain membranes. J Pharmacol Exp Ther 271:1630–1637

51. Gear RW, Miaskowski C, Gordon NC, Paul SM, Heller PH, Levine JD (1999) The kappa opioid nalbuphine produces gender- and dose-dependent analgesia and antianalgesia in patients with postoperative pain. Pain 83:339–345

52. Giardina G, Clarke GD, Dondio G, Petrone G, Sbacchi M, Vecchietti V (1994) Selective κ-opioid agonists: synthesis and structure-activity relationships of piperidines incorporating an oxo-containing acyl group. J Med Chem 37:3482–3491

53. Wang Y, Tang K, Inan S, Siebert D, Holzgrabe U, Lee DYW, Huang P, Li J-G, Cowan A, Liu-Chen L-Y (2005) Comparison of pharmacological activities of three distinct κ ligands

(Salvinorin A, TRK-820 and 3FLB) on κ opioid receptors in vitro and their antipruritic and antinociceptive activities in vivo. J Pharmacol Exp Ther 312:220–230

54. Ostresh JM, Schoner CC, Hamashin VT, Nefzi A, Meyer J-P, Houghten RA (1998) Solid-phase synthesis of trisubstituted bicyclic guanidines via cyclization of reduced n-acylated dipeptides. J Org Chem 63:8622–8623

55. Harding WW, Tidgewell K, Byrd N, Cobb H, Dersch CM, Butelman ER, Rothman RB, Prisinzano TE (2005) Neoclerodane diterpenes as a novel scaffold for μ opioid receptor ligands. J Med Chem 48:4765–4771

56. Prisinzano TE, Tidgewell K, Harding WW (2005) κ Opioids as potential treatments for stimulant dependence. AAPS J 07:E592–E599

57. Tidgewell K, Groer CE, Harding WW, Lozama A, Schmidt M, Marquam A, Hiemstra J, Partilla JS, Dersch CM, Rothman RB, Bohn LM, Prisinzano TE (2008) Herkinorin analogues with differential β-arrestin-2 interactions. J Med Chem 51:2421–2431

58. Lin C-E, Takemori AE, Portoghese PS (1993) Synthesis and κ-opioid antagonist selectivity of a norbinaltorphimine congener. Identification of the address moiety required for κ-antagonist activity. J Med Chem 36:2412–2415

59. Jones RM, Hjorth SA, Schwartz TW, Portoghese PS (1998) Mutational evidence for a common κ antagonist binding pocket in the wild-type κ and mutant μ[K303E] opioid receptors. J Med Chem 41:4911–4914

60. Metzger TG, Paterlini MG, Ferguson DM, Portoghese PS (2001) Investigation of the selectivity of oxymorphone- and naltrexone-derived ligands via site-directed mutagenesis of opioid receptors: exploring the 'address' recognition locus. J Med Chem 44:857–862

61. Martin WR (1983) Pharmacology of opioids. Pharmacol Rev 35:283–323

62. Feinberg AP, Creese I, Snyder SH (1976) The opiate receptor: a model explaining structure-activity relationships of opiate agonists and antagonists. Proc Natl Acad Sci USA 73:4215–4219

63. Portoghese PS (1965) A new concept on the mode of interaction of narcotic analgesics with receptors. J Med Chem 8:609–616

64. Portoghese PS, Alreja BD, Larson DL (1981) Allylprodine analogs as receptor probes. Evidence that phenolic and nonphenolic ligands interact with different subsites on identical opioid receptors. J Med Chem 24:782–787

65. Gozalbes R, Barbosa F, Nicolaï E, Horvath D, Froloff N (2009) Development and validation of a pharmacophore-based QSAR model for the prediction of CNS activity. ChemMedChem 4:204–209

66. Medina-Franco JL, Martnez-Mayorga K, Bender A, Marn RM, Giulianotti MA, Pinilla C, Houghten RA (2009) Characterization of activity landscapes using 2D and 3D similarity methods: consensus activity cliffs. J Chem Inf Model 49:477–491

67. Yamaotsu N, Fujii H, Nagase H, Hirono S (2010) Identification of the three-dimensional pharmacophore of κ-opioid receptor agonists. Bioorg Med Chem 18:4446–4452

68. Fujii H, Narita M, Mizoguchi H, Murachi M, Tanaka T, Kawai K, Tseng LF, Nagase H (2004) Drug design and synthesis of ε opioid receptor agonist: 17-(cyclopropylmethyl)-4,5α-epoxy-3,6β-dihydroxy-6,14-endoethenomorphinan-7α-(N-methyl-N-phenethyl)carboxamide (TAN-821) inducing antinociception mediated by putative ε opioid receptor. Bioorg Med Chem 12:4133–4145

69. Kuhl U, von Korff M, Baumann K, Burschka C, Holzgrabe U (2001) Stereochemical behaviour of κ-agonistic 2,4-dipyridin-2-yl-3,7-diazabicyclo[3.3.1]nonanones—influence of the substituent in position N3. J Chem Soc Perkin Trans 2:2037–2042

70. Tsujishita H, Hirono S (1997) Camdas: an automated conformational analysis system using molecular dynamics. J Comput Aided Mol Des 11:305–315

71. Halgren TA (1999) MMFF VI. MMFF94s option for energy minimization studies. J Comput Chem 20:720–729

72. Halgren TA (1999) MMFF VII. Characterization of MMFF94, MMFF94s, and other widely available force fields for conformational energies and for intermolecular-interaction energies and geometries. J Comput Chem 20:730–748
73. Iwase K, Hirono S (1999) Estimation of active conformations of drugs by a new molecular superposing procedure. J Comput Aided Mol Des 13:499–512
74. Nagase H, Osa Y, Nemoto T, Fujii H, Imai M, Nakamura T, Kanemasa T, Kato A, Gouda H, Hirono S (2009) Design and synthesis of novel delta opioid receptor agonists and their pharmacologies. Bioorg Med Chem Lett 19:2792–2795

Index